

EIDESSTATTLICHE ERKLÄRUNG

Ich erkläre an Eides statt, dass ich die vorliegende Arbeit selbstständig verfasst, andere als die angegebenen Quellen/Hilfsmittel nicht benutzt, und die den benutzten Quellen wörtlich und inhaltlich entnommenen Stellen als solche kenntlich gemacht habe. Das in TUGRAZonline hochgeladene Textdokument ist mit der vorliegenden Dissertation identisch.

Datum

Unterschrift

Danksagung

Begeistert durch die exzellenten Vorlesungen, das enorme Fachwissen und den hochinteressanten Forschungsschwerpunkt wollte ich meine Dissertation unbedingt bei Prof. Dr. Rolf Breinbauer durchführen. In den drei Jahren meines Doktoratsstudiums wurde ich in meiner hohen Meinung über Rolf Breinbauer bestätigt. Rolf, ich möchte Dir meinen tiefsten Dank, nicht nur für die Ermöglichung meiner Dissertation, sondern auch für das große Vertrauen, deine Unterstützung, deinen extremen Einsatz und die freundschaftliche Betreuung ausdrücken. Mir hat die Zeit wirklich sehr großen Spaß gemacht und ich konnte sehr viel lernen. Es ist mir ein Anliegen zu erwähnen, dass ich begeistert von deiner überaus motivierten und positiven Einstellung bin. Ich hätte mir keinen besseren Betreuer wünschen können! Vielen vielen Dank Rolf!!

Meinen großen Dank möchte ich auch gegenüber Prof. Dr. Robert Saf ausdrücken, der sich dazu bereit erklärt hat mein zweiter Gutachter zu sein. Darüber hinaus bin ich für die HRMS Messungen und für die großartige Unterstützung bei der Interpretation dankbar.

Des Weiteren bin ich meinen Bürokollegen Melanie Trobe, Patrick Dobrounig und Sebastian Grimm dankbar für die produktive und sehr lustige Zeit.

Ein großes Dankeschön gebührt meinen großartigen Studenten Harald Podversnik, Michaela Wernik, Roland Pichler-Nagl, Sebastian Tassoti und Thomas Schlatzer. Ihr seid wirklich außergewöhnlich begabte Studenten und es ehrt mich, dass ihr bei mir eure Bachelorarbeiten bzw Masterlabore gemacht habt. Ihr wart eine große Bereicherung für das Gelingen meiner Dissertation und habt fantastische Arbeit geleistet.

Speziell hervorheben möchte ich Felix Anderl und Mario Leypold, die bei kniffligen Synthesproblemen immer eine große Hilfe waren. Extra erwähnen möchte ich auch Jakov Ivkovic und Dr. Gernot Strohmeier, die mir wertvolle Tipps betreffend HPLC gaben.

Ich bin wirklich dankbar so tolle Kollegen zu haben. Die Zeit mit euch war sehr freundschaftlich und bereichernd. Danke an Carina Doler, Christian Lembacher-Fadum, Christian Leypold, Christian Pichler, Julia Blesl, Jakob Pletz, Jakov Ivkovic, Felix Anderl, Kathrin Heckenbichler, Marko Kljajic, Mario Faber, Mario Leypold, Melanie Trobe, Patrick Dobrounig, Sebastian Grimm, Stefan Holler und Xuepu Yu.

Einen Riesendank möchte ich Astrid Nauta für die wirklich wertvolle und kompetente Unterstützung nicht nur in organisatorischen Angelegenheiten ausdrücken.

Immer wenn es Probleme mit der EDV gab, war Peter Plachota sofort zur Stelle und hat jedes einzelne Problem behoben. Vielen vielen Dank!

Einen großen Dank an das NMR-Team Prof. Dr. Jörg Weber und Carina Illaszewicz-Trattner für die aufopferungsvolle Hilfe bei der Spektreninterpretation und den unzähligen Messungen.

Vielen Dank an Karin Bartl und Pål William Wallace für die HRMS Messungen.

Ein herzliches Dankeschön an meine Freunde, meinen Bruder Jakob und meine Familie für die großartige Unterstützung. Einen besonderen Dank möchte ich meiner Freundin Lydia für ihr großes Verständnis ausdrücken, das sie mir in extrem zeitintensiven Phasen meiner Dissertation entgegenbracht hat. Du hast mich immer unterstützt. Danke!

Ein außerordentlicher Dank gebührt meinen wunderbaren Eltern Friederike und Helmut für ihre aufopferungsvolle Unterstützung jederzeit und in jeglicher Hinsicht. Ich bin euch unendlich dankbar.

Diese Arbeit ist meinen Eltern Friederike und Helmut gewidmet.

1 Table of contents

1	Table of contents.....	iv
2	Abstract.....	1
3	Kurzfassung.....	2
4	Introduction.....	3
5	Theoretical background.....	4
5.1	Characteristics of phenazines.....	4
5.2	History of phenazines.....	6
5.3	Cystic fibrosis.....	7
5.4	Biosynthesis of phenazines.....	7
5.5	Chorismate-utilizing enzymes.....	11
5.6	PhzE.....	15
5.6.1	Active sites of PhzE.....	16
5.6.2	Inhibition of PhzE and anthranilate synthase (AS).....	16
5.6.3	Mechanistic considerations.....	18
5.6.4	Differences between PhzE and AS.....	18
5.7	Carbenoid-based OH-insertion reactions.....	20
5.7.1	Carbenoid-based OH-insertion reactions in chemical biology.....	21
5.7.2	O-H insertion reactions with diazocarbonyl compounds.....	21
6	Aim of this work.....	26
7	Results and discussion.....	27
7.1	Aromatic inhibitors.....	27
7.2	Cyclohexane-derived inhibitors.....	32
7.3	ADIC-derived inhibitors.....	36
7.3.1	General considerations.....	36
7.3.2	First ADIC-derived inhibitor.....	39
7.3.3	Etherification screening.....	41
7.3.4	Additional ADIC-derived inhibitors.....	45
7.4	Cyclohexadiene-derived inhibitors.....	48
7.4.1	Fully-conjugated substrates.....	48
7.4.2	Cross-conjugated substrates.....	51
7.5	Investigations towards mechanism-based inhibitors.....	53
7.5.1	Birch-reduction.....	55
7.5.2	Esterification.....	61
7.5.3	Reduction.....	63
7.5.4	Synthesis of the putative inhibitor 48	63
7.5.5	Introduction of the second double bond.....	64

7.5.6	Deprotection.....	68
7.5.7	Summary.....	68
7.5.8	Investigation of 4-fluorobenzoic acid as alternative starting material	70
7.5.9	Alternative access to a 4-methylated cyclohexadiene intermediate	72
7.6	Systematic investigation of carbenoid based OH-insertion reactions for labile substrates	74
7.6.1	GC-FID Screening.....	74
7.6.2	¹ H-NMR Screening.....	76
8	Summary and outlook	82
8.1	Summary.....	82
8.1.1	Aromatic inhibitors.....	82
8.1.2	Cyclohexane-derived inhibitors	83
8.1.3	ADIC-derived inhibitors	85
8.1.4	Cyclohexadiene-derived inhibitors.....	86
8.1.5	Mechanism-based inhibitors.....	86
8.1.6	Etherification of unstable alcohols	87
8.2	Outlook.....	88
8.2.1	Enzymatic activity tests	88
9	Experimental section	89
9.1	General	89
9.2	Solvents	89
9.3	Reagents.....	91
9.4	Analytical Methods	93
9.4.1	Thin-layer chromatography.....	93
9.4.2	Flash column chromatography	93
9.4.3	High performance liquid chromatography	93
9.4.4	Nuclear magnetic resonance spectroscopy	94
9.4.5	High resolution mass spectrometry	94
9.4.6	Determination of the melting point.....	95
9.4.7	Gas chromatography.....	95
9.5	General procedure for the ¹ H-NMR screening of OH-insertion reactions	96
9.6	General procedure for cracking paraformaldehyde.....	96
9.7	General setup of the Birch-reduction	97
9.8	Experimental procedures and analytical data	98
9.8.1	Methyl 2-diazo-2-(dimethoxyphosphoryl)acetate (R-1)	98
9.8.2	Methyl 2-diazoacetate (R-2)	99
9.8.3	Methyl 2-diazopropanoate (R-3)	100
9.8.4	Dimethyl 2-diazomalonate (R-4).....	101

9.8.5	Methyl-2-diazo-2-(trimethylsilyl)acetate (R-5)	102
9.8.6	Rh ₂ (1-adaman) ₄ dimer.....	103
9.8.7	Methyl 3-hydroxy-4-methylbenzoate (1)	104
9.8.8	Methyl 3-((1-methoxy-1-oxobutan-2-yl)oxy)-4-methylbenzoate (2)	105
9.8.9	Methyl 3-hydroxy-4-methylbenzoate (3)	106
9.8.10	Methyl 3-((1-methoxy-1-oxobut-2-en-2-yl)oxy)-4-methylbenzoate (4)	108
9.8.11	Methyl 3-((1-methoxy-1-oxopropan-2-yl)oxy)-4-methylbenzoate (5)	110
9.8.12	Methyl 3-(2-methoxy-2-oxoethoxy)-4-methylbenzoate (6)	111
9.8.13	3-(1-Carboxypropoxy)-4-methylbenzoic acid (7).....	112
9.8.14	3-((1-Carboxyvinyl)oxy)-4-methylbenzoic acid (8)	113
9.8.15	3-((1-Carboxyprop-1-en-1-yl)oxy)-4-methylbenzoic acid (9)	114
9.8.16	3-(1-Carboxy-ethoxy)-4-methyl benzoic acid (10).....	115
9.8.17	3-(Carboxymethoxy)-4-methylbenzoic acid (11)	116
9.8.18	8-Hydroxy-2,2-dimethyl-4H-benzo[d][1,3]dioxin-4-one (12)	117
9.8.19	Ethyl 2-(((2,2-dimethyl-4-oxo-4H-benzo[d][1,3]dioxin-8-yl)oxy)methyl)acrylate (13)	118
9.8.20	Methyl 2-(((2,2-dimethyl-4-oxo-4H-benzo[d][1,3]dioxin-8-yl)oxy)butanoate (14) 119	
9.8.21	3-(1-Carboxypropoxy)-2-hydroxybenzoic acid (15).....	120
9.8.22	<i>cis</i> -3-((1-Carboxyvinyl)oxy)cyclohexane-1-carboxylic acid (16)	121
9.8.23	<i>cis</i> -3-(Carboxymethoxy)cyclohexane-1-carboxylic acid (17).....	122
9.8.24	Methyl-3-hydroxycyclohexane-1-carboxylate (18)	123
9.8.25	Methyl 3-oxocyclohexane-1-carboxylate (19)	124
9.8.26	5-Oxocyclohex-1-ene-1-carboxylic acid (20)	126
9.8.27	Methyl 3-(2-methoxy-2-oxoethoxy)cyclohexane-1-carboxylate (21).....	127
9.8.28	Methyl 3-((3-methoxy-3-oxoprop-1-en-2-yl)oxy)cyclohexane-1-carboxylate (22)	128
9.8.29	Ethyl-6-((tert-butoxycarbonyl)amino)-5-(2-ethoxy-2-oxoethoxy)cyclohex-1-ene- 1-carboxylate (23)	130
9.8.30	Ethyl 6-((tert-butoxycarbonyl)amino)-5-hydroxycyclohex-1-ene-1-carboxylate (24)	131
9.8.31	Ethyl 3-((tert-butoxycarbonyl)amino)-7-oxabicyclo[2.2.1]heptane-2-carboxylate (25)	132
9.8.32	Ethyl <i>endo</i> -3-((tert-butoxycarbonyl)amino)-7-oxabicyclo[2.2.1]hept-5-ene- <i>exo</i> -2- carboxylate (26)	133
9.8.33	Ethyl <i>endo</i> -3-nitro-7-oxabicyclo[2.2.1]hept-5-ene- <i>exo</i> -2-carboxylate (27)....	135
9.8.34	Ethyl (<i>E</i>)-3-nitroprop-2-enoate (28).....	136
9.8.35	Ethyl 2-hydroxy-3-nitropropanoate (29).....	137
9.8.36	Ethyl <i>trans</i> -6-((tert-butoxycarbonyl)amino)-5-hydroxycyclohexa-1,3-diene-1- carboxylate (30)	138

9.8.37	Ethyl <i>trans</i> -6-((tert-butoxycarbonyl)amino)-5-(2-methoxy-2-oxoethoxy)cyclohexa-1,3-diene-1-carboxylate (31)	139
9.8.38	<i>trans</i> -2-Carboxy-6-(carboxymethoxy)cyclohexa-2,4-dien-1-ammonium 2,2,2-trifluoroacetate (32)	141
9.8.39	<i>rac</i> -Ethyl (5 <i>S</i> ,6 <i>S</i>)-5-(2-amino-2-oxoethoxy)-6-((tert-butoxycarbonyl)amino)cyclohexa-1,3-diene-1-carboxylate (33).....	143
9.8.40	Methyl 5-(2-methoxy-2-oxoethoxy)cyclohexa-1,3-diene-1-carboxylate (34)... 144	
9.8.41	Methyl 5-hydroxycyclohexa-1,3-diene-1-carboxylate (35).....	145
9.8.42	Methyl 7-oxabicyclo[2.2.1]hept-5-ene-2-carboxylate (36)	146
9.8.43	Dimethyl 2-((5-(methoxycarbonyl)cyclohexa-2,4-dien-1-yl)oxy)malonate (37)147	
9.8.44	Cyclohexa-2,5-diene-1-carboxylic acid (38).....	148
9.8.45	Methyl cyclohexa-2,5-diene-1-carboxylate (39)	149
9.8.46	Methyl 7-oxabicyclo[4.1.0]hept-3-ene-2-carboxylate (40)	150
9.8.47	Methyl 3-hydroxycyclohexa-1,5-diene-1-carboxylate (41).....	151
9.8.48	Methyl 3-(2-methoxy-2-oxoethoxy)cyclohexa-1,5-diene-1-carboxylate(42)... 152	
9.8.49	3-Methoxy-4-methylbenzoic acid (43).....	153
9.8.50	4-Methyl-5-oxocyclohex-2-enecarboxylic acid (44).....	154
9.8.51	Methyl 4-methyl-5-oxocyclohex-2-enecarboxylate (45).....	156
9.8.52	Methyl 5-hydroxy-4-methylcyclohex-2-enecarboxylate (46)	157
9.8.53	Methyl 5-((3-methoxy-3-oxoprop-1-en-2-yl)oxy)-4-methylcyclohex-2-ene-1-carboxylate (47)	159
9.8.54	Ammonium 5-((1-carboxylatovinyl)oxy)-4-methylcyclohex-2-ene-1-carboxylate (48)	161
9.8.55	Methyl 4-methyl-5-((trimethylsilyl)oxy)cyclohex-2-enecarboxylate (49).....	162
9.8.56	Methyl 1-hydroxy-4-methyl-5-((trimethylsilyl)oxy)cyclohex-2-enecarboxylate (50)	163
9.8.57	Methyl 4-methyl-5-((triisopropylsilyl)oxy)cyclohex-2-enecarboxylate (51)	164
9.8.58	Methyl 1-hydroxy-4-methyl-5-((triisopropylsilyl)oxy)cyclohex-2-enecarboxylate (52)	165
9.8.59	Methyl 4-methyl-3-((triisopropylsilyl)oxy)cyclohexa-1,5-dienecarboxylate (53)	166
9.8.60	Methyl 5-hydroxy-4-methylcyclohexa-1,3-diene-1-carboxylate (54).....	167
9.8.61	2,2,2-Trifluoroethyl 5-methyl-7-oxabicyclo[2.2.1]hept-5-ene-2-carboxylate (55).. ..	168
9.8.62	2,2,2-Trifluoroethyl 5-hydroxy-4-methylcyclohexa-1,3-diene-1-carboxylate (56)	169
9.8.63	Methyl (<i>E</i>)-5-hydroxy-5-phenylpent-2-enoate (57)	170
9.8.64	Methyl (<i>E</i>)-5-(2-ethoxy-2-oxoethoxy)-5-phenylpent-2-enoate (58)	171
9.8.65	<i>rac-trans</i> -Ethyl-6-((tert-butoxycarbonyl)amino)-5-(2-ethoxy-2-oxoethoxy)cyclohexa-1,3-diene-1-carboxylate (59)	172
9.8.66	“Rh ₂ (tfacam) ₄ ” –batch 1	173

9.8.67	"Rh ₂ (tfacam) ₄ " –batch 2.....	175
10	Abbreviations.....	177
11	References.....	182
12	Appendix.....	187

2 Abstract

Phenazines are a large class of redox-active secondary metabolites, mainly produced by *Streptomyces* and *Pseudomonas*. In order to compete with hostile organisms these secondary metabolites equip bacteria with a competitive advantage, making them to a potential source of antibiotics and anti-proliferate drugs against cancer. In addition, new data suggest that phenazines also play a role in the primary metabolism of their producers.

In the first step of the biosynthesis towards strain-specific phenazines, chorismate, an important intermediate of the shikimate pathway, is converted to 2-amino-2-deoxyisochorismic acid (ADIC). This reaction is catalyzed by PhzE, an enzyme related to anthranilate synthase (AS). Other than in PhzE, where ADIC is transported to PhzD for the synthesis towards strain-specific phenazines, AS catalyzes the elimination of pyruvate in ADIC to give anthranilate. These different modes of action are somewhat surprising as the active site of PhzE and AS is nearly identical. There is evidence that pyruvate elimination in AS proceeds via a pericyclic mechanism and that the methylene group of the enolpyruvyl moiety in ADIC has to be properly oriented towards the hydrogen atom at C-2. It is likely that the different modes of action may derive from a different release path or the time ADIC remains in the active center.

This thesis presents the synthesis of a diverse set of compounds, which will be used to study binding differences between PhzE and anthranilate synthase. These compounds may present potent lead structures for the development of new antibiotics, upon testing for their inhibitory potential.

Some synthesized intermediates are rather labile and a strategy for the etherification of unstable alcohols was developed, which is of general use.

3 Kurzfassung

Phenazine sind redoxaktive Sekundärmetaboliten und werden hauptsächlich von *Pseudomonas* und *Streptomyces* produziert. Sie statten ihre Produzenten nicht nur mit einem kompetitiven Vorteil aus, sondern können sogar im Primärmetabolismus eine wichtige Rolle spielen. Die Erforschung der Biosynthese von Phenazinen könnte zur Entwicklung von neuartigen Antibiotika beitragen.

In der ersten Stufe der Biosynthese von Phenazinen wird Chorisminsäure in 2-Amino-2-desoxyisochorisminsäure (ADIC) umgewandelt- eine Reaktion die von PhzE katalysiert wird, ein Enzym das mit Anthranilatsynthase (AS) verwandt ist. Anders als in PhzE, wo ADIC zur Synthese von stammspezifischen Phenazinen zu PhzD transportiert wird, katalysiert AS die Eliminierung von Brenztraubensäure in ADIC für die Synthese von Anthranilsäure. Diese unterschiedlichen mechanistischen Wege sind überraschend, da das aktive Zentrum der beiden Enzyme weitgehend identisch ist. Es gibt Hinweise darauf, dass die Eliminierung von Brenztraubensäure in AS über einen pericyclischen Mechanismus verläuft und dass die Methylengruppe in ADIC in richtiger Anordnung zum Wasserstoff am C-2 Atom stehen muss. Es ist wahrscheinlich, dass die beiden mechanistischen Möglichkeiten des unterschiedlichen Freisetzungsweges von ADIC oder dessen Verbleibdauer im aktiven Zentrum entstammen.

In dieser Arbeit wird die Synthese von einem Ensemble diverser Substanzen vorgestellt, die zur Ergründung der unterschiedlichen mechanistischen Wege von PhzE und Anthranilatsynthase verwendet werden. Diese Substanzen könnten einen wichtigen Beitrag für die Entwicklung von neuartigen Antibiotika leisten.

Darüberhinaus wird ein für die Veretherung von instabilen Alkoholen entwickeltes Konzept vorgestellt das nicht nur für die Synthese von PhzE und AS Inhibitoren vorteilhaft sein kann, sondern auch für generelle Syntheseherausforderungen.

4 Introduction

Antibiotic drug resistance has become a global threat. Nevertheless, research and development into antibiotics has declined because of its low profitability.^[1,2]

The discovery of penicillin in a mould culture by Alexander Fleming in 1928 clearly constitutes one of the most important medicinal accomplishments. Howard Walter Florey and Ernst Boris Chain were the first to produce this useful antibiotic.^[3] Growing resistance among pathogenic bacteria necessitates research into alternative antibiotics,^[3] but only two new classes of antibiotics have been launched since 1967:^[4] oxazolidinones in 2000 and lipopeptides in 2003.^[2]

Phenazines are a large class of redox-active secondary metabolites. This class of natural products is mainly produced by *Streptomyces* and *Pseudomonas*. *Pseudomonas aeruginosa* accounts for 10-15 % of all nosocomial infections worldwide.^[5] This germ represents a major problem as it is resistant to many drug classes and able to acquire further resistance mechanisms.^[6] The disease cystic fibrosis is made even worse through infection with *Pseudomonas aeruginosa*. In the deeper layer of the biofilm in the lungs of these patients, phenazines act to sustain glycolysis via reoxidation of NADH and the oxidative activity of patients has shown to be fatal.^[7-9]

Secondary metabolites are molecules produced at late stages of microbial growth in laboratory cultures. Until recently, it has been thought that secondary metabolites do not contribute to the growth or survival of their producers, but in the last years it has been realized that they are of greater importance for their host organisms.^[10] In order to compete with hostile organisms these secondary metabolites equip bacteria with a competitive advantage,^[11] making them a potential source of antibiotics and anti-proliferative drugs against cancer. In addition, new data suggest that phenazines also play a role in the primary metabolism of their producers.^[12] A mouse model of lung infection with strains of *Pseudomonas aeruginosa* that are not capable of producing phenazines showed less virulence than their phenazine producing counterparts,^[13] which underlines the importance of phenazines.

5 Theoretical background

5.1 Characteristics of phenazines

Phenazines are a large class of redox-active secondary metabolites produced by many Gram-positive (e.g. *Streptomyces*) and Gram-negative bacteria (e.g. *Pseudomonas*) or by archaeal *Methanosarcina* species. It has been shown that some phenazines exhibit antibiotic, antitumor, antimalarial, and antiparasitic activities. These secondary metabolites are produced by cells that have stopped dividing and it has been shown that phenazine-producing organisms show a longer lifespan in the natural environment than their non phenazine-producing counterparts.^[3]

Phenazines act as antibiotics and are produced in huge quantities when it comes to the protection from competitors.^[10,14] It turned out that these secondary metabolites are advantageous for their producers.^[11] However, new data suggest that phenazines also play a role in the primary metabolism of their producers.^[12] Various features^[3,12,15] of phenazines are known, which include:

- Reduction of molecular oxygen to reactive oxygen species that are toxic to other microorganisms. These toxic intermediates trigger also tissue damage in human infectious disease;^[7]
- Retention of glycolysis under anaerobic conditions through reoxidation of NADH. These conditions are for example met in the deeper layer of a biofilm from patients suffering from cystic fibrosis;^[8,9]
- Contribution to iron homeostasis through the reduction of Fe³⁺-containing minerals to the more soluble Fe²⁺ forms and subsequent siderophore uptake;^[16]
- Activation of the iron-containing transcription factor SoxR,^[17] which is responsible for the production of signalling molecules for oxidative stress defence;^[18]
- Inhibition of the DNA-template controlled RNA synthesis through DNA intercalation (π - π stacking).^[19]

Despite massive supply of phenazines, the physical importance has not yet been fully understood.^[10] There are over 150 phenazine natural products known in the literature^[12] and thousands of derivatives have been synthesized so far.^[3,15,20] In Figure 5.1 a few naturally occurring phenazines are exemplified.

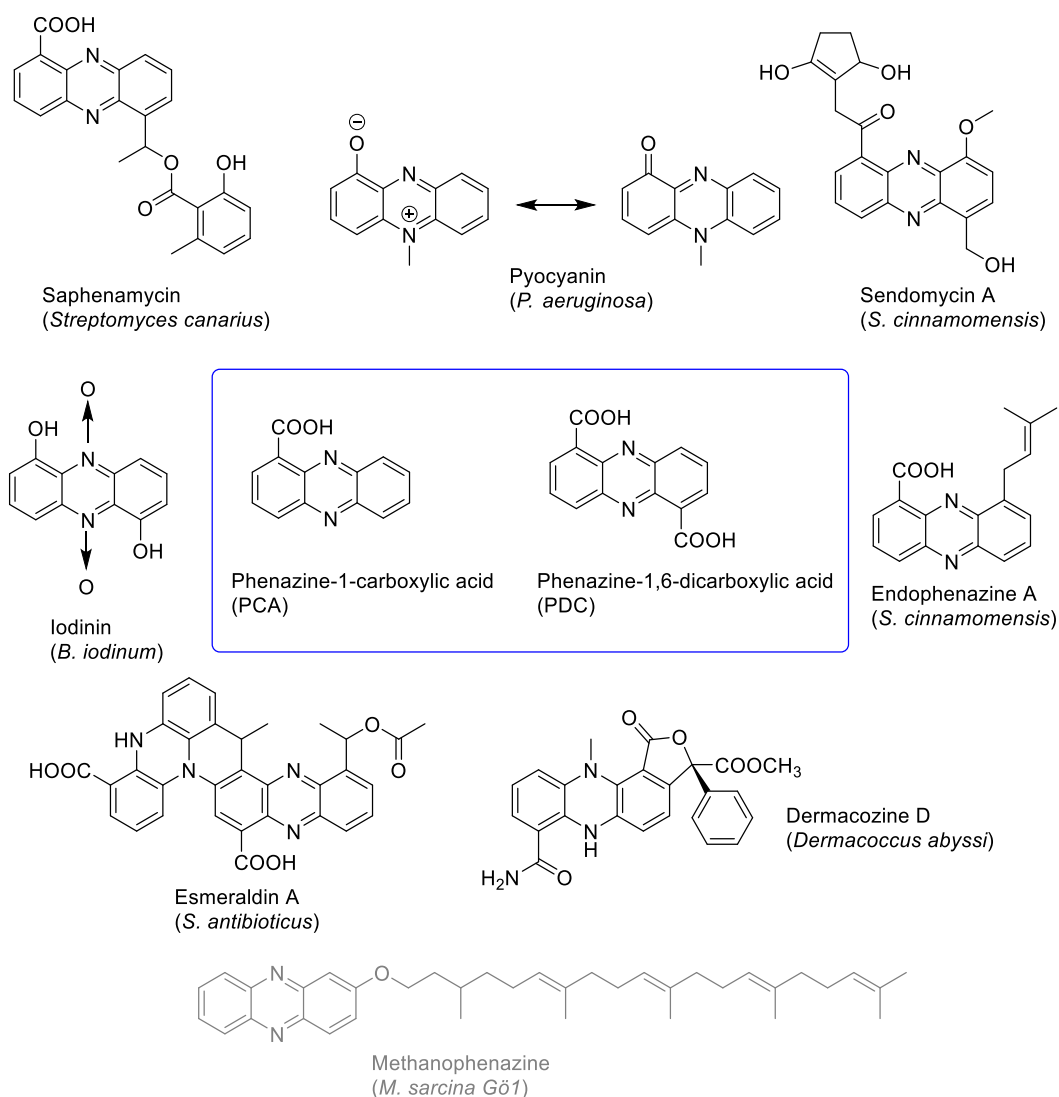


Figure 5.1: Examples of naturally occurring phenazine derivatives.^[12,15] All depicted molecules derive from either PCA or PDC (blue box) with the exception of methanophenazine (grey), for which the biosynthetic pathway is not known to date and which is from archaeal origin.

The variety of colors upon substitution of the core phenazine structure is quite impressive (Figure 5.2). Only small modifications of the phenazine core result in differently colored products. For instance 5-methyl-7-amino-1-carboxyphenazinium betaine (aeruginosin A) is deep red, while phenazine-1-carboxylic acid (PCA) is lemon yellow.^[10]

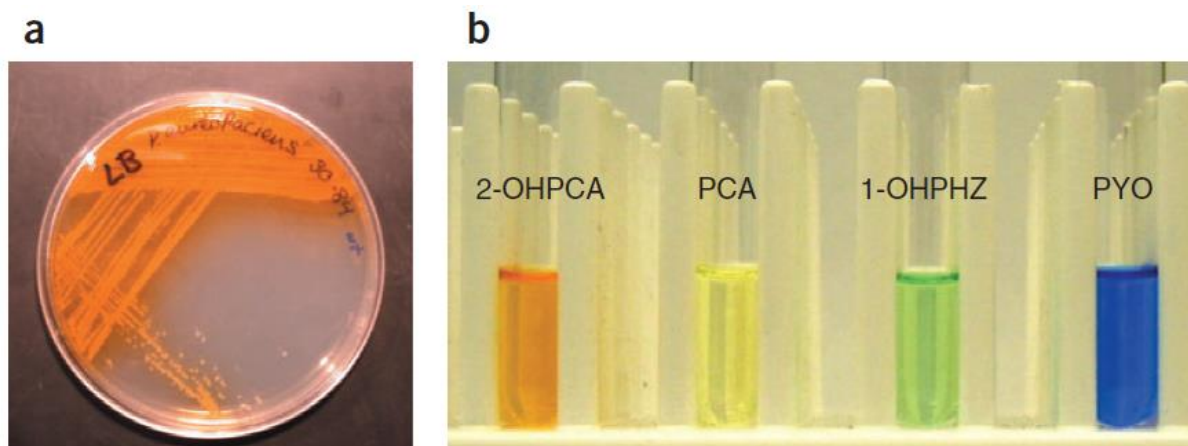


Figure 5.2: a: 2-OHPCA colors the agar orange; b: Phenazine solutions in aqueous medium (figure taken from Price-Whelan et al.)^[10]

The core structure of phenazines is a pyrazine (1,4-diazabenzene) containing two annulated benzenes. The unique properties of phenazines derive from its electronic and steric properties. The flat structure of the aromatic core has structural similarity to known intercalators such as acridines, chromomycin or ethidium bromide and allows therefore for DNA intercalation through π - π interactions with the base pairs.^[19] Another impressive example for structure-related properties of phenazines is the occurrence of a charge transfer, which is attributed to the large electron-rich chromophore. For instance 2-hydroxyphenazine and its reduced form have been found to be electron carriers in the metabolic pathway to produce methane in methanogenic archaea, along with other phenazines.^[3,21,22]

Phenazines are most commonly produced by *Pseudomonas* and *Streptomyces*, minor producers are *Brevibacterium*, *Microbispora* and *Sorangium*.^[23] *Pseudomonas* strains produce most commonly simple phenazines (hydroxyl- and carboxyl-substituted as well as methoxy- and methylester derivatives).^[3] *Streptomyces* generally produce more complex phenazines, along with simple phenazines like those produced by *Pseudomonas*. Some examples for more complex structures include aldehydes, thioethers, esters, amides as well as terpenoidal, carbohydrate- and amino acid-containing phenazines.^[3] Larger derivatives can even consist of two phenazine moieties (e.g. esmeraldin A). *Streptomyces* produces several optically active phenazines that are derivatives of natural amino acids or natural terpenes.^[3]

5.2 History of phenazines

The fact that phenazines are colored pigments, led to their early discovery in the mid-19th century.^[12] The first discovered phenazines were pyocyanin, chlororaphine and iodinin (Figure 5.1).^[23] In 1859 Mathurin-Joseph Fordos described the extraction of a blue pigment, which is

responsible for the coloration of the 'blue pus', observed in patients suffering from severe purulent wounds. Fordos named the blue pigment 'pyocyanine' (PYO) from the Greek words for 'pus' and 'blue'. Pyocyanine is nowadays more commonly spelled as 'pyocyanin'.^[24,25] In 1882, Carl Gessard named a microorganism associated with pyocyanin *Bacillus pyocyaneus*.^[12] Numerous studies about the chemical composition of pyocyanin have been published so far and it was found that pyocyanin is a redox-active compound that changes its color depending on pH and oxidation state. This microorganism is today known as *Pseudomonas aeruginosa* and it took more than 50 years before the correct chemical structure of pyocyanin was established.^[3,12,15]

5.3 Cystic fibrosis

Pseudomonas aeruginosa is an important opportunistic and nosocomial pathogen,^[12] as well as a common cause of death for patients suffering from cystic fibrosis due to chronic infections of the lungs. Biofilm formation in patients from cystic fibrosis is exceptionally harmful, because it renders bacteria under this biofilm less accessible to immune-response and medication. For billions of years bacterial cells have grown in biofilms as a part of their successful strategy to colonize most life forms. In the deeper layer of the biofilm of this immunocompromised patients, these germs act as respiratory pigments that sustain glycolysis via reoxidation of NADH under anaerobic conditions. An electrochemical gradient is sustained when the reduced phenazines diffuse to the surface of the biofilm and is reoxidized.^[8,9,26,27]

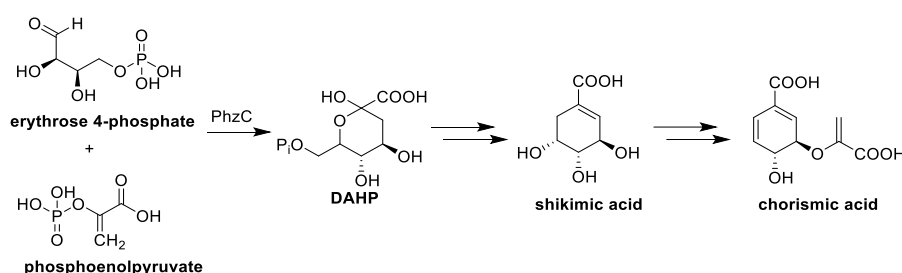
5.4 Biosynthesis of phenazines

Initial research into phenazine biosynthesis was conducted in the second half of the 19th century, when culture media composition of microbial pyocyanin production was studied. It could be shown that the culture conditions and the origin of the bacteria greatly influence the amount of pyocyanin formed. In addition, it was found that *Pseudomonas aeruginosa* produces a variety of additional colored compounds.^[15] In the 1950s Blackwood and Neish discovered that alanine, leucine and isoleucine were the preferred amino acid substrates for phenazine biosynthesis and that ¹⁴C-incorporated glycerol and dihydroxyacetone is incorporated into pyocyanin.^[28] Additional studies with ¹⁴C-labeled compounds were performed by Millican in the early 1960s when he discovered that different to anthranilate, shikimic acid is efficiently incorporated into pyocyanin, which illustrated that chorismate is not converted to anthranilate in the biosynthesis of pyocyanin.^[29] In the early 1970s, it could be shown that phenazines derive from two molecules of chorismic acid^[30,31] and Floss and co-workers found that 2-amino-2-deoxyisochorismic acid (ADIC) is completely inserted into phenazine-1,6-dicarboxylic acid

(PCA), which indicated that phenazine biosynthesis branches off at this point. Most commonly *Pseudomonas* strains are used for the research into phenazines, but it is thought that phenazine biosynthesis in *Streptomyces* proceeds similarly to *Pseudomonas*.^[3,12,15,32]

Research into the biosynthesis of strain-specific phenazines had been complicated because of difficulties in the isolation of unstable intermediates, but the identification of specific genes has leveraged our current knowledge of the biosynthetic pathway towards phenazines.^[15]

The shikimate pathway provides chorismate, the first substrate in the biosynthesis of phenazines (Scheme 5.1).^[3] Chorismic acid is the starting material for many primary and secondary metabolites such as aromatic amino acids, vitamin K, ubiquinone, folate and the siderophores.^[33] *Pseudomonas* and some other bacteria possess PhzC, which catalyzes the first step in the shikimate pathway, the reaction of erythrose 4-phosphate with phosphoenolpyruvate. The *phzC* gene encodes a type-II 3-deoxy-D-arabinoheptulosonate 7-phosphate (DAHP) synthase. In the case of the inhibition of other DAHP synthases, it is thought that PhzC ensures sufficient metabolite flow used in the phenazine biosynthesis.^[15]



Scheme 5.1: Biosynthesis of chorismic acid via the shikimate pathway.^[3]

Genes for phenazine biosynthesis have been found in all bacterial phenazine producers^[34] and five enzymes are encoded in an operon, which catalyze the biosynthesis of phenazine-1,6-dicarboxylic acid (PDC) and phenazine-1-carboxylic acid (PCA), the central building blocks for the biosynthesis of strain-specific phenazines. The so called *phz*-operon was discovered in the late 1990s and further investigations enabled the elucidation of the biochemical pathway for the synthesis of phenazines (Scheme 5.2).^[15]

Five genes are required for the core phenazine biosynthesis, namely *phzB*, *phzD*, *phzE*, *phzF* and *phzG* (Figure 5.3). All phenazine-producing *Pseudomonas* contain an approximately 80 % sequence identical copy of the *phzB* gene, namely *phzA*.^[15] No eubacterial-like *phz* gene cluster has yet been identified in the only known archaeal phenazine producer *Methanosarcina mazei* Gö1.^[15,21,35]

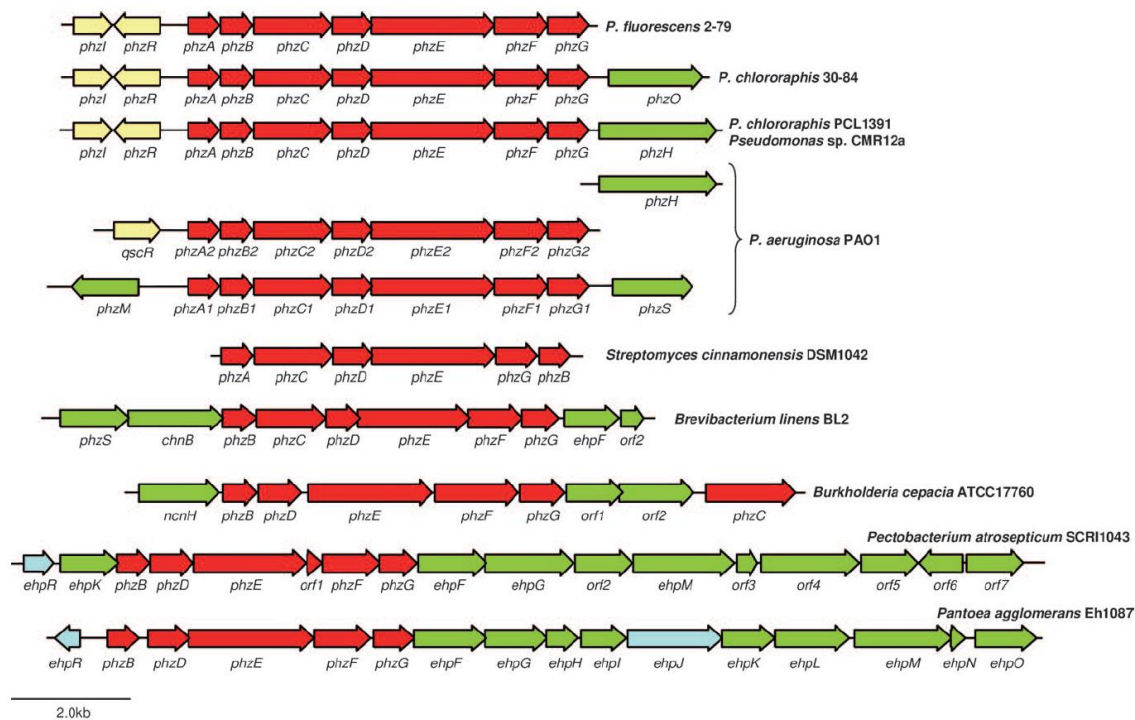
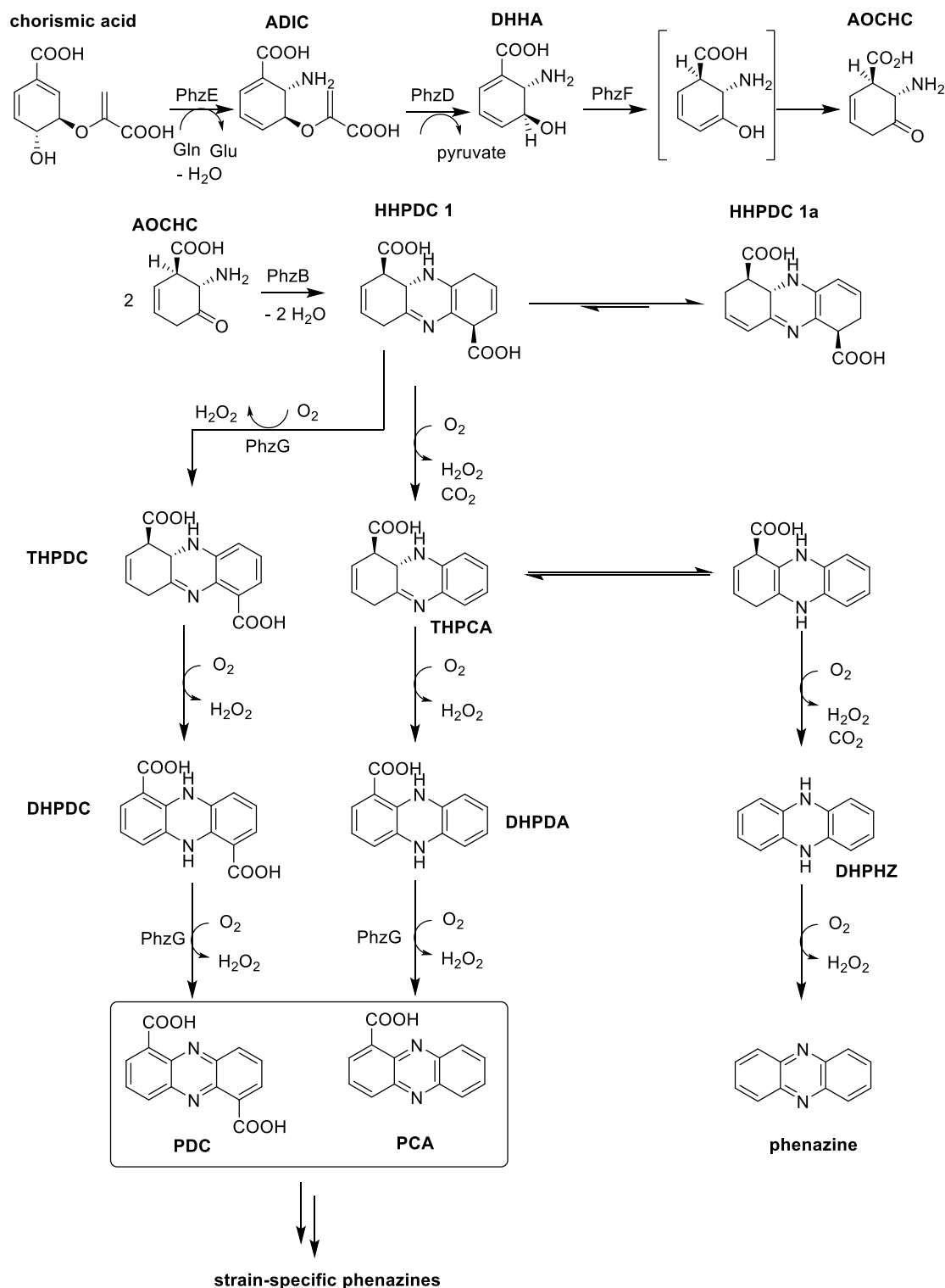


Figure 5.3: Some bacterial biosynthesis clusters. Red: core phenazine biosynthesis, green: phenazine modification, yellow: regulation, cyan: transport and resistance. Figure taken from Mentel et al.^[15]

Chorismic acid is converted to 2-amino-2-deoxy isochorismate (ADIC) by PhzE, in the first step of the biocatalytic cascade. PhzE is a homodimeric enzyme, similar to anthranilate synthase, but lacking the ability to eliminate pyruvate to give anthranilate (see chapter 5.6.4). ADIC is unstable (half-life of 34 h),^[33,36] and is cleaved to *trans*-2,3-dihydro-3-hydroxyanthranilate (DHHHA) by the enzyme PhzD in the second step of the strain-specific biosynthesis of phenazines. DHHA is the last stable intermediate in the pathway. Double bond isomerization catalyzed by PhzF (structurally related to diaminopimelate epimerase,^[37] proline racemase,^[38] 2-methylaconitate isomerase^[39] and 3-methylitaconate- Δ -isomerase^[40])^[12] gives an unstable enol, which isomerizes spontaneously to 6-amino-5-oxocyclohex-2-ene-1-carboxylic acid (AOCHC), which in turn is also unstable. The mechanism for the PhzF catalyzed step is still under investigation, and it is possible that the underlying mechanism is a sigmatropic suprafacial [1,5]-proton shift, rather than an acid-base catalysis.^[41] The next step in the biosynthesis involves the PhzB-catalyzed condensation of the two ketones AOCHC in a head-to tail fashion yielding HHPDC, which is in equilibrium with its fully conjugated isomer.^[15] HHPDC can undergo spontaneous oxidative decarboxylation yielding DHPDA. Oxidation, catalyzed by PhzG, yields PCA. PhzG is also able to oxidize HHPDC twice without decarboxylation (the third oxidation step proceeds uncatalyzed) leading to PDC. As mentioned above, PCA and PDC are the central precursors for strain-specific phenazines. Final modifications of the “core” PCA or PDC isolated from *Pseudomonas* include most commonly the introduction of hydroxyl groups at any position of PCA, methylation,

decarboxylation, *N*-oxidation or other classical biosynthetic transformations.^[42] *Phzh* was identified as a phenazine modifying gene in the biosynthesis of phenazine-1-carboxamide, which is observed in chlororaphine in *P. chlororaphis*.^[43] Carbon-substituted phenazines from *Streptomyces* strains include more sophisticated and yet unknown transformations.^[3,15,20,44]



Scheme 5.2: Biosynthetic pathway of strain-specific phenazines starting from chorismic acid.^[12]

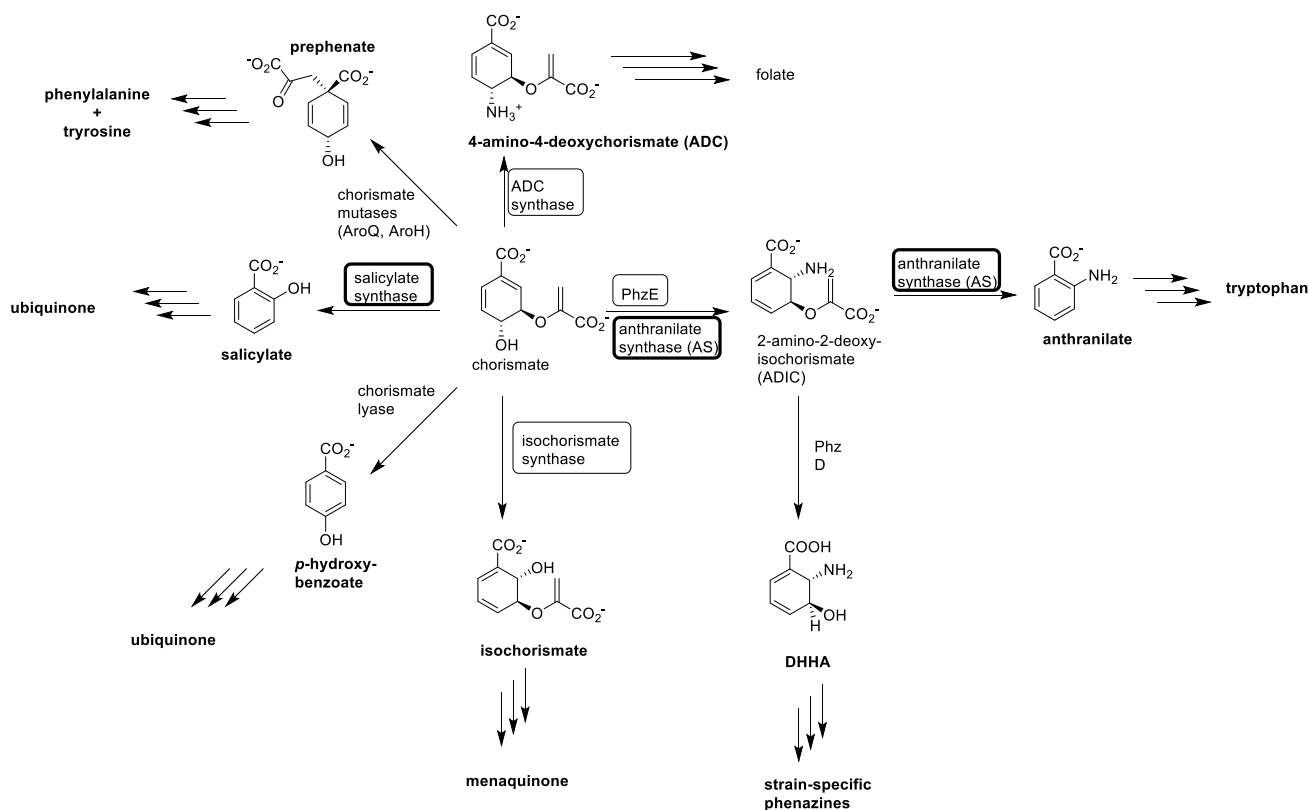
5.5 Chorismate-utilizing enzymes

In the shikimate pathway, phosphoenolpyruvate and erythrose-4-phosphate are converted into chorismate and seven enzymatic steps are included.^[45,46] As the shikimate pathway does not occur in mammals, but in algae, higher plants, bacteria, fungi and apicomplexan parasites, the enzymes involved in this pathway are thought to be attractive targets for the development of antimicrobial drugs and herbicides.^[46–48] Considerable research into chorismate-utilizing enzymes (CUE) has been conducted so far, resulting in a number of inhibition and mechanism studies.^[49–66]

It was realized that this enzyme family shares intriguing similarities concerning the active site and the three-dimensional fold and it may be possible that chorismate-utilizing enzymes have diverged from a common ancestor.^[49,67,68] Sequence identities range from 21-27 %.^[66]

Scheme 5.3 gives an overview of the chorismate-utilizing enzymes, which consist of four families:^[33]

- Chorismate mutases (two unrelated types of AroQ and AroH), which catalyze the transformation of chorismate to prephylate;
- Chorismate lyases, which catalyze the transformation of chorismate to *p*-hydroxybenzoate with concomitant release of pyruvate;
- Menaquinone, siderophore, tryptophan (MST) biosynthesis family, which utilize water or ammonia for a Mg²⁺ dependant nucleophilic substitution reaction at the six-membered ring in chorismate. Two members of this family, namely anthranilate synthase (AS) and salicylate synthase, catalyze the concomitant release of pyruvate via a presumable sigmatropic elimination reaction in the active center.

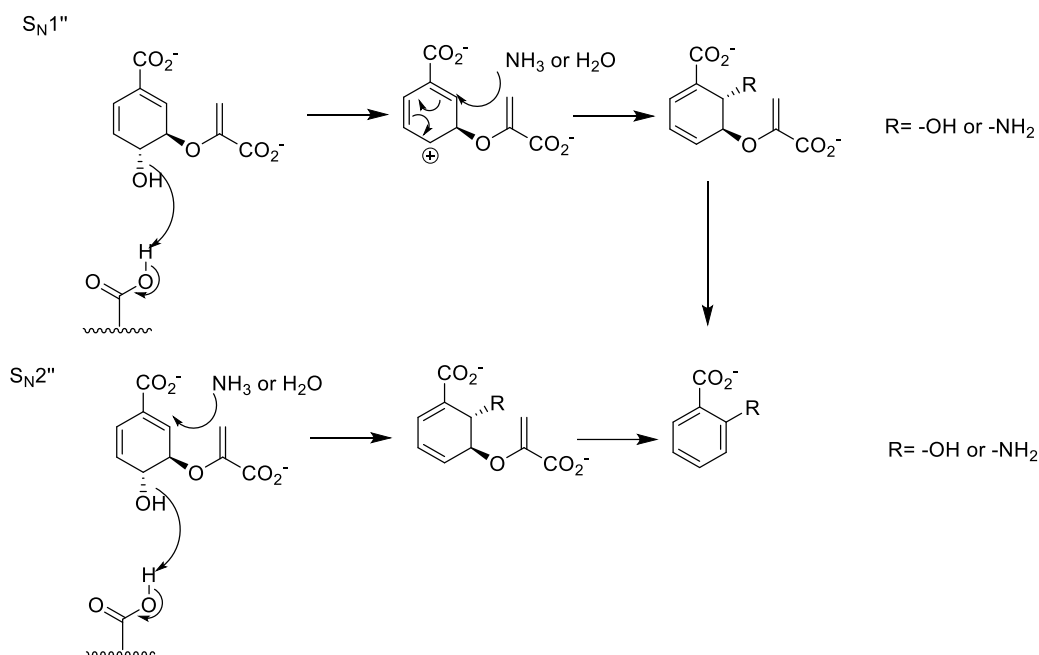


Scheme 5.3: Chorismate-utilizing enzymes. Framed enzymes belong to the MST family. Bold: These enzymes of the MST family catalyze a concomitant release of pyruvate.^[33,49]

It is hypothesized that three members of the MST family, namely anthranilate synthase (AS), isochorismate synthase and salicylate synthase share unifying features in their mechanism.^[53,65,69,70] There are many possible mechanisms and two are outlined in Scheme 5.4:

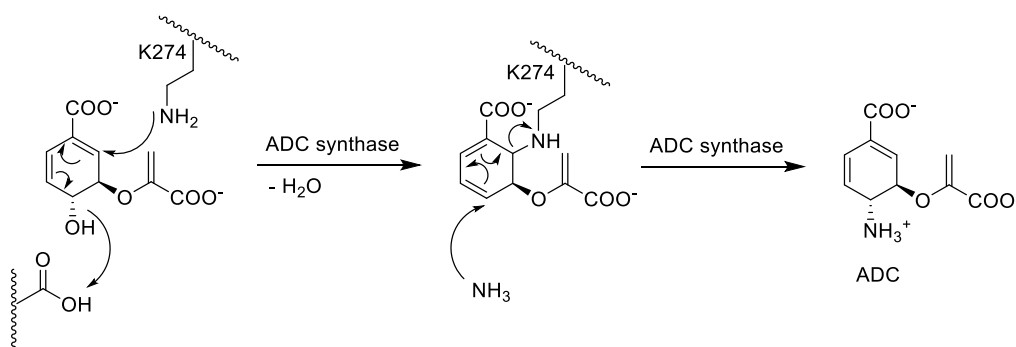
- S_N1'' mechanism:^[65,71] The hydroxyl group of chorismate is protonated by a glutamate residue in the active site with concomitant elimination of water to give the corresponding carbocation. The incoming nucleophile (NH₃ or H₂O) then attacks on C-2 to yield ADIC (in the case of AS) or isochorismate (in the case of isochorismate and salicylate synthase);
- S_N2'' mechanism:^[65] This mechanism proceeds through a direct attack of either ammonia or water on C-2 of chorismic acid and ADIC (in the case of AS) or isochorismate (in the case of isochorismate and salicylate synthase) is released.

For the synthesis of anthranilate or salicylate an additional step involves the elimination of the C-3 enol pyruvyl side chain. There is evidence that this transformation may proceed via a pericyclic rearrangement, which is relatively rare.^[65,72–74]



Scheme 5.4: Two possible mechanisms of the first step in AS, isochorismate synthase and salicylate synthase.^[65]

The mechanism towards 4-amino-4-deoxychorismate (ADC) catalyzed by ADC synthase involves the attack of an amino side chain of an active site lysine residue (K274 in the *E. coli* enzyme),^[69,70] resulting in an enzyme-bound intermediate which is released upon attack of ammonia at C-4 to give ADC (Scheme 5.5).^[66]



Scheme 5.5: Putative mechanism of the biosynthesis towards ADC.^[66]

The lysine residue is conserved as an alanine in anthranilate synthase and isochorismate synthase.^[46] In the case of ADC synthase and anthranilate synthase, there must be a mechanism of preventing water from acting as a nucleophile.^[46]

The three most potent inhibitors of AS reported to date were published in 1995 by Kozlowski et al.^[53] (Figure 5.4).^[66]

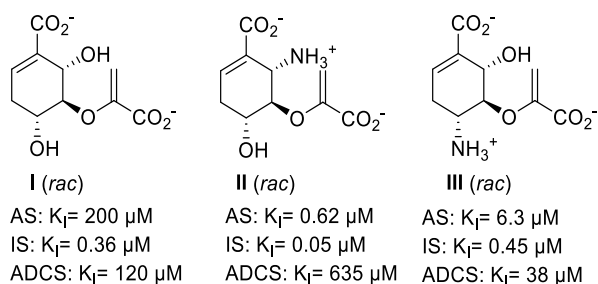


Figure 5.4: Most potent inhibitors of the chorismate-utilizing enzymes to date. Values are not corrected for the presence of the enantiomer. AS= *S. marcescens* anthranilate synthase, IS= *E. coli* isochorismate synthase and ADCS= *E. coli* ADC synthase.^[53,66]

The inhibitors **I-III** are based on the proposed transition state of IS and AS (Figure 5.5).

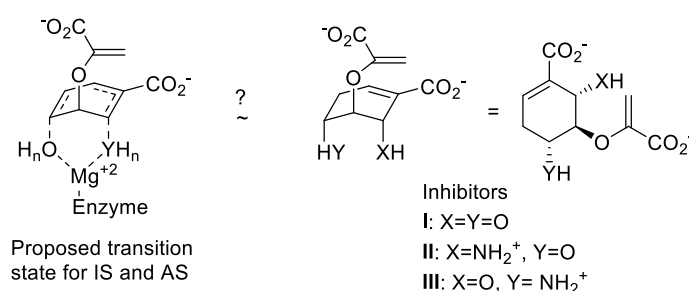


Figure 5.5: Proposed transition state for IS and AS.^[53]

The findings of Kozlowski et al.^[53] are briefly discussed:^[66]

Inhibitor **II** turned out to be the best inhibitor for IS and AS. Compound **II** was initially believed to be a selective inhibitor of AS, because of the ammonium group in position C-6, which mimics the incoming ammonia in the transition state. It was argued that **II** is also a good inhibitor for IS, due to a great axial proportion of the substituents (approx. 20-28% axial composition in **II**, compared to 12 % axial composition of chorismate^[75] in water). The equatorial to axial ratio present at equilibrium is greatly influenced by thermodynamics (which favours the equatorial arrangement) but also by hydrogen bonding and salt bridge formation. The percentage of the axial conformers was determined by NMR and the coupling constants were compared with similar compounds with locked conformation. The poor binding of **I** in the case of AS was explained due to the evolutionary pressure in AS to select against hydroxyl groups, whereas in the case of IS, NH₃ is not available *in vivo*, omitting the evolutionary pressure. The relatively modest binding affinity of **I-III** against ADCS was later explained due to steric crowding at C-6 (a side chain amino group of the lysine residue would be in close proximity).^[66]

It should be noted that many of the literature known inhibitors were tested against several chorismate-utilizing enzymes, but we will focus on the inhibition of AS due to the striking similarities in the active site to PhzE.

5.6 PhzE

In the first reaction of the biosynthesis towards strain-specific phenazines, chorismate is converted to 2-amino-2-deoxyisochorismate (ADIC) catalyzed by PhzE in a Mg^{2+} -dependent reaction (Scheme 5.2). An enzyme related to PhzE, namely anthranilate synthase, catalyzes the same transformation, but in addition also the consecutive conversion to anthranilate, which succeeds via the elimination of pyruvate. PhzE is incapable to catalyze the elimination of pyruvate and therefore the produced ADIC can follow the biosynthetic pathway towards strain-specific phenazines. Direct proof of the generation and release of ADIC had not been provided until 2011, when Blankenfeldt and coworkers could prove that PhzE is an ADIC synthase. The converted chorismic acid was trapped in crystals of an inactive mutant of PhzD and by means of mass spectrometric analysis the product was confirmed as ADIC. PhzE exhibits two domains, namely the menaquinone, siderophore, tryptophan biosynthesis (MST) domain, where chorismate is utilized to give ADIC, and a second type-1 glutamine amidotransferase (GATase1) domain, where ammonia is produced from glutamate, connected by a 45-residue linker (Figure 5.6). It was found that binding of chorismic acid leads to structural rearrangements, which induces an ammonia channel (approx. 25 Å in length) within each of the two MST/GATase1 functional units of the dimer.^[33]

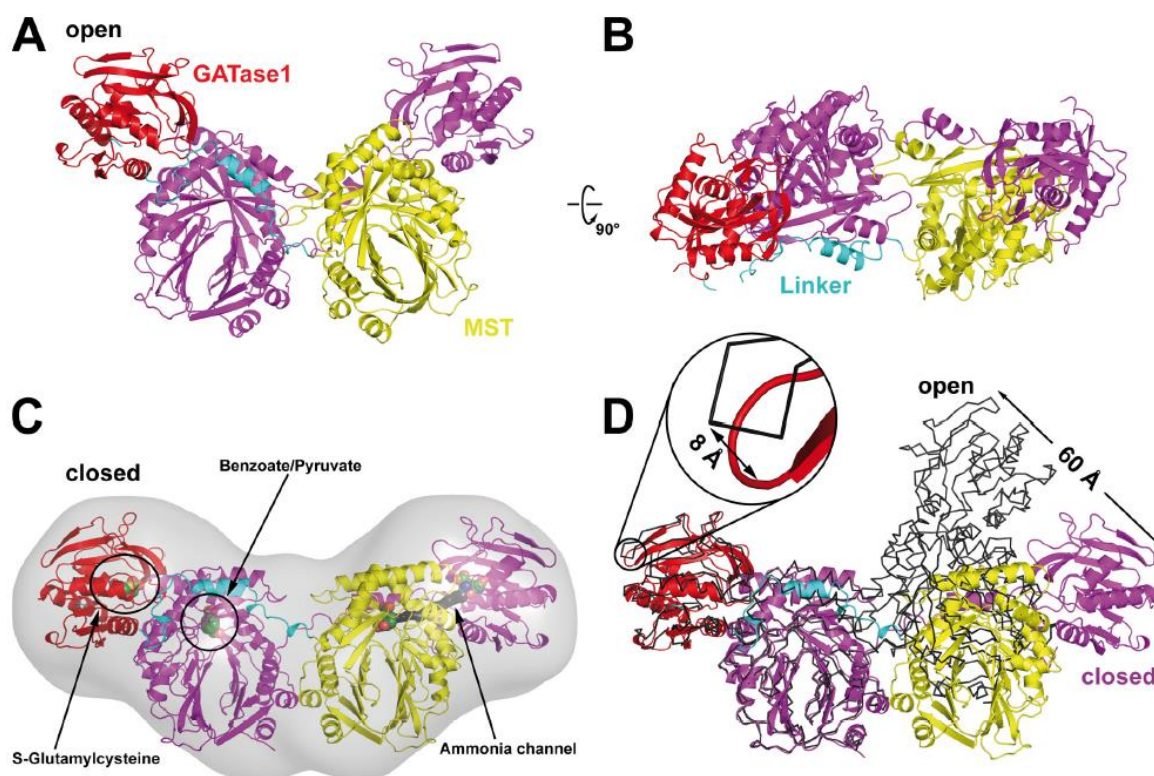


Figure 5.6: PhzE structure from *Burkholderia lata* 383. A: Open form; B: Open form, from top; C: Ligand-bound closed form; D: Comparison of the open (thin lines) and closed structures (ribbons). One MST domain is superimposed from each crystal form. Figure taken from Li et al.^[33]

5.6.1 Active sites of PhzE

It was found that Mg^{2+} and chorismic acid bind simultaneously to PhzE in an endothermic fashion, enabling the GATase1 domain to capture glutamine for hydrolysis. The requirement for Mg^{2+} is thought to derive from neutralization of the negative charges of the active site. It is interesting to note that benzoate and pyruvate were found in the MST active site of the closed crystal form but the required reducing agent remained unclear. The active center of the MST domain is located in the core and is constructed of residues of a large β -sandwich structure with amino acids from α -helices. The active site of the GATase1 domain is located close to the surface and solvents can diffuse in the ligand-free structure.^[33]

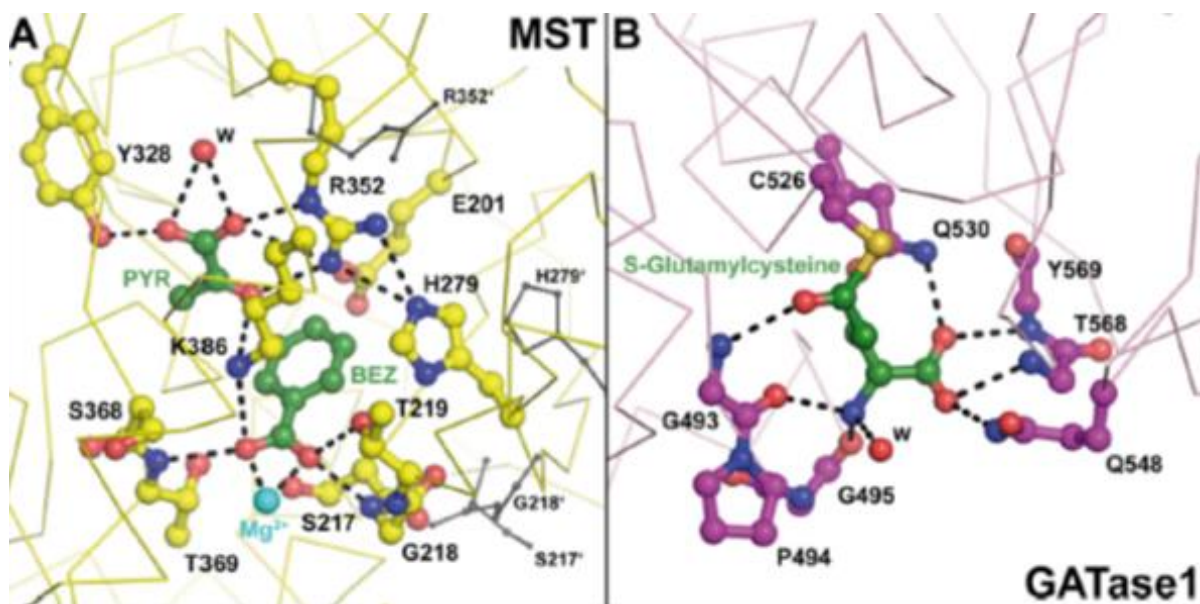


Figure 5.7: Active sites of PhzE (from *Burkholderia lata* 383). A: Active site of the MST domain. The positions of important moving residues in the open form are shown in black; B: Covalent modifications of Cys526 in the GATase1 active site. Figure taken from Li et al.^[33]

5.6.2 Inhibition of PhzE and anthranilate synthase (AS)

Some AS show feedback inhibition by L-tryptophan, the major downstream product of anthranilate in primary metabolism. No feedback inhibition of L-tryptophan or phenazine-1-carboxylic acid from *B. lata* or from *Pseudomonas* strains was found in PhzE and it is argued that Arg26 and Trp184 residues of the protein block the potential regulatory site (Figure 5.8). Zn^{2+} , Mn^{2+} , and Ni^{2+} were found to be inhibitors of PhzE.^[33]

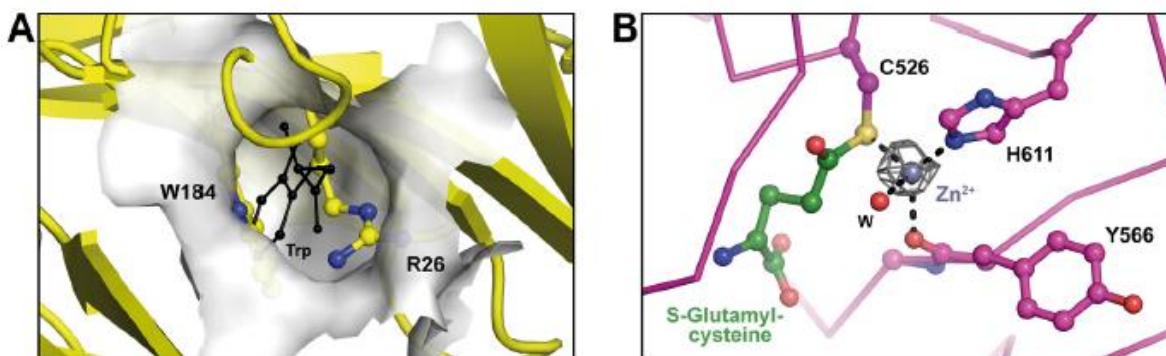


Figure 5.8: Inhibition of PhzE. A: The allosteric tryptophan binding site in PhzE of *S. marcescens* anthranilate synthase (AS) is blocked by Arg26 and Trp184; B: Zn^{2+} binds to the GATase1 active site. Figure taken from Li *et al.*^[33]

The design of highly specific inhibitors against the family of chorismate-utilizing enzymes may be an important contribution for the development of selective antibacterials and many inhibition studies have been published,^[65] but no inhibitor of PhzE is known to date. Figure 5.9. gives an overview of some inhibitors of chorismate-utilizing enzymes. Due to clarity reasons, only inhibition constants of AS are depicted.

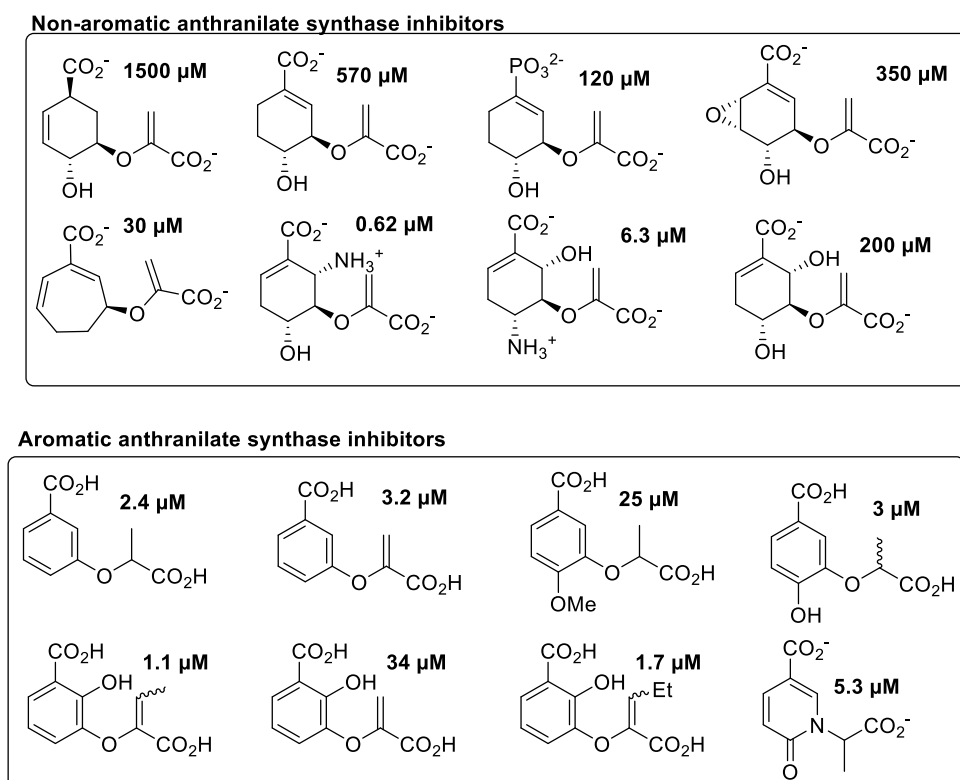
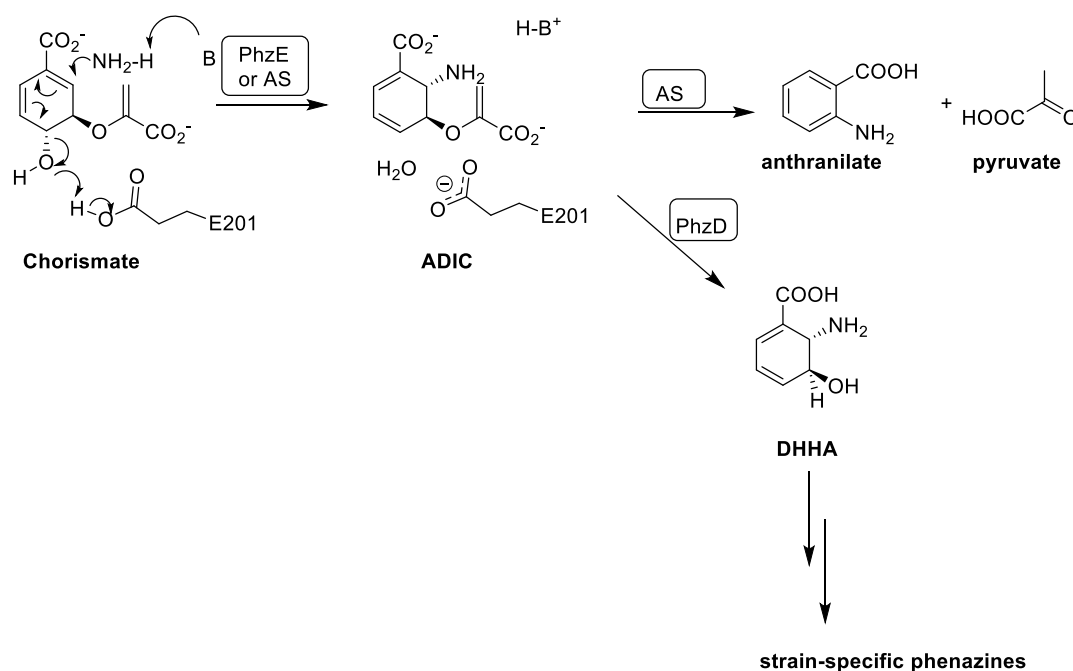


Figure 5.9: Some inhibitors of anthranilate synthase (AS). Inhibition constants for the other chorismate-utilizing enzymes are not depicted due to clarity reasons.^[49,53,59,65,66,76]

5.6.3 Mechanistic considerations

The proposed mechanism of the PhzE-catalyzed conversion of chorismate to ADIC is outlined in Scheme 5.6.

It is thought that the carbonyl groups of Ile216, Thr304, along with the side chains of Ser217 and Thr369 act as hydrogen bond acceptors, thus assisting in the deprotonation of NH_3 . The stereochemical outcome of the reaction is mainly attributed to the ammonia channel, which ends at C-2 of the *Si-face* of chorismic acid. Glu201 assists in protonation of the hydroxyl-group at C-4 of chorismic acid. Upon mutation to glutamine, the enzyme becomes inactive.^[33]



Scheme 5.6: Comparison between PhzE and anthranilate synthase (AS). NH_3 derives from glutamine.

5.6.4 Differences between PhzE and AS

Anthranilate synthase consists of a small TrpG and a large TrpE subunit encoded by *trpG* and *trpE* genes, respectively. TrpG hydrolyses the amido side chain of glutamine and the produced ammonia is believed to be transferred through an intramolecular channel to TrpE, where chorismate is processed.^[76,77]

The coordination sphere of PhzE and AS is nearly identical. Nevertheless, pyruvate eliminates from ADIC to give anthranilate in AS catalyzed reactions, whereas ADIC becomes not converted to anthranilate in the case of PhzE (Scheme 5.6). From a thermodynamic point of view, the transformation into anthranilate and pyruvate is much more favourable and it remains still unclear why these enzymes behave differently.

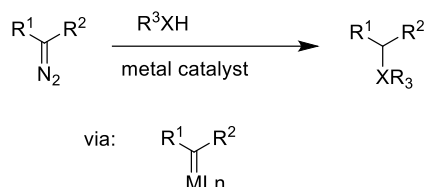
Various experiments^[33] have been conducted in order to study differences between AS and PhzE:

- PhzE was transformed into a possible AS, by mutating three amino acid residues which account for the different first coordination sphere and an increase of anthranilate production was not observed;
- The mutation of His398 to methionine in AS from *Salmonella enterica* created an ADIC synthase, deactivating pyruvate lyase activity (it has to be noted that the corresponding His279 is also conserved in PhzE);
- Upon crystallization, pyruvate elimination was observed in PhzE, but not in solution.

There is evidence that pyruvate elimination in AS and salicylate synthase proceeds via a pericyclic^[74] reaction and therefore it is believed that the binding properties in AS account for pyruvate lyase activity, as the methylene group of the enolpyruvyl moiety in ADIC has to be properly oriented towards the hydrogen atom at C-2. It is likely that ADIC synthases provide a different release path or shortens the time ADIC remains in the active center.^[33]

5.7 Carbenoid-based OH-insertion reactions

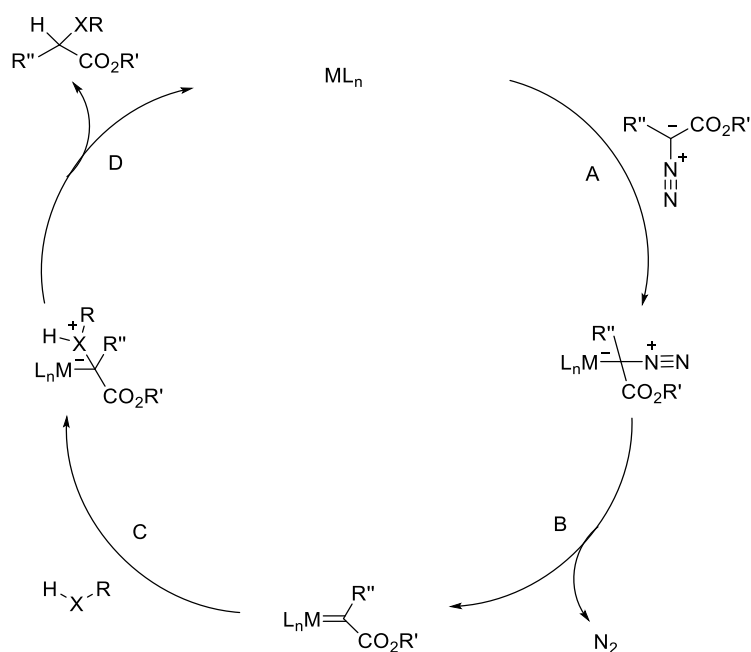
Carbenoid-based X-H insertions (XHIs) with X being heteroatoms like oxygen, nitrogen, sulfur, selenium, phosphorus or halogens are reactions where a metal-carbenoid is normally generated *in situ* from a diazo precursor to give a newly formed C-X bond upon attack of the heteroatom at the electrophilic carbenoid (Scheme 5.7).^[78]



Scheme 5.7: Insertion of RXH into an *in-situ* generated metal-carbenoid.^[78]

Different metals like Ru or Fe have been applied in carbenoid based XHIs but Rh and Cu are yet most commonly used. The positive aspects of Rh are the high turnover numbers and frequencies as well as the large substrate scope. Limitations of Rh are the restricted stereocontrol and common side reactions like C-H insertion or β -elimination. Cu in turn scores with being inexpensive and chemoselective but is susceptible to inhibition by Lewis bases. Not only the metal is important, but certain ligands can dramatically alter selectivity and reactivity in XHIs.^[78]

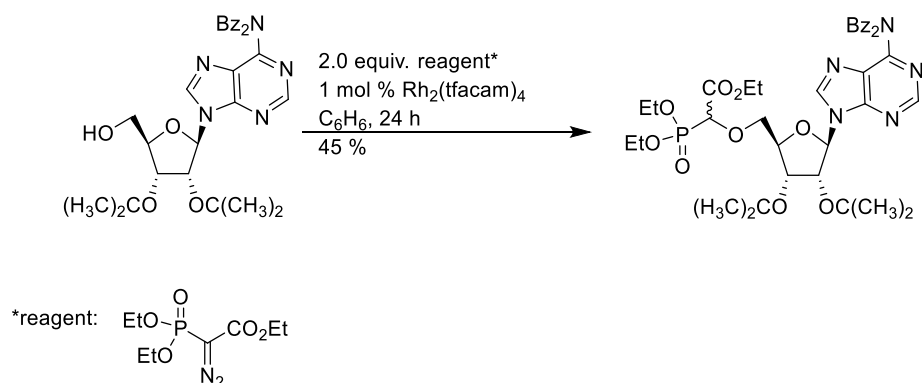
As each metal behaves somewhat different, there is no single universally valid mechanism of polar XHIs. However, there are similarities and a general outline of the believed stepwise mechanism for polar XHIs is given in Scheme 5.8.^[78] In step A the diazo ylide coordinates to the catalyst ML_n . The following carbene formation is accompanied by the loss of nitrogen (step B) and allows for an attack of HXR (step C). The last step of the catalytic cycle includes a [1,2]-proton shift with concomitant release of the catalyst.^[78]



Scheme 5.8: General outline for polar XHIs. Scheme taken from D. Gillingham and N. Fei.^[78]

5.7.1 Carbenoid-based OH-insertion reactions in chemical biology

It is impressive that metal-carbenoids can be applied to modify intact proteins, nucleic acids, and complex natural products.^[78] One example for the utilization of carbenoid based OH-insertion reactions in an adenosine derivative is given in Scheme 5.9.^[79]

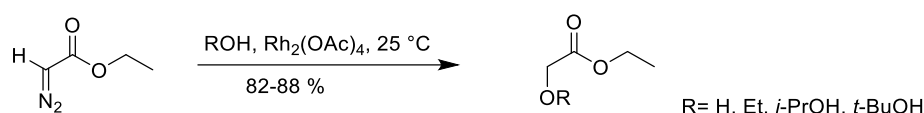


Scheme 5.9: Carbenoid based OH-insertion in an adenosine derivative.^[79]

5.7.2 O-H insertion reactions with diazocarbonyl compounds

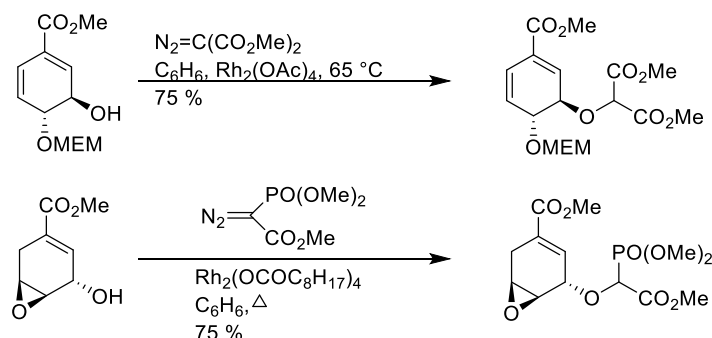
Diazocarbonyl compounds have been widely used in synthesis due to its stability and availability. These substrates can be either decomposed under thermal, photochemical, acid or transition-metal catalyzed conditions.^[80]

Transition metal-catalyzed OH-insertion reactions are known since the early 1900s^[81] and have become increasingly popular as these reactions are carried out under relatively mild conditions. $\text{Rh}_2(\text{OAc})_4$ was reported in 1973 by Paulissen et al.^[82] to be an extremely efficient catalyst for the decomposition of ethyl diazoacetate (EDA) to give the corresponding alkoxyacetates upon treatment with water or alcohols (Scheme 5.10).^[80]



Scheme 5.10: OH-insertion reaction using $\text{Rh}_2(\text{OAc})_4$ as a catalyst.^[80,82]

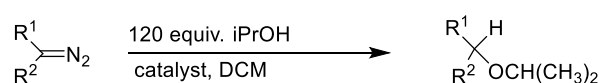
Rhodium-catalyzed O-H insertion reactions have found many applications, one of which is the etherification of highly functionalized cyclohexanols such as shikimate or chorismate derivatives (Scheme 5.11).^[80,83]



Scheme 5.11: Instable compounds can be effectively derivatized using transition metal catalyzed OH-insertion reactions.^[80]

Influence of EWG groups

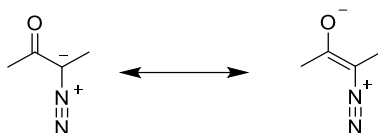
It has been shown that stabilized diazo compounds are less readily decomposed. Stabilization is achieved upon installation of EWGs and the degree of stabilization decreases in the order: $\text{PO}(\text{OEt})_2 > \text{Ph}_2\text{PO} > \text{EtO}_2\text{C} \sim \text{PhSO}_2 > \text{Me}_2\text{NCO} > \text{CN} > \text{PhCH}_2 > \text{Ph} \sim \text{H}$ (Scheme 5.12). It is worth noting that $\text{Rh}_2(\text{tfacam})_4$ proved to be a superior catalyst for the decomposition of stabilized diazo compounds.^[84,85]



$\text{R}^1, \text{R}^2 = \text{H}, \text{CO}_2\text{Et}, \text{Ph}, \text{PhCH}_2, \text{Ph}_2\text{PO}, (\text{EtO})_2\text{PO}, \text{PhSO}_2, \text{CN}.$
 catalyst = $\text{Rh}_2(\text{OAc})_4$ or $\text{Rh}_2(\text{tfacam})_4$.

Scheme 5.12: Transition metal-catalyzed OH-insertion reactions using stabilized diazo compounds.^[85]

The increased stability of diazo phosphonates over diazo carbonyl compounds was explained with the mesomeric enolate form in diazocarbonyl compounds, where the negative charge is on oxygen rather than in close proximity to N_2^+ , rendering the diazo carbonyl compound prone to decomposition.^[85,86]

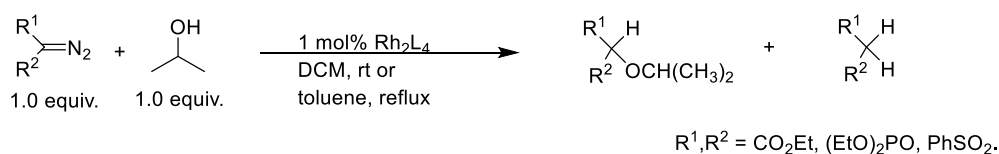


Scheme 5.13: Mesomeric structures of diazo carbonyl compounds.^[85]

A selective decomposition of less stabilized diazo functionalities in the presence of stabilized one is possible using $Rh_2(OAc)_4$ as a catalyst.^[87]

Influence of the catalyst

For a given reaction (Scheme 5.14), Moody et. al could show that the rate of decomposition decreases with electron-poor ligands, when rhodium carboxylates were used as a catalyst. However, $Rh_2(tfacam)_4$ proved to be the most effective catalyst for this system.^[85]



Scheme 5.14: OH- insertion reaction by Cox et al.^[85]

Influence of the diazoester alkoxy group

Teyssié et. al. could show that there is an effect of the diazoester alkoxy group and ether formation increased with the number of carbon atoms in the diazoester alkoxy group.^[88]

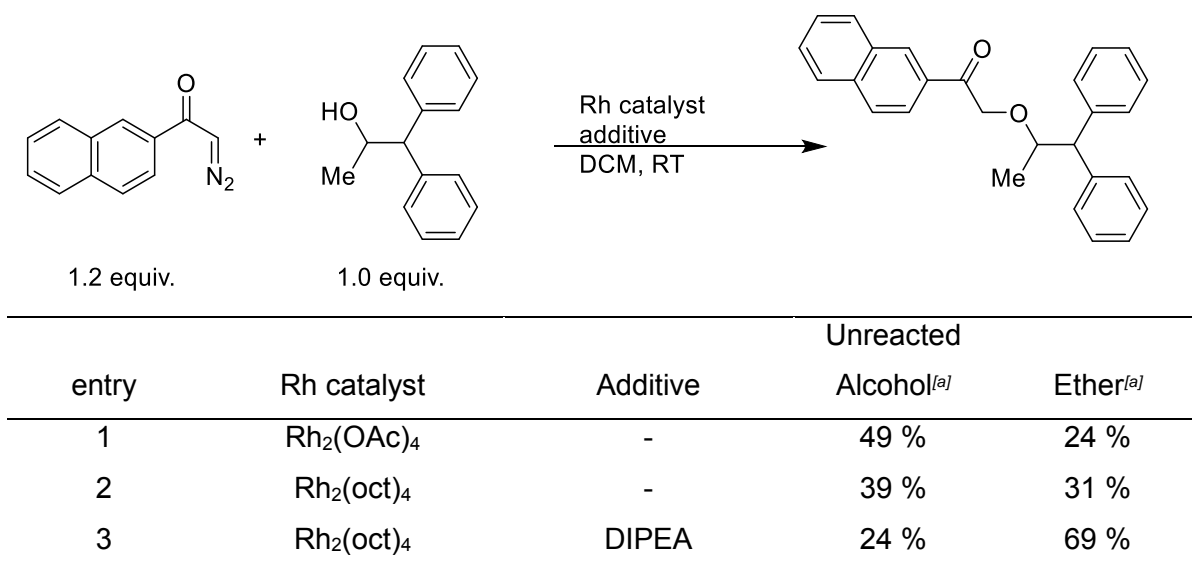
Regiochemistry

Experiments using a mixture of simple non-allylic and allylic alcohols revealed that the latter ones are more reactive. When a mixture of 1-hexanol and 1-hexene with $Rh_2(OAc)_4$ as the catalyst was subjected to different diazoacetates, methyl diazoacetate showed the highest ratio of OH-insertion to double-bond addition (6.7, compared to 2.7 when *n*-butyl diazoacetate was used). However, when the catalyst was changed to rhodium ferrocenate, *n*-butyl diazoacetate gave the highest ratio of OH-insertion (2.6).^[88]

Additives

In their synthesis towards an ascomycin derivative, Nelson et. al. found that by simply adding an additive, the yield of OH-insertion reactions can be drastically enhanced. Initial attempts centered on rhodium octanoate [$\text{Rh}_2(\text{oct})_4$] catalyzed insertion reactions and afforded the desired ascomycin derivative in low yields (25-30%). Upon typical parameter optimization of the addition rate, mode of addition, ascomycin concentration, catalyst charge, diazoketone charge, temperature and solvent, the yield was slightly increased to 36 %. Their next attempts centered on the addition of additives and the isolated yield could be increased to 54 % when DCM/TMU (125:1) was used as a solvent. The generality of this method was explored using DIPEA instead of TMU and is outlined in Table 5.1.^[89]

Table 5.1 The effect of additives on the O-H insertion reaction.^[89]

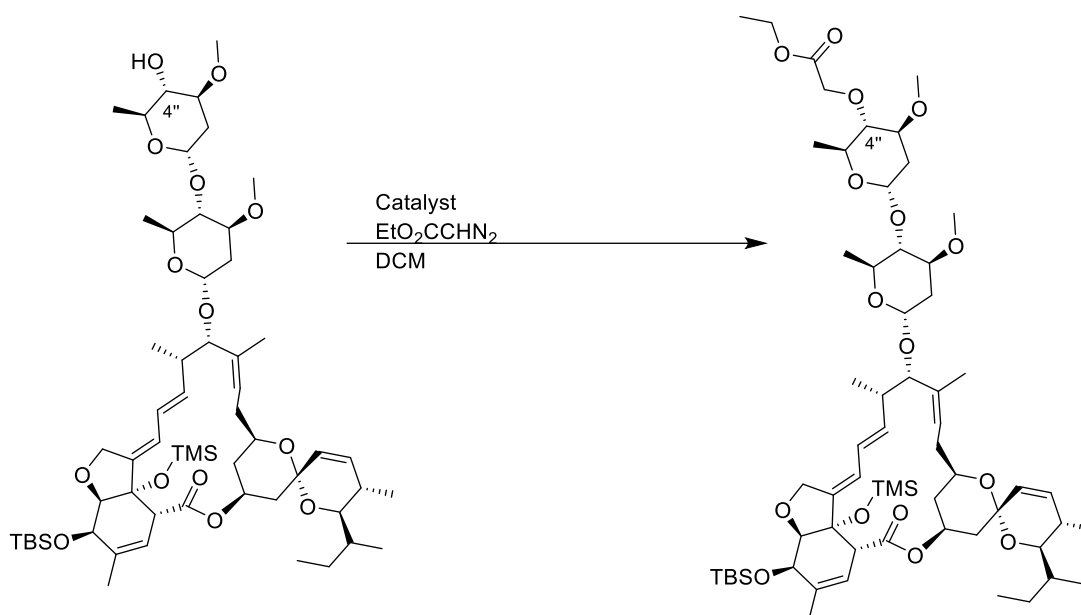


^[a] HPLC assay.

^[b] Isolated yield

In their synthesis towards 4''-alkoxy avermectin derivatives, Nagai et al. tested various conditions using metal-catalyzed OH-insertion reactions (Table 5.2).^[90] An increase in yield was not observed when additives were added.

Table 5.2 Effect of the catalyst on the O-H insertion reactions. Table taken from Nagai et al.^[90]



Entry[a]	Conditions	Yield (%)
1	0.02 equiv. $\text{Rh}_2(\text{OAc})_4$, RT, 4 h	62
2	0.01 equiv. $\text{Rh}_2(\text{O}_2\text{CC}_7\text{H}_{15})_4$, RT, 2 h	42
3	0.01 equiv. $\text{Rh}_2(\text{O}_2\text{CCF}_3)_4$, RT, 12 h	7 (99) ^[b]
4	0.01 equiv. $\text{Rh}_2(\text{OAc})_4$, 0.1 equiv. TMU, RT, 12 h	11 (80) ^[b]
5	0.01 equiv. $\text{Rh}_2(\text{OAc})_4$, 0.1 equiv. Me_2S , RT, 5 h	33 (70) ^[b]
6	0.05 equiv. $\text{Cu}(\text{OTf})_2$, RT, 12 h	18
7	0.1 equiv. $\text{BF}_3 \cdot \text{Et}_2\text{O}$, 0 °C, 2 h	Decomposed
8	0.02 equiv. $\text{Sc}(\text{OTf})_3$, RT, 1 min	Decomposed

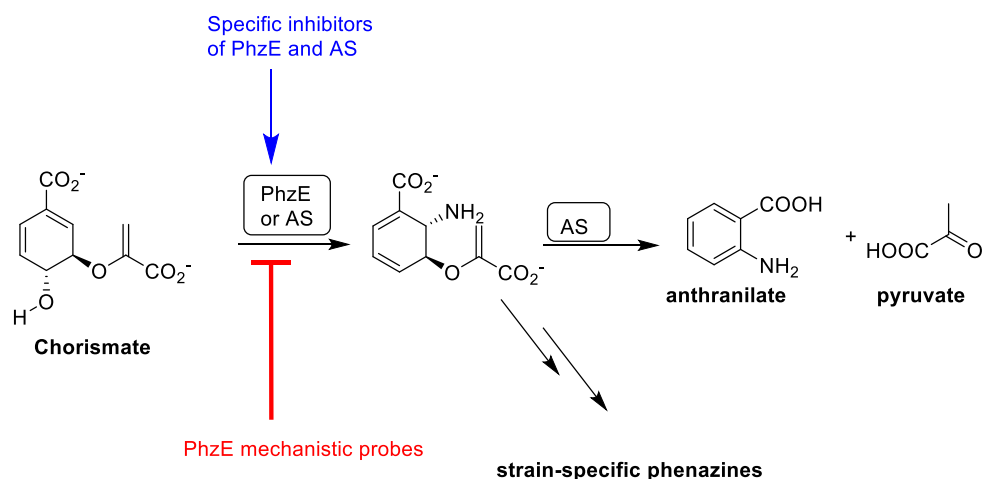
^[a] The reactions were carried out using 2.0 equiv. of ethyl diazoacetate.

^[b] Based on recovered starting material.

6 Aim of this work

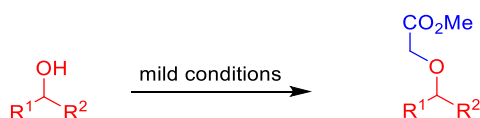
Enzymes that are involved in the metabolism of chorismate are attractive targets for the development of biologically active compounds, because only prokaryotic microorganisms, plants and fungi are capable to produce and metabolize chorismate.^[33,91]

The active site of anthranilate synthase (AS) and PhzE is nearly identical, but it remains unclear why in the case of AS the intermediate 2-amino-2-deoxyisochorimsate (ADIC) is converted to anthranilate and pyruvate, whereas ADIC exits PhzE and is further transformed to strain-specific phenazines. Although there are a lot of mechanistic and inhibition studies of the chorismate-utilizing enzymes, there is no inhibition study of PhzE known to date. In order to elucidate binding differences between PhzE and AS, ligands should be synthesized that are stable throughout crystallization experiments. In addition, this thesis is aimed at the synthesis of specific inhibitors of PhzE and AS (Scheme 6.1).



Scheme 6.1: Synthesis of mechanistic probes for PhzE and specific inhibitors for both PhzE and AS.

The most potent inhibitors of anthranilate synthase (AS) to date exhibit an enol pyruvyl side chain.^[53,59] The introduction of a side chain may pose a considerable challenge when it comes to the stability of our proposed inhibitors. In the course of this thesis, a robust methodology for the introduction of a glycolate side chain under mild conditions should be developed (Scheme 6.2). In addition, the developed methodology should be of general use.



Scheme 6.2: Methodology development for the mild introduction of a glycolate side chain into unstable alcohols.

7 Results and discussion

7.1 Aromatic inhibitors

Traditional inhibitors of anthranilate synthase are either cyclohexene or cyclohexadiene derivatives.^[53,62,76] Abell and co-workers have introduced aromatic analogues of chorismic acid as a new type of inhibitors. Additionally, 4- and 5-carboxypyridone derivatives have been introduced by the same group and proved to be a good starting point for the development of second or third generation inhibitors.^[65]

Chorismate was docked into the vacant active site of *S. marcescens* anthranilate synthase (benzoate and pyruvate ligands were first removed). It was shown that chorismate forms an electrostatic interaction with an enzyme bound magnesium ion at C-1 carboxylate and the C-4 hydroxyl is in vicinity of a glutamate residue (Glu309) (Figure 7.1 (A)). The pyruvate side chain at C-3 is in a binding pocket in close proximity to Arg469 and Tyr449, where it can form hydrogen bonds. A docking study of several putative aromatic inhibitors was performed (see docking of the (*R*)-enantiomer of **IV** in Figure 7.1 (B)) and it was shown that these ligands would bind similarly compared to chorismate. The C-1 carboxylate would interact with the metal ion and the *para*-functionality would be in close proximity to Glu309. The C-3 side chains dock into the same binding pocket as the pyruvate side chain in chorismate. The aromatic ring was slightly shifted when larger C-3 side chains were introduced.^[59]

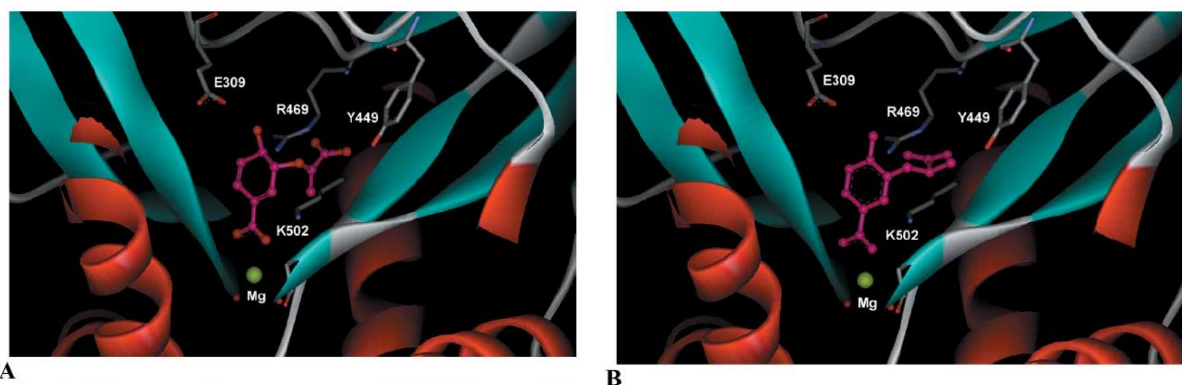


Figure 7.1: (A) chorismate and (B) an aromatic analogue docked into the active site of *S. marcescens* anthranilate synthase (117Q).^[77] Figure taken from Payne et al.^[76]

Some intriguing results were obtained concerning the different substitution pattern in aromatic chorismic acid analogues. Figure 7.2 captures some aromatic chorismic acid analogues with different substitution pattern at C-2-4. Interestingly, good inhibition constants were achieved with varying substituents at C-3. Different substituents were attached at C-4 and it turned out that a hydroxyl group is comparable to a hydrogen group and that a methyl group is comparable to a hydroxymethyl or aminomethyl group at C-4. This lack of sensitivity is somewhat surprising as hydrogen bonding with Glu309 is expected and it is argued that having only hydrogen at C-4 would allow a water molecule to bind between C-4 and Glu309. It was

found that a different stereochemistry in the side chain of the lactate group has an effect on inhibition.

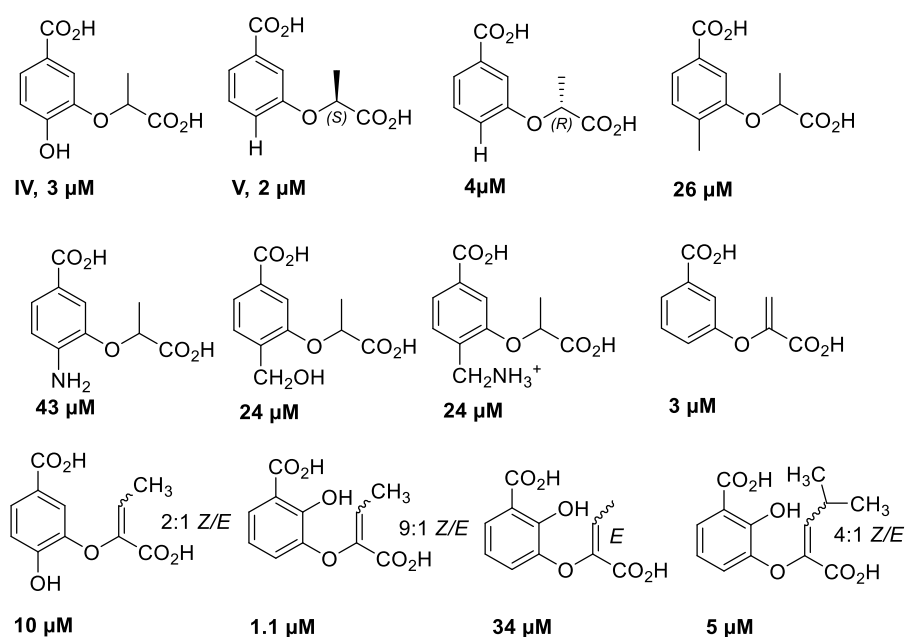


Figure 7.2: Some aromatic chorismic acid analogues. Inhibition constants are only given for *S. marcescens* anthranilate synthase.^[59]

It has to be noted that the shown effects may only apply for aromatic inhibitors. Payne et al. could show for their cyclohexene derived inhibitors of AS that by the substitution of a pyruvate side chain at position C-3 with either a lactate or glycolate the inhibition is dramatically decreased (Figure 7.3).^[66]

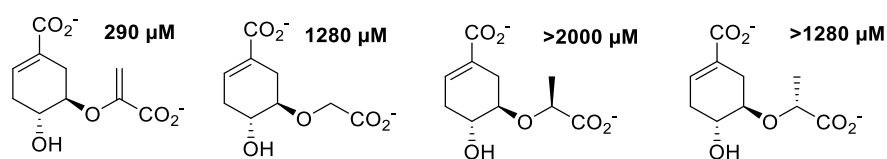
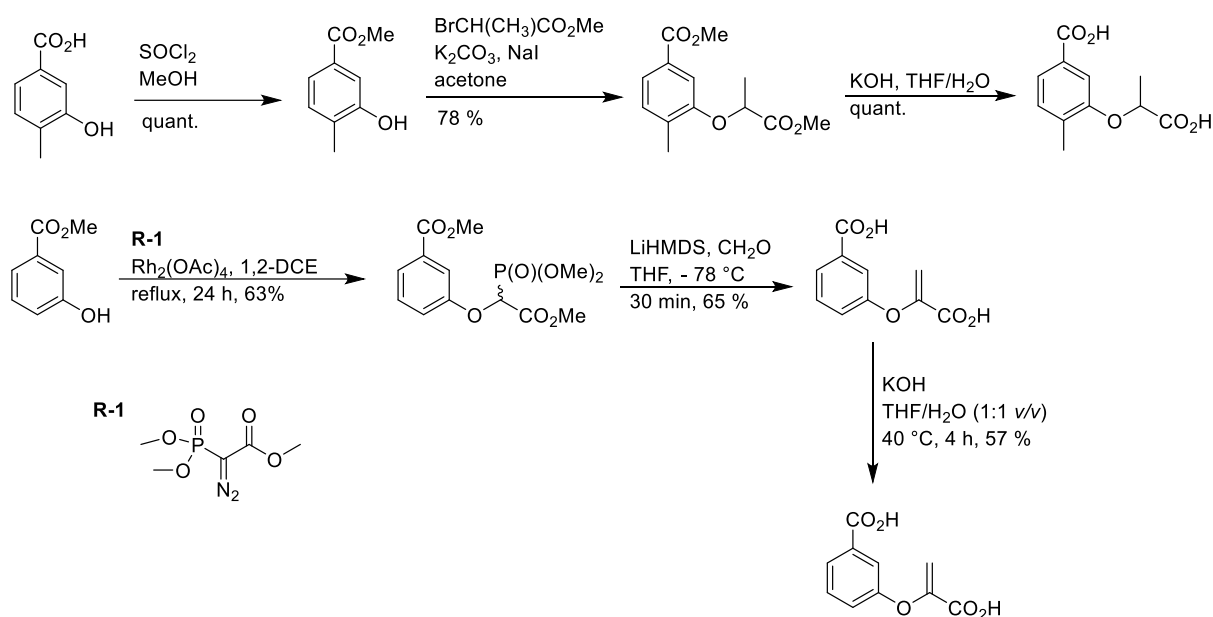


Figure 7.3: Cyclohexene derived inhibitors of the chorismate-utilizing enzymes.^[66] Due to clarity reasons, inhibition constants are only depicted for AS (*S. marcescens*)

Driven by the findings of Abell et al. and Payne et al. that aromatic chorismate analogues show comparably good inhibition constants against the *S. marcescens* anthranilate synthase compared to traditional inhibitors (ranging from sub-micromolar to millimolar),^[53,76] and the easy synthetic accessibility towards these compounds, several putative inhibitors of PhzE and AS were synthesized (Scheme 7.2). At the outset of the project, it was decided to use **1** as a starting material for the synthesis of putative inhibitors **7-11**. In order to explore the influence of a different substitution pattern at C-3, pyruvate, lactate, butanoate and butenoate side chains were installed.

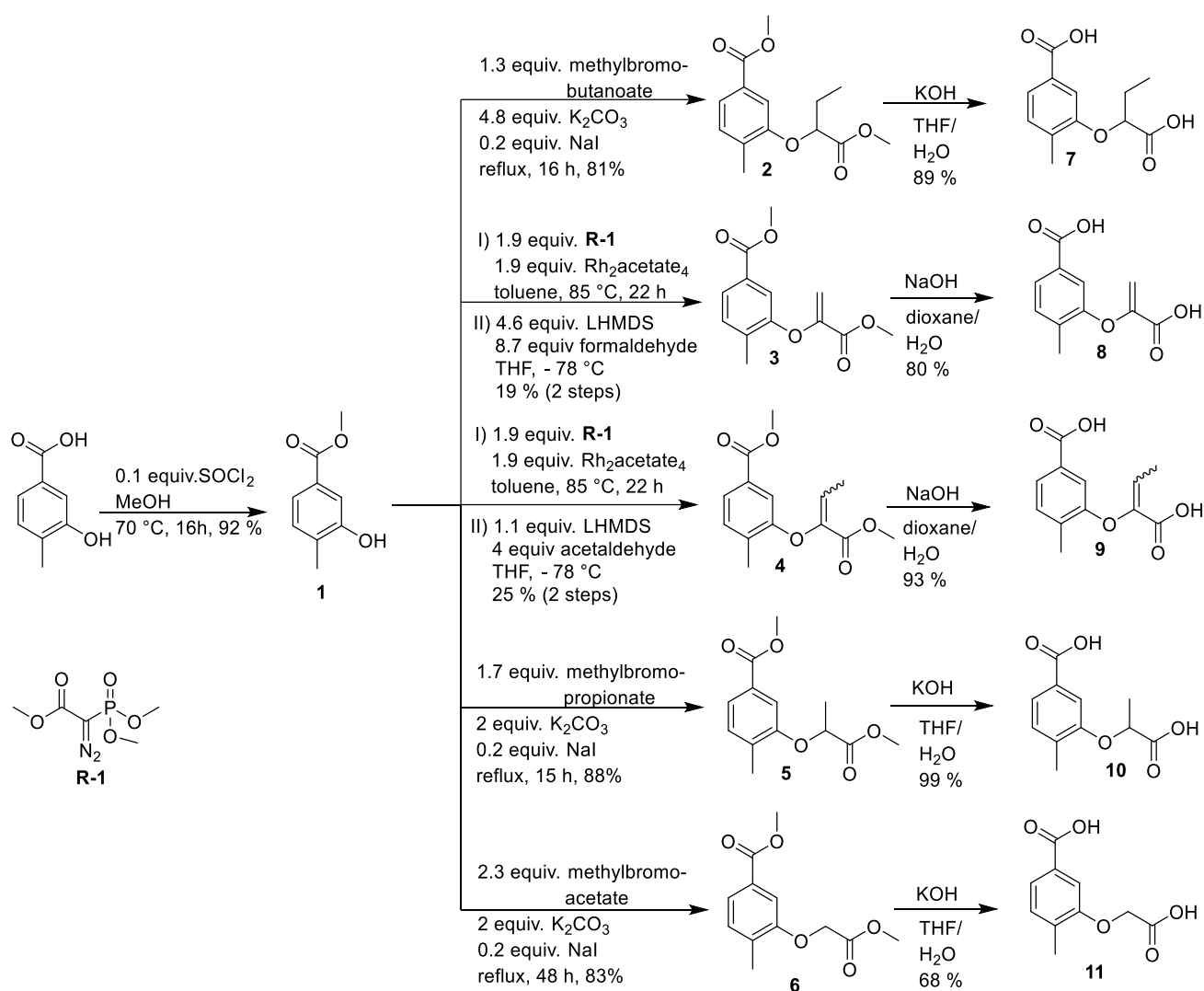
Abell et al. and Payne et al. have developed robust strategies for the introduction of a C-3 side chain in aromatic chorismic acid analogues (Scheme 7.1).^[49,59]



Scheme 7.1: Robust strategy for the introduction of the C-3 side chain in aromatic chorismate analogues by Abell et al. and Payne et al.^[49,59]

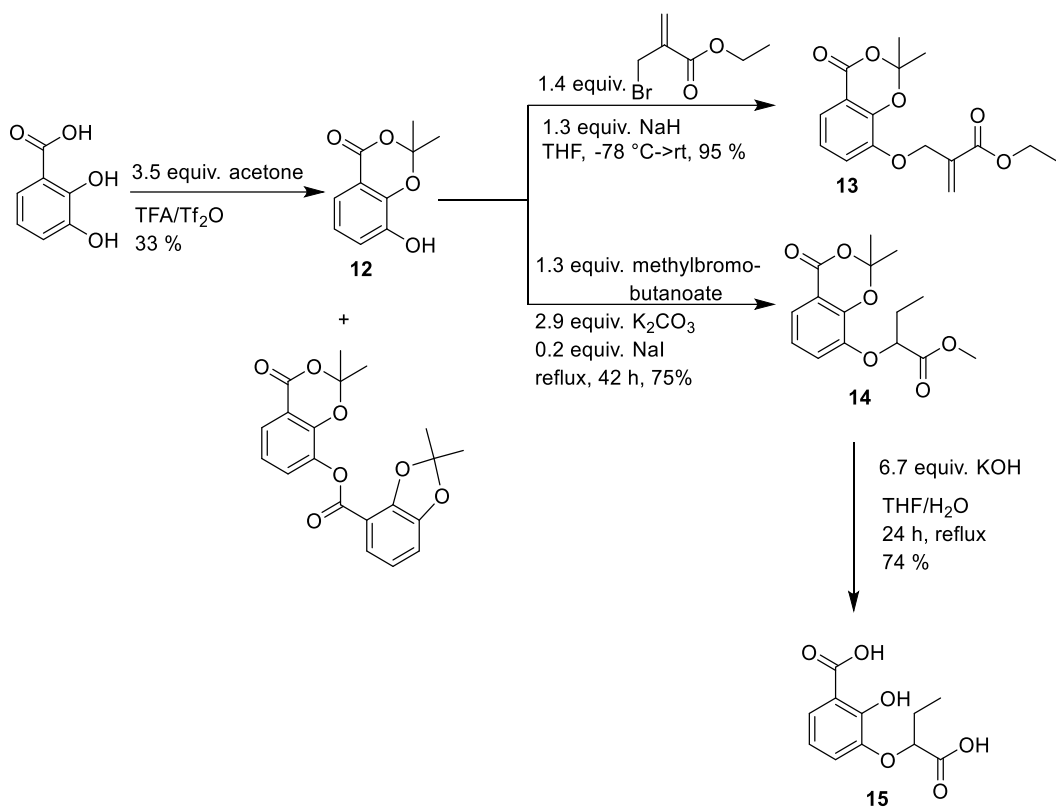
It was decided to exploit the successful strategy described above for the synthesis of putative inhibitors of PhzE and anthranilate synthase (Scheme 7.2). As a starting point, the already known **10** was synthesized following the literature procedure of Payne et al.^[59] Differently decorated compounds **7-11** were synthesized using the described methods.

The installation of an unsaturated side chain in **1** was achieved in good yields (81-88 %) for substrates **2**, **5** and **6**. The introduction of the corresponding enoether at C-3 was achieved in two steps. First, a $\text{Rh}_2(\text{OAc})_4$ catalyzed etherification using diazophosphonoacetate gave the corresponding phosphonoacetate side chain. A subsequent Horner-Wadsworth Emmons reaction afforded **3** and **4** in a combined yield of 19 % and 25 %, respectively. Saponification of the diesters occurred straightforwardly using either KOH in THF/ H_2O or NaOH in 1,4-dioxane.



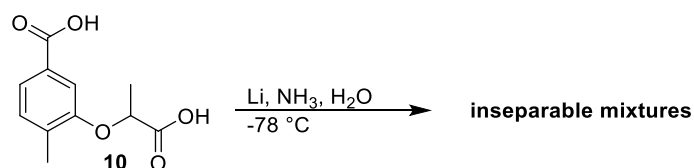
Scheme 7.2: Synthetic access to putative aromatic inhibitors **7-11**.

In order to enlarge diversity, compounds **13-15** were synthesized. Compound **12** is described in the literature and was synthesized accordingly.^[92] The transformation of 2,3-dihydroxy benzoic acid to **12** was plagued by the undesired dimerization of **12** (approx. 11 %) and the low yield can be additionally attributed to difficulties in product isolation as **12** and the dimer exhibit nearly identical R_f values. Upon finding a lead, this step will be subjected to further optimization in order to minimize undesired dimer formation. The introduction of a side chain in **12** gave **13** and **14** in good yields (95 % and 75 % respectively). Saponification of **14** was achieved using the method of Shen et al.^[93] to give **15** in a satisfactory 74% yield. Saponification of **13** was tested but the reaction was plagued by side reactions and product isolation turned out to be challenging.



Scheme 7.3: Synthesis of aromatic chorismic acid analogues exhibiting a hydroxyl group at C-2.

In order to investigate if the synthesized aromatic putative inhibitors can be easily converted into cyclohexadiene derivatives, **10** was subjected to a Birch-reduction using Li as the reducing agent and H₂O as the proton source. Unfortunately, only inseparable mixtures were obtained and it is assumed that the substitution pattern on the aromatic ring is too complex to give specific products (Scheme 7.4).



Scheme 7.4: Birch-reduction of compound **10** yielded inseparable mixtures as suggested by NMR and HPLC-MS.

Compounds **7-11** and **13-15** will be used in crystallization experiments for PhzE and AS. In addition, inhibition experiments will be performed.

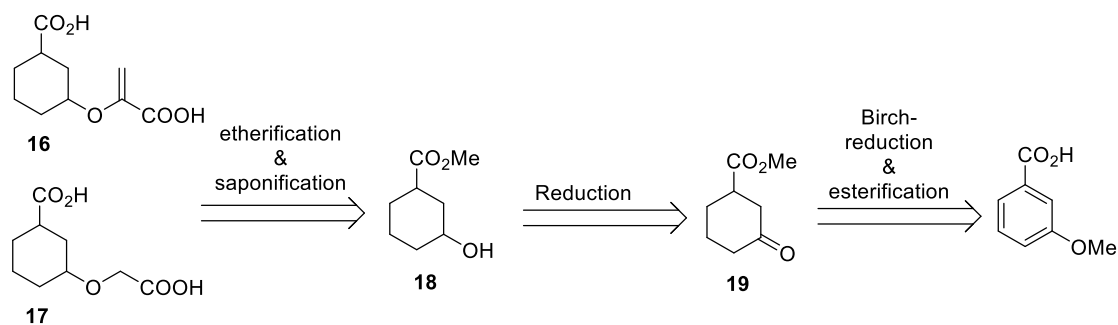
7.2 Cyclohexane-derived inhibitors

Some limitations of aromatic inhibitors may arise from the fact that the hydroxyl at C-4 in chorismate adopts a more axial orientation prior to departure and this property can be poorly mimicked by aromatic inhibitors as the substituent at C-4 is pointing out in the same plane as the aromatic ring.^[59] To this end, we scouted for alternative scaffolds that meet the following demands:

- sp^3 hybridisation at C-4;
- Inexpensive starting material;
- Target molecule should be accessible via a short synthetic route;
- Stable target compound;
- A late intermediate should give easy access to a diverse set of compounds, upon finding a lead.

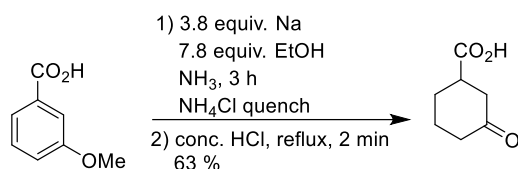
As the carboxylate in chorismate at position C-1 forms electrostatic interactions with an enzyme-bound magnesium and as the pyruvate side chain at C-3 fits into a binding pocket, we sought to design an inhibitor that exhibits a C-1 carboxylate and a side chain at position C-3. Influenced by the fact that plain aromatic structures can effectively inhibit AS, the simplest alternative scaffold we could think of was a cyclohexane derivative and we propose **16** and **17** as putative inhibitors for PhzE and AS (Scheme 7.5). Compound **16**, like the natural substrate chorismate, exhibit a pyruvate side chain at position C-3. In order to increase diversity, **17** was proposed as an additional putative inhibitor, exhibiting a glycolate, rather than a pyruvate side chain. Both structures lack a hydroxyl at position C-4, as it has been shown that a hydrogen at position C-4 in aromatic AS inhibitors displays a respectable replacement. To our surprise, cyclohexane derivatives for AS and PhzE inhibition have so far received no attention.

Scheme 7.5 depicts a retrosynthetic analysis towards **16** and **17**. The side chains present in **16** and **17** would be installed via etherification of **18**. Subsequent hydrolysis would then give rise to the free carboxylic acids present in **16** and **17**. The alcohol functionality in **18** would be accessible via reduction of the corresponding keto group in **19**. Compound **19** represents a product of the Birch-reduction and would be accessible starting from 3-methoxy benzoic acid followed by an esterification.



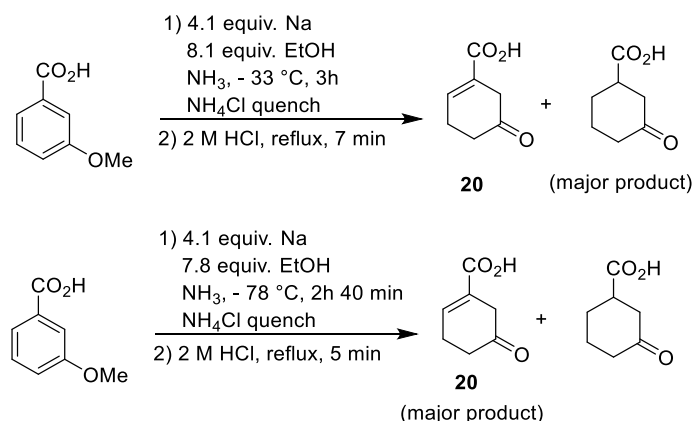
Scheme 7.5: Retrosynthetic analysis of **16** and **17**.

On the basis of literature examples,^[94,95] it was expected that Birch-reduction of 3-methoxy benzoic acid using Na in in NH₃ with EtOH as the proton source would lead to the fully reduced 3-oxocyclohexane-1-carboxylic acid (Scheme 7.6).



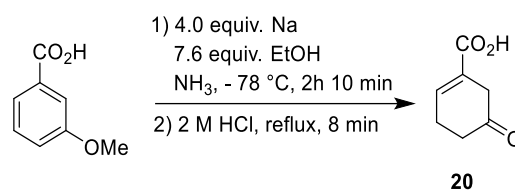
Scheme 7.6: Birch-reduction of 3-methoxy benzoic acid by Allan *et al.*^[94]

Unfortunately, no reaction temperature was given in the literature and therefore we performed two experiments at two different temperatures using the method by Allan *et al.* (Scheme 7.7).^[94] In the first experiment we performed the reaction at -33 °C (boiling point of ammonia), in the second experiment we ran the reaction at -78 °C. When the reaction was run at -33 °C, the major product was 3-oxocyclohexane-1-carboxylic acid with large amounts of **20**. Again, a mixture of **20** and 3-oxocyclohexane-1-carboxylic acid was obtained, when the reaction was performed at -78 °C, but **20** being the major product.



Scheme 7.7: The outcome of the Birch reduction of 3-methoxy benzoic acid is influenced by temperature.

In order to study the influence of the quenching agent, NH_4Cl addition was omitted in the next experiment (Scheme 7.8). It turned out that 3-methoxybenzoic acid was quantitatively converted to **20**, when NH_4Cl addition was omitted.

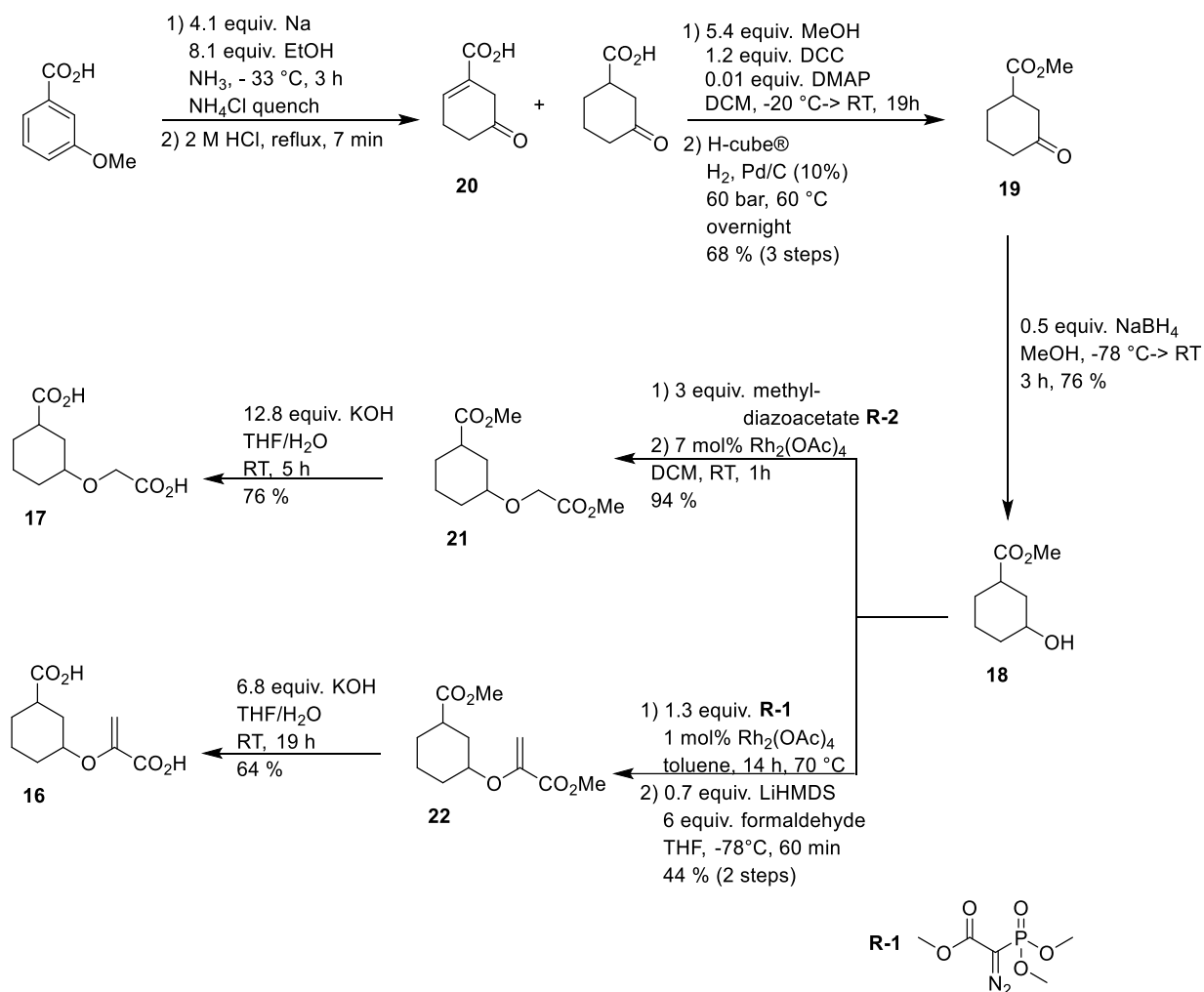


Scheme 7.8: Birch-reduction of 3-methoxy benzoic acid lead to **20**, when NH_4Cl quench was omitted.

For the synthesis towards **19**, we decided to take the already synthesized mixture of **20** and 3-oxocyclohexane-1-carboxylic acid. We proceeded with an esterification using the conditions by Neises et al.^[96] In order to obtain **19** as a pure compound, we performed a hydrogenation using the H-cube[®] flow reactor. Starting from 3-methoxybenzoic acid, we obtained pure **19** in 68 % yield over three steps. The next step in our synthetic route called for a reduction of **19** and we followed the synthesis by Haerter et al.^[97] using NaBH_4 in MeOH at $-78\text{ }^\circ\text{C}$ to give literature known **18** in a yield of 76 %. **18** is the central intermediate of our synthetic route and would easily allow for derivatisation upon finding a lead. In order to get access to the putative inhibitor **16**, we first attached a trimethylphosphonoacetate moiety to the alcohol at position C-3. Then, we performed a Horner-Wadsworth-Emmons reaction using formaldehyde (freshly synthesized via cracking of paraformaldehyde) as the electrophile. We obtained **22** in an acceptable yield of 44 % over two steps. For the last step in the synthesis towards **16**, we performed a saponification using KOH. We obtained **16** in a yield of 64 %.

For the synthesis towards **17**, we first performed a $\text{Rh}_2(\text{OAc})_4$ catalyzed OH-insertion using methyl diazoacetate to give **21** in an excellent yield of 94 %. Upon hydrolysis using KOH, we obtained **17** in a yield of 76 %.

In summary, we established a simple route towards the stable putative inhibitors **16** and **17**. Compounds **16** and **17** will be used to study binding differences between AS and PhzE and it will be interesting to see, how this new type of substrate will bind to PhzE and AS. In addition, inhibition assays will be performed. The central intermediate **18** will give access to alternative substrates, upon finding a lead.



Scheme 7.9: Synthetic access to the putative inhibitors of PhzE and anthranilate synthase (AS) **16** and **17**.

7.3 ADIC-derived inhibitors

7.3.1 General considerations

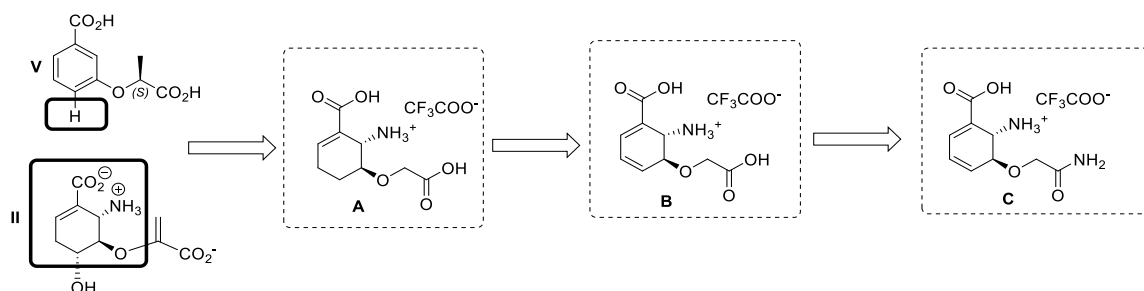
We envisioned to establish new putative inhibitors in a rational design, which could be the basis for novel inhibitors of PhzE and anthranilate synthase. Our design was guided by the most potent inhibitor^[53] of anthranilate synthase to date (see **II** in Scheme 7.10). In devising our approach, we became intrigued by the work of Abell and co-workers, who could show that a hydrogen atom is an improved substituent for a hydroxyl group at the C-4 position in aromatic anthranilate synthase inhibitors.^[59] We sought to design putative inhibitors that combine the above mentioned structural elements and would be readily accessible. Upon finding a lead, the developed strategy should easily allow for diversification.

We propose the following ADIC derivatives as putative inhibitors for PhzE and anthranilate synthase (Scheme 7.10, dashed frame):

Compound A: this compound exhibits the key structural elements found in compound **II** and has a hydrogen at C-4, which in our rationale may be beneficial. Other than ADIC, this compound lacks one double bond and exhibits a glycolate side chain at position C-3 rather than a pyruvate.

Compound B: introducing a second double bond in the ring of **A** would give rise to **B**. Other than ADIC, the proposed inhibitor would exhibit a glycolate side chain, rather than a pyruvate at position C-3. It is anticipated that the glycolate side chain would not be susceptible for ether cleavage and would therefore represent a stable ADIC analogue that may also find interesting use in crystallization experiments for PhzD.

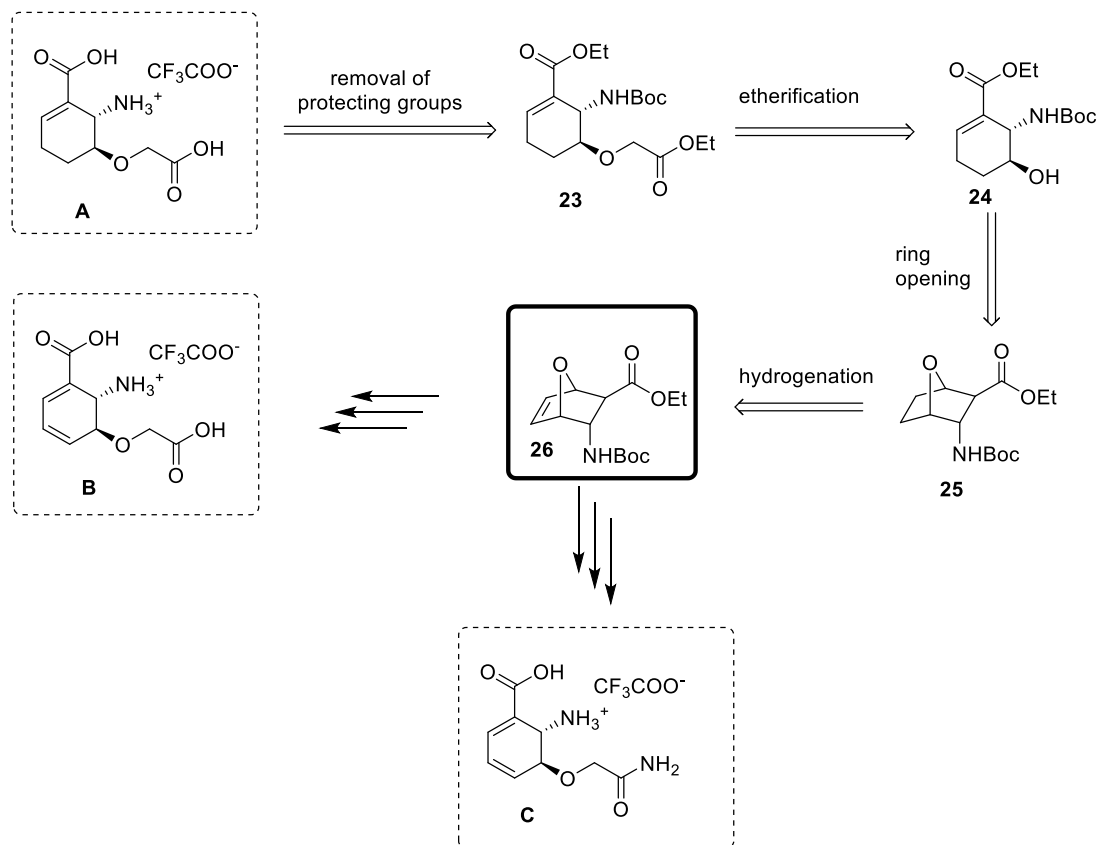
Compound C: this compound exhibits an 2-hydroxyacetamide side chain at C-3 rather than the glycolate in **B**.



Scheme 7.10: Rationale for a new type of PhzE and anthranilate synthase inhibitor.

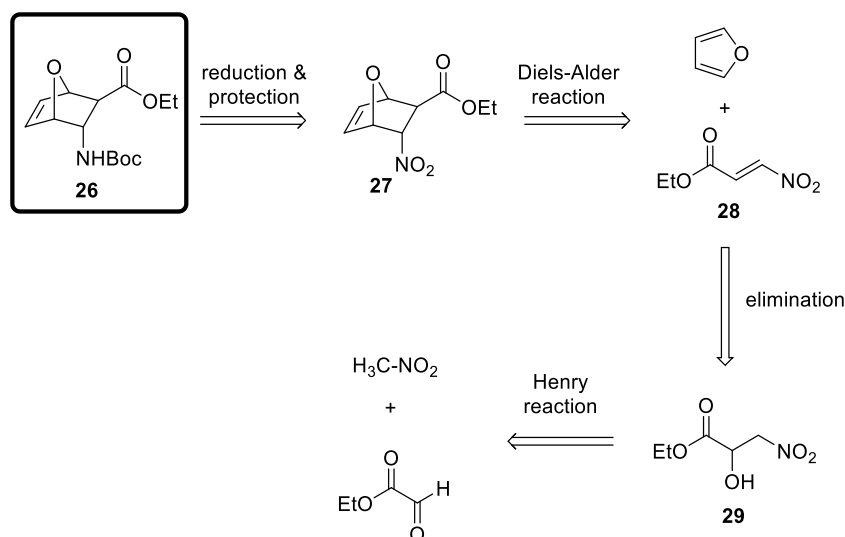
Scheme 7.11 presents a retrosynthetic analysis of the proposed cyclohexene derivative **A** and a demonstration that the central intermediate **26** can be exploited for the synthesis of the aforementioned putative inhibitors **B** and **C**. Starting from **23**, deprotection of the Boc group and hydrolysis of the two carboxylic acid ester groups would give **A**. **23** in turn could be synthesized via a Williamson-ether synthesis starting from **24**. Intermediate **24** would be

accessible via a base-mediated opening of **25**. The hydrogen would be abstracted at the most acidic position of **25**. Starting from **26**, which represents the central intermediate (bold frame), **25** is accessible via a hydrogenation reaction.^[98] The central intermediate **26** is known in the literature^[99] and would give rise to our proposed alternative inhibitors.



Scheme 7.11: Retrosynthetic analysis towards putative inhibitors of PhzE and anthranilate synthase.

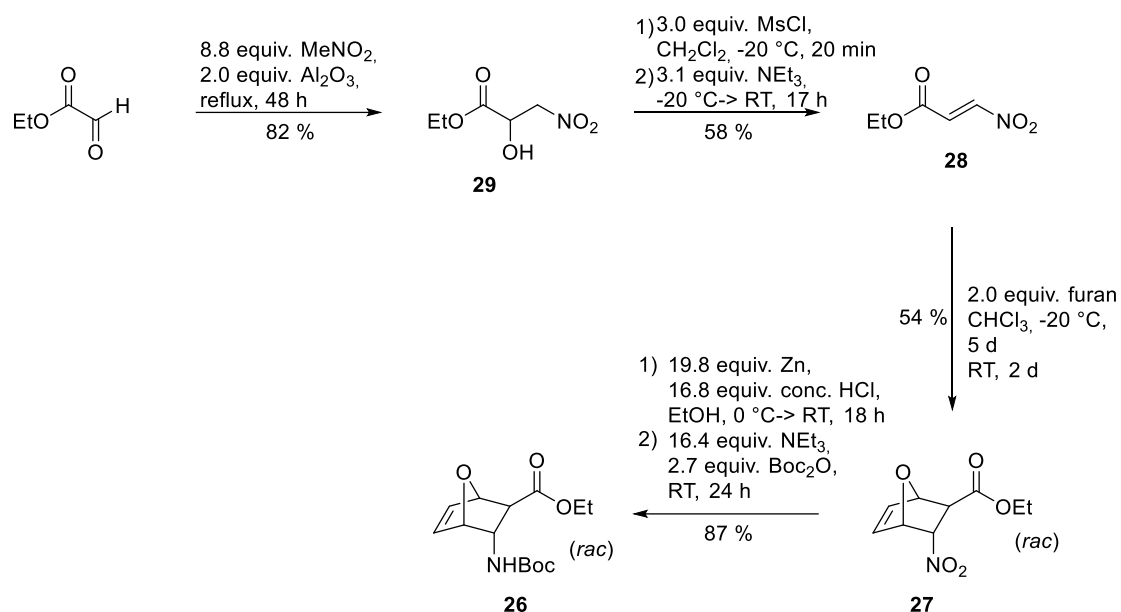
Scheme 7.12 gives a retrosynthetic analysis towards literature known **26**. Central Intermediate **26** can be synthesized via a reduction of the nitro group in **27**, followed by an *in-situ* protection with Boc_2O . **27** in turn is accessible via a highly *endo*-selective Diels-Alder-reaction starting from furan and **28**. Starting from ethyl glyoxylate, **29** is accessible via a Henry-reaction with nitromethane. Upon elimination of water from **29**, compound **28** is generated. All steps towards literature known **26** were performed following the procedures of Mesesane et al.^[99] Some steps were slightly modified.



Scheme 7.12: Retrosynthetic analysis of central intermediate **26**.

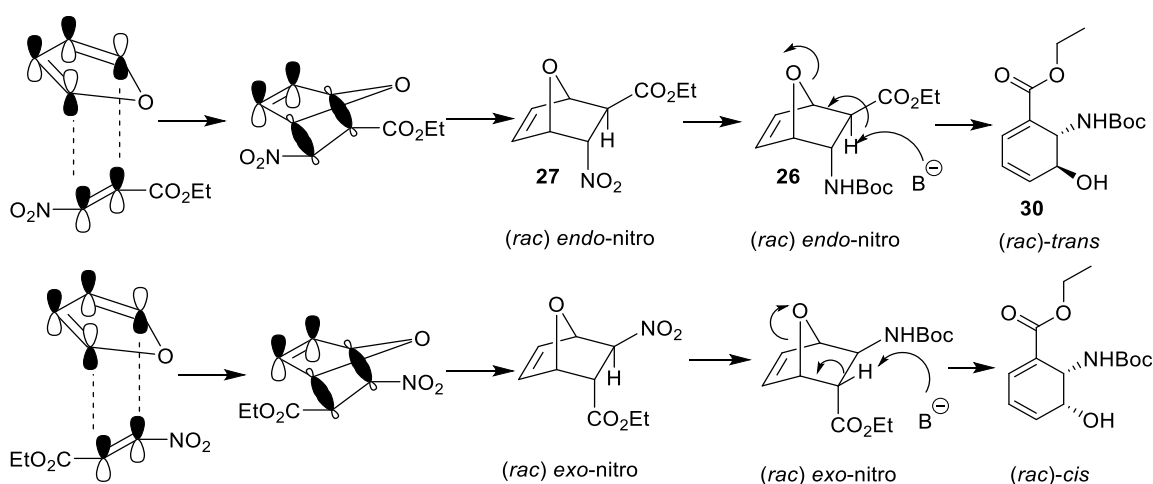
The synthesis of the central intermediate **26** (Scheme 7.13.) started with the synthesis of the dienophile **28**, according to a slightly modified procedure of Addo et al.^[100] Henry-reaction using a ca. 50 % solution of ethyl glyoxylate in toluene was reacted with nitromethane under neutral Al₂O₃ catalysis to give nitroalcohol **29** in a yield of 82 %. Subsequent treatment with MsCl and elimination using Et₃N as a base allowed for the synthesis of **28** in a yield of 58 %.

Following the protocol by Masesane et al.,^[99] dienophile **28** was then reacted with furan using kinetically controlled conditions in order to end up with the (*rac*)-*endo*-nitro isomer of **27**. The reaction was carried out in CHCl₃ at -20 °C for five days and at RT for two days to give the *endo*-nitro isomer in a yield of 54 %. The Diels-Alder reaction was plagued by the formation of the thermodynamically favoured *exo*-nitro isomer and product isolation proved to be challenging as the crude mixture of diastereomers had to be separated via three consecutive flash column chromatographies. The conversion of the oxanorbornene **27** into the corresponding amine, followed by Boc-protection was performed in a one-pot reaction following the procedure by Masesane et al.^[99] The reduction of the nitro group in **27** was achieved using Zn/HCl and the subsequent Boc-protection was performed using Et₃N and Boc₂O. The last step towards the central intermediate **26** was performed in 87 % yield.



Scheme 7.13: Synthesis towards the central intermediate **26**.

High *endo*-selectivity in the Diels-Alder reaction for the construction of **27** is especially important, as only the *endo* isomer can be further transformed to the corresponding *trans* isomer upon base-mediated ring opening. A ring opening of the corresponding (*rac*)-*exo*-nitro isomer would give the *cis* isomer (Scheme 7.14).^[99]

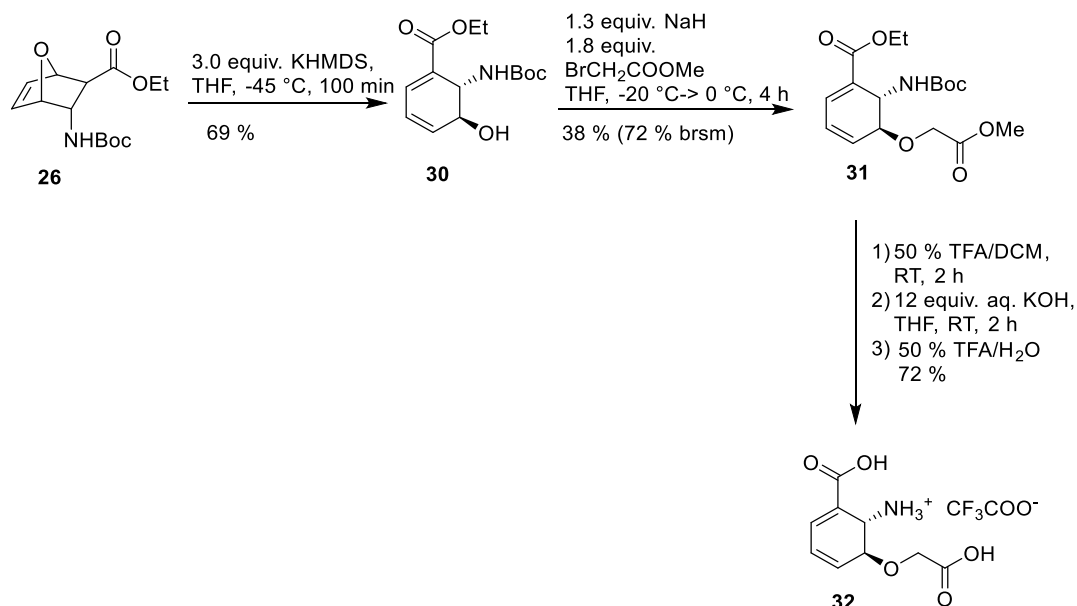


Scheme 7.14: Stereochemical influence of the Diels-Alder reaction on the base-mediated ring opening. Scheme adapted from Masesane et al.^[99]

7.3.2 First ADIC-derived inhibitor

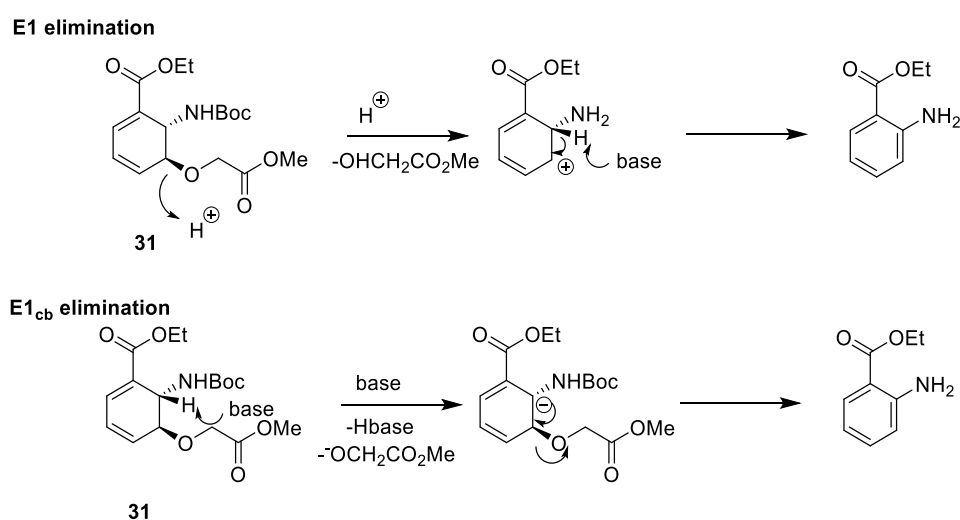
Having the late intermediate **26** in hand, we approached the synthesis of the first ADIC derived putative inhibitor **32**. Scheme 7.15 captures the remaining steps towards **32**. Starting from **26**, a base-mediated ring opening using KHMDS afforded **30** in a yield of 69 %. The reaction towards **30** was performed at -45 °C following the protocol of Bunnage et al.^[101] The next step

included an etherification of **30** to give **31**. After assessment of various reaction conditions (see chapter 7.3.3), it was found that Williamson-etherification at 0 °C gives proper results. Although Rh₂(OAc)₄-catalyzed OH-insertion using methyl diazoacetate gave slightly better results, it was decided to stick to the standard Williamson-etherification conditions in order to avoid the carcinogenic methyl diazoacetate and expensive Rh₂(OAc)₄ catalyst. Starting from **30**, late intermediate **31** was isolated in a yield of 38 % (72 % brsm).



Scheme 7.15: Synthesis towards the putative inhibitor **32** starting from the oxanorbornene intermediate **26**.

The last step towards **32** included a protecting group removal of **31**. As aromatization could not be ruled out at this stage (Scheme 7.16), a screening for proper conditions was performed.



Scheme 7.16: Two possible elimination mechanisms in ADIC analogue **31**.

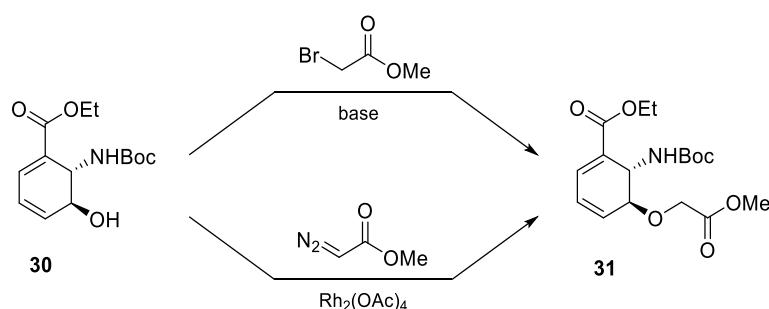
A brief screening of the protecting group removal, namely the deprotection of the amine and the hydrolysis of the ester groups, showed that the order in which the protecting groups are

cleaved is crucial. When hydrolysis is performed prior to Boc-deprotection, aromatization occurred upon solvent removal of the crude reaction mixture, as indicated via $^1\text{H-NMR}$. When **31** was stirred in a 50 % TFA/DCM solution to remove the Boc-group, followed by ester hydrolysis with aqueous KOH in THF and subsequent acidification with TFA, a mixture of **32** and CF_3COOK in a yield of 72 % was obtained upon concentration *in vacuo*. The putative inhibitor **32** was obtained as a pure compound in CF_3COOK and no further purification was therefore performed. Further screening revealed, that a selective cleavage of the methyl ester side chain is possible, when porcine liver esterase (PLE) is used (pH= 7.6, $\text{NaH}_2\text{PO}_4/\text{Na}_2\text{HPO}_4$, cosolvent= DCM, 30 °C, 3 days), suggested by HPLC-MS.

In conclusion, a promising rationally designed inhibitor was synthesized. The synthetic sequence proceeded through two steps in an overall yield of 27 % (52 % brsm), starting from the literature known **30**. In addition, the developed methodology was used for the synthesis of additional putative inhibitors (see chapter 7.3.4). Our strategy allows for diversification as the side chain is introduced at a late stage. Furthermore, we were able to saponify selectively one carboxylic acid ester functional group, which could be exploited to introduce further diversity. The ADIC derivative proved to be stable in D_2O for at least 5 days (duration of the experiment).

7.3.3 Etherification screening

Two different approaches for the etherification of **30** were tested (Scheme 7.17). In the first approach, an α -bromoester was used as electrophile in the presence of a base to deprotonate the alcohol **30**. Several different bases and solvents were tested for this purpose. The second approach included the Rh(II)-catalyzed O-H insertion of an α -diazoester.

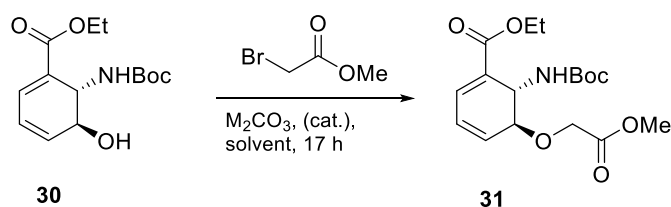


Scheme 7.17: Two different strategies for the etherification of intermediate **30**.

First attempts for the introduction of a side chain in **30** centred on the α -bromoester approach using Ag_2O in Et_2O and DBU in DMF, respectively. To our dismay, no conversion of the starting material was observed at RT. It is noteworthy that elevation of the temperature to 50 °C resulted only in minor product formation.

A brief screening using alternative bases and solvents with and without the use of NaI and KI showed only little conversion, as observed with HPLC analysis (Table 7.1). No product formation was observed when the reaction was run at RT in acetone using Na₂CO₃ as base (entry 1). The addition of 0.4 equiv. KI to the reaction mixture did not result in any product formation (entry 2). Using completely different conditions (K₂CO₃ as base, DMF, NaI, 50 °C) resulted in minor product formation (entry 3). The replacement of K₂CO₃ by Cs₂CO₃ led to a slight improvement (entry 4). The best results were obtained, when acetone was used as a solvent instead of DMF (entry 5), but the reaction was accompanied with the formation of an uncharacterized side product (approx. equal amount of formed product and side product). Unsatisfied with the obtained results, we moved on to a second screening, using totally different conditions for etherification.

Table 7.1: Screening of reaction conditions for the etherification of **30** using M₂CO₃ as base.



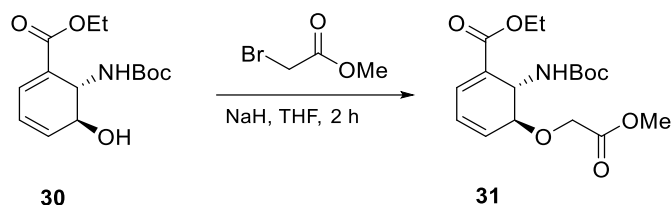
α-						
Entry	Bromoester	M ₂ CO ₃	Catalyst	Solvent	Temp.	Yield ^[a]
1	5.6 equiv.	1.3 equiv. Na ₂ CO ₃	-	acetone	RT	n.d. ^[b]
2	5.5 equiv.	1.4 equiv. Na ₂ CO ₃	0.4 equiv. KI	acetone	RT	n.d. ^[b]
3	5.8 equiv.	1.8 equiv. K ₂ CO ₃	0.3 equiv. NaI	DMF	50 °C	4 %
4	6.1 equiv.	1.8 equiv. Cs ₂ CO ₃	0.3 equiv. NaI	DMF	50 °C	7 %
5	5.8 equiv.	1.8 equiv. Cs ₂ CO ₃	0.3 equiv. NaI	acetone	50 °C	16 %

[a] Calculated from relative intensities of peaks in the HPLC-chromatograms ($\lambda = 210 \text{ nm}$) without internal standard. HPLC-method: "standard-1", $t_R(\mathbf{31}) = 3.57 \text{ min}$ ($m/z = 378$). [b] Not detectable.

In the second esterification screening (Table 7.2) we used NaH as a base in THF. Gratifyingly, the alternative conditions resulted in a substantial improvement. The highest amount of product formation was detected when the reaction was run at 0 °C, although a large amount of uncharacterized side product was formed (entry 1). In an attempt to lower the amount of side product, we reduced the temperature to -10 °C (entry 2) and it turned out that these conditions

represent a substantial improvement compared to the previously applied, as side product formation could be lowered to approx. 7 % of the total peak area.

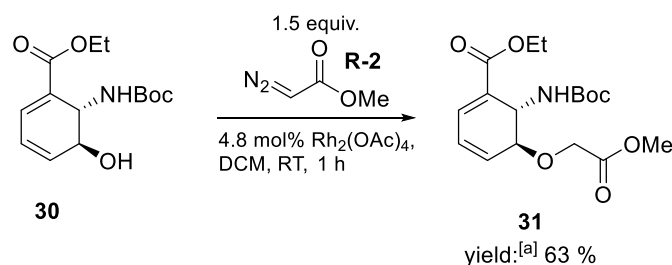
Table 7.2: Screening of reaction conditions for the etherification of **30** using NaH as base.



Entry	α -			Product ^[a]	Educt ^[b]	Side-Product ^[c]
	Bromoester	NaH	Temp.			
1	1.8 equiv.	1.9 equiv.	0 °C	42 %	13 %	28 %
2	1.7 equiv.	1.2 equiv.	-10 °C	34 %	49 %	7 %
3	3.0 equiv.	1.3 equiv.	0 °C	27 %	38 %	17 %

[a] Calculated from relative intensities of peaks in the HPLC-chromatograms ($\lambda = 210$ nm) without internal standard. HPLC-method: "standard-1", $t_R(\mathbf{31}) = 3.57$ min ($m/z = 378$). [b] $t_R(\mathbf{30}) = 2.53$ min ($m/z = 306$). [c] $t_R = 5.85$ min.

In order to test an alternative approach for the etherification of **30**, a $\text{Rh}_2(\text{OAc})_4$ catalyzed OH-insertion using methyl diazoacetate was tested. When standard conditions were applied, **31** was formed in a yield of 63 %, as detected by HPLC-MS.



Scheme 7.18: Etherification of **30** using methyl diazoacetate as electrophile. [a] Calculated from relative intensities of the HPLC-chromatogram ($\lambda = 210$ nm) without internal standard. HPLC-method: "standard-1", $t_R(\mathbf{31}) = 3.57$ min ($m/z = 378$).

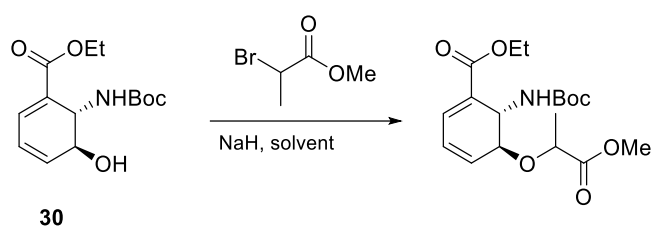
In order to increase diversity, the feasibility of the introduction of a lactyl side chain rather than a glycolate side chain was next subjected to further investigation.

When the optimized conditions for the Williamson etherification were applied using methyl bromopropionate as an electrophile using a reduced amount of NaH in order to minimize side reactions, only minor product formation was detected (Table 7.4, entry 1). This outcome can be explained primarily to the additional steric hindrance in methyl bromopropionate compared to methyl bromoacetate. Another reason may be that methylbromopropionate is prone to

elimination and the formed unsaturated product may act as a Michael acceptor, which in turn would lead to side product formation.

The use of DMF as a solvent turned out to be beneficial (entry 2), as the amount of formed product could be increased to 26 %. It turned out that the use of lower temperatures resulted not in an improvement in yield, as determined via HPLC-MS.

Table 7.3 Screening of reaction conditions for the introduction of a lactyl side chain in **30** using NaH as a base.

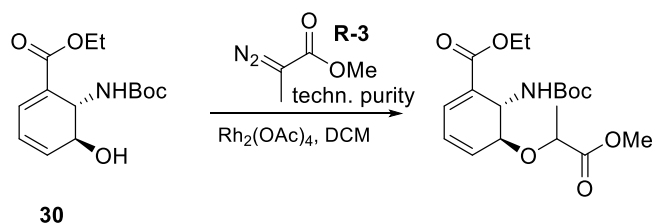


α-							
Entry	Bromoester	NaH	Solvent	Temp.	Time	Product ^[a]	Educt ^[b]
1	1.7 equiv.	1.2 equiv.	THF	-10 °C	2.5 h	3 %	47 %
2	1.7 equiv.	1.2 equiv.	DMF	-10 °C	6.5 h	26 %	36 %
3	1.7 equiv.	1.3 equiv.	DMF	-60 °C	6.5 h	19 %	66 %

[a] Calculated from relative intensities of peaks in the HPLC-chromatograms ($\lambda = 210$ nm) without internal standard. HPLC-method: "standard-1", $t_R(\text{product}) = 3.89$ min ($m/z = 392$). [b] $t_R(\mathbf{30}) = 2.53$ min ($m/z = 306$).

Unsatisfied with the outcome of the first screening for the introduction of a lactyl side chain in **30**, we turned our attention to the $\text{Rh}_2(\text{OAc})_4$ catalyzed OH-insertion of methyl diazopropionate into **30** (Table 7.4). When standard conditions were applied, encouraging 39 % product were formed. This result could be improved when the reaction was run at -10 °C (entry 2) to give 53 % product, as observed via HPLC.

Table 7.4: Screening of the reaction conditions for the introduction of a lactyl side-chain in **30** using methyl diazopropionate.

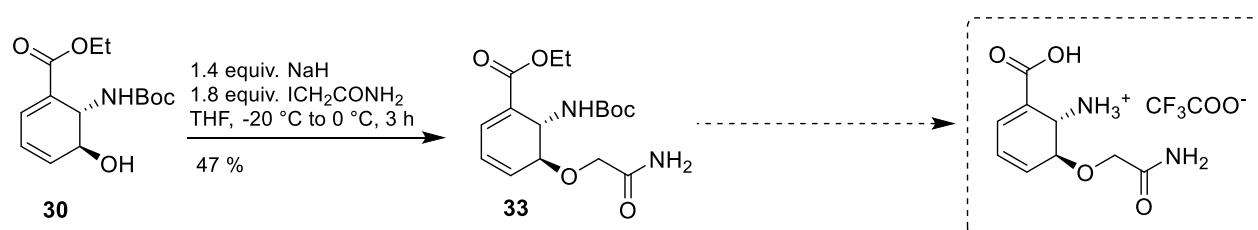


Diazo						
Entry	compound	$\text{Rh}_2(\text{OAc})_4$	Temp.	Time	Product ^[a]	Educt ^[b]
1	1.6 equiv.	4.8 mol%	RT	1 h	39 %	35 %
2	2.0 equiv.	5.0 mol%	-10 °C	5.5 h	53 %	18 %

[a] Calculated from relative intensities of the HPLC-chromatograms ($\lambda = 210$ nm) without internal standard. HPLC-method: "standard-1", $t_R(\text{product}) = 3.89$ min ($m/z = 392$). [b] $t_R(\mathbf{30}) = 2.53$ min ($m/z = 306$).

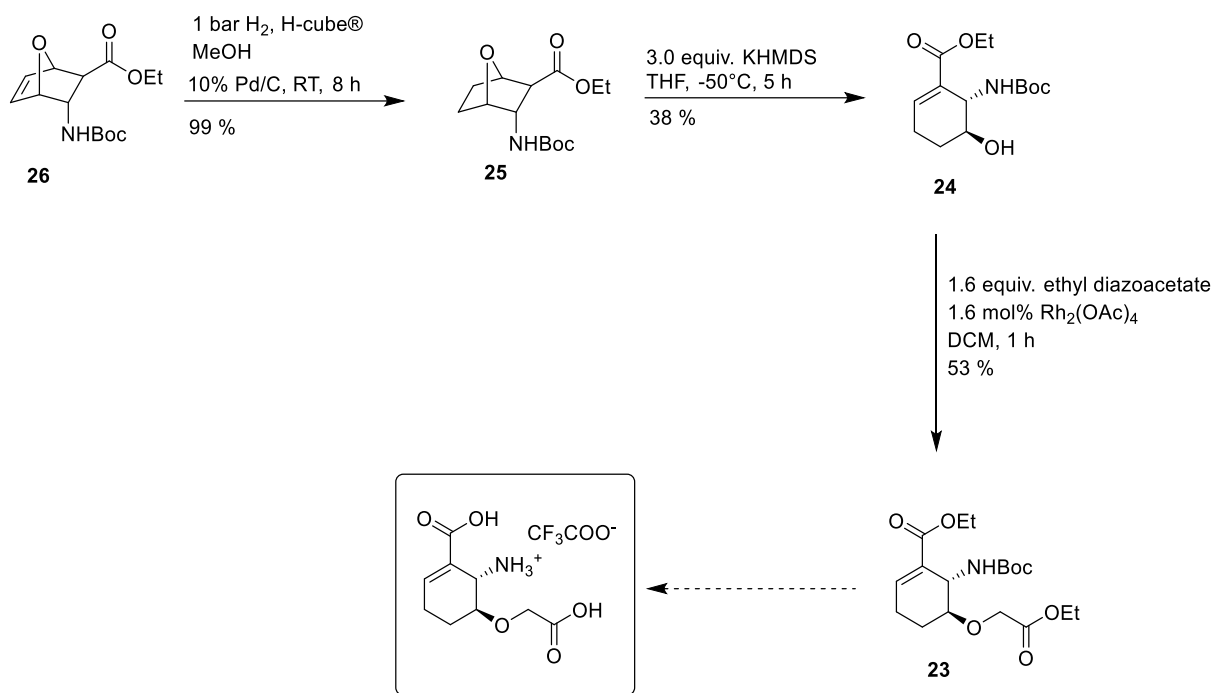
7.3.4 Additional ADIC-derived inhibitors

In order to increase diversity, compound **30** was subjected to an alternative electrophile in the etherification reaction. Upon treatment of **30** with 1.4 equiv. NaH and 1.8 equiv. iodoacetamide, intermediate **33** was isolated in 47 % yield (Scheme 7.19). Only little side product formation was observed via TLC. What remains to be done for the synthesis towards the corresponding putative inhibitor (dashed frame) is the deprotection of both the Boc-protecting group and the hydrolysis of the carboxylic acid ester group, which will be performed directly prior biological testing. The analogue of ADIC exhibiting a 2-hydroxy acetamide side chain at position C-3 could be a promising inhibitor for PhzE and anthranilate synthase.



Scheme 7.19: Synthesis of **33**.

Scheme 7.20 captures the overall synthesis towards the strategic intermediate **23**, which was synthesized starting from **26** in three steps with an overall 20 % yield. As the stability of our target compound (frame) is not known, the final deprotection of the amine and the esters will be applied directly prior biological testing. Starting from **24**, several alternative putative inhibitors could be synthesized, simply by using alternative electrophiles.



Scheme 7.20: Synthesis towards the strategic intermediate **23**.

The synthesis towards **23** started with hydrogenation of **26**, which was performed using the H-cube® flow reactor (1 bar H₂, 10 % Pd/C, RT, 1 h). Literature^[98] known **25** was isolated without purification as a pure compound in 99 % yield. The next step involved a base-mediated opening of bicycle **25**. Several conditions were tested and it turned out that the reaction is very temperature dependent. Higher temperatures (-25 °C) result in massive side product formation. When freshly prepared LiHMDS was used as base at -45 °C, only little side product formation was observed, but only minor conversion took place, as 65 % of the starting material could be recovered. When KHMDS was used as a base, full conversion was detected after 5 h, but significant side product formation was observed via TLC. Compound **24** was obtained in a yield of 38 % when the latter conditions were applied. A base-mediated opening of **25** was also performed in the PhD thesis of Mario Leypold.^[41]

Table 7.5: Screening of the reaction conditions for the synthesis of **24**.



Entry	Base	Temp.	Time	Product ^[a]	Educt ^[a]
1	3.2 equiv. LiHMDS	-45 °C	5.5 h	19 %	65 %
2	3.0 equiv. KHMDS	-45 °C to -25 °C	5.5 h	-[b]	-[b]
3	3.0 equiv. KHMDS	-45 °C	5 h	38 %	-

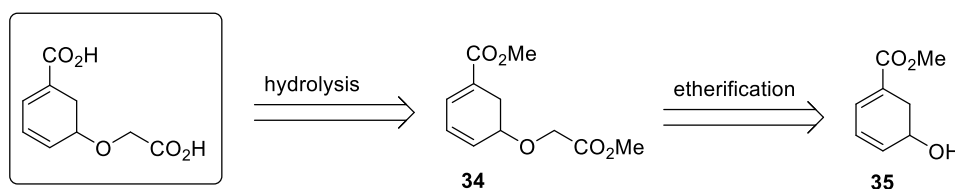
[a] isolated yield [b] massive side product formation according to TLC

The next step in the synthetic route called for an introduction of the glycolate side chain. It is assumed that **24** is more susceptible for a base-promoted aromatization compared to **30** and it was decided to use a neutral $\text{Rh}_2(\text{OAc})_4$ catalyzed OH-insertion using methyl diazoacetate for the etherification. Compound **23** was isolated in 53 % yield starting from **24**. What remains to be done is the deprotection of both the Boc-protecting group and the hydrolysis of the two carboxylic acid ester groups, which will be performed directly prior biological testing.

7.4 Cyclohexadiene-derived inhibitors

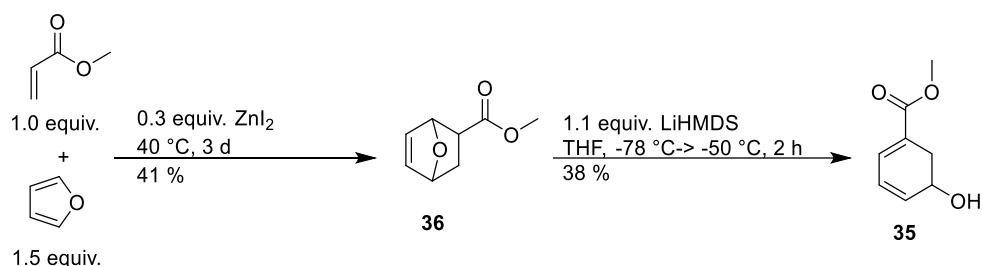
7.4.1 Fully-conjugated substrates

In order to increase our library of compounds that will be tested for inhibition and applied to study binding differences between PhzE and anthranilate synthase (AS), we proposed cyclohexadiene derivative 5-(carboxymethoxy)cyclohexa-1,3-diene-1-carboxylic acid as interesting candidate (see framed compound, Scheme 7.21). The target compound is a fully conjugated cyclohexadiene derivative and the carboxylic acid functionality at position C-1 is supposed to form electrostatic interaction to the Mg^{2+} bound to PhzE and AS. The glycolate side chain at C-3 is supposed to form hydrogen bonds within the corresponding binding pocket. Scheme 7.21 gives a retrosynthetic analysis, starting from the literature known intermediate **35**.^[102] An etherification of the alcohol at position C-3 in **35** would give access to **34**, which upon hydrolysis would yield our target compound.



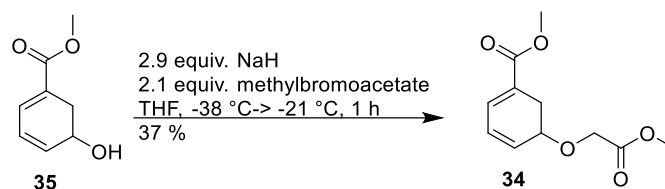
Scheme 7.21: Retrosynthetic analysis towards a fully conjugated cyclohexadiene derivative.

Intermediate **35** was obtained in two steps, following a literature procedure (Scheme 7.22).^[102] Starting from furan and methyl acrylate, a Diels-Alder reaction afforded **36** in 41 % yield. The bicycle **36** was opened using freshly prepared LiHMDS as a base to give the desired intermediate **35** in 38 % yield. It has to be noted that the obtained oil **35** became increasingly viscous upon storage at $-20\text{ }^{\circ}\text{C}$, which was accompanied by an additional spot formation on TLC ($R_f = 0$, cyclohexane/EtOAc = 1/1). It is hypothesized that oligomerization may occurred.



Scheme 7.22: Synthesis towards **35** following the procedure by Brion.^[102]

After assessment of various reaction conditions, late intermediate **34** was obtained in 37 % yield starting from **35** via a Williamson-etherification (Scheme 7.23).



Scheme 7.23: Williamson-etherification of **35**.

Fortunate to have the late stage intermediate in hand, our next attempts centered on the hydrolysis of the two methyl esters in **34**. Compound **34** is fairly unstable as elimination of the glycolate side chain would lead to a stable aromatic system. To address this challenge, we first applied 4.2 equiv. TMSOK^[103] as a rather mild reagent in THF. Unfortunately, aromatization was observed at RT after 2.5 h via ¹H-NMR. The next approach centered on the use of KOH (15.5 equiv. in H₂O/THF) and partial aromatization was observed after 2 h according to ¹H-NMR. We next examined the use of NaOH in H₂O with and without the addition of cosolvents. The most promising result was obtained, when 2.05 equiv. NaOH were used in H₂O without the use of a cosolvent (Figure 7.4)

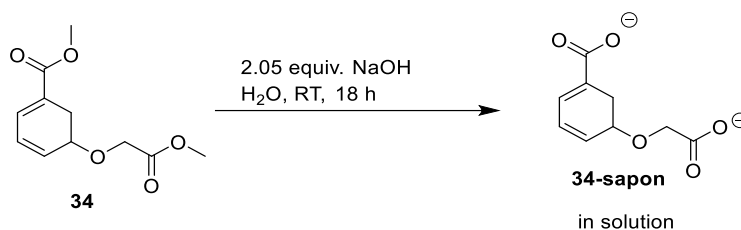


Figure 7.4: Saponification of **34** in H₂O without the use of a cosolvent

Reaction monitoring of the crude mixture indicated clean conversion to hydrolysed **34** (Figure 7.5). It should be noted that solubility of the starting material might be an issue here and the amount of starting material conversion was not determined. However, when the reaction mixture was gently concentrated *in vacuo* under the exclusion of oxygen (2 days, oil-pump), aromatization occurred and ¹H-NMR indicated a 1:1:1 mixture of benzoate/ **34-sapon**/ 2-hydroxyacetate (Figure 7.6).

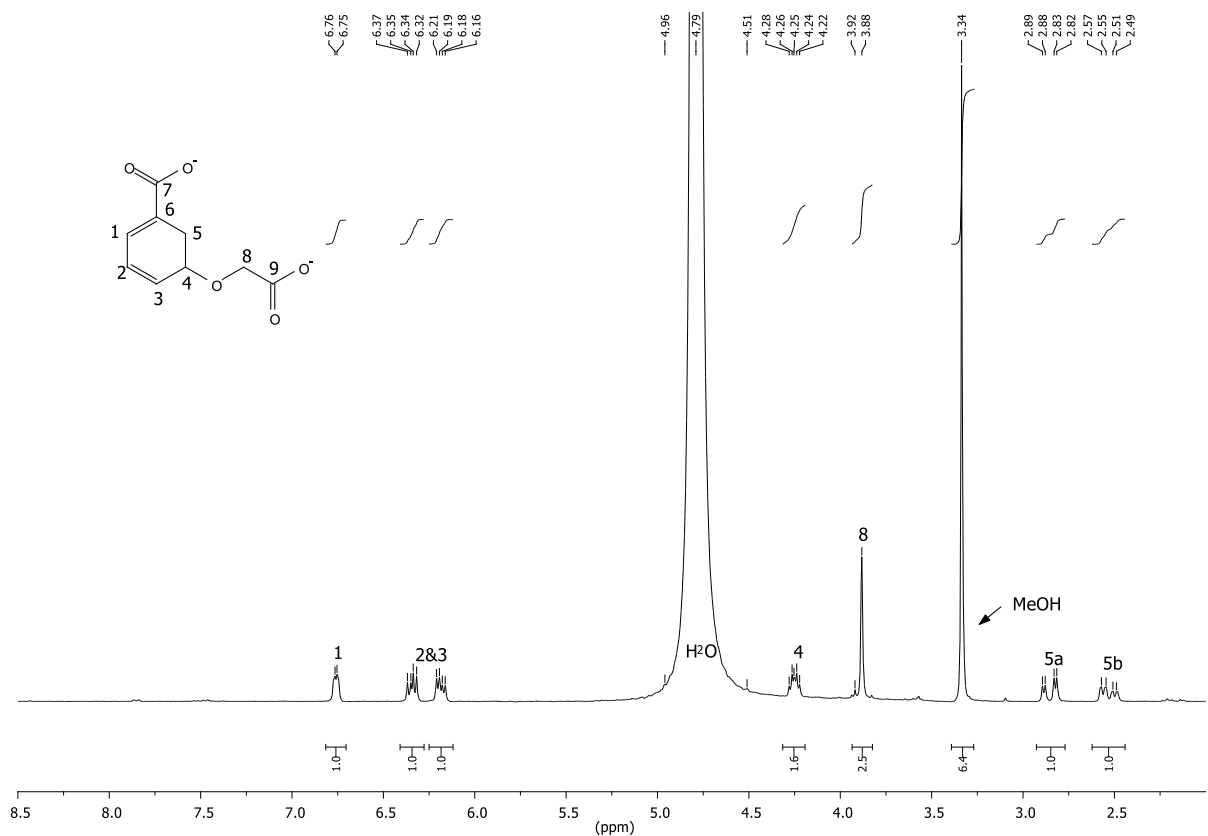


Figure 7.5: ¹H-NMR (300 MHz, D₂O) of hydrolysed **34** without workup in H₂O.

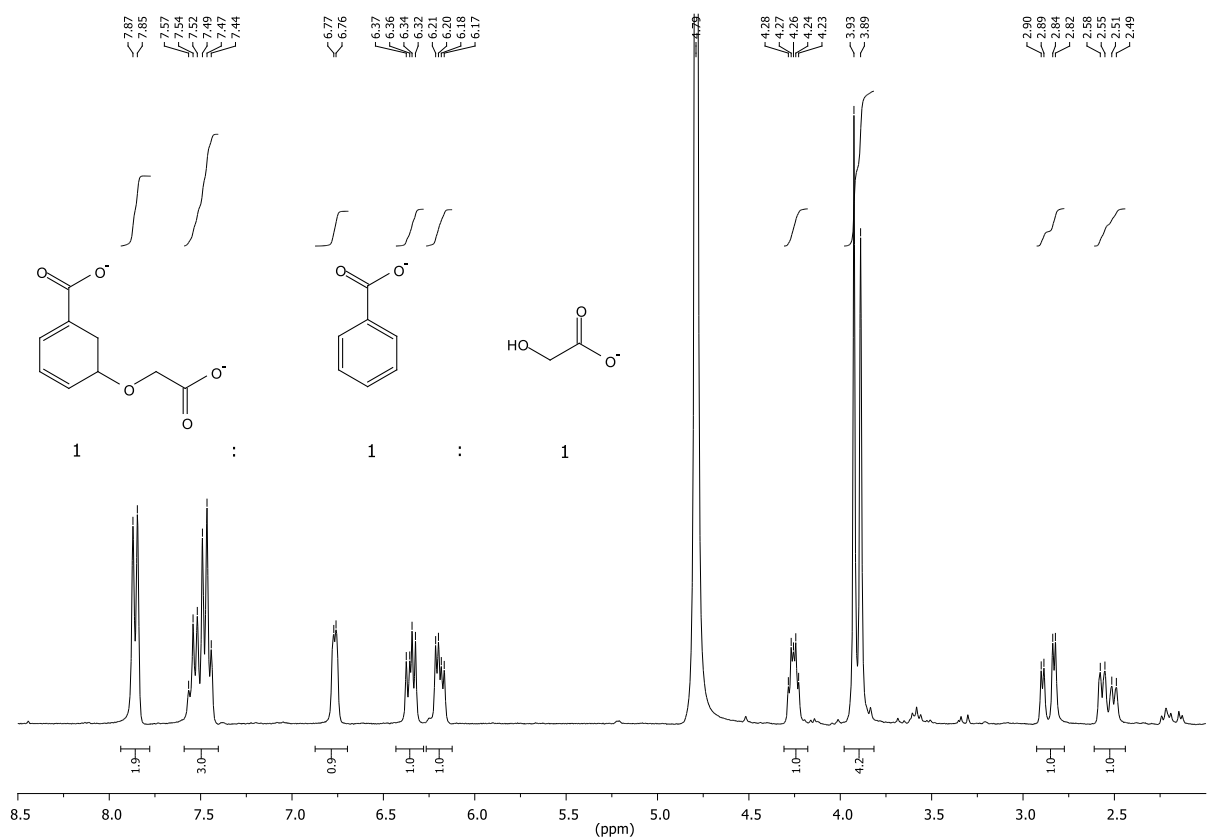
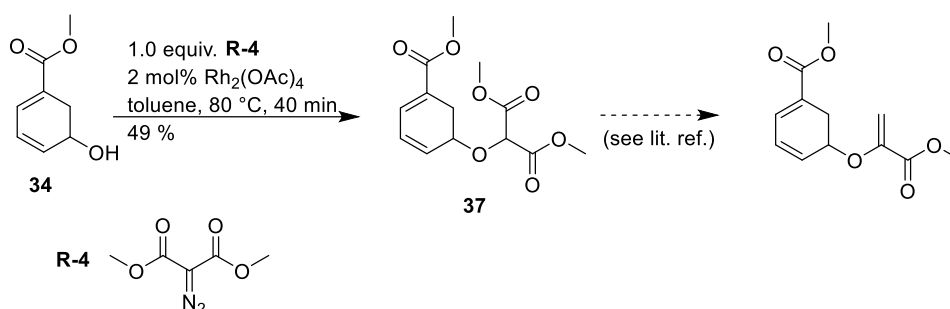


Figure 7.6: ¹H-NMR (300 MHz, H₂O) of hydrolysed **34** in H₂O after solvent evaporation.

Importantly, we could show that saponification of **34** is possible and that the corresponding product is stable in solution at RT for at least 18 h (reaction time). In order to study binding differences between PhzE and AS, **34** will be hydrolysed directly prior to the crystallization experiments.

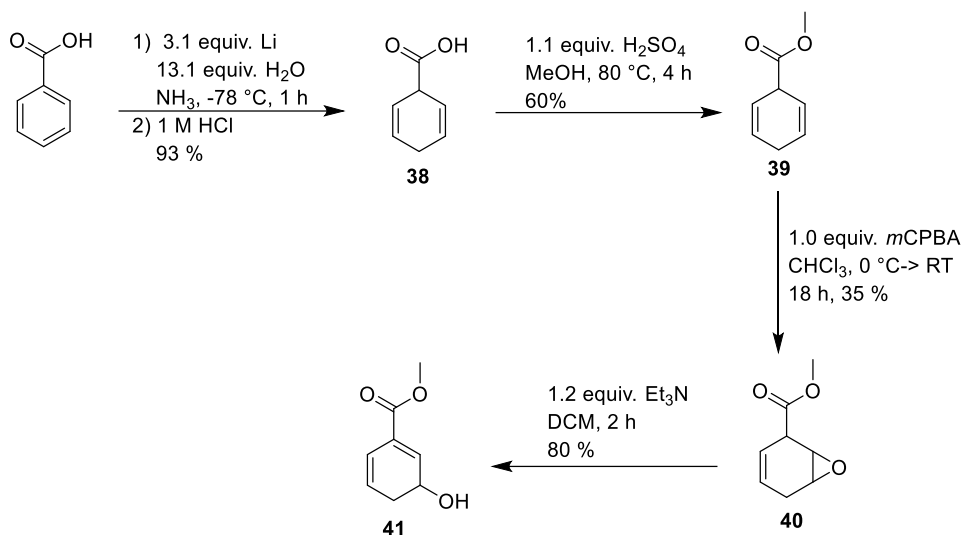
Compound **37** was synthesized following a literature procedure and will be also subjected to hydrolysis upon first crystallization experiments turn out to be successful (Scheme 7.24).^[104]



Scheme 7.24: Synthesis of **37**.

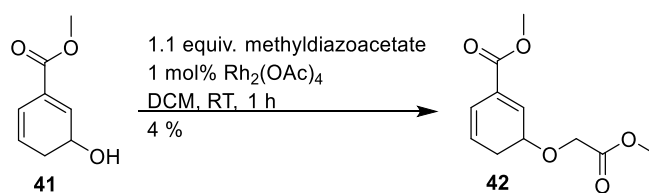
7.4.2 Cross-conjugated substrates

In order to get access to cross-conjugated **42**, we first synthesized **41** following a literature procedure (Scheme 7.25). All steps towards **41** were performed following the procedure by O'Mahony et al.,^[105] except the Birch-reduction which was performed following the procedure of G. A. Kraus and Frazier.^[106] The synthesis towards **41** started with Birch-reduction of benzoic acid using Li in H₂O/NH₃. Compound **38** was obtained in 93 % yield. The carboxylic acid in **38** was esterified via a Fischer esterification to produce **39** in 60 % yield. Desymmetrisation using 1.0 equiv. *m*CPBA afforded **40** in 35 % yield. The epoxide in **40** was opened using Et₃N as a base. Late intermediate **41** was obtained in 80 % yield. It has to be noted that the obtained oil **41** became increasingly viscous upon storage at -20 °C, which was accompanied by formation of an additional spot on TLC (*R_f* = 0, cyclohexane/EtOAc = 1/1).



Scheme 7.25: Synthesis towards **41** following a literature procedure.^[105,106]

With **41** in hand we next proceeded to the installation of a glycolate moiety at position C-3 via a $\text{Rh}_2(\text{OAc})_4$ catalyzed OH-insertion reaction. Unfortunately, **42** was isolated in a yield of only 4 %. This disappointing result may originate from the previously hypothesized oligomerization of the starting material **41**. The etherification of **41** will be revisited in the future again.

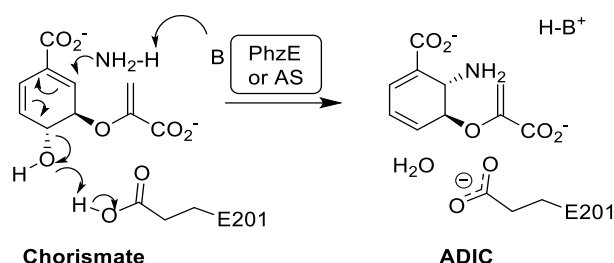


Scheme 7.26: Etherification of **41** gave access to **42**.

Compound **42** presents an interesting late stage intermediate and will be hydrolysed using the same method as for the hydrolysis of **34** in order to perform crystallization experiments.

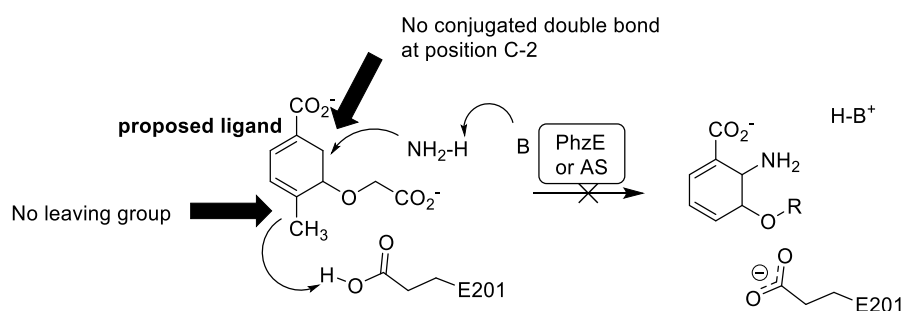
7.5 Investigations towards mechanism-based inhibitors

PhzE and anthranilate synthase (AS) catalyze the conversion of chorismate to 2-amino-2-deoxyisochorismate (ADIC). This transformation proceeds via an attack of ammonia at the C-2 position of chorismate with the subsequent loss of water (Scheme 7.27).



Scheme 7.27: Conversion of chorismate into 2-amino-2-deoxyisochorismate (ADIC) catalyzed by PhzE and anthranilate synthase (AS).

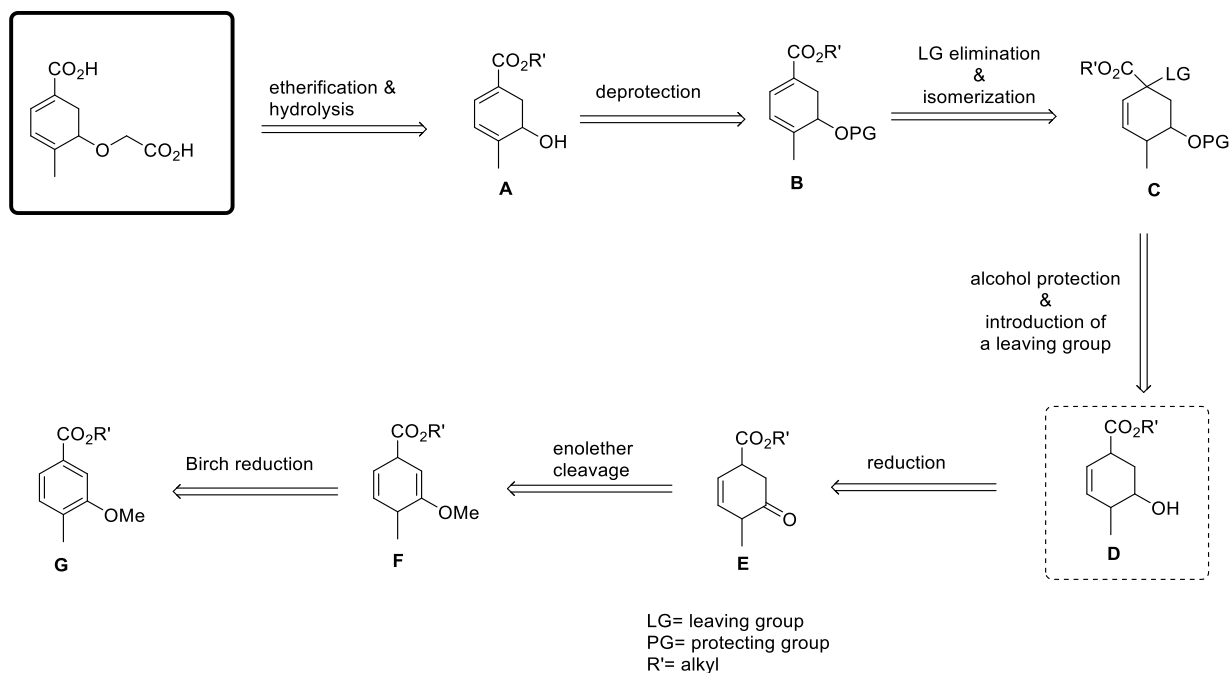
Our rationale is to design a ligand that is sufficiently similar to chorismate, as the ligand must enter the active site, but should be inert to amination at position C-2 (Scheme 7.28). We speculate that the installation of a methyl group instead of a hydroxyl group at position C-4 in the natural substrate would render the enzyme inactive as a methyl group is not prone to elimination. In addition, our alternative core structure lacks the cross-conjugated double bond at position C-2. We propose the alternative side chain glycolate instead of pyruvate in position C-3 in order to increase stability. The proposed ligand would not only serve to study binding differences between PhzE and AS, but would represent a putative inhibitor of the aforementioned enzymes.



Scheme 7.28: Analog of chorismate that is thought to be inert to amination at the C-2 position.

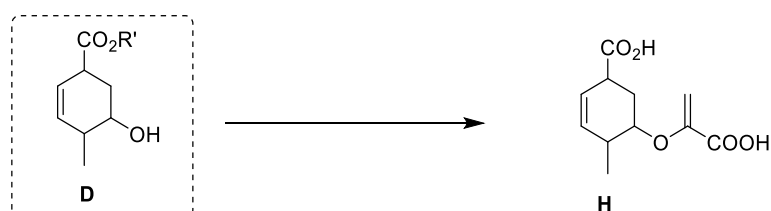
Scheme 7.29 gives a retrosynthetic analysis of our proposed ligand. The side chains of our target molecule (framed) would be installed via an etherification of the proposed late stage intermediate **A**. A following hydrolysis would then give access to the putative inhibitor. The second double bond, which is present in **A** could be introduced via an elimination of a leaving group, and we proposed **C** as an intermediate for **A**. The introduction of a leaving group in α -position of an enolisable ester may be achieved via a base-mediated α -deprotonation of **D**, followed by the introduction of an electrophile. In order to reduce possible side reactions, the

alcohol functionality present in **D** would have to be protected prior to the introduction of the leaving group. **D** would be the central intermediate in our proposed strategy. In order to get access to the alcohol functionality, we proposed a reduction of the ketone group in **E**. The ketone itself may be accessible via cleavage of the corresponding enoether in **F**. The structural features present in **F** are a retron of the Birch-reduction and we proposed inexpensive and commercially available **G** as the starting material for the overall synthesis towards the proposed putative inhibitor (framed).



Scheme 7.29: Retrosynthetic approach towards a putative inhibitor of PhzE and AS (framed). The central intermediate of this strategy is highlighted with a dashed frame.

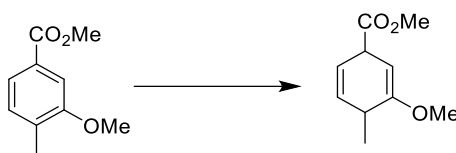
A central aspect in devising our approach was to introduce an intermediate, which can be exploited for the synthesis of an additional putative inhibitor. We proposed **D** as a central intermediate which would meet our requirements as it exhibits an alcohol functionality in position C-3, that could serve for the introduction of a pyruvate moiety to give **H** (Scheme 7.30).



Scheme 7.30: Central intermediate **D** could serve for the synthesis of additional putative inhibitors.

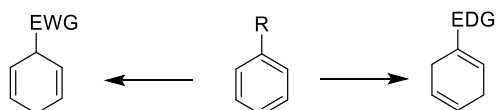
7.5.1 Birch-reduction

Our initial attempts for the synthesis of our proposed inhibitor centered on the Birch-reduction of methyl 3-methoxy-4-methylbenzoate (Scheme 7.31).



Scheme 7.31: Birch reduction of methyl 3-methoxy-4-methylbenzoate.

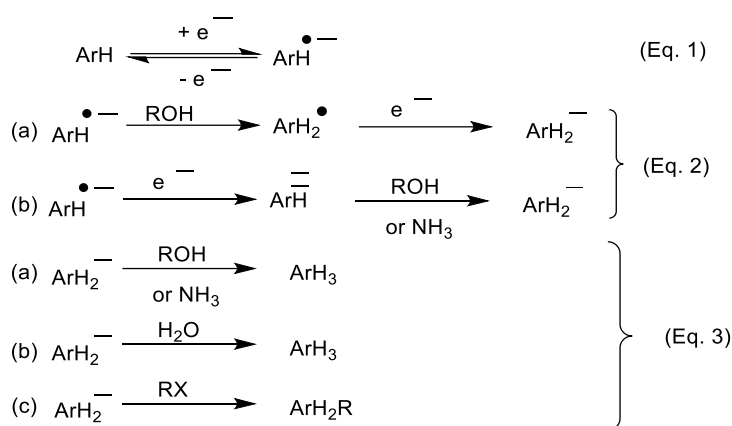
The reduction of aromatic compounds by alkali metals in liquid ammonia to give partially unsaturated six-membered rings is called the Birch-reduction. Wooster and Godfrey were the first to discover the reaction, but it is named after A. J. Birch, who had made major contributions to this type of reduction.^[107–109] Most commonly Na or Li are applied as metals and cosolvents like Et₂O or THF are used to improve solubility of the substrate. Especially for the reduction of benzene and inactivated derivatives thereof, weak acids like alcohols are needed as a proton source. The regiochemical outcome of the Birch reduction is greatly influenced by substituents attached to the aromatic ring (Scheme 7.32).^[109] The stereochemical outcome of such reactions follows the “Birch rule”: “electron-donating substituents direct reduction so that the major product has the maximum number of such groups attached to the residual double bonds, and a maximum of EWG groups are located at the allylic sites.”^[109,110]



Scheme 7.32: Influence of substituents on the regiochemistry in the Birch reduction.^[109]

The mechanism of the Birch-reduction is outlined in Scheme 7.33:^[109] Upon attack of an electron on an aromatic system ArH, a radical anion is formed, which is in equilibrium with the reactant (Eq. 1). This radical anion can be protonated by a proton donor like an alcohol to give the radical ArH₂[•]. Upon additional of an electron, ArH₂^{•-} is formed (Eq. 2a)

The same ArH₂^{•-} can be formed in the absence of a proton donor, when an electron attacks the radical anion ArH^{•-} to give a dianion, which in turn can be protonated by either an alcohol or ammonia to give ArH₂^{•-} (Eq. 2b). ArH₂^{•-} can either be protonated to give ArH₃ (Eq. 3a and 3b) or alkylated to give ArH₂R (Eq. 3c). The protonation of the final radical anion determines the stereochemical outcome of nonrigid systems.



Scheme 7.33: Mechanism of the Birch reduction. Scheme adapted from Rabideau and Marcinow^[109]

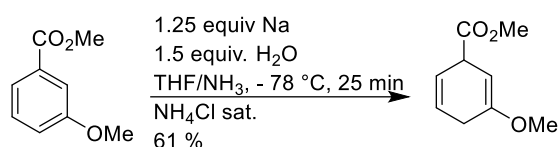
When performing a Birch-reduction a number of things have to be considered that significantly influence the outcome of the reaction:^[109]

- Nature of the metal. Most often Li, Na and K are used. Lithium is often chosen over the other metals as it is the most reactive and the most soluble metal in NH₃. In addition, lithium amide is less soluble than sodium or potassium amide and therefore isomerisation is less likely when Li is used;
- Temperature;
- Cosolvents are often added in order to increase solubility of the substrate;
- Proton donors are sometimes needed for reduction, but for example the addition of alcohols to benzoates can be detrimental as overreduction may occur when more than one equivalent of alcohol is used. The choice of the proton source is crucial and it is assumed that the basicity of the formed base influences the rate of isomerization (e.g. isomerization proceeds faster when sodium ethoxide is formed compared to sodium methoxide);^[111]
- The final quenching process is crucial for the outcome of the reaction and can serve one or more of the following purposes: the destruction of the remaining metal, the protonation of anionic intermediates or the shift of an equilibrium.
The quenching process may be applied via the addition of an alcohol, NH₄Cl or a saturated NH₄Cl solution. The quenching process can be either fast (e.g. via an inverse quench) or slow. Fast quenching can be important and overreduction throughout the quenching process is possible for example when an alcohol serves as the quenching agent, as the metal is destroyed only slowly;
- The purity of ammonia and reagents may also play a crucial role.

On the basis of literature precedence (Scheme 7.34),^[112] it was expected that a reduction of methyl 3-methoxy-4-methylbenzoate would give rise to the corresponding 1,4-dihydro compound. Although it is known that carboxylic acid esters can be reduced to the

corresponding alcohols in metal-ammonia-alcohol solution in the so called Bouveault-Blanc-reaction,^[113] Rabideau et al.^[112] could show that aromatic carboxylic acid esters can be effectively reduced to the corresponding 1,4-dihydro analogues when 1.25 equiv. of H₂O are present prior to the metal addition. They hypothesized that water serves to rapidly protonate the formed radical anion before dimerization and ester cleavage can occur. Rabideau et al. obtained good results, when aromatic ethyl and *tert*-butyl esters were applied but methyl esters provided only poor results. In addition, they could show that *p*-methylbenzoate can be reduced to its *cis* and *trans* 1,4-dihydro isomers.

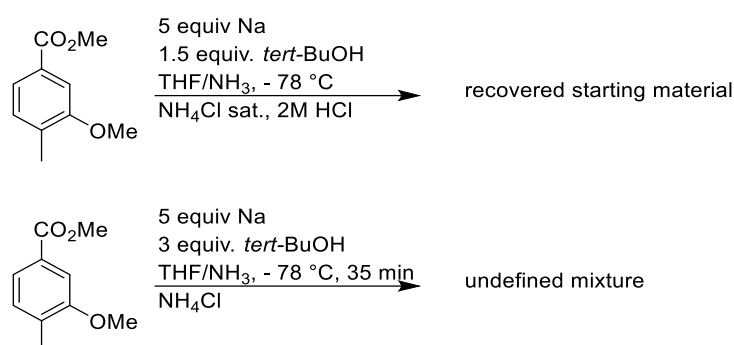
In their synthesis towards dimethyl mycosporulone, Kraus and Cui succeeded in the reduction of methyl 3-methoxybenzoate to the corresponding 1,4-dihydro compound via a Birch-reduction (Scheme 7.34).^[114] For their reduction, they used a protocol of Rabideau et al.^[112]



Scheme 7.34: Reduction of methyl 3-methoxybenzoic acid by Kraus and Cui.^[114]

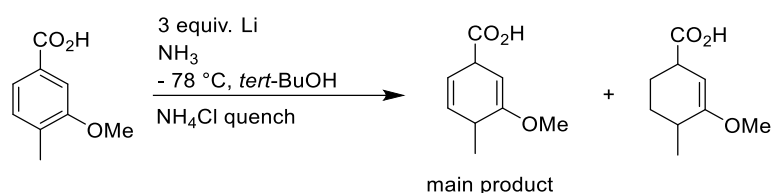
Inspired by these intriguing examples for the reduction of aromatic carboxylic acid esters, we envisaged to test the specific applicability of the described method for the reduction of our proposed starting material. To this end, we modified the procedure of Kraus and Cui^[114] for the reduction of methyl 3-methoxy-4-methylbenzoate. The amount of Na was increased (3.1 equiv. were applied) as our initial attempts centered on the reduction of the aromatic ring, irrespective of ester reduction or hydrolysis. The inverse quench into a sat. NH₄Cl solution was delayed until NH₃ was evaporated (G. A. Kraus and W. Cui quenched the reaction after 25 min)^[114]. To our dismay, the corresponding 1,4-dihydro compound was not observed. According to the crude NMR, it is assumed that either a partial saponification, ammonolysis or the reduction to the corresponding alcohol took place. Unsatisfied with the obtained results, we moved on to test *tert*-BuOH as an alternative proton source instead of H₂O (Scheme 7.35). Methyl 3-methoxy-4-methylbenzoate was stirred in a mixture of THF, NH₃ and 1.5 equiv. *tert*-BuOH as a proton source at – 78 °C and Na (5 equiv.) was added until a blue colour persisted and the mixture was poured into an excess of aqueous sat. NH₄Cl. It was acidified to a pH of 6-7 using 2 M HCl and extracted with Et₂O. To our dismay, only starting material was recovered. When the applied method was changed (3 equiv. instead of 1.5 equiv. *tert*-BuOH, prolonged stirring (35 min) after the blue colour of the mixture persisted and the use of solid NH₄Cl instead of an aqueous NH₄Cl solution) an undefined mixture was detected. The occurrence of aliphatic

protons in the $^1\text{H-NMR}$ spectrum suggest that at least partial reduction of the aromatic ring system took place.



Scheme 7.35: *tert*-BuOH was tested as a proton source for the Birch reduction of methyl 3-methoxy-4-methylbenzoate.

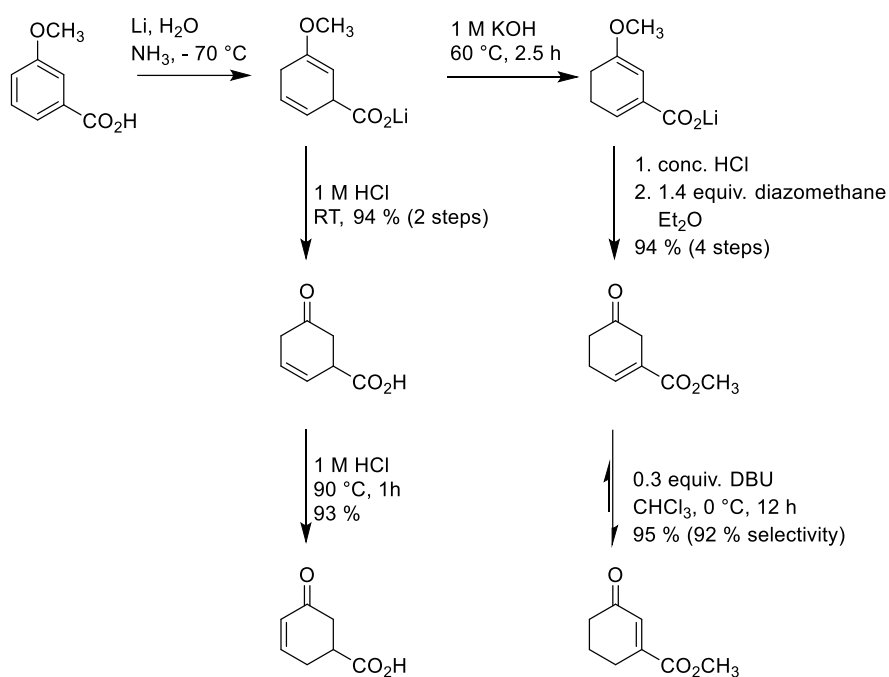
Guided by the successful reduction of 3-methoxy-4-methylbenzoic acid to the corresponding 1,4-dihydro derivative by Subba Rao and Ramanathan (Scheme 7.36),^[115] we decided to change our strategy and tested 3-methoxy-4-methylbenzoic acid as a starting material for the Birch-reduction.



Scheme 7.36: Birch-reduction of 3-methoxy-4-methylbenzoic acid by Subba Rao and Ramanathan.^[115]

The reduction of aromatic carboxylic acids is well known and the carboxyl group strongly activates the ring system. In addition, the carboxyl group generally outweighs other functionalities when it comes to regiochemistry.^[109]

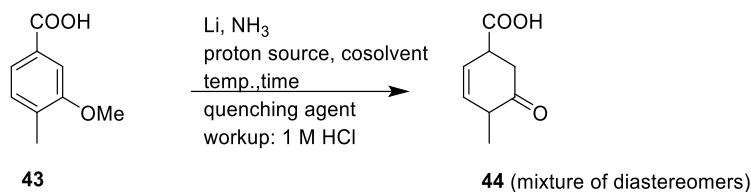
Webster and Silverstein showed in their studies about the Birch reduction of *m*-anisic acid that upon control of the conditions specific 3-oxocyclohexenecarboxylic acids are accessible when 3-methoxycarboxylic acid is used as the starting material. (Scheme 7.37). It is argued when water is used as a proton source with excess Li that only a relatively weak, mostly insoluble base is formed at a slow rate^[111]



Scheme 7.37: Synthesis of specific 3-oxocyclohexenecarboxylic acids by Webster and Silverstein.^[111]

Intrigued by the results of Webster and Silverstein,^[111] we decided to perform both the Birch-reduction and the ensuing enoether cleavage in one pot and tested several conditions for the conversion of **43** to **44** (Table 7.6). Our brief screening using the methods of Subba Rao et al. and Webster et al.,^[111,115] showed that both H₂O and *tert*-BuOH are suitable proton sources for our purpose. Entries 1, 3 and 4 showed good results, although some impurities were observed in the crude reaction mixture. Poor results were obtained when the reaction was run at – 33 °C (entry 2).

Table 7.6: Screening using **43** as a starting material

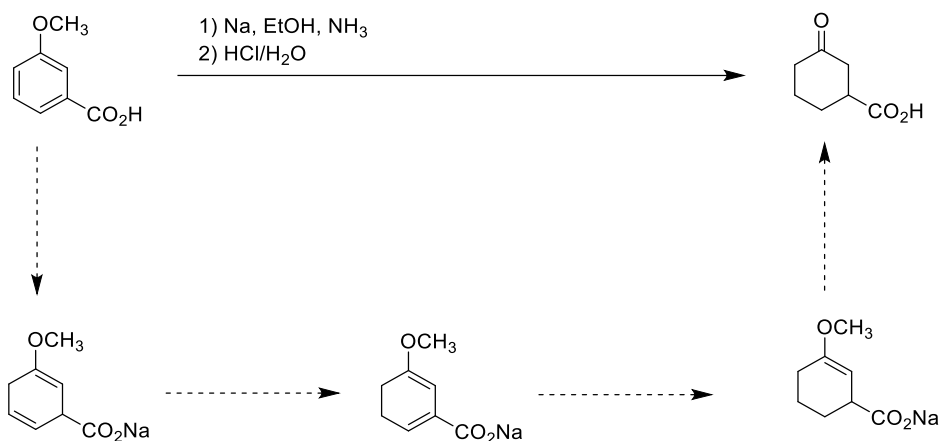


Entry	Conditions	NMR
1 ^[b]	2.8 equiv. Li, 2.5 equiv. <i>tert</i> -BuOH - 78 °C, 25 min, THF, NH ₄ Cl	product + some side products
2 ^[a]	3.4 equiv. Li, 2.7 equiv. <i>tert</i> -BuOH - 33 °C, 25 min, THF, NH ₄ Cl	undefined mixture
3 ^[b]	3.4 equiv. Li, 2.5 equiv. <i>tert</i> -BuOH - 78 °C, 5 min, THF, NH ₄ Cl	product + some side products
4 ^[b]	3.1 equiv. Li, 13 equiv. H ₂ O - 78 °C -> RT	product + some side products

[a] product distribution was estimated according to crude ¹H-NMR and crude ¹³C,APT-NMR

[b] product distribution was estimated according to crude ¹H-NMR

Impurities in the crude reaction mixture may be attributed to isomerization and double reduction. Such reactions are known to occur in the Birch reduction (Scheme 7.38).^[95,111]



Scheme 7.38: Possible transformations in the Birch-reduction. Scheme adapted from Webster and Silverstein.^[111]

We decided to use the conditions of entry 4 for the scale-up. Unfortunately, we realized that upon scaling up (2 mmol in the test reaction, 35 mmol in the scale-up reaction), significantly poorer results were obtained (Figure 7.7). The side products in the 35 mmol batch are presumably unreacted starting material, double bond isomers and the fully reduced cyclohexane derivative. We decided to use the crude material in the following step.

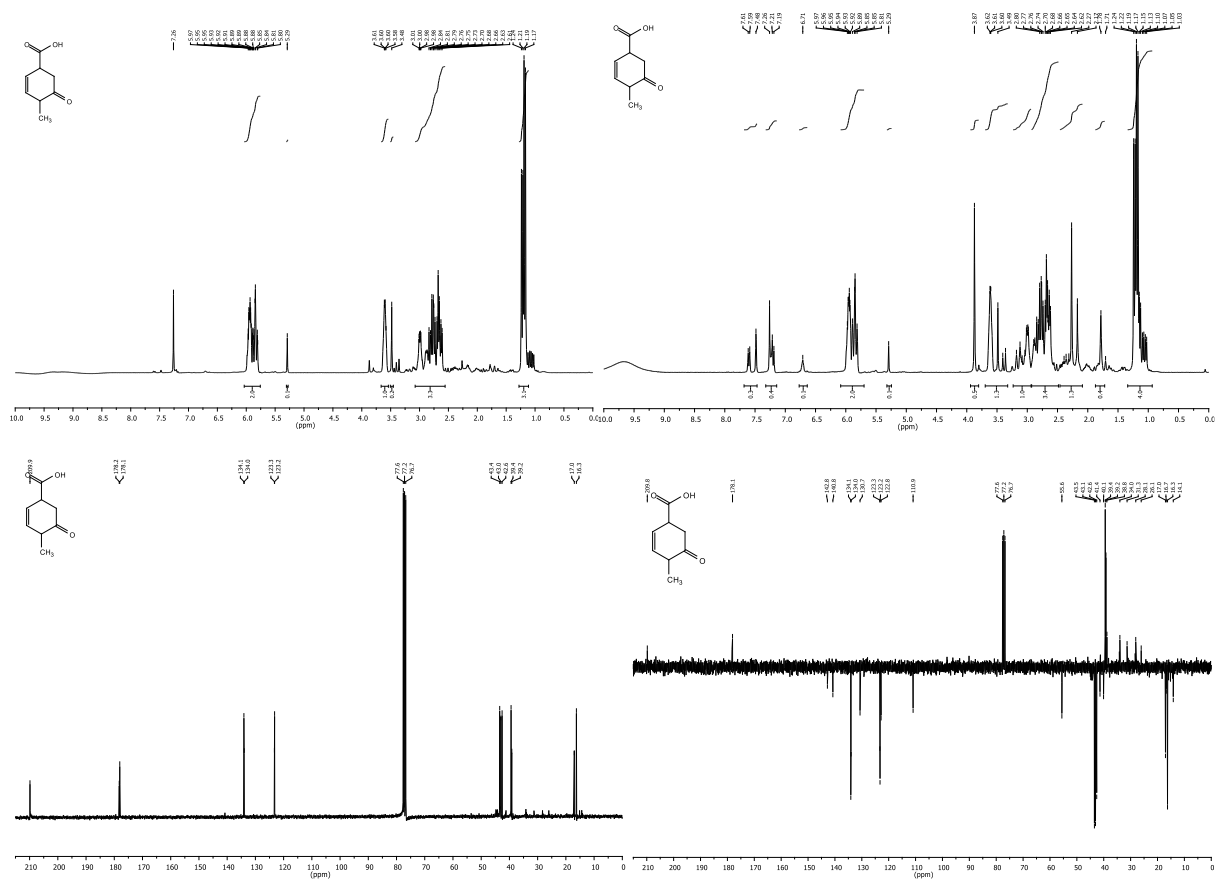
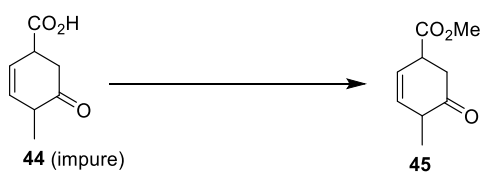


Figure 7.7: Influence of the batch size on the outcome of the reaction. 2 mmol batch ($^1\text{H-NMR}$ top left, $^{13}\text{C-NMR}$ bottom left) versus 35 mmol batch ($^1\text{H-NMR}$ top right, $^{13}\text{C-NMR}$, APT bottom right).

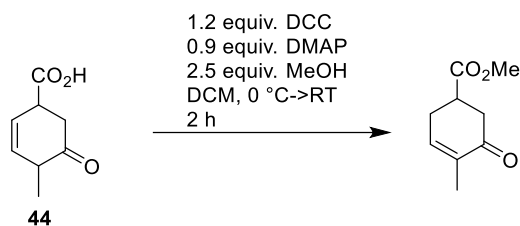
7.5.2 Esterification

The next step in our synthetic route called for an esterification of the carboxylic acid group present in **44** (Scheme 7.39).



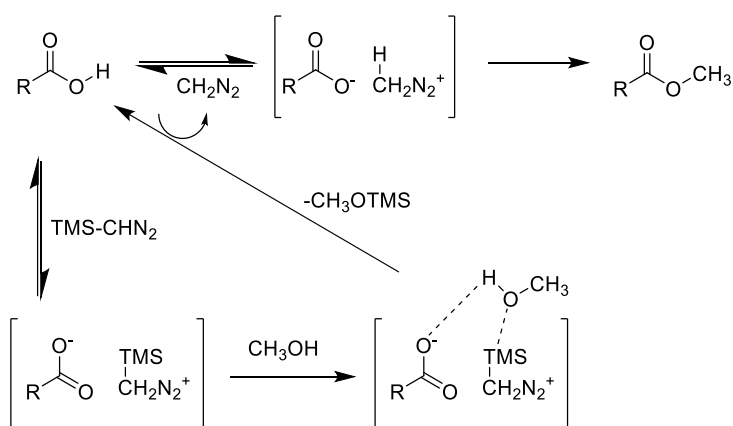
Scheme 7.39: Esterification of **44**.

Initially, we applied the conditions by Neises et al. using DCC and DMAP in MeOH. Unfortunately, the esterification was plagued by an isomerisation of the double bond (Scheme 7.40).



Scheme 7.40: Esterification of **44** was plagued by an isomerisation of the double bond.

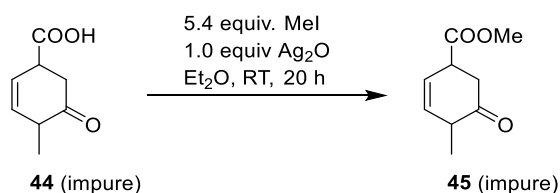
In an attempt to avoid double bond isomerization, we next examined base-free TMS-diazomethane as an alkylation reagent using Aoyama-Shiori conditions^[116]. TMS-diazomethane is a commercially available and stable alternative to the gaseous diazomethane. The mechanism of the TMS-diazomethane mediated esterification in toluene/MeOH was proposed by Hashimoto and Aoyama (Scheme 7.41).^[116] It was found that the carboxylic acid both acts as the reagent and catalyst for the formation of diazomethane. As the very toxic and explosive diazomethane is generated *in situ*, the reaction should be performed with care.



Scheme 7.41: Proposed mechanism for a methyl esterification using TMS-diazomethane in toluene/MeOH.^[116]

Gratifyingly, **44** underwent methyl esterification without isomerization when TMS-diazomethane in toluene/MeOH was used.

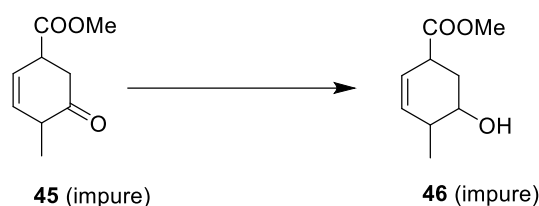
Motivated by our successful methyl esterification of **44**, we scouted for methods that avoid the generation of the extremely toxic diazomethane. Gratifyingly, the same results as with TMS-diazomethane were obtained, when 5.4 equiv. MeI and 1.0 equiv. Ag₂O were used (Scheme 7.42).



Scheme 7.42: Methyl esterification of **44**.

7.5.3 Reduction

In order to gain access to the central intermediate **46**, the ketone present in **45** had to be reduced (Scheme 7.43).



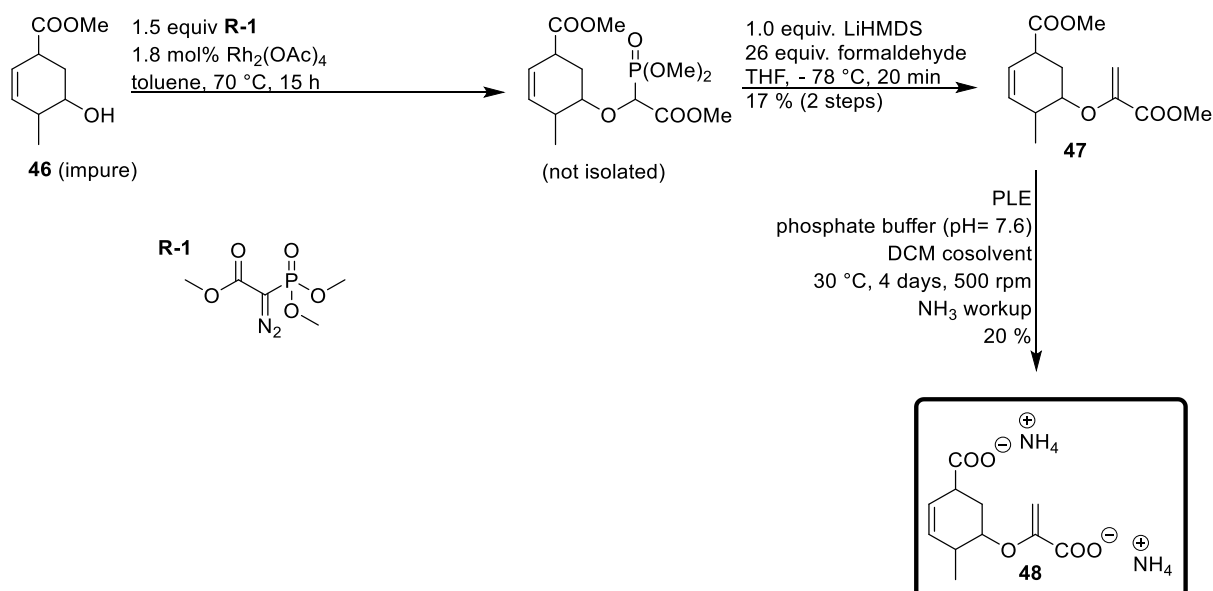
Scheme 7.43: Reduction of **45**.

Several reducing agents (DIBAL-H, LiAlH_4 , NaBH_4 , $\text{NaBH}_4 + \text{CeCl}_3 \cdot 6\text{H}_2\text{O}$, $\text{NaBH}_4 + \text{AlCl}_3$, NaCNBH_3 , Red-Al, $\text{NaBH}(\text{OAc})_3$, $\text{BH}_3 \cdot \text{Me}_2\text{S}$) were tested and reactions were carried out in either THF, MeOH, *i*PrOH or toluene at low temperatures (varied from -78°C to 0°C). The reaction mixtures were either poured into 1 M HCl or 10 % Rochelle salt solution for crude GC-MS analysis. Due to the impure intermediate **45** (side products presumably derived from the Birch-reduction were not separable), the occurrence of a mixture of diastereomers and peak overlap, only messy chromatograms were obtained on GC-MS. A legitimate statement of the product distribution was therefore impossible. The method of Gemal and Luche^[117] using 0.5 equiv. NaBH_4 and 0.2 equiv. $\text{CeCl}_3 \cdot 6\text{H}_2\text{O}$ in MeOH at -78°C (entry 15) gave the best results and **46** could be obtained (although not pure).

7.5.4 Synthesis of the putative inhibitor **48**

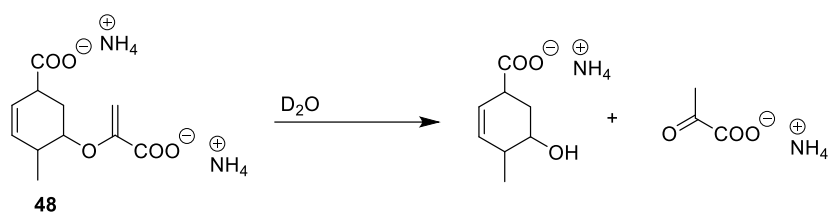
With **46** in hand, we could move on in the synthesis of the putative inhibitor **48**. What remained to be done was the introduction of a pyruvate moiety at position C-3, followed by hydrolysis of the two ester groups in **47** (Scheme 7.44). The phosphonoacetate was synthesized according to literature known procedures via an OH-insertion reaction using $\text{Rh}_2(\text{OAc})_4$ as the catalyst.^[49,66] A subsequent Horner-Wadsworth-Emmons reaction using LiHMDS and freshly prepared formaldehyde solution (via cracking of paraformaldehyde) gave **47** in a combined yield of 17 %. To get access to **48**, the two methyl ester functionalities in **47** had to be saponified. As **47** is supposed to be a rather unstable compound (base-mediated double bond isomerization may occur as well as acid-mediated pyruvate cleavage), we focused on rather neutral enzyme-catalyzed methods. For that purpose, we tested Novozyme 435 (resin-bound), CAL-B (resin-bound) and pig liver esterase (PLE) as ester cleaving enzymes. PLE gave the best results (as observed by HPLC) and produced **48** after 4 days at 30°C in 20 % yield starting from **47**. As only little amounts of **47** were available, we performed 48 small batches in order to avoid upscaling experiments. As it turned out, **48** is susceptible to pyruvate cleavage

upon acid catalysis and was therefore quenched with NH_3 directly after separation on semi-preparative HPLC. **48** will be applied to study binding differences between PhzE and anthranilate synthase (AS). In addition, **48** may serve as an inhibitor of PhzE and anthranilate synthase and could be the starting point for the development of new antibiotics. Once **48** turns out to be an effective inhibitor, reaction procedures will be improved to achieve better yields.



Scheme 7.44: Synthesis of the putative inhibitor **48**.

It has to be noted that **48** is unstable in D_2O and the pyruvate moiety is quantitatively cleaved off after several days in D_2O , as indicated by $^1\text{H-NMR}$.

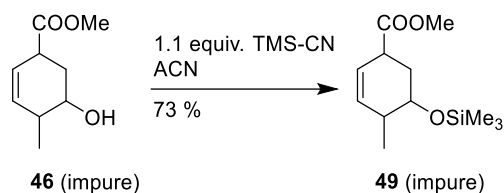


Scheme 7.45: Pyruvate elimination in **48** after several days in D_2O .

7.5.5 Introduction of the second double bond

Having the central intermediate **46** in hand, we next aimed for the introduction of a second double bond. For that purpose, the alcohol functionality in **46** had to be protected first, because of possible side reactions during the introduction of the second double bond.

Initially, we protected **46** as the corresponding silylether **49**. Compound **46** was readily protected using the mild reagent TMS-CN (Scheme 7.46). This method was previously described by Mai and Patil.^[118]

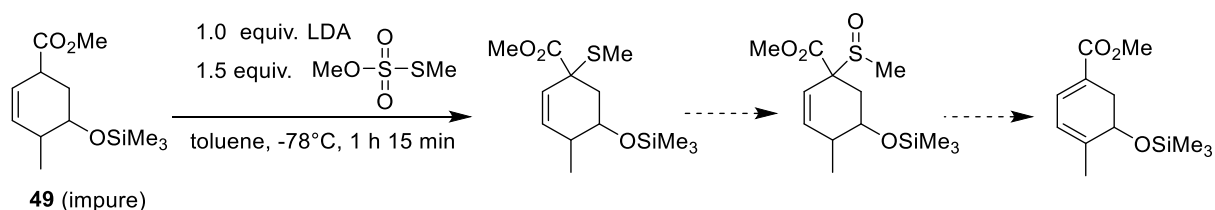


Scheme 7.46: Alcohol **46** was readily protected using TMS-CN

In order to introduce a second double bond, we decided to install a leaving group in α -position to the carboxylic acid ester. Upon installation, a leaving group may be eliminated to give the corresponding cyclohexadiene.

Our initial attempts centered on the introduction of sulfides and selenides in α -position to the enolisable carboxylic acid ester. On the basis of examples in the literature, it was hypothesized that upon introduction, these sulfides and selenides may be eliminated by oxidation and elevation of the temperature.^[119–122] The following electrophiles were tested: Me_2S_2 , Ph_2S_2 , $\text{Me}_2\text{S}_2\text{O}_3$, I_2 , PhSeCl , PhSeBr , *N*-(phenylseleno)phthalimide. The reactions were carried out in THF without any additive but in some cases the solvent was changed to DMF or 1,2-DME, or HMPA and NMP were added in order to increase polarity. Reaction monitoring was carried out via GC-MS.

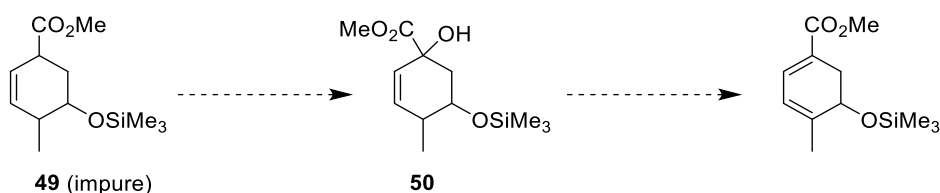
The most promising results were obtained, when $\text{Me}_2\text{S}_2\text{O}_3$ was used as an electrophile. **49** underwent good conversion into the corresponding methyl sulfide within 1 h, as indicated by GC-MS ($t_R = 6.26$ min (double-peak), $[\text{M}-\text{CH}_3]^+ = 273$ m/z , method= NG-standard, see Scheme 7.47).



Scheme 7.47: Introduction of a leaving group in **49**.

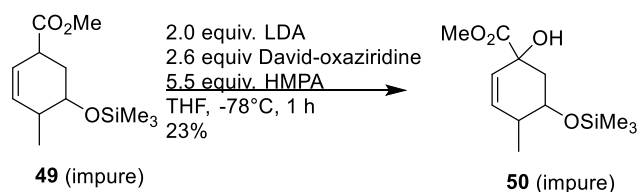
We next examined if a subsequent oxidation to the corresponding sulfoxide is possible in order to generate a proper leaving group. For efficiency reasons, we continued to work with test solutions, where a conversion to the methylsulfide took place. We either skipped the workup and added the oxidation agent directly to the reaction mixture or performed an aqueous workup and added the oxidation reagent and a proper solvent. Reaction monitoring was performed via

GC-MS and we tested the following oxidizing agents: Davis-oxaziridine, *m*CPBA and H₂O₂. Although some experiments indicated partial conversion to a product corresponding to the cyclohexadiene derivative (*t*_R = 5.75 min, [M]⁺ = 240 m/z, method NG-standard, the overall picture of the chromatogram was not satisfying. We decided to move on and examined the introduction of alternative leaving groups. For this purpose, we next tested the introduction of a hydroxyl group in α -position to the enolisable ester **49** (Scheme 7.48).



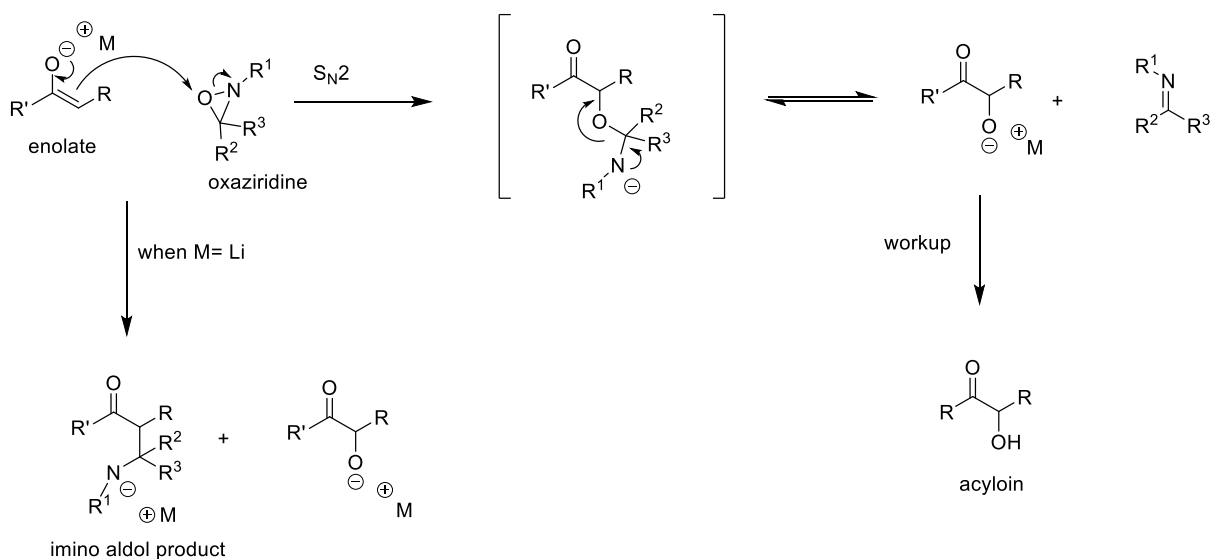
Scheme 7.48: Planned route for the synthesis towards the cyclohexadiene analogue of **46**.

The α -hydroxylation of **49** using the Davis-oxaziridine^[123,124] as an electrophile was successful and yielded **50** (Scheme 7.49). The addition of HMPA turned out to be favourable, as a cleaner chromatogram was observed (GC-MS). Future reaction optimization will be aimed at avoiding this extremely toxic and carcinogenic additive.



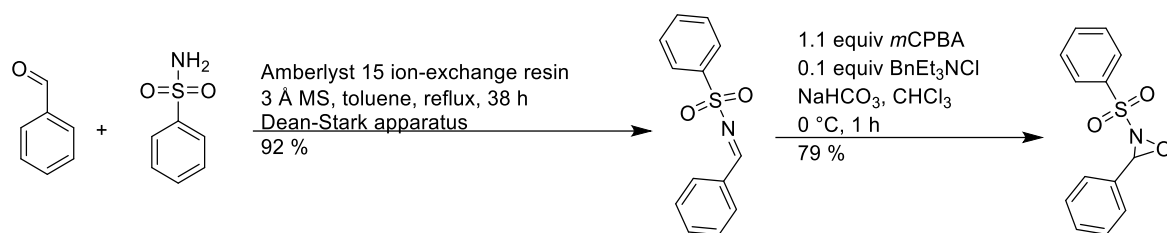
Scheme 7.49: α -Hydroxylation of **49**.

The mechanism for the α -hydroxylation of enolisable carboxylates using the Davis-oxaziridine proceeds via an attack of the corresponding enolate on the oxygen in the oxaziridine (Scheme 7.50).



Scheme 7.50: Mechanism for the α -hydroxylation of enolisable carbonyls.^[125]

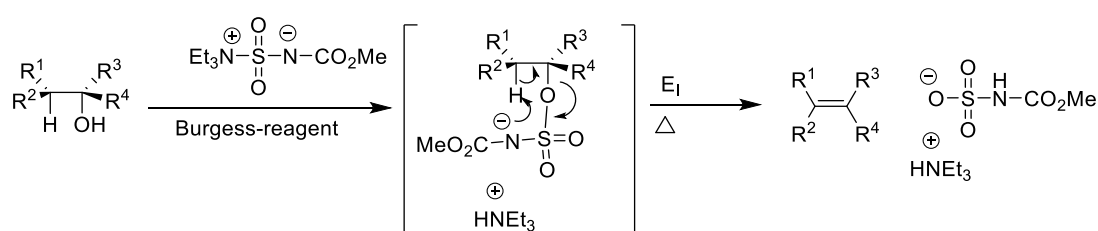
The Davis-oxaziridine was synthesized in a two-step procedure accordingly to Vishwakarma et al. (Scheme 7.51).^[123]



Scheme 7.51: Synthesis of the Davis-oxaziridine following the two step procedure by Vishwakarma et al.^[123]

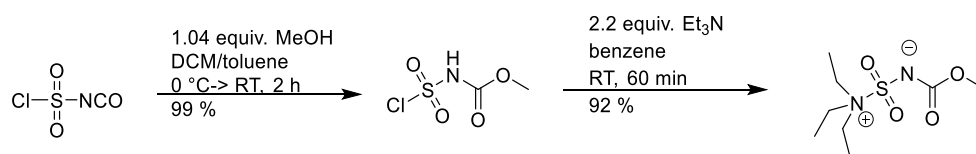
Having **50** in hand, we next scouted for methods for the elimination of H₂O to give the cyclohexadiene analogue of **49** (Scheme 7.48). Our attempts centered on the use of Martin-sulfurane,^[126–128] the introduction of a triflate as a leaving group, the reagent triphenylphosphine-iodine,^[129] acid catalysis using amberlyst-15,^[130] and CuCl-DIC pseudourea formation.^[131] Unfortunately, none of the listed methods turned out to be successful.

Further attempts for the dehydration of **50** centered on the Burgess-reagent. Discovered in the early 1970s, the inner salt of (methoxycarbonylsulfamoyl)triethylammonium hydroxide, namely the Burgess-reagent was found to readily dehydrate secondary and tertiary alcohols to give olefins. This dehydration method presents a neutral process for the selective *syn*-elimination of alcohols (Scheme 7.53).^[125,132] In addition, the Burgess-reagent has found many further applications such as the conversion of primary alcohols to its carbamates,^[133] or the conversion of primary amides to the corresponding nitriles^[125,134]



Scheme 7.52: Mechanism for the dehydration of alcohols using the Burgess reagent.^[125]

The Burgess reagent was synthesized following the two-step procedure by Burgess et al. (Scheme 7.53)^[135]

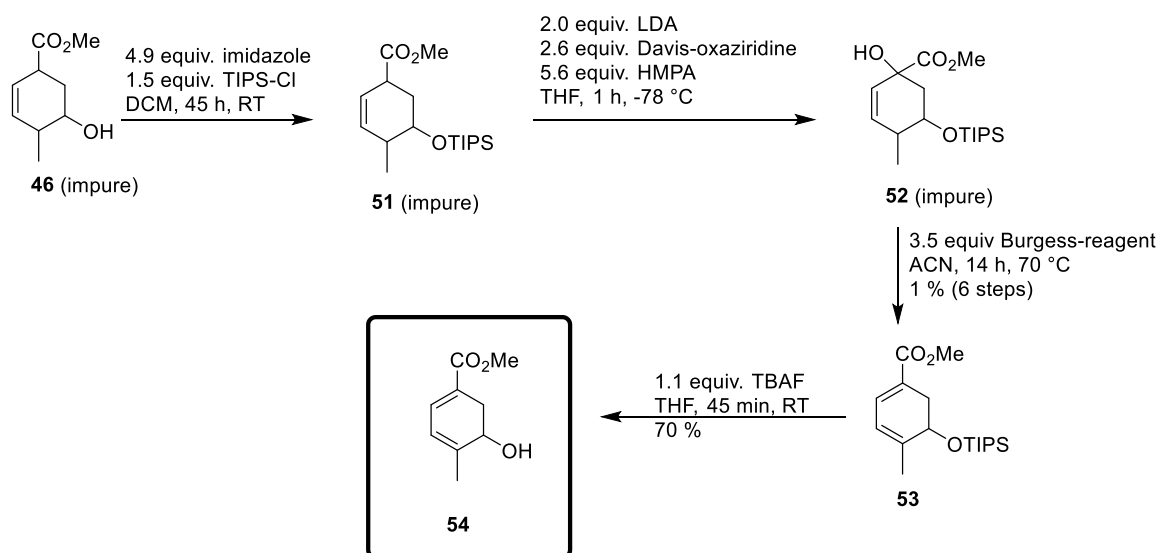


Scheme 7.53: Synthesis of the Burgess reagent following the two-step procedure by Burgess et al.^[135]

Although we were able to observe full conversion to a product which mass corresponded to the cyclohexadiene analogue of **49** (as observed via GC-MS: $t_R = 5.74$ min, $[M]^+ = 240$ m/z, method= NG-standard), we were only able to isolate minute quantities and full characterization was therefore not possible. In order to get better insights into the reaction, we performed a time-dependant $^1\text{H-NMR}$ experiment (abs. deg. C_6D_6 , 1.1 equiv. Burgess-reagent, 50°C) and several aromatic protons were observed but interpretation turned out to be challenging because of massive peak formation. We hypothesized that the installation of a TIPS protecting group would render the molecule more stable because of steric bulk. Therefore, we protected **46** using TIPS-Cl to achieve **51** (Scheme 7.54). Subsequent α -hydroxylation using the same methods as for the synthesis towards **50** gave **52** and we were pleased that the elimination of water from **52**, accompanied with double bond isomerisation, yielded pure **53** (1%, 6 steps from **43**). We also tested some of the previously described methods for elimination of water from **52**, but to no avail.

7.5.6 Deprotection

Gratifyingly, the following cleavage of the TIPS protecting group afforded **54** in a yield of 70%. **54** will serve as a promising key intermediate for the synthesis of a diverse set of PhzE and anthranilate synthase (AS) inhibitors.



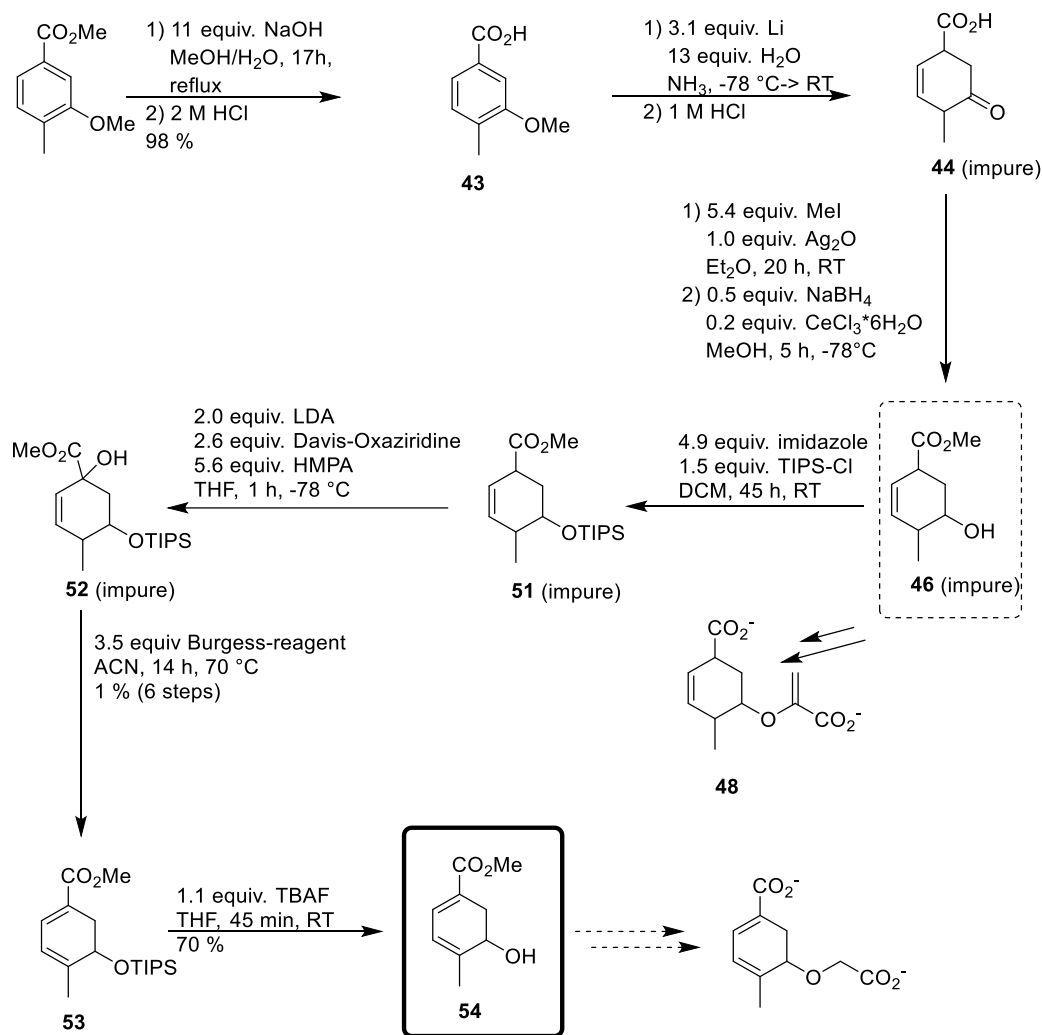
Scheme 7.54: Synthetic route from **46** to the key intermediate **54**.

7.5.7 Summary

A straightforward synthesis for the key compounds **46** and **54** was established, which involved the handling of some instable intermediates (Scheme 7.55). Both compounds can be used for the synthesis of a diverse set of putative inhibitors of PhzE and anthranilate synthase, upon

installation of a glycolate side chain at position C-3 and subsequent hydrolysis. Gratifyingly, we were able to achieve **48**, which will be used in crystallization and inhibition studies of PhzE and anthranilate synthase (AS). Furthermore, the synthetic pathway revealed insights into the extraordinary properties of some instable intermediates.

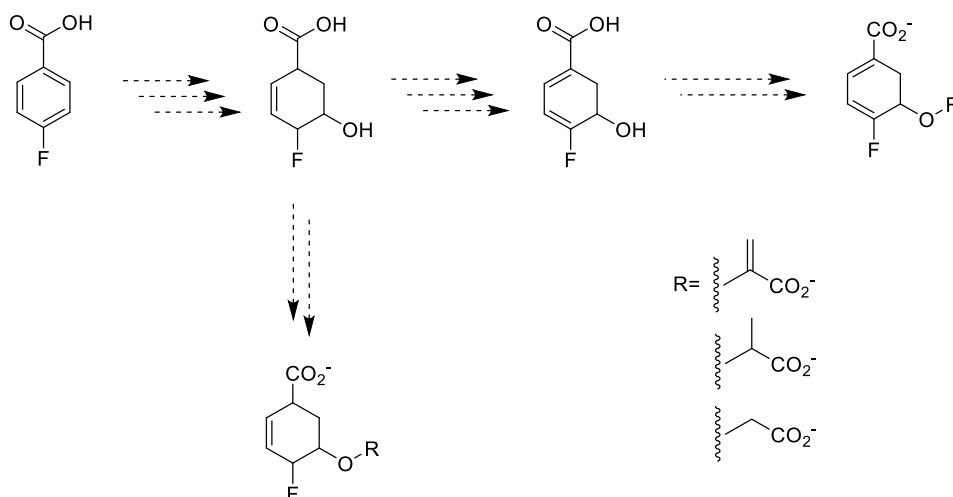
Starting from inexpensive methyl 3-methoxy-4-methylbenzoate, saponification followed by Birch-reduction and aqueous hydrolysis afforded **44**. The thermodynamically instable intermediate **44** was esterified and reduced to give **46**, the central intermediate in the synthesis. Compound **46** can be exploited for the synthesis of additional putative inhibitors, upon installation of various side chains at position C-3. Alcohol **46** was protected using TIPS-Cl to produce **50**. A screening of several double-bond formation methods identified the introduction of an α -hydroxyl group followed by elimination of water via the Burgess reagent as the most appropriate method to introduce unsaturation. It has to be noted that all intermediates (**44**, **46**, **51**, **52**) were not obtained pure, presumable because of physically similar side products derived from the Birch reduction. Gratifyingly, the elimination of water from **52**, followed by a spontaneous rearrangement yielded pure compound **53**, which was converted to **54** by deprotection of the alcohol. **54** is the key compound as it will serve for the synthesis of putative inhibitors. First attempts for the installation of a glycolate side chain at position C-3 failed and we decided to first put up an efficient and robust methodology for the etherification of labile compounds before revisiting the etherification of **54**, as only minute quantities of **54** were available. An overview of these experiments is given in chapter 7.6. In chapter 7.4.1 we could show that methyl esters can be effectively cleaved in fully conjugated cyclohexadiene structures. This methodology will be applied in due course.



Scheme 7.55: Straightforward synthesis towards **54**, the central intermediate **46** and the putative inhibitor **48**.

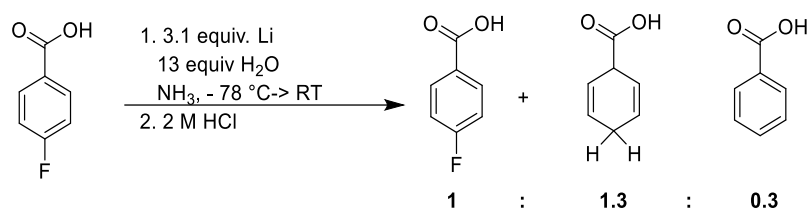
7.5.8 Investigation of 4-fluorobenzoic acid as alternative starting material

Motivated by our successful synthesis towards **54**, we wondered if our established route could serve as a template for the synthesis of 4-fluoro analogs of **54** (Scheme 7.56).



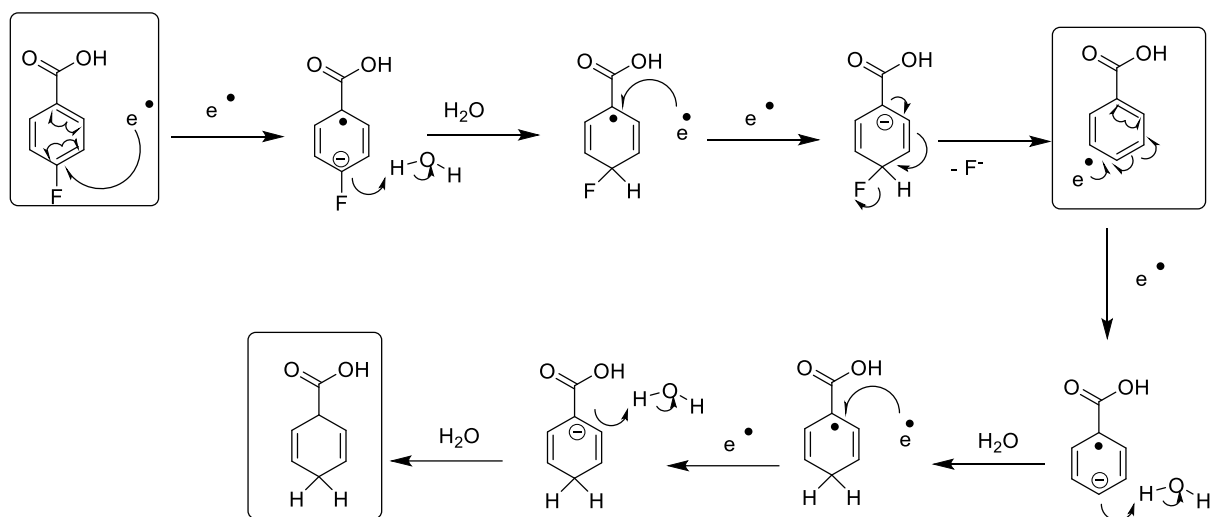
Scheme 7.56: Rationale for the synthesis of a diverse set of 4-fluoro substituted putative inhibitors of PhzE and anthranilate synthase.

In an attempt to study the feasibility of our strategy, we first had to test if the starting material 4-fluorobenzoic acid is not prone to defluorination under Birch-conditions. When we performed a Birch reduction using the same conditions as for the synthesis towards **44**, we obtained a 1/1.3/0.3 starting material/1,4-dihydro benzoic acid/benzoic acid mixture (Scheme 7.57).



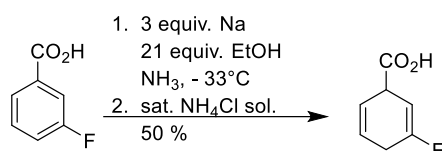
Scheme 7.57: Birch reduction of 4-fluorobenzoic acid

We propose the following mechanism for the Birch reduction of 4-fluorobenzoic acid (Scheme 7.58): upon attack of an electron at position C-1, a radical anion is formed, which instantly gets protonated by water to give a radical. The radical in turn can form an anion by the attack of an additional electron. Upon double bond shift, the fluoro substituent in position C-4 is eliminated to give benzoic acid, which is further reduced to the corresponding 1,4-dihydro derivative.



Scheme 7.58: Supposed mechanism for the reduction of 4-fluorobenzoic acid.

It has to be noted that a Birch reduction of *m*-benzoic acid is possible (Scheme 7.59), and would be consistent with our suggested mechanism.

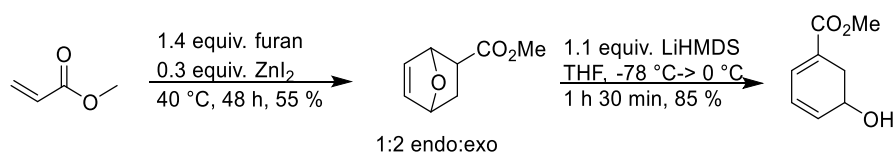


Scheme 7.59: Birch-reduction of 3-fluorobenzoic acid by Rabideau et al.^[109,136]

7.5.9 Alternative access to a 4-methylated cyclohexadiene intermediate

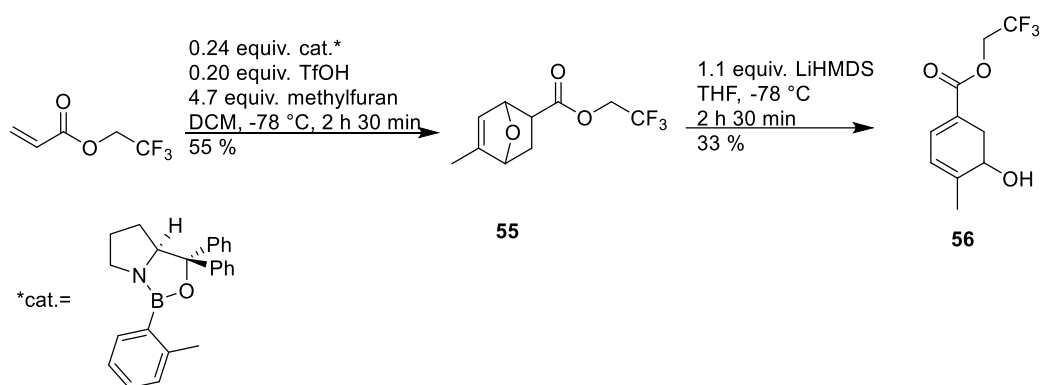
In 7.5.7 we present the synthesis towards **46** and **54**. Upon installation of different side chains on position C-3 and hydrolysis of the carboxylic acid ester functionalities, a diverse set of 4-methylated cyclohexene and cyclohexadiene derivatives would be accessible. In our rationale these compounds would present potent inhibitors for PhzE and anthranilate synthase (AS). However, our designed route lacks in efficiency, as the synthesis towards the late intermediate **54** requires 8 steps with an overall yield of ca. 1%. In order to increase efficiency, we scouted for alternative routes that would give access to analogues of **54**.

Inspired by the effective synthesis towards methyl 5-hydroxycyclohexa-1,3-diene-1-carboxylate by Brion via a base-catalyzed opening of a oxanorbornene (Scheme 7.60),^[102] we aimed at the synthesis of a 4-methyl derivative of **54**.



Scheme 7.60: Synthetic access to methyl 5-hydroxycyclohexa-1,3-diene-1-carboxylate by Brion.^[102]

To address this challenge, we synthesized **55**, following the literature procedure of Corey et. al.^[137] Compound **55** was obtained in 55 % yield starting from trifluoroethyl acrylate. The next step called for a base-mediated ring opening in **55** and we applied the conditions of Brion to achieve compound **56** in 33 % yield after 2.5 h min at -78 °C using 1.1 equiv. LiHMDS as a base (Scheme 7.61).



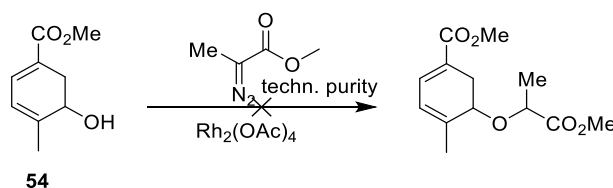
Scheme 7.61: Synthesis towards **56**.

In summary, we were able to produce **56** in two steps with an overall yield of 18 %. Compound **56** represents an analog of **54**, with the only difference in the ester functionality. Reaction optimization for the base-mediated ring opening will be performed in due course.

7.6 Systematic investigation of carbenoid based OH-insertion reactions for labile substrates

Guided by the successful synthesis of **54** and **56**, which represent late stage intermediates for the synthesis of mechanism-based PhzE and anthranilate synthase (AS) inhibitors, we aimed at the installation of a side chain in position C-3.

Our initial attempts centered on the introduction of a lactyl side chain in **54** using methyl diazoacetate for a carbenoid based OH-insertion reaction, as this type of reaction usually allows for a mild installation of various ethers (Scheme 7.62). We chose $\text{Rh}_2(\text{OAc})_4$ as a catalyst, which is often used for OH-insertion reactions.^[78,90] Several conditions were tried out but it quickly became apparent that this is a rather challenging task. Reaction control turned out to be difficult as **54** is instable on GC. To our dismay, first experiments for the etherification of **54** were unsuccessful as indicated by multiple spots on TLC. Upon purification via flash column chromatography, $^1\text{H-NMR}$ analysis suggested some formation of the desired product. However, only minute quantities of impure material could be obtained.



Scheme 7.62: Attempts for the etherification of **54**.

7.6.1 GC-FID Screening

Given the fact that first attempts for the installation of a lactyl side chain into **54** were rather unsatisfying and only little quantities of the late intermediates **54** and **56** were available, we decided to use model substrates to find optimal conditions. In order to address this challenge, we took commercially available alcohols as model substrates that in our rationale reflect the thermodynamic lability of **54** and **56**. Compounds **A-C** (Table 7.7) were chosen, as for **54** and **56**, an elimination of water would give conjugated compounds. Substrate **B** exhibit a double bond that should reflect the diene functionality in **54** and **56** and might be subjected to cyclopropanation in our screening, a known side reaction for carbenoid based OH-insertion reactions.^[88]

The results for the $\text{Rh}_2(\text{OAc})_4$ catalyzed OH-insertion of methyl diazoacetate into compounds **A-C** show an increase in conversion for compound **A** when the addition time was prolonged from 15 to 60 min (compare entries 1 and 2). Gratifyingly, very promising results were obtained as compounds **A-C** could be quantitatively converted using the following conditions: 1 mol% $\text{Rh}_2(\text{OAc})_4$, 1.6 equiv. methyl diazoacetate, RT, addition time= 60 min.

Table 7.7: OH-insertion screening with a diverse set of alcohols

A-D

A

B

C

Entry	Substrate	Temp.	Addition time	Diazo compound ^[a]	Rh ₂ (OAc) ₄	Conversion ^{[b][c][d][e]}
1	A	RT	15 min	0.9 equiv	1 mol %	64 %
2	A	RT	60 min	0.9 equiv	1 mol %	70 %
3	A	0°C	120 min	0.8 equiv	1 mol %	64 %
4	A	RT	60min	1.6 equiv	1 mol %	>99 %
5 ^[f]	A	RT	60 min	0.8 equiv	1 mol %	21 %
6	B	RT	60 min	0.9 equiv	1 mol %	66 %
7	B	RT	60 min	1.1 equiv	1 mol %	78 %
8	B	RT	60 min	1.6 equiv	1 mol %	>98 %
9	B	RT	60 min	1.4 equiv	0.2 mol %	55 %
10	C	RT	60 min	0.9 equiv	1 mol %	64 %
11	C	0°C	120 min	0.8 equiv	1 mol %	76 %
12	C	RT	60 min	1.6 equiv	1 mol %	>99 %
13	C	0°C	120 min	1.6 equiv	1 mol %	>99 %
14	C	RT	120 min	1.6 equiv	1 mol %	>99 %
15	C	RT	60 min	1.4 equiv	0.2 mol %	76 %

[a] added via a syringe pump, concentration of methyl diazoacetate was calculated via ¹H-NMR using 1,3,5-trimethoxybenzene as internal standard. [b] calculated after complete addition of the diazo compound via integration of GC-FID signals

[c] conversion% = 100 - [(area remaining starting material/area standard)/initial ratio] * 100;

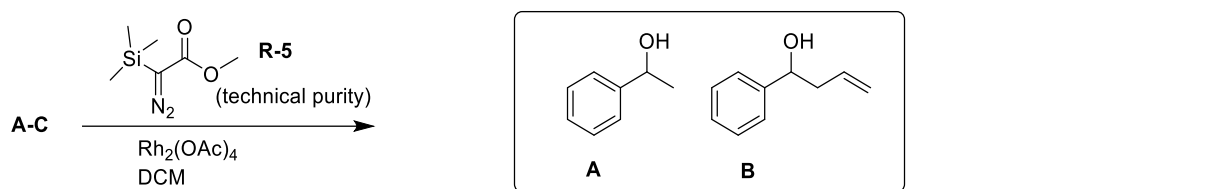
initial ratio = (area starting material)/(area standard); nonane was used as an internal standard

[d] workup: it was filtered through ca. 2 cm SiO₂ and rinsed with DCM/EtOAc = 3/1.

[e] results should be treated with care: double determination of initial ratio was performed and massive deviations were observed in some cases- these results were dismissed; only deviations <5 % in initial ratio were not dismissed

[f] 0.35 equiv. DIPEA were added to the reaction mixture

We also tested TMS-diazoacetate (**R-5**) as an alternative reagent for the Rh₂(OAc)₄ catalyzed OH-insertion reaction using compounds **A** and **B**. Surprisingly, we observed the formation of two new peaks on GC-FID. It may be that two products were obtained or that the formed product is instable throughout analysis or workup. We will take a deeper look at this observation in due course.

Table 7.8: OH-insertion screening with a diverse set of alcohols


Entry	Substrate	Temp.	Addition time	Diazo compound ^[a]	Rh ₂ (OAc) ₄	Conversion ^{[b][c][d][e][f]}
1	B	RT	60 min	1.4 equiv	0.2 mol %	16 %
2	B	RT	60 min	2.0 equiv	0.2 mol %	38 %
3	A	RT	60 min	2.1 equiv	0.4 mol %	31 %

[a] added via a syringe pump [b] calculated after complete addition of the diazo compound via integration of GC-FID signals

[c] conversion% = 100 - [(area remaining starting material/area standard)/initial ratio] * 100;

initial ratio = (area starting material)/(area standard); nonane was used as an internal standard

[d] workup: it was filtered through ca. 2 cm SiO₂ and rinsed with DCM/EtOAc = 3/1.

[e] formation of two new peaks was observed in all entries

[f] results should be treated with care: double determination of initial ratio was performed and massive deviations were observed in some cases -these results were dismissed; only deviations <5 % in initial ratio were not dismissed

7.6.2 ¹H-NMR Screening

Having in hand optimized reaction conditions for carbenoid mediated OH-insertion reactions of compounds **A-C**, we next examined to expand the methodology to (*E*)-5-hydroxy-5-phenylpent-2-enoate (**57**), which in our rationale represents an improved model substrate for **54** and **56**, as upon elimination of water from **57**, a highly conjugated compound would be formed. In addition, the double bond present in **57** might be prone to cyclopropanation.

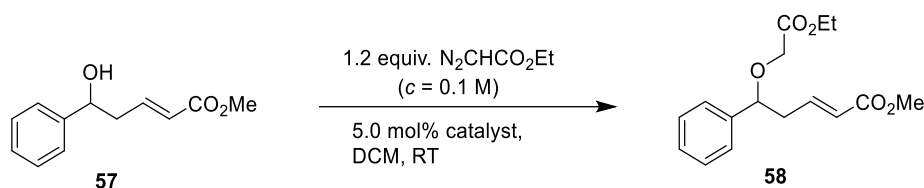
In order to get a deeper look into carbenoid based insertion reactions for unstable alcohols, we used ¹H-NMR to monitor our reactions. The geminal proton to the hydroxyl group in **57** gives a signal that is clearly distinguishable from the corresponding proton in **58**, allowing for quantification with SiPhMe₃ as an internal standard.

Initially, we tested different catalysts for the transformation of **57** to **58** using ethyl diazoacetate as the insertion reagents. We used a catalyst loading of 5 mol% for this screening, accounting for possible differing catalyst stabilities. The results are captured in Table 7.9. Interestingly, the best results were obtained using Cu(OTf)₂ and “Rh₂(tfacam)₄”^{*} as a catalyst. It was decided not to proceed with Cu(OTf)₂ in the subsequent screenings as Cu(OTf)₂ is very hygroscopic

^{*} The composition and purity of this catalyst remains unclear. See section “ Experimental procedures and analytical data”.

and requires full protection from air, which would constitute disproportional additional expenses. When 5.0 mol% “Rh₂(tfacam)₄” was used, a yield of 61 % could be obtained according to ¹H-NMR. It became apparent that longer reaction times (20 h) did not increase the amount of the desired product, indicating that the conversion of **57** to **58** takes place very fast. This is corroborated by the finding that the addition of more ethyl diazoacetate after 20 h led to an increase in product formation.

Table 7.9: Catalyst screening

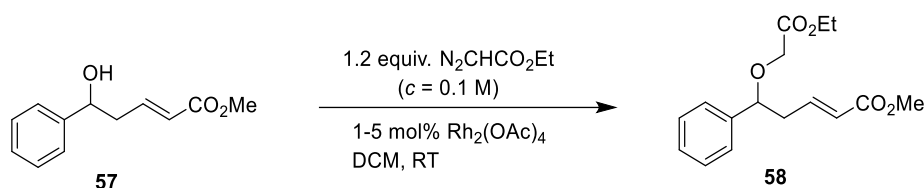


Entry ^[a]	Catalyst	Time ^[b]	Educt ^[c]	Product ^[d]	Remainder
1	Rh ₂ (adaman) ₄	30 min	68 %	8 %	24 %
		20 h	64 %	7 %	29 %
2	Rh ₂ (Oct) ₄	30 min	64 %	11 %	25 %
		20 h	63 %	12 %	25 %
3	Rh ₂ (OAc) ₄	30 min	41 %	27 %	31 %
		20 h	35 %	26 %	38 %
4	Rh ₂ (Tfa) ₄	30 min	59 %	33 %	8 %
		20 h	54 %	29 %	17 %
5	Cu(OTf) ₂ ^[e]	30 min	48 %	43 %	8 %
		20 h	47 %	39 %	13 %
6	“Rh ₂ (tfacam) ₄ ”	30 min	34 %	61 %	5 %
		20 h	38 %	62 %	0 %

[a] quantification via ¹H-NMR (d1= 16 sec, 32 scans, SiPhMe₃ was added as internal standard). A solution of the diazo compound was added over the course of 60 min to a solution of **57** via a syringe pump. [b] time after complete addition of the diazo compound. Sample was diluted in CDCl₃ (filtered through Al₂O₃) for NMR analysis. [c] signal at 4.8 ppm [d] signal at 4.5 ppm [e] colorless solid, which turned blue on contact with air.

For our further investigations, we decided to proceed with “Rh₂(tfacam)₄” as a catalyst for which the best results were obtained. Also Rh₂(OAc)₄ was further investigated, being a standard catalyst for OH-insertion reactions.^[78,90]

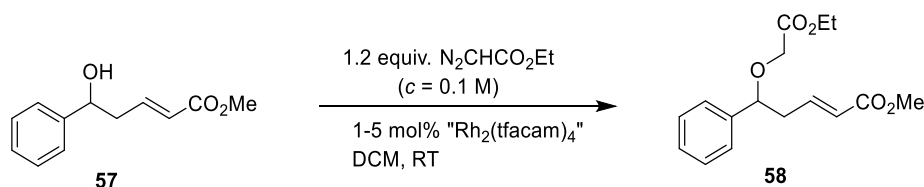
We next conducted a brief screening of different catalyst loadings. Using Rh₂(OAc)₄, the best results were obtained with a catalyst loading of 2.5 mol%, although a catalyst loading of 1 % showed comparable results (Table 7.10).

Table 7.10: Catalyst loading screening with $Rh_2(OAc)_4$ 

Entry ^[a]	Catalyst loading	Time ^[b]	Educt ^[c]	Product ^[d]	Remainder
1	2.5 mol%	30 min	37 %	37 %	27 %
		20 h	41 %	36 %	23 %
2	1.0 mol%	30 min	35 %	33 %	32 %
		20 h	34 %	30 %	36 %

[a] quantification via 1H -NMR ($d1 = 16$ sec, 32 scans, $SiPhMe_3$ was added as internal standard). A solution of the diazo compound was added over the course of 60 min to a solution of **57** via a syringe pump. [b] time after complete addition of the diazo compound. Sample was diluted in $CDCl_3$ (filtered through Al_2O_3) for NMR analysis. [c] signal at 4.8 ppm [d] signal at 4.5 ppm.

Pleasingly, " $Rh_2(tfacam)_4$ " gave dramatically better results compared to $Rh_2(OAc)_4$. When we used 2.5 mol % catalyst, 73 % product were obtained, according to 1H -NMR (Table 7.11). When we used a catalyst loading of 1.0 mol%, an acceptable yield of 57 % was achieved and we were optimistic to further increase the yield with this catalyst loading, as 31 % unreacted starting material was observed on 1H -NMR.

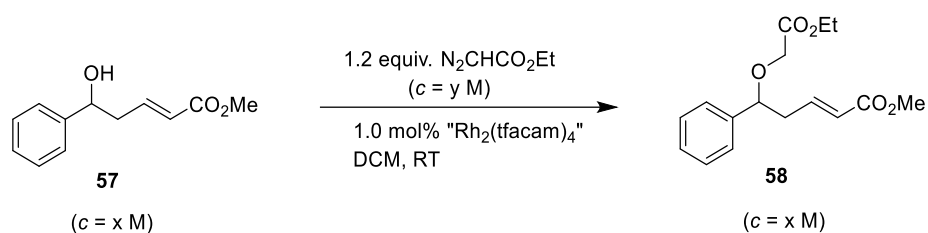
Table 7.11: Catalyst loading screening with $Rh_2(tfacam)_4$ 

Entry ^[a]	Catalyst loading	Time ^[b]	Educt ^[c]	Product ^[d]	Remainder
1	2.5 mol%	30 min	18 %	73 %	9 %
		20 h	11 %	71 %	18 %
2	1.0 mol%	30 min	31 %	57 %	12 %
		20 h	33 %	57 %	10 %

[a] quantification via 1H -NMR ($d1 = 16$ sec, 32 scans, $SiPhMe_3$ was added as internal standard). A solution of the diazo compound was added over the course of 60 min to a solution of **57** via a syringe pump. [b] time after complete addition of the diazo compound. Sample was diluted in $CDCl_3$ (filtered through Al_2O_3) for NMR analysis. [c] signal at 4.8 ppm [d] signal at 4.5 ppm.

In terms of cost efficiency, we next aimed to increase yields with a catalyst loading of 1.0 mol%. For that purpose we varied the molarity of both **57** and ethyl diazoacetate (Table 7.12). We were surprised to see that this variation had a significant impact on the outcome of the reaction. The best results were obtained when both **57** and ethyl diazoacetate were used in a concentration of 0.5 M (entry 3, 69 %).

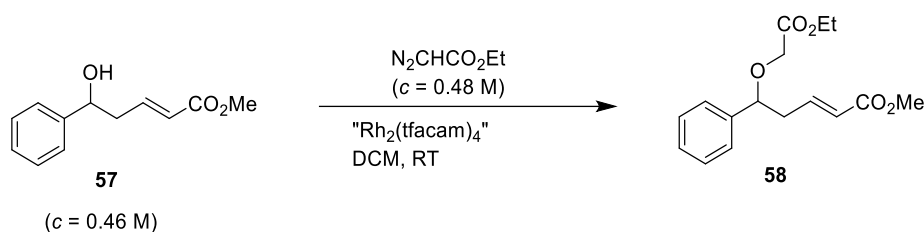
Table 7.12: Concentration screening with $Rh_2(tfacam)_4$



Entry ^[a]	Time ^[b]	x	y	Educt ^[c]	Product ^[d]	Remainder
1	30 min	0.5	0.1	47 %	48 %	6 %
	20 h			42 %	48 %	11 %
2	30 min	0.1	0.5	17 %	64 %	19 %
	20 h			18 %	69 %	13 %
3	30 min	0.5	0.5	24 %	69 %	7 %
	20 h			24 %	70 %	6 %

^[a] quantification via ¹H-NMR (*d*₁ = 16 sec, 32 scans, SiPhMe₃ was added as internal standard). A solution of the diazo compound was added over the course of 60 min to a solution of **57** via a syringe pump. ^[b] time after complete addition of the diazo compound. Sample was diluted in CDCl₃ (filtered through Al₂O₃) for NMR analysis. ^[c] signal at 4.8 ppm ^[d] signal at 4.5 ppm.

Inspired by our drastic improvements in methodology, we aimed to further improve results by increasing the amount of used ethyl diazoacetate. Pleasingly, we were able to further improve the formation of **58** when using 1.9 equiv. of ethyl diazoacetate (Table 7.13). Much to our delight, best results were obtained with a catalyst loading of 1.1 % (entry 5). Importantly, under identical conditions and in the absence of catalyst, no reaction occurred (entry 4).

Table 7.13: Catalyst screening

Entry ^{[a][b][e]}	Catalyst loading	Diazo compound	Educt ^[c]	Product ^[d]	Remainder
1	1.1 mol%	1.9 equiv.	<10 %	81 %	>10 %
2	2.8 mol%	1.9 equiv.	0 %	85 %	15 %
3	1.1 mol%	1.2 equiv.	30 %	60 %	10 %
4	-	1.2 equiv.	97 %		3 %
5	1.1 mol%	1.9 equiv.	>5 %	88 %	<7%
6	2.8 mol%	1.9 equiv.	0 %	82 %	18 %

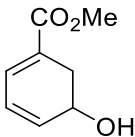
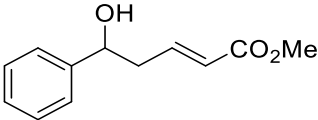
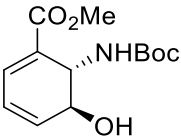
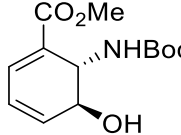
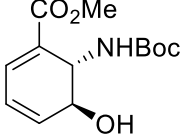
[a] quantification via ¹H-NMR (*d*₁ = 16 sec, 32 scans, SiPhMe₃ was added as internal standard). A solution of the diazo compound was added over the course of 60 min (entries 1-4) or 120 min (entries 5-6) to a solution of **57** via a syringe pump. [b] NMR analysis was performed directly after complete addition of the diazo compound. CDCl₃ (filtered through Al₂O₃) was used as an NMR solvent.

[c] signal at 4.8 ppm [d] signal at 4.5 ppm. [e] a new batch of "Rh₂(tfacam)₄" (=batch 2) was used

Having in hand good reaction conditions for the transformation of **57** to **58**, our next goals will be to determine isolated yields using this methodology for a diverse set of instable alcohols. In addition, we will compare our methodology to the standard reaction for the formation of ethers from alcohols, the Williamson etherification.

Our initial investigations of the Williamson-etherification centered on the thermodynamically instable compounds **30**, **35** and **57** using NaH as a base (Table 7.14). Only poor yields were obtained with this method, although significant amounts of unreacted starting material could be isolated, suggesting that upon methodology development yields could be increased.

Table 7.14: Williamson-etherification

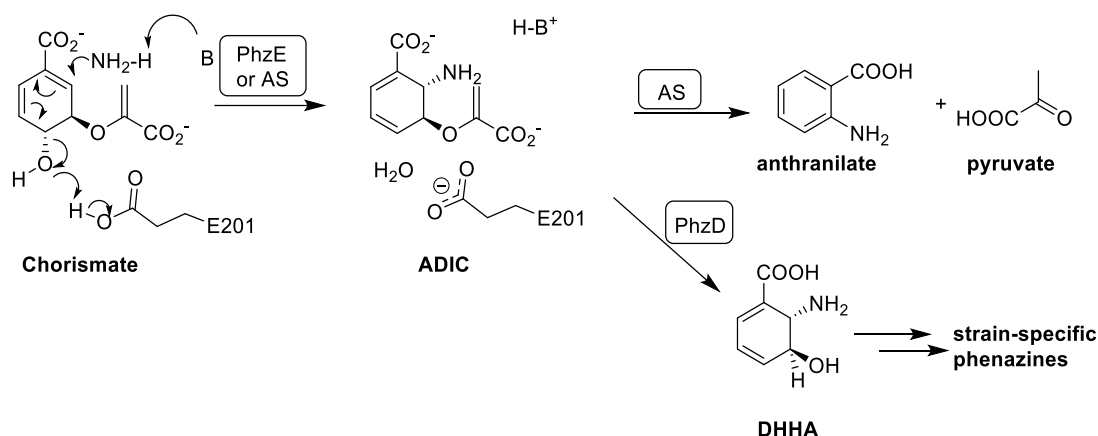
Entry	Starting material	Conditions	Product ^[a]	Educt ^[a]
1	 35 (4 mmol)	2.9 equiv. NaH 2.1 equiv. methylbromoacetate THF, -78°C->-20°C, 1 h	37 %	-
2	 57 (0.4 mmol)	1.6 equiv. NaH 1.7 equiv. ethyliodoacetate THF, -30°C->RT, 6 h	33 %	38 %
3	 30 (0.24 mmol)	1.5 equiv. NaH 1.8 equiv. ethyliodoacetate THF, -20°C->RT, 6h	26 %	33 %
4	 30 (0.29 mmol)	1.6 equiv. NaH 1.8 equiv. ethyliodoacetate THF, -22°C->RT, overnight	24 %	<42 % ^[b]
5	 30 (2.5 mmol)	1.3 equiv. NaH 1.8 equiv. methylbromoacetate THF, -20°C->0°C, 4h	38 %	34 %

[a] isolated yield, [b] residual solvent

8 Summary and outlook

8.1 Summary

Phenazines are secondary metabolites mainly produced by *Streptomyces* and *Pseudomonas*. In the first step of the biosynthesis towards strain-specific phenazines, chorismate is converted to 2-amino-2-deoxyisochorismic acid (ADIC) (Scheme 8.1). This step is catalyzed by PhzE, an enzyme with striking similarities to anthranilate synthase (AS). Surprisingly, ADIC is converted to anthranilate and pyruvate in AS, whereas ADIC is further transformed to strain-specific phenazines in the case of PhzE. In order to study binding difference between PhzE and AS, a whole set of different inhibitors have been synthesized for crystallization experiments. As phenazines equip bacteria with a competitive advantage,^[11] our synthesized compounds may present a potential source of antibiotics.



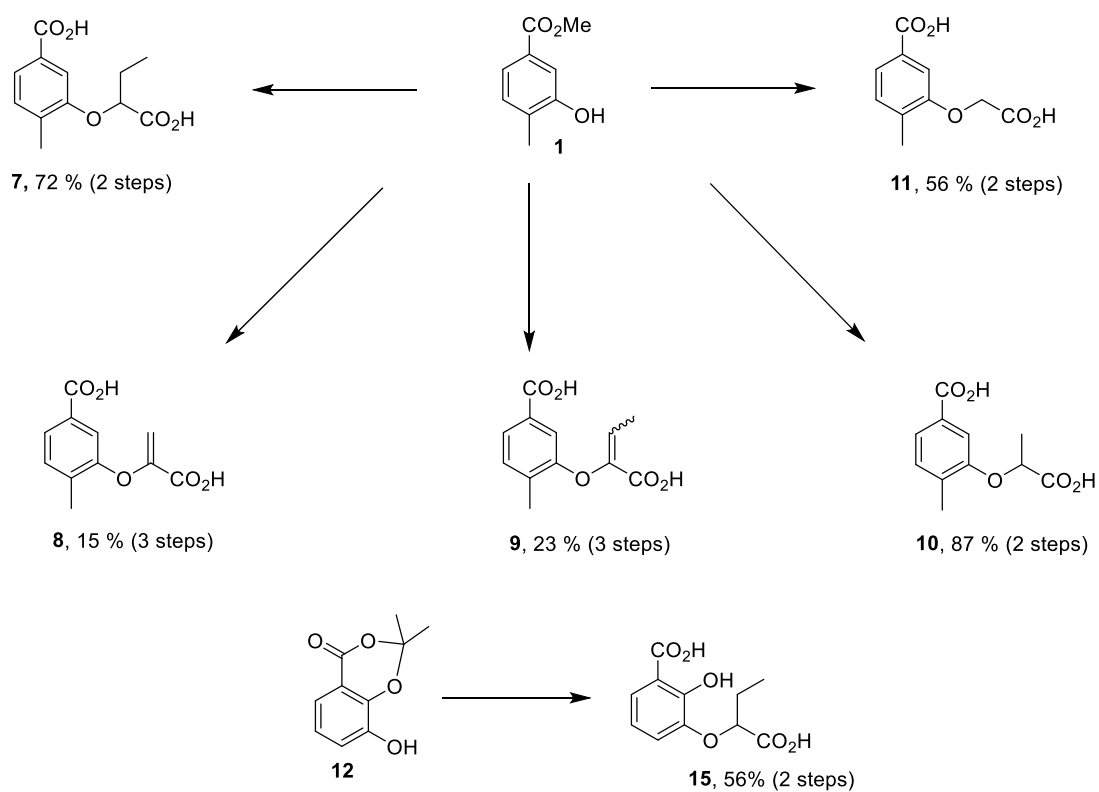
Scheme 8.1: Differences between PhzE and anthranilate synthase (AS).

We have synthesized aromatic, cyclohexane, cyclohexene, cyclohexadiene and ADIC derived putative inhibitors for PhzE and AS.

8.1.1 Aromatic inhibitors

Based on the fact that crystallization experiments of PhzE in the presence of chorismate in the group of Blankenfeldt showed only benzoate and pyruvate in the active site and that ADIC has a half-life of only 34 h,^[33] we aimed for the synthesis of stable ligands for crystallization experiments. Driven by the easy synthetic accessibility towards aromatic chorismate analogues and that Abell et al. and Payne et al. have shown that some of these analogues show comparably good inhibition constants against *S. marcescens* anthranilate synthase compared to traditional inhibitors,^[76] we synthesized a set of aromatic compounds that in our rationale are suited for crystallization experiments and may represent potent inhibitors (Scheme 8.2).

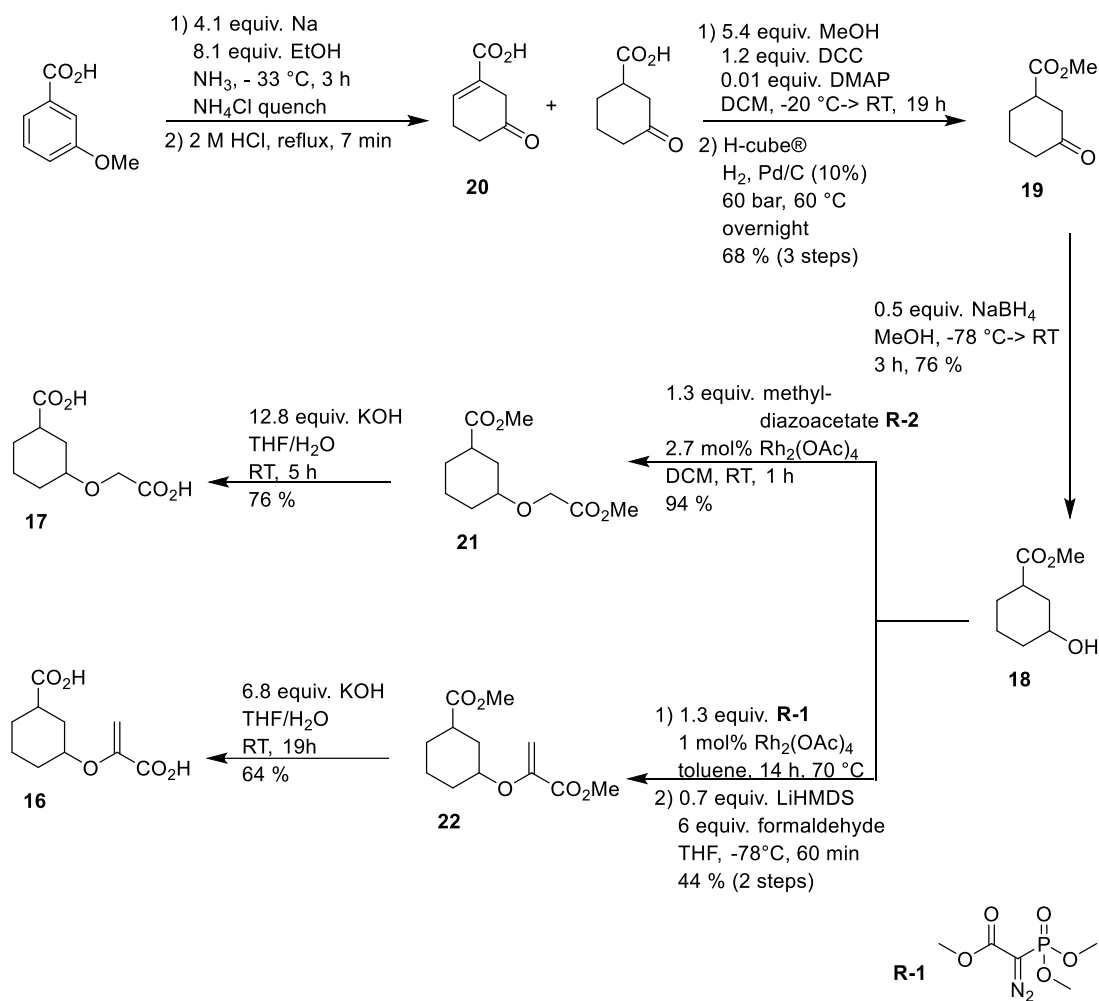
It was decided to exploit the already existing methodology of Abell et al. and Payne et al. for the introduction of a C-3 side chain into literature known **1**.^[49,59]



Scheme 8.2: Synthesized putative aromatic inhibitors of PhzE and AS.

8.1.2 Cyclohexane-derived inhibitors

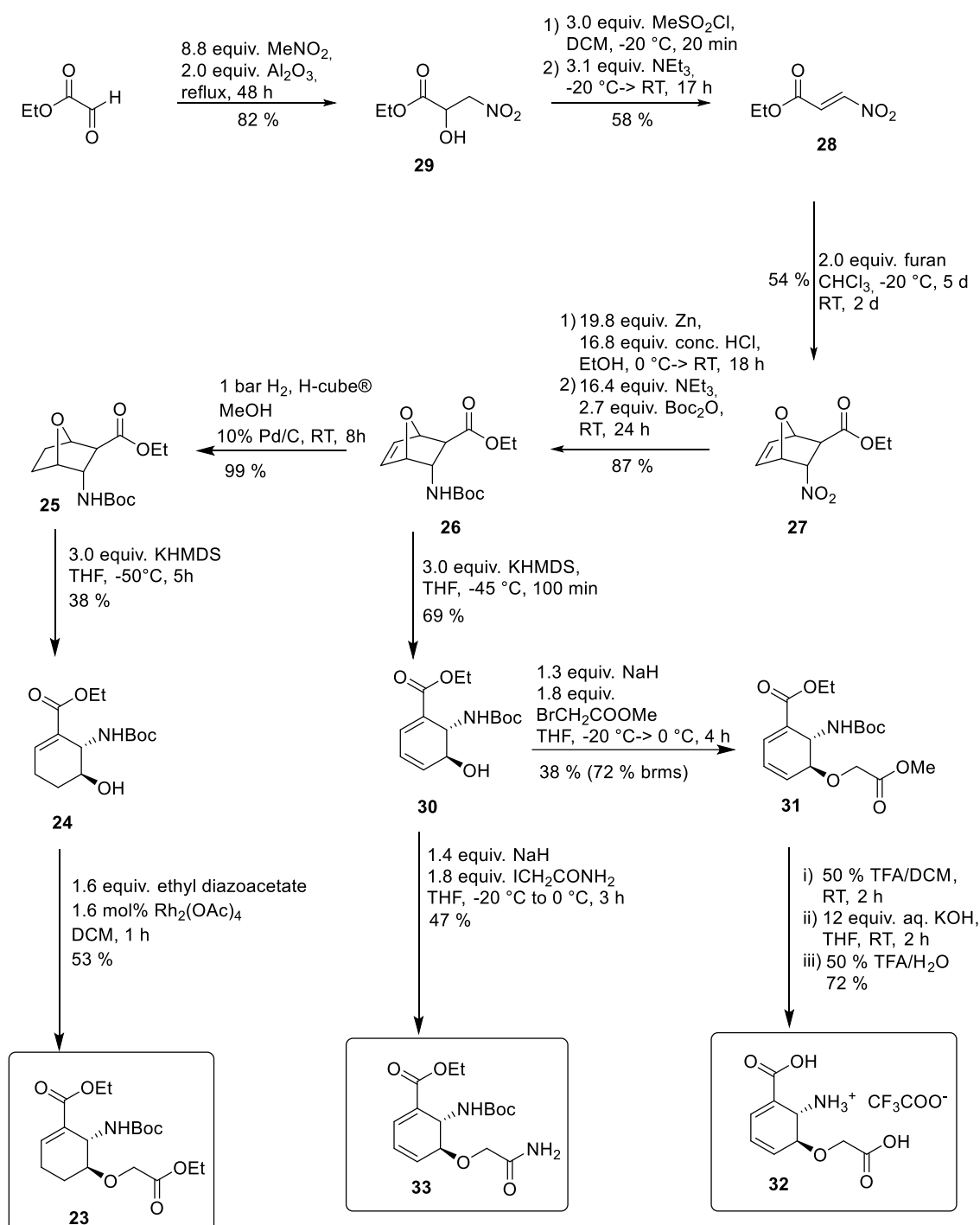
In order to increase diversity, we synthesized cyclohexane derivatives **16** and **17** (Scheme 8.3). Starting from the literature known **18**, differently decorated substrates were easily accessible.



Scheme 8.3: Synthetic access to the putative inhibitors of PhzE and anthranilate synthase (AS) **16** and **17**.

8.1.3 ADIC-derived inhibitors

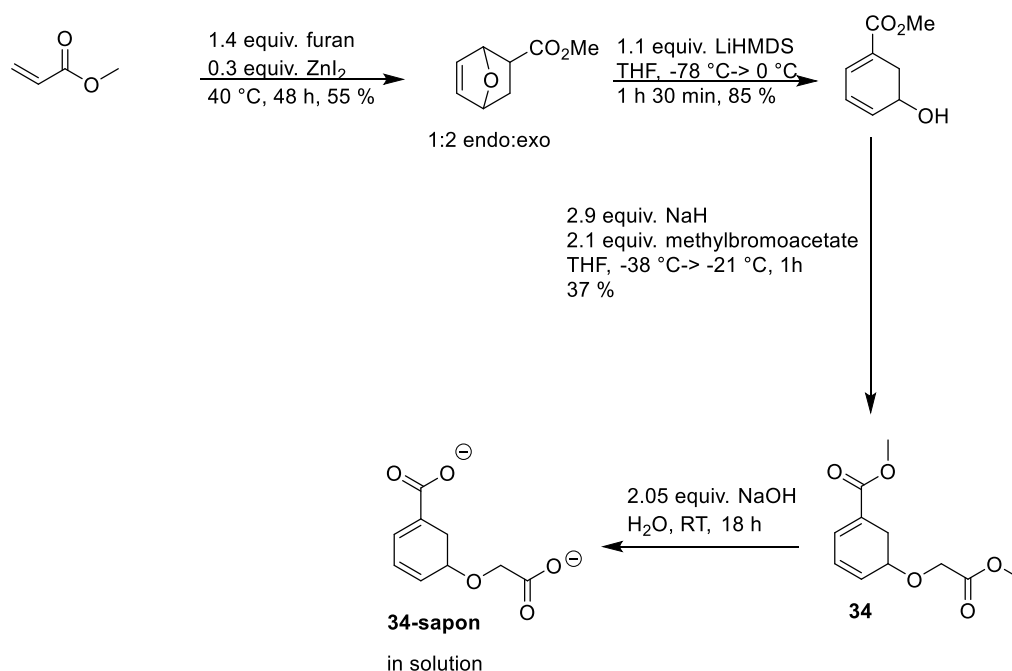
We aimed to design putative inhibitors that combine promising structural elements and would readily allow for diversification upon finding a lead (Scheme 8.4). We suppose that compound **23**, **32** and **33** represent interesting lead structures for the development of different inhibitors.



Scheme 8.4: ADIC derived inhibitors

8.1.4 Cyclohexadiene-derived inhibitors

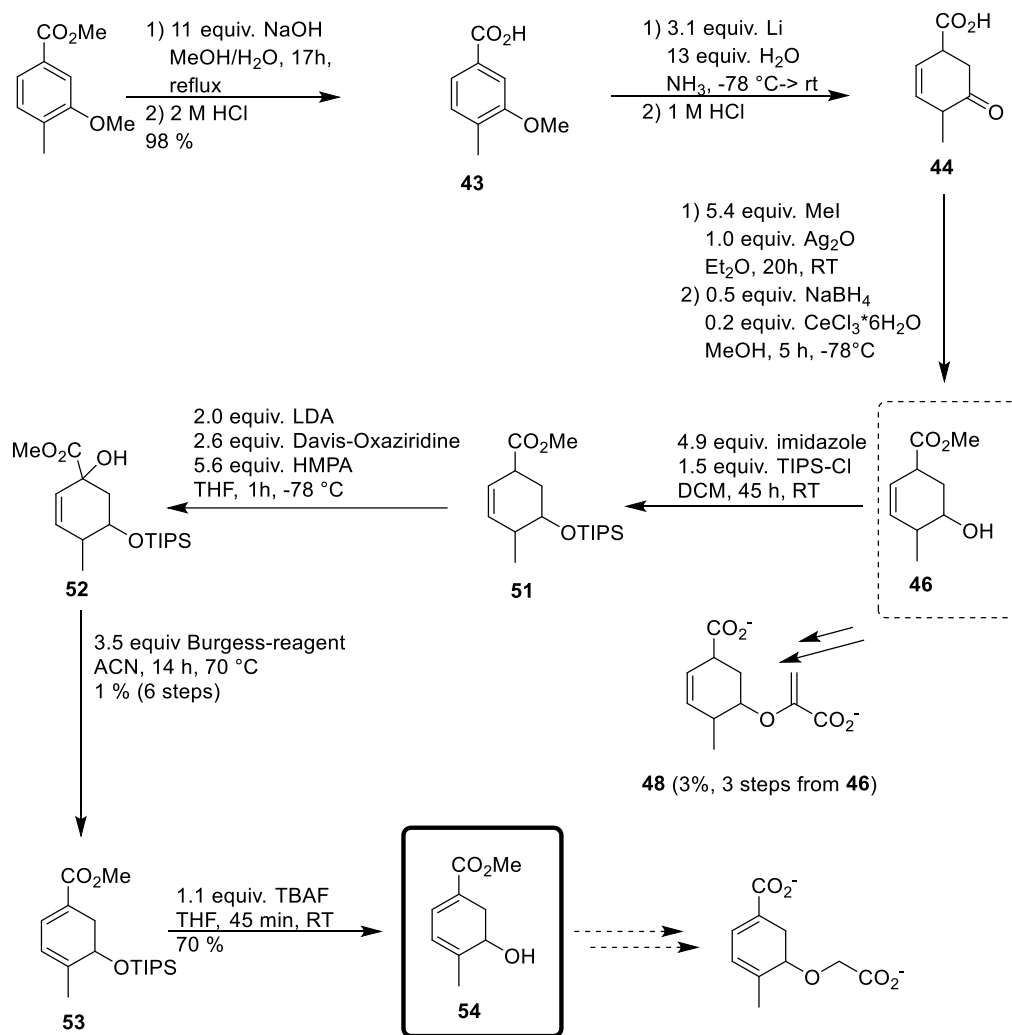
Having established aromatic, cyclohexane and ADIC derived inhibitors, we sought to design cyclohexadiene derived inhibitors as alternative lead structures for the inhibition of PhzE and AS (Scheme 8.5).



Scheme 8.5: Synthesis of a cyclohexadiene derived inhibitor.

8.1.5 Mechanism-based inhibitors

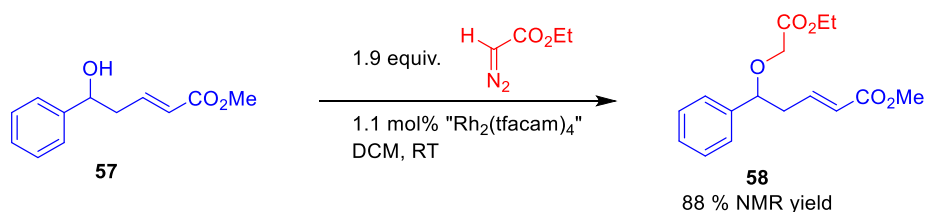
We hypothesized that the introduction of a methyl in position C-4 of cyclohexadiene-derived inhibitors may be beneficial. To this end, we developed a synthetic strategy towards strategic intermediate **54**, which will serve for the development of putative inhibitors of PhzE and AS. In addition, cyclohexene derivative **48** was synthesized as putative inhibitor (Scheme 8.6).



Scheme 8.6: Synthesis of **48** as a cyclohexene derived inhibitor and **54** as a strategic intermediate.

8.1.6 Etherification of unstable alcohols

Motivated by difficulties in etherification of some unstable substrates, a general strategy for the etherification of unstable alcohols was developed, which can be of central importance for the development of additional inhibitors of PhzE and AS (Scheme 8.7).



Scheme 8.7: Methodology development for the mild introduction of a side chain into instable alcohols.

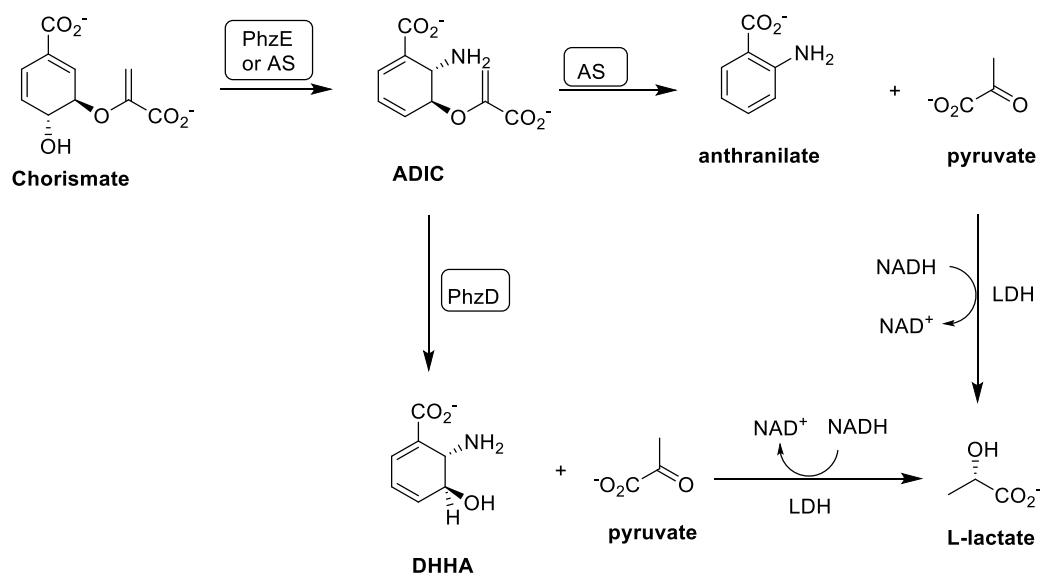
8.2 Outlook

In order to study binding differences between PhzE and anthranilate synthase (AS), thermodynamic and crystallographic experiments will be performed. Determination of the inhibition constant will be performed using enzymatic activity tests.

8.2.1 Enzymatic activity tests

We expect that some of the synthesized compounds are inhibitors of PhzE or AS. In order to determine inhibition constants, *in vitro* studies will be performed. As it is expected that our putative inhibitors would interfere in UV or fluorescence assays, coupled assays will be performed (Scheme 8.8). Pyruvate liberation can be determined using lactate dehydrogenase (LDH). As pyruvate is converted to L-lactate by LDH, NADH is oxidized to NAD⁺ what can be measured by a decrease in absorption at 340 nm.^[49] Contrary to AS, pyruvate is not released in the case of PhzE. In order to cause pyruvate liberation in PhzE, a coupling with PhzD will be performed.

Alternatively, the enzyme-ligand mixture will be quenched with ACN and quantification will be performed via HPLC-MS.



Scheme 8.8: Coupled assay of PhzE and anthranilate synthase (AS).

9 Experimental section

9.1 General

Reactions were carried out using standard Schlenk techniques under an inert atmosphere of argon or nitrogen and absolute and degassed solvents (if necessary) were used, unless otherwise indicated. Molecular sieves were activated by filling a 500 mL round-bottom flask to one third of its volume with molecular sieves (Sigma-Aldrich, beads, 8-12 mesh) and heating the flask in a heating mantle (~150°C) under oil pump vacuum for 1 d, followed by cooling to RT under an atmosphere of argon. Degassing was carried out by passing a stream of argon through the reaction mixture/solvent. This means, a balloon filled with argon was placed on a syringe with needle, and the needle was punched through a septum and dipped into the reaction mixture. Additionally, the vessel was immersed in an ultrasonic bath with a needle punched through the septum as gas outlet. Temperatures were measured externally. When working at 0 °C, an ice-water bath served as the cooling agent. Temperatures between -78 °C and 0 °C were achieved using dry ice/acetone mixtures. Reactions carried out at higher temperatures than RT were heated in a silicon oil bath on a hot plate (RCT basic IKAMAG® safety control) equipped with a temperature controller.

9.2 Solvents

Acetone: Acetone used for non-inert conditions was purchased from Brenntag and distilled using a rotary evaporator.

Acetonitrile: Acetonitrile was purchased from Alfa Aesar (99.9%). For inert conditions, acetonitrile was passed through an aluminium oxide column (solvent purification system: Puresolv™ from Innovative Technology Inc.) under inert conditions and stored over molecular sieves in a brown 1 L Schlenk bottle under argon atmosphere.

Chloroform: Chloroform used for non-inert conditions was purchased from VWR and was used as obtained.

Cyclohexane: Cyclohexane used for non-inert conditions was purchased from Fisher Scientific as analytical grade (99.99 %) and was used as obtained.

Dichloromethane: Dichloromethane used for inert conditions was purchased from Alfa Aesar (stabilized with EtOH), heated at reflux temperature for 1 d on phosphorus pentoxide, distilled, then heated at reflux temperature for 1 d over calcium hydride and then distilled under argon atmosphere into a dry brown 1 L Schlenk bottle with activated 4 Å molecular sieves. Dichloromethane used for non-inert conditions was purchased from Fisher Scientific as analytical grade (99.99 %) and was used as obtained.

Diethyl ether: Diethyl ether used for non-inert conditions was purchased from Roth and the stabilizer was removed by distillation using a rotary evaporator. The solvent was stored over KOH pellets in a brown-glass bottle.

1,4-Dioxane: 1,4-Dioxane used for non-inert conditions was purchased from Sigma Aldrich and the stabilizer was removed by distillation using a rotary evaporator. The solvent was stored over KOH pellets in a brown-glass bottle.

N,N-Dimethylformamide: *N,N*-Dimethylformamide was purchased from ACROS Organics as extra dry solvent (<50 ppm water, over 3 Å molecular sieves, AcroSeal®) and was transferred to a dry brown 1 L Schlenk bottle with activated 3 Å molecular sieves and stored under argon atmosphere.

Dimethylsulfoxide: Dimethylsulfoxide was purchased from ACROS Organics and stored over 4 Å molecular sieves in a brown 1 L Schlenk bottle.

Ethanol: Ethanol used for non-inert conditions was purchased from Merck (stabilized with 1 % methylethyl ketone) and was used without further purification.

Ethyl acetate: Ethyl acetate used for non-inert conditions was purchased from Fisher Scientific as analytical grade (99.99 %) and was used as obtained.

HMPA: HMPA was stored over 4 Å molecular sieves in a 100 mL Schlenk bottle under argon atmosphere.

Methanol: Methanol used for non-inert conditions was purchased from Fisher Scientific as analytical grade (99.99%) solvent and used directly without any purification. For inert conditions, methanol was distilled over magnesium turnings and iodine under argon atmosphere and stored over 3 Å molecular sieves. Alternatively, it was purchased from Sigma-Aldrich as anhydrous solvent (99.8%) and stored over 3 Å molecular sieves in an 1 L Schlenk bottle under argon atmosphere

Tetrahydrofuran: Tetrahydrofuran used for non-inert reactions was purchased from Roth and the stabilizer was removed by distillation using a rotary evaporator. The solvent was stored over KOH pellets in a brown-glass bottle. For inert conditions stabilizer free tetrahydrofuran was heated at reflux temperature under argon atmosphere over sodium until benzophenone indicated dryness by a deep violet color and distilled. The dried THF was stored over 4 Å molecular sieves in a brown 1 L Schlenk bottle under argon atmosphere.

Toluene: Toluene used for non-inert conditions was purchased from Sigma Aldrich and was used as obtained. For inert conditions, toluene was passed through an aluminium oxide column (solvent purification system: Puresolv™ from Innovative Technology Inc.) under inert conditions and stored over 4 Å molecular sieves in a brown 1 L Schlenk bottle under argon atmosphere.

Water: For work-up purposes and quenching of reactions deionized water was used.

9.3 Reagents

All chemicals and reagents were purchased from the companies ABCR, ACROS Organics, Alfa Aesar, Brenntag, Fisher Scientific, Fluka, Merck, Roth, Sigma Aldrich or VWR and were used without further purification, unless otherwise stated. ¹H-NMR spectra for all synthesized reagents are provided (see Appendix)

PLE was purchased from Sigma Aldrich: E3019-20KU ~20U/mg.

Burgess reagent: This reagent was prepared following a two-step literature procedure ^[133]

Corey's oxazaborolidinium catalyst: This catalyst was prepared following a two-step literature procedure.^[138]

Davis-oxaziridine: This reagent was prepared following a two-step literature procedure ^[123]

Dimethyl 2-diazomalonate (R-4): This compound was prepared following a literature procedure.^[139] See chapter 9.8.4.

Ethyldiazoacetate: This compound was purchased from Aldrich. The concentration of the DCM solution was calculated via ¹H-NMR using 1,3,5-trimethoxybenzene as an external standard.

mCPBA: mCPBA was purchased from Sigma Aldrich as a ≤ 77 % mixture. Before starting a reaction with mCPBA the exact concentration of the applied solution was determined by titration.

A 250 mL round-bottom flask was charged with 640 mg of the used mCPBA/CHCl₃ solution (2.5 g mCPBA, 80 mL CHCl₃, sonification via ultra-sound bath). Consecutively, 50 mL H₂O, 5 mL CHCl₃, 5 mL HOAc glacial and 1.5 g NaI were added. It was stirred vigorously and titrated with a previously prepared 0.1 M Na₂S₂O₃ solution. The color changes from brown to colorless. The concentration was calculated as following:

$$\text{wt \%} = [\text{mg Na}_2\text{S}_2\text{O}_3] * 0.5 / [\text{mg mCPBA-CHCl}_3 \text{ solution}]$$

Methyl 2-diazoacetate (R-2): Methyl 2-diazoacetate was prepared according to the literature.^[140] The concentration of the obtained DCM/CHCl₃ solution was calculated via ¹H-NMR using 1,3,5-trimethoxybenzene as an external standard. See chapter 9.8.2.

Methyl 2-diazopropionate (R-3): Methyl 2-diazopropionate was prepared following a literature procedure.^[141] The concentration of the obtained DCM/CHCl₃ solution was calculated via ¹H-NMR using 1,3,5-trimethoxybenzene as an external standard. See chapter 9.8.3.

Methyl 2-diazo-2-(dimethoxyphosphoryl)acetate (R-1): This compound was prepared following a literature procedure.^[142] See chapter 9.8.1.

Methyl-2-diazo-2-(trimethylsilyl)acetate (R-5): This compound was prepared following a literature procedure.^[143] See chapter 9.8.5.

3-Methylfuran: This compound was prepared following a two-step literature procedure.^[144]

n-Butyllithium: *n*-Butyllithium was purchased from ACROS Organics as a 2.5 M solution in hexane. Before starting a reaction with *n*-BuLi the exact concentration of the solution was determined by a titration method from Kofron and Baclawsk.^[145]

A 100 mL Schlenk tube was flame dried under vacuum, filled with nitrogen and charged with 250.0 mg diphenyl acetic acid and 10 mL abs. THF. To this solution *n*-BuLi was added dropwise by using a syringe until the color of the solution turned from colorless to yellow. The added amount of *n*-BuLi corresponds to the weighed amount of diphenylacetic acid. This procedure was repeated twice and the average was used to calculate the exact concentration of *n*-BuLi.

LDA solution: 1.05 equiv. of diisopropylamine were dissolved in an appropriate amount of abs. THF. It was cooled to -78 °C (dry ice/acetone) and 1.0 equiv. *n*-BuLi (in hexane) were slowly added. The dry ice/acetone cooling bath was replaced by an ice bath and it was stirred for 10 min at 0 °C.

A 15 mL Schlenk tube was flame dried, filled with nitrogen and charged with 115.0 mg diphenyl acetic acid and 1 mL abs. THF. To this solution, the LDA solution was added dropwise by using a syringe until the color of the solution turned from colorless to pale yellow. The added amount of LDA corresponds to the weighed amount of diphenylacetic acid. This procedure was repeated twice and the average was used to calculate the exact concentration of the LDA solution.

NaH₂PO₄/Na₂HPO₄-buffer (pH = 7.6): The NaH₂PO₄/Na₂HPO₄-buffer was prepared by dissolving 12.0 g NaH₂PO₄ (purchased from Fluka) in 1.0 L deionised water followed by the dropwise addition of NaOH (3.0 M) to the stirred solution to a pH of 7.6.

Rh₂(1-adaman)₄: This catalyst was prepared following a literature procedure.^[89] See chapter 9.8.6.

Triethylamine: Triethylamine was first distilled over KOH and then distilled over calcium hydride under argon atmosphere and stored over 4 Å molecular sieves in a 1 L Schlenk bottle under argon atmosphere.

9.4 Analytical Methods

9.4.1 Thin-layer chromatography

Analytical thin layer chromatography was performed using TLC-plates purchased from Merck (TLC aluminium foil, silica gel 60 F₂₅₄). The TLC plates were generally screened using a UV lamp with $\lambda = 254$ nm (fluorescence quenching) and $\lambda = 366$ nm (immanent fluorescence of the analytes). Alternatively, a stain reagent was applied and the plates were developed using a stream of hot air.

CAM: 2.0 g cerium(IV)-sulfate, 50.0 g ammonium molybdate and 50 mL conc. H₂SO₄ were dissolved in 400 mL water.

Ninhydrin: 250.0 mg ninhydrin were dissolved in 100 mL ethanol.

KMnO₄: 3.0 g KMnO₄ and 20.0 g K₂CO₃ dissolved in 300 mL 5 % NaOH solution.

9.4.2 Flash column chromatography

Preparative column chromatography was performed using silica gel 60 from ACROS Organics (particle size 35-70 μ m) at an air pressure of \sim 1.5 bar. The mobile phase was forced through the column by means of a rubber bulb pump. Additional details such as amount of silica gel, column size, composition/gradient of mobile phase and fraction size are indicated in the corresponding experimental procedures.

9.4.3 High performance liquid chromatography

Analytical HPLC measurements were performed on a Shimadzu Nexera Liquid Chromatograph. The separation of the analytes was carried out using a "C-18 reversed-phase" column of the type "Poroshell[®] 120 SB-C18, 3.0 x 100 mm, 2.7 μ m" by Agilent Technologies. Detection of the substances was accomplished with a "Shimadzu SPD-M20A Prominence Diode Array Detector" at a wavelength of $\lambda = 210$ nm and with the mass selective detector "Shimadzu LCMS-2020 Liquid Chromatograph Mass Spectrometer" in the modes "ESI positive" and "ESI negative". As eluents acetonitrile and water with 0.01% formic acid as an additive were used.

Methods:

"standard-1": 0.00-0.50 min 70 % water/HCOOH and 30 % CH₃CN, 0.50-6.50 min linear to 100 % CH₃CN, 6.50-7.20 min 100 % CH₃CN, 7.20-7.30 min linear to 30 % CH₃CN, 7.30-9.00 min 30 % CH₃CN; 0.7 mL·min⁻¹; 40 °C.

“standard-2”: 0.00-1.50 min 100 % water/HCOOH and 0 % CH₃CN, 1.50-5.50 min linear to 80 % CH₃CN, 5.50-6.00 min 80 % CH₃CN, 6.00-6.05 min linear to 100 % CH₃CN, 6.05-6.70 min 100 % CH₃CN, 6.70-6.80 min linear to 0 % CH₃CN, 6.80-8.00 min 0 % CH₃CN; 0.7 mL·min⁻¹; 40 °C.

For semi-preparative HPLC a Thermo Scientific Dionex Ulti Mate 3000 Instrument was used. Semi-preparative HPLC was carried out utilizing a Macherey-Nagel VP 125/21 Nucleodur 100-5 C18 ec column. Demineralized water was additionally purified by filtering through a 0.2 µm cellulose nitrate membrane filter.

High pressure hydrogenation experiments were performed using the H-Cube™ continuous hydrogenation unit (HC-2.SS) from Thales Nanotechnology Inc. running with a Knauer Smartline pump 100 and equipped with a 10 mL ceramic pump head. As hydrogenation catalyst 10% Pd/C catalyst cartridges were used (Thales Nanotechnology inc., THS01111, 10% Pd/C CatCart™).

9.4.4 Nuclear magnetic resonance spectroscopy

The described nuclear resonance spectra were acquired with the following instruments:

Bruker AVANCE III with Autosampler: 300.36 MHz ¹H-NMR, 75.53 MHz ¹³C-NMR

Varian Unity Inova: 499.91 MHz ¹H-NMR, 125.69 MHz ¹³C-NMR, 470.35 MHz ¹⁹F-NMR

Bruker MSL 300 MHz: 282 MHz ¹⁹F-NMR

Chemical shifts δ are referenced to the residual protonated solvent signals as internal standard (CDCl₃: δ = 7.26 ppm (¹H), 77.16 ppm (¹³C), C₆D₆: δ = 7.16 ppm (¹H), 128.06 ppm (¹³C), D₂O: δ = 4.79 ppm (¹H)), MeOD-d₄: 3.31 ppm (¹H), 49.0 ppm (¹³C), DMSO-d₆: 2.50 ppm (¹H), 39.5 ppm (¹³C), ¹³C-NMR and APT spectra were acquired proton-decoupled. Signal multiplicities are abbreviated as s (singlet), bs (broad singlet), d (doublet), dd (doublet of doublet), t (triplet), q (quadruplet) and m (multiplet). For the correct assignment of the signals HH-COSY, HSQC, HMQC and HMBC were recorded if necessary. The deuterated solvent, the chemical shifts δ in ppm (parts per million), the coupling constants J in Hertz (Hz) and the integral and assignment of the respective signal are given. Deuterated solvents for nuclear resonance spectroscopy were purchased from Euriso top® (CDCl₃, C₆D₆) and Deutero® (D₂O).

9.4.5 High resolution mass spectrometry

TOF MS EI:

High resolution mass spectrometry was performed on a Waters GCT premier micromass. The products were ionized by an Electron Impact Ionization (EI)-source with 70 eV. Probes were

injected via an Agilent Technologies GC 7890A with capillary column (DB-5MS, 30 m x 0.25 mm x 0.25 μ m film).

FT-ICR MS ESI:

HRMS was determined by FT-MS on a LTQ FT Ultra instrument (Thermo Scientific) equipped with an ESI source. Samples were dissolved in 0.01 % formic acid in either acetonitrile or methanol (HPLC grade) and directly injected using a syringe pump with a flow of 3 μ L \cdot min⁻¹. Capillary temperature was set to either 200 °C or 270 °C and the sheath gas flow to 5. 5-10. Data were analysed with Xcalibur 2.1.0 (Thermo Fisher Scientific).

9.4.6 *Determination of the melting point*

Melting points are uncorrected and were determined using a “Mel-Temp®” apparatus with integrated microscopical support by the company Electrothermal. The temperature was measured using a mercury thermometer.

9.4.7 *Gas chromatography*

GC-MS analyses were carried out on an Agilent Technologies 7890A GC system equipped with a 5975C mass selective detector (inert MSD with Triple Axis Detector system, EI, 70 eV). In both systems samples were injected by employing autosampler 7683B in a split mode 1/175 (inlet temperature: 250°C; injection volume: 2.0 μ L) and separated on an Agilent Technologies J&W GC HP-5MS capillary column ((5%-phenyl)-methylpolysiloxane; 30 m \times 0.25 mm \times 0.25 μ m) at a constant helium flow rate (He 5.0 (Air Liquide), 1.085 mL/min, average velocity 41.6 cm/sec).

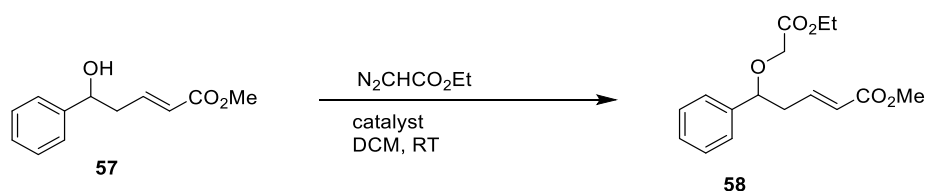
As a general gradient temperature method was used NG-STANDARD: (initial temperature: 50°C for 1 min, linear increase 40°C/min to 300°C, hold for 5 min, 1 min post-run at 300°C, detecting range: 50.0 to 550.0 amu, solvent delay of 2.80 min). When reactions were monitored by GC-MS, the samples were prepared using a microscale workup. This means, an aliquot was taken from the reaction mixture, quenched with 1 mL sat. NaHCO₃ solution and 1 mL DCM or EtOAc. After proper mixing and phase separation, the organic layer was collected, dried over MgSO₄ and filtered through cotton in a Pasteur-pipette. Reaction mixtures containing transition metals were additionally filtered through a short pad of silica gel (ca. 1 cm) over cotton in a Pasteur-pipette (elution via EtOAc or MeOH).

GC-FID analyses were carried out on an Agilent Technologies 6890N GC system equipped with a FID detector (250°C, 30 mL/min He-flow, 300 mL/min air flow, makeup-flow N₂). Samples were injected by employing autosampler 7683B in a split mode 1/100 (inlet temperature:

280°C; injection volume: 5.0 µL) and separated on an Agilent Technologies J&W Scientific DB-1701 GC capillary column (14%-Cyanopropyl-phenyl)-methylpolysiloxane; 30 m × 0.25 mm × 0.25 µm) at a constant N₂ flow rate (0.8 mL/min, average velocity 28 cm/sec).

General method: Testmethode-1701: (initial temperature: 80°C for 1 min, linear increase 30°C/min to 280°C, hold for 0 min). When reactions were monitored by GC-FID, the samples were prepared using a microscale workup. This means, an aliquot was taken from the reaction mixture, quenched with ~1 mL sat. NaHCO₃ solution and ca. 1 mL DCM or EtOAc. After proper mixing and phase separation, the organic layer was collected, dried over MgSO₄ and filtered through cotton in a Pasteur-pipette. Reaction mixtures containing transition metals were additionally filtered through a short pad of silica gel (ca. 1 cm) over cotton in a Pasteur-pipette (eluted with EtOAc or MeOH).

9.5 General procedure for the ¹H-NMR screening of OH-insertion reactions



Scheme 9.1: OH insertion reaction of **57**.

A flame dried and nitrogen flushed Schlenk flask with magnetic stirring bar was charged with the catalyst.* An aliquot of a stock solution containing the starting material **57** and 0.1 equiv. trimethylphenylsilane in DCM was added. To the stirred mixture an aliquot of a stock solution of ethyl 2-diazoacetate was added over the course of 1 h using a syringe pump. The reaction mixture was kept stirring at RT and samples for reaction monitoring by ¹H-NMR (CDCl₃) were taken after a given time.

9.6 General procedure for cracking paraformaldehyde

A flame dried and nitrogen flushed two-neck round-bottom flask equipped with a Schlenk adapter was charged with an appropriate amount of paraformaldehyde. The two-neck flask was connected to a three-neck flask equipped with a bubbler. The three-neck flask was charged with an appropriate amount of THF and placed in an acetone/dry-ice bath (-78 °C). The two-neck flask was transferred to a pre-heated oil-bath (170 °C) and it was heated until all paraformaldehyde was cracked. A formaldehyde solution in THF at -78 °C was obtained.

* If less than 2 mg of catalyst was used, an aliquot of a stock solution of the catalyst was pipetted into the Schlenk flask and the solvent was removed using the oil pump (~14 h)

9.7 General setup of the Birch-reduction

A general setup of the Birch-reduction is depicted in Figure 9.1.

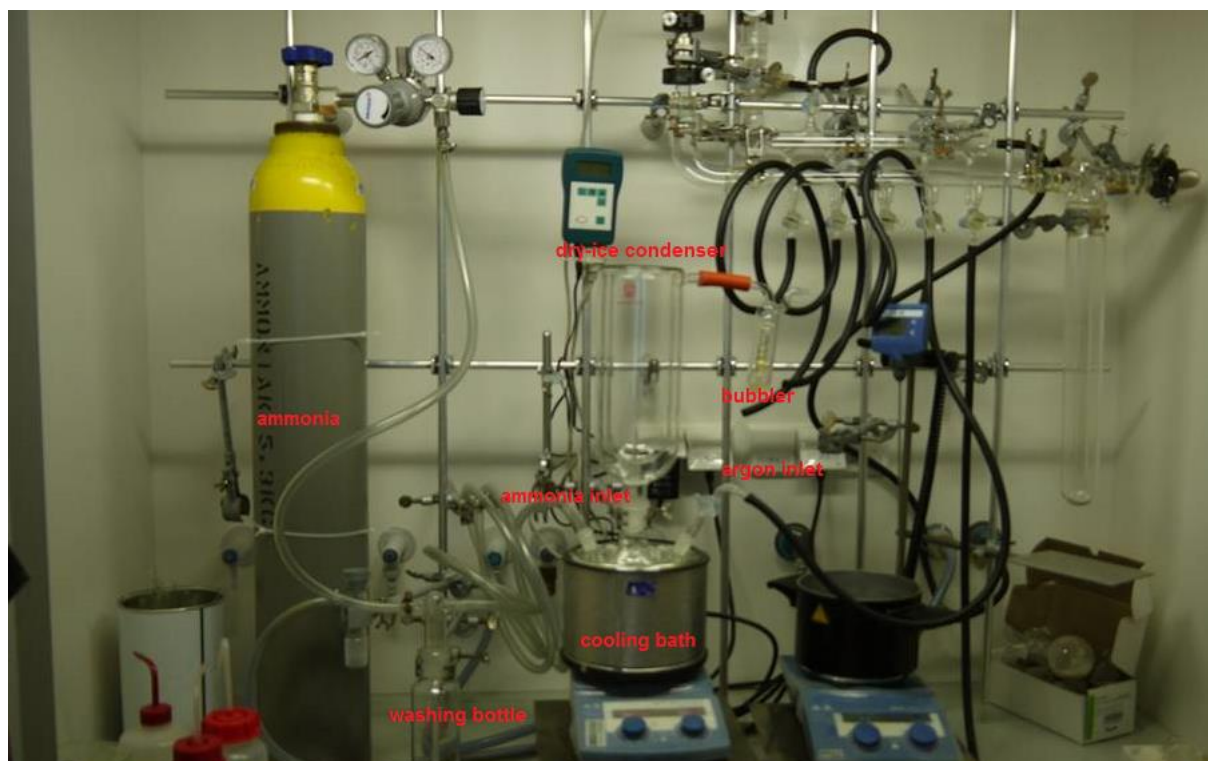
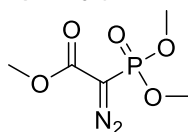


Figure 9.1: General setup of the Birch-reduction. Picture kindly provided by Xuepu Yu.

9.8 Experimental procedures and analytical data

9.8.1 Methyl 2-diazo-2-(dimethoxyphosphoryl)acetate (**R-1**)



This compound was prepared following a literature procedure.^[142]

A flame dried and argon flushed 500 mL three-neck round-bottom flask equipped with magnetic stirring bar was consecutively charged with 763 mg (19.1 mmol, 1.4 equiv.) 60 w% NaH dispersion in mineral oil, 24.95 g (ca. 13.90 mmol, 1 equiv.) 11-15 w% sol. *p*-toluenesulfonylazide in toluene and 100 mL abs. THF. The flask was cooled to 0 °C (ice bath) and 2.94 mL (18.16 mmol, 1.3 equiv.) trimethylphosphonoacetate were added over a period of 5 min. It was stirred for 40 min at 0 °C. Subsequently, the ice-bath was removed and it was stirred for another 6 h at RT. The colorless, cloudy solution was quenched by careful addition of 200 mL Et₂O and 200 mL H₂O, the layers were separated and the aqueous layer was extracted with Et₂O (5x100 mL). The combined organic layers were dried over Na₂SO₄, filtered and concentrated *in vacuo*. The product was purified via flash column chromatography (140 g SiO₂, 15 x 4.5 cm, cyclohexane/EtOAc = 1/1, 160 mL frac., frac. 9-15 pooled).

Yield= 1.60 g (7.69 mmol, 54 %) pale yellow oil

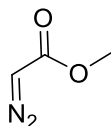
C₅H₉N₂O₅P [208.11 g·mol⁻¹]

R_f= 0.19 (cyclohexane/ EtOAc = 1/1, CAM)

GC-MS (EI, 70 eV, NG-STANDARD): t_R= 5.18.

¹H-NMR (300 MHz, CDCl₃): δ= 3.85 (s, 3 H), 3.81 (s, 6 H).

9.8.2 Methyl 2-diazoacetate (**R-2**)



This compound was prepared according to a literature procedure.^[140]

A 100 mL, three-neck round-bottom flask, equipped with magnetic stirring bar was charged with 3.78 g (30.1 mmol, 1 equiv.) glycine methyl ester hydrochloride, 18 mL CHCl₃ and 7.6 mL H₂O. It was cooled to 0 °C (ice bath). Vigorous stirring was begun and 2.49 g (36.1 mmol, 1.2 equiv.) NaNO₂ in 7.6 mL H₂O were added over a period of two min. Subsequently, it was cooled to -10 °C (dry-ice/acetone) and 2.86 mL sulfuric acid (5 % in H₂O) were added over a period of 4 min. It was stirred at this temperature for additional 20 min after which the solution was transferred to a separatory funnel. The organic phase was diluted with DCM (30 mL) and washed with a 5 % NaHCO₃ sol. The organic phase was dried over Na₂SO₄, filtered and gently concentrated *in vacuo*.

Yield= 2.21 g mixture of desired product in DCM and CHCl₃

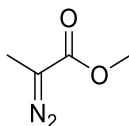
The concentration of the obtained DCM/CHCl₃ solution was calculated via ¹H-NMR using 1,3,5-trimethoxybenzene as an external standard.

C₃H₄N₂O₂ [100.08 g·mol⁻¹]

R_f= 0.50 (DCM, UV)

¹H-NMR (300 MHz, CDCl₃): δ= 4.74 (s, 1H), 3.74 (s, 3H).

9.8.3 Methyl 2-diazopropanoate (**R-3**)



This compound was prepared according to a literature procedure.^[141]

A 250 mL, one-neck round-bottom flask, equipped with magnetic stirring bar was charged with 2.03 g (14.5 mmol, 1 equiv.) L-alanine methyl ester hydrochloride and 100 mL CHCl₃. Vigorous stirring was begun and 2.01 mL (14.5 mmol, 1 equiv.) Et₃N were added. The colorless precipitate was filtered off and the solution was transferred to a 250 mL Schlenk flask. Subsequently, 203 μL (3.5 mmol, 0.24 equiv.) HOAc and 2.35 mL (17.5 mmol, 1.2 equiv.) isopentyl nitrite were added. The reaction mixture was heated at 70 °C for 3 h, after which it was cooled to RT, diluted with DCM (30 mL) and washed with sat. NaHCO₃ (1x30mL). The organic phase was dried over Na₂SO₄, filtered and gently concentrated *in vacuo*. The product was purified via flash column chromatography (75 g SiO₂, 12 x 4.0 cm, DCM, 50 mL frac., frac. 3-6 pooled).

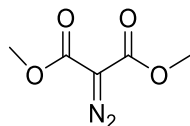
Yield= 259 mg (2.3 mmol, 16 %) yellow liquid

C₄H₆N₂O₂ [114.1 g·mol⁻¹]

R_f= 0.66 (DCM, UV)

¹H-NMR (300 MHz, CDCl₃): δ= 3.76 (s, 3H), 1.96 (s, 3H).

9.8.4 Dimethyl 2-diazomalonate (**R-4**)



This compound was prepared following a literature procedure.^[139]

A flame dried and argon flushed 100 mL two-neck round-bottom flask equipped with magnetic stirring bar was charged with 320 mg (2.42 mmol, 1 equiv.) dimethyl malonate, 10 mL abs. ACN and 0.50 mL (3.6 mmol, 1.5 equiv.) Et₃N. It was stirred vigorously and 600 mg (2.50 mmol, 1.01 equiv.) 4-acetamidobenzenesulfonylazide were added. After stirring overnight, the solid material was filtered off. The reaction mixture was diluted with 50 mL EtOAc and washed with H₂O (1x30 mL). The aqueous phase was back-extracted with EtOAc (1x30 mL). The combined organic layers were dried over MgSO₄, filtered and concentrated *in vacuo*. The product was purified via flash column chromatography (26 g SiO₂, 8.3 x 3.3 cm, cyclohexane/EtOAc = 2/1, 10 mL frac., frac. 3-11 pooled).

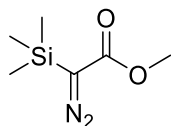
Yield= 252 mg (1.59 mmol, 66 %) yellow liquid

C₅H₆N₂O₄ [158.11 g·mol⁻¹]

R_f= 0.41 (cyclohexane/ EtOAc = 2/1, CAM)

¹H-NMR (300 MHz, CDCl₃): δ= 3.84 (s, 6 H).

9.8.5 Methyl-2-diazo-2-(trimethylsilyl)acetate (**R-5**)



This compound was prepared following a literature procedure.^[143]

A flame dried and argon flushed 250 mL, two-neck round-bottom flask, equipped with a magnetic stirring bar and an argon-inlet, was charged with 1.014 g (10.1 mmol, 1 equiv.) methyl-2-diazoacetate, 50 mL abs. Et₂O and 2.1 mL (15.0 mmol, 1.5 equiv.) *N,N*-diisopropylethylamine. The yellowish reaction mixture was cooled to -78°C (dry ice/acetone). Vigorous stirring was begun and 1.8 mL (10.0 mmol, 1 equiv.) TMS-OTf were added over a period of 10 min, which resulted in a yellow cloudy solution. The reaction mixture was stirred at -78 °C for 30 min. Subsequently, the cooling bath was removed and the mixture was stirred at RT for 40 h. The insoluble materials were filtered off using a Schlenk frit. The residue was washed with abs. Et₂O (1x10 ml) to obtain a crude product, which was purified via vacuum distillation (50°C, 1.6 mbar; the use of a condensation trap was necessary).

Yield= 0.847 g (4.91 mmol, 49 %) yellow/brown oil

C₆H₁₂N₂O₂Si [172.26 g·mol⁻¹]

¹H-NMR (300 MHz, CDCl₃): δ= 3.72 (s, 3H), 0.25 (s, 9H).

9.8.6 $Rh_2(1\text{-adaman})_4$ dimer

This compound was prepared following a literature procedure.^[89]

A flame dried and argon flushed 10 mL Schlenk flask equipped with magnetic stirring bar, was charged with 500 mg (2.77 mmol, 24.5 equiv.) adamantanecarboxylic acid and 1.0 mL ACN. Vigorous stirring was begun and 50 mg (0.113 mmol, 1 equiv.) $Rh_2(OAc)_4$ dimer were added. The flask was transferred into a pre-heated oil bath (160 °C) and stirred for 3 h. After cooling to RT, the mixture was concentrated *in vacuo* and mixed with a solution of 25 mL ACN and 2.5 mL DCM. The solution turned purple and it was stirred for 3 h, after which the solution was sucked off and the solid was washed with 10 mL ACN/DCM (10/1 v/v). It was dried by an oil pump at 80 °C and a blue solid was obtained.

Yield= 85 mg (0.092 mmol, 82 %) colorless oil

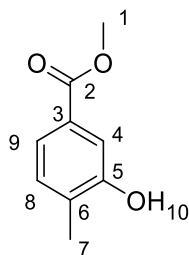
$C_{44}H_{60}O_8Rh_2$ [922.77g·mol⁻¹]

R_f = 0.31 (cyclohexane/ EtOAc = 40/1, CAM)

¹H-NMR (300 MHz, CDCl₃): δ = 1.71 (br s, 3 H), 1.45 (br s, 12 H).

¹³C-NMR (76 MHz, CDCl₃): δ = 41.9, 39.1, 36.1, 27.8.

9.8.7 Methyl 3-hydroxy-4-methylbenzoate (**1**)



This compound was prepared following a literature procedure.^[59]

A flame dried and argon flushed 250 mL Schlenk flask equipped with magnetic stirring bar, was consecutively charged with 2.40 g (15.8 mmol, 1 equiv.) 3-hydroxy-4-methylbenzoic acid, 40 mL abs. MeOH and 0.1 mL (1.38 mmol, 0.09 equiv.) thionyl chloride. Vigorous stirring was begun and it was stirred at 70 °C for 16 h. After cooling to RT the mixture was poured into 50 mL H₂O and the aqueous phase was extracted with EtOAc (3x40 mL). The combined organic layers were dried over Na₂SO₄, filtered and concentrated *in vacuo*. The crude product was purified via flash column chromatography (70 g SiO₂, 19 x 3.3 cm, cyclohexane/EtOAc = 3/1, 20 mL frac., frac. 5-16 pooled).

Yield= 2.41 g (14.5 mmol, 92 %), colorless solid

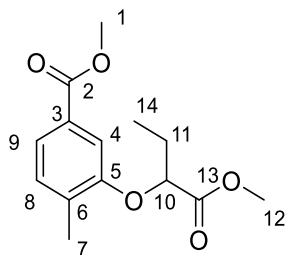
C₉H₁₀O₃ [166.18 g·mol⁻¹]

R_f= 0.41 (cyclohexane/ EtOAc = 3/1, CAM)

GC-MS (EI, 70 eV, NG-STANDARD): t_R= 5.76; m/z (%)= 166.0 (100 [M⁺]), 135.0 (213), 77.1 (67).

¹H-NMR (300 MHz, CDCl₃): δ = 7.55 (m, 2H), 7.18 (d, *J*= 7.70 Hz, 1H), 5.52 (bs, 1H), 3.90 (s, 3H), 2.30 (s, 3H).

9.8.8 Methyl 3-((1-methoxy-1-oxobutan-2-yl)oxy)-4-methylbenzoate (**2**)



A 50 mL round-bottom flask equipped with magnetic stirring bar, was consecutively charged with 400 mg (2.41 mmol, 1 equiv) **1**, 20 mL acetone, 401 μ L (3.12 mmol, 1.3 equiv.) methylbromobutanoate, 665 mg (4.81 mmol, 2.0 equiv.) K_2CO_3 and 65 mg (0.43 mmol, 0.18 equiv.) NaI. Vigorous stirring was begun and it was stirred at reflux temperature for 16 h. After cooling to RT the solvent was removed *in vacuo*. The residue was redissolved in 40 mL EtOAc and washed with H_2O (1x20 mL). The organic layer was dried over Na_2SO_4 , filtered and concentrated *in vacuo*. The crude product was purified via flash column chromatography (40 g SiO_2 , 12 x 3.5 cm, cyclohexane/DCM/acetone 10/1/0.5, 15 mL frac., frac. 4-13 pooled).

Yield= 522 mg (5.73 mmol, 81 %) colorless oil

$C_{14}H_{18}O_5$ [266.29 $g \cdot mol^{-1}$]

R_f = 0.33 (cyclohexane/EtOAc/acetone = 20/2/0.1, CAM)

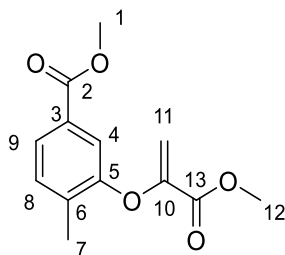
HRMS (TOF MS EI): m/z : calcd for $C_{14}H_{18}O_5^+$ [M] $^+$: 266.1154;

found: 266.1150.

1H -NMR (300 MHz, $CDCl_3$): δ = 7.57 (dd, 1H, J = 7.7 Hz, 1.1 Hz, H-9), 7.32 (d, 1H, J = 1.0 Hz, H-4), 7.20 (d, 1H, J = 7.7 Hz, H-8), 4.70 (t, 1 H, J = 6.0 Hz, H-10), 3.87 (s, 3H), 3.75 (s, 3H), 2.34 (s, 3H, H-7), 2.10–1.97 (m, 2H, H-11), 1.09 (t, J = 7.4 Hz, 3H, H-14).

^{13}C -NMR, APT (76 MHz, $CDCl_3$): δ = 172.0, 167.1, 156.0, 133.5, 131.0, 129.0, 122.8, 112.2, 77.6, 52.2, 26.3, 16.7, 9.7.

9.8.9 Methyl 3-hydroxy-4-methylbenzoate (**3**)



A flame dried and argon flushed 500 mL Schlenk flask equipped with magnetic stirring bar and a bubbler, was consecutively charged with 1.50 g (9.03 mmol, 1 equiv) **1**, 60 mL abs. toluene, 2.56 g (12.3 mmol, 1.4 equiv.) **R-1** and 61 mg (0.138 mmol, 1.5 mol %) Rh₂(OAc)₄. Vigorous stirring was begun and it was stirred at 85 °C for 14 h (reaction monitoring via GC-MS (GC-MS (EI, 70 eV, NG-STANDARD): t_R= 7.76; m/z (%)= 346.1 (100 [M⁺]), 314.1 (185), 286.1 (223), 182.0 (277), 124.0 (208), 93.0 (150)). Subsequently, 1.00 g (4.81 mmol, 0.5 equiv.) **R-1** and 15 mg (0.034 mmol, 0.4 mol %) Rh₂(OAc)₄ were added and it was stirred another 8 h. After no starting material was further converted to the product as observed via GC-MS, the solution was cooled to RT and concentrated *in vacuo*. The crude product was purified via flash column chromatography (250 g SiO₂, 16 x 5.8 cm, cyclohexane/EtOAc = 1/2, 120 mL frac., frac. 10-21 pooled). 1.70 g of a yellow oil were obtained. It was used without further purification.

In a flame dried and argon flushed 100 mL one-neck flask equipped with a Schlenk adapter and magnetic stirring bar 1.58 g (4.56 mmol, 1 equiv.) of the obtained yellow oil were dissolved in 30 mL abs. THF. It was cooled to -78 °C (dry ice/acetone) and 15.3 ml LiHMDS (0.3 M in abs. THF, 4.59 mmol, 1.0 equiv.) were added. The solution was stirred for 30 min at this temperature, until a formaldehyde solution, produced by cracking paraformaldehyde (approx. 39.8 mmol in 20.0 mL THF, 8.7 equiv.) was transferred via a cannula. It was stirred for another 90 min and the solution was poured into a flask containing 150 mL sat. NH₄Cl solution. The aqueous phase was extracted with EtOAc (3x100 mL). The combined organic layers were dried over Na₂SO₄, filtered and concentrated *in vacuo*. The crude product was purified via two consecutive flash column chromatographies (1: 90 g SiO₂, 17 x 3.5 cm, cyclohexane/EtOAc 7/1, 6 mL frac., frac. 2-6 pooled; 2: 50 g SiO₂, 11.0 x 3.7 cm, cyclohexane/DCM/acetone 10/1.5/0.3, 30 mL frac., frac. 11-15 pooled).

Yield= 400 mg (1.60 mmol, 19 %, 2 steps) colorless oil

C₁₃H₁₄O₅ [250.25 g·mol⁻¹]

R_f= 0.33 (cyclohexane/ EtOAc = 6/1, CAM)

GC-MS (EI, 70 eV, NG-STANDARD): t_R= 6.52; m/z (%)= 250.1 (100 [M⁺]), 219.1 (84), 191.1 (226), 159.0 (111), 119.0 (68), 89.0 (105), 59.0 (84).

HRMS (TOF MS EI):

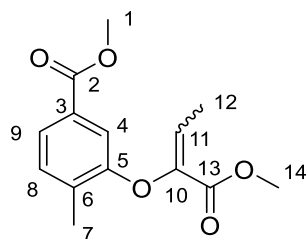
m/z: calcd for $C_{13}H_{14}O_5^+$ [M]⁺: 250.0841;

found: 250.0829.

¹H-NMR (300 MHz, CDCl₃): δ = 7.76 (dd, *J* = 7.9 Hz, 1.3 Hz, 1H, H-9), 7.61 (d, *J* = 1.1 Hz, 1H, H-4), 7.30 (d, *J* = 7.8 Hz, 1H, H-8), 5.66 (d, *J* = 2.3 Hz, 1H, H-11a), 4.70 (d, *J* = 2.2 Hz, 1H, H-11b), 3.89 (s, 3H, H12/H1), 3.85 (s, 3H, H12/H1), 2.29 (s, 3H, H-7).

¹³C-NMR, APT (76 MHz, CDCl₃): δ = 166.5, 163.0, 153.3, 150.2, 135.6, 131.6, 129.7, 126.1, 120.6, 102.9, 52.7, 52.3, 16.3.

9.8.10 Methyl 3-((1-methoxy-1-oxobut-2-en-2-yl)oxy)-4-methylbenzoate (**4**)



A flame dried and argon flushed 500 mL Schlenk flask equipped with magnetic stirring bar and a bubbler, was consecutively charged with 1.50 g (9.03 mmol, 1 equiv.) **1**, 60 mL abs. toluene, 2.56 g (12.3 mmol, 1.4 equiv.) **R-1** and 61 mg (0.138 mmol, 1.5 mol %) Rh₂(OAc)₄. Vigorous stirring was begun and it was stirred at 85 °C for 14 h (reaction monitoring via GC-MS). Subsequently, 1.00 g (4.81 mmol, 0.5 equiv.) **R-1** and 15 mg (0.034 mmol, 0.4 mol %) Rh₂(OAc)₄ were added and it was stirred another 8 h. After no starting material was further converted to the product, as observed via GC-MS (GC-MS (EI, 70 eV, NG-STANDARD): t_R= 7.76; m/z (%)= 346.1 (100 [M⁺]), 314.1 (185), 286.1 (223), 182.0 (277), 124.0 (208), 93.0 (150).), the solution was cooled to RT and concentrated *in vacuo*. The crude product was purified via flash column chromatography (250 g SiO₂, 16 x 5.8 cm, cyclohexane/EtOAc = 1/2, 120 mL frac., frac. 10-21 pooled). 1.70 g of a yellow oil were obtained. It was used without further purification.

In a 25 mL one-neck round-bottom flask equipped with a Schlenk adapter and magnetic stirring bar 388 mg (1.12 mmol, 1 equiv.) of the yellow oil were dissolved in 6.0 mL abs. THF. It was cooled to -78 °C (dry ice/acetone) and 2.70 mL freshly prepared LiHMDS (0.442 M in abs. THF, 1.19 mmol, 1.1 equiv.) were slowly added. The reaction mixture turned orange and it was stirred for 10 min, after which 250 µL (4.46 mmol, 4.0 equiv.) acetaldehyde were added (reaction control via TLC). After 2.5 h, 10 mL sat. NH₄Cl solution were added dropwise. The aqueous phase was extracted with EtOAc (5x15 mL). The combined organic layers were dried over Na₂SO₄, filtered and concentrated *in vacuo*. The crude product was purified via flash column chromatography (25 g SiO₂, 21.5 x 2.1 cm, cyclohexane/DCM/acetone 20/3/0.6, 15 mL frac., frac. 5-8 pooled).

Yield= 194 mg (0.734 mmol, 25 %, 2 steps), slightly yellow oil

C₁₄H₁₆O₅ [264.28 g·mol⁻¹]

R_f= 0.17 (cyclohexane/DCM/acetone = 20/3/0.6)

HRMS (TOF MS EI): m/z: calcd for C₁₄H₁₆O₅⁺ [M]⁺: 264.0998;

found: 264.0981.

^1H NMR (300 MHz, CDCl_3): δ = 7.45 (dt, J = 7.7 Hz, 1.3 Hz, 1H, H-9), 7.23 (d, J = 1.2 Hz, 0.5 H, H-4), 7.12 – 7.03 (m, 1.5 H, H-4, H-8), 6.59 (q, J = 7.2 Hz, 0.5 H, H-11), 5.75 (q, J = 7.6 Hz, 0.5 H, H-11), 3.69-3.54 (2x d, J = 4.1 Hz, J = 7.5 Hz, 6 H, H-1, H-14), 2.23 (s, 1.5 H, H-7), 2.13 (s, 1.5 H, H-7), 1.96 (d, J = 7.6 Hz, 1H, H-12), 1.61 (d, J = 7.2 Hz, 1.5H, H-12).

The isomers could not be separated. They are assigned according to peak height.

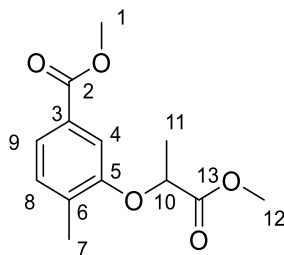
diastereomer 1:

^{13}C -NMR (76 MHz, CDCl_3): δ = 166.9, 163.3, 155.5, 142.0, 132.9, 131.2, 129.1, 127.8, 123.6, 113.2, 52.3, 52.2, 16.6, 11.7

diastereomer 2:

^{13}C -NMR (76 MHz, CDCl_3): δ = 166.9, 163.6, 155.6, 142.1, 133.8, 131.2, 129.2, 126.5, 124.1, 115.8, 52.2, 52.0, 16.6, 13.1.

9.8.11 Methyl 3-((1-methoxy-1-oxopropan-2-yl)oxy)-4-methylbenzoate (**5**)



This compound was prepared following a literature procedure.^[59]

A flame dried and argon flushed 100 mL Schlenk flask equipped with magnetic stirring bar, was consecutively charged with 201 mg (1.21 mmol, 1 equiv.) **1**, 10 mL acetone, 223 μ L (2.00 mmol, 1.7 equiv.) methylbromopropionate, 338 mg (2.45 mmol, 2.0 equiv.) K_2CO_3 and 33 mg (0.22 mmol, 0.18 equiv) NaI. Vigorous stirring was begun and it was stirred at reflux temperature for 15 h. After cooling to RT the solvent was removed *in vacuo*. The residue was redissolved in EtOAc (50 mL) and washed with H_2O (1x25 mL). The organic layer was dried over Na_2SO_4 , filtered and concentrated *in vacuo*. The product was purified via flash column chromatography (10 g SiO_2 , 17 x 0.7 cm, cyclohexane/EtOAc/acetone 20/2/0.1, 7 mL frac., frac. 5-10 pooled).

Yield= 270 mg (1.1 mmol, 88 %) colorless oil

$C_{13}H_{16}O_5$ [252.27 $g \cdot mol^{-1}$]

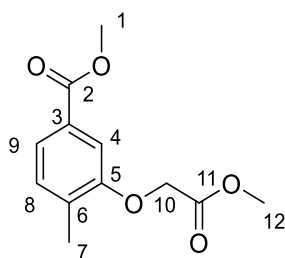
R_f = 0.56 (cyclohexane/EtOAc = 3/1, CAM)

GC-MS (EI, 70 eV, NG-STANDARD): t_R = 6.50; m/z (%)= 252.2 (100 $[M^+]$), 221.1 (37), 193.1 (67), 193.1 (137), 161.1 (67), 135.1 (102).

1H -NMR (300 MHz, $CDCl_3$): δ = 7.55 (dd, 1H, J = 1.2 Hz, J = 7.9 Hz, H-9), 7.32 (d, J = 1.2 Hz, 1H, H-4), 7.18 (d, J = 7.9 Hz, 1 H, H-8), 4.84 (q, J = 6.7 Hz, 1 H, H-10), 3.85 (s, 3H), 3.73 (s, 3H), 2.30 (s, 3H, H-7), 1.62 (d, J = 6.7 Hz, 3 H, H-11).

^{13}C -NMR, APT (76 MHz, $CDCl_3$): = δ 172.5, 167.1, 155.8, 133.6, 131.0, 129.0, 122.9, 112.6, 72.9, 52.4, 52.2, 18.7, 16.8.

9.8.12 Methyl 3-(2-methoxy-2-oxoethoxy)-4-methylbenzoate (**6**)



A 50 mL Schlenk flask equipped with magnetic stirring bar was consecutively charged with 300 mg (1.81 mmol, 1 equiv.) **1**, 15 mL acetone, 0.400 mL (4.21 mmol, 2.3 equiv.) methylbromoacetate, 500 mg (3.62 mmol, 2.0 equiv.) K₂CO₃ and 65 mg (0.434 mmol, 0.24 equiv.) NaI. Vigorous stirring was begun and it was stirred at reflux temperature for 48 h. After cooling to RT the solvent was removed *in vacuo*. The residue was redissolved in EtOAc (50 mL) and washed with H₂O (1x30 mL). The aqueous layer was back-extracted with EtOAc (1x20 mL). The combined organic layers were dried over Na₂SO₄, filtered and concentrated *in vacuo*. The product was purified via flash column chromatography (20 g SiO₂ gel, 19 x 4.0 cm, cyclohexane/DCM/acetone 20/2/1, 15 mL frac., frac. 4-7 pooled).

Yield= 357 mg (0.424 mmol, 83 %) colorless solid

C₁₂H₁₄O₅ [238.24 g·mol⁻¹]

R_f= 0.41 (cyclohexane/EtOAc = 3/1, CAM)

m.p. = 70-71 °C

GC-MS (EI, 70 eV, NG-STANDARD): t_R= 6.48. M+ 238 (100%), 207.1 (68), 179.1 (41) 165.1 (83), 147.1 (50).

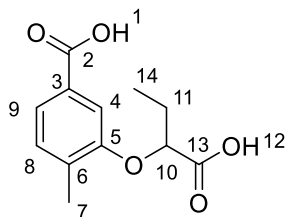
HRMS (TOF MS EI): m/z: calcd for C₁₃H₁₄O₅⁺ [M]⁺: 238.0841;

found: 238.0826.

¹H-NMR (300 MHz, CDCl₃): δ = 7.60 (dd, J = 7.7 Hz, 1.2 Hz, 1H, H-9), 7.36 (d, J = 0.8 Hz, 1H, H-4), 7.21 (d, J = 7.7 Hz, 1H, H-8), 4.72 (s, 2H, H-10), 3.89 (s, 3H), 3.80 (s, 3H), 2.34 (s, 3H).

¹³C-NMR, APT (76 MHz, CDCl₃): δ = 169.3, 167.0, 156.0 (C-5), 133.4, 131.0 (C-8), 129.0, 123.1 (C-9), 111.8 (C-4), 65.5 (C-10), 52.4, 52.2, 16.7 (C-7).

9.8.13 3-(1-Carboxypropoxy)-4-methylbenzoic acid (**7**)



A 50 mL one-neck round-bottom flask equipped with magnetic stirring bar, was consecutively charged with 364 mg (1.37 mmol, 1 equiv.) **2**, 9.0 mL THF, 468 mg (8.34 mmol, 6.1 equiv.) KOH and 10 mL H₂O. The reaction mixture was stirred for 90 min at RT (reaction monitoring via TLC). Subsequently, 20 mL H₂O was added and it was washed with EtOAc (2x20 mL), after which the aqueous phase was acidified using 1 M HCl to pH=1. The solution became cloudy and it was extracted with EtOAc (3x20 mL). The combined organic layers were dried over Na₂SO₄, filtered and concentrated *in vacuo*. No further purification was necessary.

Yield= 289 mg (1.21 mmol, 89 %), colorless solid

C₁₂H₁₄O₅ [238.24 g·mol⁻¹]

R_f= 0.14 (cyclohexane/EtOAc/HOAc = 3/2/0.05, CAM)

m.p. = 187-188 °C

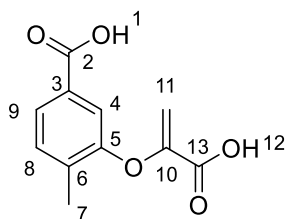
HRMS (FTICR MS ESI): m/z: calcd for C₁₂H₁₃O₅⁻ [M-H]⁻: 237.0768;

found: 237.0767.

¹H-NMR (300 MHz, MeO-d₄): δ = 7.55 (dd, *J* = 7.7 Hz, 1.1 Hz, 1H), 7.38 (s, 1H), 7.24 (d, *J* = 7.7 Hz, 1H), 4.92 (bs, 2H), 4.70 (dd, *J* = 6.5, 5.3 Hz, 1H), 2.33 (s, 3H), 2.15–1.92 (m, 2H), 1.12 (t, *J* = 7.4 Hz, 3H).

¹³C-NMR, APT (76 MHz, MeO-d₄): δ = 174.9, 169.7, 157.4, 134.2, 131.7, 130.6, 123.7, 113.2, 78.4, 27.2, 16.7, 10.0.

9.8.14 3-((1-Carboxyvinyl)oxy)-4-methylbenzoic acid (**8**)



In a 25 mL one-neck round-bottom flask equipped with magnetic stirring bar 239 mg (0.955 mmol, 1 equiv.) **3** were dissolved in a mixture of 1.0 mL 1,4 dioxane and 1.0 mL 3.0 M NaOH. The reaction mixture was stirred overnight at RT. Subsequently, the solvent was removed *in vacuo* and 7 mL H₂O were added. The aqueous phase was washed with Et₂O (1x15 mL), after which the aqueous phase was acidified using 1 M HCl to a pH=3-4. The solution became cloudy and NaCl was added to saturation and it was extracted with EtOAc (7x20 mL). The combined organic layers were dried over Na₂SO₄ and concentrated *in vacuo* to give a colorless solid. No further purification was necessary.

Yield= 168 mg (0.763 mmol, 80 %) colorless solid

C₁₁H₁₀O₅ [220.20 g·mol⁻¹]

R_f= 0.58 (MeOH/EtOAc/HOAc = 1/1/0.01, CAM)

m.p. = 206-209 °C

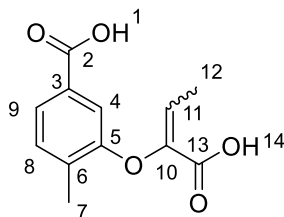
HRMS (TOF MS EI): m/z: calcd for C₁₃H₁₄O₅⁺ [M]⁺: 222.0528;

found: 222.0541.

¹H-NMR (300 MHz, MeO-d₄): δ = 7.79–7.69 (m, 1H, H-9), 7.55 (d, *J* = 1.3 Hz, 1H, H-4), 7.37 (d, *J* = 7.8 Hz, 1H, H-8), 5.70 (d, *J* = 2.1 Hz, 1H, H-11a), 4.80 (d, *J* = 2.1 Hz, 1H, H-11b), 2.30 (s, 3H, H-7).

¹³C-NMR, APT (76 MHz, MeO-d₄): δ = 169.0, 165.4, 154.9, 151.7, 136.3, 132.6, 131.4, 126.9, 120.8, 103.9, 16.2.

9.8.15 3-((1-Carboxyprop-1-en-1-yl)oxy)-4-methylbenzoic acid (**9**)



In a 10 mL one-neck round-bottom flask equipped with magnetic stirring bar 81.3 mg (0.308 mmol, 1 equiv) **4** were dissolved in a mixture of 0.5 mL 1,4-dioxane and 0.5 mL 3 M NaOH. The reaction mixture was stirred for 18 h at RT. Subsequently, 30 mL H₂O were added and the aqueous phase was washed with Et₂O (2x5 mL), after which the aqueous phase was acidified using 1M HCl to a pH=1. The solution became cloudy and the aqueous layer was extracted with EtOAc (5x10 mL). The combined organic layers were dried over Na₂SO₄, filtered and concentrated *in vacuo*. No further purification of the product was necessary.

Yield= 68 mg (0.288 mmol, 93 %) colorless solid

C₁₂H₁₂O₅ [236.22 g·mol]

m.p. = 280-290 °C

R_f= 0.13 (cyclohexane/EtOAc/HOAc = 3/1/0.04)

HRMS (TOF MS EI): m/z: calcd for C₁₄H₁₆O₅⁺ [M+ K]⁺: 275.0322;

found: 275.0315.

¹H-NMR (300 MHz, DMSO-d₆): δ = 7.52 (d, *J* = 7.7 Hz, 1H), 7.33 (m, 1H), 7.23 (d, *J* = 1.0 Hz, 0.2 H), 7.13 (d, *J* = 1.0 Hz, 0.7 H), 6.71 (q, *J* = 7.0 Hz, 0.8 H), 6.09 (q, *J* = 7.5 Hz, 0.2 H), 2.33, 2.27 (2xs, 3H, H-7), 2.07, 1.71 (2xd, *J* = 7.1 Hz, 3H, H-12).

The isomers could not be separated. They are assigned according to peak height.

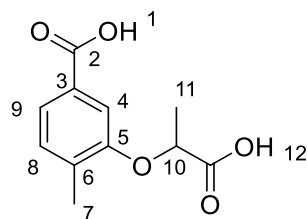
diastereomer 1:

¹³C-NMR (126 MHz, DMSO-d₆): δ = 166.9, 163.3, 155.1, 142.0, 131.5, 131.1, 129.6, 126.8, 122.9, 112.3, 16.1, 11.3.

diastereomer 2:

¹³C-NMR (126 MHz, DMSO-d₆): δ = 166.9, 163.8, 155.7, 141.6, 131.9, 131.5, 129.6, 127.0, 123.0, 113.7, 16.1, 12.9.

9.8.16 3-(1-Carboxy-ethoxy)-4-methyl benzoic acid (**10**)



This compound was prepared following a literature procedure.^[59]

In a 100 mL round-bottom flask equipped with magnetic stirring bar 1.00 g (3.96 mmol, 1 equiv.) **5** were dissolved in 25 mL THF. Subsequently, 957 mg (17.1 mmol, 4.3 equiv.) KOH, dissolved in 25 mL H₂O were added dropwise. It was stirred at 40 °C for 2 h, after which 50 mL H₂O were added and the solution was washed with EtOAc (2x40 mL). The aqueous phase was acidified using 1 M HCl to pH=1 and extracted with EtOAc (3x50 mL). The combined organic layers were dried over Na₂SO₄, filtered and concentrated *in vacuo*.

Yield= 881 mg (3.93 mmol, 99 %), colorless solid

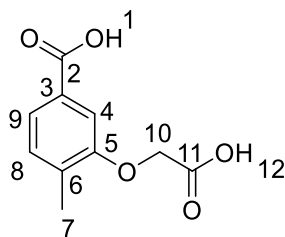
C₁₁H₁₂O₅ [224.21g·mol⁻¹]

R_f= 0.11 (cyclohexane/EtOAc/HOAc = 3/2/0.05)

¹H-NMR (300 MHz, MeO-d₄): δ= 7.55 (dd, 1H, *J*= 1.2 Hz, *J*= 7.9 Hz, H-9), 7.43 (d, *J*= 1.2 Hz, 1H, H-4), 7.24 (d, *J*= 7.9 Hz, 1 H, H-8), 4.86 (q, *J*= 6.7 Hz, 1 H, H-10), 2.31 (s, 3H, H-7), 1.64 (d, *J*= 6.7 Hz, 3 H, H-11).

¹³C-NMR, APT (76 MHz, MeO-d₄): δ= 175.6, 169.7, 157.2, 134.3, 131.7, 130.6, 123.8, 113.4, 73.6, 18.9, 16.7.

9.8.17 3-(Carboxymethoxy)-4-methylbenzoic acid (**11**)



In a 50 mL one-neck round-bottom flask equipped with magnetic stirring bar 30.0 mg (1.26 mmol, 1 equiv) **6** were dissolved in a mixture of 8.5 mL THF, 16 mL H₂O and 484 mg KOH (8.63 mmol, 6.9 equiv.). The reaction mixture was stirred for 15 h at RT. Subsequently, 25 mL H₂O were added and the aqueous phase was washed with Et₂O (2x25 mL) and acidified using 1M HCl to pH=1. The solution became cloudy and the aqueous layer was extracted with Et₂O (3x30 mL). The combined organic layers were dried over Na₂SO₄, filtered and concentrated *in vacuo*. No further purification of the product was necessary.

Yield= 179 mg (0.852 mmol, 68 %) colorless solid

C₁₀H₁₀O₅ [210.19 g·mol⁻¹]

R_f= 0.08 (cyclohexane/EtOAc/HOAc = 3/2/0.05)

m.p. = 241-243 °C

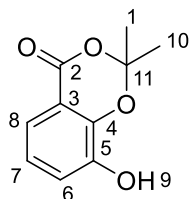
HRMS (TOF MS EI): m/z: calcd for C₁₄H₁₆O₅⁺ [M+ K]⁺: 249.0165;

found: 249.0106.

¹H-NMR (300 MHz, MeO-d₄): δ = 7.56 (d, *J* = 7.7 Hz, 1H), 7.42 (s, 1H), 7.24 (d, *J* = 7.7 Hz, 1H), 4.74 (s, 2H), 2.32 (s, 3H).

¹³C-NMR, APT (76 MHz, MeO-d₄) δ = 172.4, 169.7, 157.5, 134.1, 131.7, 130.6, 123.9, 112.8, 66.0, 16.6.

9.8.18 8-Hydroxy-2,2-dimethyl-4H-benzo[d][1,3]dioxin-4-one (**12**)



This compound was prepared following a literature procedure.^[92]

A 50 mL round-bottom flask equipped with magnetic stirring bar was charged consecutively with 2.01 g (13.04 mmol, 1 equiv.) 2,3-dihydroxy benzoic acid, 20 mL TFA and 10 mL triflic acid anhydride. The cloudy solution was cooled to 0 °C (ice-bath) and stirred vigorously, after which 3.4 mL (46.25 mmol, 3.5 equiv.) acetone were added over the course of 60 min. It was stirred at 0 °C for further 4 h. Subsequently it was warmed to RT and stirred for further 3.5 h. Acetone was removed *in vacuo* and the remainder was poured into 100 mL H₂O (precooled to 0 °C) and NaHCO₃ was added until the solution reached pH=9. A brown, sticky solid precipitated. The aqueous phase was extracted with EtOAc (3x90 mL) and the combined organic layers were dried over Na₂SO₄, filtered and concentrated *in vacuo*. The product was purified via flash column chromatography (90 g SiO₂, 19.0 x 3.5 cm, cyclohexane/EtOAc 5/1, 60 mL frac., frac. 12-19 pooled).

Yield= 838 mg (4.32 mmol, 33 %) colorless solid

C₁₀H₁₀O₄ [194.19 g·mol⁻¹]

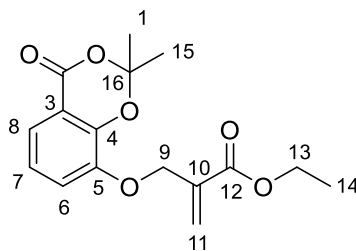
R_f= 0.56 (cyclohexane/EtOAc = 1/1)

GC-MS (EI, 70 eV, NG-STANDARD): t_R= 5.95; m/z (%)= 194.0 (100 [M⁺]), 136.1 (1300), 108.1 (200).

¹H-NMR (300 MHz, CDCl₃): δ = 7.50 (dd, J = 7.8 Hz, 1.4 Hz, 1H), 7.19 (dd, J = 8.0 Hz, 1.4 Hz, 1H), 7.01 (t, J = 7.9 Hz, 1H), 5.57 (s, 1H), 1.74 (s, 6H).

¹³C-NMR (76 MHz, CDCl₃): δ= 160.8, 144.8, 143.5, 122.9, 122.0, 120.9, 114.0, 107.3, 26.0.

9.8.19 Ethyl 2-(((2,2-dimethyl-4-oxo-4H-benzo[d][1,3]dioxin-8-yl)oxy)methyl)acrylate (**13**)



In a flame dried and argon flushed 50 mL Schlenk flask equipped with magnetic stirring bar 213 mg (1.10 mmol, 1 equiv.) **12** were dissolved in 10 mL abs. THF. It was stirred vigorously and cooled to -78 °C (dry ice/acetone) and 56 mg (1.40 mmol, 1.3 equiv.) 60 % dispersion NaH were slowly added. It was stirred at -78 °C for 20 min, after which 198 µL (1.52 mmol, 1.4 equiv.) ethyl-2-(bromomethyl) acrylate were added. The cooling bath was removed and it was warmed to RT. It was stirred for 2 h, after which complete consumption of the starting material was observed (reaction monitoring via TLC) and the solution was poured into 50 mL sat. NH₄Cl solution. It was extracted with EtOAc (4x20 mL) and the combined organic layers were dried over Na₂SO₄, filtered and concentrated *in vacuo*. The product was purified via flash column chromatography (5 g SiO₂, 7.5 x 1.6 cm, cyclohexane/EtOAc 5/1, 3 mL frac., frac. 2-18 pooled).

Yield= 321 mg (1.05 mmol, 95 %) colorless crystals

C₁₆H₁₈O₆ [306.31 g·mol⁻¹]

R_f= 0.53 (cyclohexane/EtOAc = 2/1, CAM)

m.p.: 31-33 °C

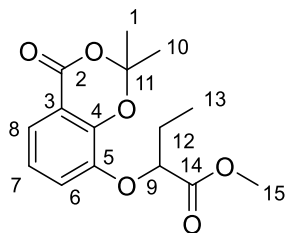
HRMS (TOF MS EI): m/z: calcd for C₁₃H₁₄O₅⁺ [M]⁺: 306.1104;

found: 306.1111.

¹H-NMR (300 MHz, CDCl₃): δ = 7.58 (dd, *J* = 7.8 Hz, 1.4 Hz, 1H), 7.14 (dd, *J* = 8.1 Hz, 1.3 Hz, 1H), 7.02 (t, *J* = 8.0 Hz, 1H), 6.41 (d, *J* = 1.1 Hz, 1H), 5.96 (d, *J* = 1.1 Hz, 1H), 4.83 (s, 2H), 4.25 (q, *J* = 7.3 Hz, 2H), 1.77 (s, 6H), 1.32 (t, *J* = 7.16, 3H).

¹³C-NMR, APT (76 MHz, CDCl₃): δ =165.4, 161.1, 147.2, 146.6, 135.6, 126.6, 122.3, 121.9, 120.8, 114.8, 106.8, 67.9, 61.2, 25.9, 14.3.

9.8.20 Methyl 2-((2,2-dimethyl-4-oxo-4H-benzo[d][1,3]dioxin-8-yl)oxy)butanoate (**14**)



A 50 mL Schlenk flask equipped with magnetic stirring bar was consecutively charged with 199 mg (1.03 mmol, 1 equiv.) **12**, 15 mL acetone, 0.166 mL (1.29 mmol, 1.3 equiv.) methylbromoacetate, 279 mg (2.02 mmol, 2.9 equiv.) K₂CO₃ and 33 mg (0.22 mmol, 0.2 equiv.) NaI. Vigorous stirring was begun and it was stirred at reflux temperature for 42 h. After cooling to RT the solvent was removed *in vacuo*. The residue was redissolved in EtOAc (50 mL) and washed with H₂O (1x20 mL). The aqueous layer was back-extracted with EtOAc (1x20 mL). The combined organic layers were dried over Na₂SO₄, filtered and concentrated *in vacuo*. The product was purified via flash column chromatography (20 g SiO₂, 8 x 2.3 cm, cyclohexane/EtOAc 8/1, 13 mL frac., frac. 10-20 pooled).

Yield= 226 mg (0.768 mmol, 75 %) colorless oil

C₁₅H₁₈O₆ [294.30 g·mol⁻¹]

R_f= 0.46 (cyclohexane/EtOAc = 3/1, CAM)

GC-MS (EI, 70 eV, NG-STANDARD): t_R= 7.05. M⁺ 294.1 (100%), 236.1 (600), 207.0 (425), 177.0 (1400), 136.1 (1600).

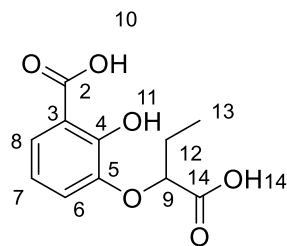
HRMS (TOF MS EI): m/z: calcd for C₁₅H₁₈O₆⁺ [M]⁺: 294.1104;

found: 294.1100.

¹H-NMR (300 MHz, CDCl₃): δ = 7.62 (dd, J = 7.8 Hz, 1.4 Hz, 1H), 7.14 (dd, J = 8.1 Hz, 1.4 Hz, 1H), 6.99 (t, J = 8.0 Hz, 1H), 4.55 (t, J = 6.2 Hz, 1H, H-9), 3.75 (s, 3H, H-15), 2.00 (dd, J = 7.2 Hz, J = 6.3 Hz, 2H, H-12), 1.75 (2 s, 6H, H-1, H-10), 1.09 (t, J = 7.4 Hz, 3H, H-13).

¹³C-NMR, APT (76 MHz, CDCl₃): δ = 171.8, 161.0, 147.0, 146.9, 123.8, 123.0, 122.4, 115.2, 106.8, 80.4 (C-9), 52.3 (C-15), 26.5 (C-12), 26.0, 25.8, 9.8 (C-13).

9.8.21 3-(1-Carboxypropoxy)-2-hydroxybenzoic acid (**15**)



A 15 mL Schlenk flask equipped with magnetic stirring bar was consecutively charged with 99.8 mg (0.339 mmol, 1 equiv.) **14**, 0.5 mL THF, 0.5 mL H₂O and 128 mg (2.28 mmol, 6.7 equiv.) KOH were added. The reaction mixture was stirred for 24 h at reflux temperature. Subsequently, 80 mL H₂O were added and it was washed with Et₂O (2x25 mL), after which the aqueous phase was acidified using 1 M HCl to pH=1. The solution became cloudy and it was extracted with EtOAc (4x40 mL). The combined organic layers were dried over Na₂SO₄, filtered and concentrated *in vacuo*. The remainder was dissolved in 10 mL Et₂O and the insoluble materials were discarded. It was again concentrated *in vacuo* and recrystallized from 7 mL Et₂O/3 mL pentane to obtain the pure product.

Yield= 60 mg (0.250 mmol, 74 %) colorless solid

C₁₁H₁₂O₆ [240.21 g·mol⁻¹]

m.p. = 157-159 °C

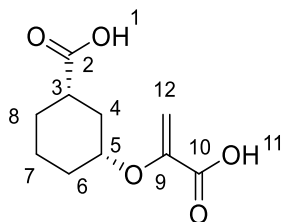
HRMS (TOF MS EI): m/z: calcd for C₁₁H₁₂O₆⁺ [M]⁺: 241.0712;

found: 241.0708.

¹H-NMR (300 MHz, MeOD-d₄): δ = 7.53 (dd, *J* = 8.0 Hz, 1.4 Hz, 1H), 7.12 (dd, *J* = 8.0 Hz, 1.3 Hz, 1H), 6.79 (t, *J* = 8.0 Hz, 1H), 4.68 (t, *J* = 6.0 Hz, 1H), 2.09–1.89 (m, 2H), 1.18–1.03 (t, *J* = 7.4 Hz, 3H, H-13).

¹³C-NMR, APT (76 MHz, MeOD-d₄): δ = 175.1, 173.7, 154.4, 147.8, 124.7, 123.1, 119.4, 114.9, 80.4, 27.1, 9.8.

9.8.22 *cis*-3-((1-Carboxyvinyl)oxy)cyclohexane-1-carboxylic acid (**16**)



In a 10 mL one-neck round-bottom flask equipped with magnetic stirring bar 76.2 mg (0.315 mmol, 1 equiv.) **22** were dissolved in 2.1 mL THF and 4.2 mL H₂O. It was stirred vigorously and 120.5 mg (2.15 mmol, 6.8 equiv.) KOH were added. It was stirred for 19 h, after which full consumption of the starting material was detected (reaction monitoring via TLC) and 10 mL H₂O were added. The solution was washed with Et₂O (2x10 mL) and the aqueous phase was acidified to pH=1 using 1 M HCl. The aqueous phase was extracted with Et₂O (3x10 mL). The combined organic layers were dried over Na₂SO₄, filtered and concentrated *in vacuo*.

C₁₀H₁₄O₅ [214.22 g·mol⁻¹]

R_f= 0.22 (MeOH/EtOAc/HOAc = 1/1/0.01, CAM)

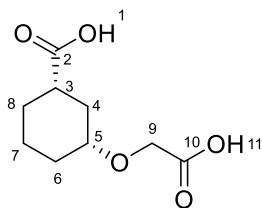
Yield= 57 mg (2.79 mmol, 64 %), colorless oil

HRMS (FTICR MS ESI): m/z: calcd for C₁₀H₁₄NaO₅⁺ [M+Na]⁺: 237.0739;
found: 237.0734.

¹H-NMR (300 MHz, MeO-d₄): δ= 5.41 (d, *J* = 2.3 Hz, 1H), 4.77 (d, *J* = 2.3 Hz, 1H), 4.13-3.99 (m, 1H), 2.50–2.28 (m, 2H), 2.11 (m, 1H), 2.01–1.79 (m, 2H), 1.52–1.22 (m, 4H).

¹³C-NMR, APT (76 MHz, MeO-d₄): δ= 178.4, 166.8, 150.7, 96.0, 76.8, 42.7, 34.7, 31.8, 29.5, 24.3.

9.8.23 *cis*-3-(Carboxymethoxy)cyclohexane-1-carboxylic acid (**17**)



In a 25 mL round-bottom flask equipped with magnetic stirring bar 102 mg (0.443 mmol, 1 equiv.) **21** was dissolved in 3.0 mL THF and 4.0 mL H₂O. It was stirred vigorously and 318 mg (5.67 mmol, 12.8 equiv.) KOH were added. It was stirred for 5 h, after which full consumption of the starting material was observed (reaction monitoring via TLC). Subsequently, the solution was diluted with 20 mL H₂O and it was washed with EtOAc (4x15 mL) and the aqueous phase was acidified to pH=1 using 1 M HCl. The aqueous layer was extracted with EtOAc (4x15 mL) and the combined organic layers were dried over Na₂SO₄, filtered and concentrated *in vacuo*.

Yield= 68.3 mg (0.338 mmol, 76 %), colorless solid

C₉H₁₄O₅ [202.21g·mol⁻¹]

R_f= 0.05 (cyclohexane/EtOAc/HOAc = 3/2/0.05)

m.p. = 125-127 °C

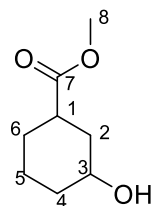
HRMS (FTICR MS ESI): m/z: calcd for C₉H₁₃O₅⁻ [M-H]⁻: 201.0768;

found: 201.0769.

¹H-NMR (300 MHz, MeO-d₄): δ= 4.89 (bs, 2H), 4.13 (s, 2H), 3.46–3.34 (m, 1H), 2.39–2.24 (m, 2H), 2.12-2.02 (m, 1H), 1.94-1.80 (m, 2H), 1.43–1.10 (m, 4H).

¹³C-NMR, APT (76 MHz, MeO-d₄): δ= 178.7, 174.4, 79.4, 66.1, 43.0, 35.7, 32.7, 29.5, 24.4.

9.8.24 Methyl-3-hydroxycyclohexane-1-carboxylate (**18**)



This compound was prepared following a literature procedure.^[97]

In an evacuated, flame dried, and N₂-flushed 250 mL round-bottom flask, equipped with a magnetic stirring bar and a drying tube, 3.17 g **19** (20.3 mmol, 1 equiv.) were dissolved in 85 mL MeOH. The colorless solution was cooled to -78 °C (dry ice/ acetone) and 0.39 g NaBH₄ (10.2 mmol; 0.5 equiv.) were added. The mixture was stirred for 3 h (reaction monitored via TLC), after which full consumption of the starting material was observed. Subsequently, the cooling bath was removed and the mixture was allowed to warm to RT. The solution was then diluted with 150 mL H₂O and extracted with EtOAc (4x70 mL). The combined organic layers were dried over MgSO₄, filtered, and concentrated *in vacuo*. The crude product was purified via flash column chromatography (50 g SiO₂, cyclohexane/EtOAc = 3/2, 15 mL frac., frac. 12-29 pooled).

Yield: 2.43 g (15.4 mmol, 76 %), colorless oil

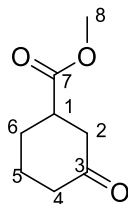
C₈H₁₄O₃ [158.20 g·mol⁻¹]

R_f = 0.24 (cyclohexane/ EtOAc = 3/2, CAM)

¹H-NMR (300 MHz, CDCl₃): δ = 3.65 (s, 3H), 3.63 – 3.52 (m, 1H), 2.34 (m, 1H), 2.23-2.11 (m, 1H), 2.02 (s, 1H, OH), 1.98–1.75 (m, 3H), 1.48–1.12 (m, 4H).

¹³C-NMR, APT (76 MHz, CDCl₃): δ = 175.7, 69.8, 51.8, 41.8, 37.7, 35.0, 28.1, 23.3.

9.8.25 Methyl 3-oxocyclohexane-1-carboxylate (**19**)



The Birch-reduction was performed following a literature procedure.^[94]

A flame dried and N₂ flushed 500 mL three-neck round-bottom flask equipped with a magnetic stirring bar, dry-ice condenser, and gas-bubbler was charged with 10.04 g (66.0 mmol, 1 equiv.) 3-methoxybenzoic acid and 31 mL EtOH (532 mmol; 8.1 equiv.). It was cooled to -33 °C (dry ice/ acetone) and 200 mL NH₃ were condensed into the flask. Subsequently, 6.22 g Na (271 mmol; 4.1 equiv.) were slowly added over the course of 2 h. It was stirred for further 60 min, after which 17.28 g NH₄Cl (323 mmol; 4.9 equiv.) were added. The cooling-bath was removed and NH₃ was evaporated overnight by a gentle stream of N₂. The remainder was dissolved in 40 mL 2 M HCl (pH=1) and heated at reflux temperature (oil-bath) for 7 min. The yellowish suspension was allowed to reach RT and extracted with DCM (4x50 mL). The combined organic layers were dried over Na₂SO₄, filtered and concentrated *in vacuo* to give an amber-colored oil, which solidified upon standing at -20°C. 8.48 g of a beige solid were obtained. It was used without purification.

In an evacuated, flame dried, and N₂ flushed 500 mL three-neck round flask equipped with a magnetic stirring bar, 8.41 g of the beige solid were dissolved in 175 mL DCM. Subsequently, 12 mL abs. MeOH (0.30 mol) and 13.45 g dicyclohexylcarbodiimide (65.2 mmol) were added. The yellowish suspension was stirred for 20 min, cooled to -20°C (dry ice/ acetone) and stirred for further 20 min. Subsequently, 0.073 g (0.60 mmol) 4-dimethylaminopyridine were added to the suspension and it was warmed to RT in the cooling bath over the course of 19 h (reaction monitoring via TLC). The mixture was filtered through a fritted funnel and the solvent removed *in vacuo* to give a beige solid. The crude product was purified via flash column chromatography (200 g SiO₂, cyclohexane/EtOAc 5/1, 100 ml frac., frac. 9-23 pooled). 7.15 g crude product were obtained.

6.69 g of the obtained oil were dissolved in 1000 mL MeOH (HPLC grade) and hydrogenated using the H-Cube[®] (60 bar, 60°C, 1 mL/min, Pd(10%)/C cat.) overnight. The solution was concentrated *in vacuo*. No additional purification was necessary.

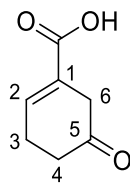
Yield: 6.48 g (41.5 mmol, 68 %, 3 steps) colorless oil

C₈H₁₂O₃ [156.18 g·mol⁻¹]

$^1\text{H-NMR}$ (300 MHz, CDCl_3): δ = 3.67 (s, 3H), 2.77 (m, 1H), 2.51 (d, J = 7.9 Hz, 2H), 2.32 (m, 2H), 2.15–1.95 (m, 2H), 1.89–1.62 (m, 2H).

$^{13}\text{C-NMR}$, APT (76 MHz, CDCl_3) δ = 209.2, 174.2, 52.1, 43.2 (2x), 41.0, 27.8, 24.6.

9.8.26 5-Oxocyclohex-1-ene-1-carboxylic acid (**20**)



This compound is known in the literature and was synthesized similarly.^[146,147]

A flame dried and N₂ flushed 100 mL three-neck round-bottom flask equipped with magnetic stirring bar, dry-ice condenser, and gas-bubbler was charged with 921 mg (6.05 mmol, 1 equiv.) 3-methoxybenzoic acid and 2.7 mL EtOH (46.3 mmol; 7.6 equiv.). It was cooled to -78°C (dry ice/ acetone) and 50 mL NH₃ were condensed into the flask. Subsequently, 559 mg Na (24.3 mmol; 4.0 equiv.) were slowly added over the course of 2 h. It was stirred further 10 min, after which the cooling-bath was removed and NH₃ was evaporated overnight via a gentle stream of N₂. The remainder was dissolved in 6 mL 2 M HCl (pH=1) and heated at reflux temperature (oil-bath) for 8 min. The yellowish suspension was allowed to reach RT, extracted with DCM (5x30 mL). The combined organic layers were dried over Na₂SO₄, filtered and concentrated *in vacuo* to give a yellow oil.

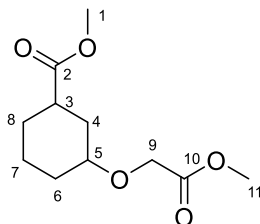
C₇H₈O₃ [140.14 g·mol⁻¹]

¹H-NMR* (300 MHz, CDCl₃): δ= 7.31 (s, 1H), 3.14 (d, *J*= 1.7 Hz, 2H), 2.75–2.62 (m, 2H), 2.51 (m, 2H).

¹³C-NMR, APT (76 MHz, CDCl₃) δ 208.1, 171.1, 141.1, 128.1, 38.8, 37.2, 25.4.

*compared with F.X Webster and R. M. Silverstein.^[111] For the (1,6)-double bond isomer see Herzog et al.^[148]

9.8.27 Methyl 3-(2-methoxy-2-oxoethoxy)cyclohexane-1-carboxylate (**21**)



A flame dried and argon flushed 50 mL Schlenk flask equipped with magnetic stirring bar was consecutively charged with 403 mg (2.55 mmol, 1equiv.) **18**, 5.0 mL abs. DCM and 3.0 mg (0.0068 mmol, 2.7 mol%) $\text{Rh}_2(\text{OAc})_4$. It was stirred vigorously and 329 mg (3.29 mmol, 1.3 equiv.) **R-2** (dissolved in 6.0 mL abs. DCM) were added over the course of 1 h, until which full consumption of the starting material was detected (reaction monitoring via TLC). The solution was concentrated *in vacuo* and the crude product was purified via flash column chromatography (9.8 g SiO_2 , 11.0 x 1.7 cm, cyclohexane/EtOAc 5/1, 7 mL frac., frac. 4-9 pooled).

Yield= 554 mg (2.41 mmol, 94 %), colorless oil

$\text{C}_{11}\text{H}_{18}\text{O}_5$ [230.26g·mol⁻¹]

R_f = 0.47 (C/EA= 2/1, CAM)

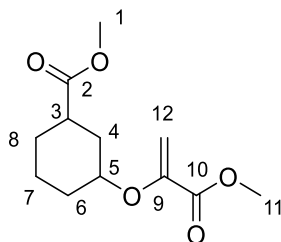
HRMS (FTICR MS ESI): m/z: calcd for $\text{C}_{11}\text{H}_{19}\text{O}_5^+$ [M+H]⁺: 231.1232;

found: 231.1227.

¹H-NMR (300 MHz, CDCl_3): δ = 4.11 (s, 2H), 3.76 (s, 3H), 3.67 (s, 3H), 3.41–3.26 (m, 1H), 2.29 (m, 2H), 2.05 (m, 1H), 1.88 (m, 2H), 1.50–1.16 (m, 4H).

¹³C-NMR, APT (76 MHz, CDCl_3): δ = 175.3, 171.3, 78.2, 65.7, 52.0, 51.8, 41.9, 34.3, 31.7, 28.3, 23.5.

9.8.28 Methyl 3-((3-methoxy-3-oxoprop-1-en-2-yl)oxy)cyclohexane-1-carboxylate (**22**)



A flame dried and argon flushed 250 mL Schlenk flask equipped with magnetic stirring bar and a bubbler was consecutively charged with 691 mg (4.37 mmol, 1 equiv.) **18**, 20 mL abs. toluene, 1.16 g (5.57 mmol, 1.3 equiv.) methyl 2-diazo-2-(dimethoxyphosphoryl)acetate and 23 mg (0.052 mmol, 1 mol%) Rh₂(OAc)₄. Vigorous stirring was begun and it was stirred at 70 °C for 14 h, after which full consumption of the starting material was detected (reaction monitoring via TLC, R_f(crude product)= 0.12, cyclohexane/EtOAc = 1/1) and the solution was cooled to RT and concentrated *in vacuo*. The crude product was purified via flash column chromatography (60 g SiO₂, 22 x 3.0 cm, cyclohexane/EtOAc 1/2 (frac. 1-13), cyclohexane/EtOAc 1/3 (frac. 14-21), EtOAc (frac. 22-28), 50 mL frac., frac. 21-27 pooled). 943 mg of a crude green oil were obtained. It was used without further purification.

In a flame dried and argon flushed 50 mL round-bottom flask equipped with a Schlenk adapter and magnetic stirring bar 855 mg of the prepared intermediate were dissolved in 10 mL abs. THF. It was cooled to -78 °C (dry ice/acetone) and 3.1 mL LiHMDS (0.87 M in THF, 2.69 mmol; freshly prepared) was slowly added. The solution was stirred for 45 min before a formaldehyde solution, produced by cracking paraformaldehyde (approximately 24.2 mmol in 8.0 mL THF) was added and it was stirred for further 60 min. The solution was poured into 100 mL sat. NH₄Cl solution. The aqueous phase was extracted with EtOAc (4x40 mL) and the combined organic layers were dried over Na₂SO₄, filtered and concentrated *in vacuo*. The product was purified via flash column chromatography (19 g SiO₂, 12.5x2.2 cm, cyclohexane/EtOAc = 4:1, 12 mL frac., frac. 7-9 pooled).

Yield= 471 mg (1.94 mmol, 44 %, 2 steps) colorless solid

C₁₂H₁₈O₅ [242.27 g·mol⁻¹]

R_f= 0.38 (cyclohexane/ EtOAc 4/1, UV)

m.p. = 38-41 °C

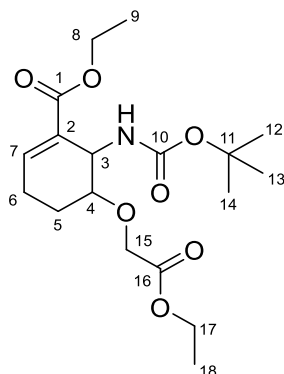
HRMS (TOF MS EI): m/z: calcd for C₁₃H₁₄O₅⁺ [M]⁺: 242.1154;

found: 242.1167.

$^1\text{H-NMR}$ (300 MHz, CDCl_3): δ = 5.43 (d, J = 2.4 Hz, 1H), 4.64 (d, J = 2.3 Hz, 1H), 4.03–3.87 (m, 1H), 3.78 (s, 3H), 3.66 (s, 3H), 2.46–2.28 (m, 2H), 2.18–2.04 (m, 1H), 2.00–1.81 (m, 2H), 1.66–1.22 (m, 4H).

$^{13}\text{C-NMR}$, APT (76 MHz, CDCl_3): δ = 174.8, 164.0, 149.4, 95.9, 75.8, 52.4, 51.8, 41.7, 33.4, 30.7, 28.1, 23.2.

9.8.29 Ethyl-6-((tert-butoxycarbonyl)amino)-5-(2-ethoxy-2-oxoethoxy)cyclohex-1-ene-1-carboxylate (**23**)



In a flame dried and argon flushed Schlenk flask equipped with a magnetic stirring bar 102.6 mg (0.360 mmol, 1 equiv.) **24** were dissolved in 1 mL abs. DCM and 2.6 mg (0.00589 mmol, 1.6 mol%) $\text{Rh}_2(\text{OAc})_4$ were added. To the stirred solution 64 mg (0.557 mmol, 1.5 equiv.) ethyl diazoacetate, dissolved in 3.0 mL abs. DCM, were added over 1 h. It was stirred for another 60 min, after which full consumption of the starting material was observed (reaction control via TLC). The solution was concentrated *in vacuo* to give a yellow oil. The crude product was purified via flash column chromatography (4.7 g SiO_2 , 8.5 x 1.3 cm, cyclohexane/EtOAc 3/1, 3 mL frac., frac. 12-22 pooled).

Yield: 70.4 mg (0.190 mmol, 53 %), colorless solid

$\text{C}_{18}\text{H}_{29}\text{NO}_7$ [371.43 $\text{g}\cdot\text{mol}^{-1}$]

$R_f = 0.20$ (cyclohexane/EtOAc = 3/1, CAM)

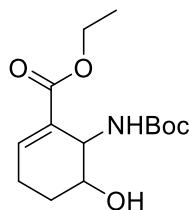
m.p. = 106-107°C

HRMS (TOF MS EI+): m/z: calcd for $\text{C}_{17}\text{H}_{25}\text{NO}_7^+$ $[\text{M}]^+$: 371.1944;

$^1\text{H-NMR}$ (300 MHz, CDCl_3): $\delta = 7.22$ (s, 1H, H-7), 4.51 (d, 1H, $J = 6.0$ Hz, H-3), 4.25-4.10 (m, 6H, H-8, H-15, H-17), 3.77 (s, 1H, H-4), 2.44 (m, 1H), 2.19 (dt, $J = 20.2$ Hz, 5.0 Hz, 1H), 2.03 (m, 1H), 1.66 (d, $J = 17.6$ Hz, 1H), 1.44 (s, 9H, H-12-14), 1.27 (2xt, $J = 7.1$ Hz, 6H, H9, H-18).

$^{13}\text{C-NMR}$ (76 MHz, CDCl_3): $\delta = 170.9$, 166.2, 154.9 (C-10), 144.1 (C-7), 127.5 (C-2), 79.8 (C-11), 77.4 (C-4), 67.0 (C-15), 60.9, 60.8, 46.0 (C-3), 28.5 (C-12-14), 21.6, 21.5, 14.3 (2 peaks).

9.8.30 Ethyl 6-((tert-butoxycarbonyl)amino)-5-hydroxycyclohex-1-ene-1-carboxylate (**24**)



A base-mediated opening of **25** was also performed in the PhD thesis of Mario Leypold.^[41]

In a flame dried and argon flushed 50 mL Schlenk flask equipped with magnetic stirring bar were placed 12 mL of abs. THF and 835 mg (4.19 mmol, 3.0 equiv.) KHMDS. The solution was cooled to -50 °C (dry ice/acetone). Subsequently, a solution of 403.5 mg (1.41 mmol, 1 equiv.) **25** in 6 mL abs. THF was added. The reaction was stirred for 5 h, when complete consumption of the starting material was observed (reaction monitoring via TLC). The solution was poured into 40 mL sat. NH₄Cl solution and the aqueous phase was extracted with EtOAc (3x40 mL). The combined organic layers were dried over Na₂SO₄, filtered and concentrated *in vacuo*. The crude product was purified via flash column chromatography (30 g SiO₂, 11.5 x 3.0 cm, cyclohexane/EtOAc 10/1 (frac. 1-15), C/EtOAc 2/1 (frac. 16-48), 20 mL frac., frac. 34-46 pooled).

Yield: 151 mg (0.53 mmol, 38 %), colorless solid

C₁₄H₂₃NO₅ [285.34 g·mol⁻¹]

R_f = 0.31 (cyclohexane/EtOAc = 1/1, KMnO₄)

m.p. = 110–112 °C

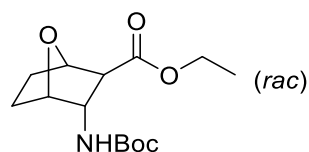
HRMS (TOF MS EI⁺): m/z: calcd for C₁₄H₂₃NO₅⁺ [M]⁺: 285.1576;

found.: 285.1574.

¹H-NMR (300 MHz, CDCl₃): δ= 7.18 (s, 1H, H-2), 4.55 (bs, 1H, O-H), 4.17 (bs, 1H, H-5), 4.17–4.11 (m, 2H, H-5, H-6), 4.03 (bs, 1H, H-8), 2.85 (bs, 1H, H-3), 2.41 (bs, 1H, H-3), 2.24 (m, 1H, H-4), 1.83-1.64 (m, 1H, H-4), 1.43 (s, 9H, H-12, H-13, H-14), 1.27 (t, *J* = 7.0 Hz, 3H, H-9).

¹³C-NMR, APT (76 MHz, CDCl₃): δ= 166.3, 155.7, 143.7, 128.0, 80.0, 69.1, 60.7, 50.9, 28.5, 24.1, 21.7, 14.3.

9.8.31 Ethyl 3-((tert-butoxycarbonyl)amino)-7-oxabicyclo[2.2.1]heptane-2-carboxylate (**25**)



This compound is known in the literature and was prepared analogously.^[98]

A colourless 5 mM solution of the substrate was prepared by dissolving 999.2 mg (3.53 mmol, 1 equiv.) **26** in 70 mL MeOH and transferred into a 150 mL beaker. For the reduction itself a continuous-flow hydrogenation reactor (H-cube) with a 10 % Pd/C catalyst cartridge was used with the following conditions:

1.0 mL/min, RT, atmospheric pressure, full H₂.

The reaction was stopped after multiple runs (ca. 6 times, 8 h). The product solution was transferred to a 250 mL round-bottom flask and the solvent was removed *in vacuo*. No further purification was needed.

Yield: 995.5 mg (3.49 mmol, 99 %), colorless solid

C₁₄H₂₃NO₅ [285.34 g·mol⁻¹]

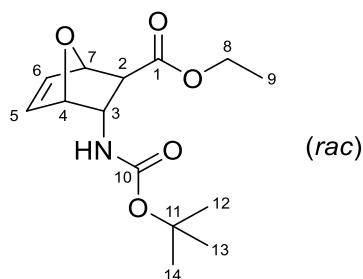
R_f = 0.73 (cyclohexane/ EtOAc = 2/3, KMnO₄)

m.p. = 113–115 °C

¹H-NMR (300 MHz, CDCl₃): δ= 4.72 (m, 2H, H-1, NH), 4.25 (d, *J* = 4.9 Hz, 1H, H-3), 4.18 (q, *J* = 7.1 Hz, 2H, H-8), 2.15 (d, *J* = 4.7 Hz, 1H, H-2), 1.92–1.75 (m, 2H, H-5, H-6), 1.75 – 1.47 (m, 3H, H-4, H-5, H-6), 1.43 (s, 9H, H-12, H-13, H-14), 1.26 (t, *J* = 7.1 Hz, 3H, H-9).

¹³C-NMR (76 MHz, CDCl₃): δ= 172.2, 155.6, 79.8, 78.5, 77.4, 61.3, 56.2, 55.2, 30.2, 28.4, 22.5, 14.3.

9.8.32 Ethyl endo-3-((tert-butoxycarbonyl)amino)-7-oxabicyclo[2.2.1]hept-5-ene-exo-2-carboxylate (**26**)



This compound was prepared following a literature procedure.^[99]

In a 2 L one-neck round-bottom flask equipped with magnetic stirring bar and gas bubbler 18.2 g (85.4 mmol, 1 equiv.) oxanorbornene **27** were dissolved in 790 mL EtOH and cooled to 0 °C (ice bath). The stirred yellow solution was treated with 120 mL (1.44 mol, 16.8 equiv.) conc. HCl, followed by the portionwise addition of 110.8 g (1.69 mol, 19.8 equiv.) activated zinc dust (activation by washing twice with 1 M HCl, H₂O, MeOH and subsequent drying *in vacuo*). The gray suspension was stirred at 0 °C for 30 min and then at RT for 18 h (reaction monitoring via TLC). Subsequently, the suspension was filtered through a pad of Celite and the filter cake was washed with EtOH (1x300 mL). The filtrate was then transferred into a 2 L one-neck round-bottom flask equipped with magnetic stirring bar, pressure-equalizing dropping funnel and gas bubbler, after which 195 mL (1.40 mol, 16.4 equiv.) triethylamine were added dropwise. The resulting colorless suspension was treated with 51.0 g (234 mmol, 2.7 equiv.) di-*tert*-butyl dicarbonate and stirred at RT for 24 h (reaction monitoring via TLC). Subsequently, the reaction mixture was concentrated *in vacuo* to give a pale yellow solid, which was washed with EtOAc (1x1.4 L). The organic phase was washed with H₂O (1x1.1 L) and the aqueous layer was then back-extracted with EtOAc (1x200 mL). The combined organic layers were washed with sat. NaHCO₃ solution (1x450 mL), dried over Na₂SO₄, filtered and concentrated *in vacuo*. The crude product was dissolved in DCM, adsorbed on 40 g SiO₂ and purified via flash column chromatography (300 g SiO₂, 15.0 x 8.0 cm, cyclohexane/EtOAc 3/1 (frac. 1-16), cyclohexane/EtOAc 2/1 (frac. 17-20), cyclohexane/EtOAc 1/1 (frac. 21-23), EtOAc (frac. 24-26), 200 mL frac., frac. 9-26 pooled).

Yield: 21.1 g (74.4 mmol, 87 %), colorless solid

C₁₄H₂₁NO₅ [283.32 g·mol⁻¹]

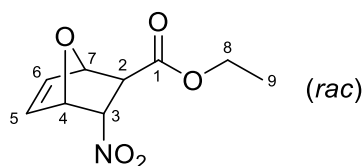
R_f = 0.29 (cyclohexane/EtOAc = 2/1, CAM)

m.p. = 101 °C

$^1\text{H-NMR}$ (300 MHz, CDCl_3): δ = 6.61 (dd, J = 5.8 Hz, 1.6 Hz, 1H, H-6), 6.47 (dd, J = 5.8 Hz, 1.4 Hz, 1H, H-5), 5.13 (s, 1H, H-7), 5.07 (bs, 1H, H-4), 4.55 (bs, 1H, H-3), 4.21 (q, J = 7.1 Hz, 3H, H-8, NH), 2.05 (d, J = 3.5 Hz, 1H, H-2), 1.44 (s, 9H, H-12, H-13, H-14), 1.29 (t, J = 7.1 Hz, 3H, H-9).

$^{13}\text{C-NMR}$, APT (76 MHz, CDCl_3): δ = 171.9 (C-1), 155.1 (C-10), 138.0 (C-6), 134.6 (C-5), 82.2 (C-7), 79.1 (C-4), 61.4 (C-8), 53.3 (C-3), 52.6 (C-2), 28.5 (C-12, C-13, C-14), 14.3 (C-9). ^{13}C -signal of quaternary C-11 could not be observed.

9.8.33 Ethyl endo-3-nitro-7-oxabicyclo[2.2.1]hepta-5-ene-exo-2-carboxylate (**27**)



This compound was prepared following a literature procedure.^[99]

In a 250 mL one-neck round-bottom flask equipped with magnetic stirring bar 23.9 mL (329 mmol, 2.00 equiv.) furan were added to a stirred and cooled (-20 °C, acetone bath/cryostat) solution of 23.8 g (164 mmol, 1 equiv.) **28** in 90 mL chloroform. The flask was covered with aluminium foil to exclude light and the reaction mixture was stirred at -20 °C for 5 d and then at RT for 2 d (reaction monitoring via TLC). Subsequently, the orange solution was concentrated *in vacuo* to give a yellow solid. The crude product was dissolved in DCM and purified via flash column chromatography (550 g SiO₂, 23.0 x 8.0 cm, cyclohexane/EtOAc 8/1, 200 mL frac., frac. 11-15 pooled). Fractions containing both diastereomers were purified via two additional flash column chromatographies (same conditions). Residual dienophile **33** was removed *in vacuo*.

Yield: 18.8 g (88.0 mmol, 54 %), colorless crystals

C₉H₁₁NO₅ [213.19 g·mol⁻¹]

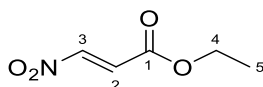
R_f = 0.40 (cyclohexane/EtOAc = 3/1, CAM)

m.p. = 49-50 °C

¹H-NMR (300 MHz, C₆D₆): δ = 5.76 (m, 2H, H-5, H-6), 5.34 (dd, *J* = 4.8 Hz, 3.1 Hz, 1H, H-3), 4.91 (s, 1H, H-7), 4.85 (d, *J* = 4.7 Hz, 1H, H-4), 3.84 (q, *J* = 7.1 Hz, 2H, H-8), 2.93 (d, *J* = 3.0 Hz, 1H, H-2), 0.85 (t, *J* = 7.1 Hz, 3H, H-9).

¹³C-NMR, APT (76 MHz, C₆D₆): δ = 169.6 (C-1), 138.7 (C-6), 133.7 (C-5), 84.7 (C-3), 83.3 (C-7), 79.1 (C-4), 61.7 (C-8), 49.3 (C-2), 14.0 (C-9).

9.8.34 Ethyl (E)-3-nitroprop-2-enoate (**28**)



This compound was prepared following a literature procedure.^[100]

In a flame dried and argon flushed 1000 mL three-neck round-bottom flask equipped with magnetic stirring bar, pressure-equalizing dropping funnel and gas bubbler 27.2 g (167 mmol, 1 equiv.) **29** were dissolved in 340 mL abs. DCM and cooled to -20 °C (dry ice/acetone). To the stirred, reddish-orange solution were added dropwise 39 mL (504 mmol, 3.0 equiv.) methanesulfonyl chloride within 20 min. Subsequently, 71 mL (509 mmol, 3.1 equiv.) abs. triethylamine were added dropwise within 30 min, whereupon a reddish-brown suspension formed. The reaction mixture was allowed to warm to RT and was stirred overnight. Upon completion of the reaction (TLC, 17 h), the suspension was poured into 1.2 L ice-cold H₂O and stirred for 10 min. The organic phase was separated and the aqueous phase was extracted with DCM (2x300 mL). The combined organic layers were washed with H₂O (3x200 mL), dried over Na₂SO₄, filtered and concentrated *in vacuo* to give a brownish oil. The crude product was purified via fractional distillation (14 cm Vigreux column, 0.72 mbar, 36-50 °C) to give impure fractions of product containing different amounts of methanesulfonyl chloride. Subsequent flash column chromatography (500 g SiO₂, 22.0 x 8.0 cm, cyclohexane/EtOAc 19/1 (frac. 1-6), cyclohexane/EtOAc 9/1 (frac. 7-8), 500 mL frac., frac. 4-8 pooled, product was detected visually).

Yield: 14.0 g (96.3 mmol, 58 %), bright yellow oil with pungent odor

C₅H₇NO₄ [145.11 g·mol⁻¹]

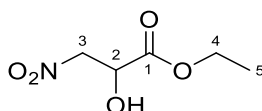
R_f = 0.62 (cyclohexane/EtOAc = 5/1, KMnO₄)

b.p. = 48-50 °C (0.70 mbar)

¹H-NMR (300 MHz, CDCl₃): δ = 7.67 (d, *J* = 13.5 Hz, 1H, H-3), 7.08 (d, *J* = 13.5 Hz, 1H, H-2), 4.32 (q, *J* = 7.1 Hz, 2H, H-4), 1.34 (t, *J* = 7.1 Hz, 3H, H-5).

¹³C-NMR, APT (76 MHz, CDCl₃): δ = 162.8 (C-1), 149.1 (C-3), 127.8 (C-2), 62.6 (C-4), 14.1 (C-5).

9.8.35 Ethyl 2-hydroxy-3-nitropropanoate (**29**)



This compound was prepared following a literature procedure.^[100]

A 500 mL two-neck round-bottom flask equipped with magnetic stirring bar, air condenser and drying tube (CaCl₂) was consecutively charged with 54 mL (0.27 mol, 1 equiv.) ethyl glyoxylate solution (ca. 50 % soln. in toluene), 126 mL (2.33 mol, 8.8 equiv.) nitromethane and 54.0 g (0.53 mol, 2.0 equiv.) aluminum oxide (activated, neutral). The reaction mixture was stirred and heated at reflux temperature until complete consumption of the starting material (TLC, 48 h). The resulting brownish-red suspension was allowed to cool to RT, filtered through a glass frit and the filter cake was washed with EtOAc (3x100 mL). The solvent was removed *in vacuo* to give a brownish-red oil, which was purified via flash column chromatography (500 g SiO₂, 22.0 x 7.5 cm, cyclohexane/EtOAc 2/1 (frac. 1-5), cyclohexane/EtOAc 1/1 (frac. 6-11), cyclohexane/EtOAc 1/2 (frac. 12-16), 250 mL frac., frac. 7-16 pooled). The resulting brownish-red oil was crystallized in the fridge overnight.

Yield: 35.4 g (0.22 mol, 82 %), orange to pale yellow crystals

C₅H₉NO₅ [163.13 g·mol⁻¹]

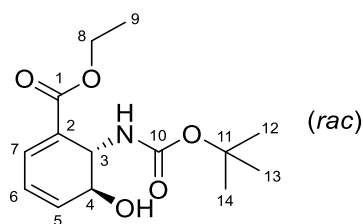
R_f = 0.26 (cyclohexane/EtOAc = 2/1, CAM)

m.p. = 35-37 °C

¹H-NMR (300 MHz, CDCl₃): δ = 4.77 (d, *J* = 4.1 Hz, 2H, H-3), 4.63 (m, 1H, H-2), 4.40-4.30 (m, 2H, H-4), 3.33 (d, *J* = 4.1 Hz, 1H, OH), 1.33 (t, *J* = 7.1 Hz, 3H, H-5).

¹³C-NMR, APT (76 MHz, CDCl₃): δ = 170.8 (C-1), 76.9 (C-3), 67.7 (C-2), 63.3 (C-4), 14.2 (C-5).

9.8.36 Ethyl trans-6-((tert-butoxycarbonyl)amino)-5-hydroxycyclohexa-1,3-diene-1-carboxylate (**30**)



This compound was prepared following a literature procedure.^[101]

In a flame dried and argon flushed 250 mL two-neck round-bottom flask equipped with magnetic stirring bar 4.22 g (21.2 mmol, 3.02 equiv.) KHMDS were dissolved in 68 mL abs. THF and cooled to -45 °C (dry ice/acetone). To the stirred solution were added 1.99 g (7.01 mmol, 1 equiv.) oxanorbornene **26** dissolved in 30 mL abs. THF and precooled to -45 °C (dry ice/acetone) via cannula, whereupon a bright yellow solution formed. The flask containing the solution of **4** was rinsed with 12 mL abs. THF. The mixture was stirred at -45 °C until complete consumption of the starting material (TLC, 100 min). Subsequently, the reaction mixture was poured into a separatory funnel containing 200 mL sat. NH₄Cl solution. The aqueous phase was extracted with EtOAc (3x90 mL). The combined organic phases were dried over Na₂SO₄, filtered and concentrated *in vacuo* to give a brownish-yellow oil. The crude product was purified via flash column chromatography (120 g SiO₂, 18.0 x 4.5 cm, cyclohexane/EtOAc 3/2 (frac. 1-16), cyclohexane/EtOAc 1/1 (frac. 17-21), 80 mL frac., frac. 13-21 pooled).

Yield: 1.37 g (4.84 mmol, 69 %), colorless solid

C₁₄H₂₁NO₅ [283.32 g·mol⁻¹]

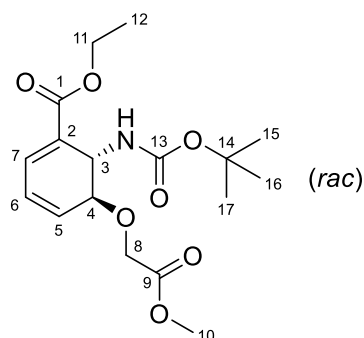
R_f = 0.36 (cyclohexane/EtOAc = 2/3, CAM)

m.p. = 96-97 °C

¹H-NMR (300 MHz, CDCl₃): 7.17 (d, *J* = 4.3 Hz, 1H, H-7), 6.27 (m, *J* = 4.2 Hz, 2H, H-5, H-6), 4.78 (d, *J* = 7.7 Hz, 1H, H-3), 4.59-4.12 (m, 5H, H-4, H-8, NH), 2.63 (bs, 1H, OH), 1.44 (s, 9H, H-12, H-13, H-14), 1.30 (t, *J* = 7.1 Hz, 3H, H-9).

¹³C-NMR, APT (76 MHz, CDCl₃): 155.6 (C-10), 133.6 (C-7), 132.8 (C-5), 124.7 (C-6), 68.1 (C-4), 61.0 (C-8), 50.4 (C-3), 28.5 (C-12, C-13, C-14), 14.3 (C-9). ¹³C-signals of quaternary C-1, C-2, C-11 could not be observed.

9.8.37 Ethyl trans-6-((tert-butoxycarbonyl)amino)-5-(2-methoxy-2-oxoethoxy)cyclohexa-1,3-diene-1-carboxylate (**31**)



In a flame dried and argon flushed 100 mL Schlenk flask equipped with magnetic stirring bar 705 mg (2.49 mmol, 1 equiv.) **30** were dissolved in 32 mL abs. THF and cooled to -20 °C (dry ice/acetone). To the stirred, slightly yellowish solution 131 mg (3.28 mmol, 1.32 equiv.) NaH (60 % dispersion in mineral oil) were added, whereupon the solution became cloudy. After 15 min, 415 μ L (4.38 mmol, 1.76 equiv.) methyl bromoacetate were added dropwise to the yellow solution, while the temperature was kept at -20 °C. The mixture was stirred and allowed to warm to 0 °C within 4 h (reaction monitoring via TLC). Subsequently, the reaction mixture was poured into a flask containing 50 mL ice-cold sat. NH_4Cl solution. The aqueous phase was extracted with EtOAc (3x120 mL). The combined organic layers were dried over Na_2SO_4 , filtered and concentrated *in vacuo* to give a yellow oil. The crude product was purified via flash column chromatography (38 g SiO_2 , 25.5 x 2.5 cm, cyclohexane/EtOAc 4/1 (frac. 1-39), cyclohexane/EtOAc 2/1 (frac. 40-63), cyclohexane/EtOAc 1/2 (frac. 64-65), 20 mL frac., frac. 24-40 pooled). In addition, 240 mg starting material **36** (frac. 52-65 pooled) were recovered.

Yield: 337 mg (0.949 mmol, 38 %), colorless solid

$\text{C}_{17}\text{H}_{25}\text{NO}_7$ [355.39 g·mol⁻¹]

R_f = 0.28 (cyclohexane/EtOAc = 2/1, CAM)

m.p. = 70-71 °C

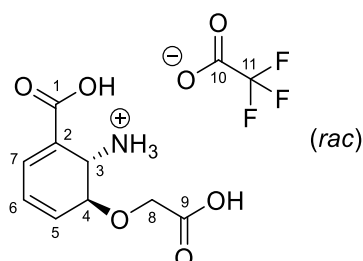
HPLC-MS ("standard-1"): t_R = 3.57 min (m/z = 378 [M+Na]⁺, λ_{max} = 279 nm).

HRMS (TOF MS EI): m/z: calcd for $\text{C}_{17}\text{H}_{25}\text{NO}_7^+$ [M]⁺: 355.1631;
found: 355.1637.

$^1\text{H-NMR}$ (300 MHz, CDCl_3): δ = 7.18 (m, 1H, H-7), 6.32 (m, 2H, H-5, H-6), 4.84 (d, J = 7.3 Hz, 1H, H-3), 4.47-4.13 (m, 5H, H-8, H-11, NH), 4.08 (s, 1H, H-4), 3.74 (s, 3H, H-10), 1.42 (s, 9H, H-15, H-16, H-17), 1.29 (t, J = 7.1 Hz, 3H, H-12).

$^{13}\text{C-NMR}$ (76 MHz, CDCl_3): δ = 171.2 (C-9), 165.8 (C-1), 155.1 (C-13), 133.7 (C-7), 130.0 (C-5), 127.6 (C-2), 125.8 (C-6), 80.0 (C-14), 75.6 (C-4), 66.2 (C-8), 61.0 (C-11), 52.0 (C-10), 46.2 (C-3), 28.5 (C-15, C-16, C-17), 14.3 (C-12).

9.8.38 *trans*-2-Carboxy-6-(carboxymethoxy)cyclohexa-2,4-dien-1-ammonium 2,2,2-trifluoroacetate (**32**)



In a 25 mL one-neck round-bottom flask with magnetic stirring bar 7.5 mL (98 mmol, 234 equiv.) trifluoroacetic acid were added dropwise within 5 min to a stirred solution of 149 mg (418 μmol , 1 equiv.) **31** in 7.5 mL DCM. Upon completion of the reaction (HPLC (“standard-2”): t_{R} = 3.57 min (m/z = 256), 2 h), the pale yellow solution was concentrated in vacuo. The resulting solid was dissolved in 4 mL THF and treated with 2.89 mL (5.02 mmol, 12 equiv.) 1.74 M KOH solution. The mixture was stirred at RT until complete consumption of the starting material (HPLC (“standard-2”): t_{R} = 2.45 min (m/z = 214), 2 h). Subsequently, the solution was diluted with 3 mL H_2O and washed with Et_2O (2x2 mL). The aqueous phase was then acidified with 50 % trifluoroacetic acid to pH=2 and concentrated *in vacuo* to afford a mixture of **38** and potassium trifluoroacetate.

The mass concentration of compound **38** was determined via $^1\text{H-NMR}$ -spectroscopy using trimethylamine hydrochloride ($\delta(\text{D}_2\text{O}) = 2.90$ ppm) as an external standard: In a NMR tube 100 μL of a 1.81 $\text{g}\cdot\text{L}^{-1}$ $\text{Me}_3\text{N}\cdot\text{HCl}$ solution in D_2O were added to a solution of 23.4 mg of the obtained mixture in D_2O using a 250 μL Hamilton syringe. The mass concentration was calculated via integration.

Yield: 738 mg (13 wt % mixture with F_3CCOOK , 300 μmol , 72 %), off-white solid

$\text{C}_{11}\text{H}_{12}\text{F}_3\text{NO}_7$ [327.21 $\text{g}\cdot\text{mol}^{-1}$]

HPLC-MS (“standard-2”): t_{R} = 2.45 min (m/z = 214 $[\text{MH}]^+$, λ_{max} = 280 nm).

HRMS (FTICR MS ESI): m/z : calcd for $\text{C}_9\text{H}_{12}\text{NO}_5^+$ $[\text{MH}]^+$: 214.0710;
found: 214.0711.

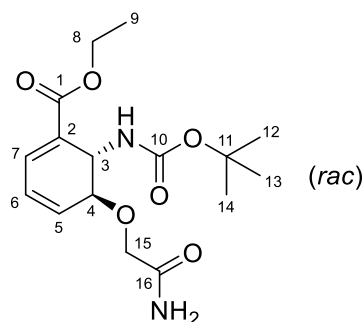
$^1\text{H-NMR}$ (500 MHz, D_2O): δ = 7.35 (d, J = 5.4 Hz, 1H, H-7), 6.52-6.42 (m, 2H, H-5, H-6), 4.57 (d, J = 5.7 Hz, 1H, H-3), 4.51-4.46 (m, 1H, H-4), 4.27 (d, J = 16.6 Hz, 1H, H-8), 4.22 (d, J = 16.7 Hz, 1H, H-8).

^{13}C -NMR (126 MHz, D_2O): δ = 175.3 (C-9), 169.1 (C-1), 162.9 (q, J = 35.5 Hz, C-10), 136.3 (C-7), 129.4 (C-5), 126.2 (C-6), 123.9 (C-2), 116.3 (q, J = 291.7 Hz, C-11), 73.5 (C-4), 66.1 (C-8), 48.2 (C-3).

^{19}F -NMR (470 MHz, D_2O): δ = -75.6 (F_3CCOO^-).

The relative stereochemistry was determined via ^1H -NMR. The coupling constant of H-6 of the ADIC analogue was determined to be 5.7 Hz. The coupling constant was compared to ADIC.^[149]

9.8.39 *rac*-Ethyl (5*S*,6*S*)-5-(2-amino-2-oxoethoxy)-6-((*tert*-butoxycarbonyl)amino)cyclohexa-1,3-diene-1-carboxylate (**33**)



In a flame dried and argon flushed Schlenk flask equipped with magnetic stirring bar 250 mg (0.886 mmol, 1 equiv) **30** were dissolved in 11 mL abs. THF and cooled to -20 °C (dry ice/acetone). To the stirred, slightly yellowish solution 48 mg (1.20 mmol, 1.4 equiv) NaH (60 % dispersion in mineral oil) were added, whereupon the solution became cloudy. After 15 min, 291 mg (1.57 mmol, 1.8 equiv.) iodoacetamide were added to the yellow solution, while the temperature was kept at -20 °C. The mixture was stirred and allowed to warm up to 0 °C within 2 h (reaction monitoring via TLC). It was stirred for another 30 min at this temperature. Subsequently, the reaction was poured into 30 mL sat. NH₄Cl solution. The aqueous phase was extracted with EtOAc (6x30 mL). The combined organic layers were dried over Na₂SO₄, filtered and concentrated *in vacuo* to give a sticky yellow gum. The crude product was purified via flash column chromatography (10 g SiO₂, 10.0 x 1.7 cm C/EA 4/1, 7 mL frac., frac. 20-40 pooled). In addition, 47 mg of the starting material (frac. 7-17 pooled) were recovered.

Yield: 141 mg (0.414 mmol, 47 %, 66 % brsm), yellowish sticky gum

C₁₆H₂₄N₂O₆ [340.38 g·mol⁻¹]

R_f = 0.28 (cyclohexane/ EtOAc = 1/4, CAM)

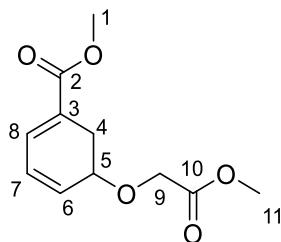
HRMS (TOF MS EI⁺): m/z: calcd for [M]⁺: 340.1634;

found: 340.1647

¹H-NMR (300 MHz, CDCl₃): δ= 7.18 (d, *J* = 5.5 Hz, 1H, H-7), 6.54 (bs, 1H, amide-H), 6.36 (m, 1H, H-6), 6.32–6.19 (m, 1H, H-5), 5.73 (bs, 1H, amide-H), 4.85 (d, *J* = 6.9 Hz, 1H, H-3), 4.42-4.00 (m, 6H, H-4, H-8, H-18, N-H), 1.42 (s, 9H), 1.30 (t, *J* = 7.1 Hz, 3H).

¹³C-NMR, APT (76 MHz, CDCl₃): δ= 172.4, 165.6, 155.2, 133.3, 129.1, 128.1, 126.8, 74.9 (C-4), 67.7 (C-15), 61.2 (C-8), 47.1 (C-3), 28.5 (C-12-C14), 14.3 (C-9).

9.8.40 Methyl 5-(2-methoxy-2-oxoethoxy)cyclohexa-1,3-diene-1-carboxylate (**34**)



In a flame dried and argon flushed 50 mL Schlenk flask equipped with magnetic stirring bar 612 mg (3.97 mmol, 1 equiv.) **30** were dissolved in 20 mL abs. THF. It was stirred vigorously and cooled to -78 °C (dry ice/acetone) and 463 mg (11.6 mmol, 2.9 equiv.) 60 % dispersion NaH were slowly added. It was stirred at -78 °C for 30 min, after which it was warmed to -38 °C, stirred at this temperature for 15 min, after which 800 µL (8.47 mmol, 2.1 equiv.) methylbromoacetate were added. Within 60 min the reaction mixture was slowly warmed to -21 °C in the cooling bath, after which complete consumption of the starting material was observed (reaction monitoring via TLC) and the solution was poured into 300 mL sat. NH₄Cl solution (pre-cooled to 15 °C). It was extracted with EtOAc (4x60 mL) and the combined organic layers were dried over Na₂SO₄, filtered and concentrated *in vacuo*. The product was purified via flash column chromatography (25 g SiO₂, 14.5 x 3.8 cm, cyclohexane/EtOAc 5/1, 20 mL frac., frac. 20-31 pooled).

Yield= 329 mg (1.45 mmol, 37 %), colorless oil

C₁₁H₁₄O₅ [226.23 g·mol⁻¹]

R_f= 0.30 (cyclohexane/EtOAc = 3/1, CAM)

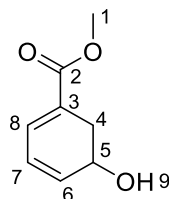
HRMS (TOF MS EI): m/z: calcd for C₁₁H₁₄O₅⁺ [M]⁺: 226.0841;

found: 226.0846.

¹H-NMR (300 MHz, CDCl₃) δ 7.12–7.02 (m, 1H, H-8), 6.27 (m, 2H, H-6, H-7), 4.29 (m, 1H, H-5), 4.15–3.99 (m, 2H, H-9), 3.77, 3.74 (2xs, 6H, H-1, H-11), 3.04–2.90 (m, 1H, H-4a), 2.60 (m, 1H, H-4b).

¹³C-NMR, APT (76 MHz, CDCl₃): δ = 171.0 (C-10), 167.3 (C-2), 131.6 (C-8), 130.1, 127.5 (C-3), 126.5, 70.9 (C-5), 64.9 (C-9), 52.0, 51.9, 27.8 (C-4).

9.8.41 Methyl 5-hydroxycyclohexa-1,3-diene-1-carboxylate (**35**)



This compound was prepared following a literature procedure.^[102]

In a flame dried and argon flushed 100 mL two-neck flask equipped with magnetic stirring bar were placed 1.28 mL (6.14 mmol, 1.2 equiv.) hexamethyldisilazane in 35 mL abs. THF. It was stirred vigorously and cooled to -78 °C (dry ice /acetone) and 2.58 mL 2.21 M *n*-BuLi (5.70 mmol, 1.1 equiv.) were slowly added. It was warmed to 0 °C for 15 min, after which it was again cooled to -78 °C. Subsequently, 790 mg (5.12 mmol, 1 equiv.) **36**, dissolved in 6.5 mL abs. THF were added over the course of 10 min. It was slowly warmed to -50 °C in the cooling-bath. After 120 min, full consumption of the starting material was observed via TLC and the solution was poured into 200 mL sat. NH₄Cl solution (pre-cooled to 0 °C). It was extracted with DCM (4x50 mL) and the combined organic layers were dried over Na₂SO₄, filtered and concentrated *in vacuo*. The product was purified via flash column chromatography (37 g SiO₂, 10 x 3.0 cm, cyclohexane/EtOAc 3/1, 20 mL frac., frac. 16-26 pooled). The obtained oil **35** became increasingly gum-like upon prolonged storage at -20°C, which was accompanied by an additional spot formation on TLC (R_f = 0, cyclohexane/EtOAc = 1/1).

Yield= 309 mg (1.95 mmol, 38 %) colorless oil

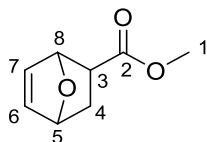
C₈H₁₀O₃ [154.16 g·mol⁻¹]

R_f = 0.50 (cyclohexane/EtOAc = 1/1, UV)

¹H-NMR (300 MHz, CDCl₃): δ = 7.14–7.01 (m, 1H, H-8), 6.30-6.17 (m, 2H), 4.37 (m, 1H, H-5), 3.77 (s, 3H, H-1), 2.99–2.84 (ddd, J =18.8 Hz, 5.1 Hz, 0.8 Hz, 1H, H-4a), 2.70-2.56 (ddd, J = 18.9 Hz, 7.6 Hz, 2.3 Hz, 1H, H-4b), 1.74 (s, 1H, H-9).

¹³C-NMR, APT (76 MHz, CDCl₃): δ = 167.6 (C-2), 133.4, 131.6 (C-8), 127.1 (C-3), 124.9, 63.3 (C-5), 52.0 (C-1), 31.3 (C-4).

9.8.42 Methyl 7-oxabicyclo[2.2.1]hept-5-ene-2-carboxylate (**36**)



This compound was prepared following a literature procedure.^[102]

A flame dried and argon flushed 30 mL Schlenk flask equipped with magnetic stirring bar was consecutively charged with 5.10 g (16.0 mmol, 0.3 equiv.) ZnI_2 , 5.60 mL (77.3 mmol, 1.5 equiv.) furan and 4.78 mL (52.8 mmol, 1 equiv.) methyl acrylate. It was stirred at 40 °C for 3 d, after which it was diluted with 150 mL EtOAc. The organic phase was washed with 1 M $Na_2S_2O_3$ solution (1x80 mL), over Na_2SO_4 , filtered and concentrated *in vacuo*. The product was purified via SiO_2 -filtration (ca. 4 cm SiO_2 , frac. 1: 230 mL cyclohexane, frac. 2: 600 mL cyclohexane/EtOAc 1/1, frac. 3: 300 mL EtOAc, frac. 2 pooled).

Yield= 4.88 g (31.7 mmol, 41 %) slightly yellow liquid

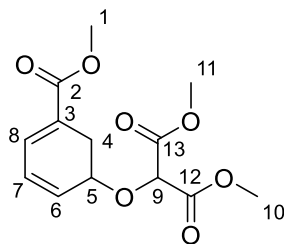
$C_8H_{10}O_3$ [154.16 g·mol⁻¹]

R_f = 0.30 (cyclohexane/EtOAc = 4/1, CAM)

¹H-NMR (300 MHz, $CDCl_3$): *endo/exo* mixture: δ = 6.49–6.13 (m, 2H), 5.21–5.09 (m, 1H), 5.03 (m, 1H), 3.67 (2xs, 3H), 3.17–3.00 (m, 0.3H), 2.42 (m, 0.7 H), 2.13 (m, 1H), 1.65–1.43 (m, 1H).

¹³C-NMR, APT (76 MHz, $CDCl_3$): *endo/exo* mixture: δ = 174.3, 172.7, 137.2, 134.8, 132.7, 81.0, 79.1, 78.8, 78.1, 52.2, 51.8, 42.8, 42.8, 29.2, 28.6.

9.8.43 Dimethyl 2-((5-(methoxycarbonyl)cyclohexa-2,4-dien-1-yl)oxy)malonate (**37**)



This compound was prepared following a literature procedure.^[150]

In a flame dried and argon flushed 8 mL Schlenk flask equipped with magnetic stirring bar 5.6 mg (0.0127 mmol, 2 mol%) $\text{Rh}_2(\text{OAc})_4$, 98.3 mg (0.638 mmol, 1 equiv.) **35** and 1.0 mL abs. toluene were consecutively added. The flask was heated to 80 °C and 102.6 mg (0.649 mmol, 1.0 equiv.) **R-4** dissolved in 0.3 mL abs. toluene (prepared in a Schlenk flask) were added over the course of 1 min. After 40 min, the solution was cooled to RT and concentrated *in vacuo*. The product was purified via flash column chromatography (4 g SiO_2 , 10.2 x 1.2 cm, cyclohexane/DCM/acetone 10/2/0.4, 3 mL frac., frac. 18-30 pooled).

Yield= 89.4 mg (0.313 mmol, 49 %), colorless oil

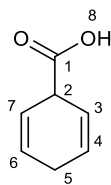
$\text{C}_{13}\text{H}_{16}\text{O}_7$ [284.26 g·mol]

R_f = 0.58 (cyclohexane/EtOAc = 1/1, KMnO_4)

$^1\text{H-NMR}$ (300 MHz, CDCl_3): δ = 7.10–7.01 (m, 1H, H-8), 6.37-6.16 (m, 2H, H-6, H-7), 4.60 (s, 1H, H-9), 4.45-4.35 (m, 1H, H-5), 3.85–3.71 (m, 9H, H-1, H-10, H-11), 3.01 (dd, J = 19.1 Hz, 5.0 Hz, 1H, H-4), 2.72–2.51 (ddd, J = 19.2 Hz, 8.4 Hz, 2.2 Hz, 1H, H-4).

$^{13}\text{C-NMR}$ (76 MHz, CDCl_3): δ = 167.4, 167.2, 167.1, 131.5, 129.2 (C-8), 127.5 (C-3), 127.2, 76.1 (C-9), 71.5 (C-5), 53.1, 53.0, 52.0 (C-1). 28.2 (C-4).

9.8.44 Cyclohexa-2,5-diene-1-carboxylic acid (**38**)



This compound was prepared following a literature procedure.^[106]

A flame dried and argon flushed 250 mL three-neck round-bottom flask equipped with magnetic stirring bar was consecutively charged with 3.10 g (25.4 mmol, 1 equiv.) benzoic acid and 6.0 mL (333 mmol, 13.1 equiv.) degassed H₂O. The flask was equipped with an argon-inlet and a dry-ice condenser. The reaction mixture was cooled to -78 °C (dry ice /acetone). The argon-inlet was replaced with an ammonia inlet and 120 mL NH₃ were collected. Vigorous stirring was begun and 0.538 g (77.5 mmol, 3.1 equiv.) Li were added in small pieces over a period of 60 min. The stirring was stopped after all Li wire was consumed and ammonia was allowed to evaporate under a stream of N₂ over a period of 18 h. The grey to yellow remainder was acidified to pH=1 using 120 mL 1 M HCl solution. The aqueous layer was extracted with Et₂O (4x50 mL). The combined organic layers were dried over Na₂SO₄, filtered and concentrated *in vacuo*. It was used without purification.

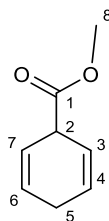
Yield= 2.94 g (23.7 mmol, 93 %) colorless solid

C₇H₈O₂ [124.14g·mol⁻¹]

¹H-NMR (300 MHz, CDCl₃): δ = 6.02–5.73 (m, 4H), 3.88–3.68 (m, 1H), 2.82–2.60 (m, 2H).

¹³C-NMR, APT (76 MHz, CDCl₃) δ = 179.3, 127.0, 121.6, 41.6, 25.9.

9.8.45 Methyl cyclohexa-2,5-diene-1-carboxylate (**39**)



This compound was prepared following a literature procedure.^[105]

A flame dried and argon flushed 50 mL Schlenk flask equipped with magnetic stirring bar, was consecutively charged with 2.94 g (24.1 mmol, 1 equiv.) **38**, 18.0 mL abs. MeOH and 1.4 mL (26.3 mmol, 1.1 equiv.) conc. H₂SO₄. It was stirred at 80 °C and full consumption of the starting material (reaction monitoring via TLC) was detected after 4 h. Subsequently, 30 mL H₂O were added. The aqueous phase was extracted with Et₂O (3x15 mL) and the combined organic layers were washed with 5 % NaHCO₃ (1x15 mL). The aqueous layer was back-extracted with Et₂O (1x15 mL) and the combined organic layers were dried over Na₂SO₄, filtered and gently concentrated *in vacuo*. The crude product was purified via flash column chromatography (50 g SiO₂, 10.0 x 4.0 cm, cyclohexane/EtOAc 30/1, 20 mL frac., frac. 5-15 pooled).

Yield= 1.99 g (14.4 mmol, 60 %) colorless oil

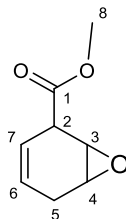
C₇H₈O₂ [138.17g·mol⁻¹]

R_f= 0.29 (cyclohexane/EtOAc= 30/1, CAM)

¹H-NMR (300 MHz, CDCl₃): δ = 5.95–5.72 (m, 4H), 3.80–3.61 (m, 4H), 2.75–2.58 (m, 2H).

¹³C-NMR (76 MHz, CDCl₃): δ = 173.8, 126.8, 122.1, 51.9, 41.8, 25.9.

9.8.46 Methyl 7-oxabicyclo[4.1.0]hept-3-ene-2-carboxylate (**40**)



This compound was prepared following a literature procedure.^[105]

In a 500 mL round-bottom flask equipped with magnetic stirring bar and a dropping funnel 13.52 g (97.9 mmol, 1 equiv.) **39** were dissolved in 80 mL CHCl_3 . It was cooled to 0 °C (ice-bath) and 357 g (97.9 mmol, 1.0 equiv.) of a 4.73 wt % *m*CPBA (pre-titrated) solution in CHCl_3 were added over the course of 60 min. It was warmed to RT and stirred for 18 h, after which complete consumption of the starting material was detected (reaction monitoring via TLC). Subsequently, the solution was filtered and washed consecutively with a 10% Na_2SO_3 solution (1x200 mL) and with a 5% NaHCO_3 solution (1x200 mL). The combined organic layers were dried over Na_2SO_4 , filtered and concentrated *in vacuo*. The product was purified via flash column chromatography (250 g SiO_2 , 12.0 x 7.8 cm, cyclohexane/EtOAc 10/1, 150 mL frac., frac. 9-18 pooled).

Yield= 5.35 g (34.7 mmol, 35 %) colorless oil

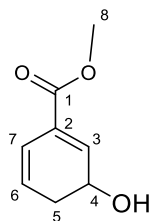
$\text{C}_8\text{H}_{10}\text{O}_3$ [154.16g·mol⁻¹]

R_f = 0.13 (cyclohexane/EtOAc= 10/1, CAM)

¹H-NMR (300 MHz, CDCl_3): δ = 5.64-5.48 (m, 2H), 3.73 (s, 3H), 3.62 (s, 1H), 3.53–3.43 (m, 1H), 3.32 (m, 1H), 2.65–2.43 (m, 2H).

¹³C-NMR, APT (76 MHz, CDCl_3): δ = 171.6, 124.6, 120.0, 52.4, 51.7, 50.7, 42.0, 25.0.

9.8.47 Methyl 3-hydroxycyclohexa-1,5-diene-1-carboxylate (**41**)



This compound was prepared following a literature procedure.^[105]

In a flame dried and argon flushed 15 mL Schlenk flask equipped with magnetic stirring bar 107 mg (0.694 mmol, 1 equiv.) **40** were dissolved in 4.5 mL DCM. It was stirred vigorously and 120 μ L (0.866 mmol, 1.2 equiv.) Et₃N were added. After 2 h, the solution was diluted with 5 mL DCM and washed with 10% CuSO₄·5H₂O (1x6 mL). The aqueous phase was back-extracted with DCM (2x10 mL) and the combined organic layers were dried over Na₂SO₄, filtered and concentrated *in vacuo*. The product was purified via flash column chromatography (4.5 g SiO₂, 13.0 x 1.2 cm, cyclohexane/EtOAc 3:1, 3 mL frac., frac. 8-12 pooled). The obtained oil **41** became increasingly gum-like upon prolonged storage at -20 °C, which was accompanied by an additional spot formation on TLC (R_f= 0, cyclohexane/EtOAc = 1/1).

Yield= 86 mg (0.558 mmol, 80 %) colorless oil

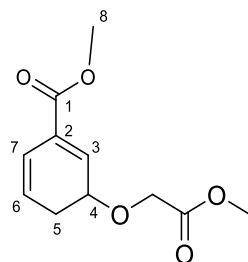
C₈H₁₀O₃ [154.16g·mol⁻¹]

R_f= 0.19 (cyclohexane/EtOAc= 3/1, CAM)

¹H-NMR (300 MHz, CDCl₃): δ = 6.93 (d, *J* = 4.6 Hz, 1H), 6.47 (dd, *J* = 9.8 Hz, 1.5 Hz, 1H), 6.05–5.90 (m, 1H), 4.55–4.37 (m, 1H), 3.79 (s, 3H), 2.57–2.43 (m, 2H), 1.84–1.69 (m, 1H).

¹³C-NMR, APT (76 MHz, CDCl₃): δ = 166.3, 135.5, 129.1, 126.6, 121.3, 64.0, 52.2, 31.8.

9.8.48 Methyl 3-(2-methoxy-2-oxoethoxy)cyclohexa-1,5-diene-1-carboxylate (**42**)



In a flame dried and argon flushed 50 mL Schlenk flask equipped with magnetic stirring bar 406 mg (2.63 mmol, 1 equiv.) **41** were dissolved in 14 mL abs. DCM and 11.1 mg (0.03 mmol, 1 mol%) Rh₂(OAc)₄ were added. It was stirred vigorously and a stock solution of **R-2** (277 mg, 2.8 mmol, 1.1 equiv. dissolved in 9.0 mL DCM) was added over the course of 1 h via a syringe pump and the solution was concentrated *in vacuo*. The product was purified via two consecutive flash column chromatographies (1: 20 g SiO₂, 14.0 x 2.3 cm, cyclohexane/EtOAc 3/1, 12 mL frac., frac. 14-17 pooled; 2: 1 g SiO₂, 5.0 x 0.6 cm, toluene/acetone 20/0.6, 1 mL frac., frac. 7-14 pooled).

Yield= 25.7 mg (0.11 mmol, 4 %), colorless oil

C₁₁H₁₄O₅ [226.23 g·mol⁻¹]

R_f= 0.15 (cyclohexane/EtOAc = 3/1, CAM)

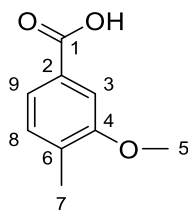
HRMS (TOF MS EI): m/z: calcd for C₁₁H₁₄O₅⁺ [M]⁺: 226.0841;

found: 226.0840.

¹H-NMR (300 MHz, CDCl₃): δ= 6.92 (d, *J* = 4.2 Hz, 1H), 6.45 (dd, *J* = 9.8 Hz, 1.3 Hz, 1H), 6.09– 5.94 (m, 1H), 4.39 (td, *J* = 8.2 Hz, 4.4 Hz, 1H), 4.11 (s, 2H), 3.77 (d, *J* = 11.3 Hz, 7H), 2.53 (dd, *J* = 4.3 Hz, 2.0 Hz, 2H).

¹³C-NMR, APT (76 MHz, CDCl₃): δ= 170.9, 166.0, 132.5, 130.4, 127.1), 121.5, 71.9, 65.4, 52.1(2xs), 28.7.

9.8.49 3-Methoxy-4-methylbenzoic acid (**43**)



This compound was prepared following a literature procedure.^[151]

In a 1 L one-neck round-bottom flask equipped with magnetic stirring bar 25.13 g (140 mmol, 1.0 equiv.) methyl 3-methoxy-4-methylbenzoate were dissolved in 550 mL MeOH and 60.9 g (1.52 mol, 10.9 equiv.) NaOH in 250 mL H₂O were added at RT. The reaction mixture was heated at reflux temperature for 17 h until complete consumption of the starting material was observed (reaction monitoring via TLC). Subsequently, MeOH was removed under reduced pressure and the remainder was diluted with 100 mL H₂O. The solution was acidified to pH=2 by the addition of 2 M HCl, which resulted in a cloudy solution. The aqueous phase was extracted with EtOAc (3x100 mL) and the combined organic layers were washed with brine (1x100 mL), dried over Na₂SO₄, filtered and concentrated *in vacuo*. No further purification of the product was necessary.

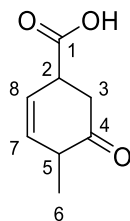
Yield= 22.9 g (138 mmol, 98 %) colorless solid

C₉H₁₀O₃ [166.17 g·mol⁻¹]

R_f = 0.48 (cyclohexane/EtOAc = 1/1, CAM)

¹H-NMR (300 MHz, CDCl₃): δ= 7.65 (d, *J* = 7.7 Hz, 1H), 7.53 (s, 1H, H-3), 7.22 (d, *J* = 7.8 Hz, 1H), 3.90 (s, 3H), 2.29 (s, 3H).

9.8.50 4-Methyl-5-oxocyclohex-2-enecarboxylic acid (**44**)



The procedure was taken from the literature.^[111]

Small test batch

In a flame dried and argon flushed 50 mL three-neck round-bottom flask equipped with magnetic stirring bar were placed 350 mg (2.10 mmol, 1.0 equiv.) **43** and 0.5 mL degassed H₂O. The flask was equipped with an argon-inlet and a dry-ice condenser and the reaction mixture was cooled to -78 °C (dry-ice/acetone). The argon-inlet was replaced with an ammonia inlet and 20 mL ammonia were collected. Vigorous stirring was begun and 45 mg (6.48 mmol, 3.1 equiv.) Li wire were added in small pieces over a period of 12 min, whereupon a light yellow solution formed in the first place, which went to deep-blue. The stirring was stopped, the dry-ice condenser was removed and ammonia was allowed to evaporate under a stream of nitrogen over a period of 90 min. The grey to yellow remainder was diluted with 10 mL 1 M HCl solution and the aqueous phase was extracted with DCM (3x20 mL). The combined organic layers were dried over Na₂SO₄ and concentrated *in vacuo*.

Ca. 250 mg of a crude colorless solid were obtained.

C₈H₁₀O₃ [154.16 g·mol⁻¹]

HRMS (FTICR MS ESI): m/z: calcd for C₈H₁₀O₃⁺ [M]⁺: 154.0630;

found: 154.0620

¹H NMR (300 MHz, CDCl₃) δ 6.08–5.73 (m, 2H), 3.60 (m, 1H), 3.09–2.54 (m, 3H), 1.20 (m, 3H).

Peaks were assigned according to peak height.

Diastereomer 1: ¹³C-NMR, APT (76 MHz, CDCl₃): δ= 209.9, 178.1, 134.1, 123.2, 43.0, 39.4, 16.3.

Diastereomer 2: ¹³C-NMR, APT (76 MHz, CDCl₃): δ= 209.9, 178.3, 134.0, 123.3, 43.0, 39.2, 17.0.

Big batch:

Four batches were carried out.

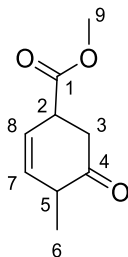
Batch 1:

In a flame dried and argon flushed 250 mL three-neck round-bottom flask equipped with magnetic stirring bar were placed 5.74 g (34.5 mmol, 1.0 equiv.) of **43** and 8.2 mL degassed H₂O. The flask was equipped with an argon-inlet and a dry-ice condenser and the reaction mixture was cooled to -78 °C (dry-ice/acetone). The argon-inlet was replaced with an ammonia inlet and 100 mL ammonia were collected. Vigorous stirring was begun and 0.683 g (98.4 mmol, 2.9 equiv.) Li wire were added in small pieces over a period of 30 min, whereupon first a blue, then a light yellow solution formed. The stirring was stopped, the dry-ice condenser was removed and ammonia was allowed to evaporate under a stream of nitrogen over a period of 4 h. The grey to yellow remainder was diluted with 230 mL 1 M HCl solution and stirred for 5 min. The aqueous layer was extracted with DCM (4x200 mL). The combined organic phases were dried over Na₂SO₄ and concentrated *in vacuo* to afford a colorless oil, which upon standing solidified. The obtained colorless solid is a mixture of the desired product and side products (presumably unreacted starting material, double bond isomers and the fully reduced cyclohexane derivative). It was used without further purification. 5.03 g crude product were obtained.

Batches 2-4 were carried out analogously.

22.88 g (0.137 mol) of **43** were used and 19.91 g crude product were obtained.

9.8.51 Methyl 4-methyl-5-oxocyclohex-2-enecarboxylate (**45**)



The total amount of **44** (19.9 g) was split into four batches. Furthermore, 1.92 g **44** that had already been synthesized during earlier experiments were added to batch 3, which influenced the diastereomeric ratio and the purity of the resulting product.

Batch 1:

A flame dried and argon flushed 500 mL one-neck round-bottom flask equipped with magnetic stirring bar was consecutively charged with 5.03 g (32.65 mmol, 1.0 equiv.) **44** and 250 mL freshly distilled Et₂O. To the stirred reaction mixture 11 mL (176 mmol, 5.4 equiv.) methyl iodide and 7.71 g (33.3 mmol, 1.0 equiv.) Ag₂O were added, and a black suspension formed.

Batches 2-4 were carried out analogously.

After 20 h, the batches were combined, Ag₂O was removed by filtration through a pad of cotton and the solution was concentrated *in vacuo*. The obtained yellow oil is a mixture of the desired product and side products (presumably methylated **43**, double bond isomers and the fully reduced cyclohexane derivative). It was used without further purification. 23.1 g crude product were obtained.

C₉H₁₂O₃ [168.19 g·mol⁻¹]

R_f = 0.70 (cyclohexane/EtOAc = 1/1, CAM)

HRMS (FTICR MS ESI): m/z: calcd for C₉H₁₂O₃⁺ [M]⁺: 168.0786;
found: 168.0792.

For NMR analysis, from Luche-reduction reisolated **45** was additionally purified via flash column chromatography (cyclohexane/DCM/acetone = 9/1/1, R_f = 0.26)

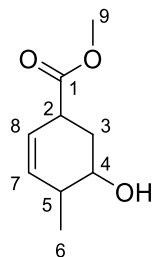
¹H-NMR (300 MHz, CDCl₃) δ 5.99–5.67 (m, 2H), 3.71 (m, 3H), 3.60–3.46 (m, 1H), 3.05–2.89 (m, 1H), 2.89–2.51 (m, 2H), 1.26–1.02 (m, 3H).

Peaks were assigned according to peak height.

diastereomer 1: ¹³C-NMR, APT (76 MHz, CDCl₃): δ = 209.6, 172.8, 133.6, 123.7, 52.5, 43.6, 42.5, 39.8, 16.1.

diastereomer 2: ¹³C-NMR, APT (76 MHz, CDCl₃): δ = 209.7, 172.9, 133.5, 123.8, 52.5, 43.2, 43.0, 39.4, 17.1.

9.8.52 Methyl 5-hydroxy-4-methylcyclohex-2-enecarboxylate (**46**)



The total amount of **45** (23.1 g) was split into four batches. Furthermore, 2.11 g of **45** that had already been synthesized during earlier experiments were added to batch 3, which influenced the diastereomeric ratio and the purity of the resulting product.

Batch 1:

In a flame dried and argon flushed 500 mL two-neck round-bottom flask with magnetic stirring bar 6.68 g (39.7 mmol, 1.0 equiv.) of **45** were dissolved in 360 mL MeOH. The reaction mixture was cooled to -78 °C (dry-ice/acetone). To the stirred yellow solution 2.49 g (7.01 mmol, 0.2 equiv.) CeCl₃·6H₂O were added over a period of 3 min. After 30 min 0.754 g (19.9 mmol, 0.5 equiv.) NaBH₄ were added over a period of 2 min. After 5 h the solution was poured into a 10 wt% 600 mL Rochelle salt solution. The organic phase was separated and the aqueous phase was extracted with DCM (3x250 mL) and EtOAc (1x50 mL). The combined organic layers were dried over Na₂SO₄, filtered and concentrated *in vacuo*.

Batches 2-4 were carried out analogously.

The batches were combined and the crude product was purified via flash column chromatography (400 g SiO₂, 20.0 x 3.5 cm, cyclohexane/EtOAc 3/1, 250 mL frac., frac. 8-20 pooled). The obtained yellow oil is a mixture of the desired product and side products (presumably double bond isomers and the fully reduced cyclohexene derivative). It was used without further purification. 12.89 g crude product were obtained. Fractions 5-7 were also pooled and concentrated *in vacuo* to recover 3.83 g **45**.

C₉H₁₄O₃ [170.21 g·mol⁻¹]

R_f = 0.60 (cyclohexane/EtOAc 1/1, CAM)

GC-MS (EI, 70 eV, NG-STANDARD): several peaks, main peak: t_R = 5.17; m/z (%) = 170.1 (100 [M⁺]), 127.1 (2500), 111.1 (3500), 93.0 (1900), 67.0 (1900).

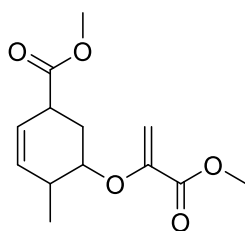
HRMS (FTICR MS ESI): m/z: calcd for C₉H₁₄O₃⁺ [M]⁺: 170.0943;
found: 170.0959.

An assignment of the ¹H-NMR is omitted.

Peaks were assigned according to peak height.

major diastereomer: ^{13}C -NMR, APT (76 MHz, CDCl_3): δ = 175.6, 133.4, 122.9, 72.4, 52.3, 41.7, 38.5, 32.5, 18.5.

9.8.53 Methyl 5-((3-methoxy-3-oxoprop-1-en-2-yl)oxy)-4-methylcyclohex-2-ene-1-carboxylate (**47**)



This compound was prepared from a different batch of starting material **46**. Purity and diastereometric ratio may be influenced.

In a flame dried and argon flushed 10 mL Schlenk flask equipped with magnetic stirring bar 200 mg (1.12 mmol, 1 equiv.) **46** were dissolved in 8 mL abs. toluene. Subsequently, 10 mg (0.02 mmol, 1.8 mol%) $\text{Rh}_2(\text{OAc})_4$ and 340 mg (1.63 mmol, 1.5 equiv.) **R-1** were added. The reaction mixture was heated to 70 °C (oil bath) and stirred for 15 h, until which complete consumption of the starting material was observed (reaction monitoring via TLC). The pale brownish solution was concentrated *in vacuo* and purified via flash column chromatography (18 g SiO_2 , 1.5x12 cm, cyclohexane/EtOAc = 1/2, 12 mL frac., frac. 6-24 pooled, R_f = 0.17, cyclohexane/EtOAc 1/2, CAM). 255 mg of a crude oil were obtained.

In a flame dried and argon flushed 10 mL Schlenk flask equipped with magnetic stirring bar 101 mg (0.29 mmol) of the crude oil were dissolved in 3 mL abs. THF. It was cooled to -78 °C (dry ice /acetone) and 0.3 ml LiHMDS (1 M in THF, 0.30 mmol) were added. The solution was stirred for 15 min at this temperature, before a formaldehyde solution, produced by cracking paraformaldehyde (approximately 7.5 mmol in 4.5 mL abs. THF) was added dropwise and the solution was stirred for further 20 min after which 10 mL sat. NH_4Cl solution were added dropwise. The aqueous phase was extracted with EtOAc (3x20 mL) and the combined organic layers were dried over Na_2SO_4 , filtered and concentrated *in vacuo*. The crude product was purified via flash column chromatography (10 g SiO_2 , 12 x 1.8 cm, cyclohexane/EtOAc 6/1, 7 mL frac., frac. 4-5 pooled).

Yield= 20 mg (0.08 mmol, 17 %, 2 steps) colorless oil

$\text{C}_{13}\text{H}_{18}\text{O}_5$ [254.28 g·mol⁻¹]

R_f = 0.28 (cyclohexane/ EtOAc= 6/1, CAM)

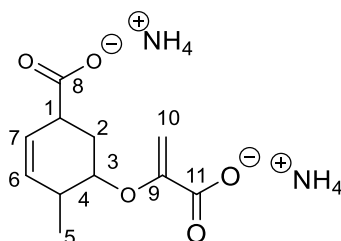
HRMS (TOF MS EI): m/z: calcd for $\text{C}_{13}\text{H}_{18}\text{O}_5^+$ [M]⁺: 254.1154;

found: 254.1167.

$^1\text{H-NMR}$ (300 MHz, CDCl_3): δ = 5.74-5.58 (m, 2H), 5.43 (m, 1H), 4.64 (m, 1H), 4.28 (m, 0.5 H), 4.00-3.80 (m, 0.5 H), 3.80 (m, 3 H), 3.70 (m, 3H), 3.23 (m, 1H), 2.70-2.45 (m, 1H), 2.40-1.83 (m, 2H), 1.09-0.95 (m, 3H).

$^{13}\text{C-NMR}$ (76 MHz, CDCl_3): δ = 173.6, 173.5, 150.2, 149.6, 133.1, 132.8, 123.3, 123.3, 95.7, 79.2, 74.7, 52.5, 52.4, 52.2, 52.2, 41.7, 36.1, 32.1, 28.5, 25.3, 18.4, 14.5.

9.8.54 Ammonium 5-((1-carboxylatovinyl)oxy)-4-methylcyclohex-2-ene-1-carboxylate (**48**)



This compound was prepared from a different batch of starting material **47**. Purity and diastereometric ratio may be influenced.

128 mg (0.503 mmol) of **47** were portioned in 48 Eppendorf vials. Subsequently, 400 μ L phosphate buffer (100 mM, pH= 7.6), 50 μ L DCM and 4.0 mg PLE (20 U/mg) were added. It was shaken for 4 d at 30 $^{\circ}$ C and 500 rpm, after which HPLC analysis (4.48 min, [M-H]⁻=225, method=standard-2) showed product formation. PLE was denatured by the addition of 600 μ L EtOH and it was subsequently centrifugated. The supernatant was filtered and transferred to a round-bottom flask and the solution was purified via prep-HPLC (method: ng-nucleodur-c18-001-hcooh-10to85; 30 $^{\circ}$ C; 12 mL/min; A: 0.01 % aqueous HCOOH, B: MeCN; min 0-3: 10 % B; min 3-11: 30 % B; min 11-16: 50 % B; min 16-19: 80 % B; min 19-22: 10 % B). Prior to the chromatographic run, the solution was acidified using aqueous 1% HCOOH to a pH=3, whereupon the solution became cloudy and was filtrated again. The obtained fractions were immediately basified to a pH of 8-9 using a 25% aqueous NH₃ solution.

The solution was then concentrated *in vacuo* to give a gum-like oil. The obtained oil is assumed to be hygroscopic.

Yield* = 31.5 mg (calc.: 5.2 mg ammonium formiate; 26.3 mg desired product, 0.10 mmol, 20 %) colorless sticky oil

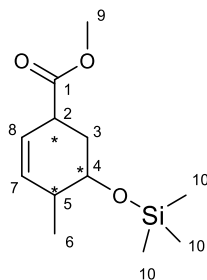
C₁₁H₂₀N₂O₅ [260.29 g/mol]

HRMS (FTICR MS ESI): m/z: calcd for C₁₁H₁₃O₅⁻ [M-H]⁻: 225.0768;
found: 225.0767.

¹H-NMR (300 MHz, D₂O): δ = 5.65 (m, 2H), 5.14 (m, 1H), 4.63 (m, 1H), 4.36 (m, 0.4H), 3.87 (m, 0.5H), 3.16 (m, 1H), 2.73 (m, 0.3H), 2.42 (m, 1H), 2.23–1.41 (m, 1.7H), 1.09–0.81 (m, 3H).

*A mixture of the desired product in ammonium acetate was obtained. According to ¹H-NMR about 26.3 mg out of the 31.5 mg are product. No standard was used.

9.8.55 Methyl 4-methyl-5-((trimethylsilyl)oxy)cyclohex-2-enecarboxylate (**49**)



This compound was prepared from a different batch of starting material **46**. Purity and diastereometric ratio may be influenced.

In a flame dried and argon flushed 100 mL three-neck round-bottom flask 2.37 g (13.92 mmol, 1 equiv.) **46** were dissolved in 80 mL abs. ACN. The flask was equipped with a bubbler and an exhaust tube was passed into a saturated KMnO_4 solution. Vigorous stirring was begun and 2.0 mL (1.58 g, 15.93 mmol, 1.1 equiv.) TMS-CN were added over a period of 15 min. After 140 min full consumption of the starting material was observed (reaction monitoring via TLC) and 50 mL H_2O was added in order to destroy excess TMS-CN. The solution was extracted with DCM (4x50 mL) and the combined organic layers were dried over Na_2SO_4 , filtered and concentrated *in vacuo*. The product was purified via flash column chromatography (125 g SiO_2 , 20 x 4.7 cm, cyclohexane/EtOAc = 20:1, 80 mL frac., frac. 3-7 pooled).

Yield= 2.46 g (10.1 mmol, 73 %), yellow oil

$\text{C}_{12}\text{H}_{22}\text{O}_3\text{Si}$ [242.39 g·mol⁻¹]

R_f = 0.89 (cyclohexane/EtOAc 2/1) (CAM, UV)

GC-MS (EI, 70 eV, NG-STANDARD): t_R = 5.50; m/z (%)= 242.1 (100 [M^+]), 227.1 (275), 199.1 (775), 183.1 (100), 116.0 (1375), 101.0 (1400), 73.0 (1025).

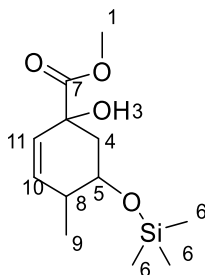
HRMS (FTICR MS ESI): m/z : calcd for $\text{C}_{12}\text{H}_{22}\text{O}_3\text{Si}^+$ [M]⁺: 242.1338;
found: 242.1357.

¹H-NMR (300 MHz, CDCl_3): δ = 5.80–5.43 (m, 2H), 4.05–3.83 (m, 0.6H), 3.79–3.61 (m, 3H), 3.49–3.32 (m, 0.5H), 3.29–3.09 (m, 0.8H), 2.33–1.73 (m, 3H), 1.10–0.81 (m, 3H), 0.23–0.00 (m, 9H).

Peaks were assigned according to peak height

main diastereomer: ¹³C-NMR (76 MHz, CDCl_3): δ = 174.3, 133.9, 123.1, 73.9, 52.1, 42.5, 39.0, 34.5, 18.6, 0.0.

9.8.56 Methyl 1-hydroxy-4-methyl-5-((trimethylsilyl)oxy)cyclohex-2-enecarboxylate (**50**)



This compound was prepared from a different batch of starting material **49**. Purity and diastereometric ratio may be influenced.

A flame dried and argon flushed 25 mL two-neck round-bottom flask was charged with 5.0 mL abs. THF and cooled to $-78\text{ }^{\circ}\text{C}$ (dry ice/ acetone). Vigorous stirring was begun and 5.9 mL of a titrated LDA stock solution in abs. THF (0.49 M, 2.90 mmol, 2.0 equiv.) were added. Subsequently, 348 mg (1.44 mmol, 1 equiv.) **49** were added over a period of 2 min. The solution turned yellow and it was stirred for another 10 min after which 1.00 g (3.80 mmol, 2.6 equiv.) Davis-oxaziridine were added over a period of 5 min. It was stirred for 10 min and 1.4 mL HMPT (8.0 mmol, 5.5 equiv.) were added. The solution turned red and after 1 h, the solution was poured into 50 mL H_2O (1 spatula NaCl was added). The solution was extracted with EtOAc (3x50 mL) and the combined organic layers were dried over Na_2SO_4 , filtered and concentrated *in vacuo*. The product was purified via flash column chromatography (100 g SiO_2 , 16.5 x 2.9 cm, cyclohexane/EtOAc = 12:1, 75 mL frac., frac. 17-20 pooled).

Yield= 85 mg (1.56 mmol, 23 %) colorless oil

$\text{C}_{12}\text{H}_{22}\text{O}_4\text{Si}$ [258.39 $\text{g}\cdot\text{mol}^{-1}$]

R_f = 0.50 (cyclohexane/EtOAc = 3/1, CAM)

GC-MS (EI, 70 eV, NG-STANDARD): t_R = 5.69; m/z (%) = 225. (100, $[\text{M} - \text{Me} - \text{H}_2\text{O}]^+$), 214.1 (400), 199.1 (500), 142.0 (1500), 119.0 (1250), 82.0 (1950).

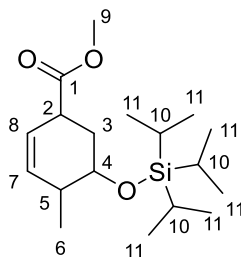
HRMS (FTICR MS ESI): m/z : calcd for $\text{C}_{12}\text{H}_{22}\text{O}_4^+$ $[\text{M}]^+$: 258.1287;
found: 258.1306.

$^1\text{H-NMR}$ (300 MHz, CDCl_3): δ = 5.85–5.40 (m, 2H), 3.78 (m, 3H), 3.73–3.57 (m, 1H), 3.29 (m, 1H), 2.26–1.81 (m, 3H), 1.05 (m, 3H), 0.20–0.02 (m, 9H).

Peaks were assigned according to peak height.

Main diastereomer: $^{13}\text{C-NMR}$ (76 MHz, CDCl_3): δ = 176.5, 137.1, 125.0, 74.3, 70.9, 53.4, 43.2, 39.4, 17.9, 0.4.

9.8.57 Methyl 4-methyl-5-((triisopropylsilyl)oxy)cyclohex-2-enecarboxylate (**51**)



In a 500 mL one-neck round-bottom flask equipped with magnetic stirring bar 12.89 g (77.1 mmol, 1.0 equiv.) **46** and 25.85 g (380 mmol, 4.9 equiv.) imidazole were dissolved in 200 mL DCM. To the stirred yellow solution 24.0 mL (112 mmol, 1.5 equiv.) TIPS-Cl were added over a period of 5 min. After 45 h (reaction monitoring via GC-MS), the reaction mixture was washed with H₂O (1x290 mL). Subsequently, the organic phase was separated and the aqueous layer was extracted with DCM (2x280 mL) and EtOAc (1x180 mL). The combined organic layers were dried over Na₂SO₄, filtered and concentrated *in vacuo*. The crude product was purified via flash column chromatography (450 g SiO₂, 20.0 x 8.5 cm, cyclohexane/EtOAc = 60/1, 250 mL frac., frac. 3-15 pooled). The obtained colorless oil is a mixture of the desired product and side products (presumably double bond isomers and the fully reduced cyclohexane derivative). 16.21 g crude product were obtained. It was used without further purification.

C₁₈H₃₄O₃Si [326.55 g·mol⁻¹]

R_f = 0.32 (cyclohexane/EtOAc = 40/1, CAM)

HRMS (FTICR MS ESI): m/z: calcd for C₁₈H₃₄O₃Si⁺ [M]⁺: 326.2277;
found: 326.2295.

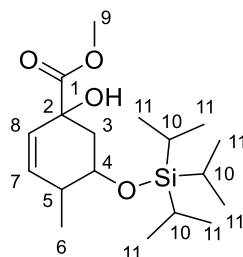
For NMR analysis, a small portion was purified via an additional column chromatography (cyclohexane/toluene = 6/1).

¹H-NMR (300 MHz, CDCl₃): δ = 5.85–5.53 (m, 2H), 4.24–3.92 (m, 1H), 3.80–3.62 (m, 3H), 3.21 (m, 1H), 2.50–2.29 (m, 1H), 2.04–1.77 (m, 2H), 1.19–0.82 (m, 24H).

Peaks were assigned according to peak height:

major diastereomer: ¹³C-NMR, APT (76 MHz, CDCl₃) δ 174.2, 134.3, 122.8, 69.6, 52.1, 43.2, 35.9, 29.4, 18.3, 14.1, 12.5.

9.8.58 Methyl 1-hydroxy-4-methyl-5-((triisopropylsilyl)oxy)cyclohex-2-enecarboxylate (**52**)



10.0 g of **51** were split into two batches.

Batch 1: A flame dried and argon flushed 500 mL two-neck round-bottom flask equipped with magnetic stirring bar was charged with 90 mL abs. THF, and cooled to -78 °C (dry-ice/acetone). Subsequently, 63.7 mL of a titrated LDA stock solution in abs. THF (0.48 M, 30.6 mmol, 2.0 equiv.) and 5.00 g (15.5 mmol, 1.0 equiv.) **51** were added portionwise over a period of 5 min. After 15 min 10.35 g (39.6 mmol, 2.6 equiv.) Davis-oxaziridine were added to the yellow solution over a period of 5 min. The yellowish-orange solution was stirred for another 20 min, whereupon 15 mL (86.2 mmol, 5.6 equiv.) HMPA were added which resulted in a red solution. After 60 min the solution was poured into 250 mL H₂O (1 spatula NaCl was added).

The batches were combined and extracted with EtOAc (3x300 mL) and the combined organic layers were dried over Na₂SO₄, filtered and concentrated *in vacuo*. The crude product was purified via flash column chromatography (500 g SiO₂, 20 x 8.5 cm, cyclohexane/EtOAc = 12/1, 250 mL frac., frac. 4-10 pooled). The obtained colorless oil is a mixture of the desired product and side products (presumably double bond isomers and the fully reduced cyclohexane derivative). It was used without further purification. 5.45 g crude product were obtained.

C₁₈H₃₄O₄Si [342.55 g·mol⁻¹]

R_f = 0.48 (cyclohexane/EtOAc = 5/1, UV)

GC-MS (EI, 70 eV, NG-STANDARD): t_R = 7.24; m/z (%) = 299.1 (100, [M- iPr]), 239.1 (36), 145.1 (26), 109.1 (86), 75.0 (76).

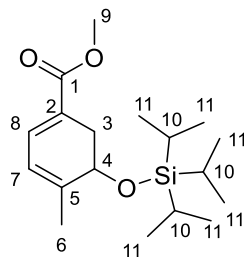
HRMS (FTICR MS ESI): m/z: calcd for C₁₈H₃₄O₄Si⁺ [M-H]⁺: 341.2148;
found: 341.2120.

¹H-NMR (300 MHz, CDCl₃): δ = 6.06–5.40 (m, 1H), 4.48–4.24 (m, 1H), 3.79 (s, 3H), 3.28 (s, 1H), 2.48 (m, 1H), 2.25–1.69 (m, 2H), 1.07 (m, 24H).

Peaks were assigned according to peak height.

Major diastereomer: ¹³C-NMR, APT (76 MHz, CDCl₃): δ = 176.6, 137.4, 124.5, 74.4, 66.5, 53.4, 38.0, 36.0, 18.2, 12.4.

9.8.59 Methyl 4-methyl-3-((triisopropylsilyl)oxy)cyclohexa-1,5-dienecarboxylate (**53**)



A flame dried and argon-flushed 500 mL three-neck round-bottom flask equipped with magnetic stirring bar and a Schlenk adapter was consecutively charged with 5.45 g (16.0 mmol, 1.0 equiv.) **52** and 200 mL degassed abs. ACN. To the stirred solution 13.24 g (55.6 mmol, 3.5 equiv.) Burgess reagent were added. Upon heating to 70 °C (oil-bath) the reaction mixture turned yellow and it was stirred for 14 h. Subsequently, the solution was allowed to cool to RT and was poured into 400 mL H₂O. The organic phase was separated, the aqueous phase was treated with small amounts of NaCl and extracted with DCM (3x300 mL). The combined organic layers were dried over Na₂SO₄, filtered and concentrated *in vacuo*. The product was purified via flash column chromatography (400 g SiO₂, 20 x 8.5 cm, pentane/DCM/EtOAc 80/5/1, 200 mL frac., frac. 8-14 pooled) to give impure product containing multiple side products. Two subsequent flash column chromatographies (50 g SiO₂, 18.5 x 3.5 cm, toluene/DCM 200/1, 30 mL frac., frac. 6-12 pooled) and (20 g SiO₂, 15 x 2.5 cm, toluene/DCM 200/1, 10 mL frac., frac. 6-10 pooled) afforded pure **50**.

Yield= 413 mg (1.3 mmol, 1 %: calculated over 6 steps from **43**) colorless oil

C₁₈H₃₂O₃Si [324.53g·mol⁻¹]

R_f= 0.45 (toluene/DCM = 200/1, CAM)

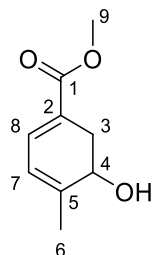
GC-MS (EI, 70 eV, NG-STANDARD): t_R= 7.22; m/z (%)= 324.2 (100, [M⁺]), 281.1 (180), 119.0 (760), 75.0 (600).

HRMS (FTICR MS ESI): m/z: calcd for C₁₈H₃₂O₃Si⁺ [M]⁺: 324.2121;
found: 324.2139.

¹H-NMR (300 MHz, CDCl₃): δ = 6.99 (d, J = 5.6 Hz, 1H), 5.87 (d, J = 5.3 Hz, 1H), 4.44 (t, J = 7.7 Hz, 1H), 3.75 (s, 3H), 2.68 (dd, J = 24.8 Hz, 7.7 Hz, 2H), 1.99 (s, 3H), 1.07 (s, 21 H).

¹³C-NMR, APT (76 MHz, CDCl₃): δ = 167.9 (C-1), 146.3 (C-5), 133.2 (C-7), 124.6 (C-8), 120.0 (C-2), 69.5 (C-4), 51.7 (C-9), 32.2 (C-3), 20.9 (C-6), 18.3 (C-10), 12.9 (C-11).

9.8.60 Methyl 5-hydroxy-4-methylcyclohexa-1,3-diene-1-carboxylate (**54**)



A 50 mL round-bottom flask equipped with magnetic stirring bar was consecutively charged with 378 mg (1.16 mmol, 1.0 equiv.) **53** and 20 mL abs. THF and was cooled to 0°C (ice-bath). To the stirred solution 334 mg (1.28 mmol, 1.1 equiv.) TBAF were added, whereupon the solution became yellow. After 45 min full consumption of the starting material was observed (reaction monitoring via TLC) and the reaction mixture was concentrated *in vacuo*. The crude product was purified via flash column chromatography (25 g SiO₂, 13 x 2.5 cm, cyclohexane/EtOAc 3/1, 15 mL frac., frac. 9-18 pooled) to give a yellow oil.

Degradation of the product was observed on TLC over a prolonged period of storage at -20 °C.

Yield= 138 mg (0.82 mmol, 70 %), yellow oil

C₉H₁₂O₃ [168.19 g·mol⁻¹]

R_f= 0.17 (cyclohexane/EtOAc = 3/1, UV)

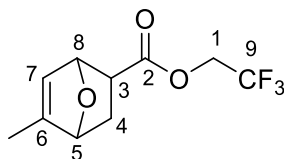
HRMS (FTICR MS ESI): m/z: calcd for C₉H₁₂O₃⁺ [M]⁺: 168.0786;

found: 168.0790.

¹H-NMR (300 MHz, CDCl₃): δ = 7.05 (m, 1 H), 5.97 (m, 1 H), 4.13 (t, *J* = 5.1 Hz, 1 H), 3.76 (s, 3 H), 2.91-2.99 (m, 1 H), 2.62 (dd, *J* = 18.7 Hz, 6.3 Hz, 1 H), 2.02 (s, 3 H), 1.48 (s, 1 H).

¹³C-NMR, APT (76 MHz, CDCl₃): δ = 167.8 (C-1), 144.1 (C-5), 132.6 (C-7), 123.8 (C-8), 120.6 (C-2), 67.7 (C-4), 51.8 (C-9), 31.7 (C-3), 21.0.

9.8.61 2,2,2-Trifluoroethyl 5-methyl-7-oxabicyclo[2.2.1]hept-5-ene-2-carboxylate (**55**)



This compound was prepared following a literature procedure.^[137]

In a flame dried and argon flushed 7 mL Schlenk flask equipped with magnetic stirring bar 57.5 mg (0.163 mmol, 0.24 equiv.) Corey's oxazaborolidinium catalyst were dissolved in 1.0 mL abs. DCM. The flask was cooled to -78 °C (dry ice/acetone) and 12 µL (0.135 mmol, 0.20 equiv.) triflic acid were added. The solution became yellow-cloudy and it was stirred at this temperature for 10 min, after which 85 µL (0.671 mmol, 1 equiv.) trifluoroethyl acrylate were added. It was stirred for further 3 min and 259 mg (3.15 mmol, 4.7 equiv.) 3-methylfuran were added. The color of the solution became first dark-yellow and changed then to orange. After 2.5 h, 20 µL Et₃N and 20 mL H₂O were added. The aqueous phase was extracted with DCM (4x20 mL), dried over Na₂SO₄, filtered and concentrated *in vacuo*. The product was purified via flash column chromatography (12 g SiO₂, 8.5 x 1.9 cm, cyclohexane/EtOAc 11/1, 8 mL frac., frac. 10-18 pooled).

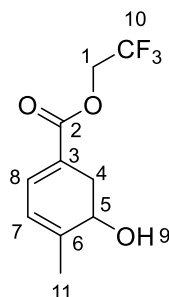
Yield= 87 mg (0.368 mmol, 55 %) slightly yellow oil

C₁₀H₁₁F₃O₃ [236.19 g·mol⁻¹]

R_f= 0.30 (cyclohexane/EtOAc 3/1, UV)

¹H-NMR (300 MHz, CDCl₃): δ = 5.74 (m, 1H), 5.11 (d, 1H, *J*= 4.0 Hz), 4.77 (d, 1H, *J*= 4.6 Hz), 4.48-4.30 (m, 2H), 3.23 (m, 1H), 2.11 (m, 1H), 1.84 (d, 3H, *J*=1.2 Hz), 1.60 (dd, *J*= 4.0 Hz, 12.0 Hz, 1H).

9.8.62 2,2,2-Trifluoroethyl 5-hydroxy-4-methylcyclohexa-1,3-diene-1-carboxylate (**56**)



A flame dried and argon flushed 8 mL Schlenk flask equipped with magnetic stirring bar was charged with 100 μL (0.483 mmol, 1.3 equiv.) hexamethyldisilazane in 0.5 mL abs. THF. It was stirred vigorously and cooled to $-78\text{ }^\circ\text{C}$ (dry ice/acetone) and 200 μL 2.09 M BuLi (0.418 mmol, 1.1 equiv.) were slowly added. It was warmed to $0\text{ }^\circ\text{C}$ for 15 min, after which it was again cooled to $-78\text{ }^\circ\text{C}$. Subsequently, 87 mg (0.368 mmol, 1 equiv.) **55**, dissolved in 0.5 mL abs. THF were added over the course of 3 min. It was stirred at $-78\text{ }^\circ\text{C}$ for 2.5 h, after which full consumption of the starting material was detected (reaction monitoring via TLC) and it was poured into 50 mL sat. NH_4Cl solution (pre-cooled to $0\text{ }^\circ\text{C}$). The aqueous phase was extracted with EtOAc (4x15 mL) and the combined organic layers were dried over Na_2SO_4 , filtered and concentrated *in vacuo*. The product was purified via flash column chromatography (15 g SiO_2 , 9.0 x 2.3 cm, cyclohexane/EtOAc = 4/1, 10 mL frac., frac. 9-14 pooled).

Yield= 29 mg (0.123 mmol, 33 %), colorless oil

$\text{C}_{10}\text{H}_{11}\text{F}_3\text{O}_3$ [236.19 $\text{g}\cdot\text{mol}^{-1}$]

R_f = 0.29 (cyclohexane/EtOAc = 3/1, UV)

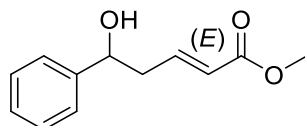
HRMS (FTICR MS ESI): m/z : calcd for $\text{C}_{10}\text{H}_{11}\text{F}_3\text{KO}_3^+$ [M+K] $^+$: 275.0297;
found: 275.0292.

$^1\text{H-NMR}$ (300 MHz, CDCl_3): δ = 7.15 (dd, J = 5.7 Hz, 2.4 Hz, 1H, H-8), 5.99 (dd, J = 5.8 Hz, 1.2 Hz, 1H, H-7), 4.61–4.46 (q, J = 8.6 Hz, 2H, H-1), 4.22–4.10 (m, 1H, H-5), 2.93 (dd, J = 18.7 Hz, 4.2 Hz, 1H, H-4a), 2.64 (dd, J = 18.7 Hz, 6.0 Hz, 1H, H-4b), 2.03 (s, 3H, H-11), 1.71 (bs, 1H, OH).

$^{13}\text{C-NMR,APT}$ (76 MHz, CDCl_3): δ = 165.5 (C-2), 145.7 (C-6), 134.7 (C-8), 123.3 (q, J = 279 Hz, C-1) 122.2 (C-3), 120.5 (C-7), 67.5 (C-5), 60.6 (q, J = 36.5 Hz, C-1), 31.4 (C-4), 21.1 (C-11).

$^{19}\text{F-NMR}$ (470 MHz, CDCl_3): δ = -73.8.

9.8.63 Methyl (*E*)-5-hydroxy-5-phenylpent-2-enoate (**57**)



This compound was prepared according to the literature.^[152]

In a flame dried and argon flushed 250 mL three-neck flask equipped with a bubbler and magnetic stirring bar 2.84 g (19.2 mmol, 1 equiv.) 1-phenylbut-3-en-1-ol were dissolved in 100 mL abs. toluene. To the stirred solution were consecutively added 3.41 mL methyl acrylate (37.6 mmol, 2.0 equiv) and 256 mg (0.41 mmol, 2 mol%) Grubbs-Hoveyda 2nd generation catalyst. It was stirred for 18 h and concentrated *in vacuo*. The crude product was purified via flash column chromatography (350 g SiO₂, 17 x 8.0 cm, cyclohexane/EtOAc 6/1, 230 mL frac., frac. 10-12 pooled). 4.32 g of a brownish oil were obtained. 2.53 g of the brownish oil were further purified via Kugelrohr distillation (0.18 mbar, 150 °C).

Yield= 2.28 g (11.1 mmol, 49 %, steps) colorless oil

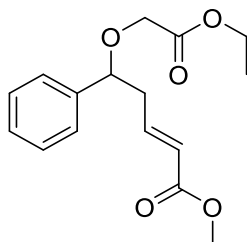
C₁₂H₁₄O₃ [206.24 g·mol⁻¹]

R_f= 0.40 (cyclohexane/ EtOAc= 4/1, CAM)

¹H-NMR (300 MHz, CDCl₃): δ= 7.43–7.26 (m, 5H), 7.09–6.83 (m, 1H), 5.91 (d, *J* = 15.7 Hz, 1H), 4.83 (dd, *J* = 7.3 Hz, 5.6 Hz, 1H), 3.71 (s, 3H), 2.83–2.49 (m, 2H), 2.02 (bs, 1H).

¹³C-NMR, APT (76 MHz, CDCl₃): δ= 166.8, 145.1, 143.5, 128.8, 128.1, 125.9, 123.8, 73.3, 51.6, 42.0.

9.8.64 Methyl (E)-5-(2-ethoxy-2-oxoethoxy)-5-phenylpent-2-enoate (**58**)



In a flame dried and argon flushed Schlenk flask equipped with a magnetic stirring bar 80.4 mg (0.390 mmol, 1 equiv.) **57** were dissolved in 1.5 mL abs. DCM and 1.7 mg (0.0039 mmol, 1.0 mol%) Rh₂(OAc)₄ were added. To the stirred solution 55 mg (0.484 mmol, 1.2 equiv.) ethyl diazoacetate, dissolved in 1.6 mL abs. DCM, were added over 1 h via a syringe pump. The reaction mixture was concentrated *in vacuo* to give a yellow oil. The crude product was purified via flash column chromatography (10 g SiO₂, cyclohexane/EtOAc 6/1, 7 mL frac., frac. 7-13 pooled).

Yield: 59 mg (0.202 mmol, 52 %), colorless oil

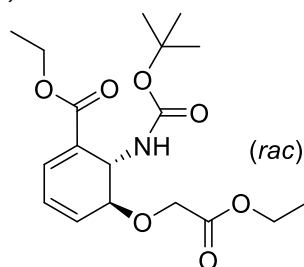
C₁₆H₂₀O₅ [292.33 g·mol⁻¹]

R_f = 0.22 (cyclohexane/EtOAc = 6/1, CAM)

¹H-NMR (300 MHz, CDCl₃): δ= 7.43–7.21 (m, 5H), 6.99 (dt, *J* = 15.5 Hz, 7.1 Hz, 1H), 5.88 (d, *J* = 15.7 Hz, 1H), 4.54 (dd, *J* = 7.5 Hz, 5.6 Hz, 1H), 4.29–4.10 (m, 2H), 4.01 (d, *J* = 16.4 Hz, 1H), 3.84 (d, *J* = 16.4 Hz, 1H), 3.71 (s, 3H), 2.79 (ddd, *J* = 14.8 Hz, 10.7 Hz, 4.2 Hz, 1H), 2.60 (ddd, *J* = 14.7 Hz, 6.9 Hz, 1.3 Hz, 1H), 1.35–1.16 (m, 3H).

¹³C-NMR (76 MHz, CDCl₃): δ= 170.3, 166.9, 145.0, 140.0, 128.8, 128.5, 126.9, 123.3, 81.2, 65.9, 61.0, 51.5, 40.8, 14.2.

9.8.65 *rac-trans*-Ethyl-6-((*tert*-butoxycarbonyl)amino)-5-(2-ethoxy-2-oxoethoxy)cyclohexa-1,3-diene-1-carboxylate (**59**)



In a flame dried and argon flushed 15 mL Schlenk flask equipped with magnetic stirring bar 68 mg (0.241 mmol, 1 equiv.) **30** were dissolved in 3 mL abs. THF and cooled to -20 °C (dry ice/acetone). To the stirred, slightly yellowish solution 14.2 mg (0.355 mmol, 1.47 equiv.) NaH (60 % dispersion in mineral oil) were added, whereupon the solution became cloudy. After 20 min, 51.8 μ L (0.438 mmol, 1.82 equiv.) ethyl iodoacetate were added dropwise to the yellow solution, while the temperature was kept at -20 °C. The mixture was stirred and allowed to warm up to RT within 6 h (reaction monitoring via TLC). Subsequently, the reaction mixture was poured into a flask containing 10 mL sat. NH₄Cl solution. The aqueous phase was extracted with EtOAc (4x20 mL). The combined organic layers were dried over Na₂SO₄, filtered and concentrated *in vacuo* to give a yellow oil. The crude product was purified via flash column chromatography (5 g SiO₂, 12.0 x 1.2 cm, cyclohexane/EtOAc 4/1 (frac. 1-23), cyclohexane/EtOAc 2/1 (frac. 24-30), cyclohexane/EtOAc 1/2 (frac. 31-40), 3 mL frac., frac. 17-24 pooled). In addition, 22 mg starting material **23** (frac. 31-34 pooled) were recovered.

Yield: 23.2 mg (0.0628 mmol, 26 %, 59 % brsm), colorless oil

C₁₈H₂₇NO₇ [206.24 g·mol⁻¹]

R_f= 0.45 (cyclohexane/ EtOAc= 2/1, CAM)

HRMS (FTICR MS ESI): m/z: calcd for C₁₈H₂₇NO₇⁺ [M]⁺: 369.1787;

found: 369.1783.

¹H-NMR (300 MHz, CDCl₃): δ = 7.18 (s, 1H), 6.32 (d, *J* = 2.2 Hz, 2H), 4.84 (d, *J* = 7.2 Hz, 1H), 4.48–4.00 (m, 8H), 1.38 (m, 9H), 1.35–1.17 (m, 6H).

¹³C-NMR, APT (76 MHz, CDCl₃): δ = 155.1, 133.7, 130.1, 127.6, 125.7, 75.6, 66.2, 61.0, 46.2, 28.5, 14.3, 14.3.

2 signals for quaternary carbons were not detected.

9.8.66 " $Rh_2(tfacam)_4$ " –batch 1

The synthesis is based on a literature procedure.^[153]

A 25 mL round-bottom flask was equipped with a short-path distillation head fitted with a 25 mL receiving flask. The reaction flask was consecutively charged with 140 mg (0.32 mmol, 1 equiv.) $Rh_2(OAc)_4$, 18.5 mL abs. chlorobenzene and 512 mg (4.5 mmol, 14 equiv. trifluoroacetamide. The apparatus was placed in an oil bath preheated to 155 °C. The solvent distilled at a rate of ~1 mL/h at this temperature. It was observed that trifluoroacetamide sublimed within the distillation apparatus. Approximately every 8 h, it was cooled to RT and an appropriate amount of chlorobenzene was added in order to restore the solvent volume of the reaction to ca. 19 mL. In addition, 512 mg (4.5 mmol, 14 equiv.) trifluoroacetamide were added after 31 h. In total, it was distilled for 72 h. The flask was cooled to RT and the solid was collected by filtration and washed with abs. DCM (4x10 mL, not amylene-free), after which 100 mL acetone were used to dissolve the solid. The solution was concentrated *in vacuo*. The crude product was purified via flash column chromatography (10 g SiO_2 , 13 x 1.8 cm, 1 mL acetone was used to dissolve the crude product, DCM/EtOAc 3/1, 10 mL frac., frac. 7-26 pooled). 153 mg of a blue solid were obtained (it was dried for 4h at 50 °C using an oil-pump)

The purity and composition of the catalyst remain unclear.

Lit.-Ref.:^[153,154] ^{19}F -NMR (282 MHz, CD_3CN , $C_6H_5CF_3$ standard at -63.7 ppm) = -74.4 ppm.

For a discussion see: Dunham et al.^[155]

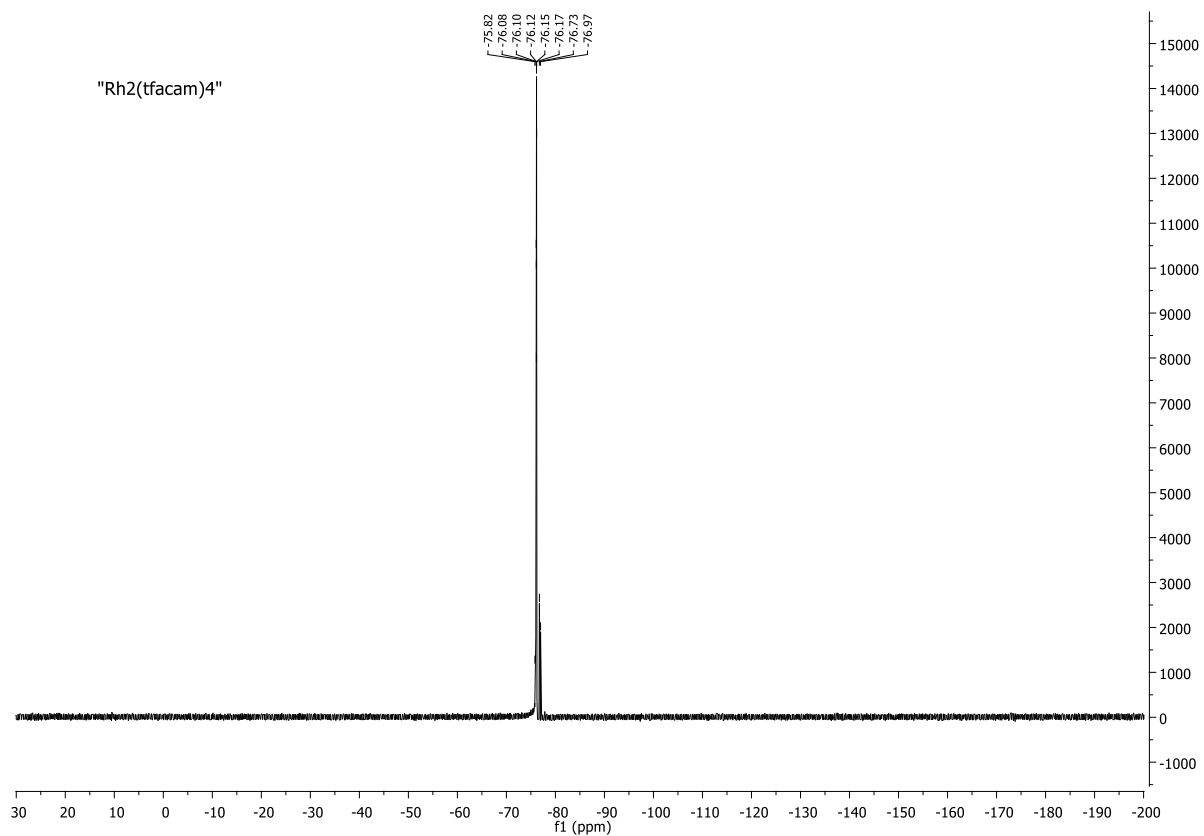


Figure 9.2: ¹⁹F-NMR (470.35 MHz, MeOD-d₄, no internal standard) of "Rh₂(tfacam)₄" batch 1.

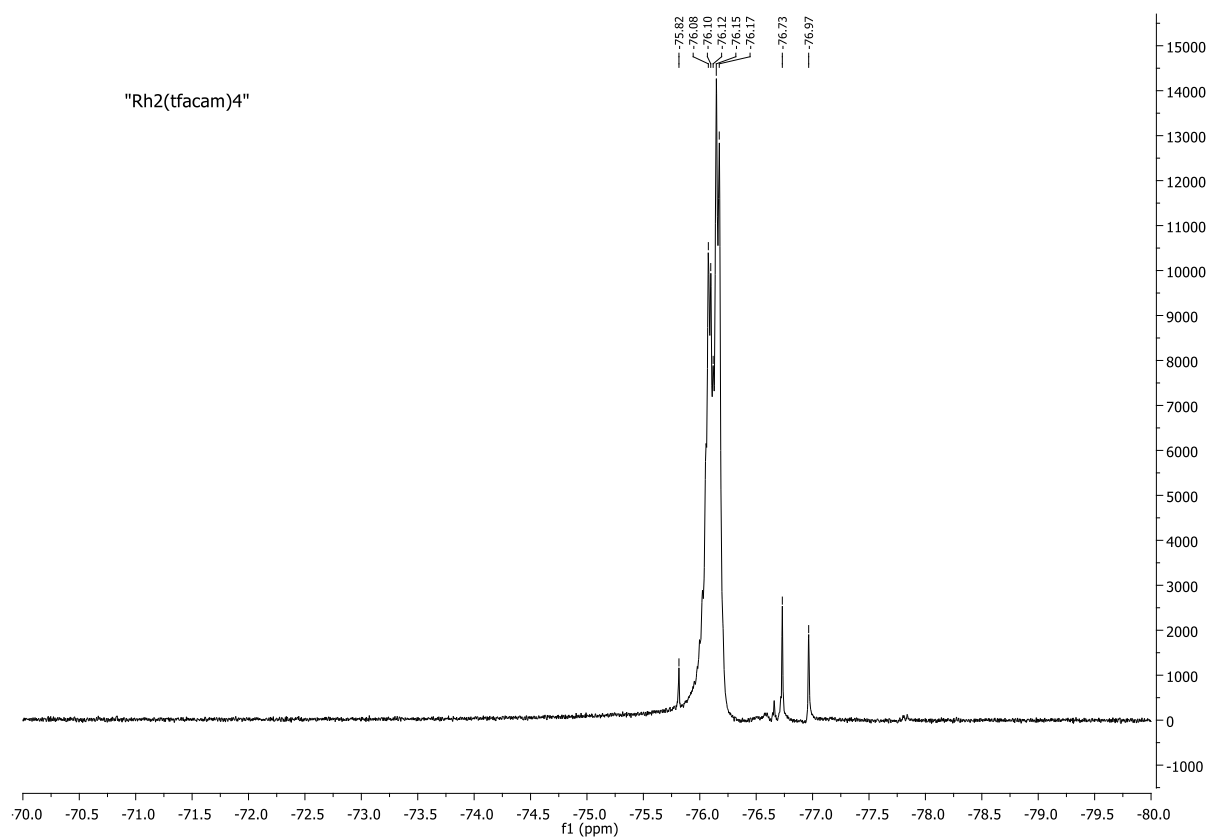


Figure 9.3: ¹⁹F-NMR (470.35 MHz, MeOD-d₄, no internal standard) of "Rh₂(tfacam)₄" batch 1.

9.8.67 " $Rh_2(tfacam)_4$ " –batch 2

The synthesis is based on a literature procedure.^[153]

A flame dried and argon flushed 50 mL two-neck round-bottom flask was equipped with a Schlenk adapter and a short-path distillation head fitted with a 50 mL receiving flask. The reaction flask was consecutively charged with 281 mg (0.635 mmol, 1 equiv.) $Rh_2(OAc)_4$, 37 mL abs. chlorobenzene and 1.03 g (9.13 mmol, 14.4 equiv. trifluoroacetamide. The reaction was carried out under N_2 . The apparatus was placed in an oil bath preheated to 155 °C. The solvent distilled at a rate of 1-2 mL/h at this temperature. It was observed that trifluoroacetamide sublimed within the distillation apparatus. Approximately every 9-15 h, the flask was cooled to RT and an appropriate amount of chlorobenzene was added in order to restore the solvent volume of the reaction to ca. 37 mL. In addition, ca. 500 mg trifluoroacetamide (4.4 mmol, 7.0 equiv.) were added every 9-15 h. In total, 3.55 g (31.4 mmol, 49 equiv.) trifluoroacetamide were used. After 72 h, the flask was cooled to RT and the following steps were performed under air. The solid was collected by filtration and washed with abs. DCM (3x10 mL, amylene-free), after which 30 mL abs. acetone (stored over 3 Å MS) were used to dissolve the solid. Subsequently, the solution was concentrated *in vacuo* and toluene was added and then removed using a rotary evaporator (3x15 mL). The same procedure was repeated using abs. DCM (2x10 mL, amylene-free) to remove residual solvent. The product was dried using an oil-pump (12 h, 50 °C). 353 mg of the crude product were obtained, which was purified via flash column chromatography (10 g SiO_2 , 17 x 1.3 cm, 1 mL acetone was used to dissolve the crude product, DCM (amylene-free)/EtOAc 3/1, 7 mL frac., frac. 2-8 pooled). 85 mg of a blue solid were obtained (which was dried for 4 h at 50 °C using an oil-pump)

The purity and composition of the catalyst remain unclear.

Lit.-Ref.:^[153,154] ^{19}F -NMR (282 MHz, CD_3CN , $C_6H_5CF_3$ standard at -63.7 ppm) = -74.4 ppm.

For a discussion see: Dunham et al.^[155]

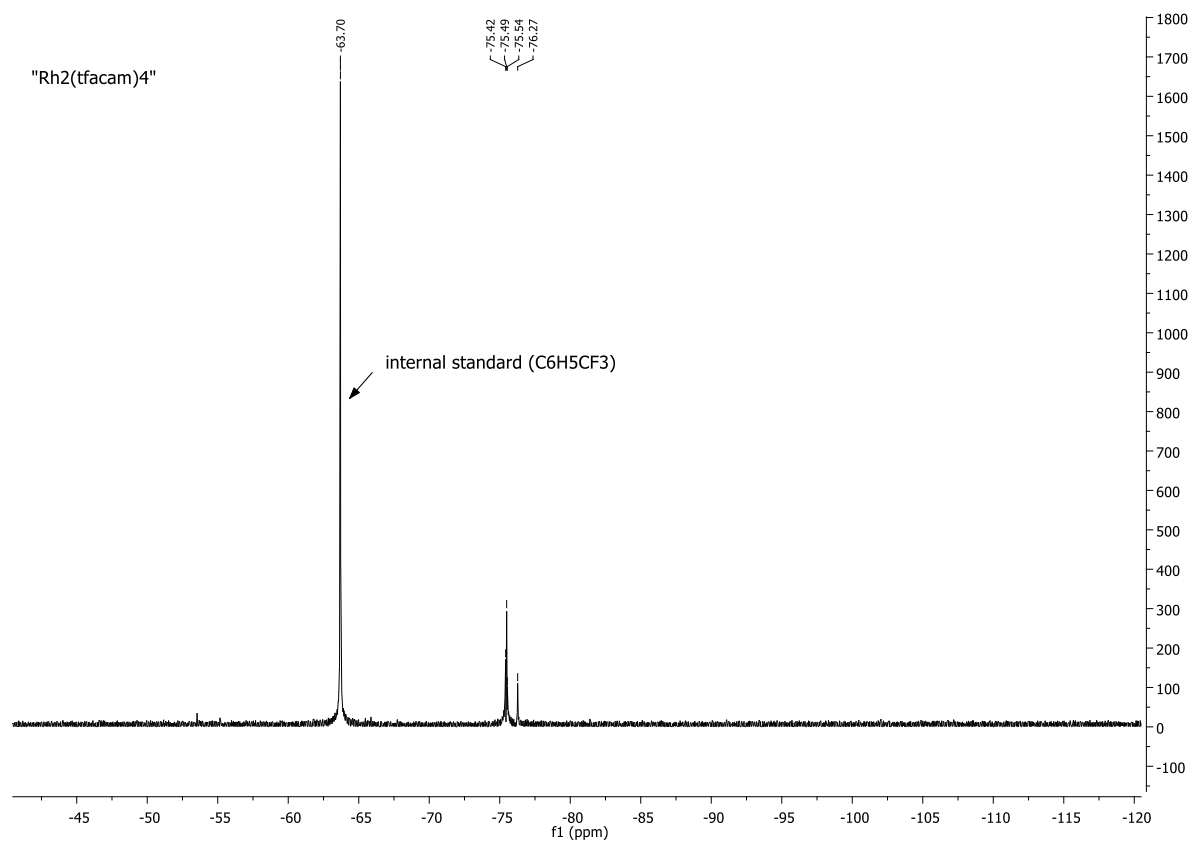


Figure 9.4: ¹⁹F-NMR (282 MHz, CD₃CN, C₆H₅CF₃ standard at -63.7 ppm) of "Rh₂(tfacam)₄" batch 2.

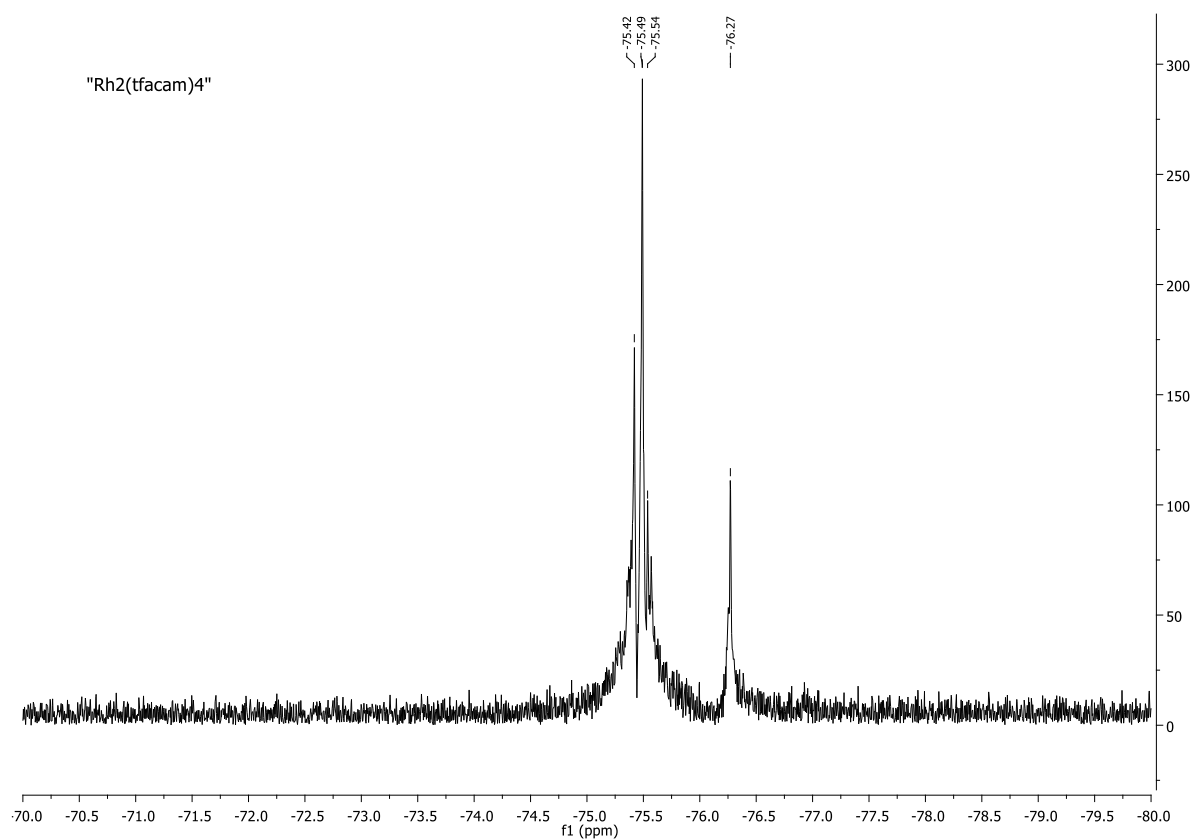


Figure 9.5: ¹⁹F-NMR (282 MHz, CD₃CN, C₆H₅CF₃ standard at -63.7 ppm) of "Rh₂(tfacam)₄" batch 2.

10 Abbreviations

δ	chemical shift
λ	wavelength
λ_{\max}	wavelength of maximum absorption
ϕ	dihedral angle
Å	ångström
°C	degree Celsius
(<i>E</i>)	entgegen (ger.: opposite)
(<i>R</i>)	rectus (lat.: right)
(<i>S</i>)	sinister (lat.: left)
(iPr) ₂ NH	diisopropylamine
μL	microliter
μm	micrometer
μM	micromolar
μmol	micromol
abs.	absolute (dry solvent)
ACN	acetonitrile
ADC	4-amino-4-deoxychorismate
ADCS	4-amino-4-deoxychorismate synthase
ADIC	2-amino-2-deoxyisochromismic acid
AOCHC	6-amino-5-oxocyclohex-2-ene-1-carboxylic acid
approx.	approximately
APT	attached proton test
Ar	argon
AS	anthranilate synthase
brsm	based on recovered starting material
b.p.	boiling point
Boc	tert-butyloxycarbonyl
ca.	circa
calcd.	calculated
CAM	cerium ammonium molybdate
cat.	catalytic
CDCl ₃	deuterated chloroform
<i>cis</i>	lat.: on this side
CL	chorismate lyase
CM	chorismate mutase
COSY	correlated spectroscopy

d	days
d	doublet
DAHP	3-deoxy-D-arabinoheptulosonate-7-phosphate
DBU	1,8-diazabicycloundec-7-ene
DCC	dicyclohexylcarbodiimide
dd	doublet of doublet
DHHA	<i>trans</i> -2,3-dihydro-3-hydroxyanthranilic acid
DHPCA	dihydrophenazine-1-carboxylic acid
DHPDC	dihydrophenazine-1,6-dicarboxylic acid
DHPHZ	dihydrophenazine
DMAP	4-(dimethylamino)pyridine
DMF	<i>N,N</i> -dimethylformamide
EDG	electron donating group
e.g.	exempli gratia (lat.: for example)
E4P	erythrose-4-phosphate
EtOAc	ethyl acetate
EI	electron impact
equiv.	equivalent
ESI	electrospray ionization
et al.	et alii (lat.: and others)
Et	ethyl
etc.	et cetera (lat.: and so on)
eV	electronvolt
EWG	electron withdrawing group
FA	formic acid
FID	flame ionization detector
frac.	fraction
FT	fourier transform
g	gram
GATase1	type 1 glutamine amidotransferase
GC	gas chromatography
GC-MS	gas chromatography- mass spectrometry
h	hour
HHPDC	hexahydrophenazine-1,6-dicarboxylic acid
HMPA	hexamethylphosphoramide
HPLC	high performance liquid chromatography
HRMS	high resolution mass spectrometry

HSQC	heteronuclear single quantum coherence
Hz	Hertz
IC	isochorismate
ICR	ion cyclotron resonance
IS	isochorismate synthase
<i>J</i>	coupling constant
KHMDS	potassium hexamethyldisilazane
K_i	inhibition constant
L	liter
m	meter
M	molar
M^+	molecular peak
m	multiplet
m.p.	melting point
<i>m/z</i>	mass to charge ratio
mAU	milli absorbance units
mbar	millibar
Me	methyl
MeO- d_4	deuterated methanol
mg	milligram
MHz	megahertz
min	minute
mL	milliliter
mmol	millimol
mol%	mol percent
Ms	methanesulfonyl chloride
MS	mass spectrometry
MST	menaquinone, siderophore, tryptophan
mV	millivolt
N_2	nitrogen
n.d.	not detectable
NAD	nicotinamide adenine dinucleotide
NADH	nicotinamide adenine dinucleotide hydride
nm	nanometer
nM	nanomolar
NMR	nuclear magnetic resonance
<i>o</i>	<i>ortho</i>

<i>p</i>	<i>para</i>
PCA	phenazine-1-carboxylic acid
PDC	phenazine-1,6-dicarboxylic acid
PEP	phosphoenolpyruvate
pH	negative decadic logarithm of the activity of H ₃ O ⁺
pKa	negative decadic logarithm of the acid dissociation constant
PLE	porcine liver esterase
ppm	parts per million
PYO	pyocyanin
q	quadruplet
quant	quantitative
RT	room temperature
<i>rac</i>	racemic
R _f	retardation factor
ROS	reactive oxygen species
s	singlet
sat.	saturated
soln.	solution
SS	salicylate synthase
t	triplet
tert	tertiary
TBS	<i>tert</i> -butyldimethylsilyl ether
Tf	trifluoromethanesulfonate
TFA	trifluoroacetic acid
THF	tetrahydrofuran
THPCA	tetrahydrophenazine-1-carboxylic acid
THPDC	tetrahydrophenazine-1,6-dicarboxylic acid
TLC	thin-layer chromatography
TMS	trimethylsilyl
TOF	time of flight
t _R	retention time
<i>trans</i>	lat.: on the other side
UV	ultraviolet
wt %	weight percent

Amino Acid Abbreviations

Amino acid	Three letter code	One letter code
Alanine	Ala	A
Arginine	Arg	R
Asparagine	Asn	N
Aspartic acid	Asp	D
Cysteine	Cys	C
Glutamic acid	Glu	E
Glutamine	Gln	Q
Glycine	Gly	G
Histidine	His	H
Isoleucine	Ile	I
Leucine	Leu	L
Lysine	Lys	K
Methionine	Met	M
Phenylalanine	Phe	F
Proline	Pro	P
Serine	Ser	S
Threonine	Thr	T
Tryptophan	Trp	W
Tyrosine	Tyr	Y
Valine	Val	V

11 References

- [1] A. Coates, Y. Hu, R. Bax, C. Page, *Nat. Rev. Drug Discov.* **2002**, *1*, 895–910.
- [2] K. T. Ziebart, S. M. Dixon, B. Avila, M. H. El-Badri, K. G. Guggenheim, M. J. Kurth, M. D. Toney, *J. Med. Chem.* **2010**, *53*, 3718–3729.
- [3] J. B. Laursen, J. Nielsen, *Chem. Rev.* **2004**, *104*, 1663–1686.
- [4] M. A. Fischbach, C. T. Walsh, *Science* **2009**, *325*, 1089–1093.
- [5] D. S. Blanc, C. Petignat, B. Janin, J. Bille, P. Francioli, *Clin. Microbiol. Infect.* **1998**, *4*, 242–247.
- [6] T. Strateva, D. Yordanov, *J. Med. Microbiol.* **2009**, *58*, 1133–1148.
- [7] G. W. Lau, D. J. Hassett, H. Ran, F. Kong, *Trends Mol. Med.* **2004**, *10*, 599–606.
- [8] A. Price-Whelan, L. E. P. Dietrich, D. K. Newman, *J. Bacteriol.* **2007**, *189*, 6372–6381.
- [9] Y. Wang, S. E. Kern, D. K. Newman, *J. Bacteriol.* **2010**, *192*, 365–369.
- [10] A. Price-Whelan, L. E. P. Dietrich, D. K. Newman, *Nat. Chem. Biol.* **2006**, *2*, 71–78.
- [11] D. Haas, G. Défago, *Nature Rev. Microbiol.* **2005**, *3*, 307–319.
- [12] W. Blankenfeldt, J. F. Parsons, *Curr. Opin. Struct. Biol.* **2014**, *29*, 26–33.
- [13] G. W. Lau, H. Ran, F. Kong, D. J. Hassett, D. Mavrodi, *Infect. Immun.* **2004**, *72*, 4275–4278.
- [14] R. D. Firn, C. G. Jones, *Nat. Prod. Rep.* **2003**, *20*, 382.
- [15] M. Mentel, E. G. Ahuja, D. V. Mavrodi, R. Breinbauer, L. S. Thomashow, W. Blankenfeldt, *Chembiochem* **2009**, *10*, 2295–2304.
- [16] M. E. Hernandez, A. Kappler, D. K. Newman, *App. Environ. Microbiol.* **2004**, *70*, 921–928.
- [17] L. E. P. Dietrich, T. K. Teal, A. Price-Whelan, D. K. Newman, *Science* **2008**, *321*, 1203–1206.
- [18] L. E. P. Dietrich, A. Price-Whelan, A. Petersen, M. Whiteley, D. K. Newman, *Mol. Microbiol.* **2006**, *61*, 1308–1321.
- [19] U. Hollstein, R. J. van Gemert, *Biochemistry* **1971**, *10*, 497–504.
- [20] J. M. Turner, A. J. Messenger, *Adv. Microbiol. Phys.* **1986**, *27*, 211–275.
- [21] H. J. Abken., M. Tietze, J. Brodersen, S. Baumer, U. Beifuss, U. Deppenmeier, *J. Bacteriol.* **1998**, *180*, 2027–2032.
- [22] U. Beifuss, M. Tietze, S. Bäumer, U. Deppenmeier, *Angew. Chem. Int. Ed.* **2000**, *39*, 2470–2472.
- [23] U. Beifuss, M. Tietze, *Top. Curr. Chem.* **2005**, *244*, 77–113.
- [24] M.-J. Fordos, *Rec. Trav. Soc. d'Émul. Sci. Pharm.* **1859**, *3*, 30.
- [25] M.-J. Fordos, *Compt. rend.* **1860**, *51*, 215–217.
- [26] J. Emerson, M. Rosenfeld, S. McNamara, B. Ramsey, R. L. Gibson, *Pediatr. Pulmonol.* **2002**, *34*, 91–100.
- [27] R. M. Donlan, J. W. Costerton, *Clin. Microbiol. Rev.* **2002**, *15*, 167–193.
- [28] A. C. Blackwood, A. C. Neish, *Can. J. Microbiol.* **1957**, *3*, 165–169.
- [29] R. C. Millican, *Biochim. Biophys. Acta* **1962**, *57*, 407–409.
- [30] D. H. Calhoun, M. Carson, R. A. Jensen, *J. Gen. Microbiol.* **1972**, *72*, 581–583.
- [31] R. P. Longley, J. E. Halliwell, J. J. R. Campbell, W. M. Ingledew, *Can. J. Microbiol.* **1972**, *18*, 1357–1363.
- [32] M. McDonald, D. V. Mavrodi, L. S. Thomashow, H. G. Floss, *J. Am. Chem. Soc.* **2001**, *123*, 9459–9460.

- [33] Q.-A. Li, D. V. Mavrodi, L. S. Thomashow, M. Roessle, W. Blankenfeldt, *J. Biol. Chem.* **2011**, *286*, 18213–18221.
- [34] D. V. Mavrodi, T. L. Peever, O. V. Mavrodi, J. A. Parejko, J. M. Raaijmakers, P. Lemanceau, S. Mazurier, L. Heide, W. Blankenfeldt, D. M. Weller et al., *App. Environ. Biol.* **2010**, *76*, 866–879.
- [35] U. Deppenmeier, A. Johann, T. Hartsch, R. Merkl, R. A. Schmitz, R. Martinez-Arias, A. Henne, A. Wiezer, S. Baumer, C. Jacobi et al., *J. Mol. Microbiol. Biotechnol.* **2002**, *4*, 453–461.
- [36] A. A. Morollo, R. Bauerle, *Proc. Natl. Acad. Sci. U.S.A.* **1993**, *90*, 9983–9987.
- [37] M. Cirilli, R. Zheng, G. Scapin, J. S. Blanchard, *Biochim. Biophys. Acta* **1998**, *37*, 16452–16458.
- [38] A. Buschiazzo, M. Goytia, F. Schaeffer, W. Degrave, W. Shepard, C. Grégoire, N. Chamond, A. Cosson, A. Berneman, N. Coatnoan et al., *Proc. Natl. Acad. Sci. U.S.A.* **2006**, *103*, 1705–1710.
- [39] G. S. Garvey, C. J. Rocco, J. C. Escalante-Semerena, I. Rayment, *Protein Sci.* **2007**, *16*, 1274–1284.
- [40] M. Velarde, S. Macieira, M. Hilberg, G. Bröker, S.-M. Tu, B. T. Golding, A. J. Pierik, W. Buckel, A. Messerschmidt, *J. Mol. Biol.* **2009**, *391*, 609–620.
- [41] Mario Leypold, *PhD thesis*, Graz University of Technology, Graz, **2015**.
- [42] U. Hollstein, L. G. Marshall, *J. Org. Chem.* **1972**, *37*, 3510–3514.
- [43] T. F. Chin-A-Woeng, J. E. Thomas-Oates, B. J. Lugtenberg, G. V. Bloemberg, *Mol. Plant. Interact.* **2001**, *14*, 1006–1015.
- [44] H. Budzikiewicz, *FEMS Microbiol. Rev.* **1993**, *104*, 209–228.
- [45] K. M. Herrmann, L. M. Weaver, *Annu. Rev. Plant Physiol. Plant Mol. Biol.* **1999**, *50*, 473–503.
- [46] O. Kerbarh, E. M. M. Bulloch, R. J. Payne, T. Sahr, F. Rébeillé, C. Abell, *Biochem. Soc. Trans.* **2005**, *33*, 763–766.
- [47] N. Amrhein, B. Deus, P. Gehrke, H. C. Steinrucken, *Plant Physiol.* **1980**, *66*, 830–834.
- [48] G. M. Kishore, D. M. Shah, *Annu. Rev. Biochem.* **1988**, *57*, 627–663.
- [49] A. Manos-Turvey, E. M. M. Bulloch, P. J. Rutledge, E. N. Baker, J. S. Lott, R. J. Payne, *ChemMedChem* **2010**, *5*, 1067–1079.
- [50] G. Chi, A. Manos-Turvey, P. D. O'Connor, J. M. Johnston, G. L. Evans, E. N. Baker, R. J. Payne, J. S. Lott, E. M. M. Bulloch, *Biochemistry* **2012**, *51*, 4868–4879.
- [51] T. R. Ioerger, T. O'Malley, R. Liao, K. M. Guinn, M. J. Hickey, N. Mohaideen, K. C. Murphy, H. I. M. Boshoff, V. Mizrahi, E. J. Rubin et al., *PloS one* **2013**, *8*, e75245.
- [52] M. C. Kozlowski, P. A. Bartlett, *J. Am. Chem. Soc.* **1991**, *113*, 5897–5898.
- [53] M. C. Kozlowski, N. J. Tom, C. T. Seto, A. M. Sefler, P. A. Bartlett, *J. Am. Chem. Soc.* **1995**, *117*, 2128–2140.
- [54] A. L. Lamb, *Biochim. Biophys. Acta* **2015**, *1854*, 1054–1070.
- [55] Z. Liu, F. Liu, C. C. Aldrich, *J. Org. Chem.* **2015**, *80*, 6545–6552.
- [56] A. Manos-Turvey, K. M. Cergol, N. K. Salam, E. M. M. Bulloch, G. Chi, A. Pang, W. J. Britton, N. P. West, E. N. Baker, J. S. Lott et al., *Org. Biomol. Chem.* **2012**, *10*, 9223–9236.
- [57] K. M. Meneely, Q. Luo, A. P. Riley, B. Taylor, A. Roy, R. L. Stein, T. E. Prisinzano, A. L. Lamb, *Biorg. Med. Chem.* **2014**, *22*, 5961–5969.
- [58] K. M. Nelson, K. Viswanathan, S. Dawadi, B. P. Duckworth, H. I. Boshoff, C. E. Barry, C. C. Aldrich, *J. Med. Chem.* **2015**, *58*, 5459–5475.
- [59] R. J. Payne, E. M. M. Bulloch, A. D. Abell, C. Abell, *Org. Biomol. Chem.* **2005**, *3*, 3629–3635.

- [60] M. Svarcova, M. Kratky, J. Vinsova, *Curr. Med. Chem.* **2015**, *22*, 1383–1399.
- [61] M. Vasan, J. Neres, J. Williams, D. J. Wilson, A. M. Teitelbaum, R. P. Remmel, C. C. Aldrich, *ChemMedChem* **2010**, *5*, 2079–2087.
- [62] C. T. Walsh, M. D. Erion, A. E. Walts, J. J. Delany, G. A. Berchtold, *Biochemistry* **1987**, *26*, 4734–4745.
- [63] C. T. Walsh, J. Liu, F. Rusnak, M. Sakaitani, *Chem. Rev.* **1990**, *90*, 1105–1129.
- [64] F. Xie, S. Dai, J. Shen, B. Ren, P. Huang, Q. Wang, X. Liu, B. Zhang, H. Dai, L. Zhang, *App. Environ. Microbiol.* **2015**, *99*, 5895–5905.
- [65] R. J. Payne, E. M. M. Bulloch, O. Kerbarh, C. Abell, *Org. Biomol. Chem.* **2010**, *8*, 3534–3542.
- [66] R. J. Payne, E. M. M. Bulloch, M. M. Toscano, M. A. Jones, O. Kerbarh, C. Abell, *Org. Biomol. Chem.* **2009**, *7*, 2421–2429.
- [67] P. Goncharoff, B. P. Nichols, *J. Bacteriol.* **1984**, *159*, 57–62.
- [68] B. A. Ozenberger, T. J. Brickman, M. A. McIntosh, *J. Bacteriol.* **1989**, *171*, 775–783.
- [69] Z. He, K. D. Stigers Lavoie, P. A. Bartlett, M. D. Toney, *J. Am. Chem. Soc.* **2004**, *126*, 2378–2385.
- [70] E. M. Bulloch, M. A. Jones, E. J. Parker, A. P. Osborne, E. Stephens, G. M. Davies, J. R. Coggins, C. Abell, *J. Am. Chem. Soc.* **2004**, *126*, 9912–9913.
- [71] K. N. Raymond, E. A. Dertz, S. S. Kim, *Proc. Natl. Acad. Sci. U.S.A.* **2003**, *100*, 3584–3588.
- [72] J. Zwahlen, S. Kolappan, R. Zhou, C. Kisker, P. J. Tonge, *Biochemistry* **2007**, *46*, 954–964.
- [73] D. E. Künzler, S. Sasso, M. Gamper, D. Hilvert, P. Kast, *J. Biol. Chem.* **2005**, *280*, 32827–32834.
- [74] M. S. DeClue, K. K. Baldrige, D. E. Künzler, P. Kast, D. Hilvert, *J. Am. Chem. Soc.* **2005**, *127*, 15002–15003.
- [75] S. D. Copley, J. R. Knowles, *J. Am. Chem. Soc.* **1987**, *109*, 5008–5013.
- [76] R. J. Payne, M. D. Toscano, E. M. M. Bulloch, A. D. Abell, C. Abell, *Org. Biomol. Chem.* **2005**, *3*, 2271–2281.
- [77] G. Spraggon, C. Kim, X. Nguyen-Huu, M. C. Yee, C. Yanofsky, S. E. Mills, *Proc. Natl. Acad. Sci. U.S.A.* **2001**, 6021–6026.
- [78] D. Gillingham, N. Fei, *Chem. Soc. Rev.* **2013**, *42*, 4918–4931.
- [79] I. Hladezuk, V. Chastagner, S. G. Collins, S. J. Plunkett, A. Ford, S. Debarge, A. R. Maguire, *Tetrahedron* **2012**, *68*, 1894–1909.
- [80] D. J. Miller, C. J. Moody, *Tetrahedron* **1995**, *51*, 10811–10843.
- [81] O. Silberrad, C. S. Roy, *J. Chem. Soc. Tans.* **1906**, *89*, 179.
- [82] R. Paulissen, H. Reimlinger, E. Hayez, A. J. Hubert, P. Teyssié, *Tetrahedron Lett.* **1973**, *14*, 2233–2236.
- [83] M. M. Campbell, M. Sainsbury, P. A. Searle, *Synthesis* **1993**, *1993*, 179–193.
- [84] G. G. Cox, J. J. Kulagowski, C. J. Moody, E.-R. H. B. Sie, *Synlett* **1992**, *1992*, 975–976.
- [85] G. G. Cox, D. J. Miller, C. J. Moody, E.-R. H. Sie, J. J. Kulagowski, *Tetrahedron* **1994**, *50*, 3195–3212.
- [86] M. Regitz, W. Bartz, *Chem. Ber.* **1970**, *103*, 1477–1485.
- [87] C. J. Moody, D. J. Miller, *Tetrahedron* **1998**, *54*, 2257–2268.
- [88] A. F. Noels, A. Demonceau, N. Petiniot, A. J. Hubert, P. Teyssié, *Tetrahedron* **1982**, *38*, 2733–2739.
- [89] T. D. Nelson, Z. J. Song, A. S. Thompson, M. Zhao, A. DeMarco, R. A. Reamer, M. F. Huntington, E. J. Grabowski, P. J. Reider, *Tetrahedron Lett.* **2000**, *41*, 1877–1881.
- [90] K. Nagai, T. Sunazuka, S. Ōmura, *Tetrahedron Lett.* **2004**, *45*, 2507–2509.

- [91] J. Bongaerts, S. Esser, V. Lorbach, L. Al-Momani, M. A. Müller, D. Franke, C. Grondal, A. Kurutsch, R. Bujnicki, R. Takors et al., *Angew. Chem.* **2011**, *123*, 7927–7932.
- [92] D. R. Magnin, R. B. Sulsky, J. A. Robl, T. J. Caulfield, R. A. Parker, 2003043624, **2003**.
- [93] R. Shen, C. T. Lin, E. J. Bowman, B. J. Bowman, J. A. Porco, *J. Am. Chem. Soc.* **2003**, *125*, 7889–7901.
- [94] R. D. Allan, G. A. Johnston, B. Twitchin, *Aust. J. Chem.* **1981**, *34*, 2231.
- [95] A. J. Birch, P. Hextall, S. Sternhell, *Aust. J. Chem.* **1954**, *7*, 256.
- [96] B. Neises, W. Steglich, *Org. Synth.* **1985**, *63*, 183.
- [97] M. Haerter, F. Wunder, H. Tinel, R. Kast, A. Geerts, E. M. Becker, P. Kolkhof, J. Hütter, J. Ergüden, *PCT Int. Appl.* 2004052839, **2004**.
- [98] I. B. Masesane, P. G. Steel, *Bull. Chem. Soc. Ethiop.* **2005**, *19*, 149–152.
- [99] I. B. Masesane, A. S. Batsanov, J. A. K. Howard, R. Mondal, P. G. Steel, *Beilstein J. Org. Chem.* **2006**, *2*, 1–6.
- [100] J. K. Addo, P. Teesdale-Spittle, J. O. Hoberg, *Synthesis* **2005**, *2005*, 1923–1925.
- [101] M. E. Bunnage, T. Ganesh, I. B. Masesane, D. Orton, P. G. Steel, *Org. Lett.* **2003**, *5*, 239–242.
- [102] F. Brion, *Tetrahedron Lett.* **1982**, *23*, 5299–5302.
- [103] M. Lovric, I. Cepanec, M. Litvic, A. Bartolincic, V. Vinkovic, *Croatica Chem. Acta* **2007**, *80*, 109–115.
- [104] J. L. Pawlak, R. E. Padykula, J. D. Kronis, R. A. Aleksejczyk, G. A. Berchtold, *J. Am. Chem. Soc.* **1989**, *111*, 3374–3381.
- [105] M. J. O'Mahony, R. A. More O'Ferrall, D. R. Boyd, C. M. Lam, A. C. O'Donoghue, *J. Phys. Org. Chem.* **2013**, *26*, 989–996.
- [106] G. A. Kraus, K. Frazier, *J. Org. Chem.* **1980**, *45*, 4820–4825.
- [107] C. B. Wooster, K. L. Godfrey, *J. Am. Chem. Soc.* **1937**, *59*, 596–597.
- [108] A. J. Birch, *J. Chem. Soc.* **1944**, 430.
- [109] P. W. Rabideau, Z. Marcinow (Eds.) *Org. React.*, Vol. 42, John Wiley & Sons, Inc., **1992**.
- [110] A. J. Birch, *Quart. Rev., Chem. Soc.* **1950**, 69.
- [111] F. X. Webster, R. M. Silverstein, *Synthesis* **1987**, *1987*, 922–924.
- [112] P. W. Rabideau, D. M. Wetzel, D. M. Young, *J. Org. Chem.* **1984**, *49*, 1544–1549.
- [113] Z. Wang, *Comprehensive organic name reactions and reagents*, Wiley, Hoboken, NJ, **2009**.
- [114] G. A. Kraus, W. Cui, *Synlett* **2003**, 95–96.
- [115] Subba Rao, G. S. R., H. Ramanathan, *Indian J. Chem., Sect. B* **1981**, *20B*, 1089.
- [116] N. Hashimoto, T. Aoyama, T. Shioiri, *Chem. Pharm. Bull.* **1981**, *29*, 1475–1478.
- [117] A. L. Gemal, J. L. Luche, *J. Am. Chem. Soc.* **1981**, *103*, 5454–5459.
- [118] K. Mai, G. Patil, *J. Org. Chem.* **1986**, *51*, 3545–3548.
- [119] B. M. Trost, T. N. Salzman, K. Hiroi, *J. Am. Chem. Soc.* **1976**, *98*, 4887–4902.
- [120] H. J. Reich, J. M. Renga, I. L. Reich, *J. Am. Chem. Soc.* **1975**, *97*, 5434–5447.
- [121] J. Cossy, N. Furet, *Tetrahedron Lett.* **1993**, *34*, 7755–7756.
- [122] F. A. Davis, O. D. Stringer, J. M. Billmers, *Tetrahedron Lett.* **1983**, *24*, 1213–1216.
- [123] L. C. Vishwakarma, O. D. Stringer, F. A. Davis, *Org. Synth.* **1988**, *66*, 203–210.
- [124] B. Chen, P. Zhou, F. A. Davis, E. Ciganek (Eds.) *Org. Reactions*, Wiley, New York, Chichester, **2003**.
- [125] L. Kürti, B. Czako, *Strategic applications of named reactions in organic synthesis. Background and detailed mechanisms ; 250 named reactions*, Elsevier Acad. Press, Amsterdam, **2005**.

- [126] J. M. Box, L. M. Harwood, J. L. Humphreys, G. A. Morris, P. M. Redon, R. C. Whitehead, *Synlett* **2002**, 2002, 358–360.
- [127] J. C. Martin, R. J. Arhart, *J. Am. Chem. Soc.* **1971**, 93, 4327–4329.
- [128] R. J. Arhart, J. C. Martin, *J. Am. Chem. Soc.* **1972**, 94, 5003–5010.
- [129] E. J. Alvarez-Manzaneda, R. Chahboun, E. Cabrera Torres, E. Alvarez, R. Alvarez-Manzaneda, A. Haidour, J. Ramos, *Tetrahedron Lett.* **2004**, 45, 4453–4455.
- [130] L. M. Frijia, C. A. Afonso, *Tetrahedron* **2012**, 68, 7414–7421.
- [131] G. Majetich, R. Hicks, F. Okha, *New J. Chem.* **1999**, 23, 129–131.
- [132] E. M. Burgess, H. R. Penton, E. A. Taylor, *J. Am. Chem. Soc.* **1970**, 92, 5224–5226.
- [133] E. M. Burgess, Penton, Harold R., Jr., E. A. Taylor, W. M. Williams, *Org. Synth.* **1977**, 56, 40–43.
- [134] D. A. Claremon, B. T. Phillips, *Tetrahedron Lett.* **1988**, 29, 2155–2158.
- [135] E. M. Burgess, H. R. Penton Jr., E. A. Taylor, W. M. Williams, *Org. Synth.* **1988**, Coll. Vol. 6, 788–791.
- [136] P. W. Rabideau, J. W. Paschal, L. E. Patterson, *J. Am. Chem. Soc.* **1975**, 97, 5700–5704.
- [137] D. H. Ryu, K. H. Kim, J. Y. Sim, E. J. Corey, *Tetrahedron Lett.* **2007**, 48, 5735–5737.
- [138] M. K. Brown, E. J. Corey, *Org. Lett.* **2010**, 12, 172–175.
- [139] F. de Nanteuil, J. Loup, J. Waser, *Org. Lett.* **2013**, 15, 3738–3741.
- [140] N. E. Searle, *Org. Synth.* **1956**, 36, 25.
- [141] N. Takamura, T. Mizoguchi, K. Koga, S.-i. Yamada, *Tetrahedron Lett.* **1971**, 12, 4495–4498.
- [142] T. Jaschinski, M. Hiersemann, *Org. Lett.* **2012**, 14, 4114–4117.
- [143] T. Allspach, H. Guembel, M. Regitz, *J. Organomet. Chem.* **1985**, 290, 33–39.
- [144] Á. M. Montaña, P. M. Grima, M. Castellví, C. Batalla, M. Font-Bardia, *Tetrahedron* **2012**, 68, 9982–9998.
- [145] W. G. Kofron, L. M. Baclawski, *J. Org. Chem.* **1976**, 41, 1879–1880.
- [146] M. E. Biffin, A. G. Moritz, D. B. Paul, *Aust. J. Chem.* **1972**, 25, 1329.
- [147] W. M. Grootaert, R. Mijngheer, P. J. de Clercq, *Tetrahedron Lett.* **1982**, 23, 3287–3290.
- [148] H. Herzog, H. Koch, H.-D. Scharf, A. J. Runsink, *Tetrahedron* **1986**, 42, 3547–3558.
- [149] A. A. Morollo, M. G. Finn, R. Bauerle, *J. Am. Chem. Soc.* **1993**, 115, 816–817.
- [150] J. J. Gajewski, J. Jurayj, D. R. Kimbrough, M. E. Gande, B. Ganem, B. K. Carpenter, *J. Am. Chem. Soc.* **1987**, 109, 1170–1186.
- [151] T. Aotsuka, H. Kanazawa, K. Kumazawa, WO 2009072581, **2009**.
- [152] C. M. Smith, G. A. O'Doherty, *Org. Lett.* **2003**, 5, 1959–1962.
- [153] K. Guthikonda, J. Du Bois, *J. Am. Chem. Soc.* **2002**, 124, 13672–13673.
- [154] B. H. Brodsky, J. Du Bois, *Org. Lett.* **2004**, 6, 2619–2621.
- [155] S. U. Dunham, T. S. Remaley, B. S. Moore, D. L. Evans, S. U. Dunham, *Inorg. Chem.* **2011**, 50, 3458–3463.

12 Appendix

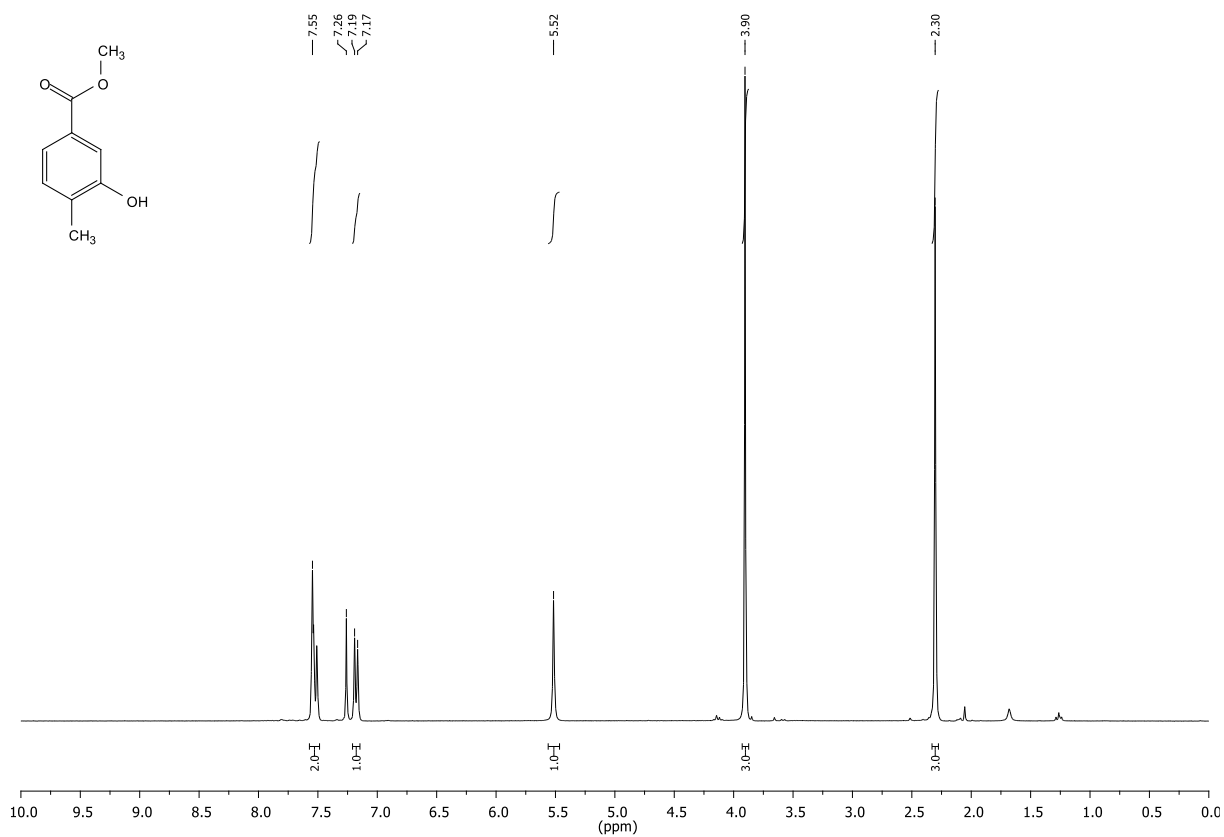


Figure 12.1: ¹H-NMR(300.36 MHz, CDCl₃) of compound 1

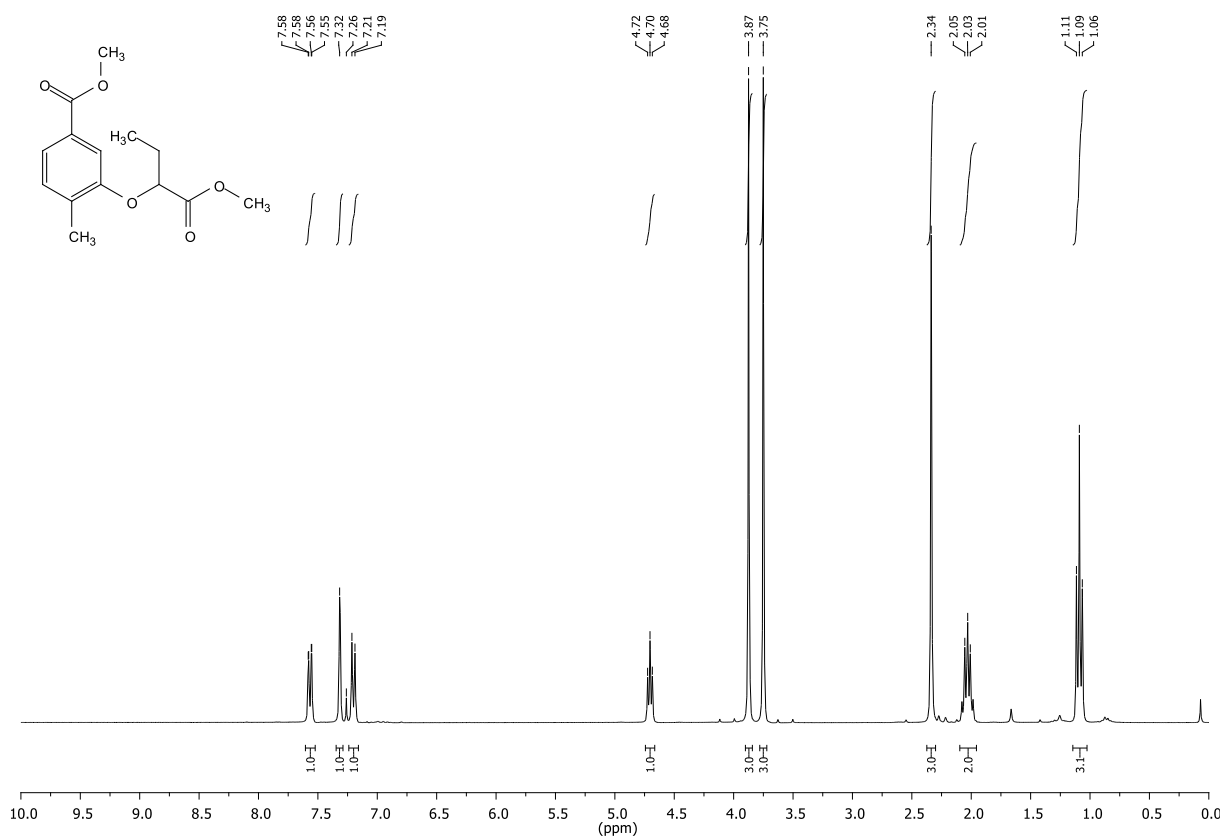


Figure 12.2: ¹H-NMR(300.36 MHz, CDCl₃) of compound 2.

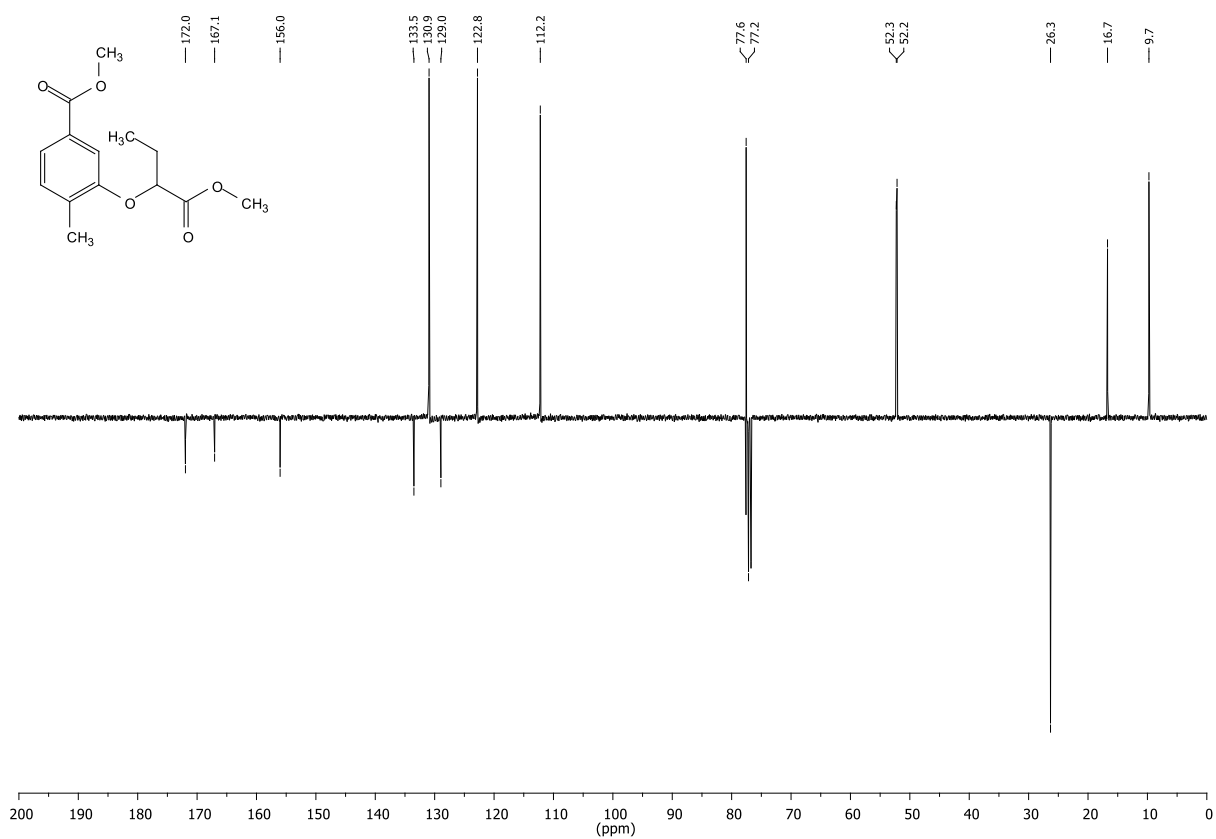


Figure 12.3: $^{13}\text{C-NMR}$, APT(75.53 MHz, CDCl_3) of compound 2.

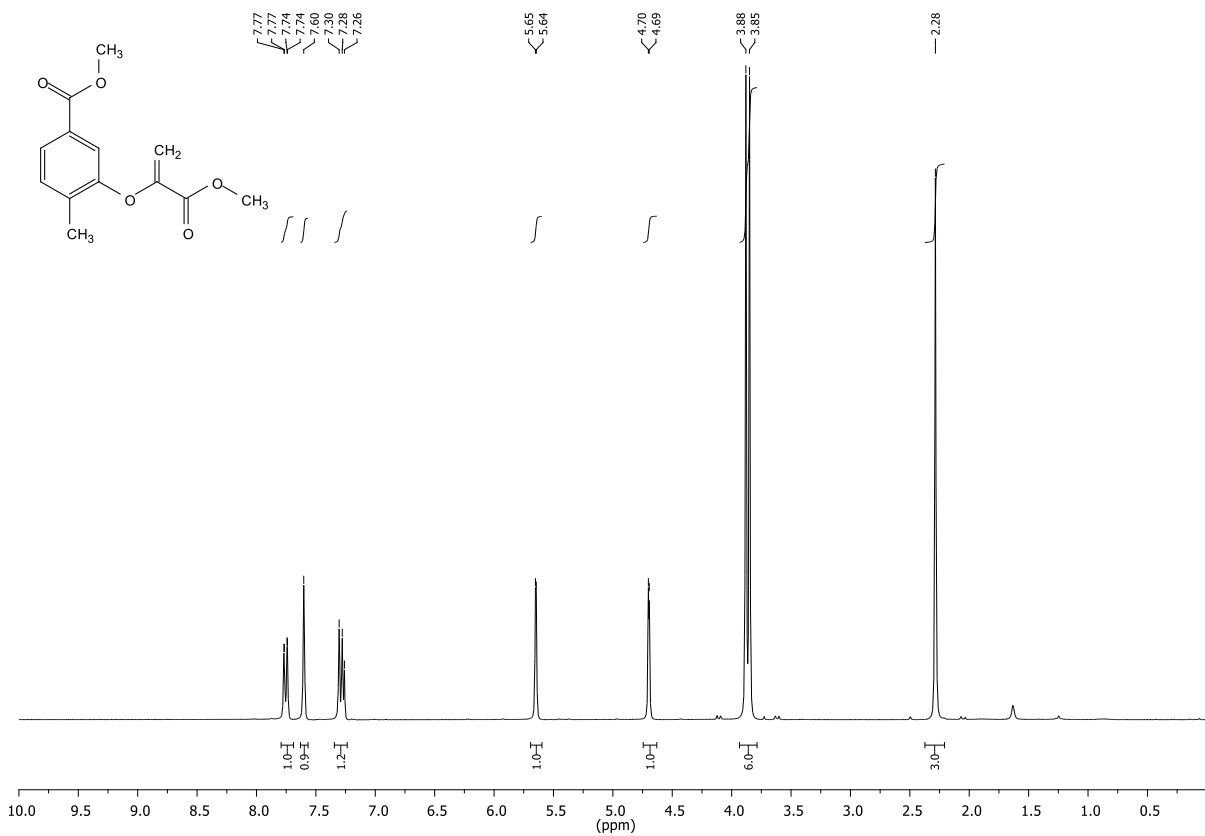


Figure 12.4: $^1\text{H-NMR}$ (300.36 MHz, CDCl_3) of compound 3.

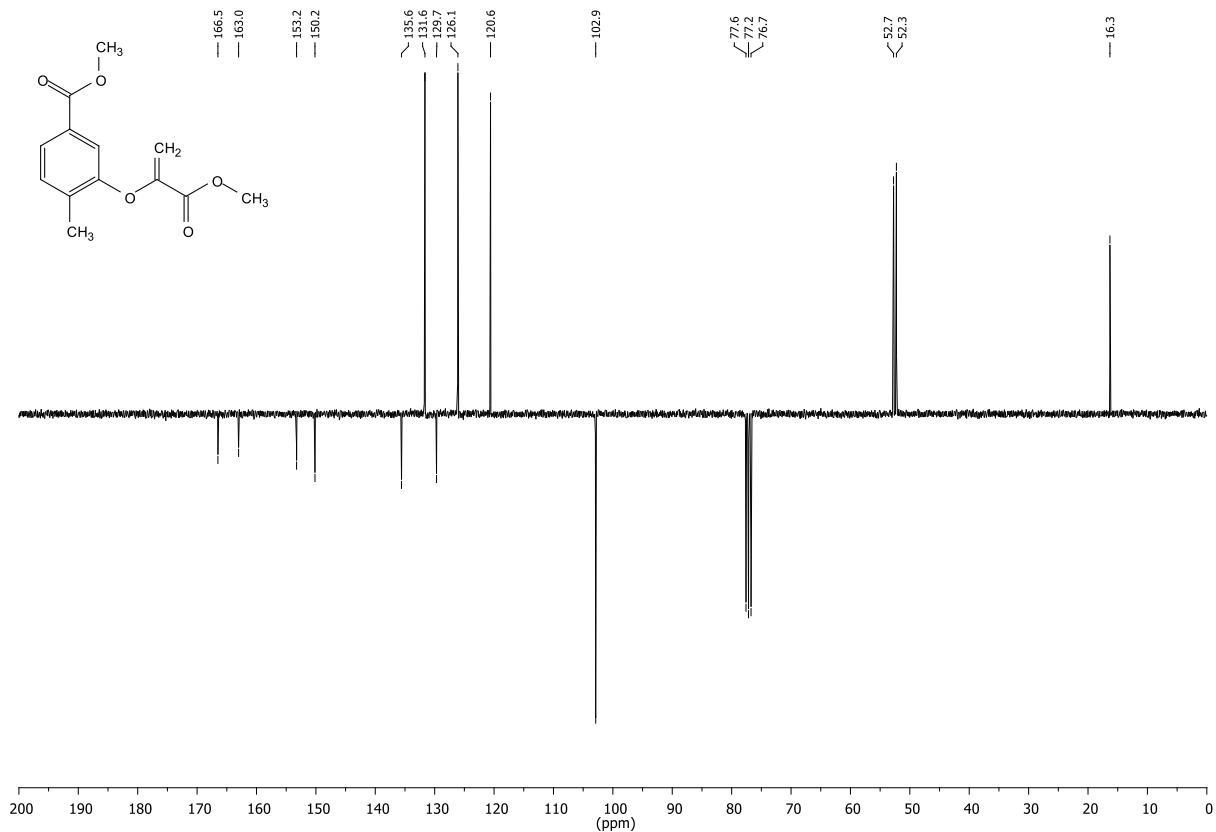


Figure 12.5: ^{13}C ,APT-NMR(75.53 MHz, CDCl_3) of compound 3

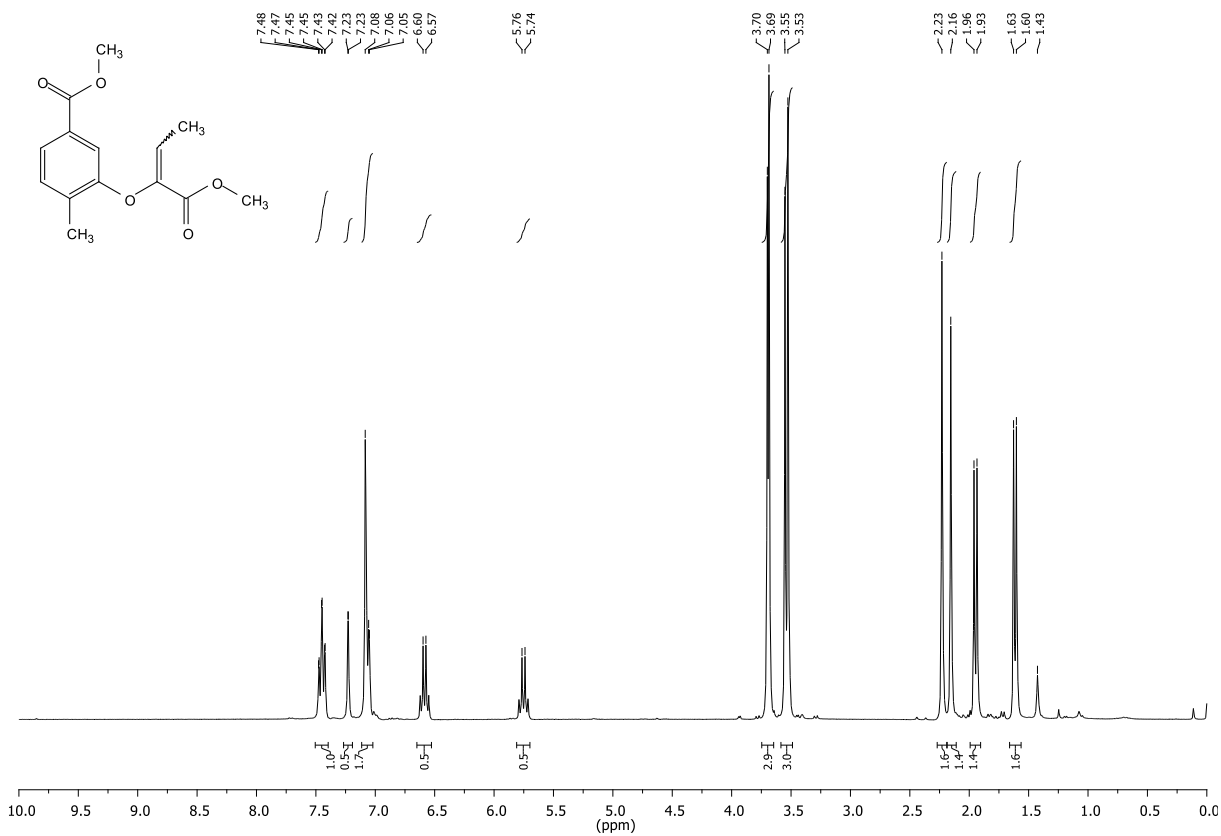


Figure 12.6: ^1H -NMR(300.36 MHz, CDCl_3) of compound 4

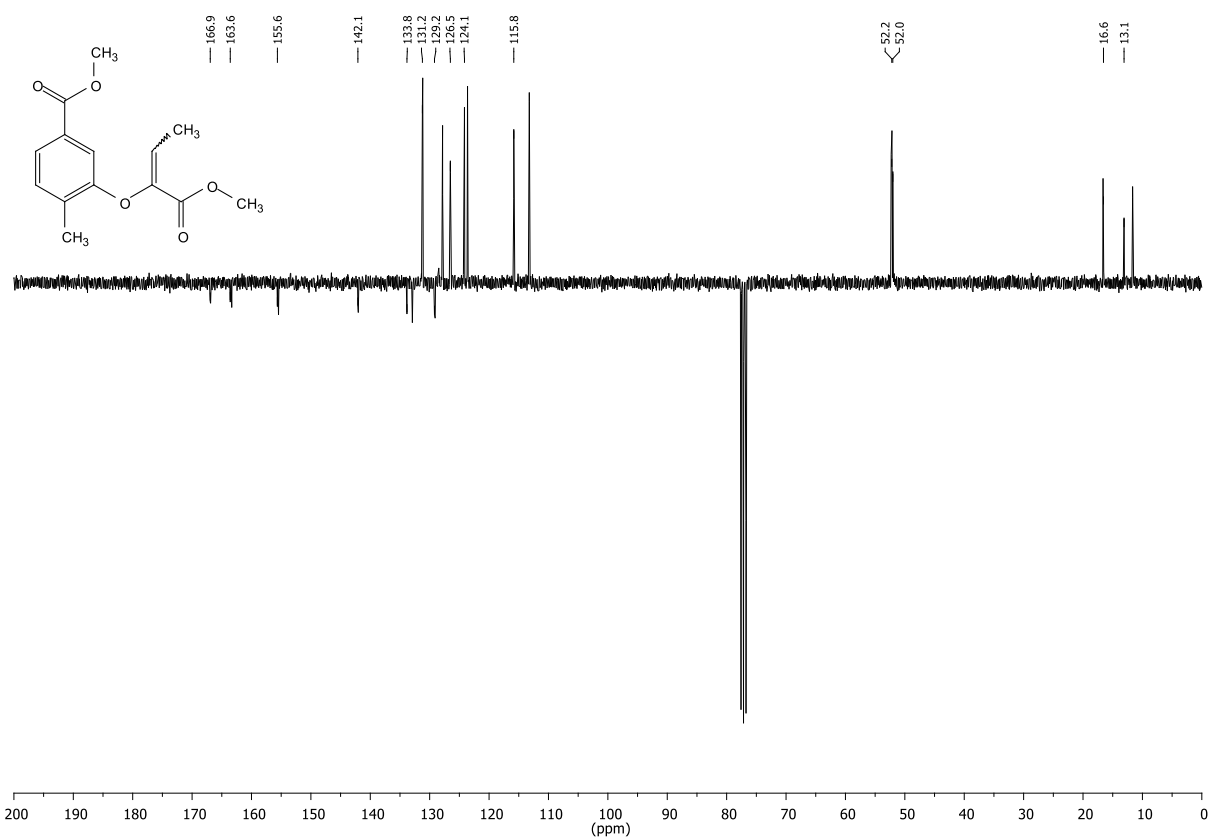


Figure 12.7: $^{13}\text{C-NMR}$, APT (75.53 MHz, CDCl_3) of compound 4

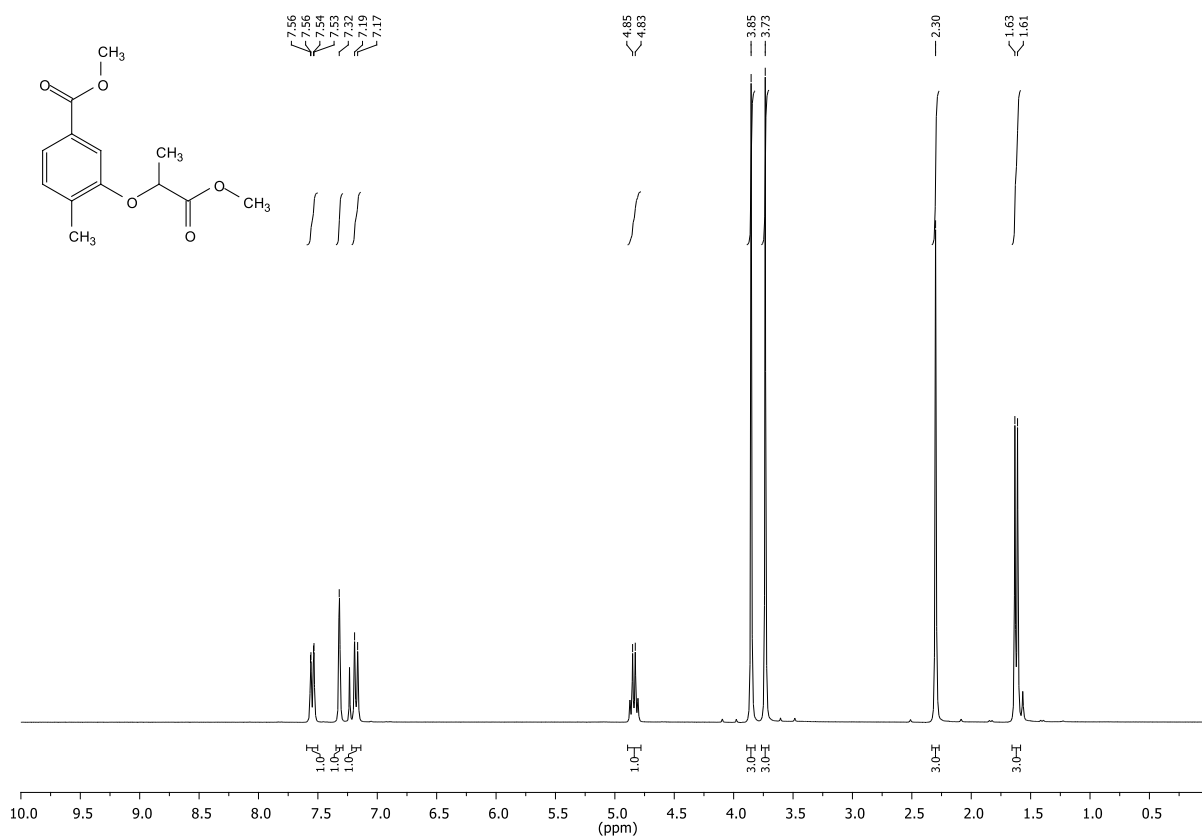


Figure 12.8: $^1\text{H-NMR}$ (300.36 MHz, CDCl_3) of compound 5.

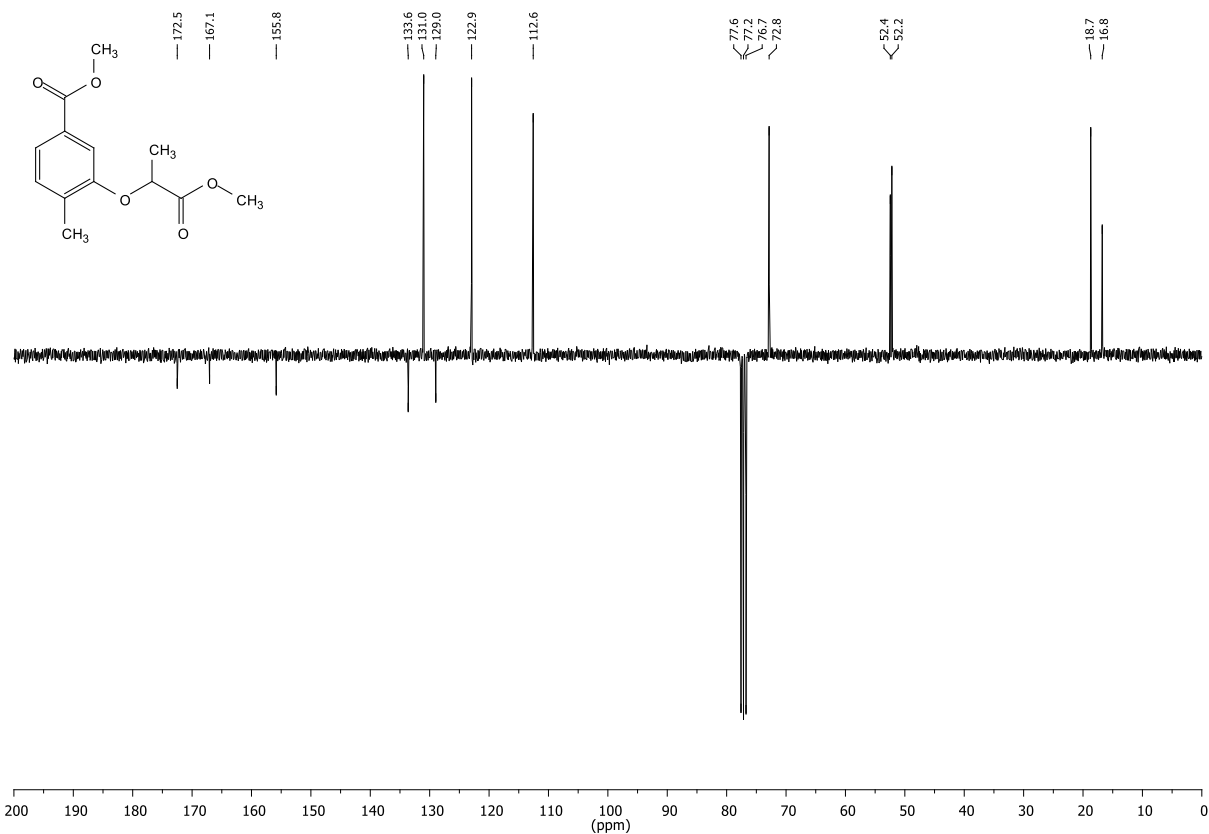


Figure 12.9: $^{13}\text{C-NMR}$, APT (75.53 MHz, CDCl_3) of compound 5.

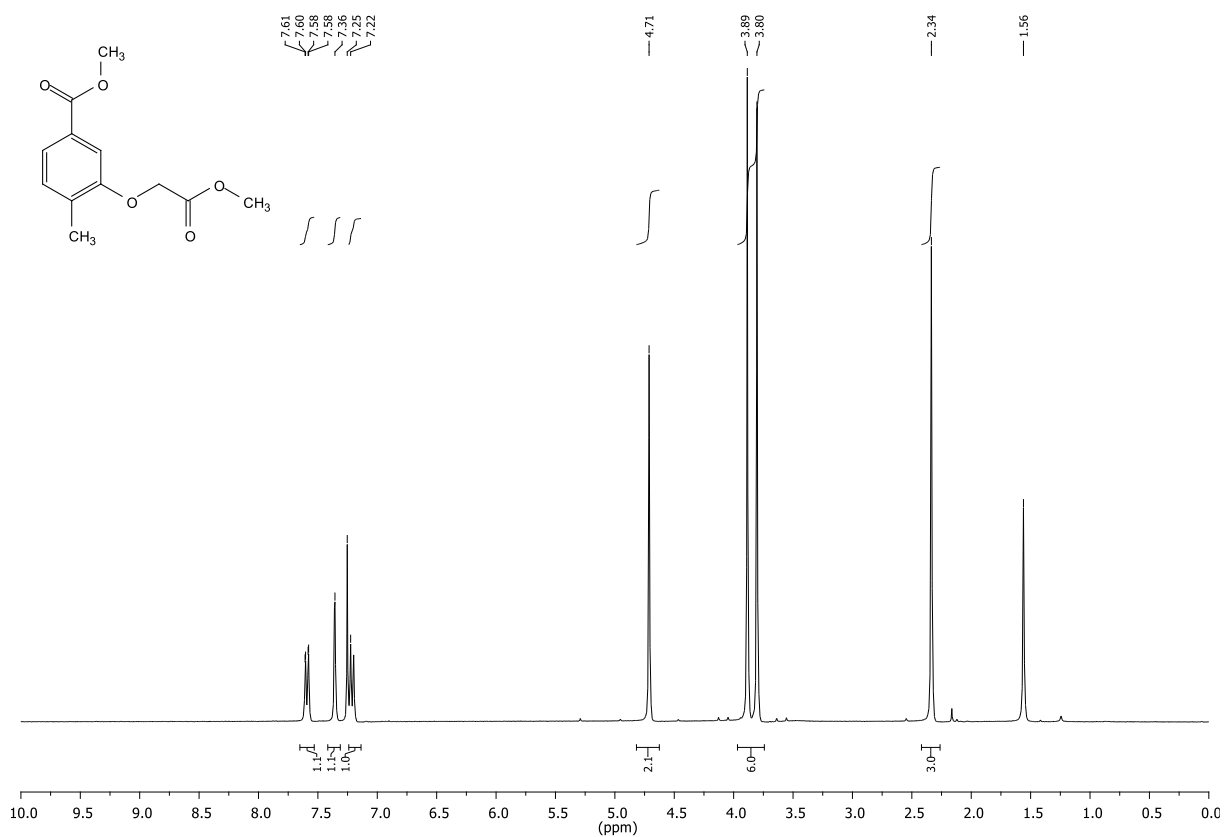


Figure 12.10: $^1\text{H-NMR}$ (300.36 MHz, CDCl_3) of compound 6

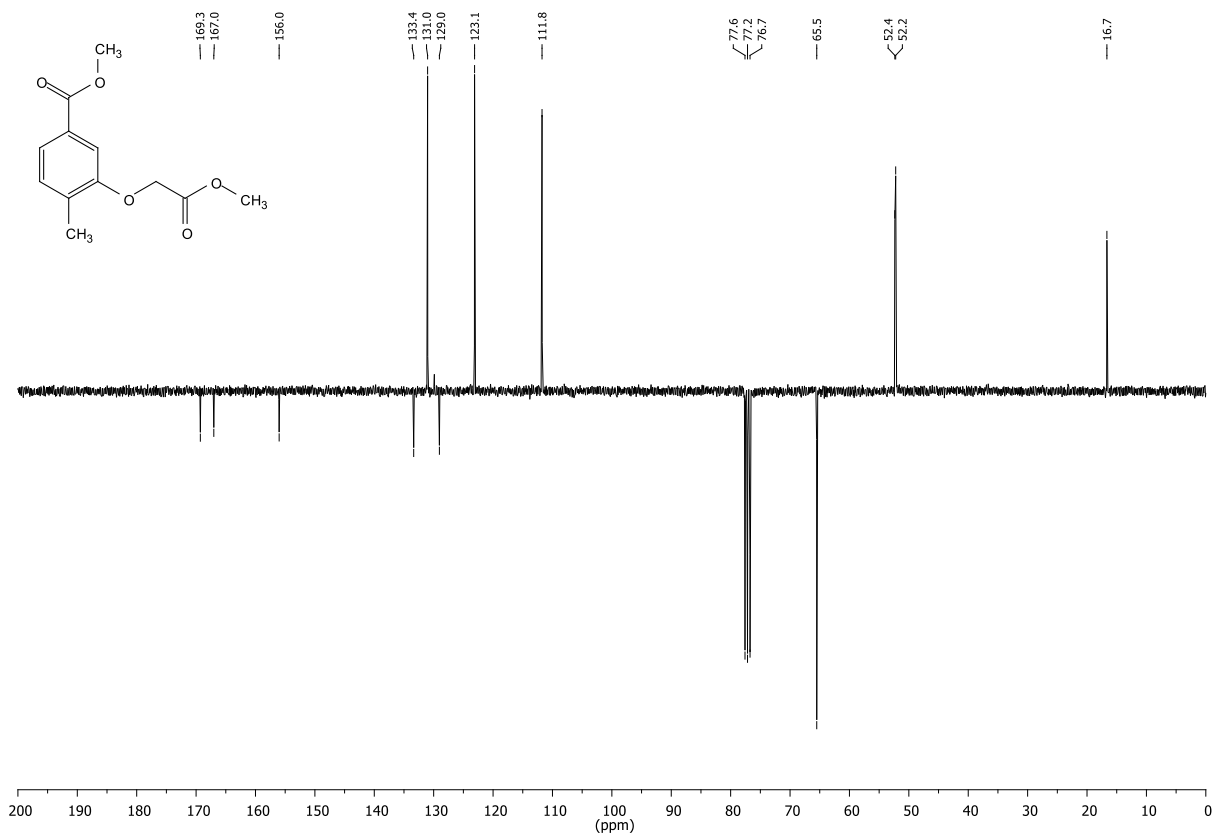


Figure 12.11: ¹³C-NMR, APT (75.53 MHz, CDCl₃) of compound 6

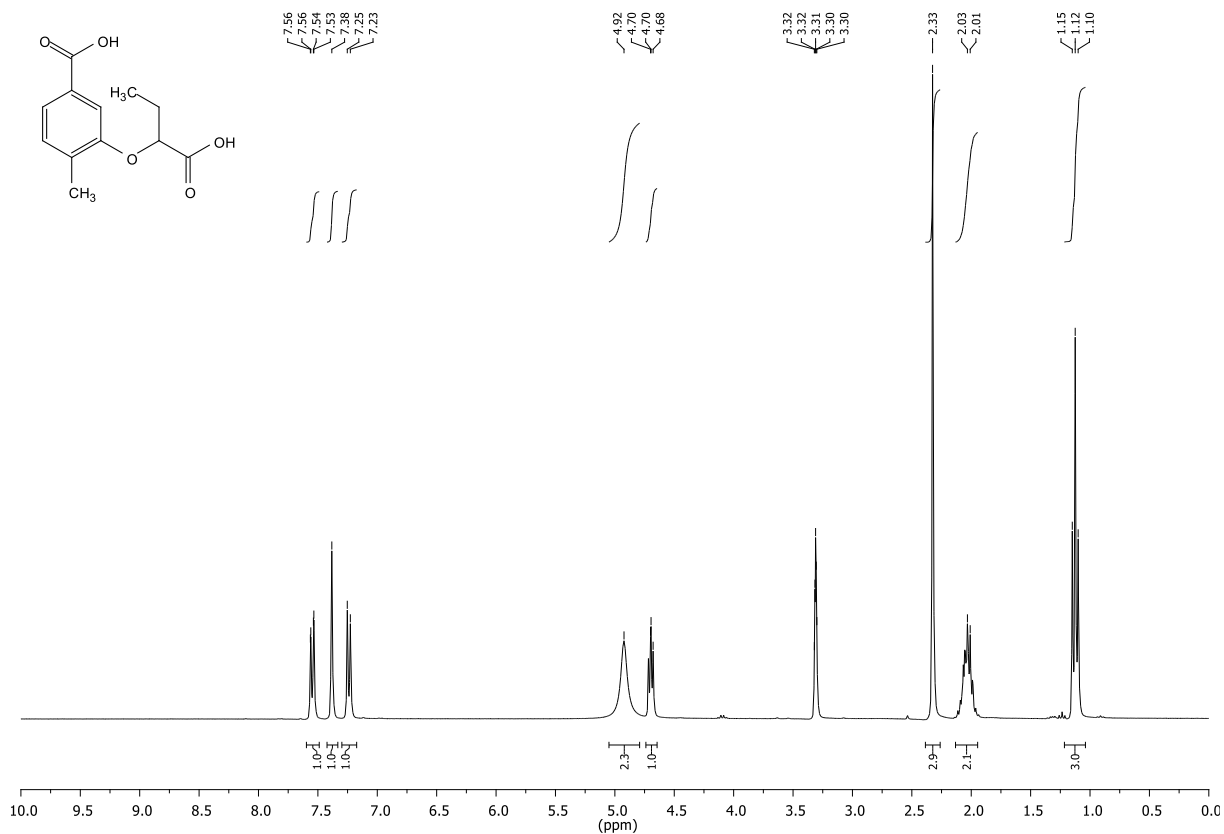


Figure 12.12: ¹H-NMR (300.36 MHz, MeOD₄) of compound 7.

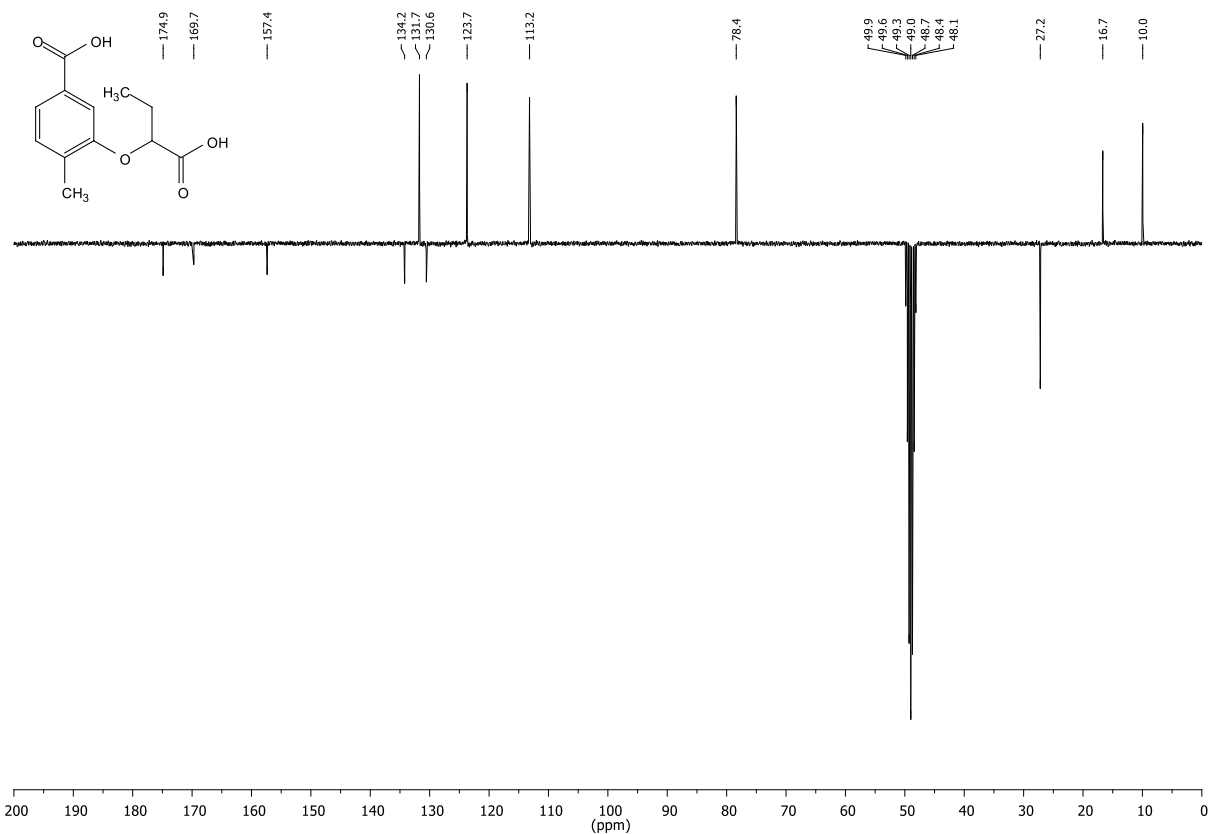


Figure 12.13: ¹³C-NMR, APT (75.53 MHz, MeOD₄) of compound 7.

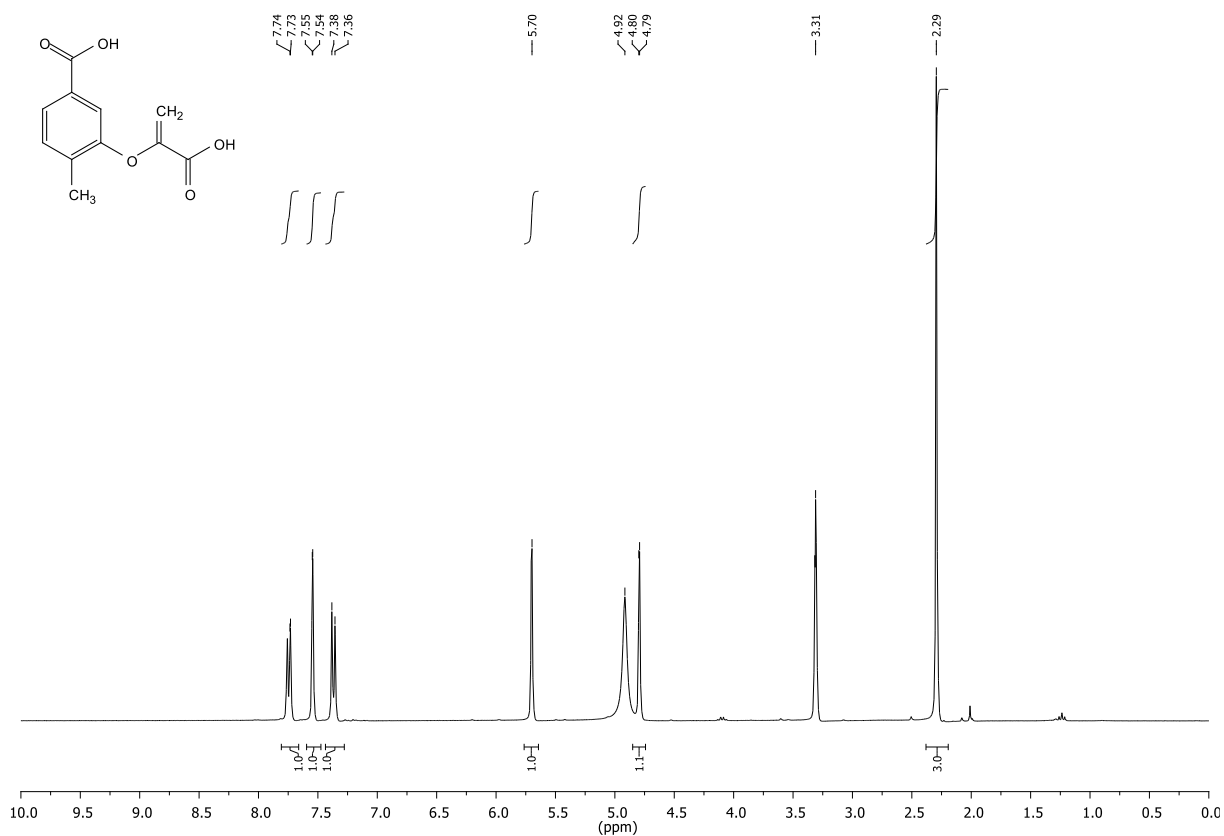


Figure 12.14: ¹H-NMR (300.36 MHz, MeOD₄) of compound 8.

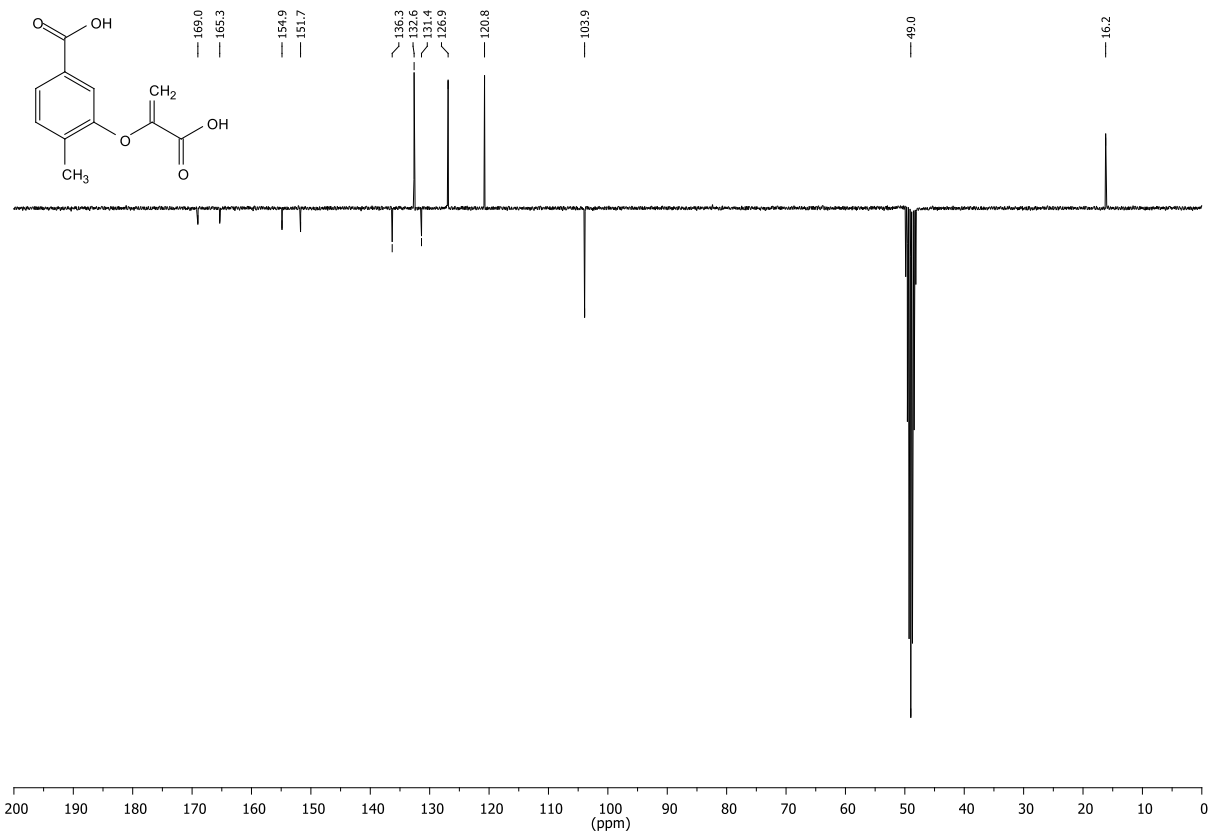


Figure 12.15: $^{13}\text{C-NMR}$, APT (75.53 MHz, MeOD_4) of compound 8.

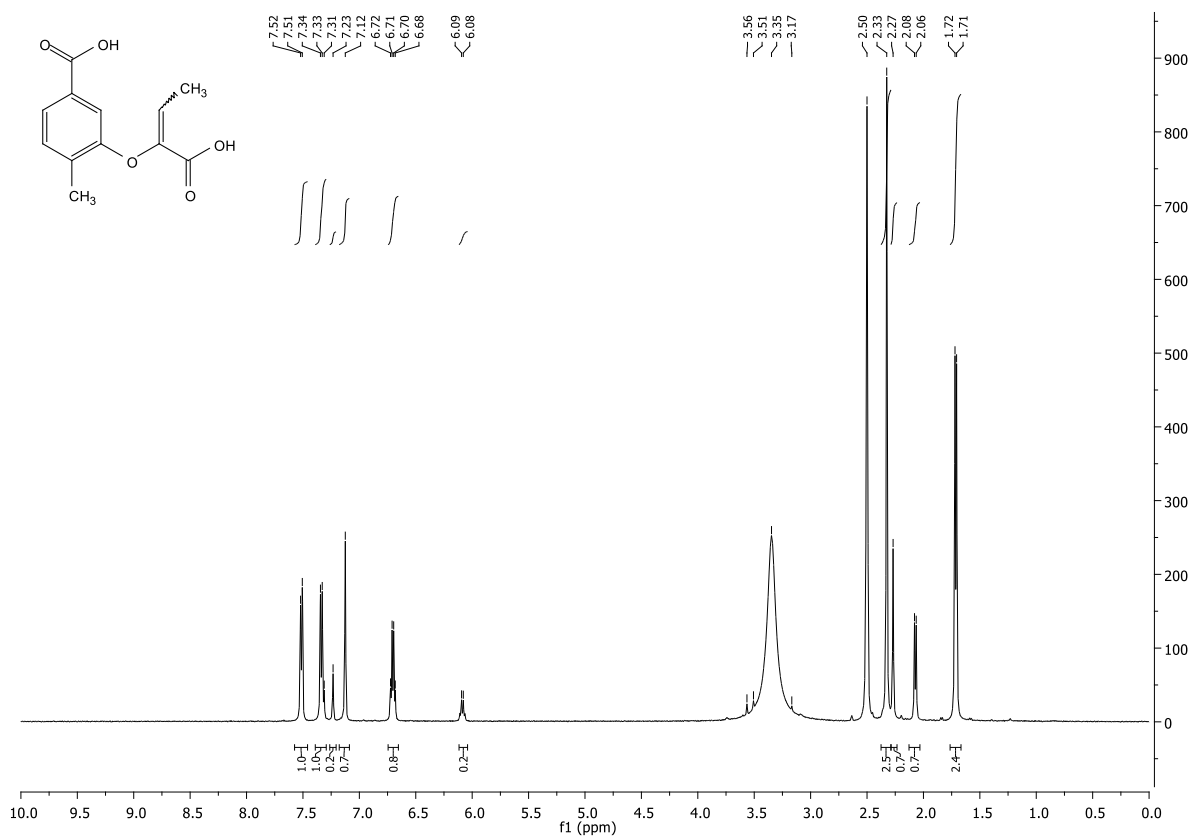


Figure 12.16: $^1\text{H-NMR}$ (499.88 MHz, DMSO-d_6) of compound 9.

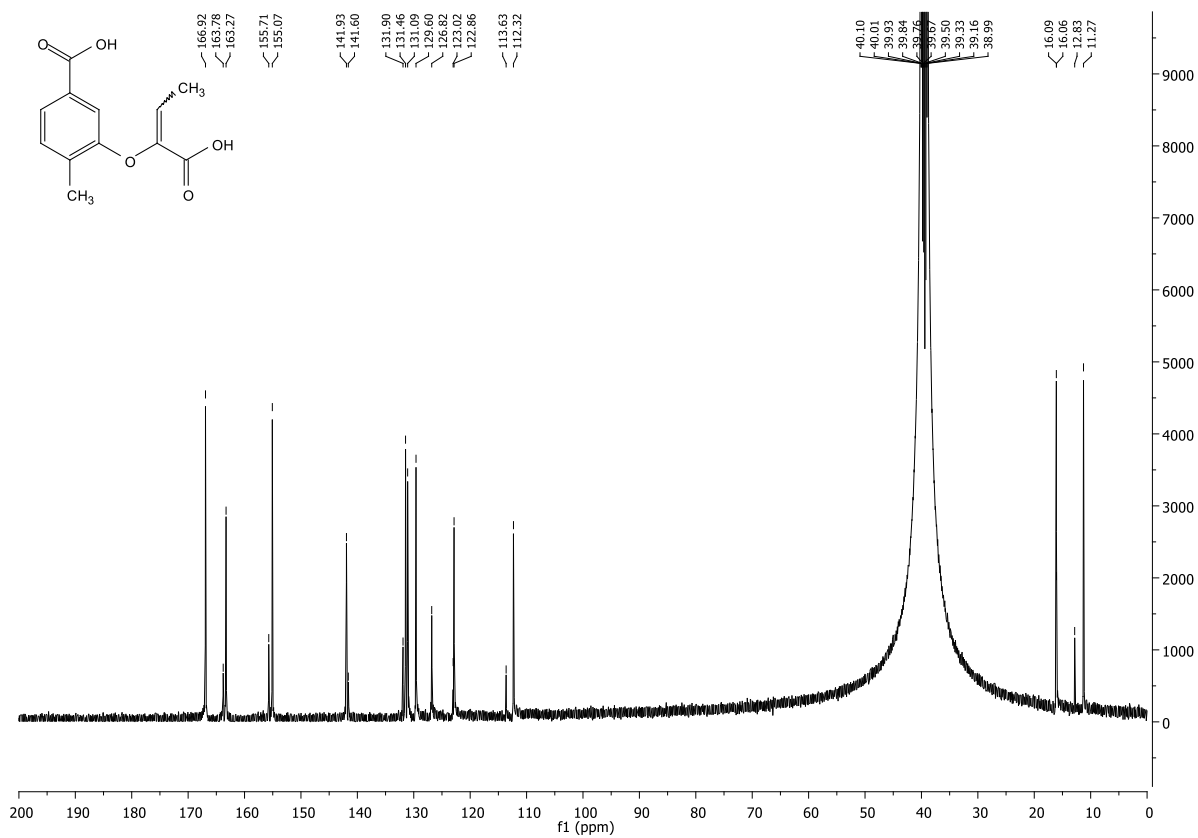


Figure 12.17: ^{13}C -NMR (125.69 MHz, DMSO-d_6) of compound 9.

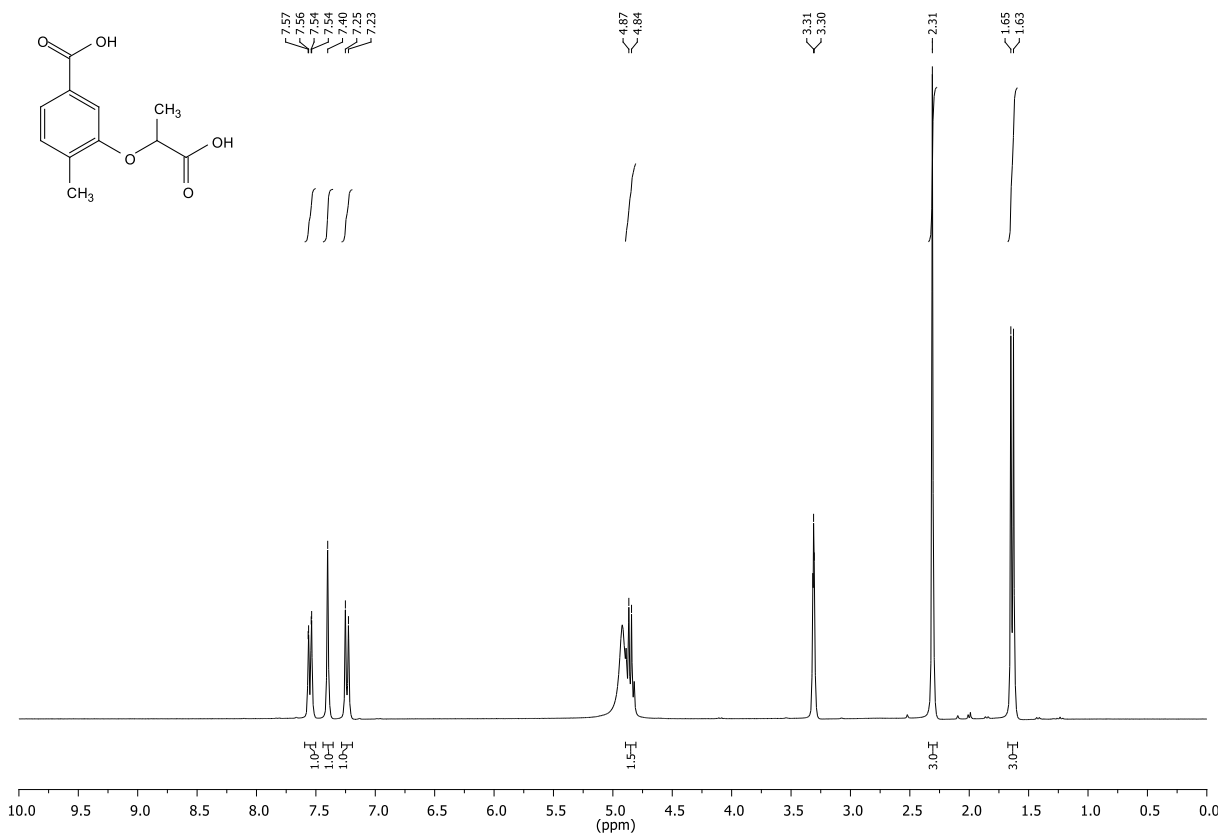


Figure 12.18: ^1H -NMR (300.36 MHz, MeOD_4) of compound 10.

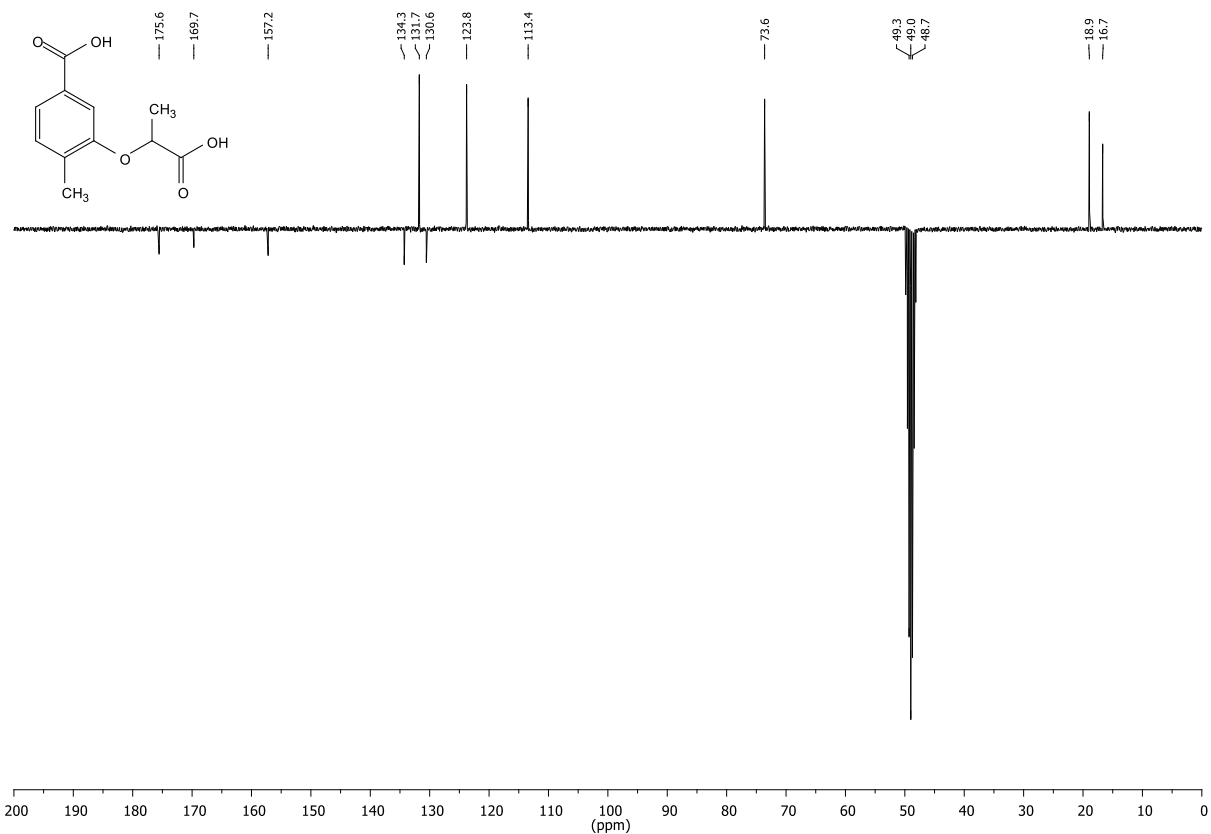


Figure 12.19: $^{13}\text{C-NMR}$, APT (75.53 MHz, MeOD_4) of compound 10.

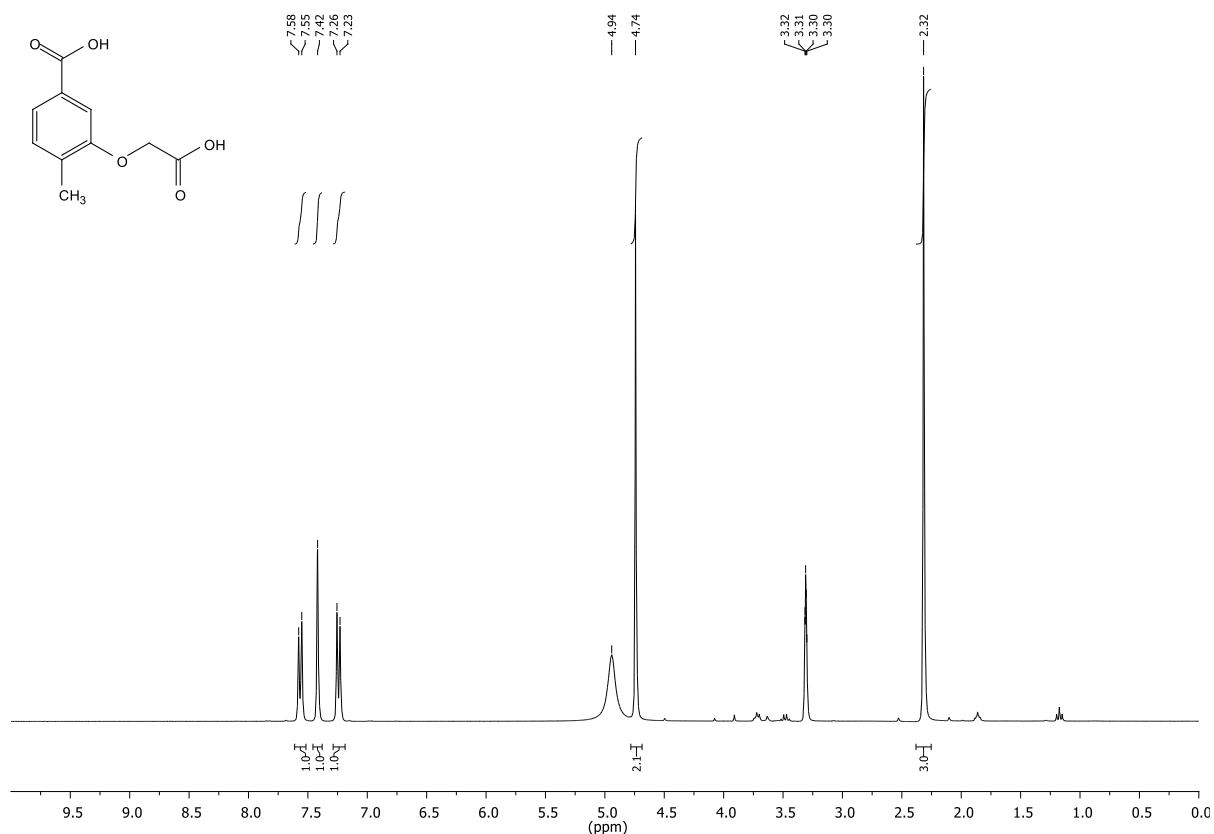


Figure 12.20: $^1\text{H-NMR}$ (300.36 MHz, MeOD_4) of compound 11.

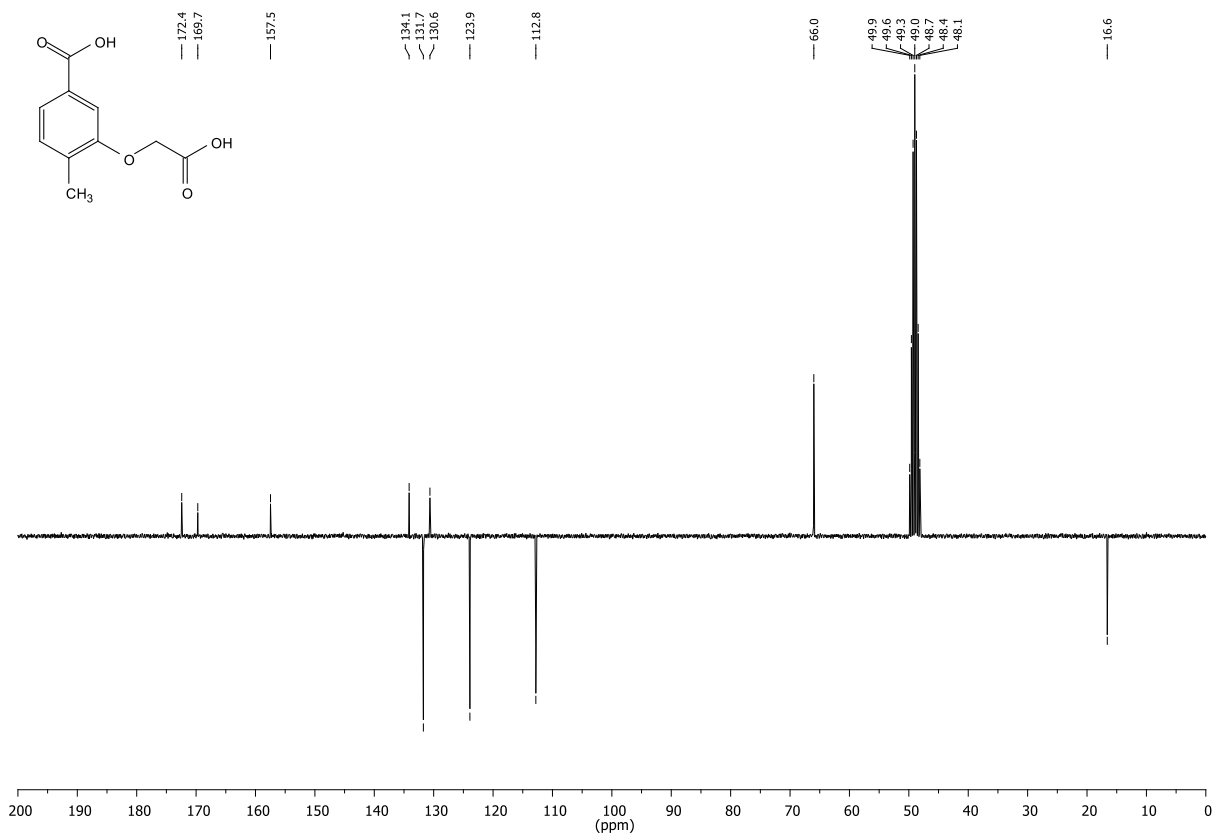


Figure 12.21: ¹³C-NMR, APT (75.53 MHz, MeOD₄) of compound 11.

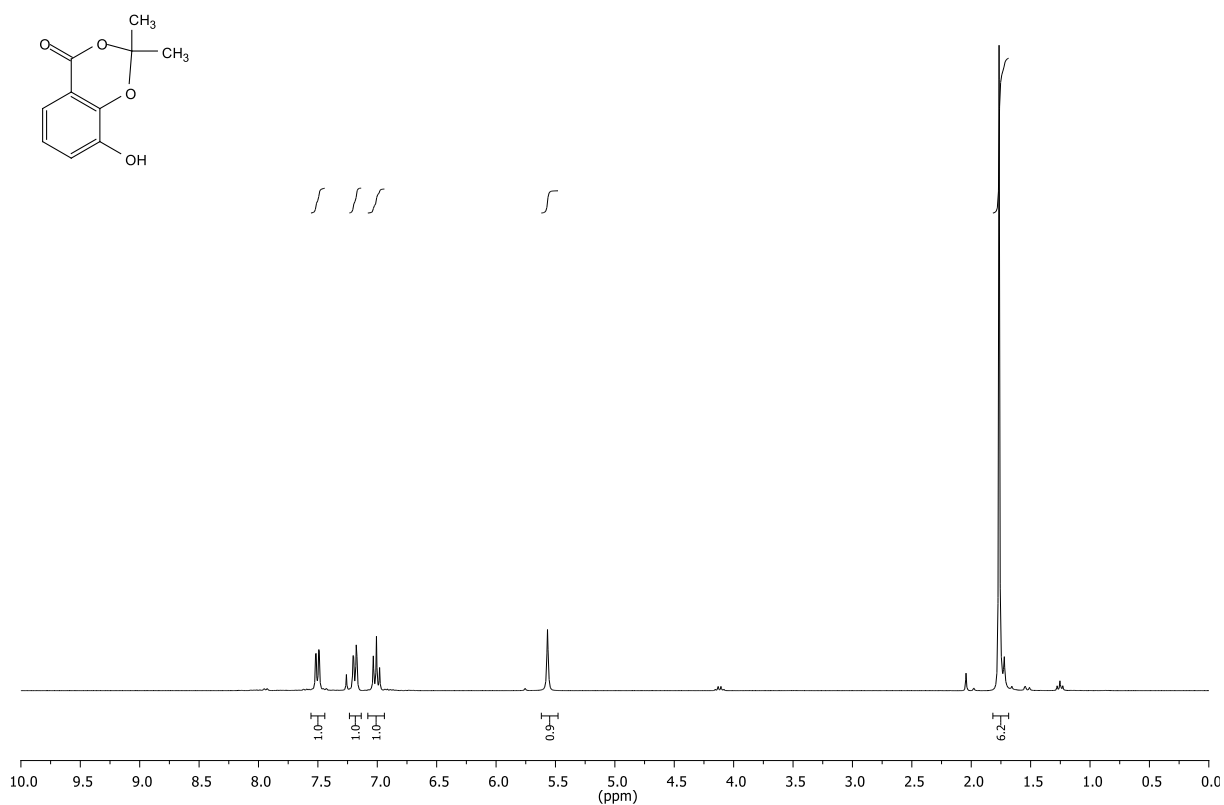


Figure 12.22: ¹H-NMR (300.36 MHz, CDCl₃) of compound 12.

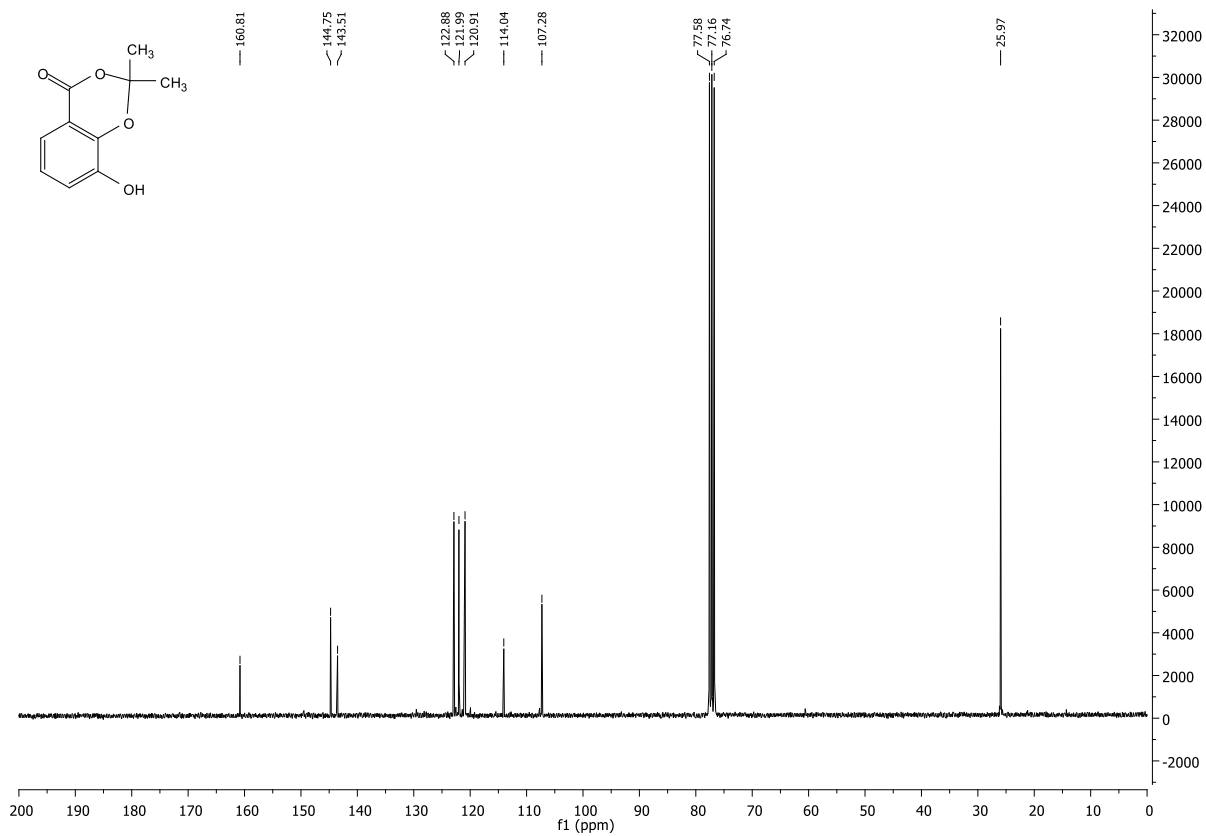


Figure 12.23: ¹³C-NMR (75.53 MHz, CDCl₃) of compound 12.

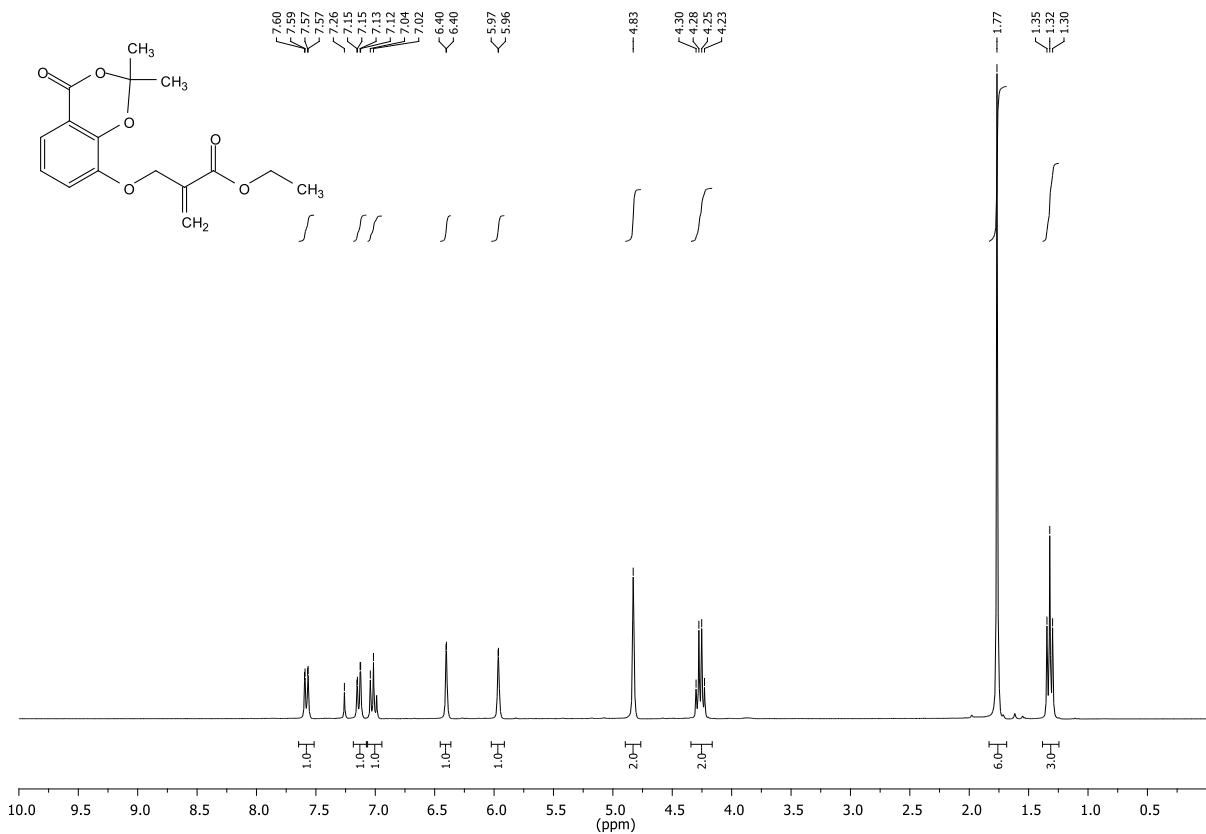


Figure 12.24: ¹H-NMR (300.36 MHz, CDCl₃) of compound 13.

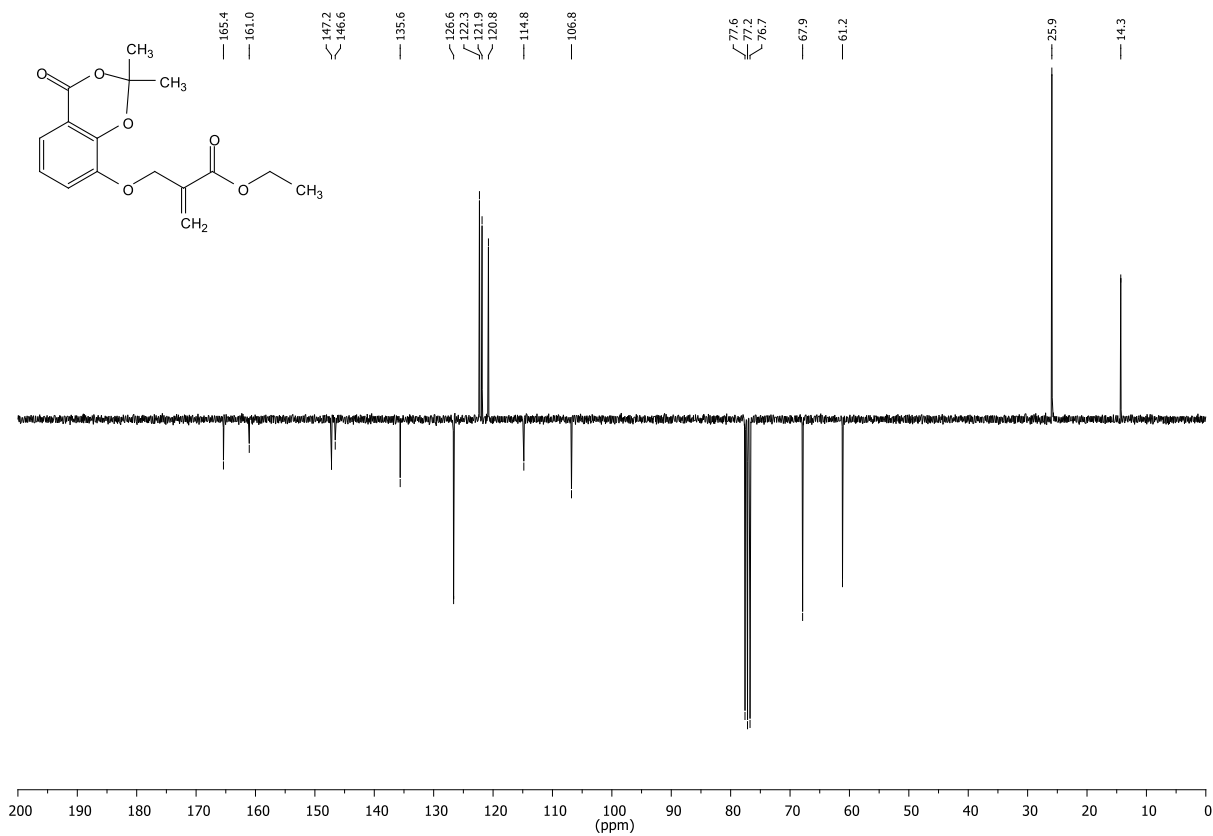


Figure 12.25: ^{13}C ,APT-NMR (75.53 MHz, CDCl_3) of compound 13.

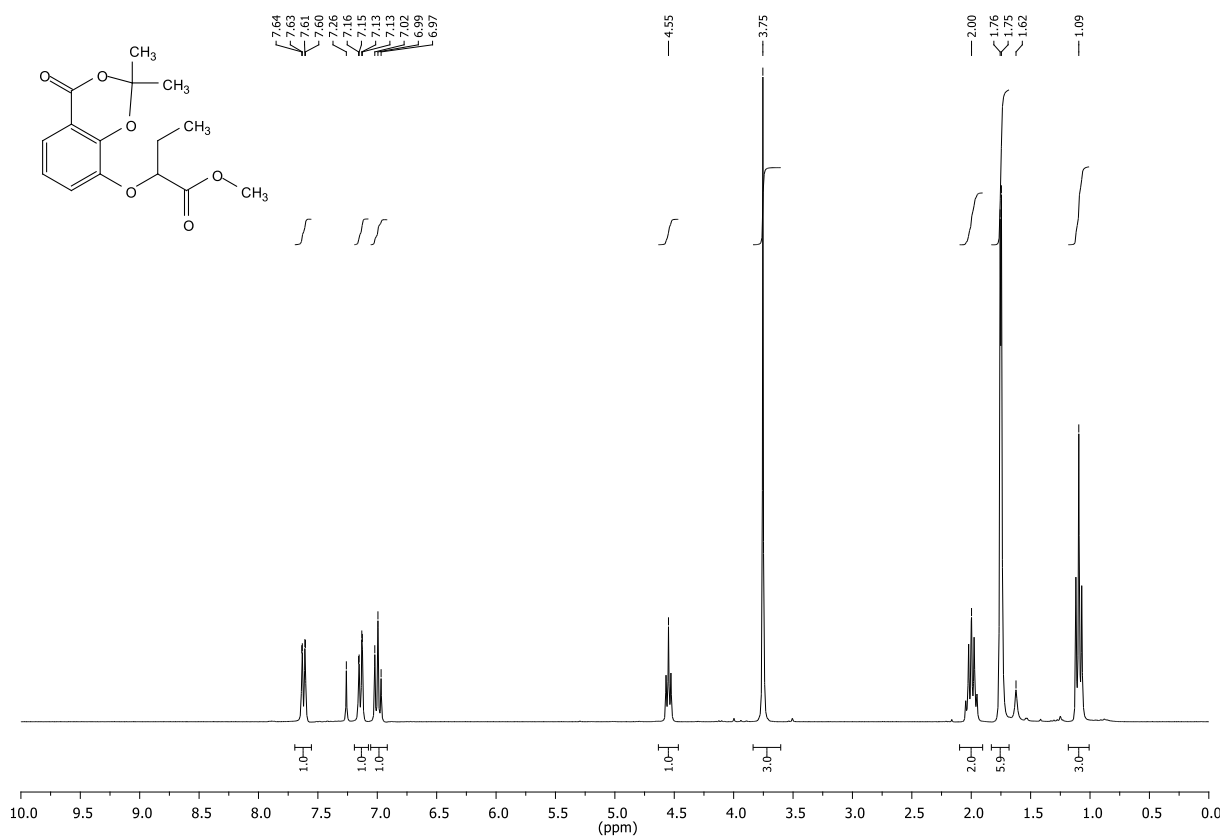


Figure 12.26: ^1H -NMR (300.36 MHz, CDCl_3) of compound 14.

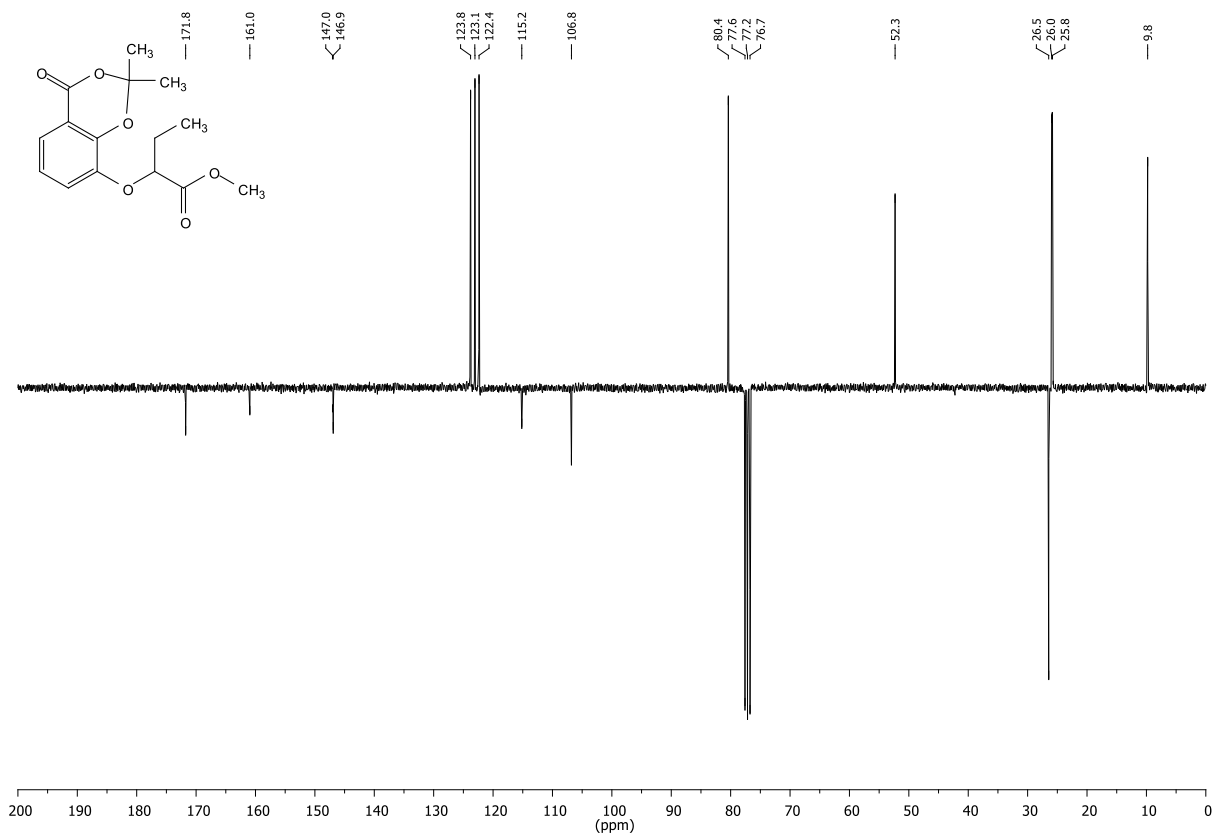


Figure 12.27: $^{13}\text{C-NMR}$,APT (75.53 MHz, CDCl_3) of compound 14.

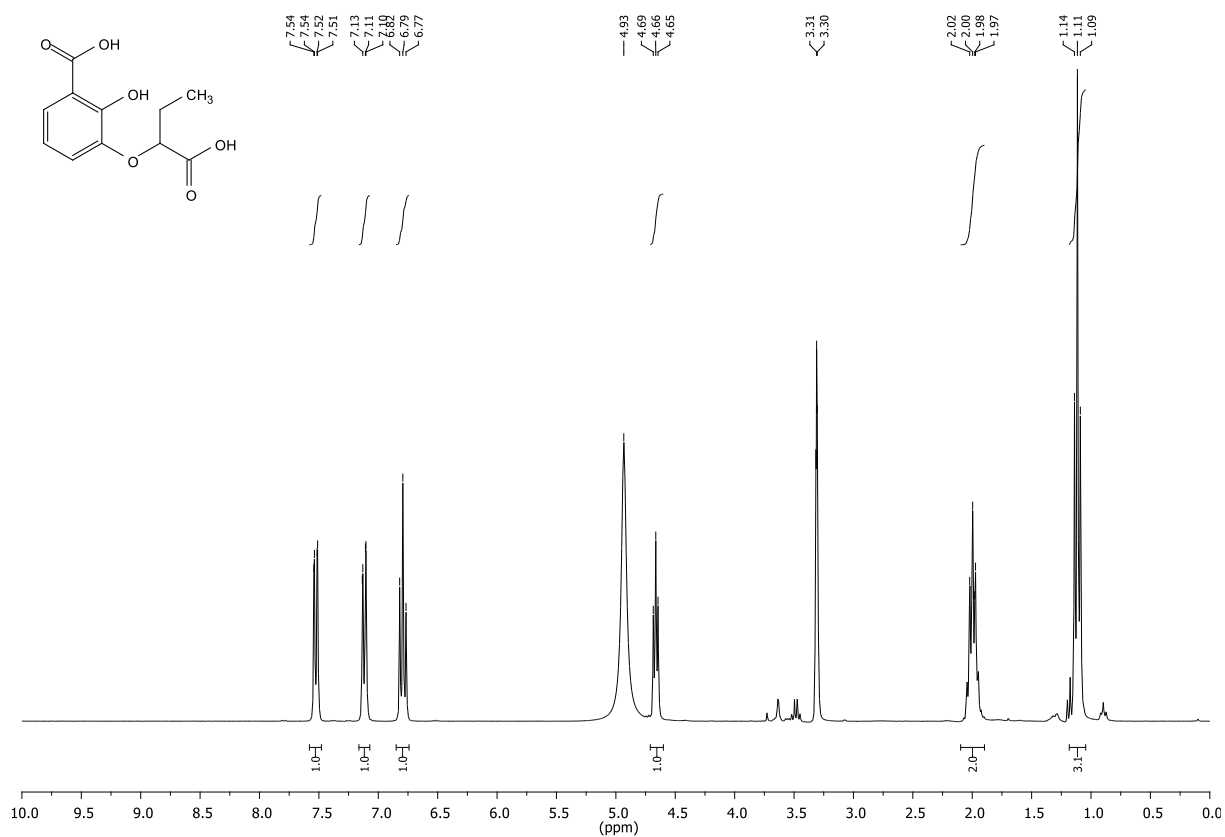


Figure 12.28: $^1\text{H-NMR}$ (300.36 MHz, MeODI_4) of compound 15.

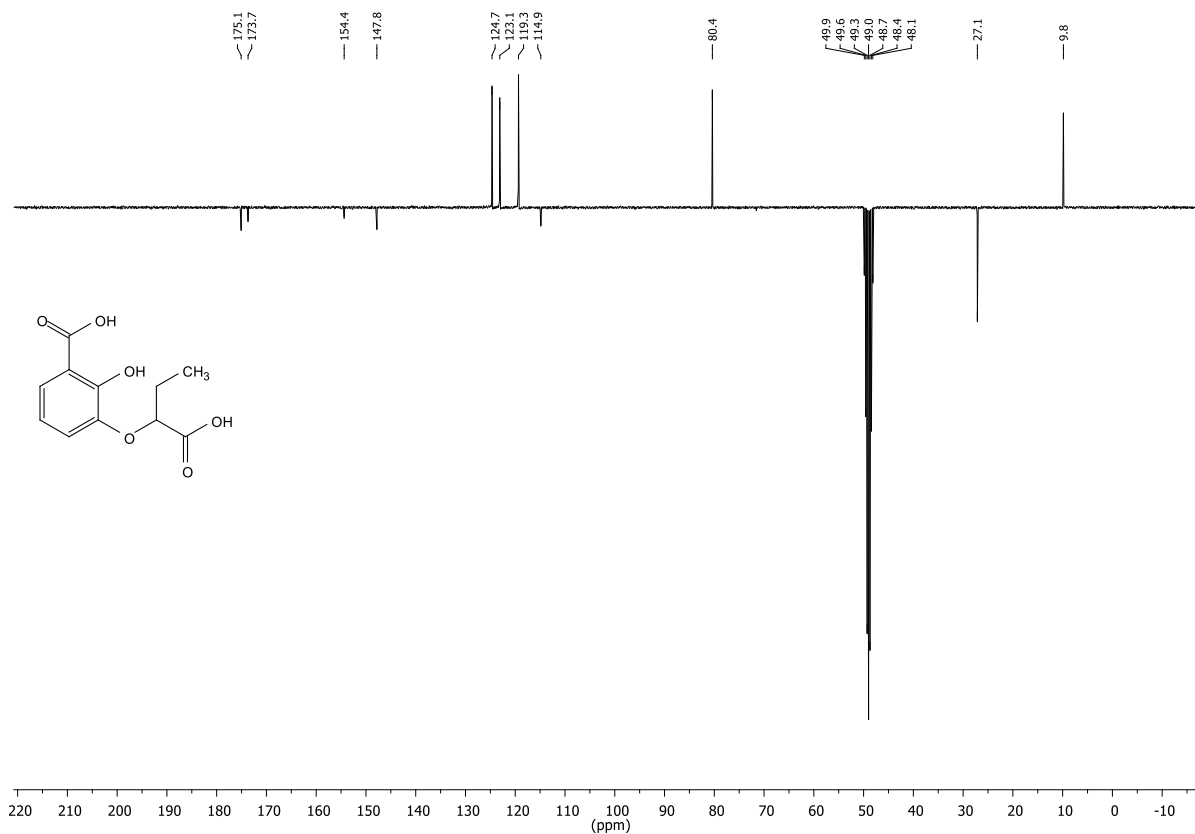


Figure 12.29: $^{13}\text{C-NMR}$,APT (75.53 MHz, MeOD_4) of compound 15.

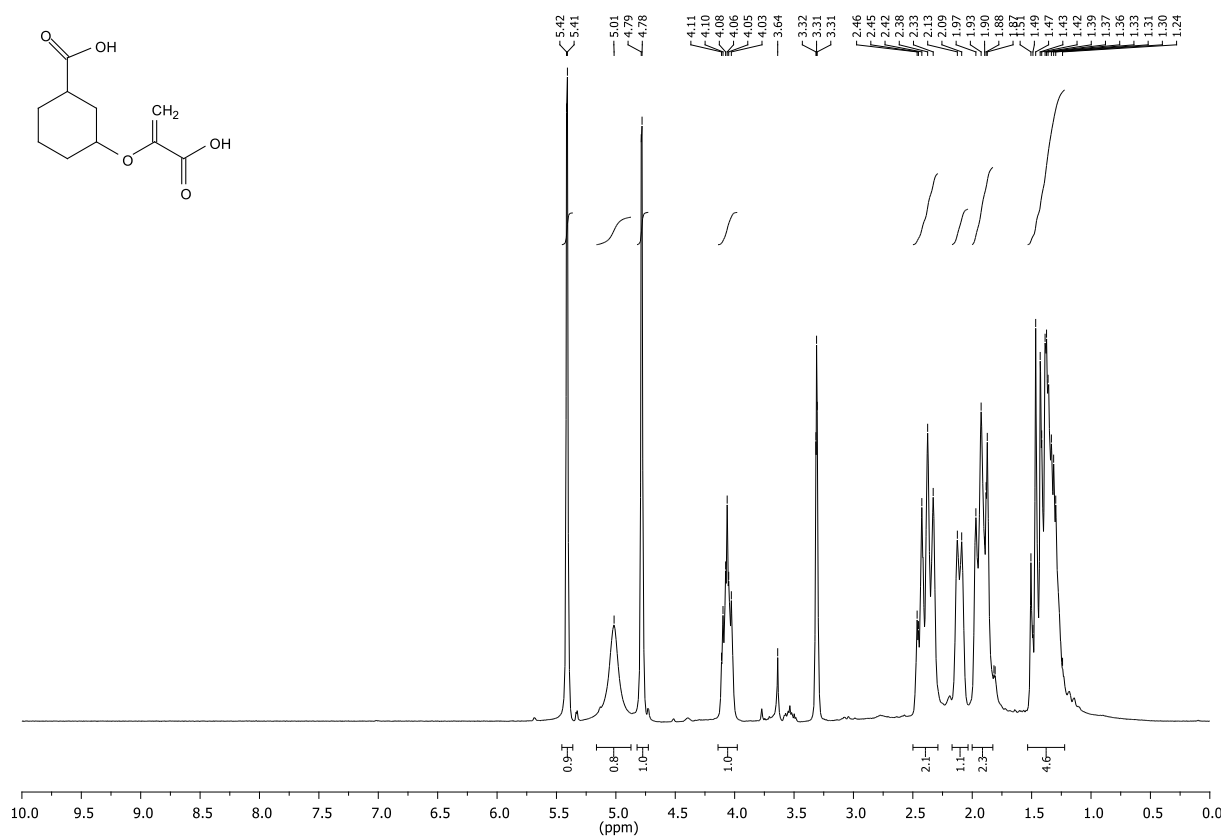


Figure 12.30 $^1\text{H-NMR}$ (300.36 MHz, MeOD_4) of compound 16.

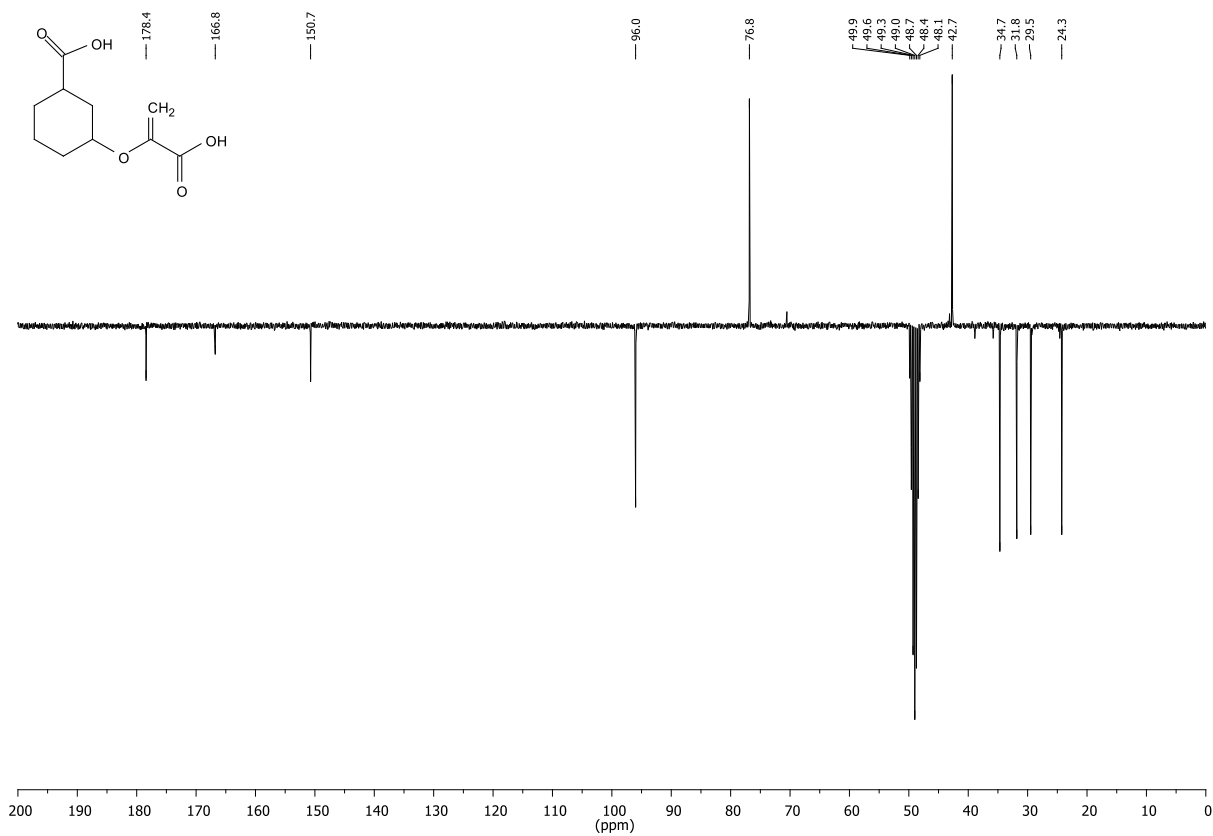


Figure 12.31 $^{13}\text{C-NMR}$, APT (75.53 MHz, MeOD_4) of compound 16.

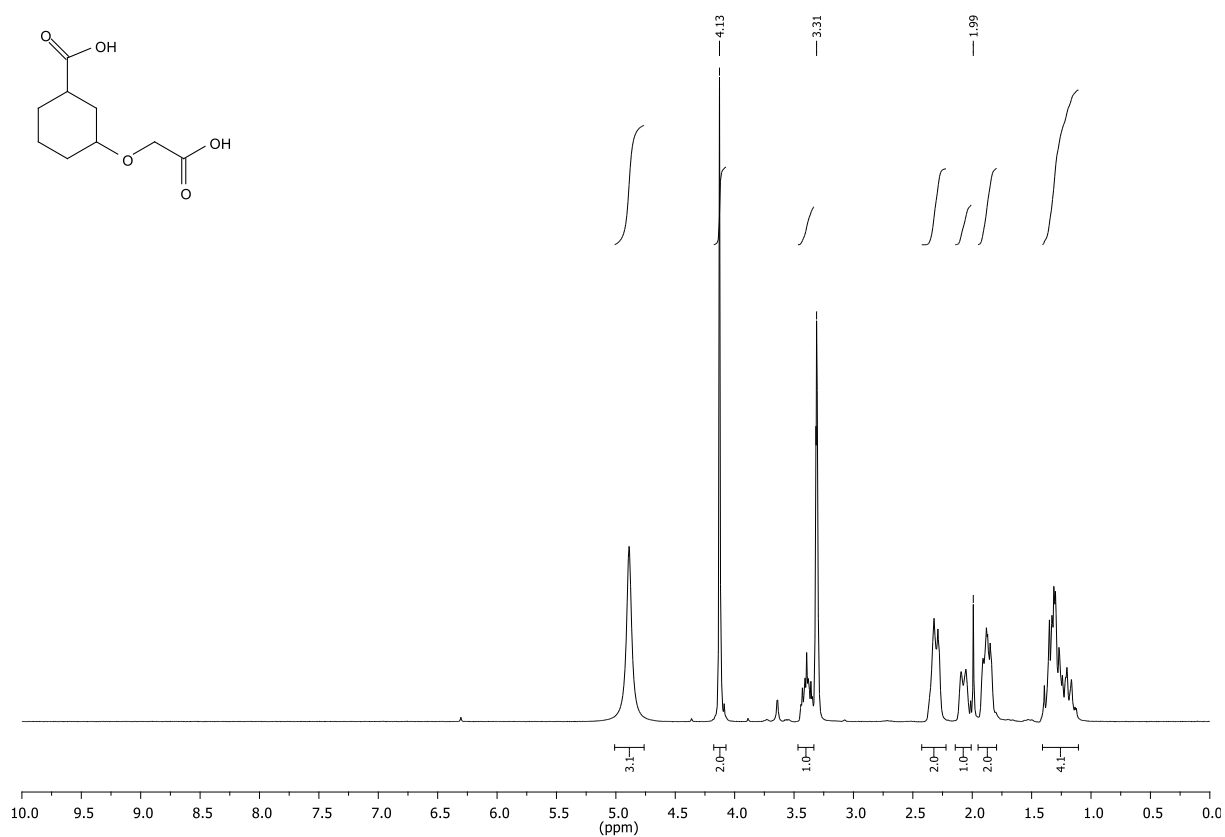


Figure 12.32: $^1\text{H-NMR}$ (300.36 MHz, MeOD_4) of compound 17.

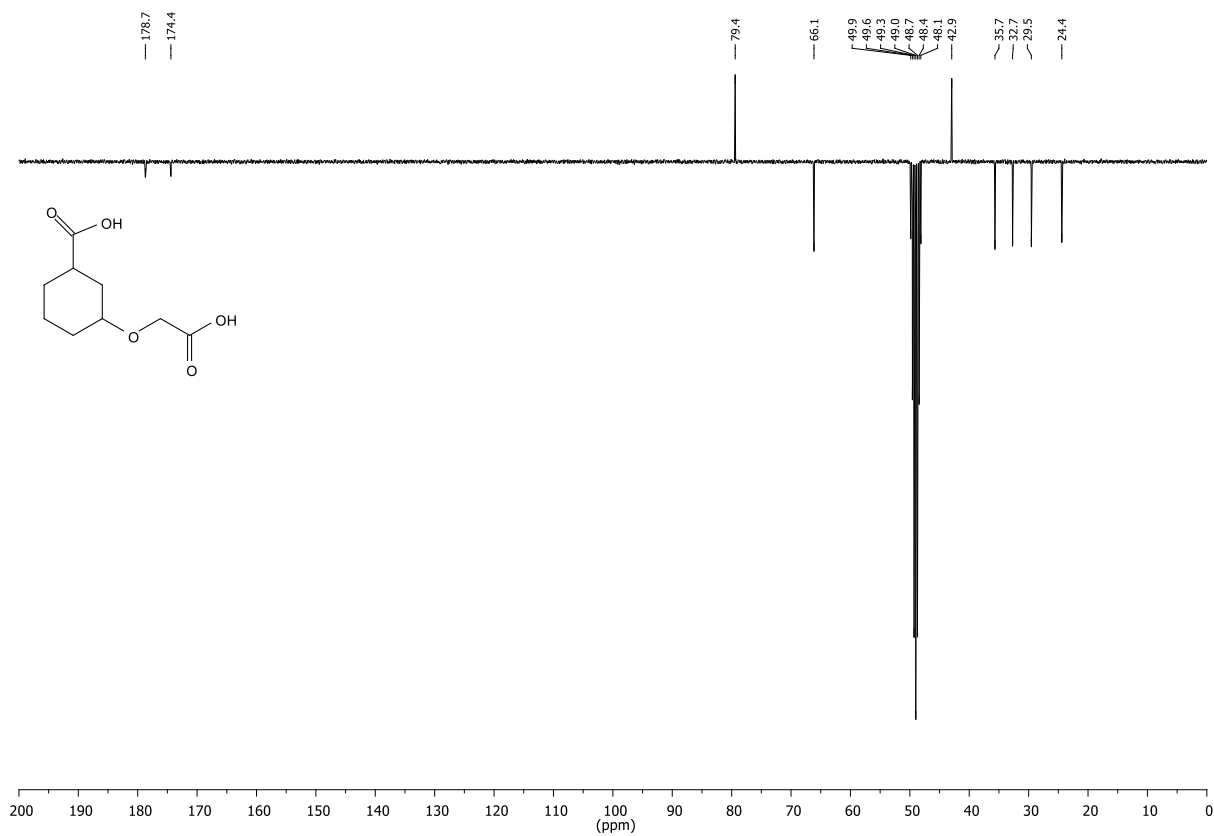


Figure 12.33: $^{13}\text{C-NMR}$,APT (75.53 MHz, CDCl_3) of compound 17.

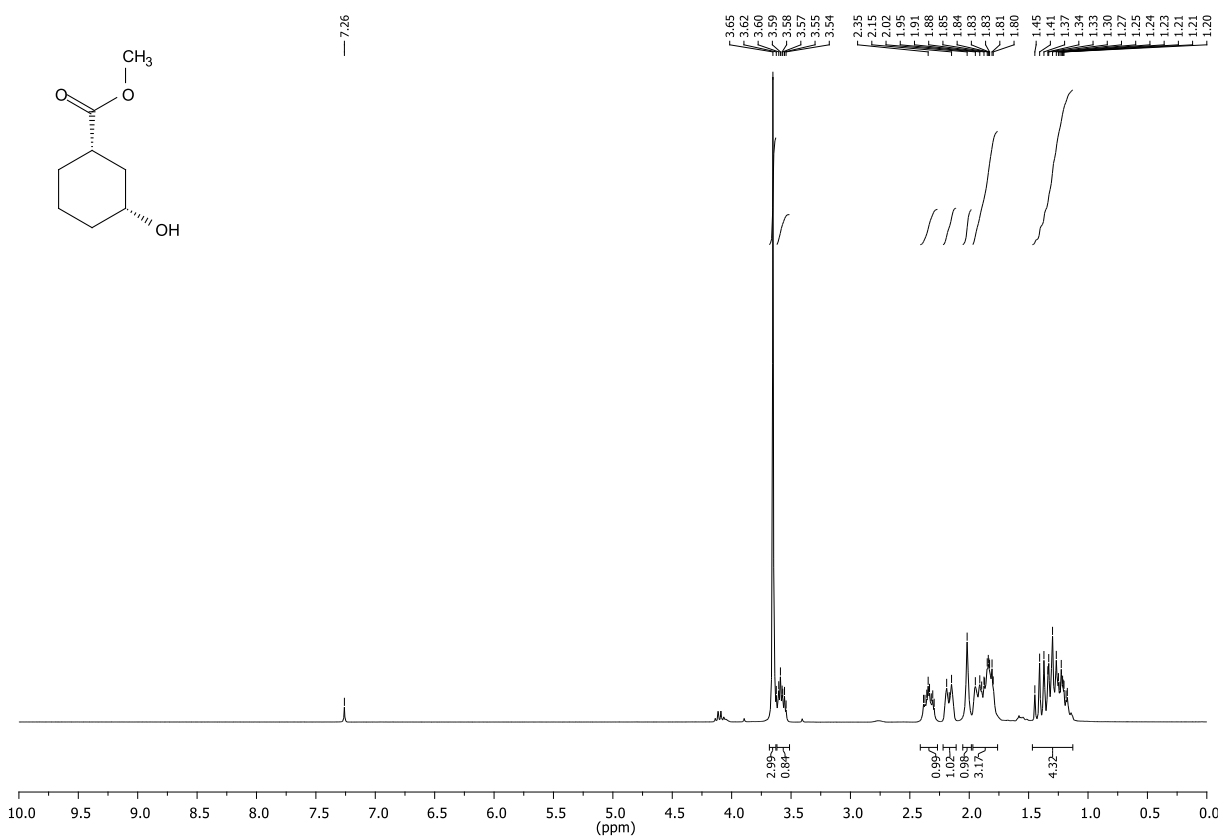


Figure 12.34: $^1\text{H-NMR}$ (300.36 MHz, CDCl_3) of compound 18.

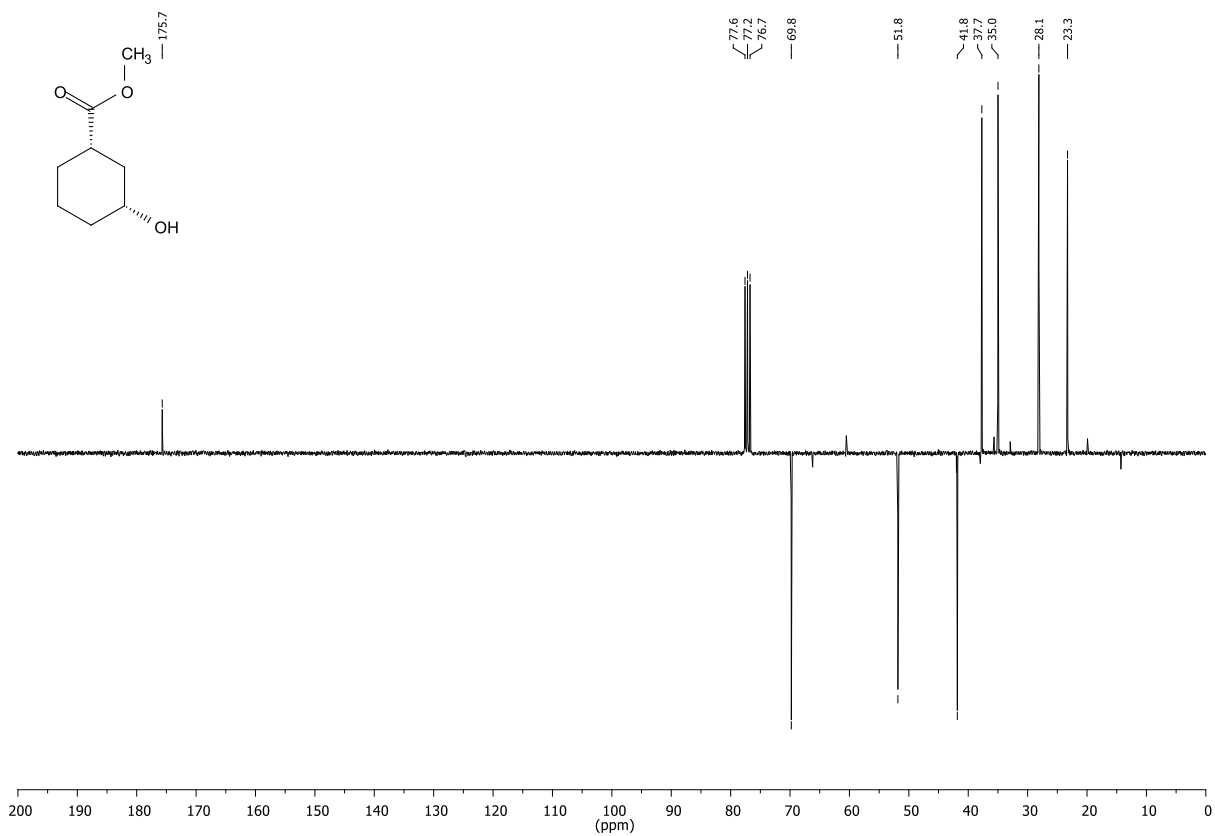


Figure 12.35: $^{13}\text{C-NMR}$,APT (77.53 MHz, CDCl_3) of compound 18.

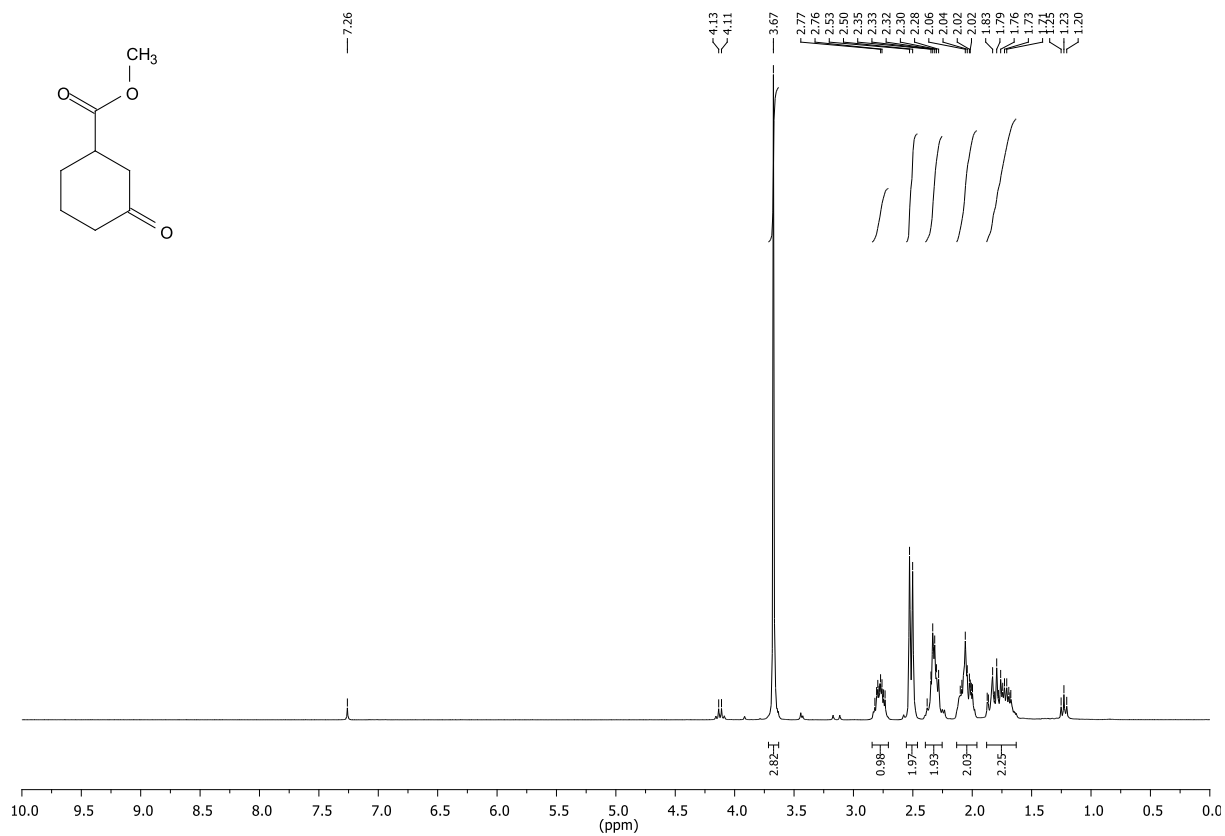


Figure 12.36: $^1\text{H-NMR}$ (300.36 MHz, CDCl_3) of compound 19.

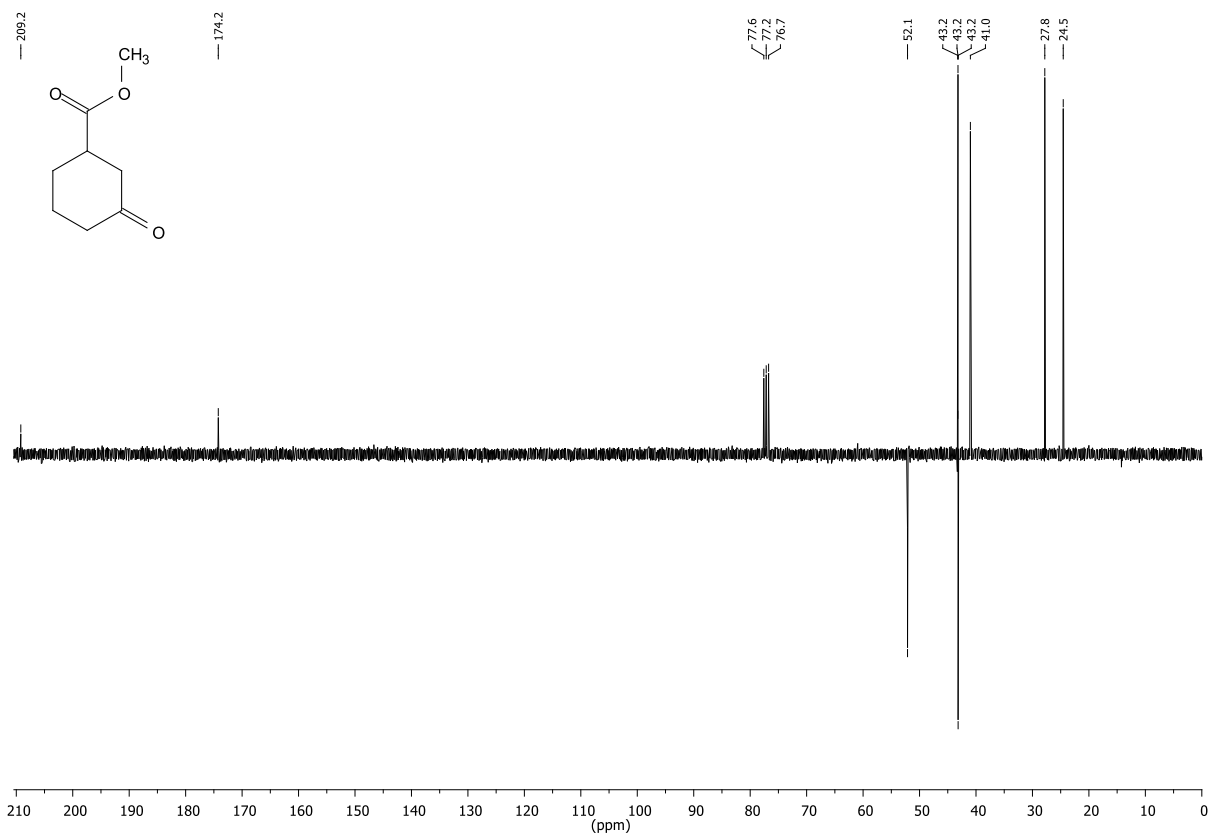


Figure 12.37: $^{13}\text{C-NMR}$,APT (77.53 MHz, CDCl_3) of compound 19.

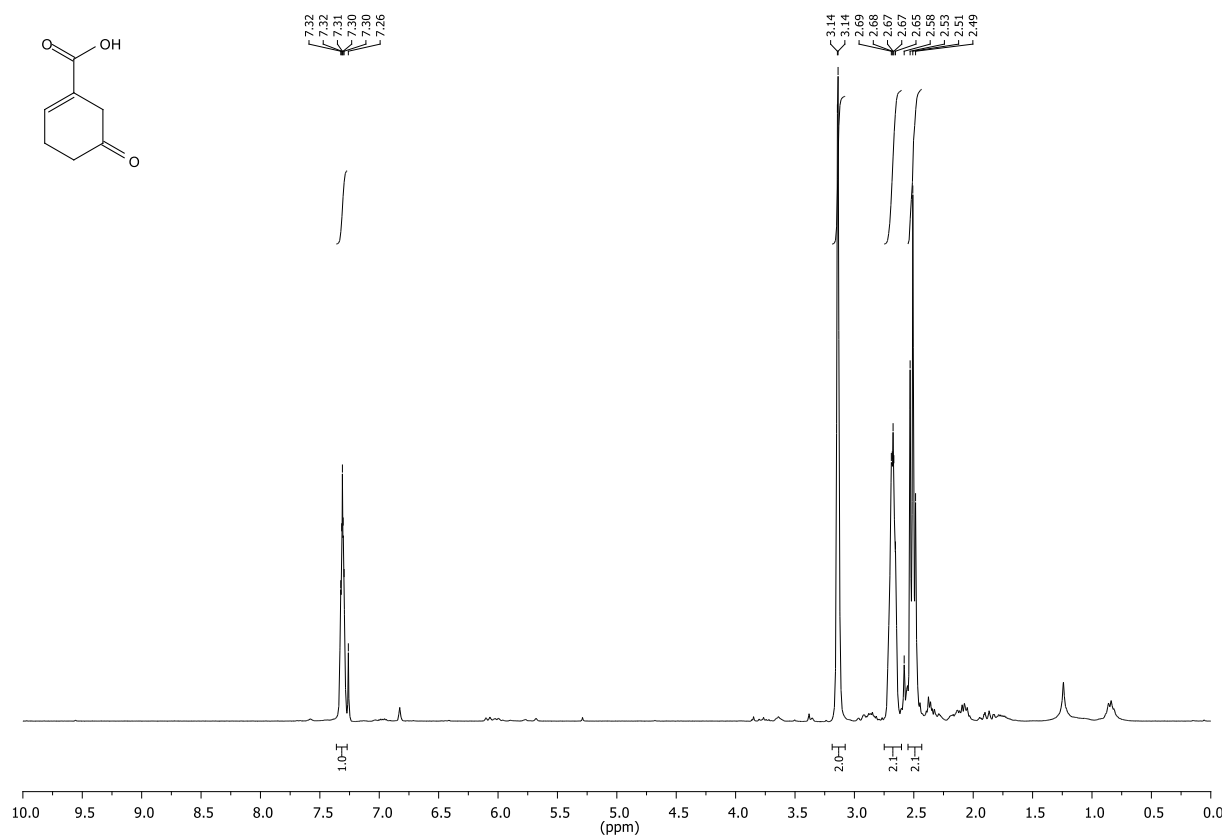


Figure 12.38: $^1\text{H-NMR}$ (300.36 MHz, CDCl_3) of compound 20.

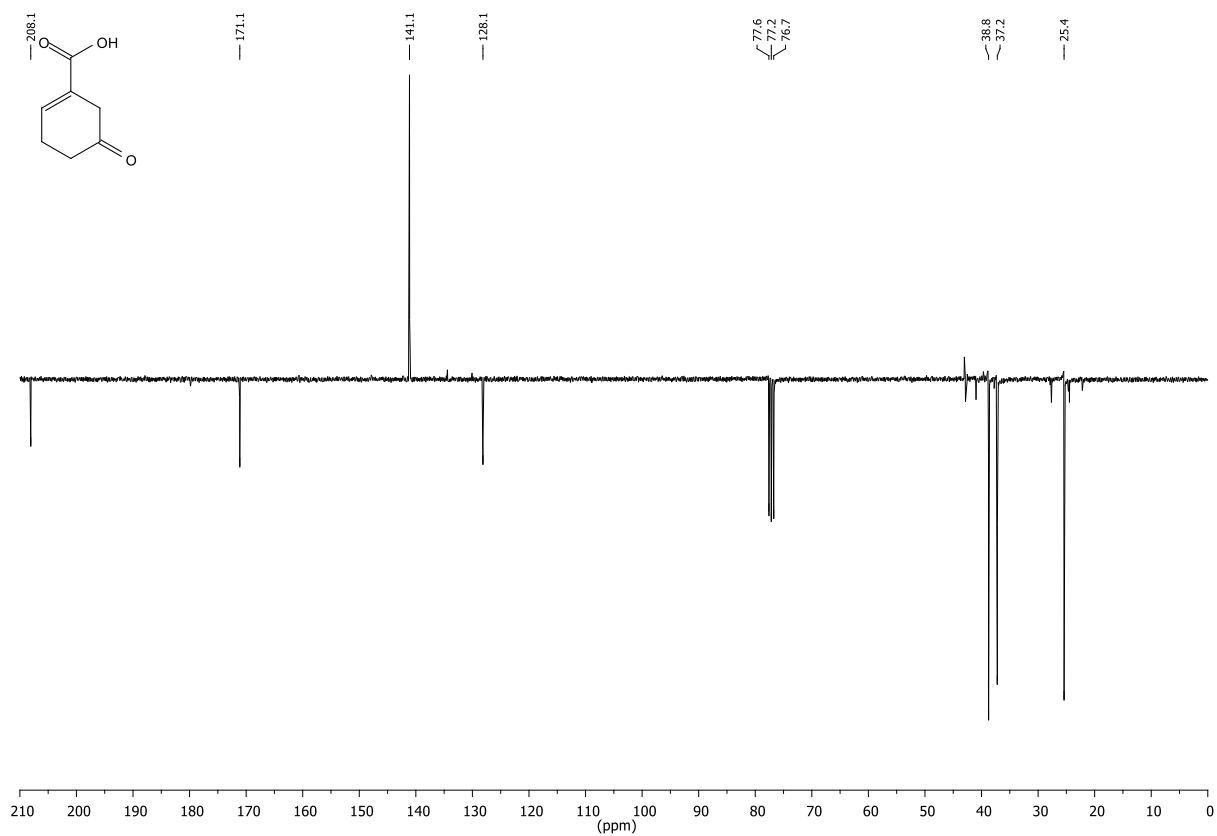


Figure 12.39: $^{13}\text{C-NMR}$,APT (77.53 MHz, CDCl_3) of compound 20.

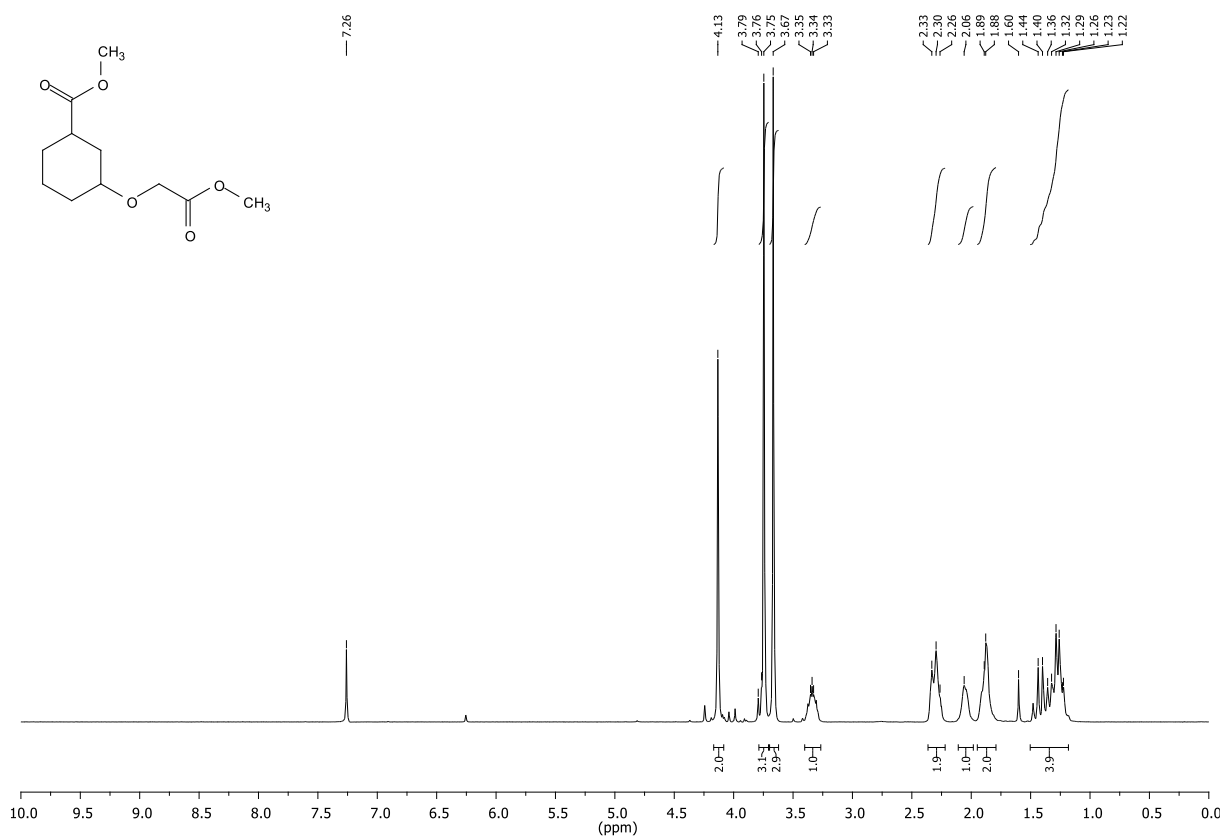


Figure 12.40: $^1\text{H-NMR}$ (300.36 MHz, CDCl_3) of compound 21.

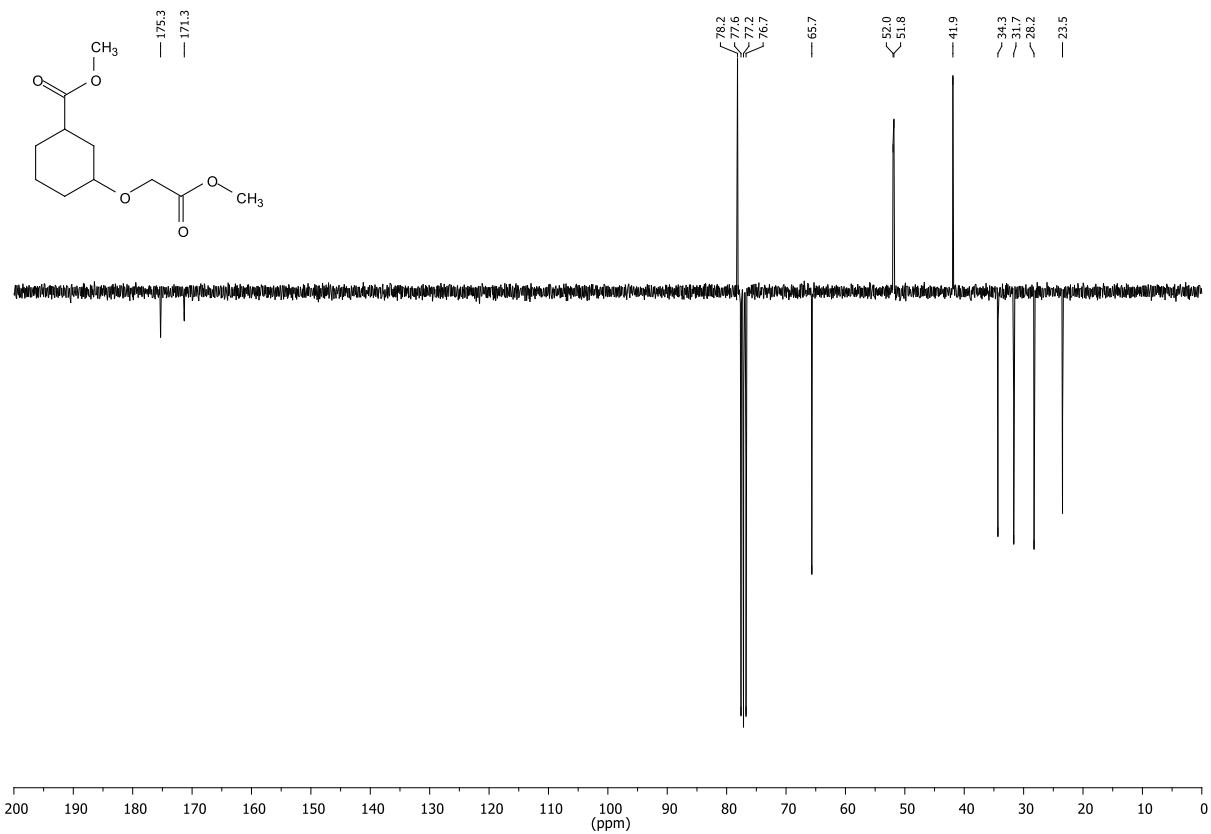


Figure 12.41: $^{13}\text{C-NMR}$ (75.53 MHz, CDCl_3) of compound 21.

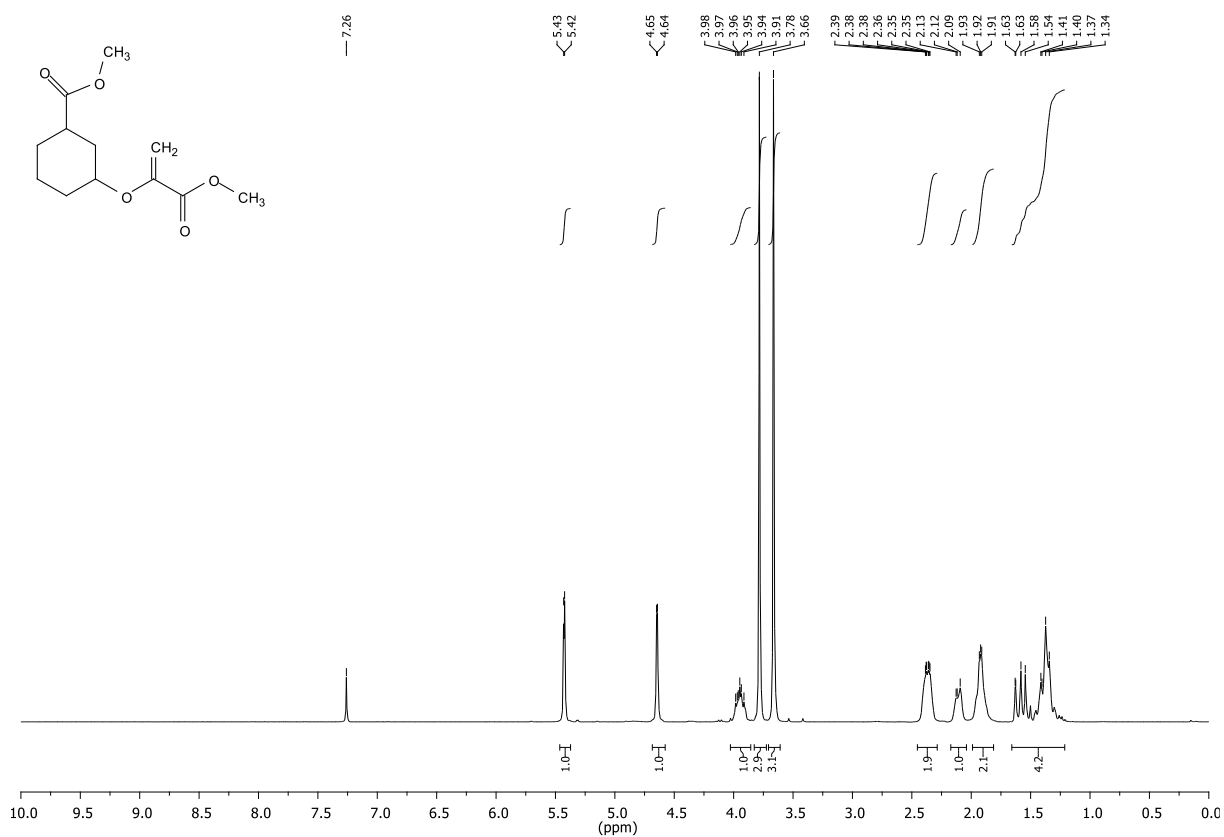


Figure 12.42: $^1\text{H-NMR}$ (300.36 MHz, CDCl_3) of compound 22.

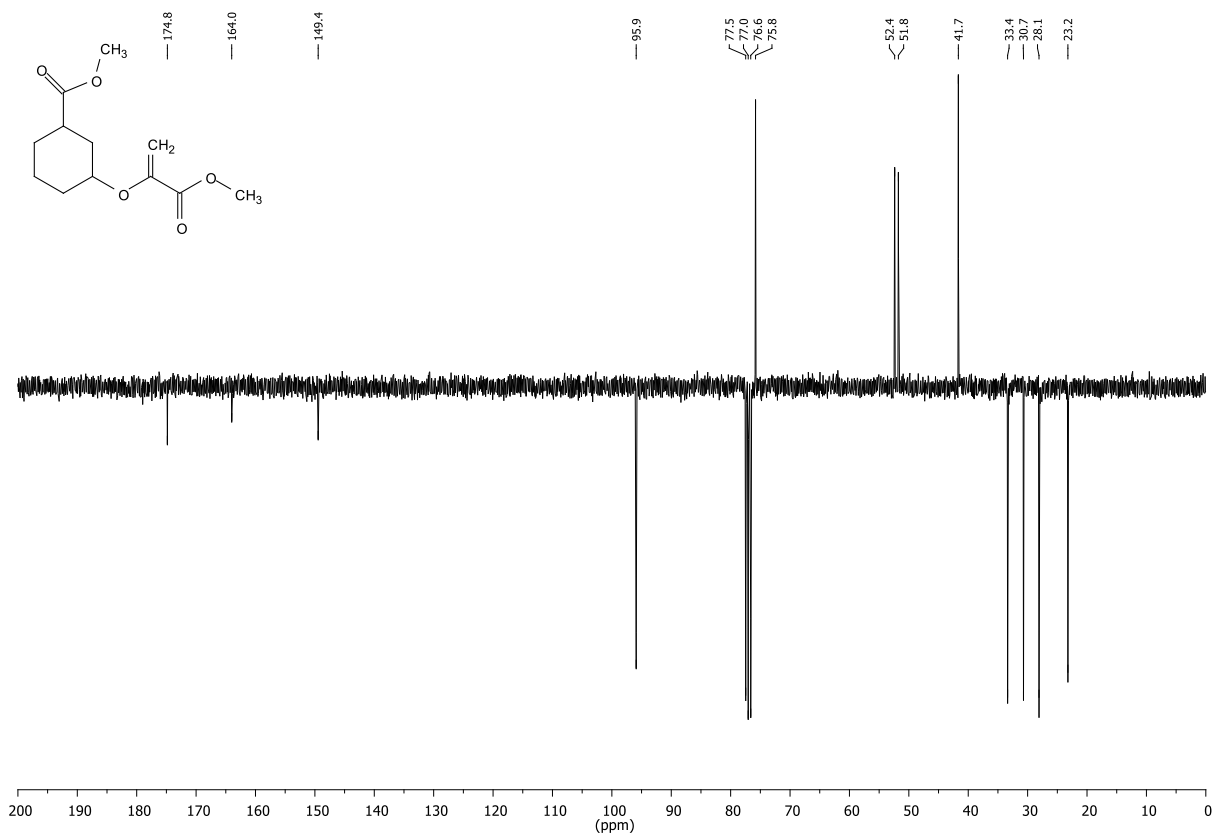


Figure 12.43: ¹³C-NMR, APT (75.53 MHz, CDCl₃) of compound 22.

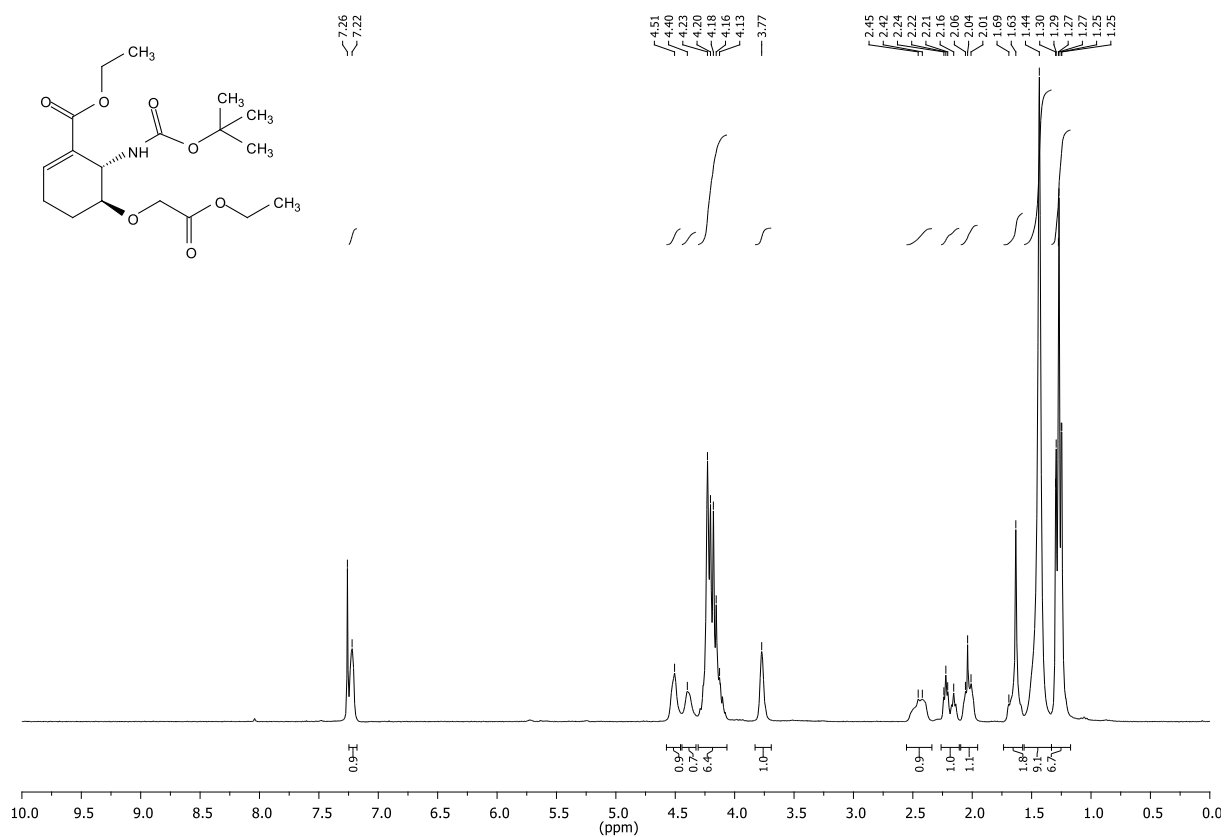


Figure 12.44: ¹H-NMR (300.36 MHz, CDCl₃) of compound 23.

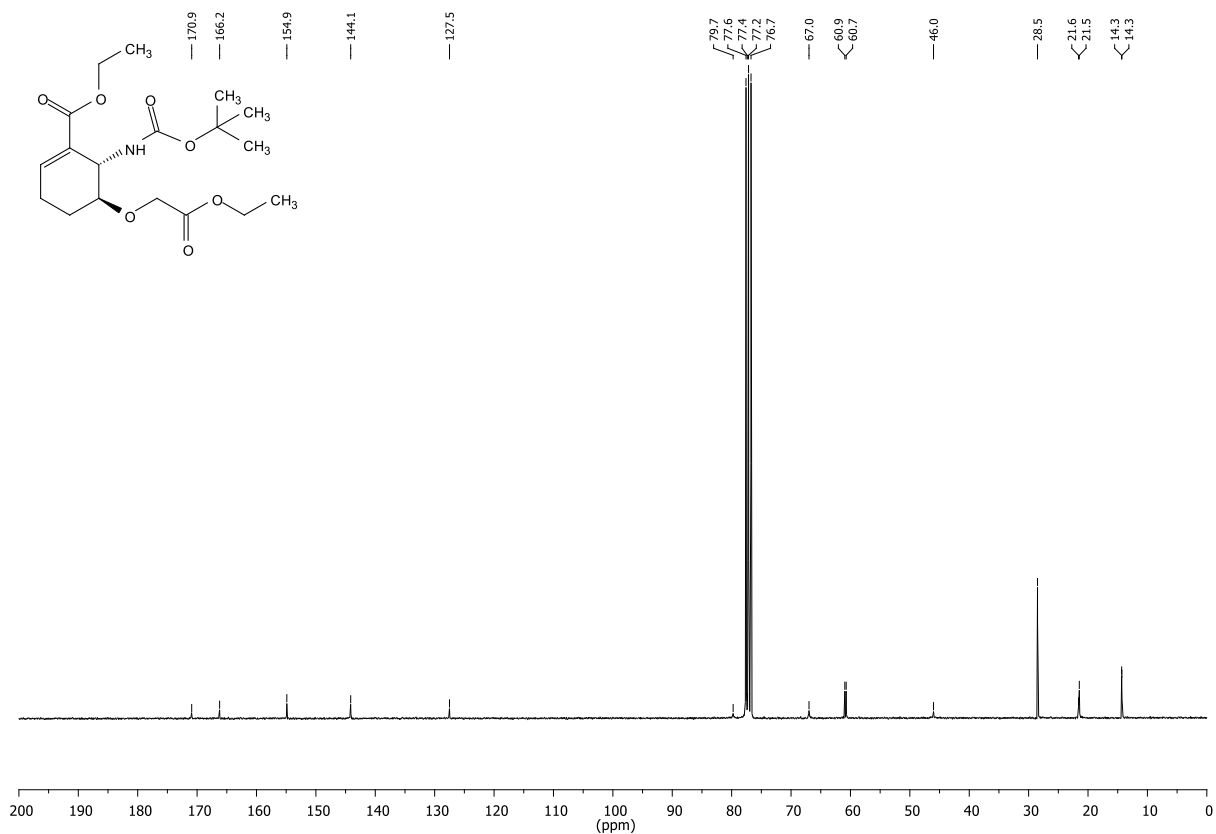


Figure 12.45: $^{13}\text{C-NMR}$ (75.53 MHz, CDCl_3) of compound 23.

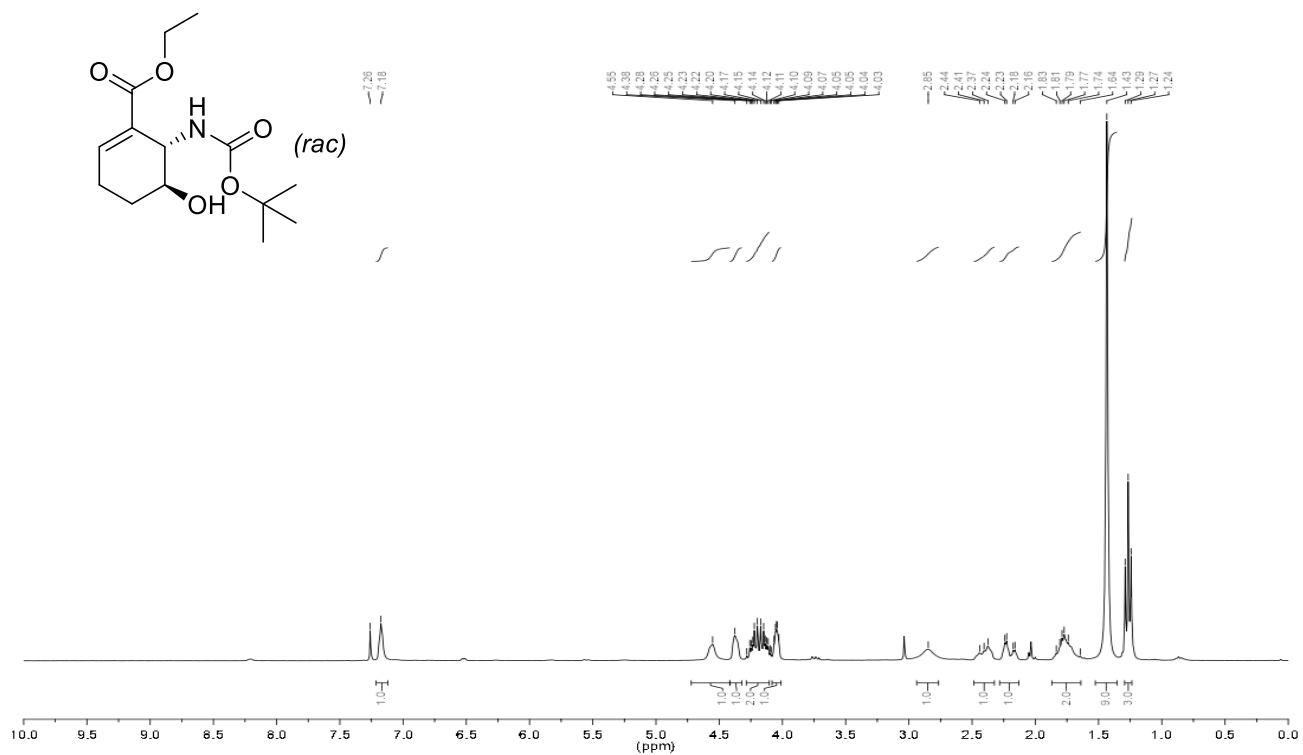


Figure 12.46: $^1\text{H-NMR}$ (300.36 MHz, CDCl_3) of compound 24.

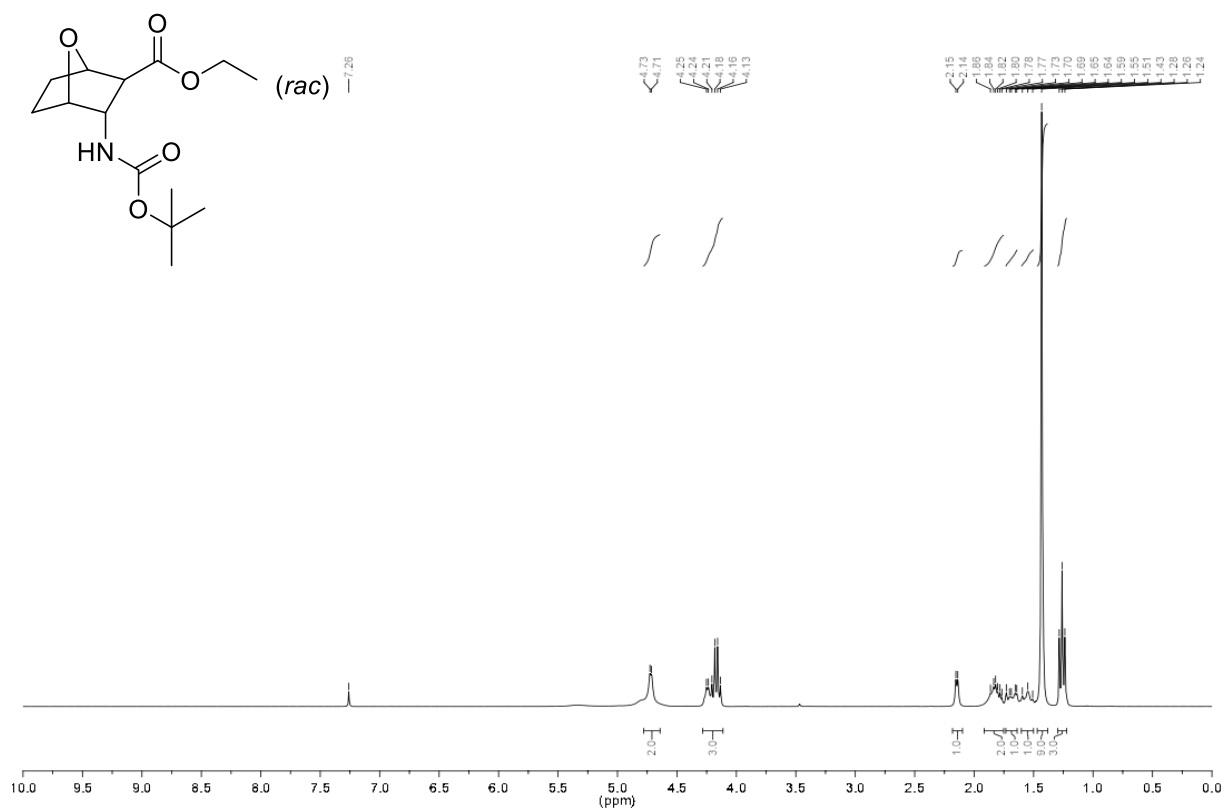


Figure 12.48: ¹H-NMR (300.36 MHz, CDCl₃) of compound 25.

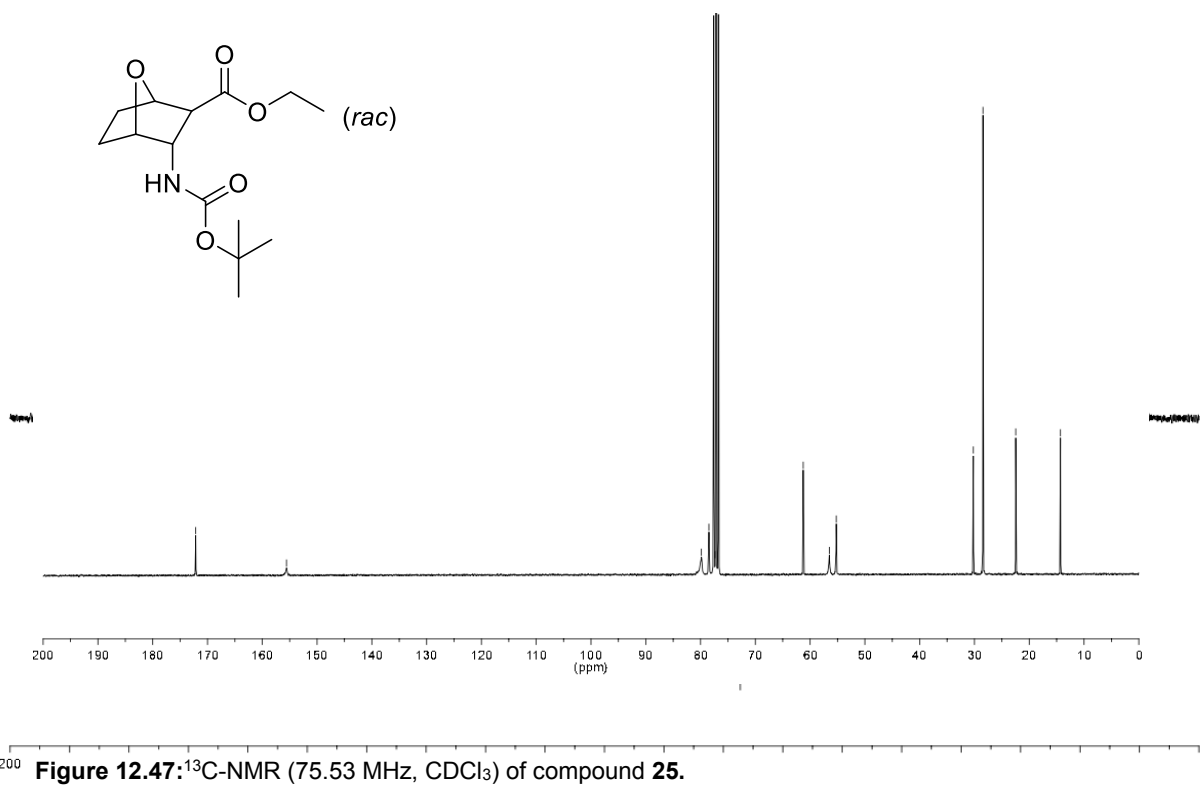


Figure 12.47: ¹³C-NMR (75.53 MHz, CDCl₃) of compound 25.

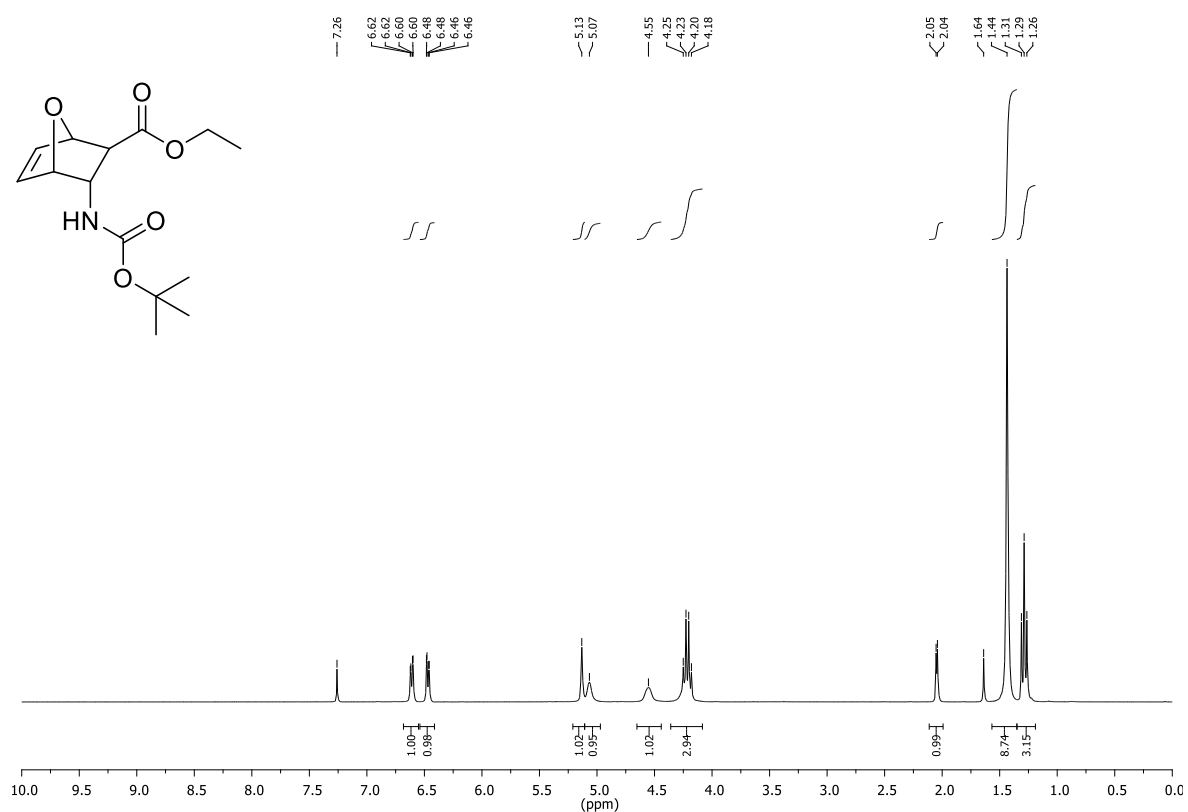


Figure 12.49: ¹H-NMR (300.36 MHz, CDCl₃) of compound 26.

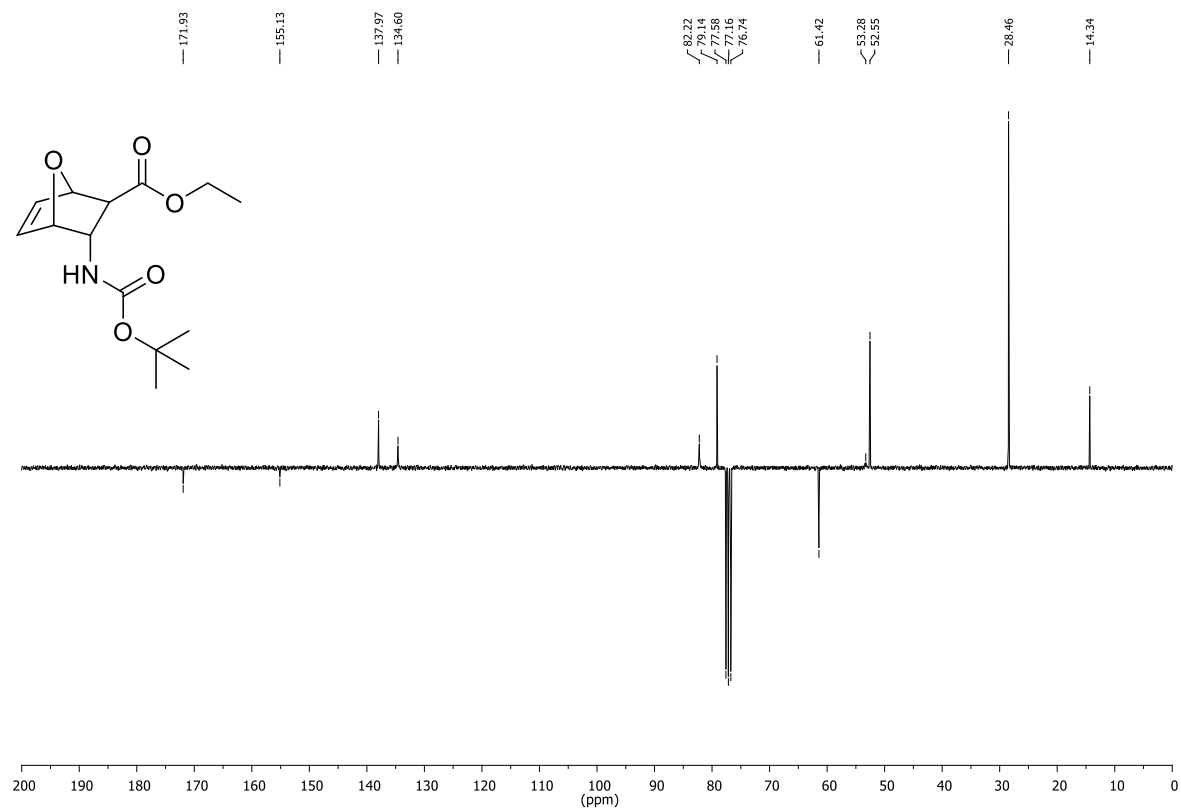


Figure 12.50: ¹³C-NMR,APT (75.53 MHz, CDCl₃) of compound 26.

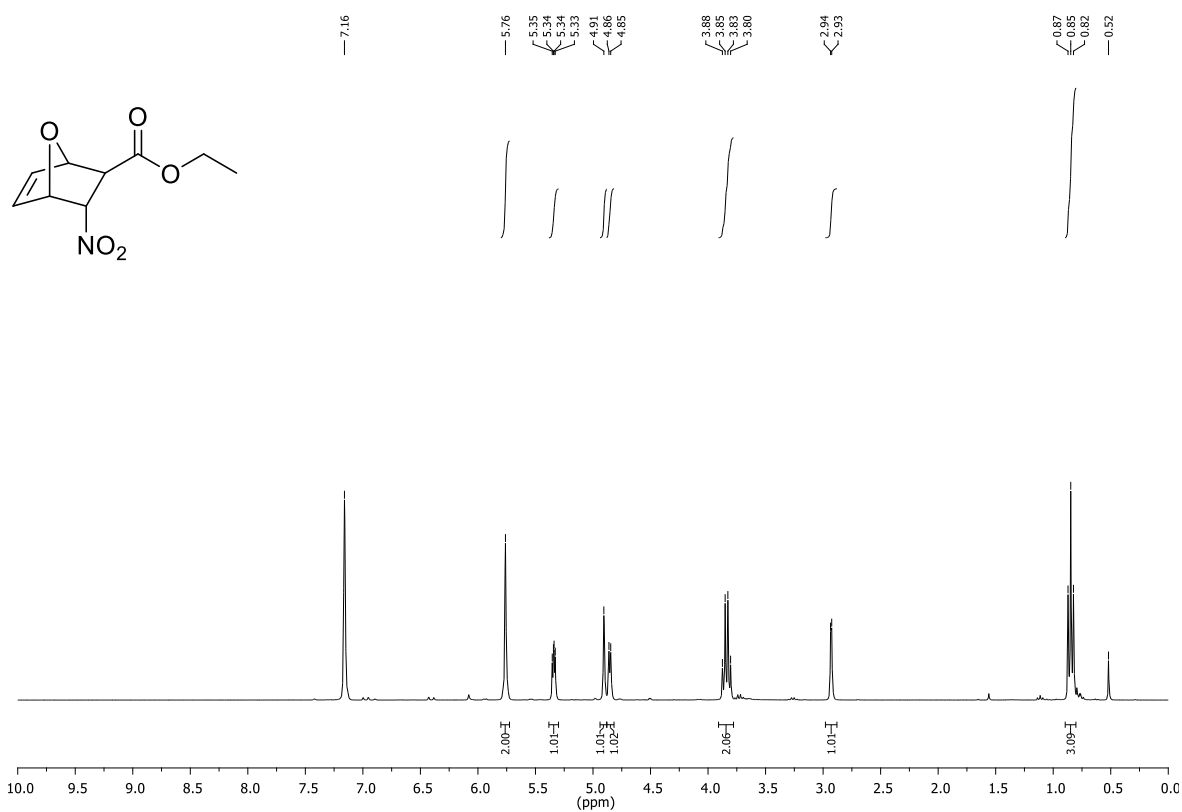


Figure 12.51: ¹H-NMR (300.36 MHz, C₆D₆) of compound 27.

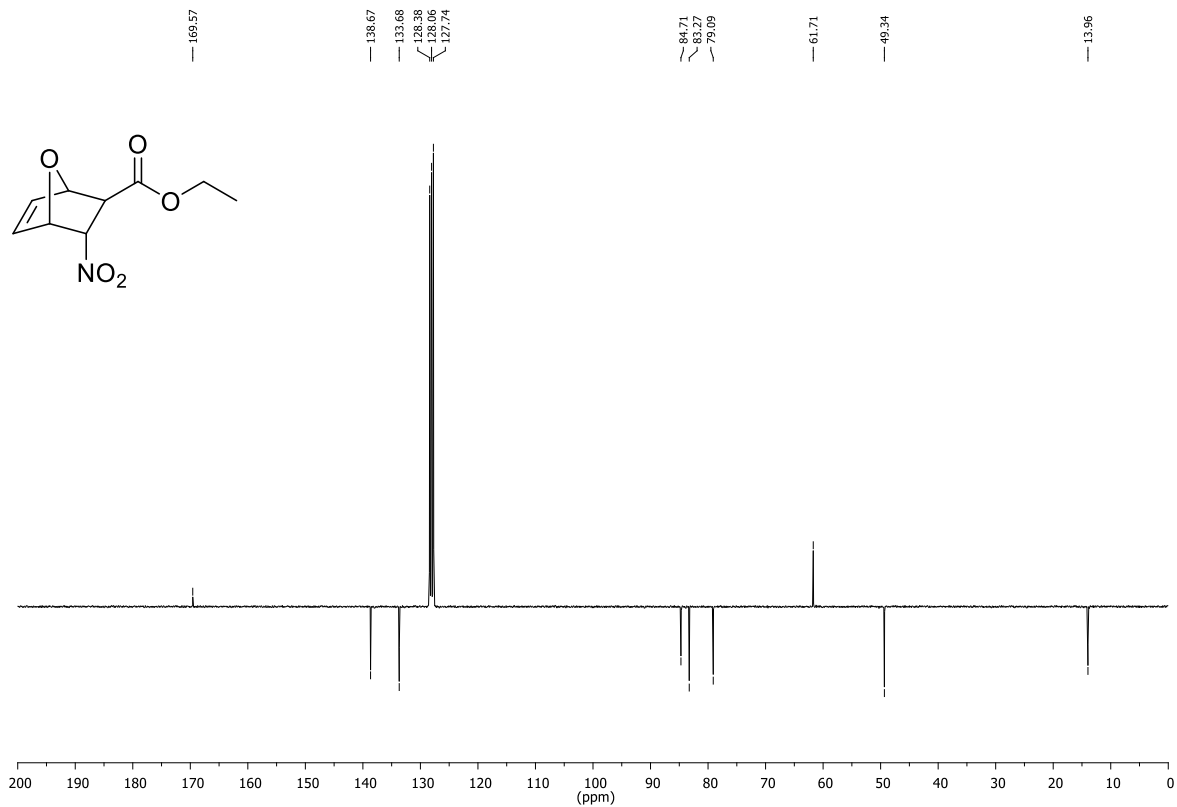


Figure 12.52: ¹³C-NMR,APT (75.53 MHz, C₆D₆) of compound 27.

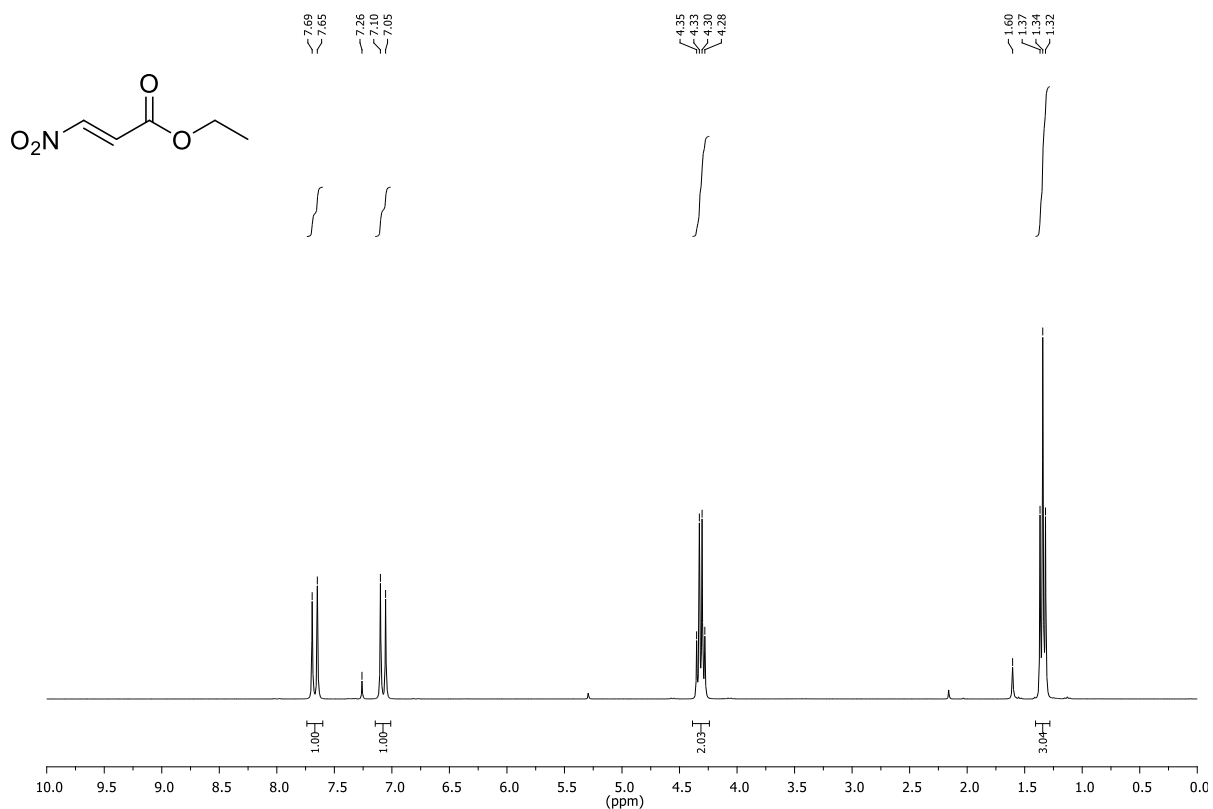


Figure 12.53: ¹H-NMR (300.36 MHz, CDCl₃) of compound 28.

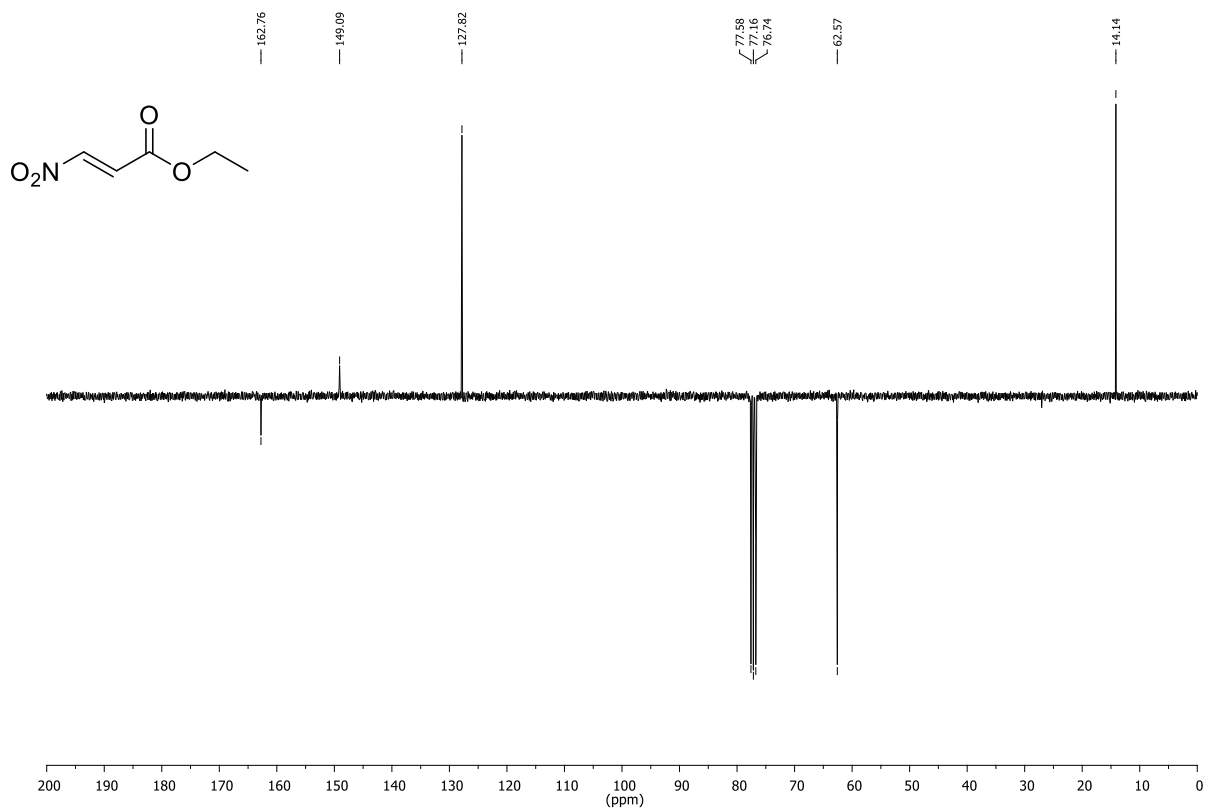


Figure 12.54: ¹³C-NMR (75.53 MHz, CDCl₃) of compound 28.

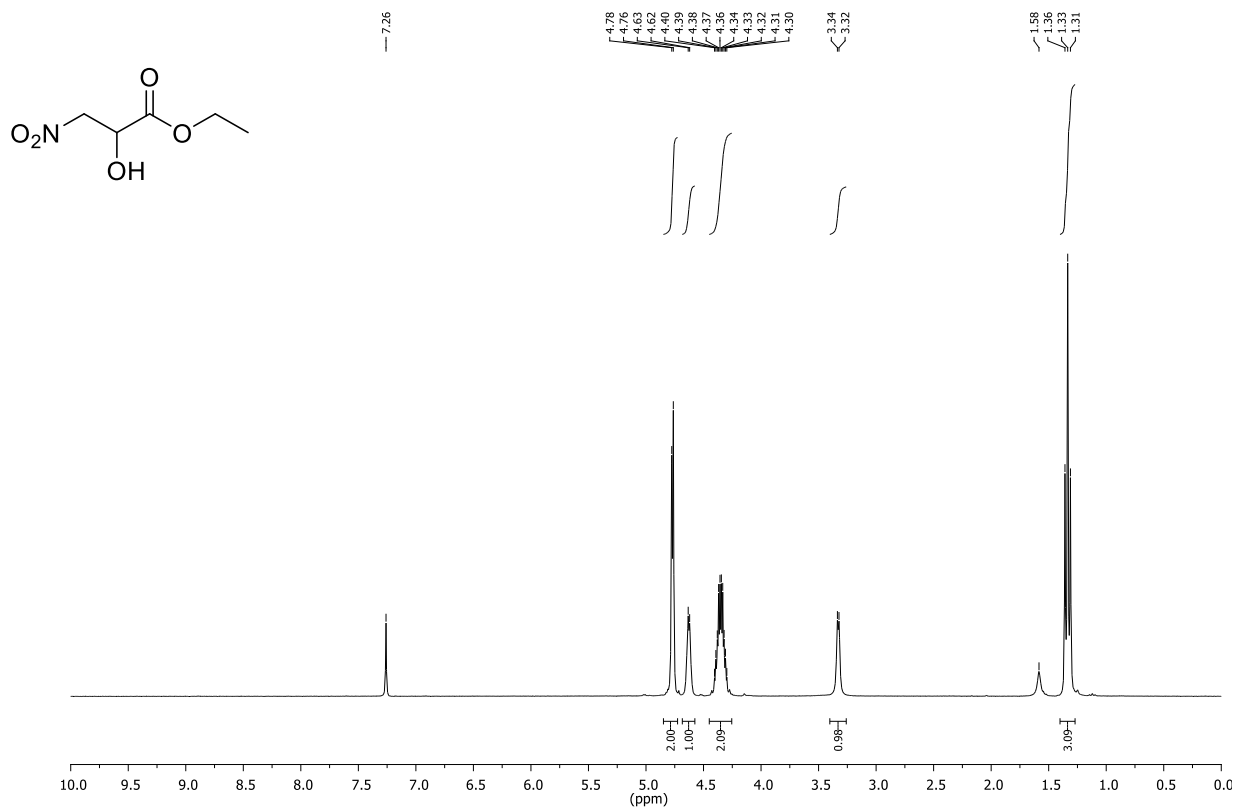


Figure 12.55: ¹H-NMR (300.36 MHz, CDCl₃) of compound **29**.

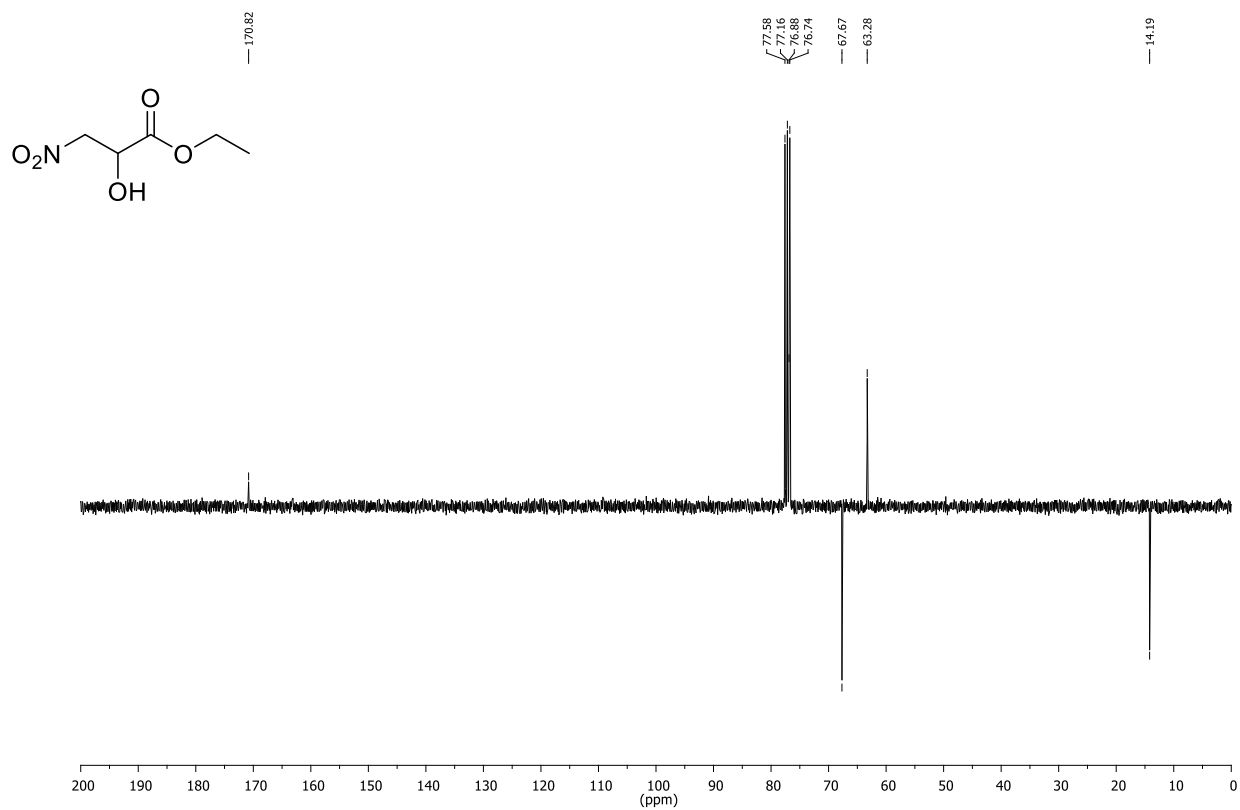


Figure 12.56: ¹³C-NMR,APT (75.53 MHz, CDCl₃) of compound **29**.

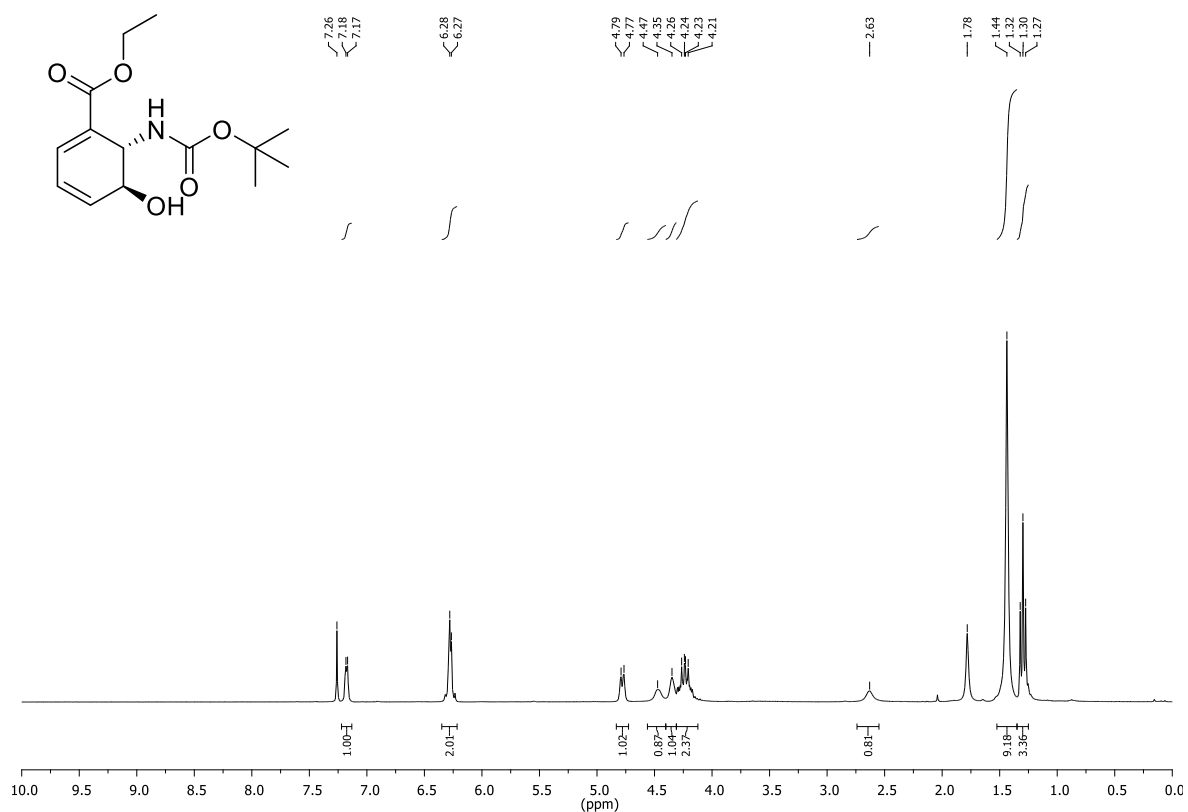


Figure 12.57: ¹H-NMR (300.36 MHz, CDCl₃) of compound 30.

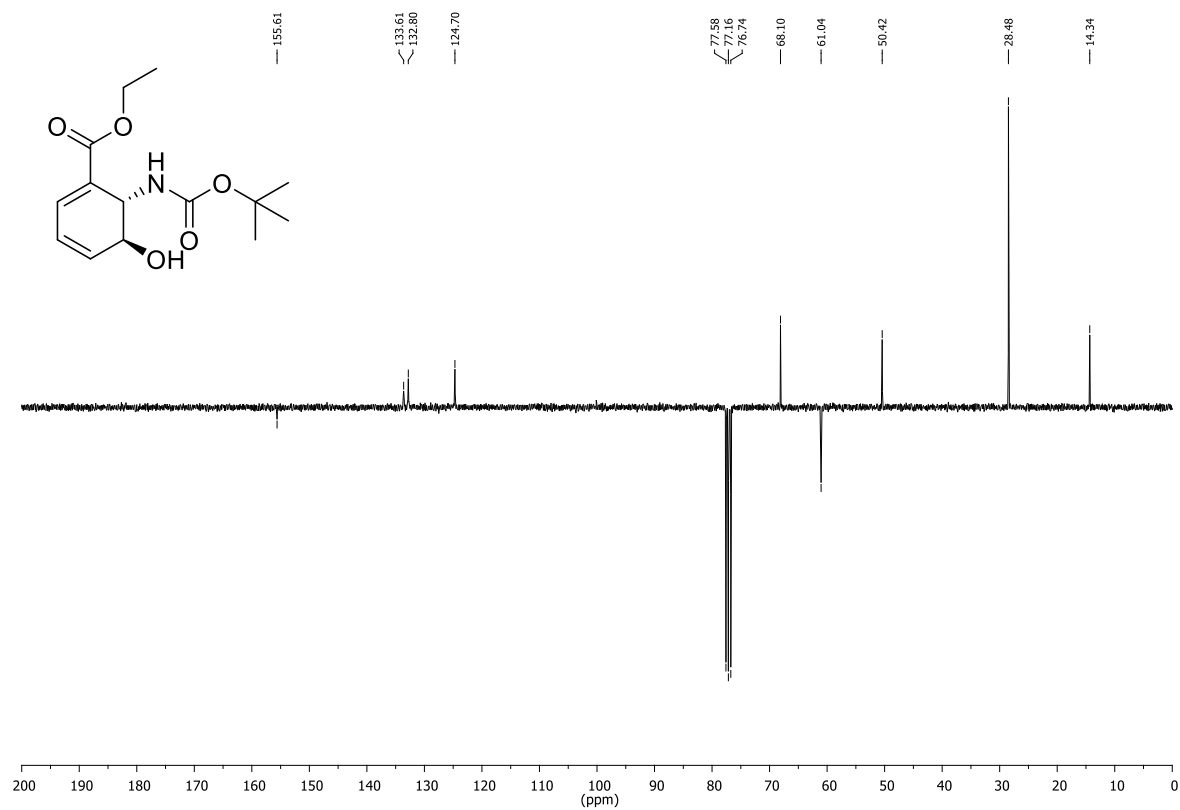


Figure 12.58: ¹³C-NMR,APT (75.53 MHz, CDCl₃) of compound 30.

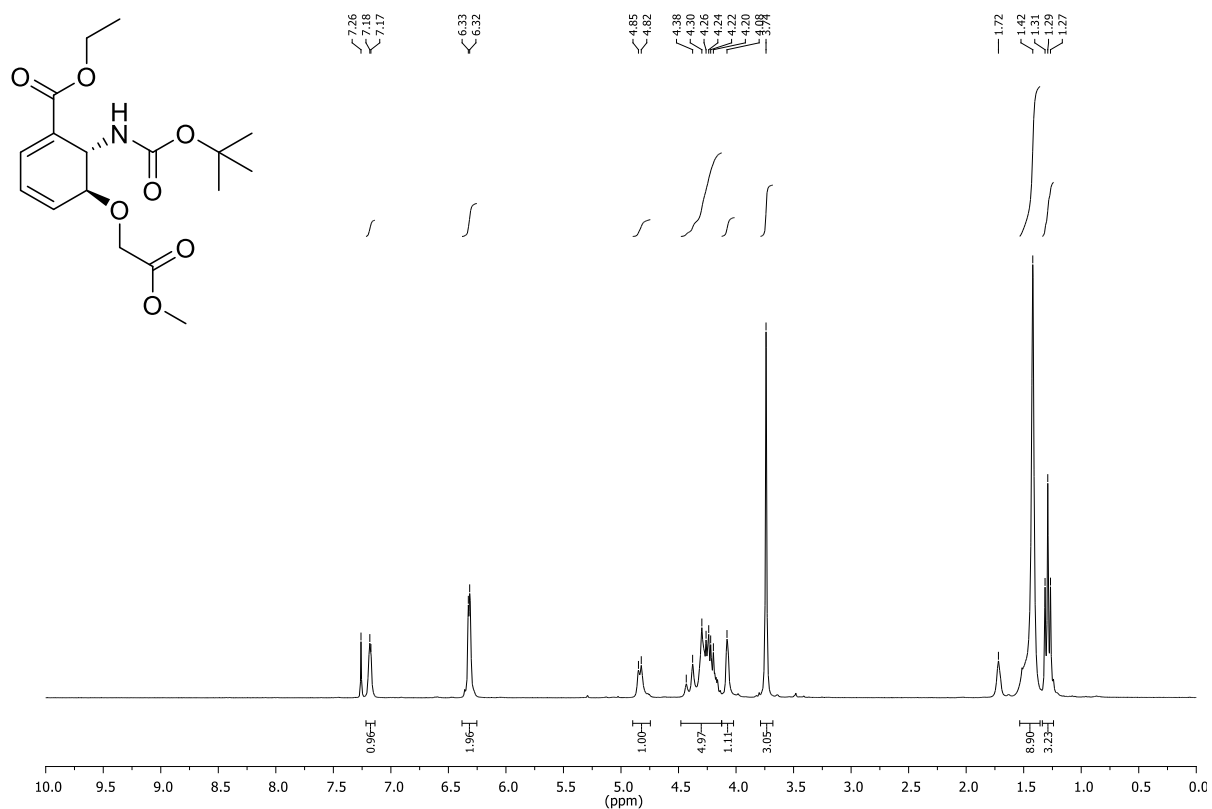


Figure 12.59: ¹H-NMR (300.36 MHz, CDCl₃) of compound 31.

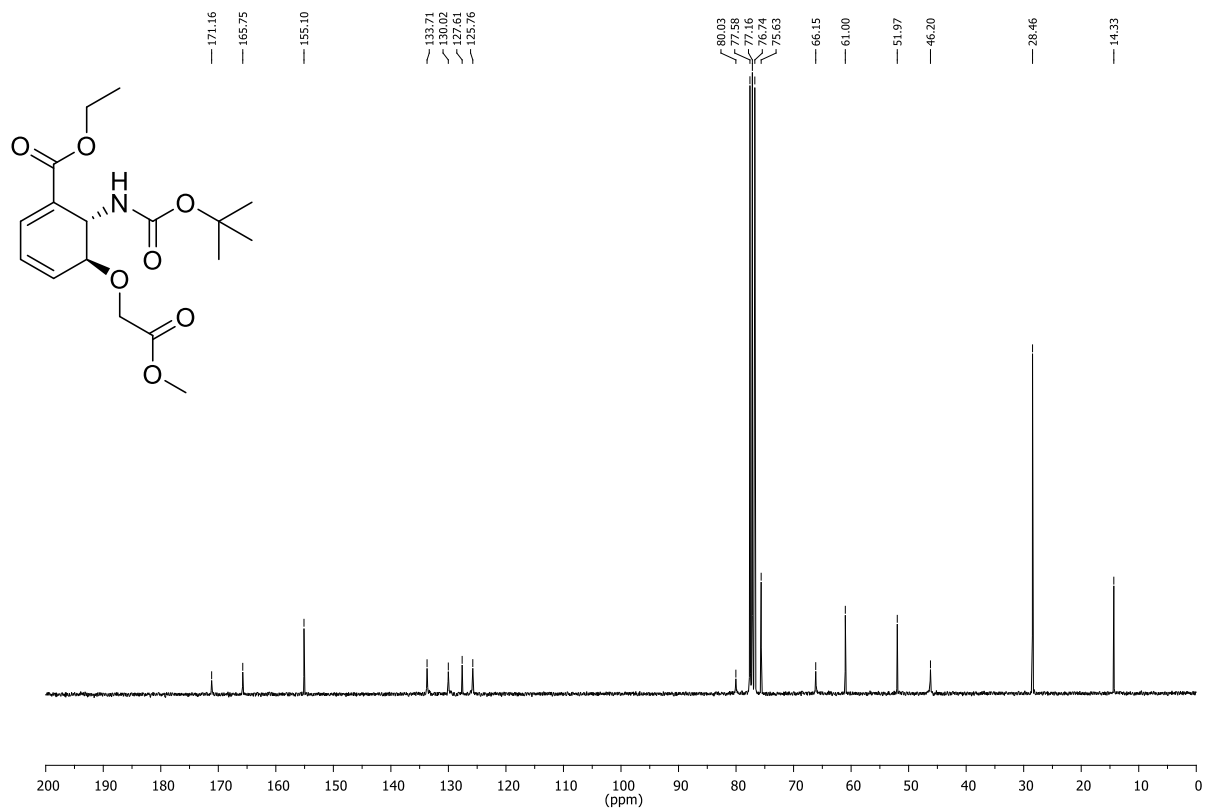


Figure 12.60: ¹³C-NMR (300.36 MHz, CDCl₃) of compound 31.

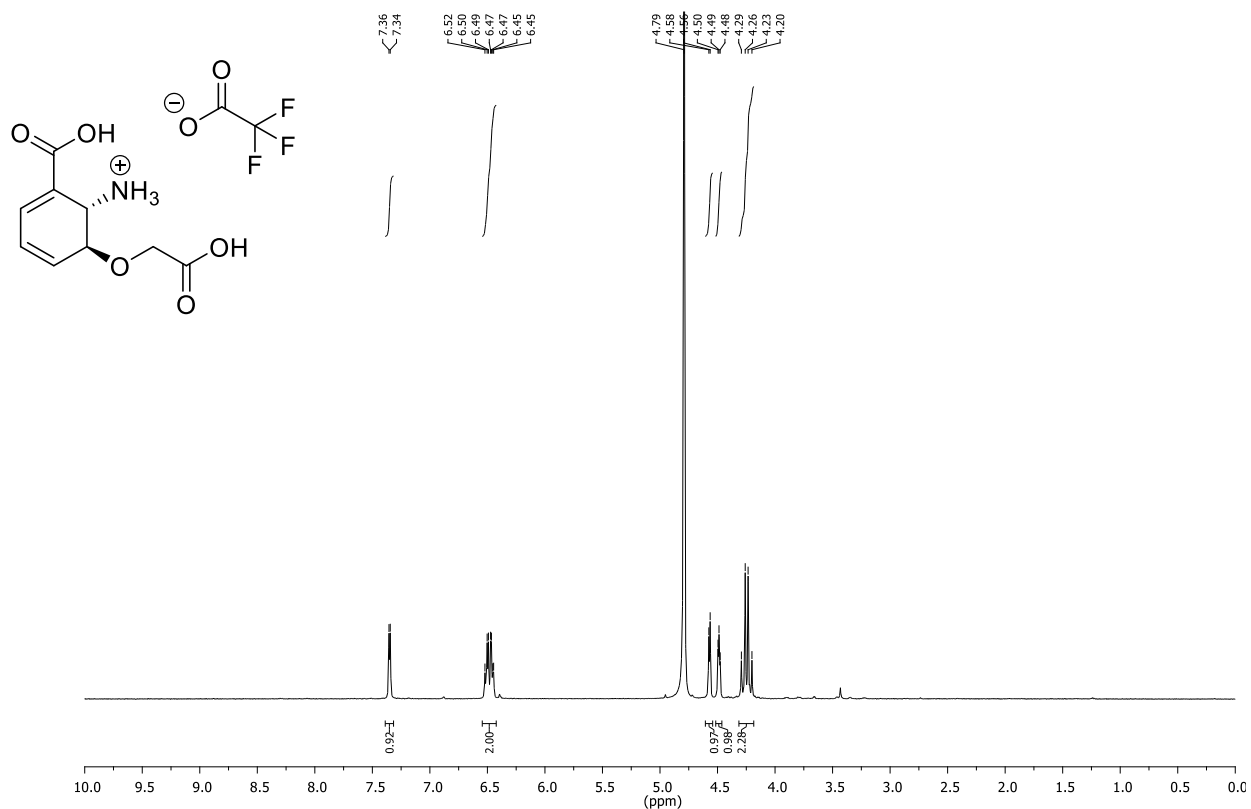


Figure 12.61: $^1\text{H-NMR}$ (499.88 MHz, D_2O) of compound 32.

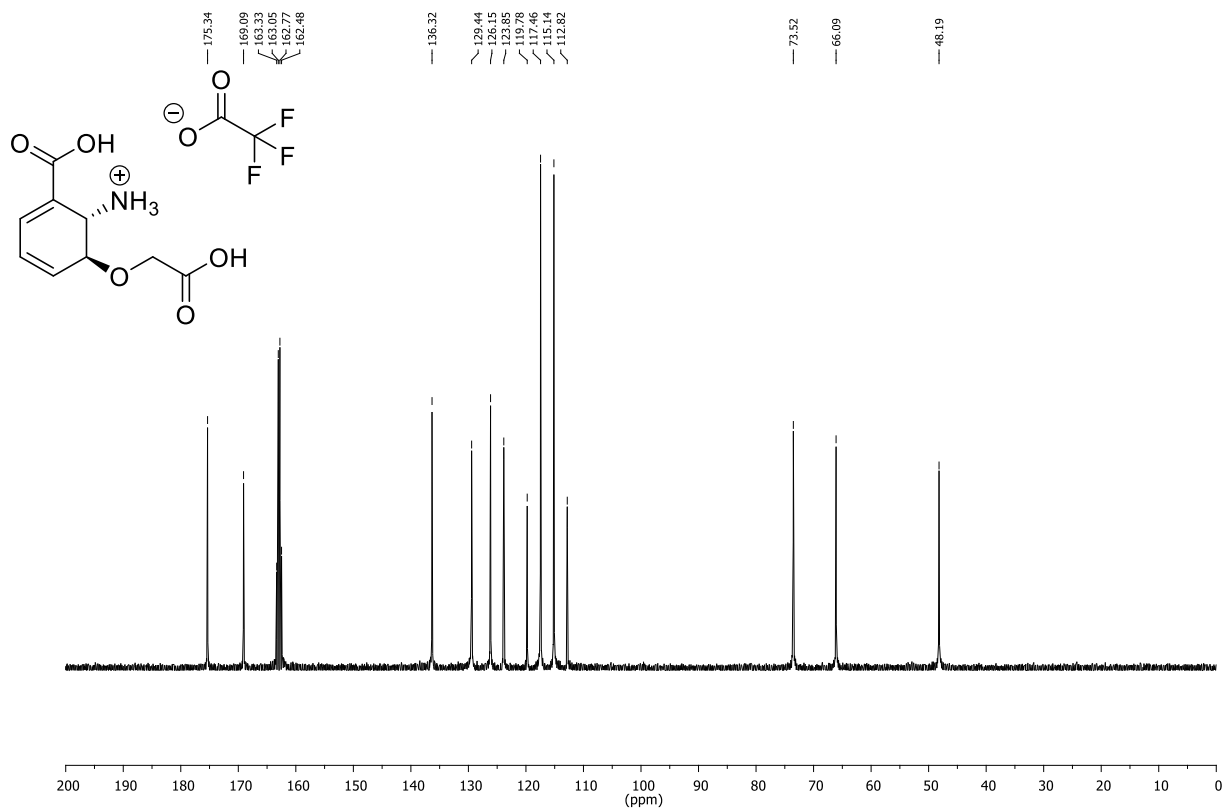


Figure 12.62: $^{13}\text{C-NMR}$ (125.69 MHz, D_2O) of compound 32.

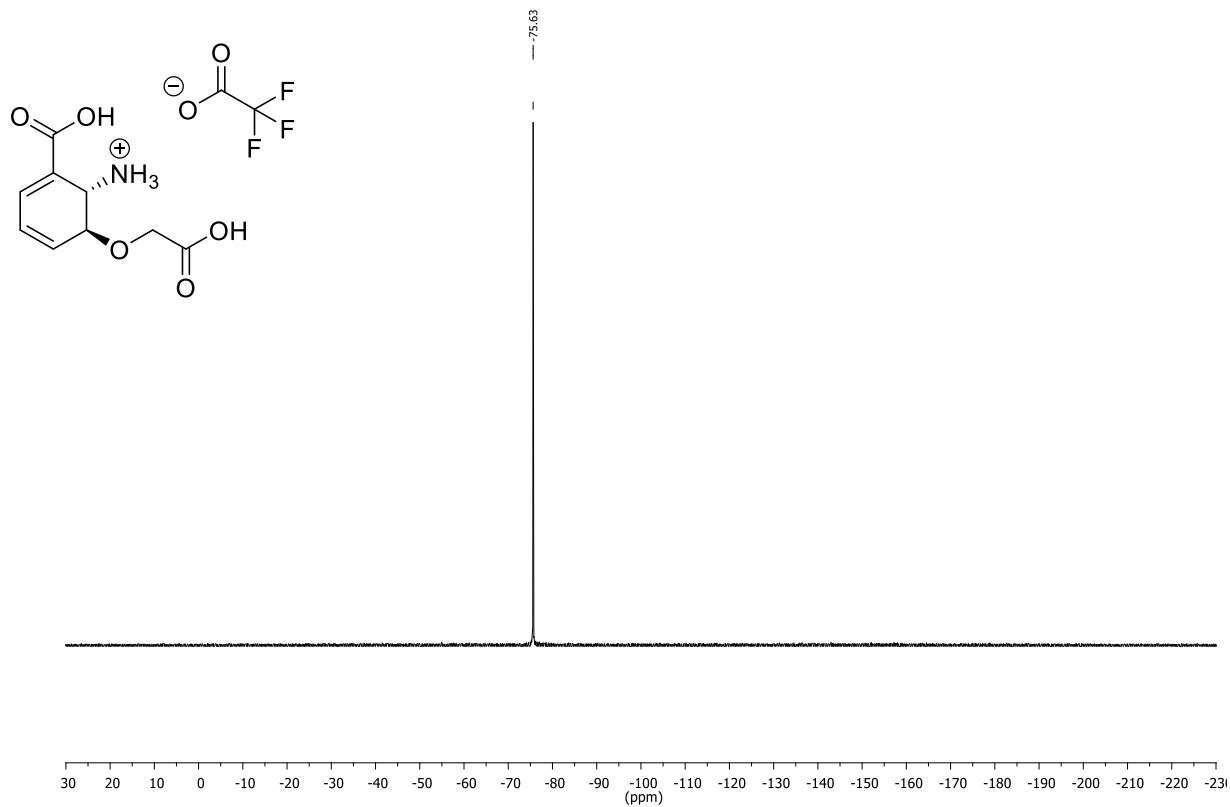


Figure 12.63: ^{19}F -NMR (470.35 MHz, D_2O) of compound 32.

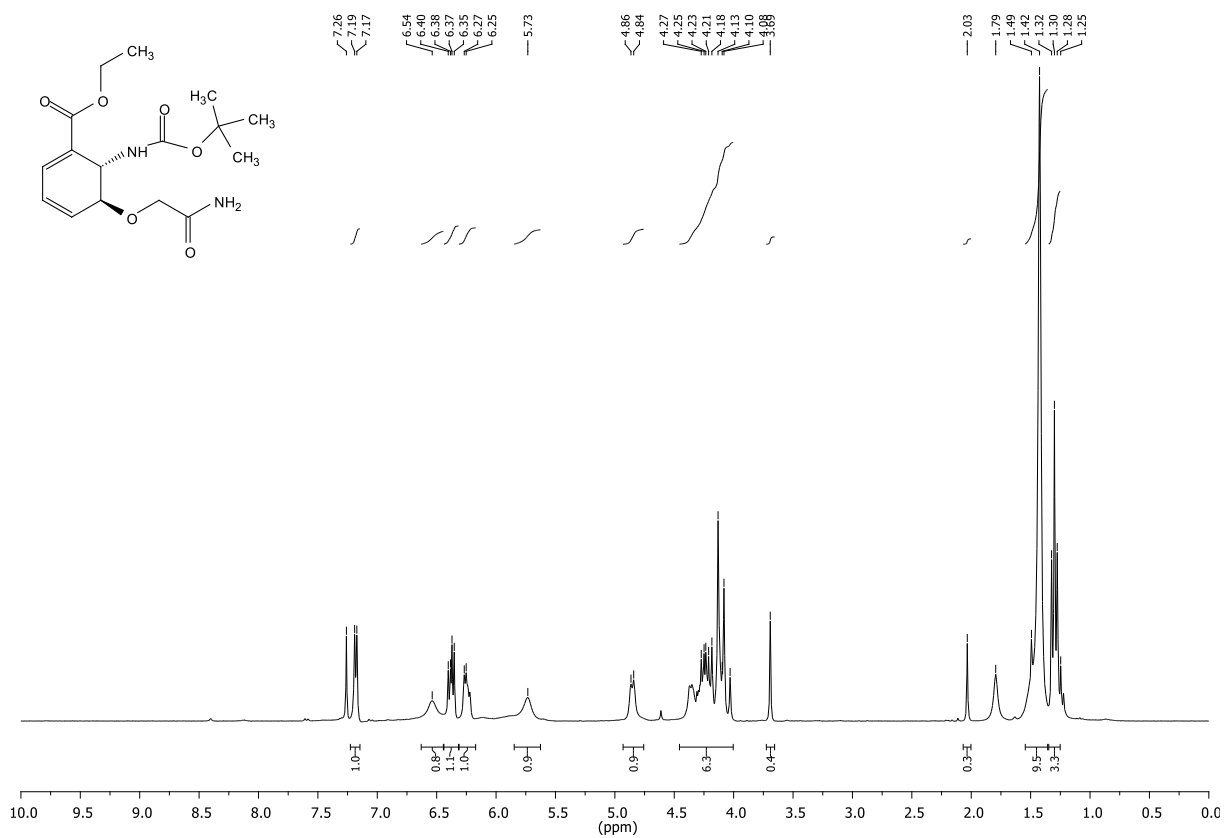


Figure 12.64: ¹H-NMR (300.36 MHz, CDCl₃) of compound 33.

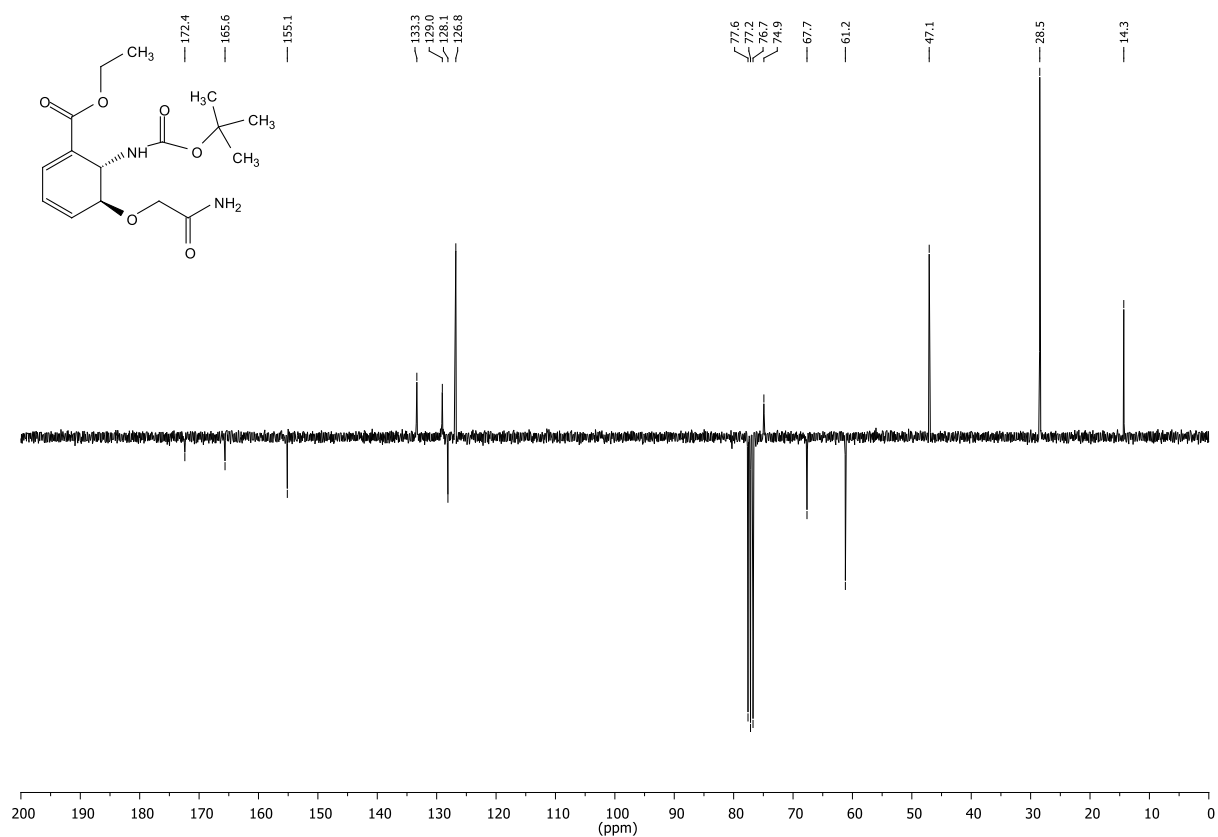


Figure 12.65: ¹³C-NMR,APT (75.53 MHz, CDCl₃) of compound 33.

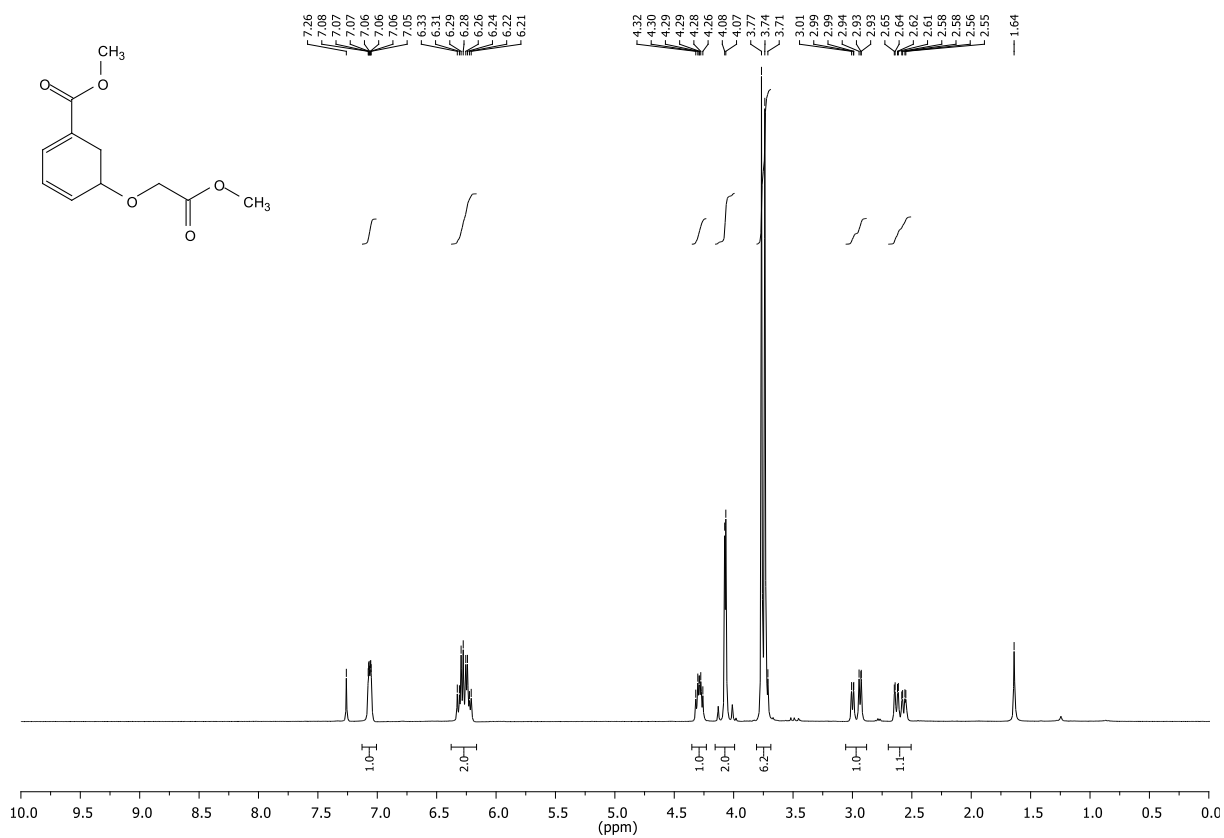


Figure 12.66: ¹H-NMR (300.36 MHz, CDCl₃) of compound 34.

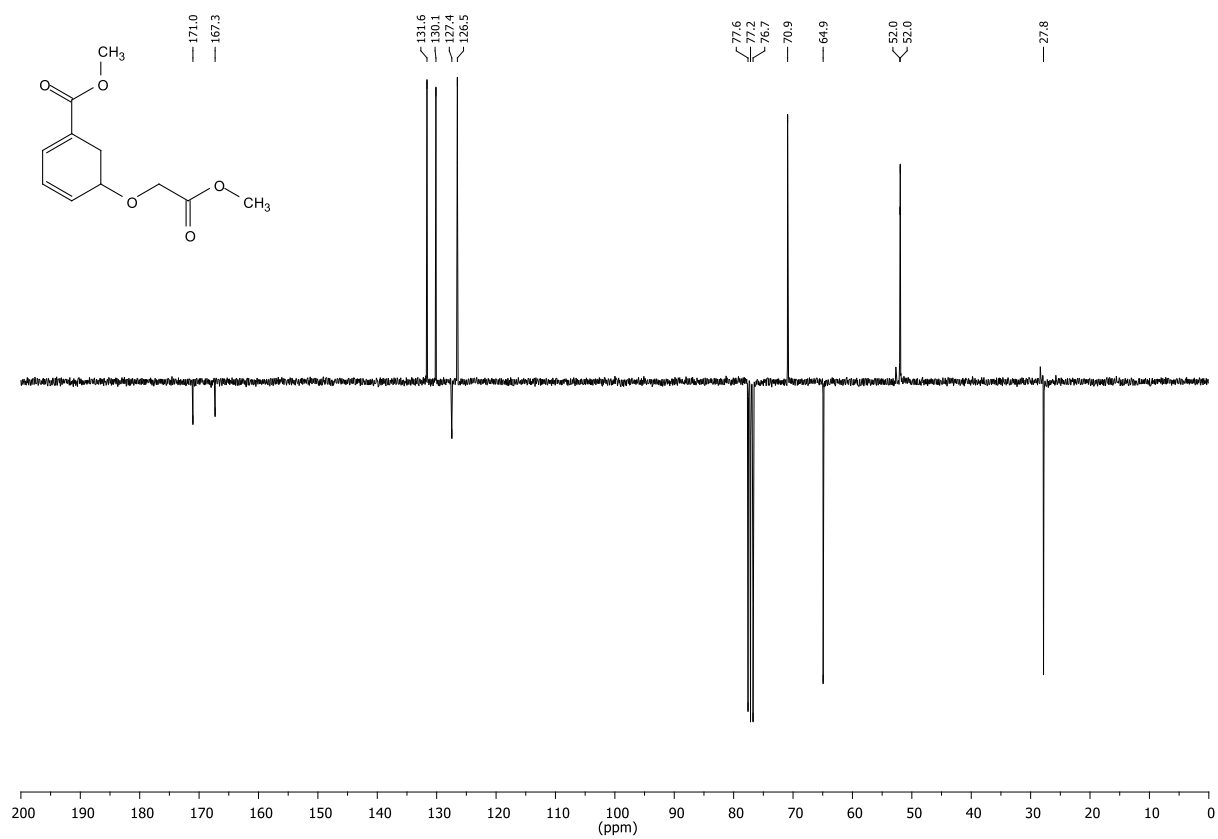


Figure 12.67: ¹³C-NMR,APT (75.53 MHz, CDCl₃) of compound 34.

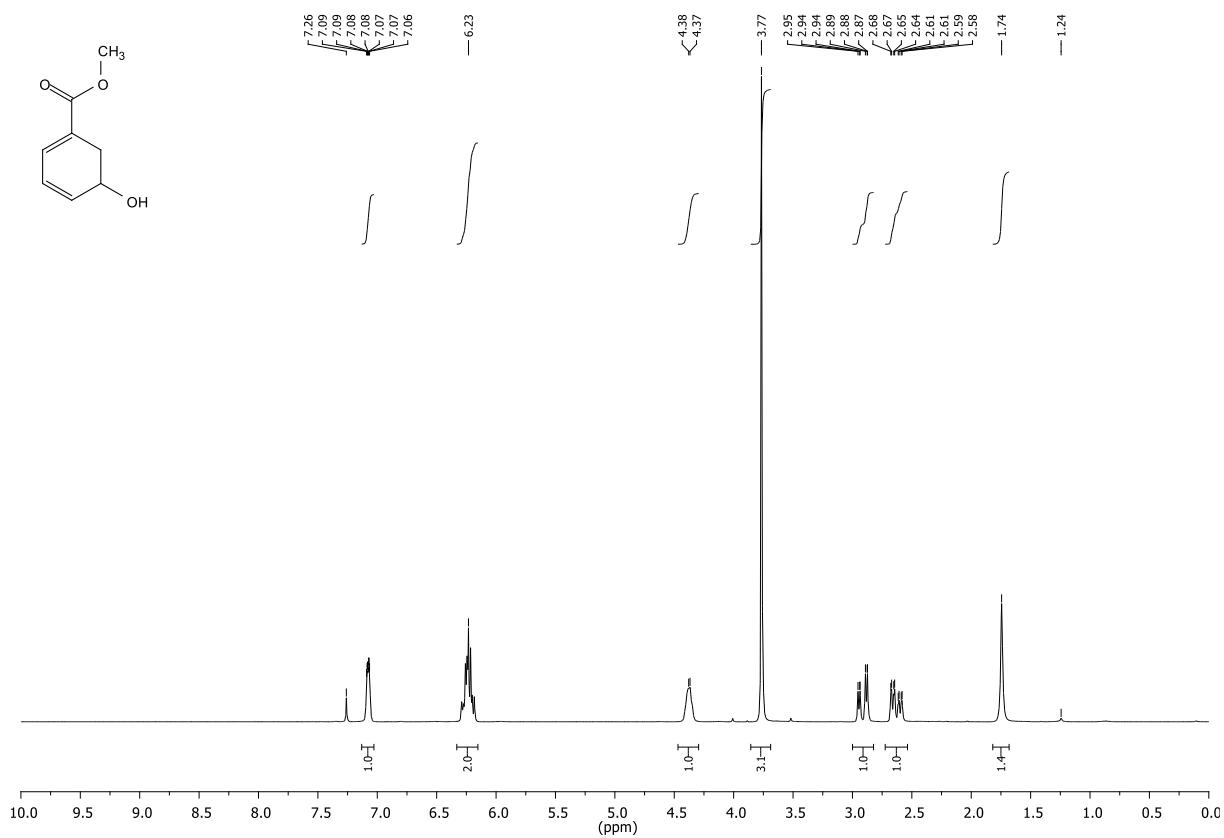


Figure 12.68: ¹H-NMR (300.36 MHz, CDCl₃) of compound 35.

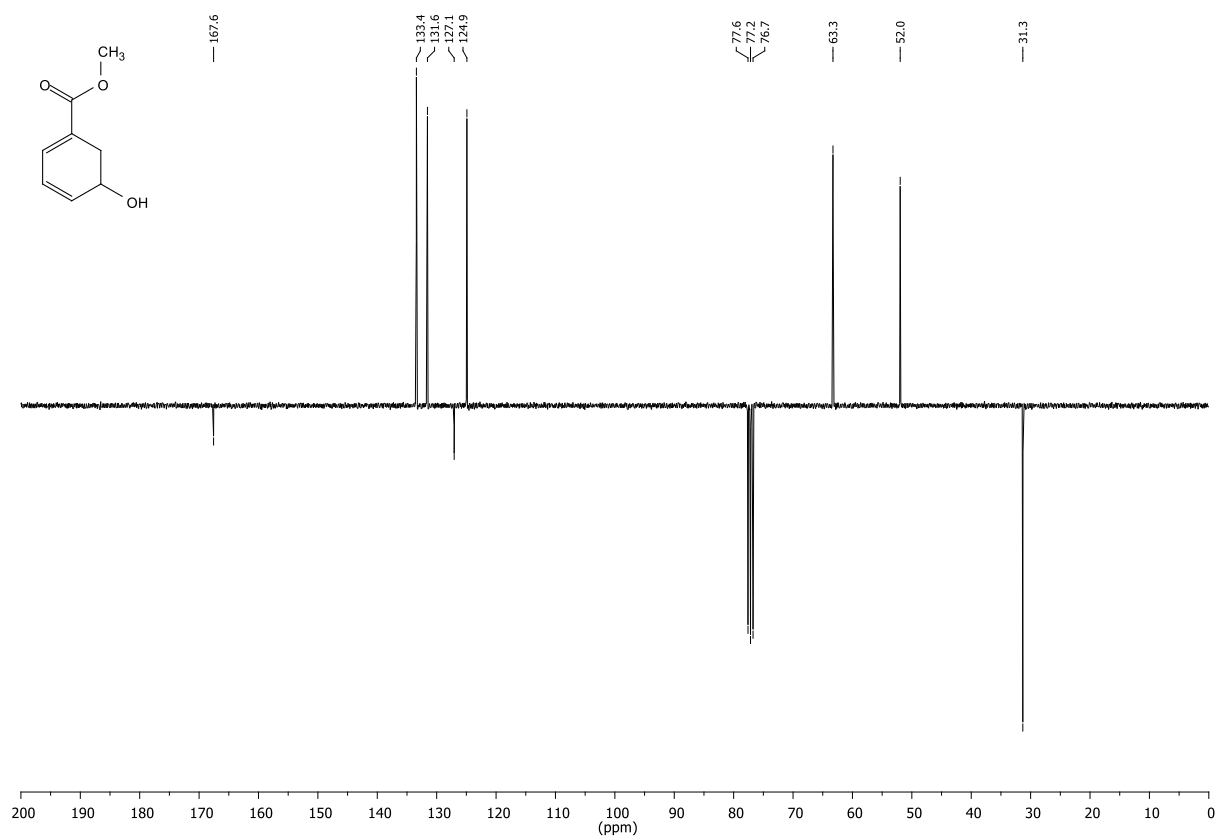


Figure 12.69: ¹³C-NMR (75.53 MHz, CDCl₃) of compound 35.

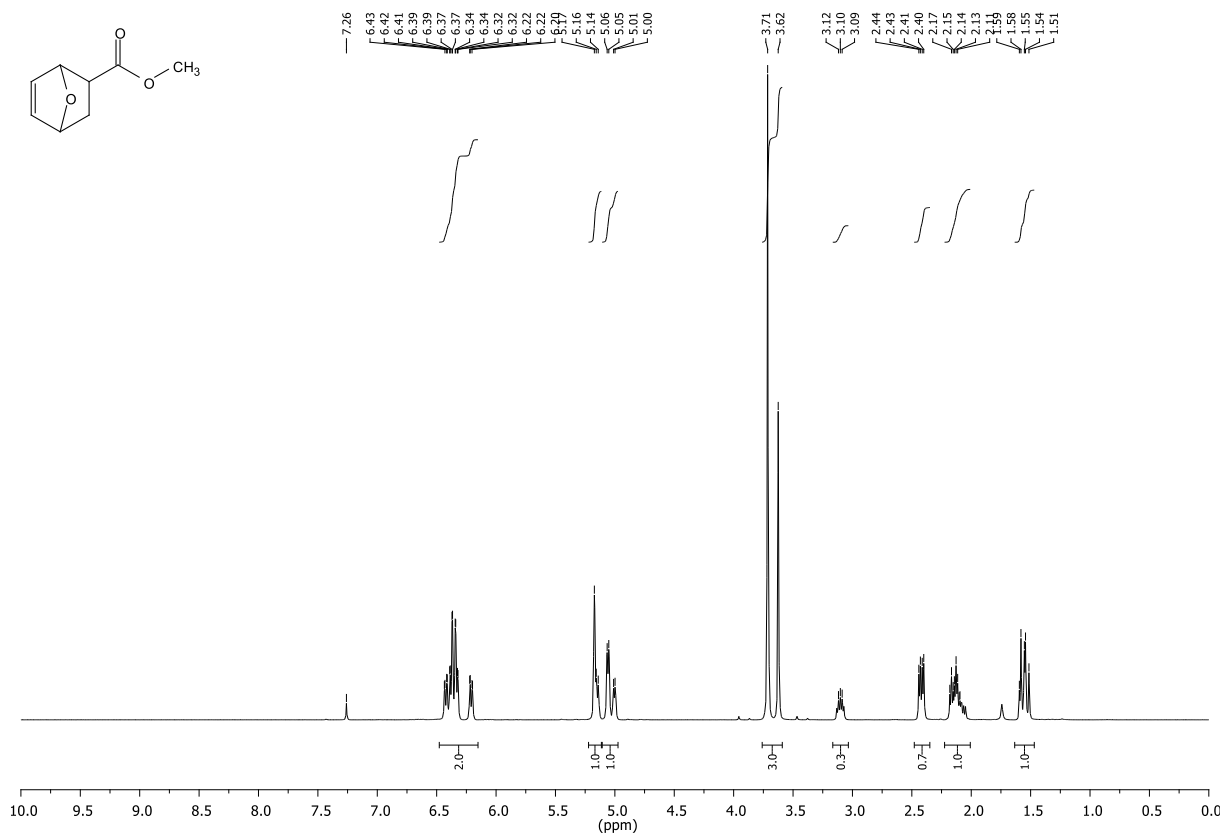


Figure 12.70: ¹H-NMR (300.36 MHz, CDCl₃) of compound 36.

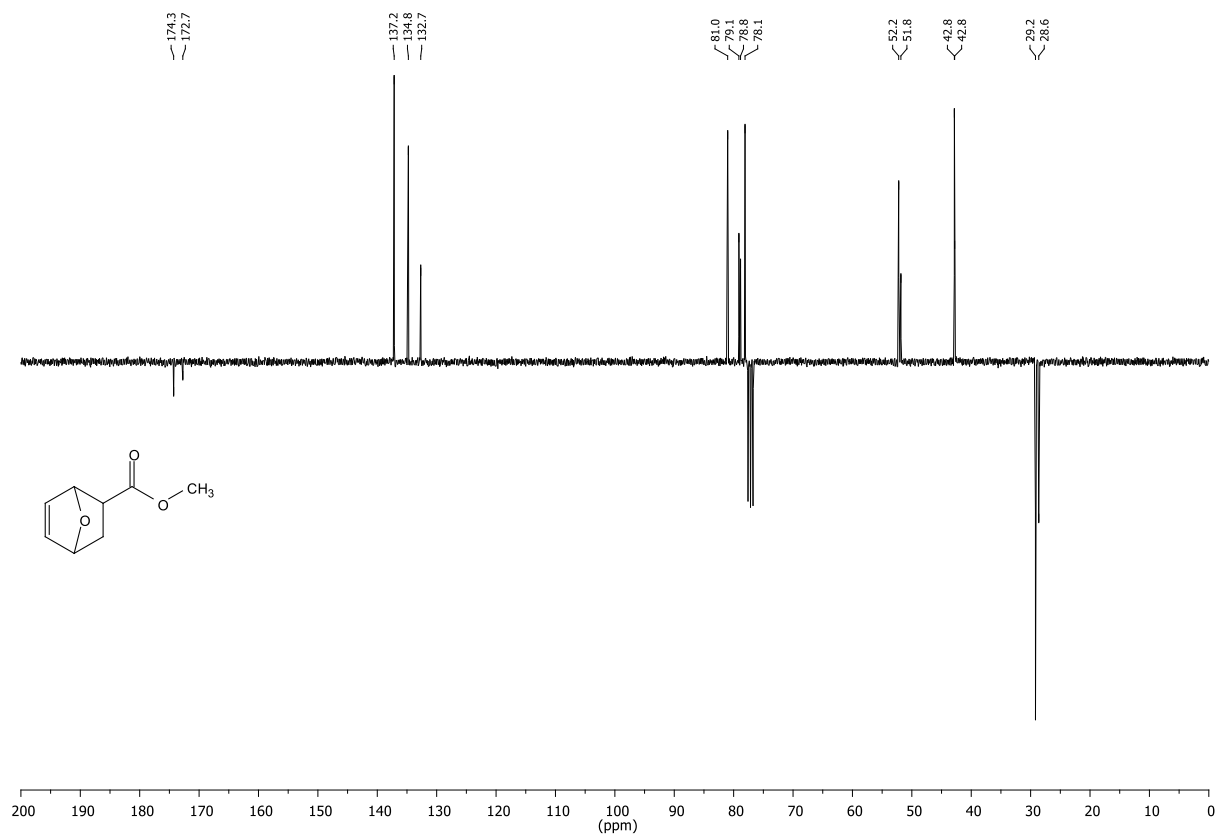


Figure 12.71: ¹³C-NMR (APT, 75.53 MHz, CDCl₃) of compound 36.

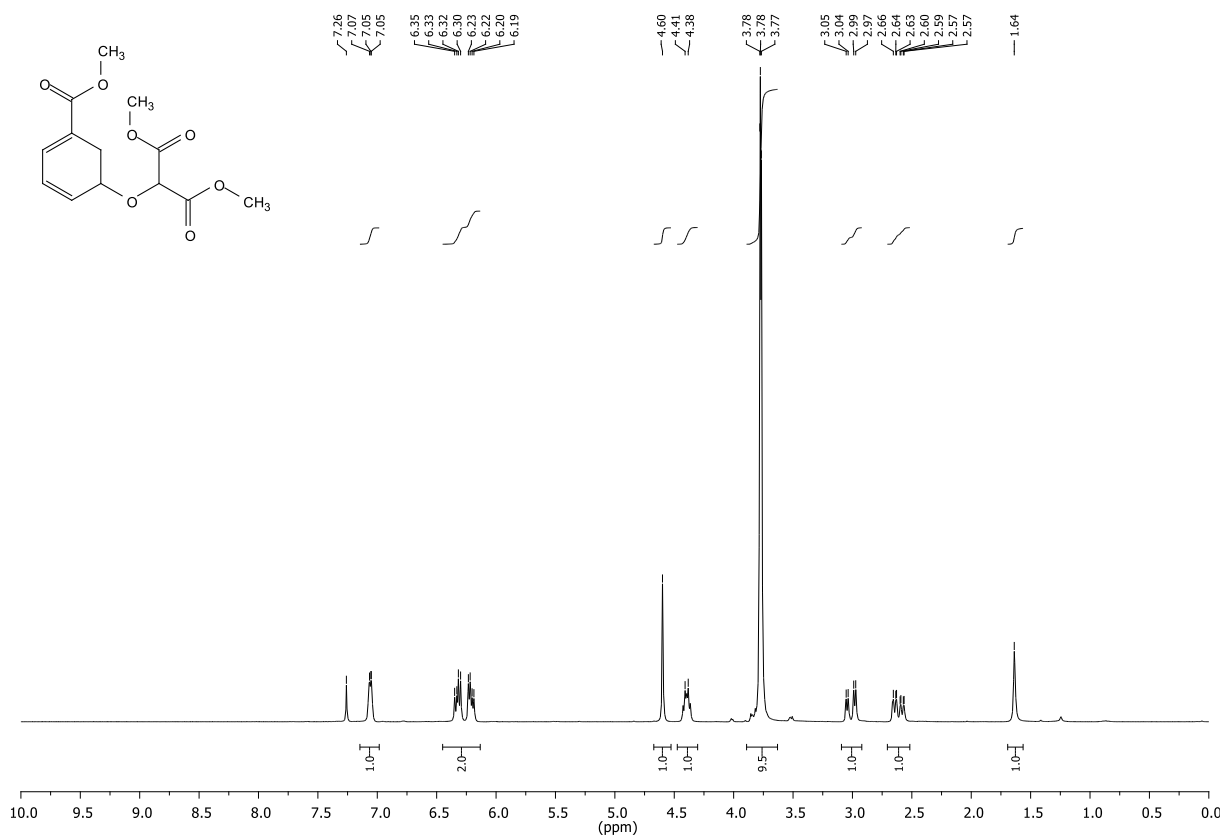


Figure 12.72: ¹H-NMR (300.36 MHz, CDCl₃) of compound 37.

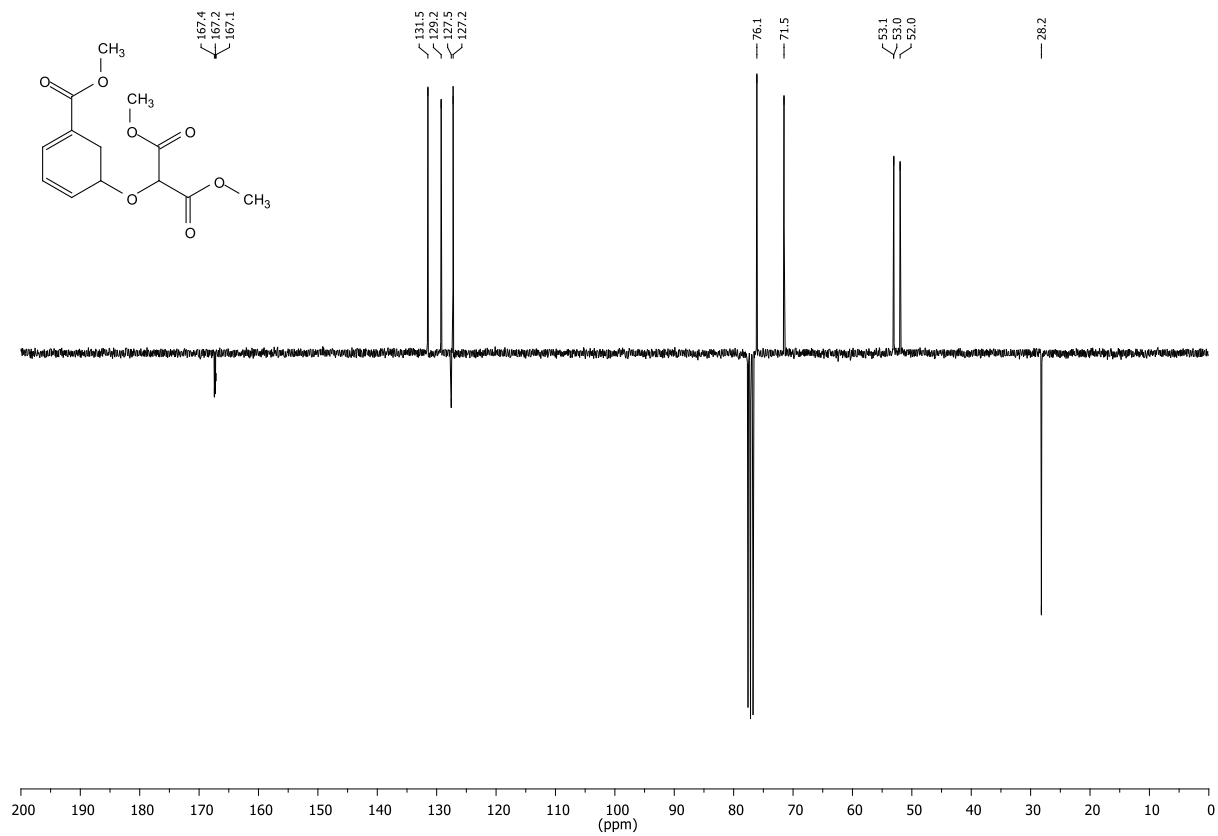


Figure 12.73: ¹³C-NMR,APT (75.53 MHz, CDCl₃) of compound 37.

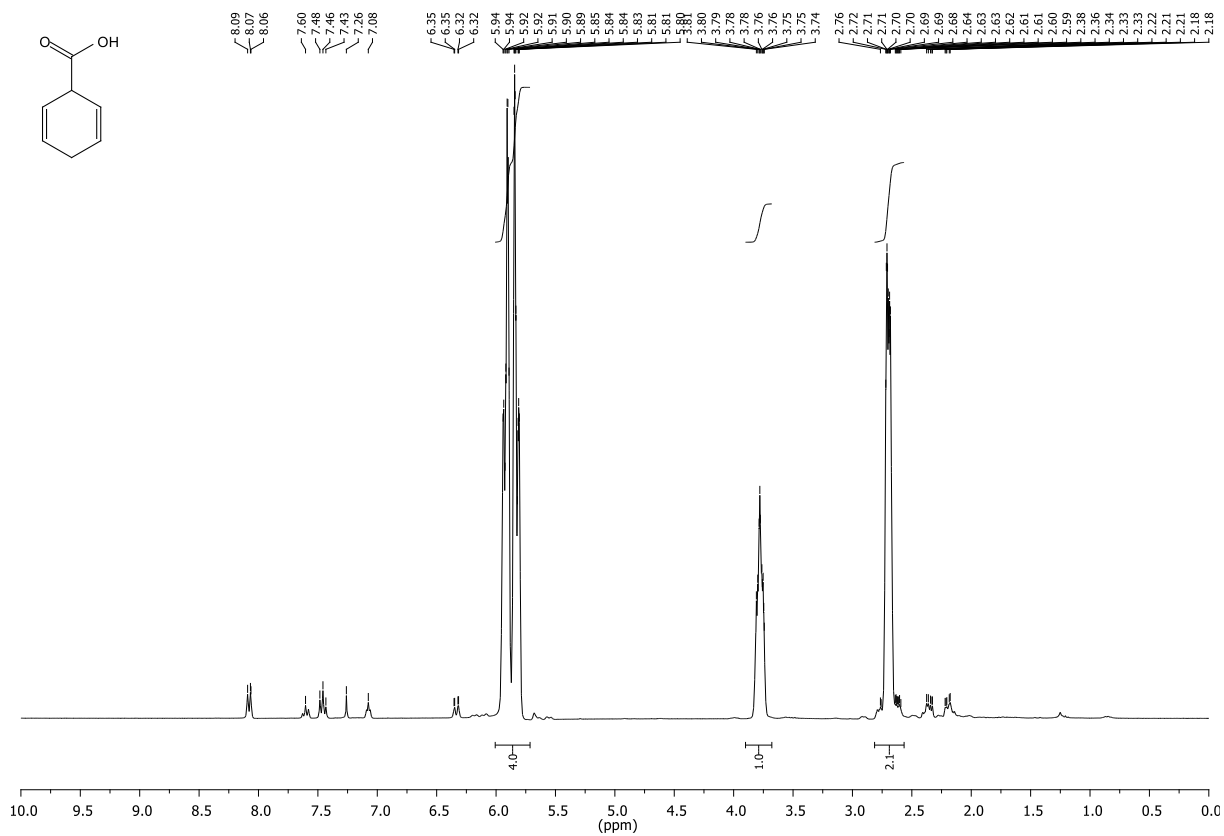


Figure 12.74: ¹H-NMR (300.36 MHz, CDCl₃) of compound 38.

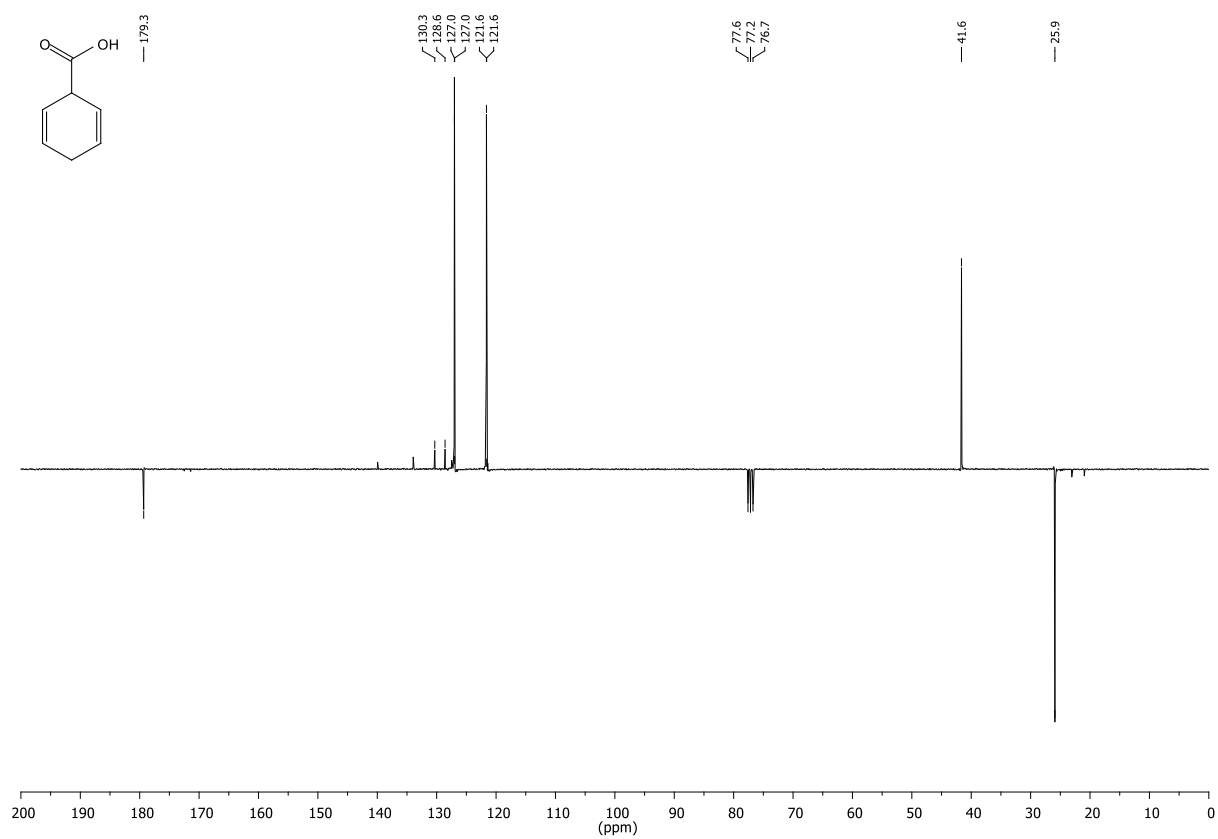


Figure 12.75: ¹³C-NMR,APT (75.53 MHz, CDCl₃) of compound 38.

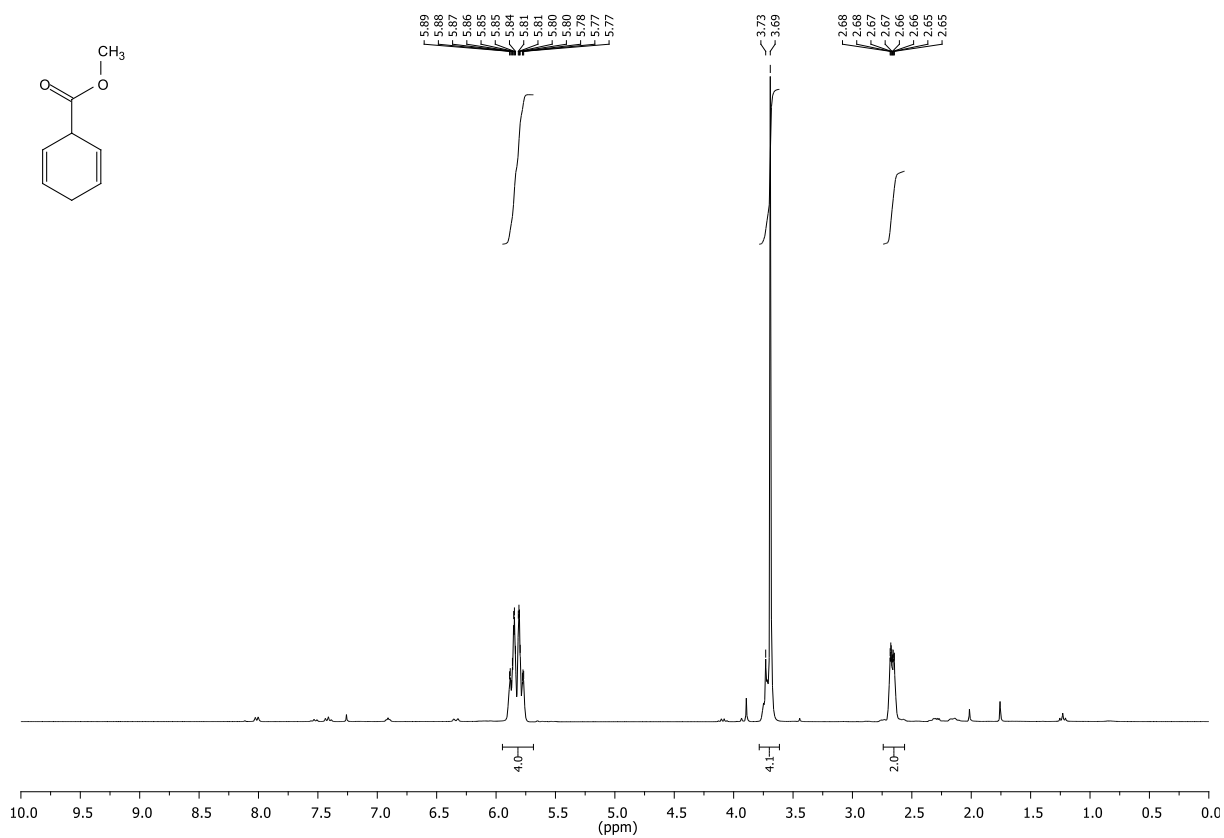


Figure 12.76: ¹H-NMR (300.36 MHz, CDCl₃) of compound 39.

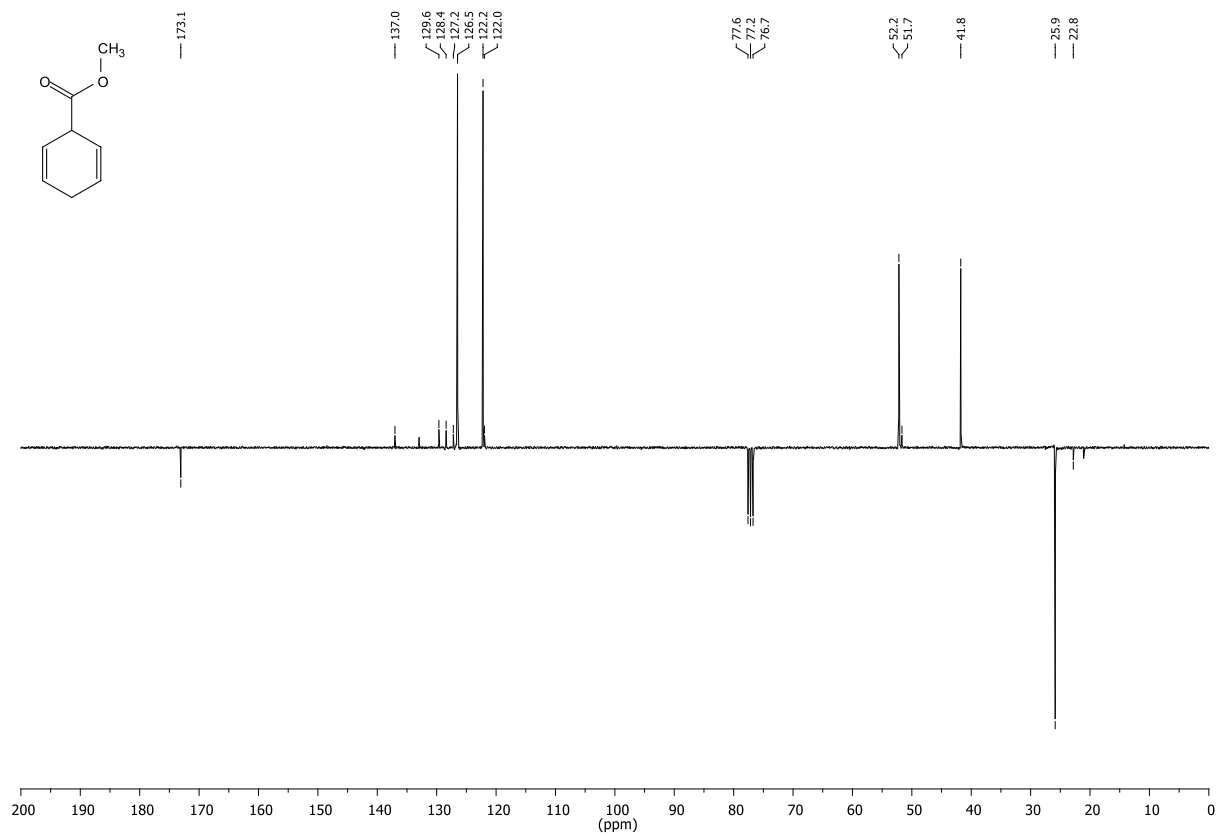


Figure 12.77: ¹³C-NMR,APT (75.53 MHz, CDCl₃) of compound 39.

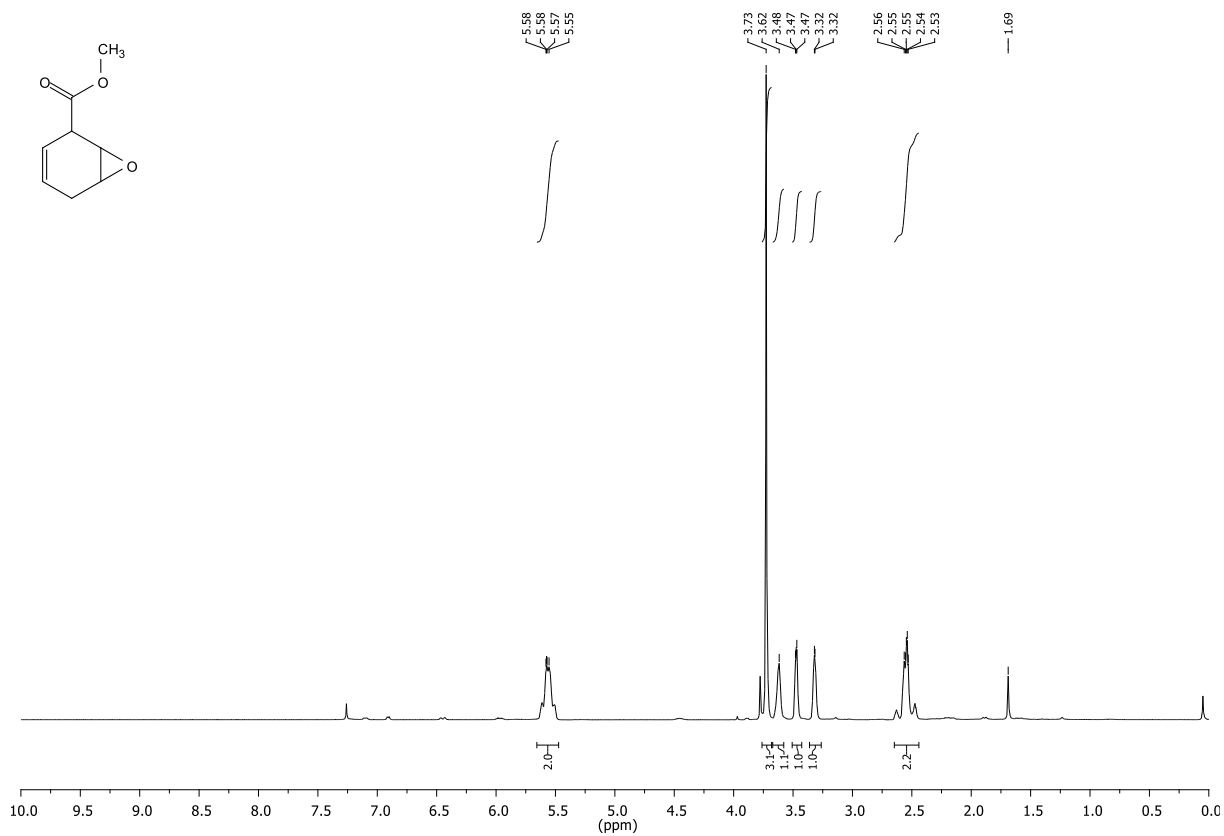


Figure 12.78: ¹H-NMR (300.36 MHz, CDCl₃) of compound 40.

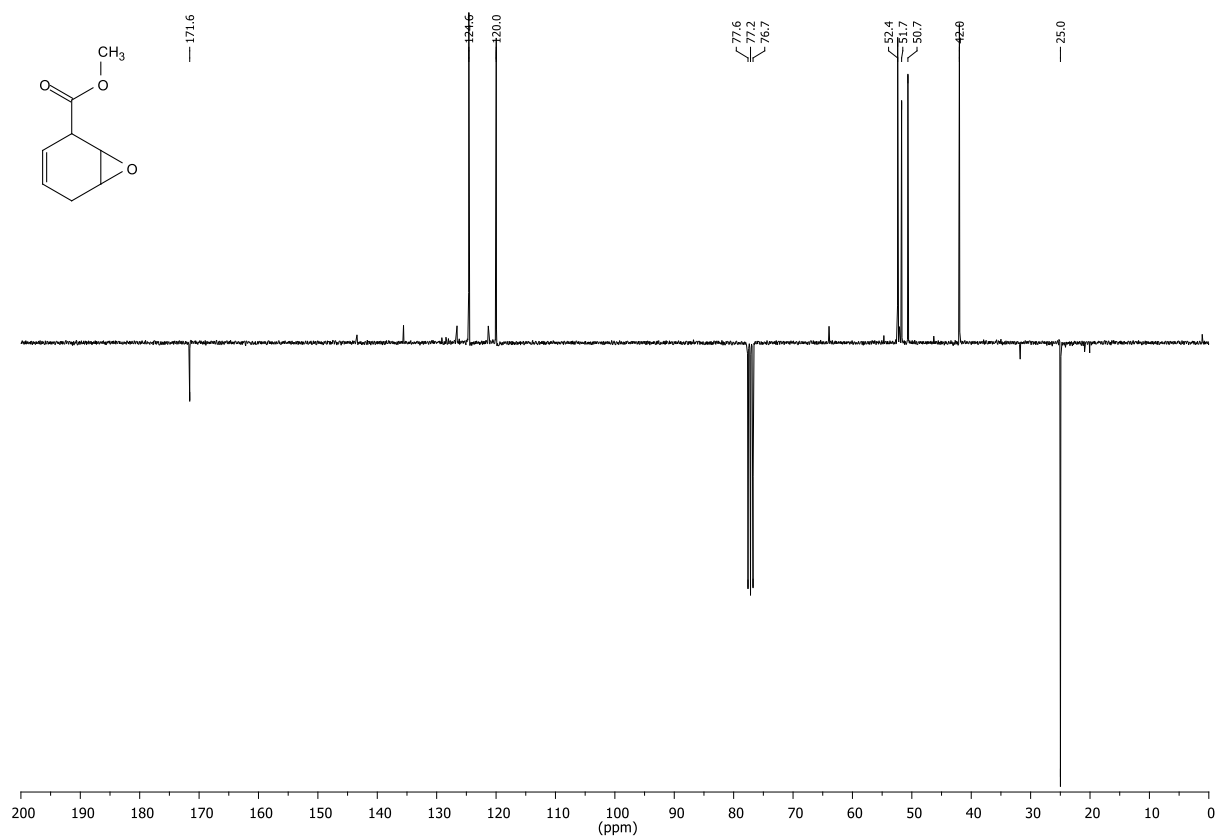


Figure 12.79: ¹³C-NMR,APT (75.53 MHz, CDCl₃) of compound 40.

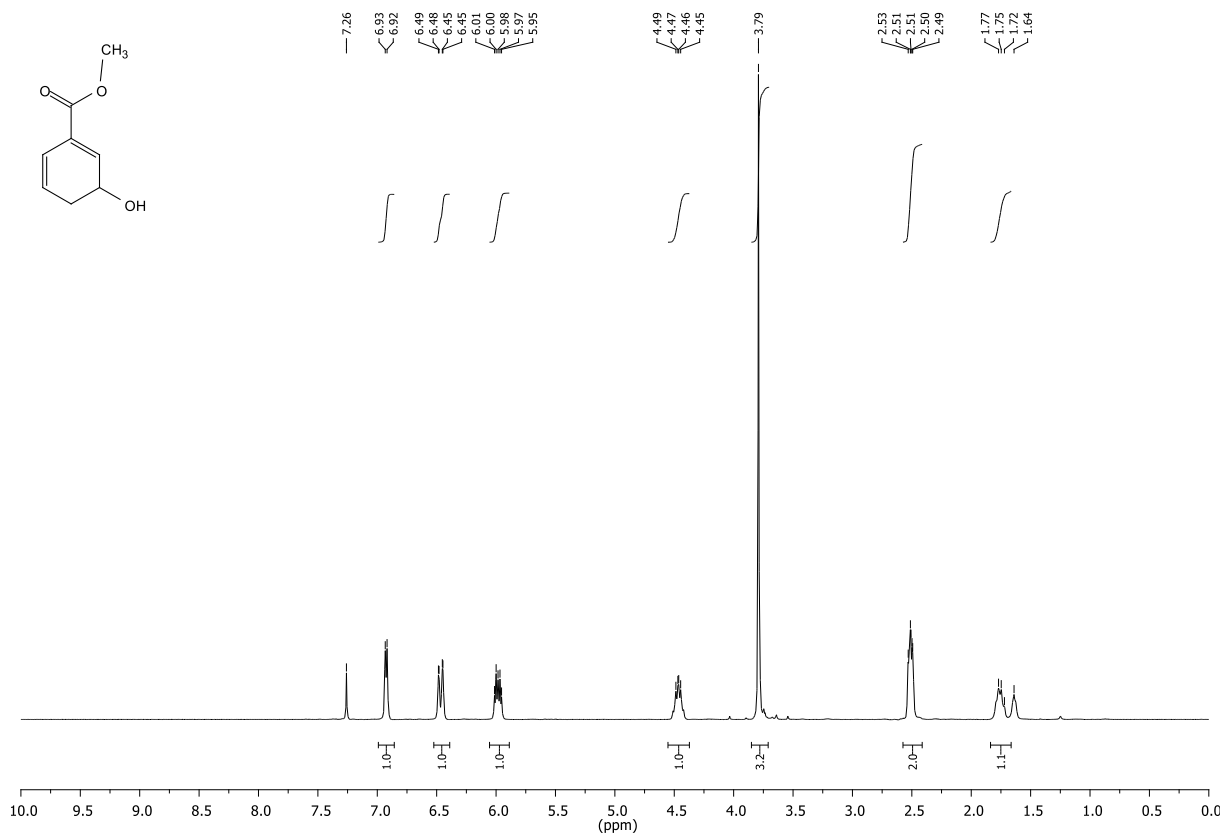


Figure 12.80: ¹H-NMR (300.36 MHz, CDCl₃) of compound 41.

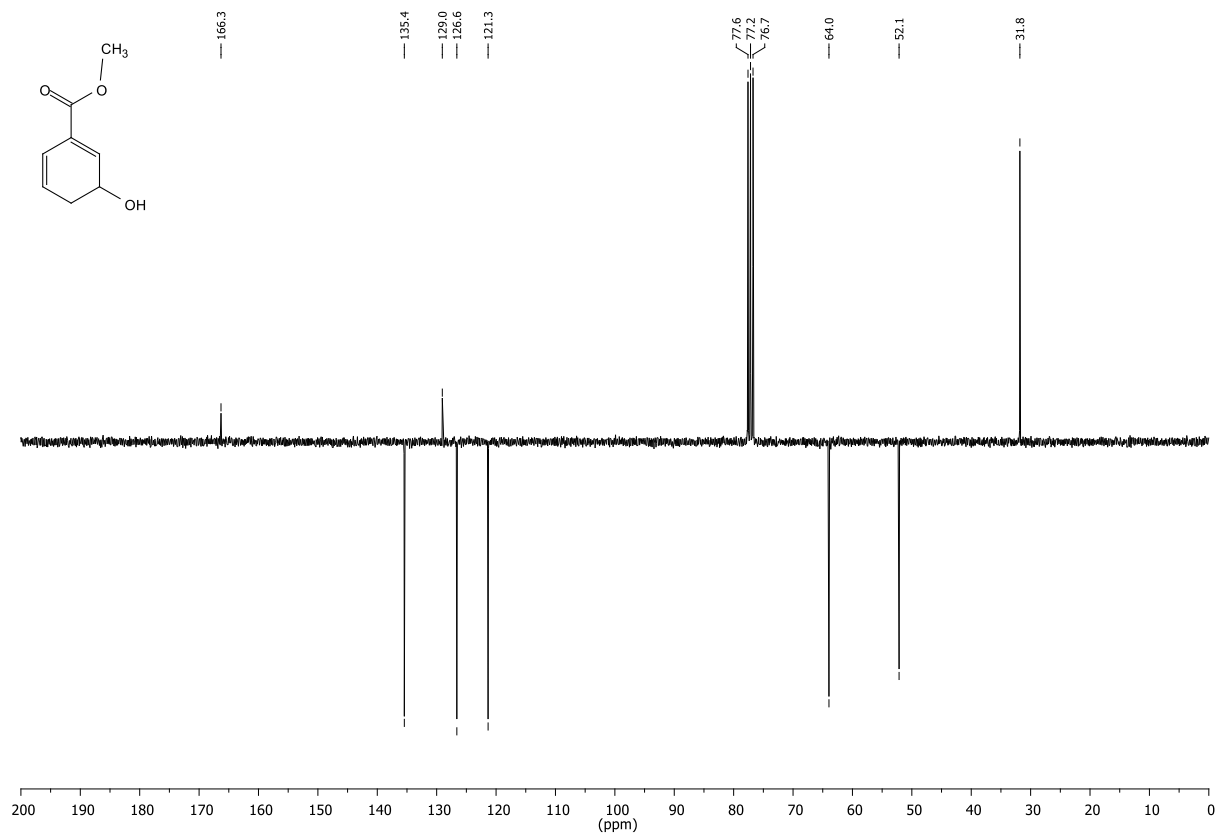


Figure 12.81: ¹³C-NMR,APT (75.53 MHz, CDCl₃) of compound 41.

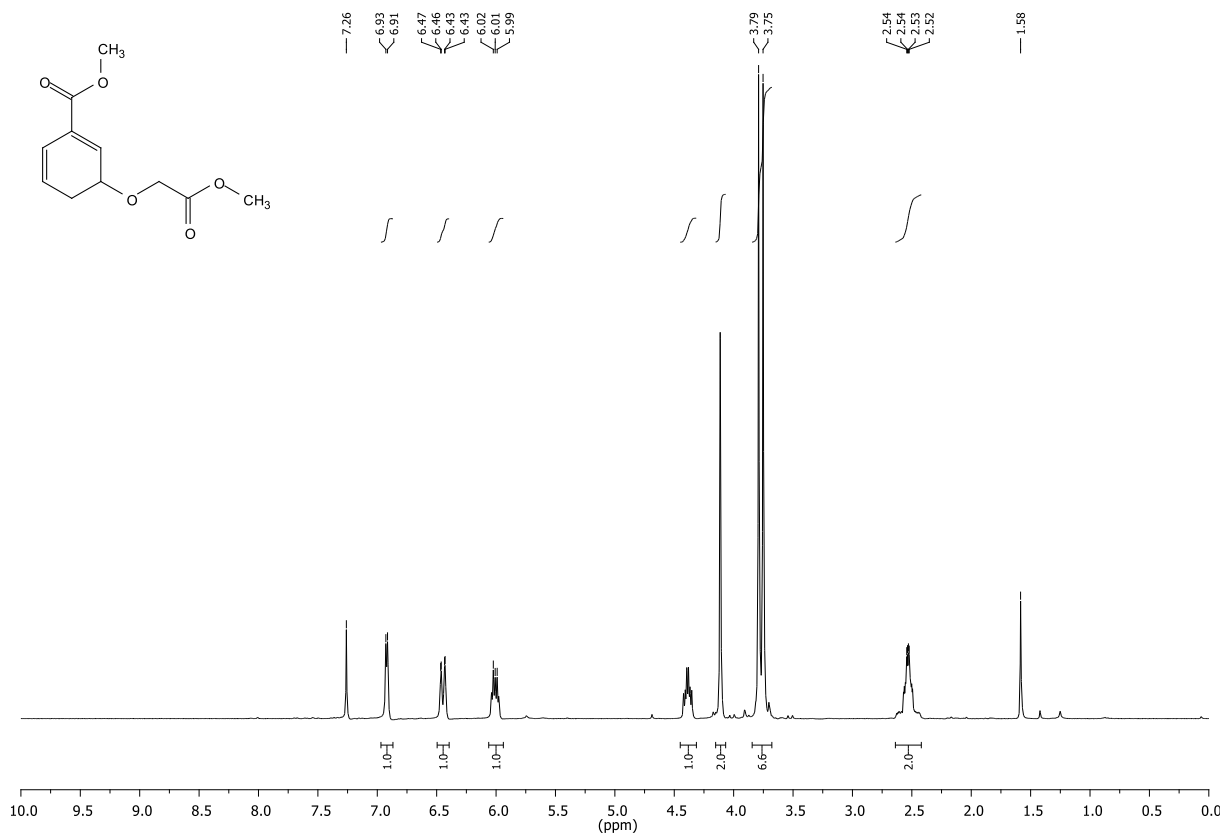


Figure 12.82: ¹H-NMR (300.36 MHz, CDCl₃) of compound 42.

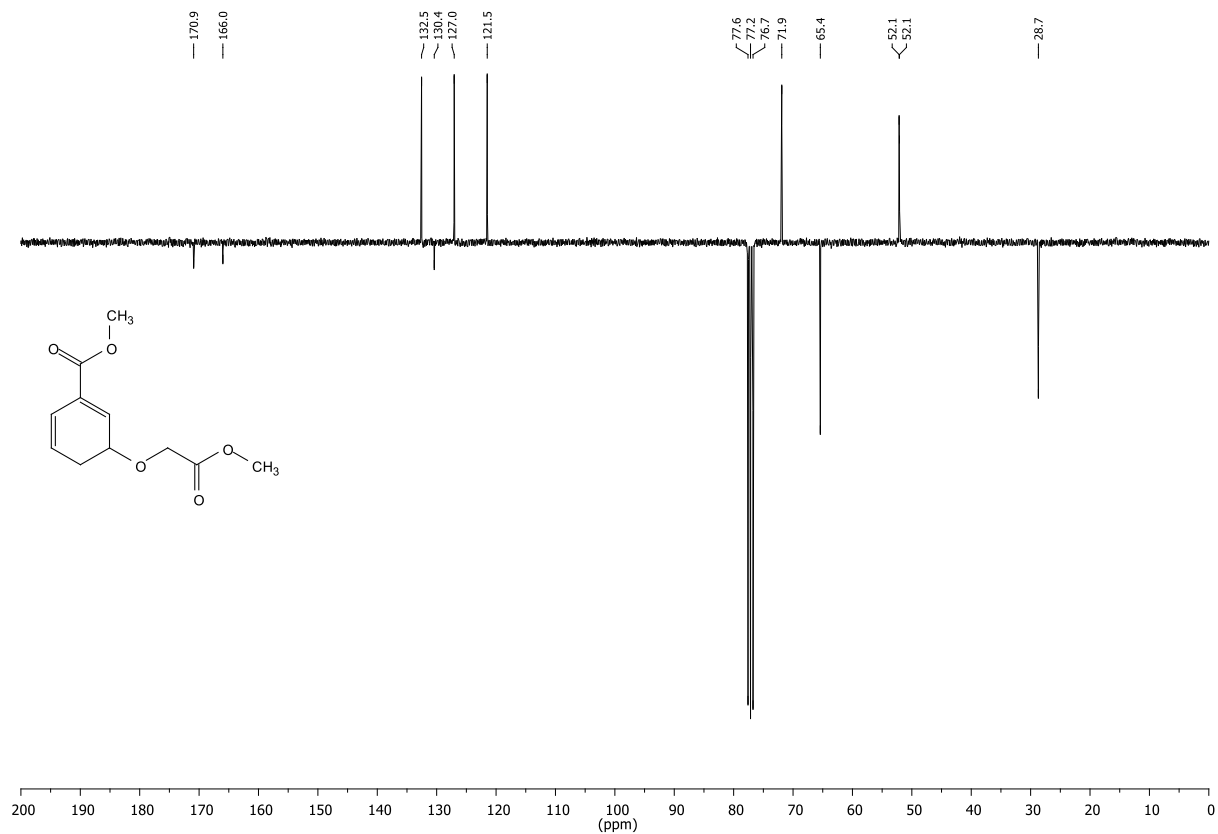


Figure 12.83: ¹³C-NMR,APT (75.53 MHz, CDCl₃) of compound 42.

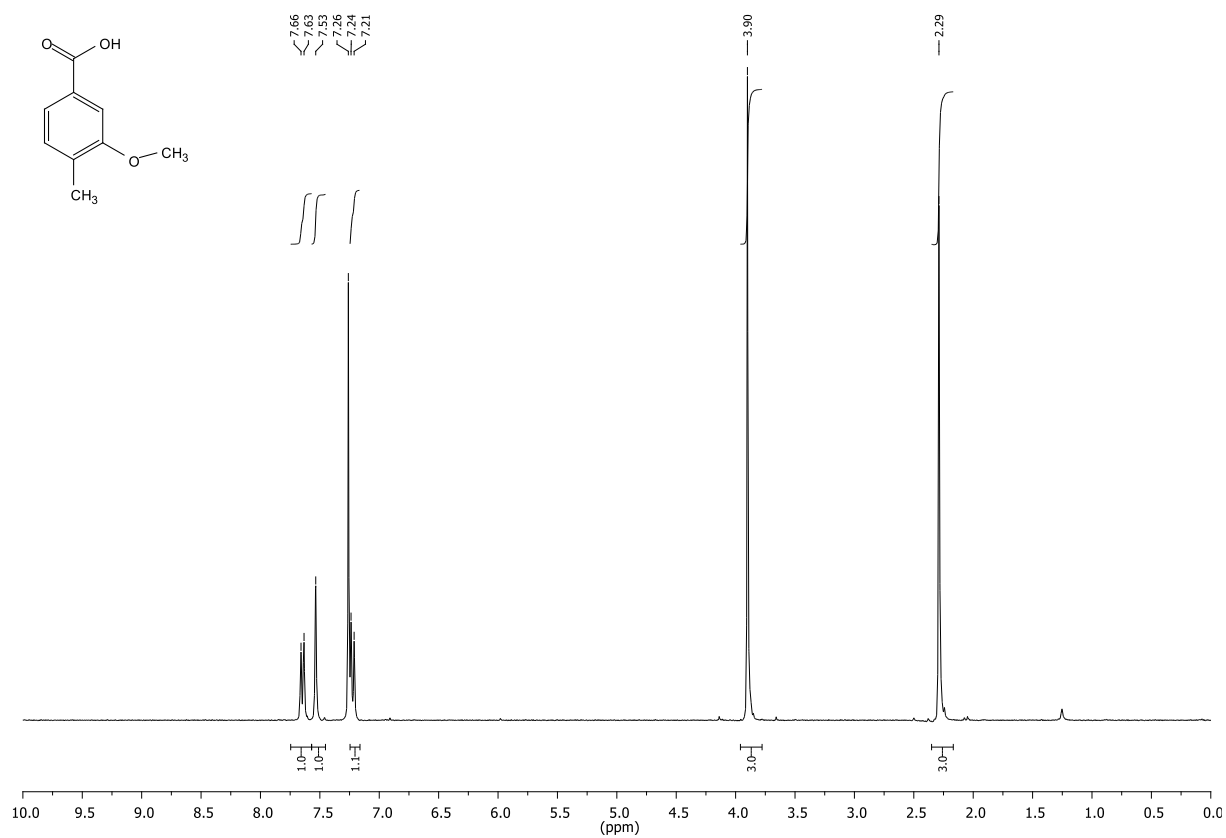


Figure 12.84: ¹H-NMR (300.36 MHz, CDCl₃) of compound 43.

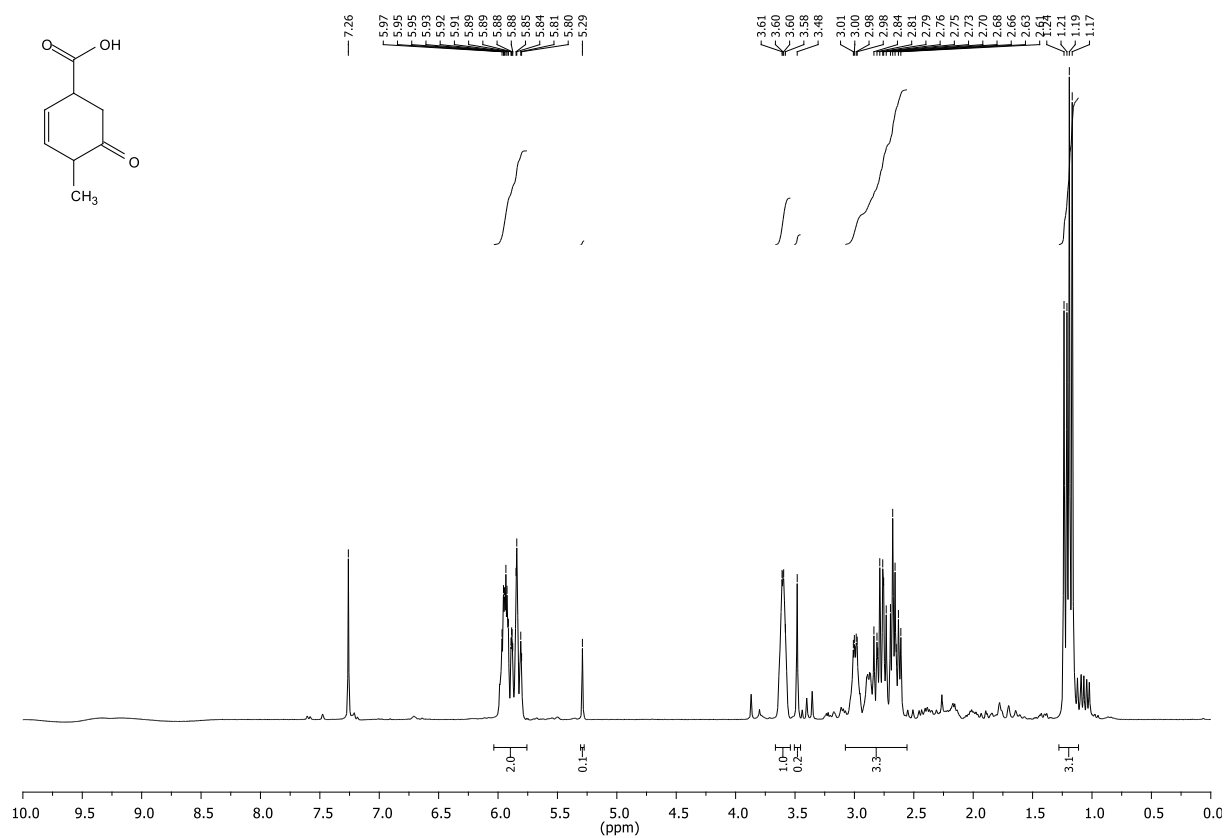


Figure 12.85: ¹H-NMR (300.36 MHz, CDCl₃) of compound 44, small test batch

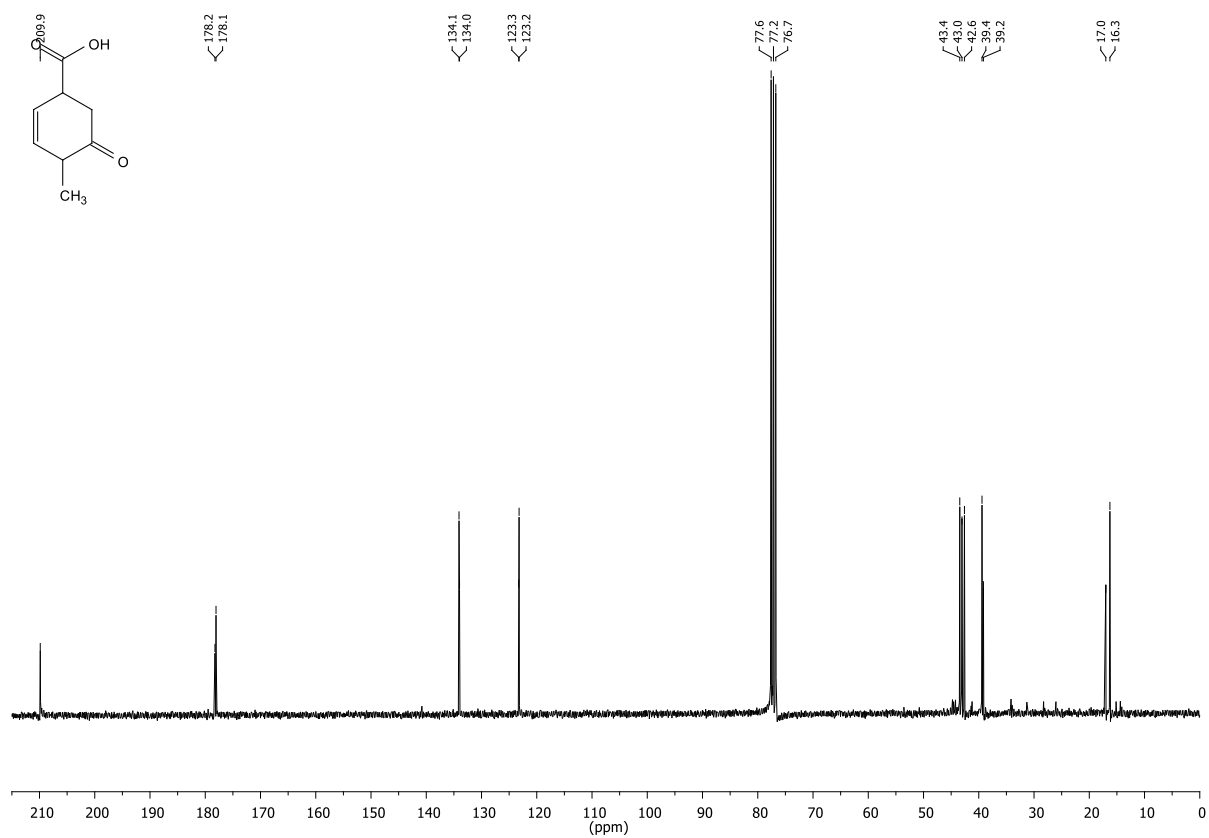


Figure 12.86 $^{13}\text{C-NMR}$ (75.53 MHz, CDCl_3) of compound **44**, small test batch

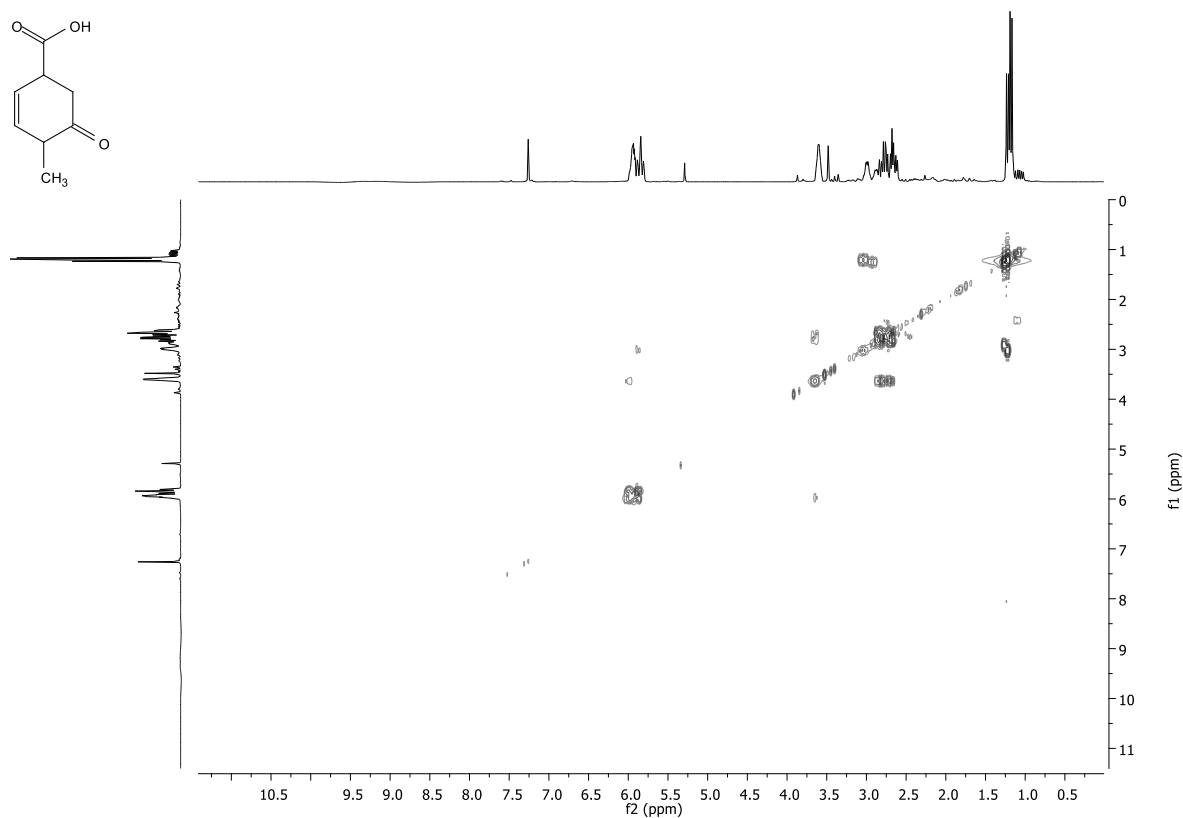


Figure 12.87: COSY-NMR (CDCl_3) of compound **44**, small test batch

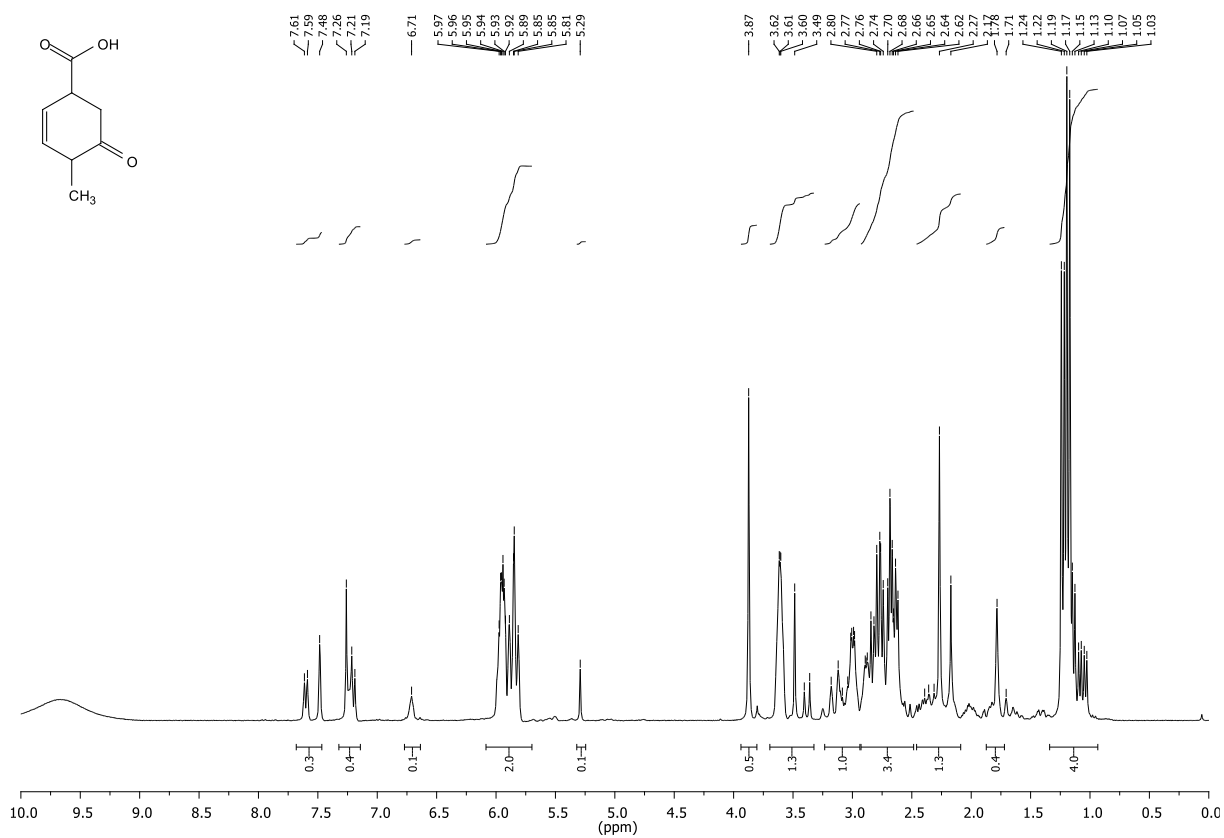


Figure 12.88: ¹H-NMR (300.36 MHz, CDCl₃) of compound 44, big batch, batch 1, impure

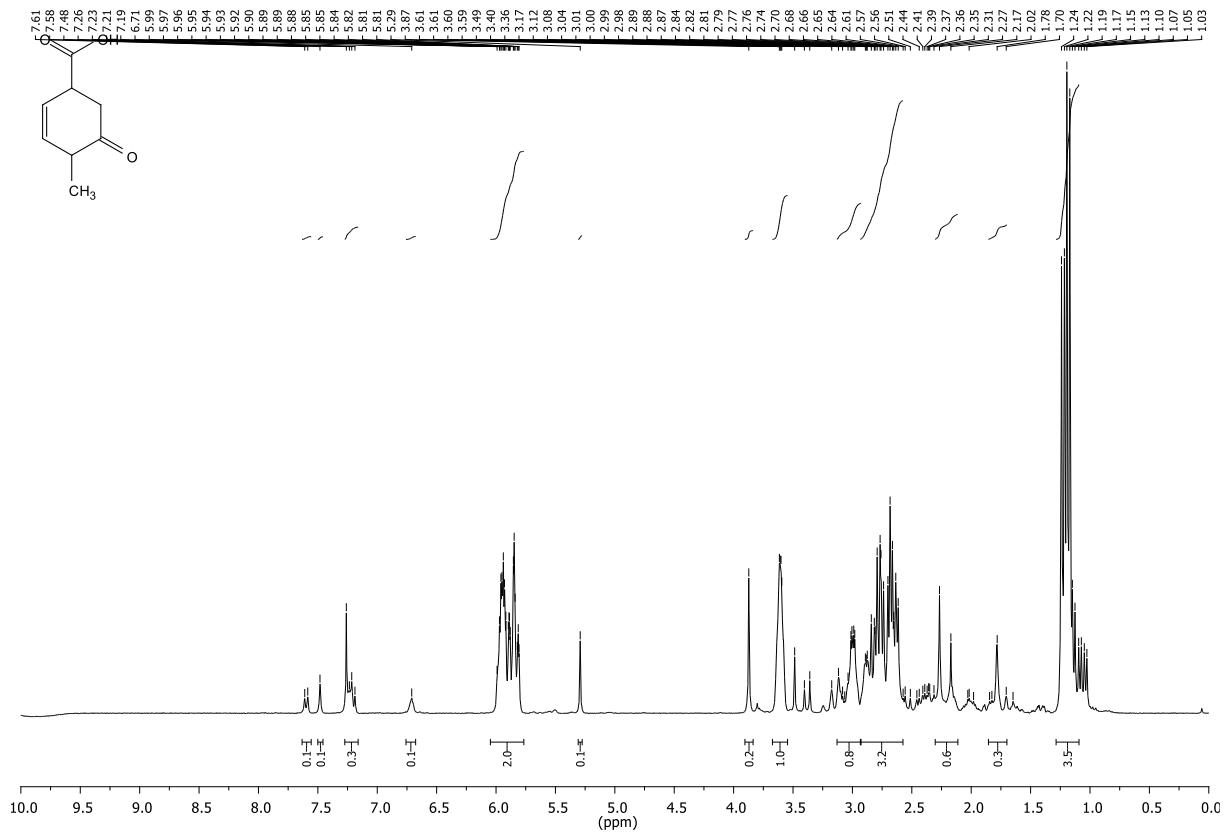


Figure 12.89: ¹H-NMR (300.36 MHz, CDCl₃) of compound 44, big batch, batch 2, impure

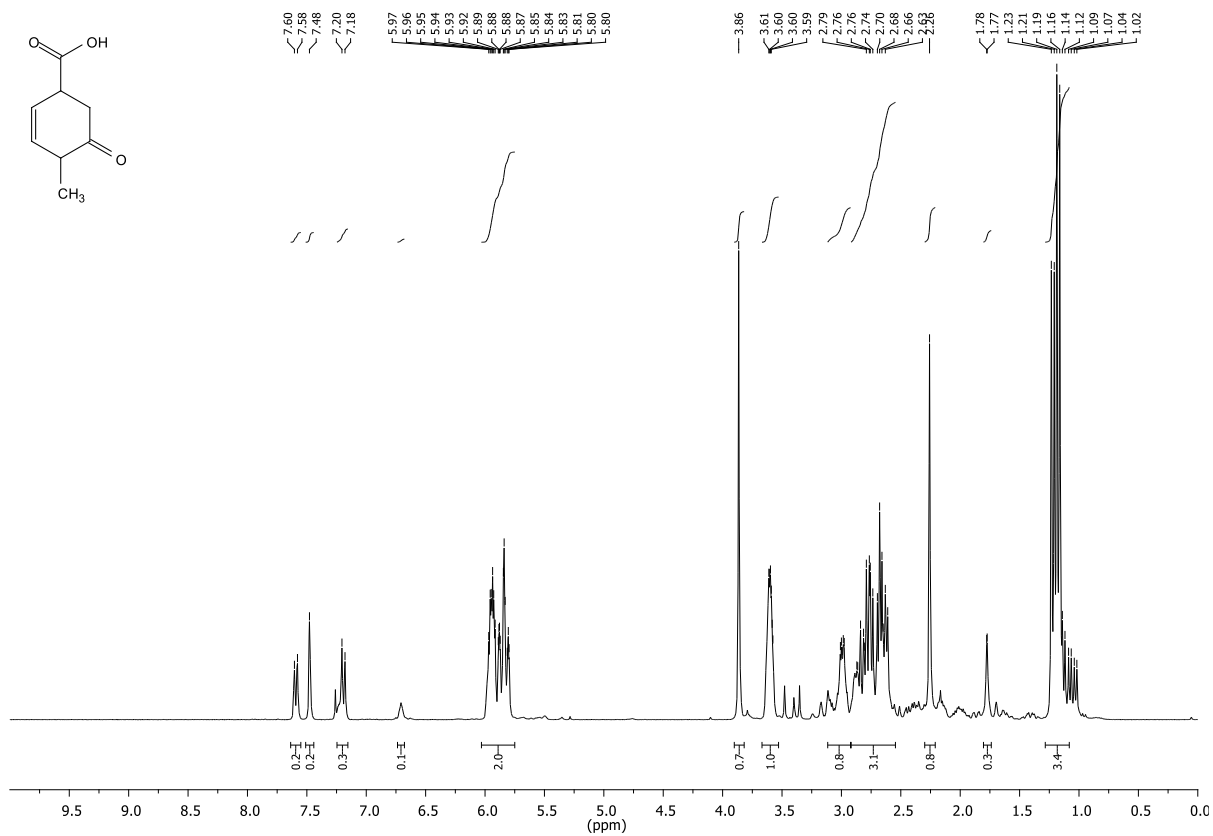


Figure 12.90: ¹H-NMR (300.36 MHz, CDCl₃) of compound 44, big batch, batch 3, impure

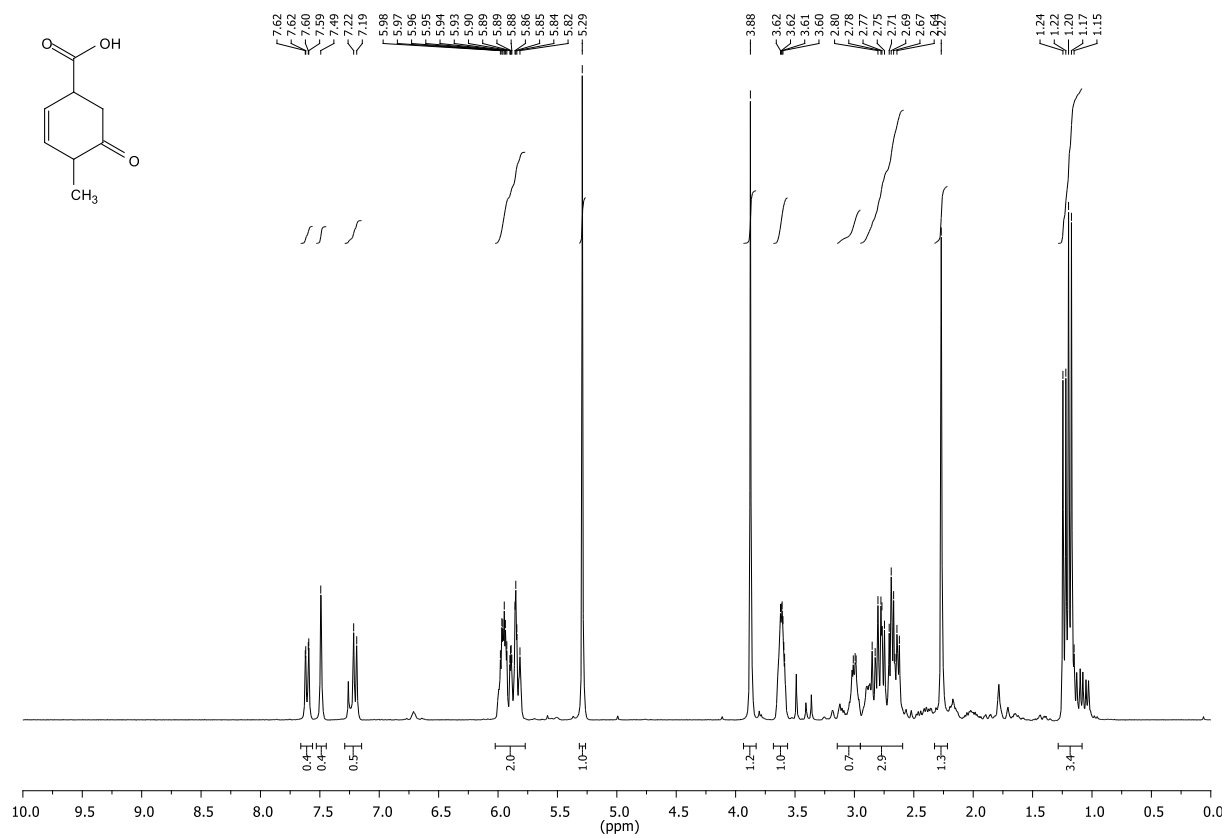


Figure 12.91: ¹H-NMR (300.36 MHz, CDCl₃) of compound 44, big batch, batch 4, impure

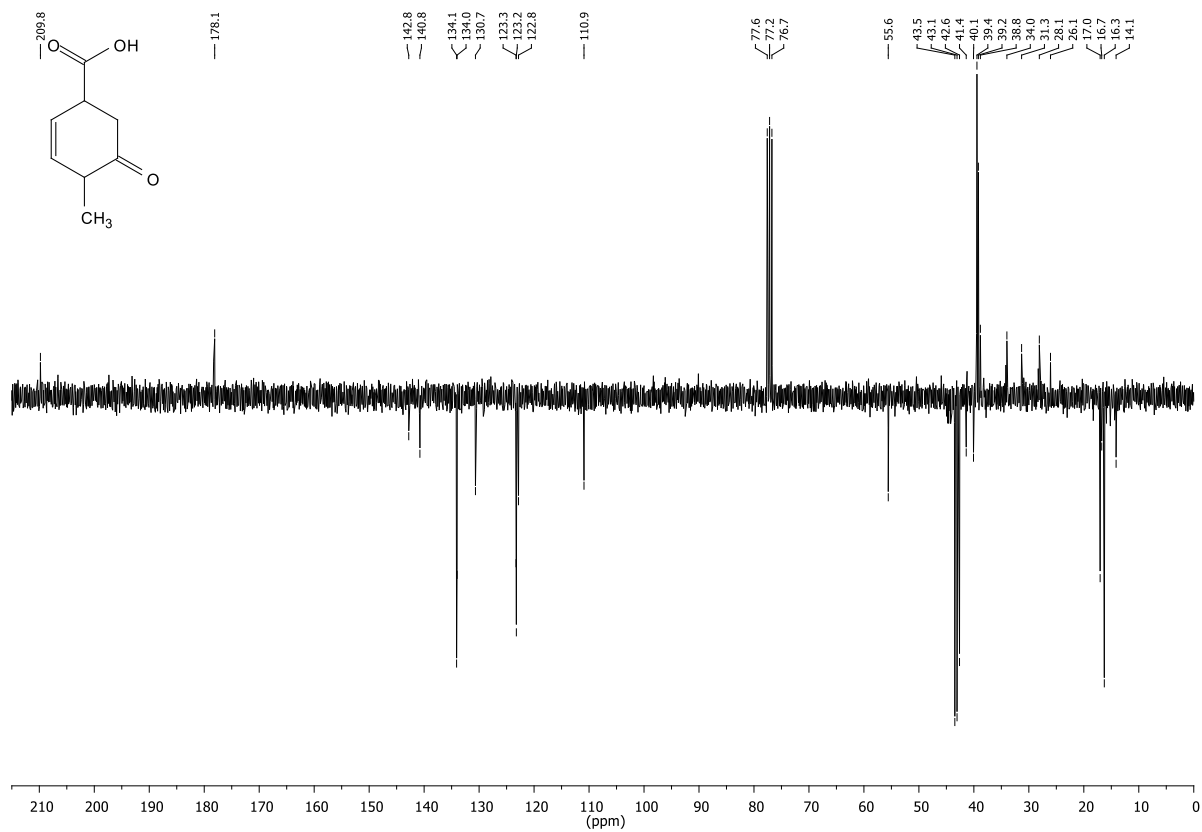


Figure 12.92: ¹³C-NMR,APT (75.53 MHz, CDCl₃) of compound 44, big batch, batch 1, impure

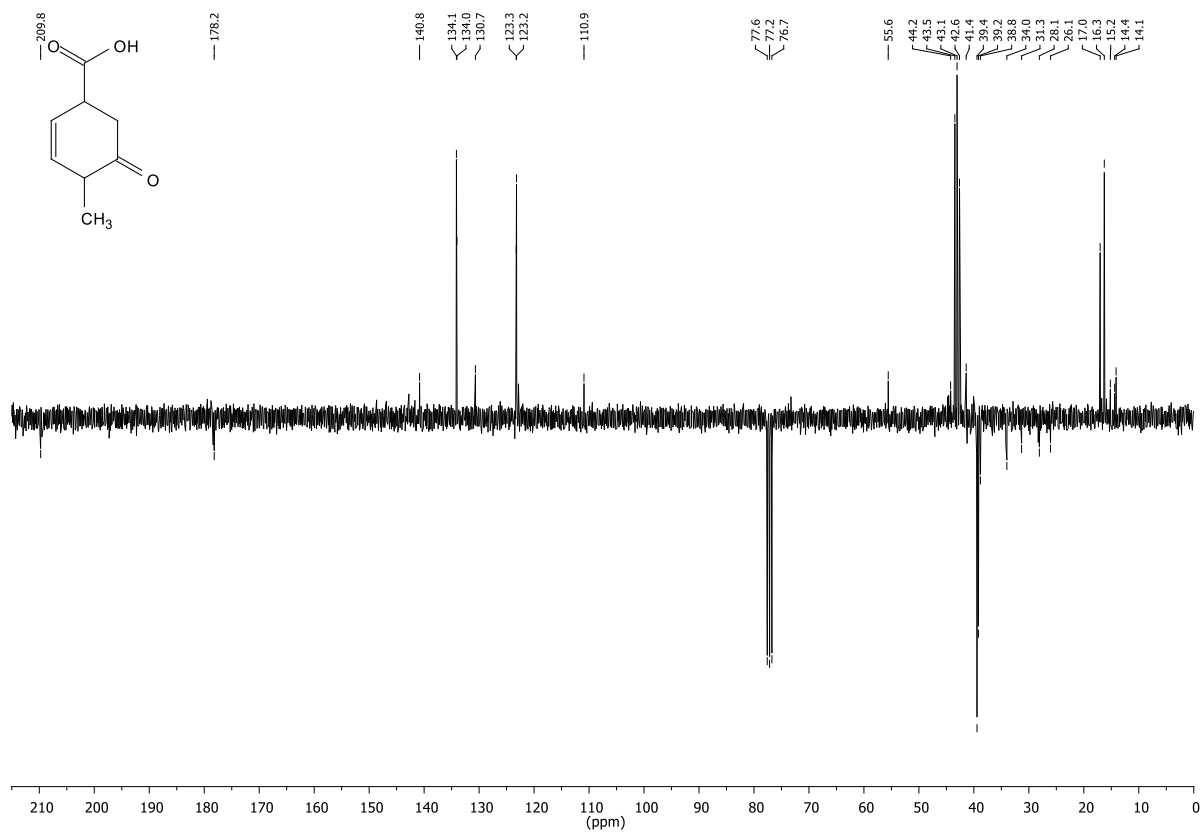


Figure 12.93: ¹³C-NMR,APT (75.53 MHz, CDCl₃) of compound 44, big batch, batch 2, impure

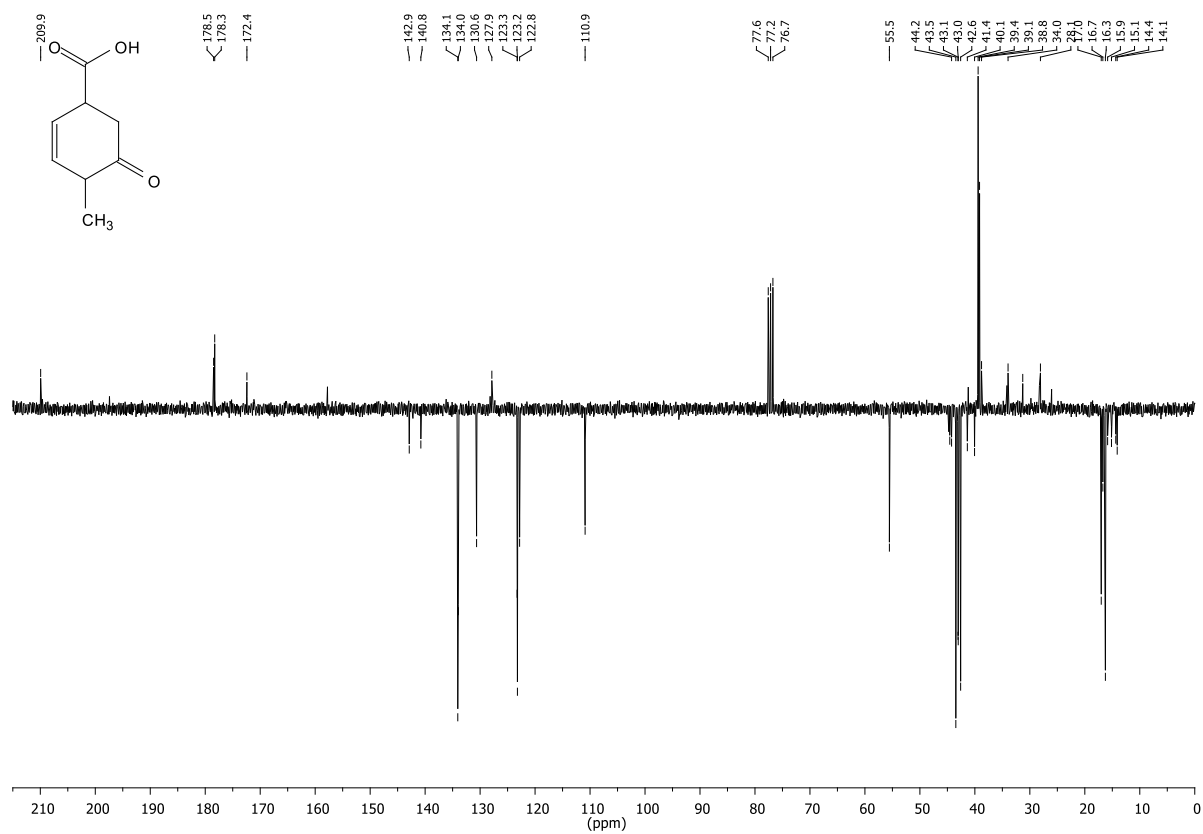


Figure 12.94: ¹³C-NMR,APT (75.53 MHz, CDCl₃) of compound 44, big batch, batch 3, impure

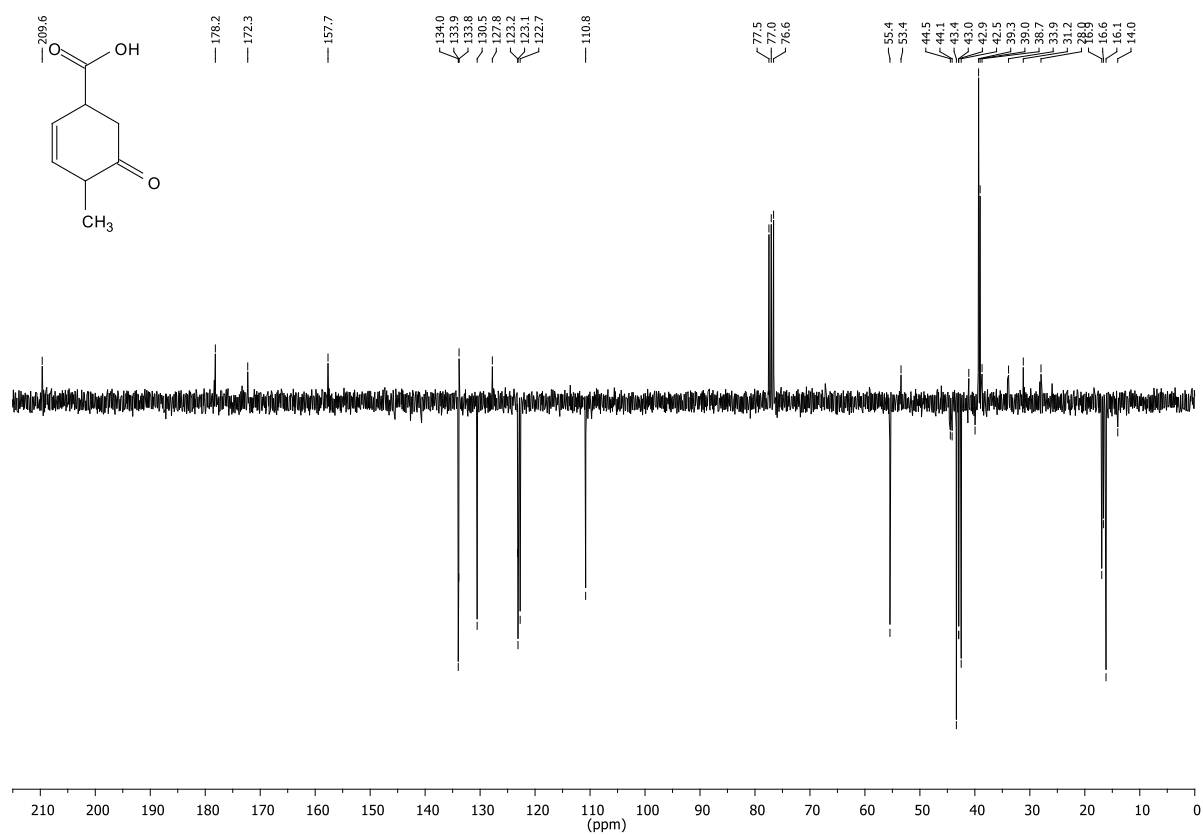


Figure 12.95: ¹³C-NMR,APT (75.53 MHz, CDCl₃) of compound 44, big batch, batch 4, impure

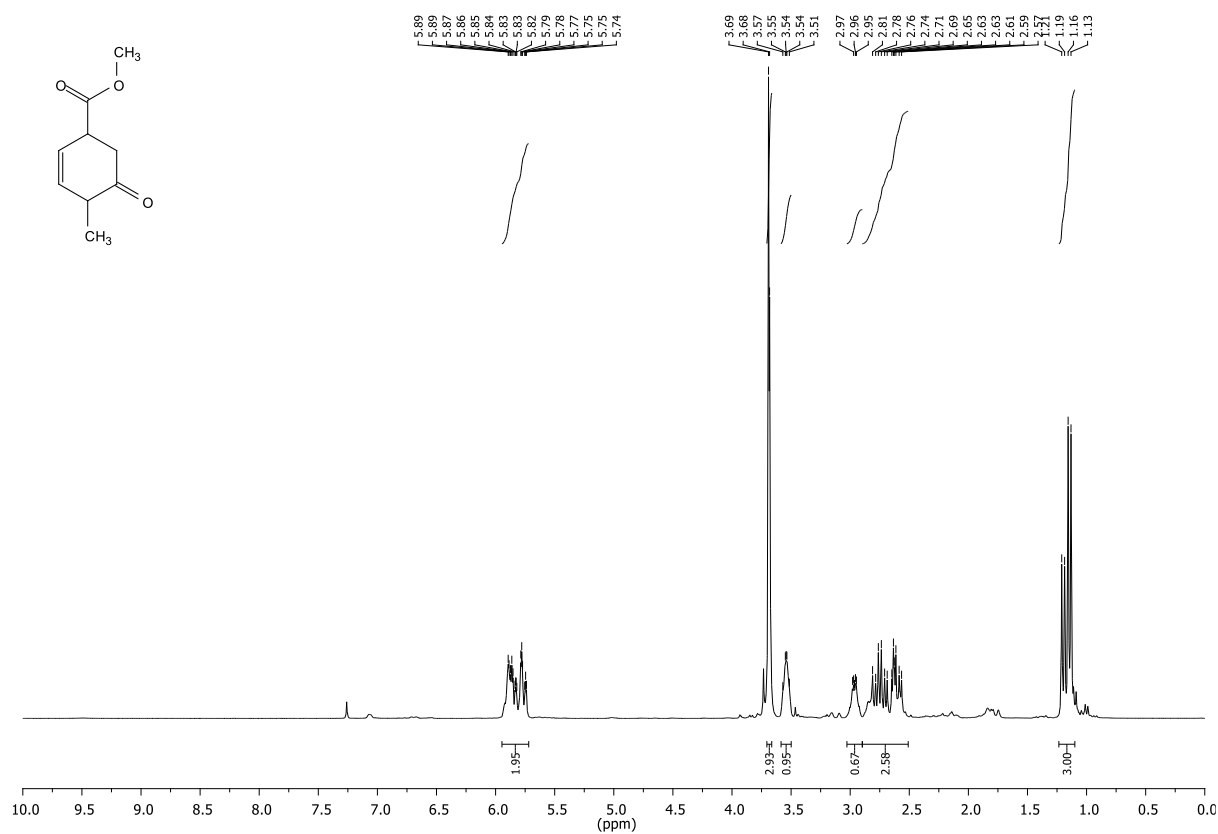


Figure 12.96: ¹H-NMR (300.36 MHz, CDCl₃) of compound 45, reisolated starting material from Luche-reduction and additional purification

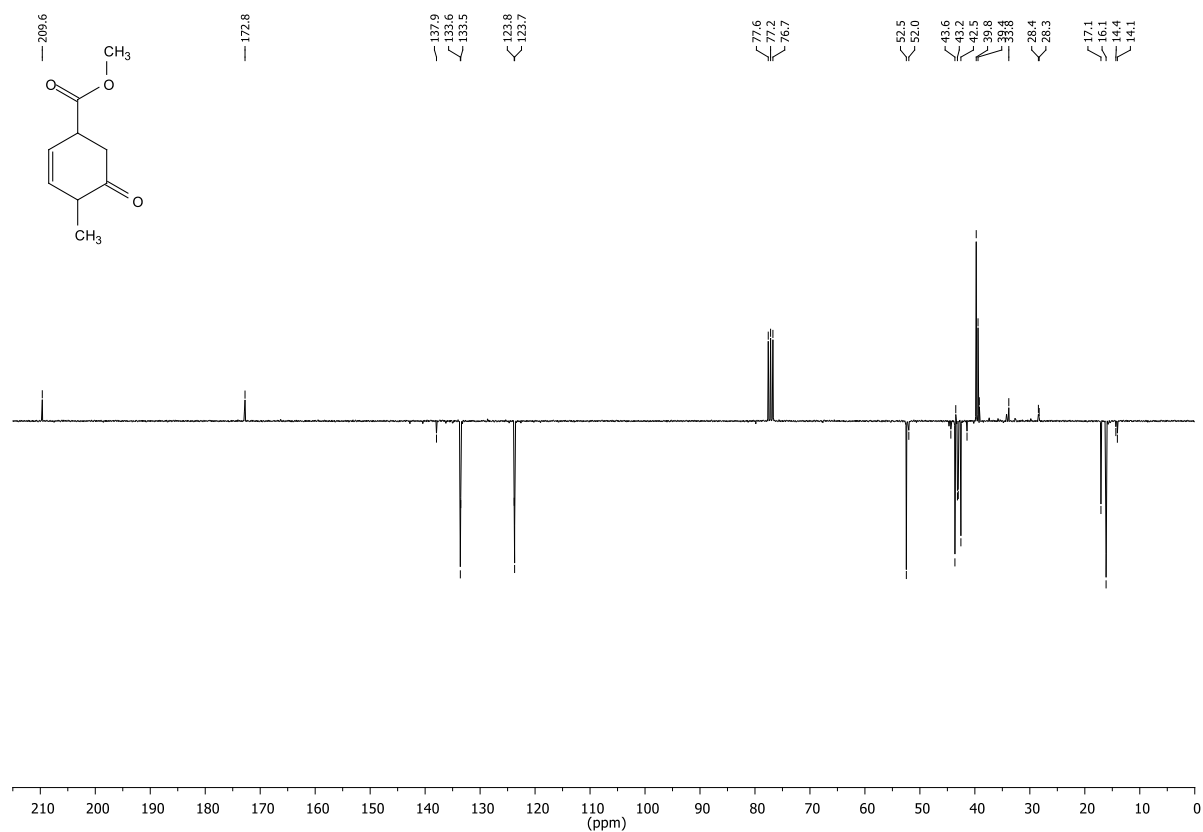


Figure 12.97: ¹³C-NMR,APT (75.53 MHz, CDCl₃) of compound 45, reisolated starting material from Luche-reduction and additional purification

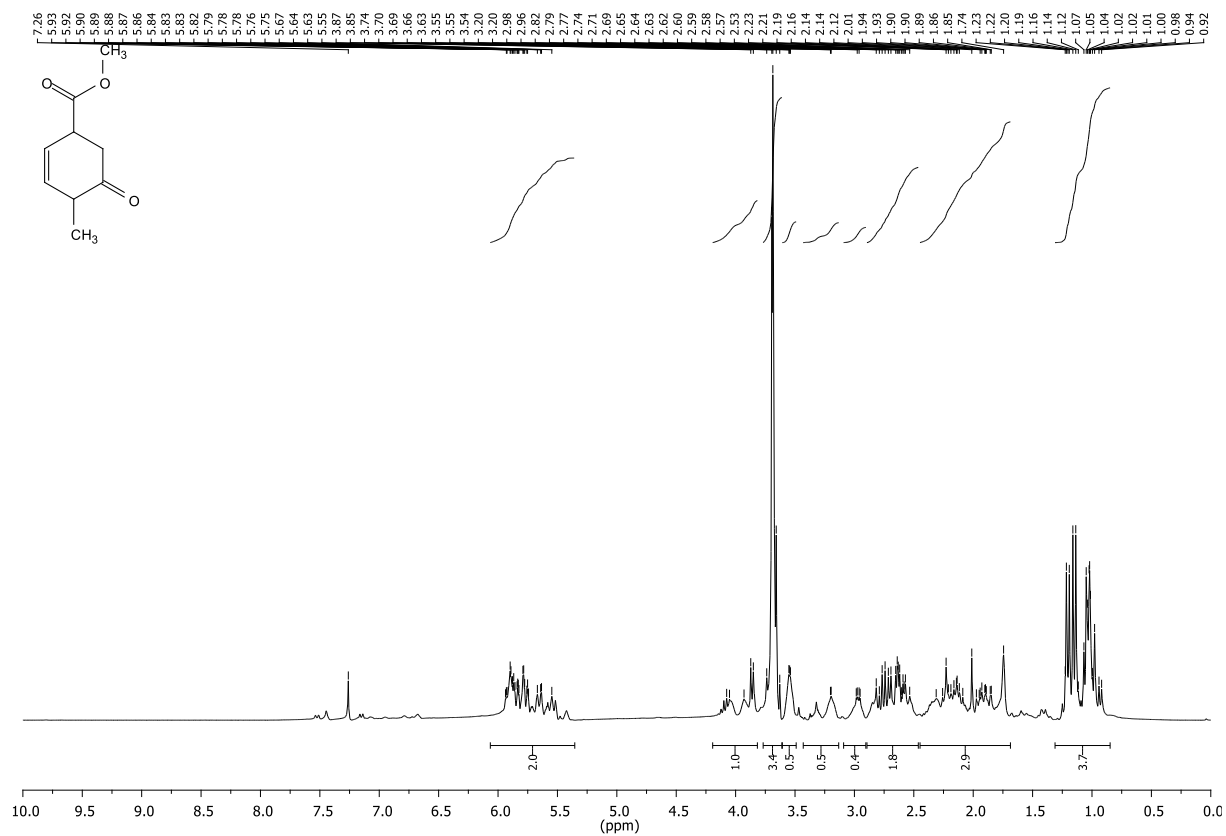


Figure 12.98: ¹H-NMR(300.36 MHz, CDCl₃) of compound **45**, reisolated starting material from Luche-reduction, impure.

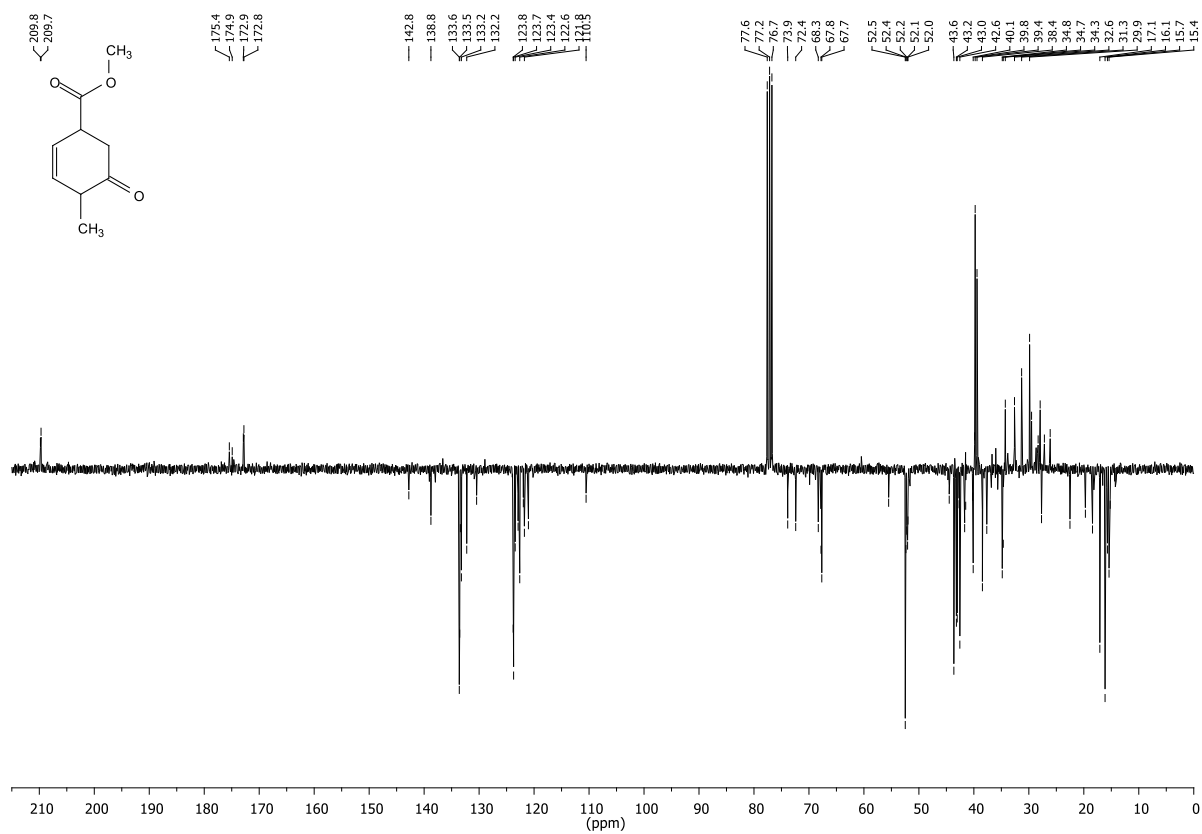


Figure 12.99: ¹³C-NMR,APT (75.53 MHz, CDCl₃) of compound **45**, reisolated starting material from Luche-reduction, impure.

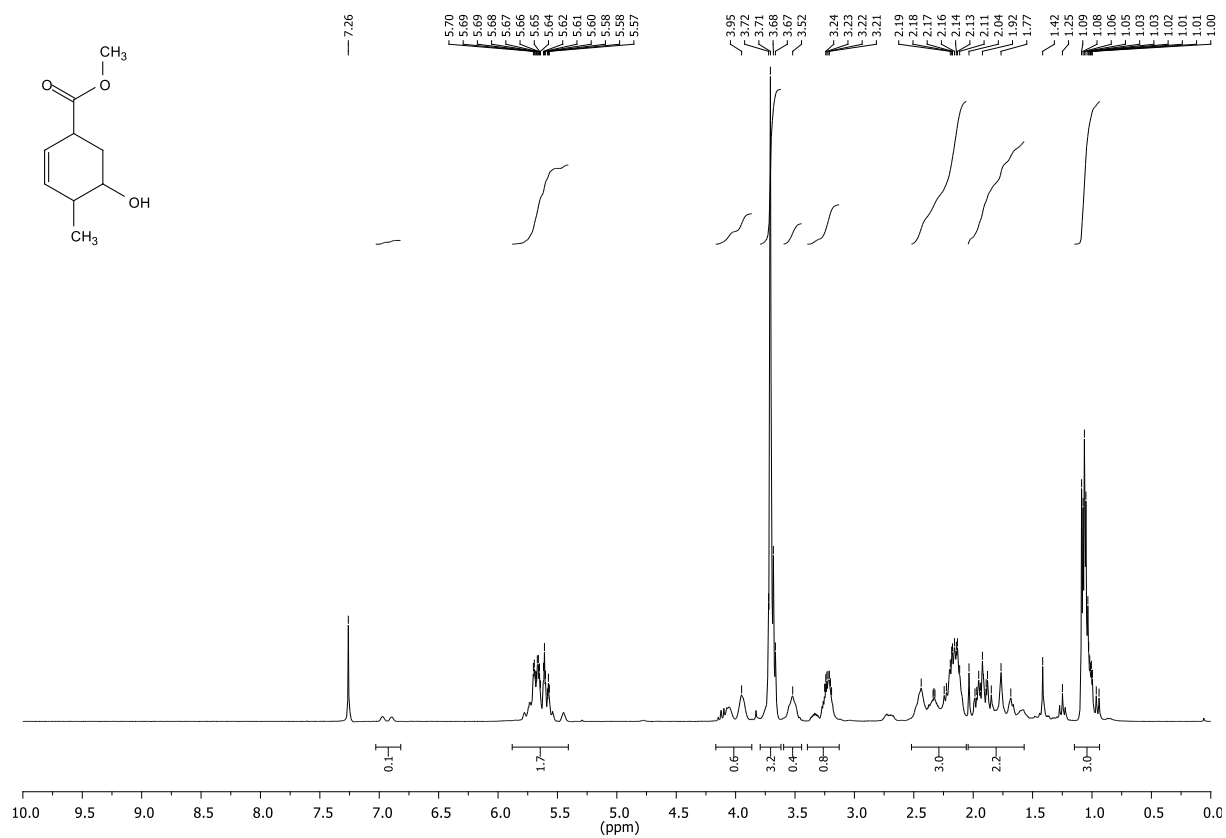


Figure 12.100: $^1\text{H-NMR}$ (300.36 MHz, CDCl_3) of compound **46**, impure

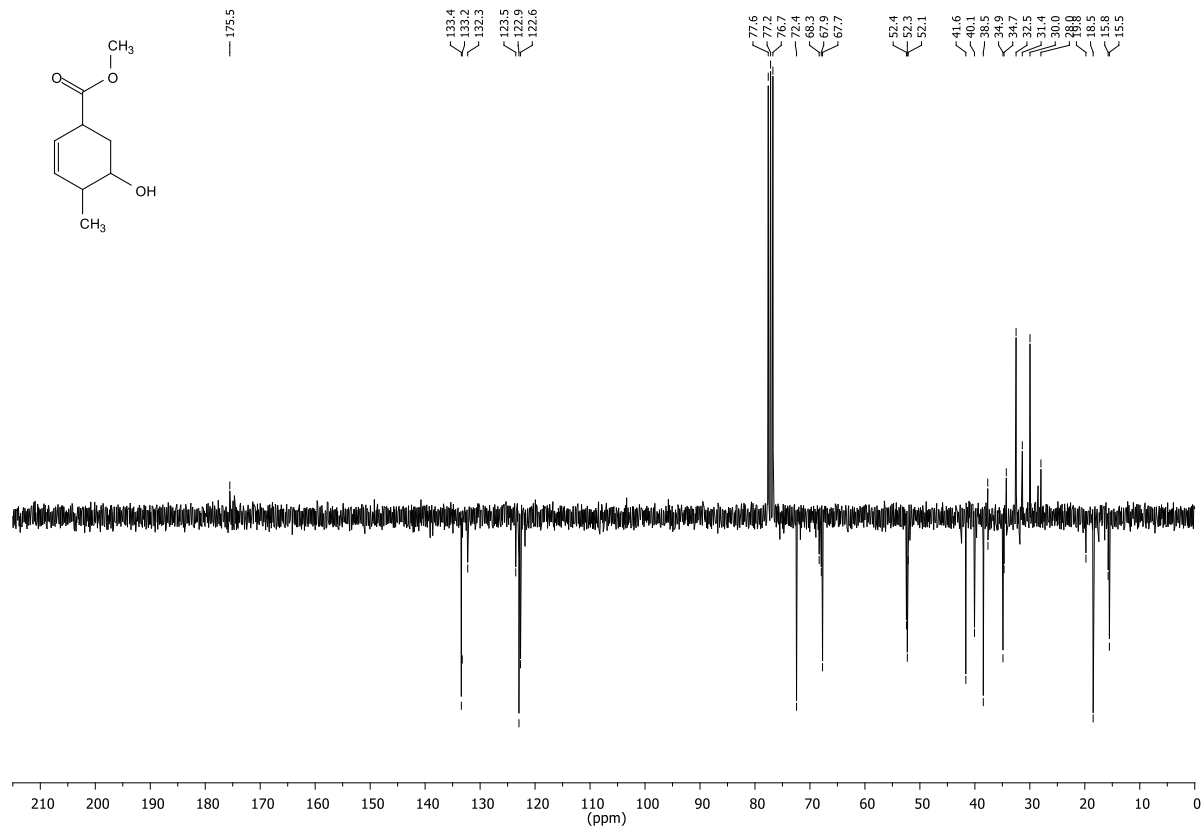


Figure 12.101: $^{13}\text{C-NMR}$,APT (75.53 MHz, CDCl_3) of compound **46**, impure.

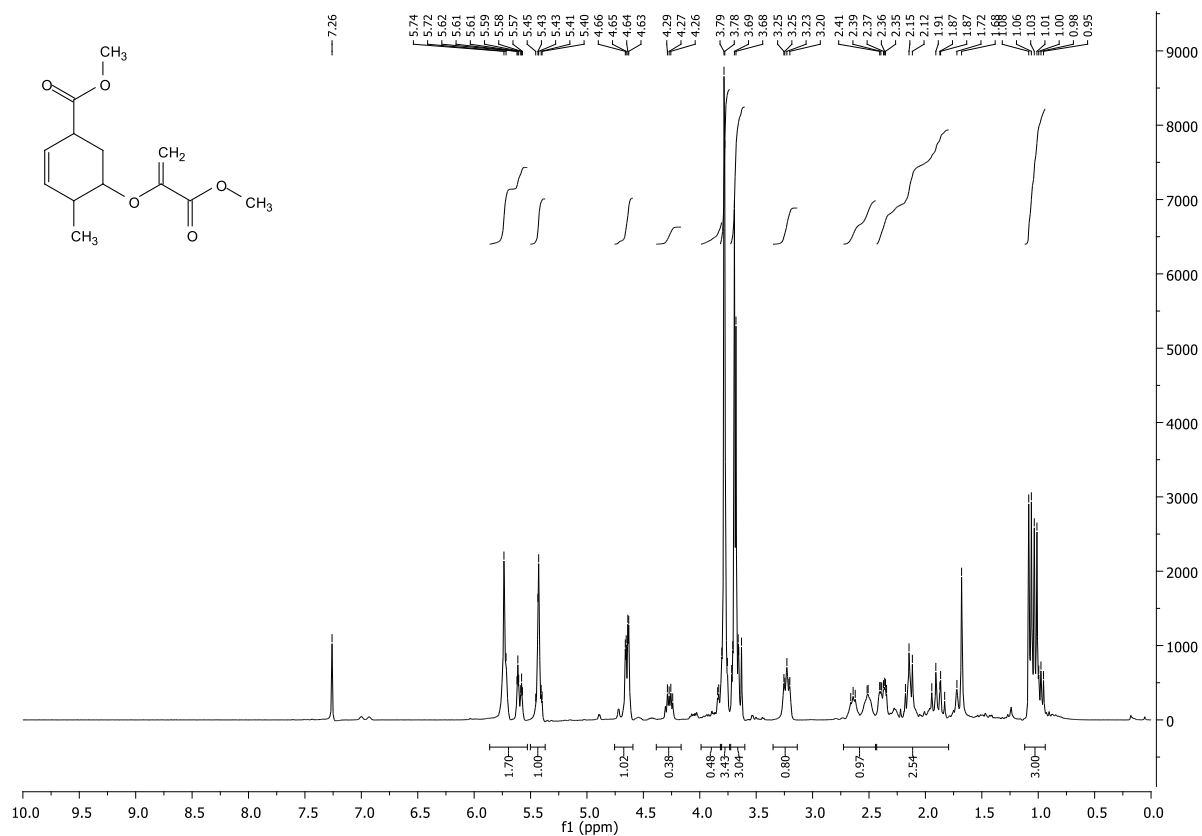


Figure 12.102: ¹H-NMR (300.36 MHz, CDCl₃) of compound 47.

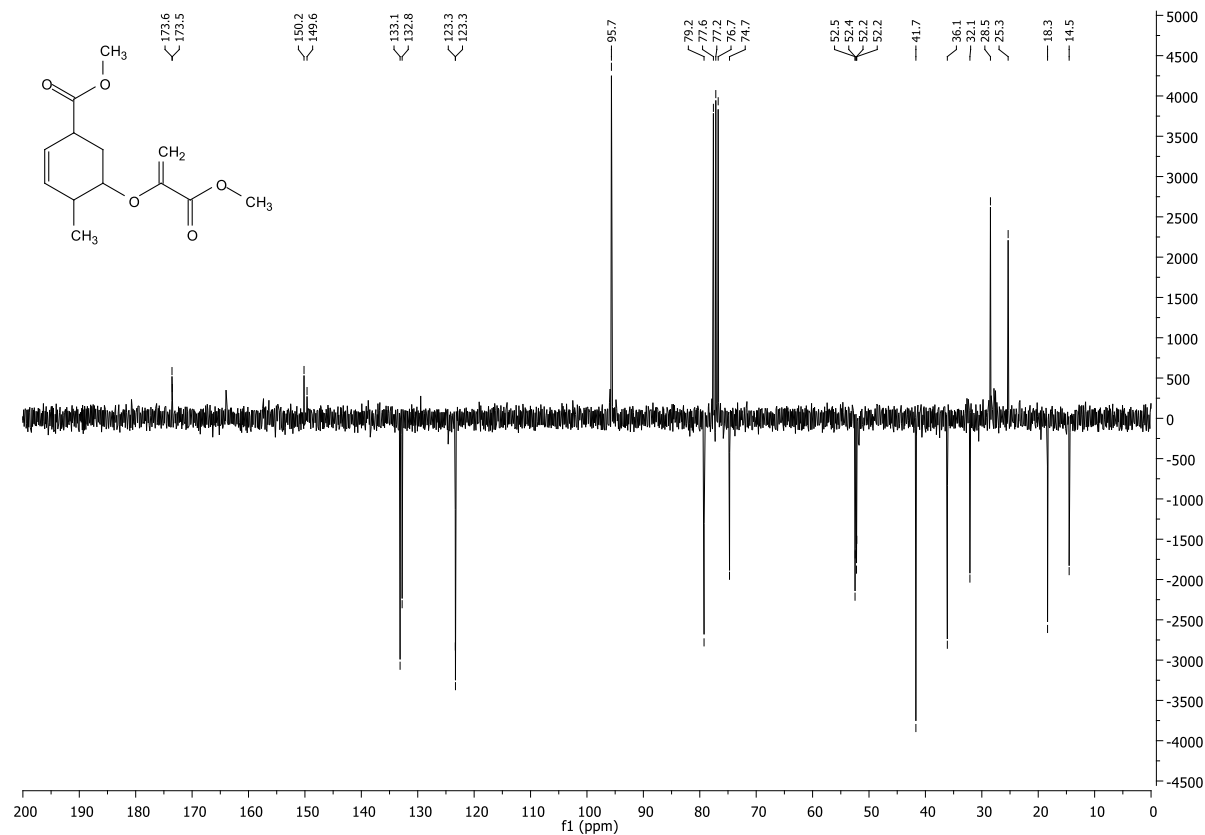


Figure 12.103: ¹³C-NMR,APT (75.53 MHz, CDCl₃) of compound 47.

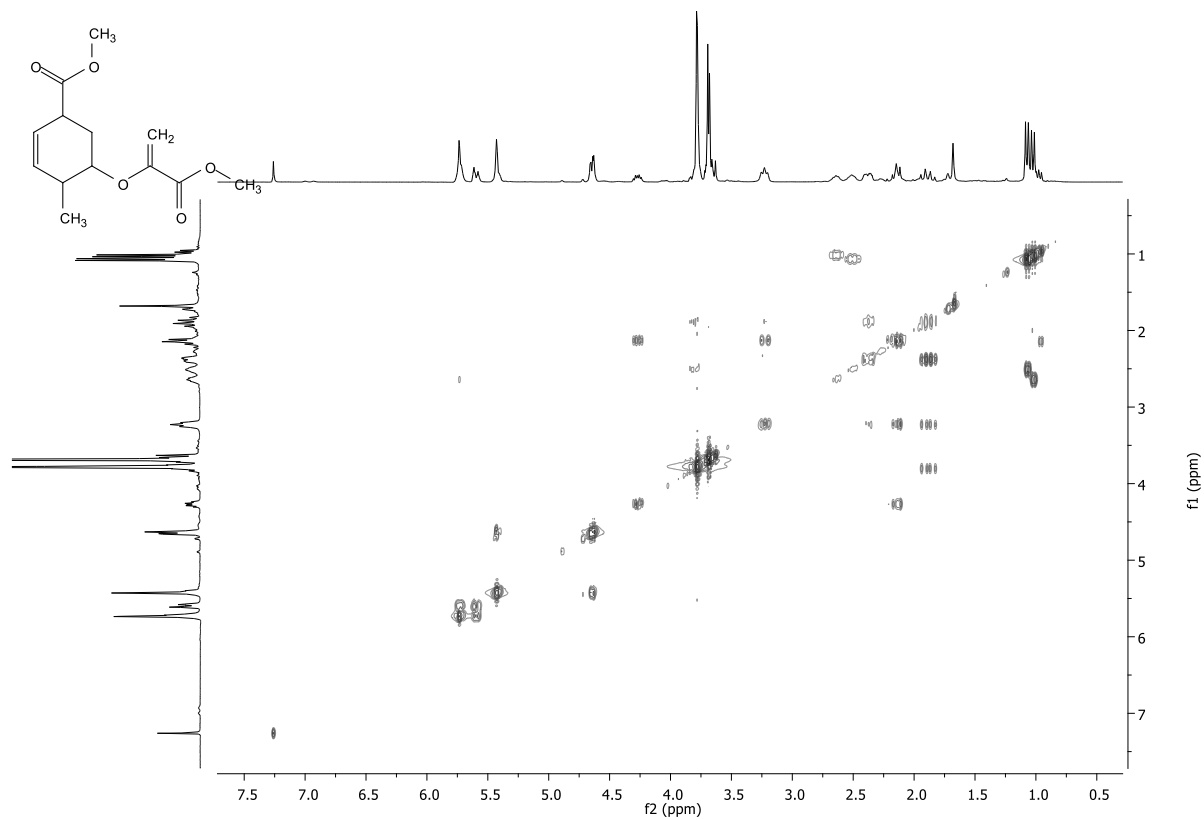


Figure 12.104: COSY-NMR (CDCl₃) of compound 47.

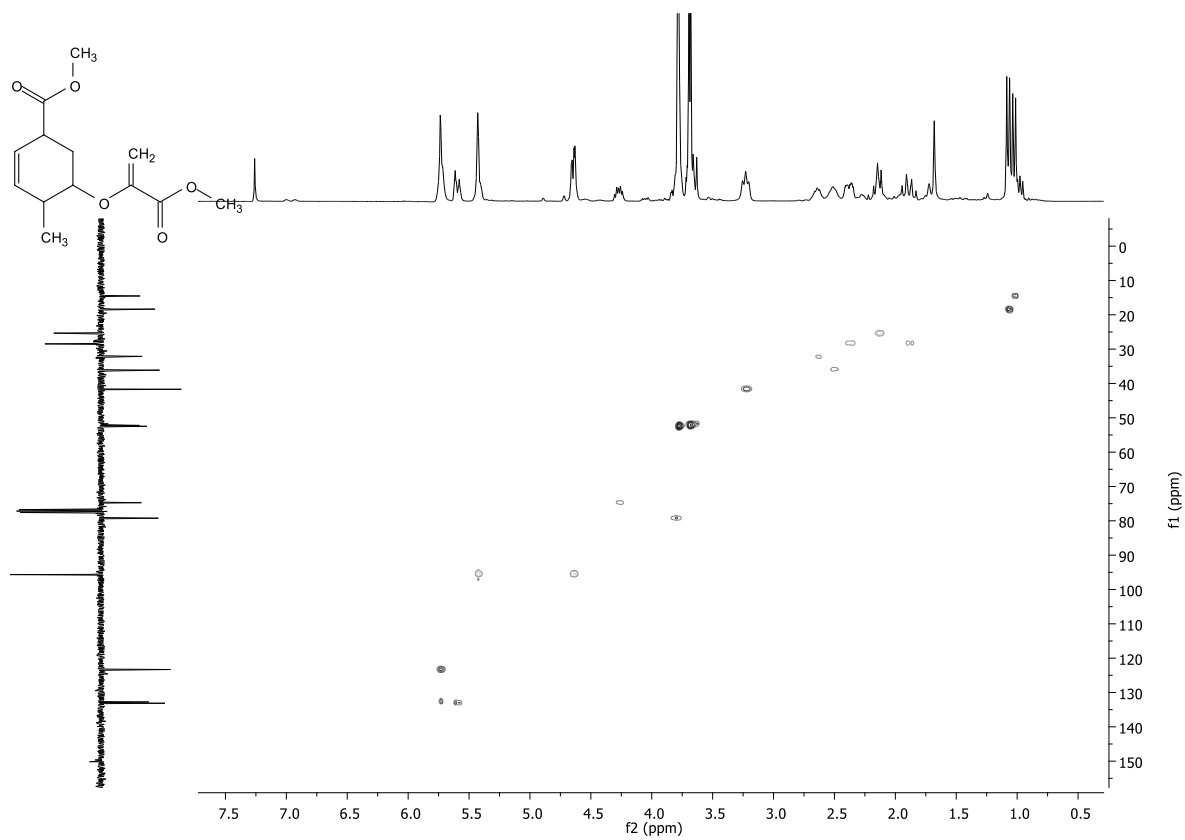


Figure 12.105: HSQC-NMR (CDCl₃) of compound 47.

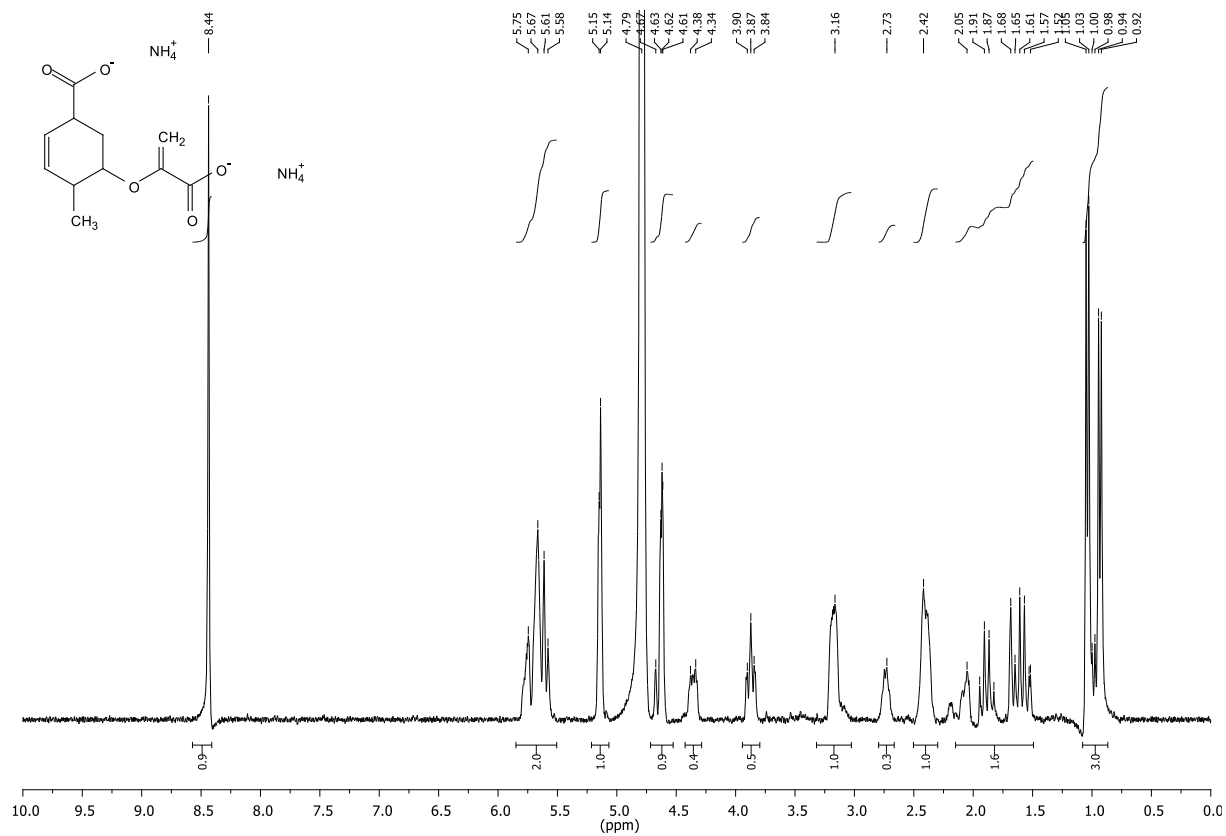


Figure 12.106: $^1\text{H-NMR}$ (300.36 MHz, D_2O) of compound 48.

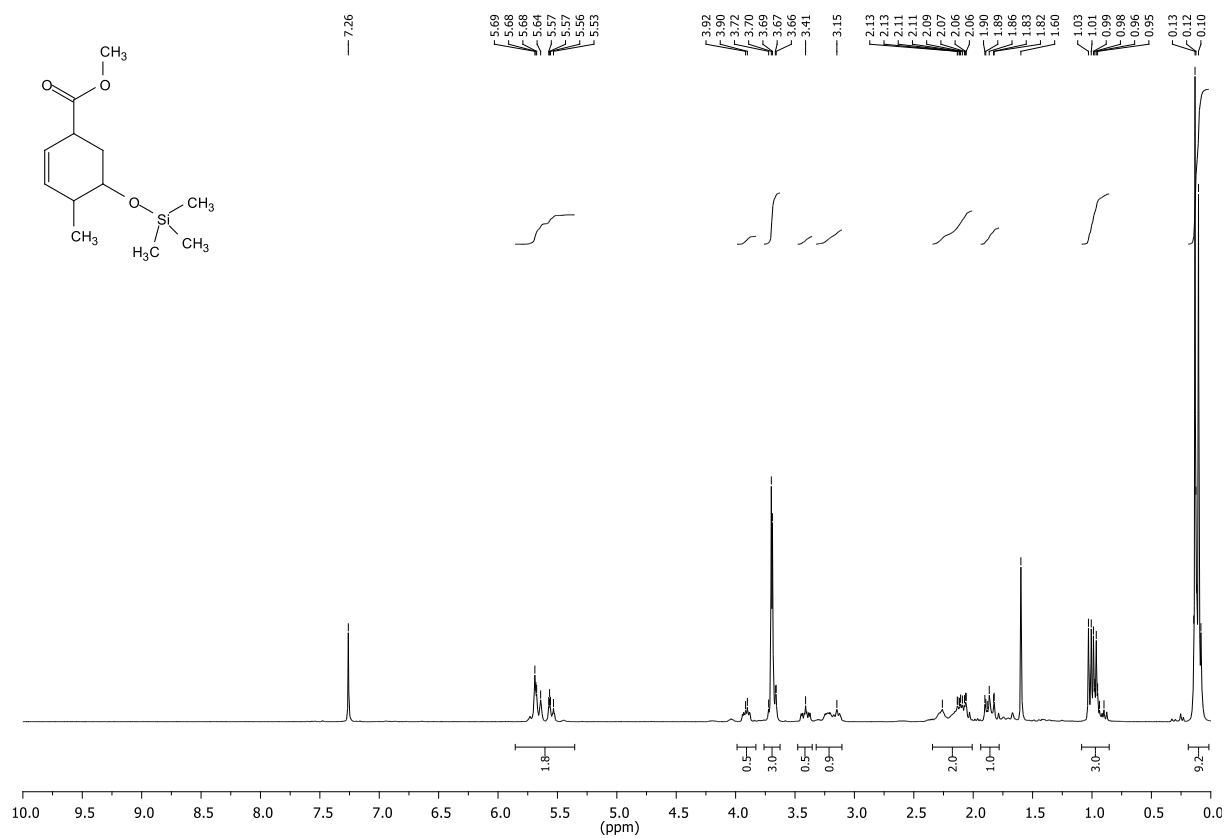


Figure 12.107: $^1\text{H-NMR}$ (300.36 MHz, CDCl_3) of compound 49.

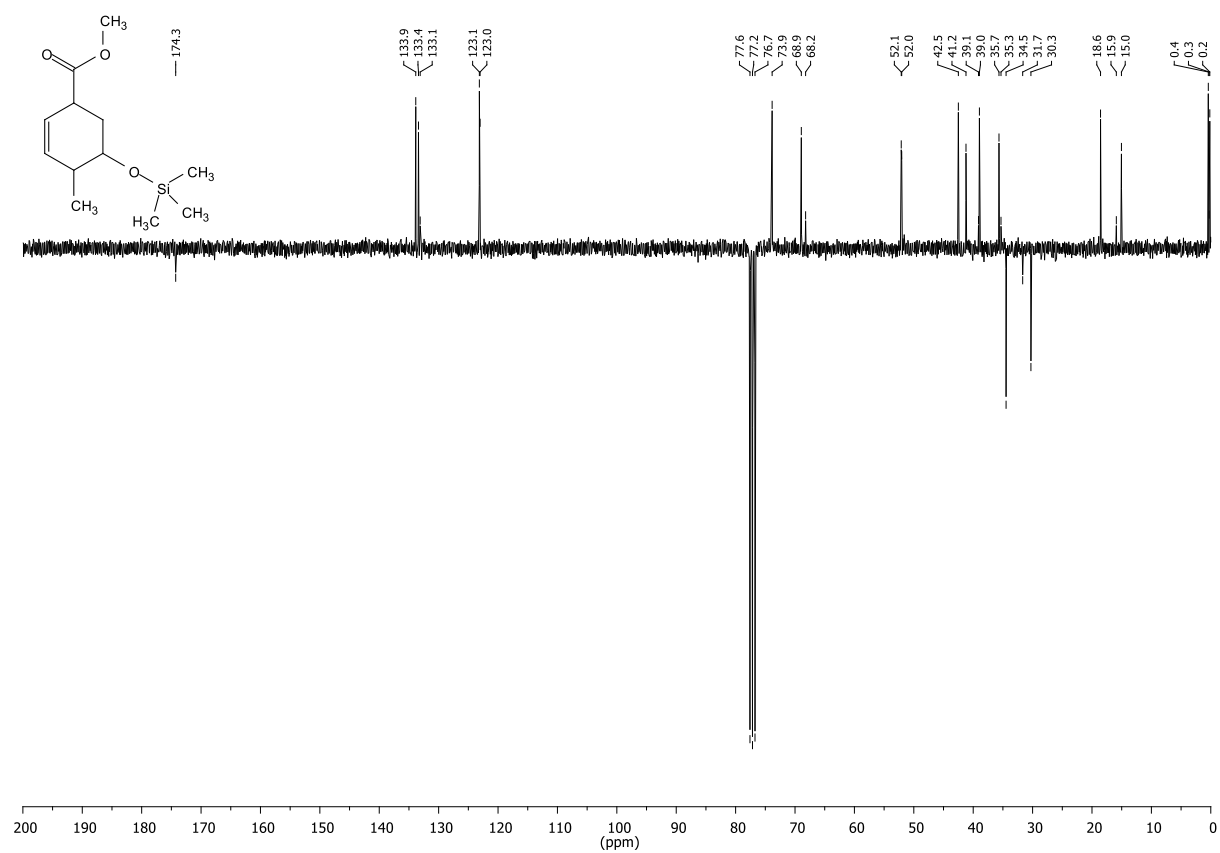


Figure 12.108: $^{13}\text{C-NMR}$, APT (75.53 MHz, CDCl_3) of compound 49.

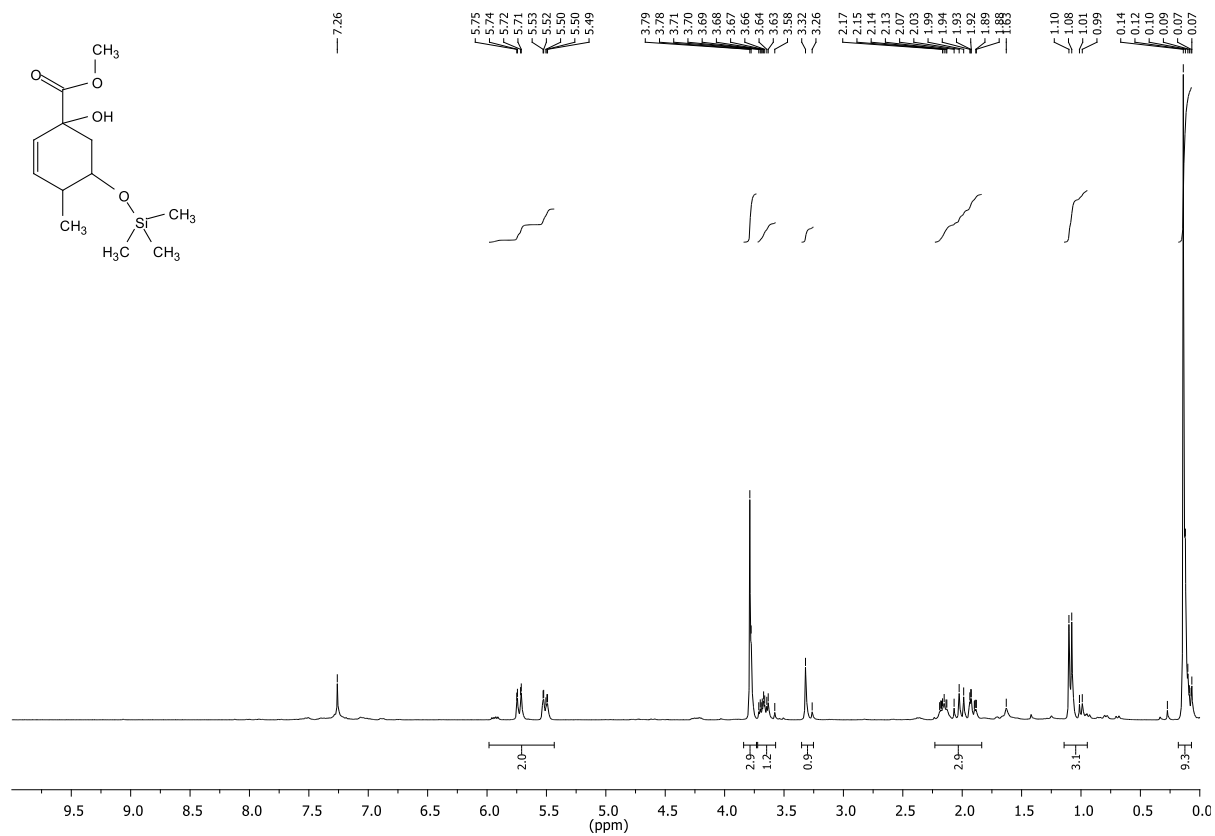


Figure 12.109: ¹H-NMR(300.36 MHz, CDCl₃) of compound 50.

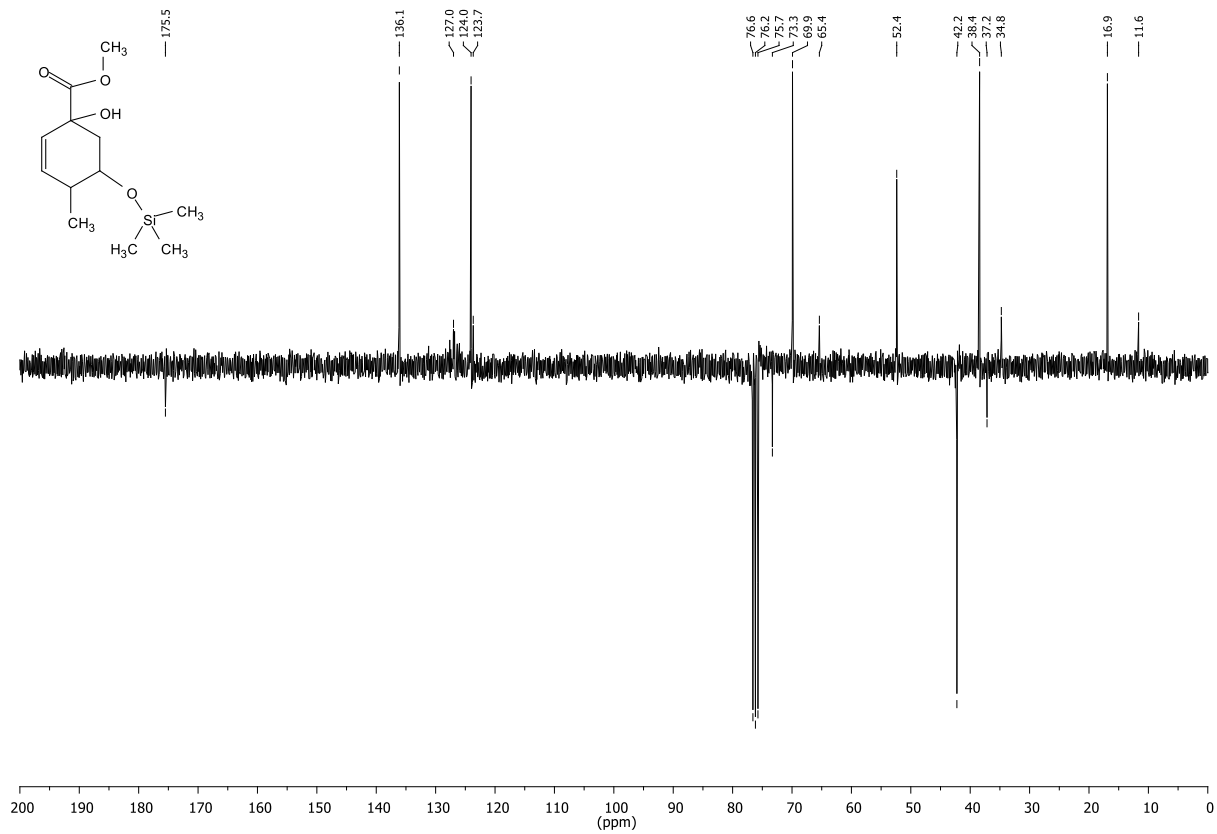


Figure 12.110: ¹³C-NMR,APT (75.53 MHz, CDCl₃) of compound 50.

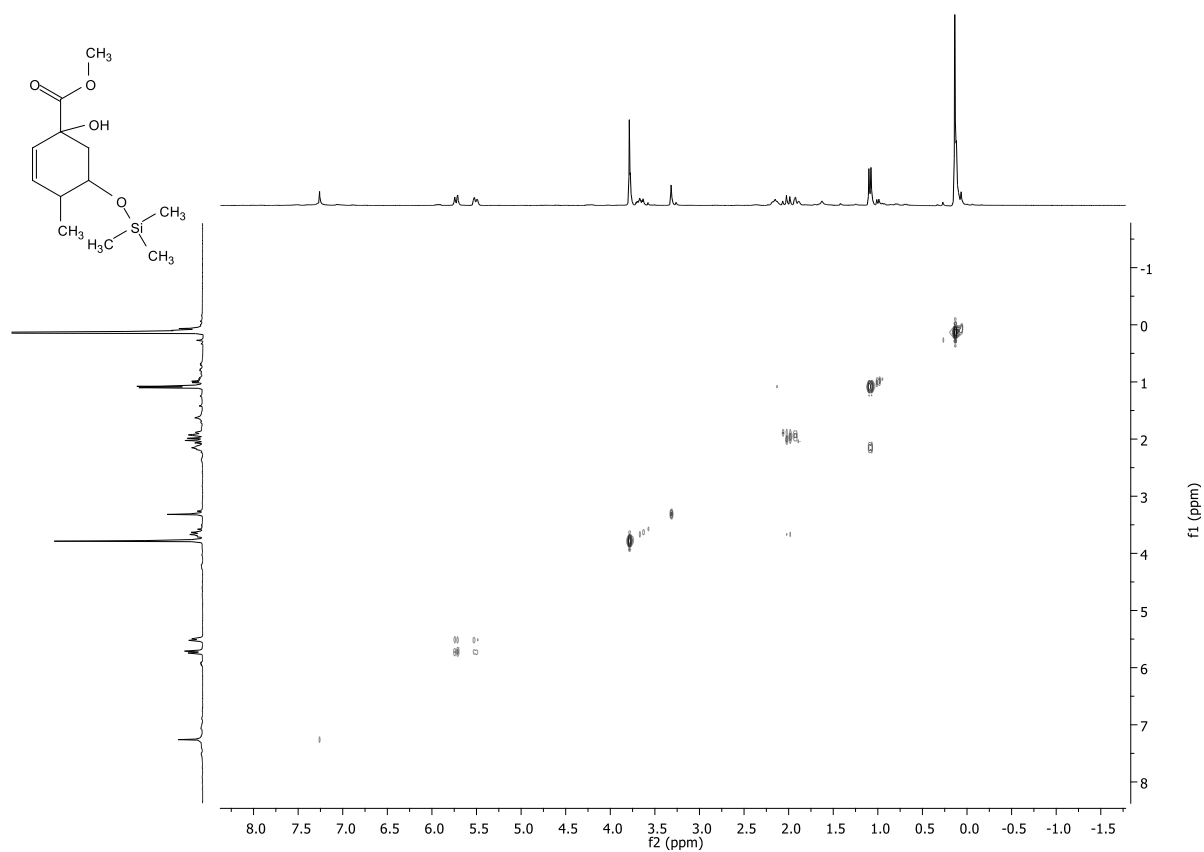


Figure 12.111: COSY-NMR of compound 50.

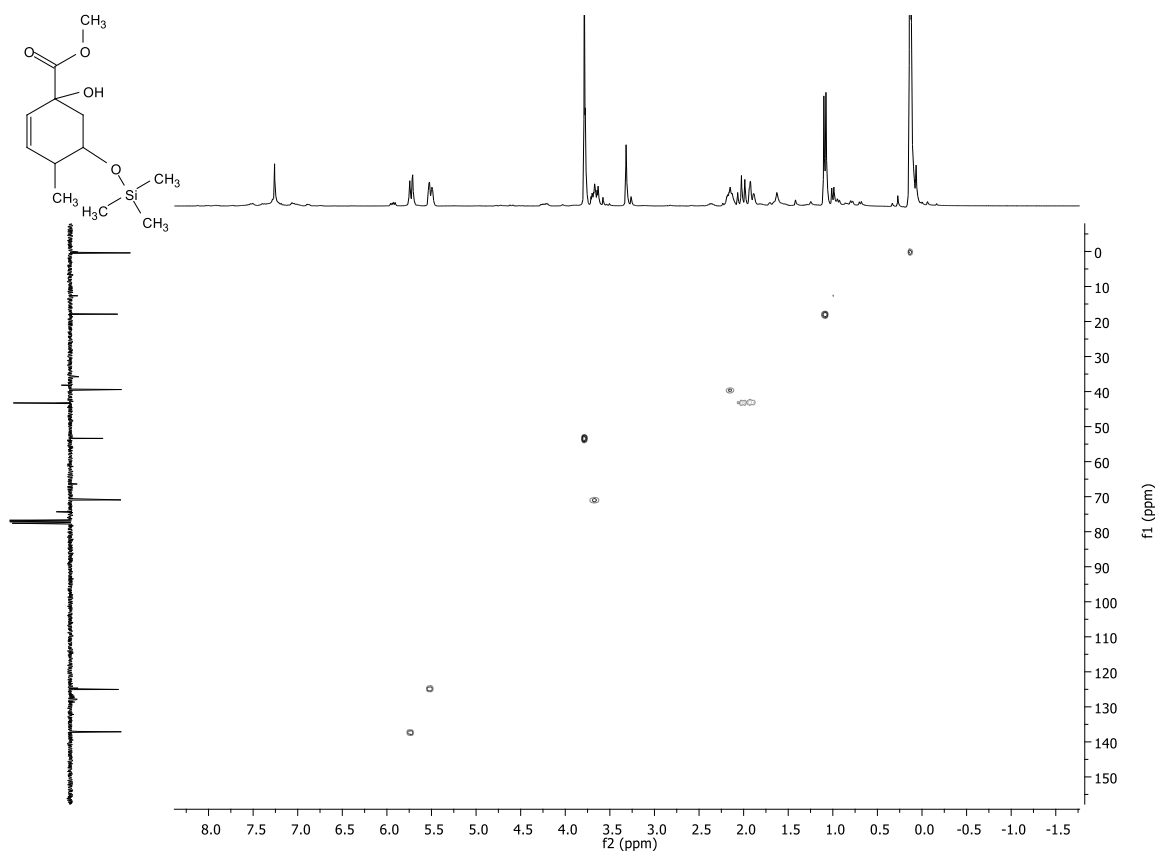


Figure 12.112: HSQC-NMR of compound 50.

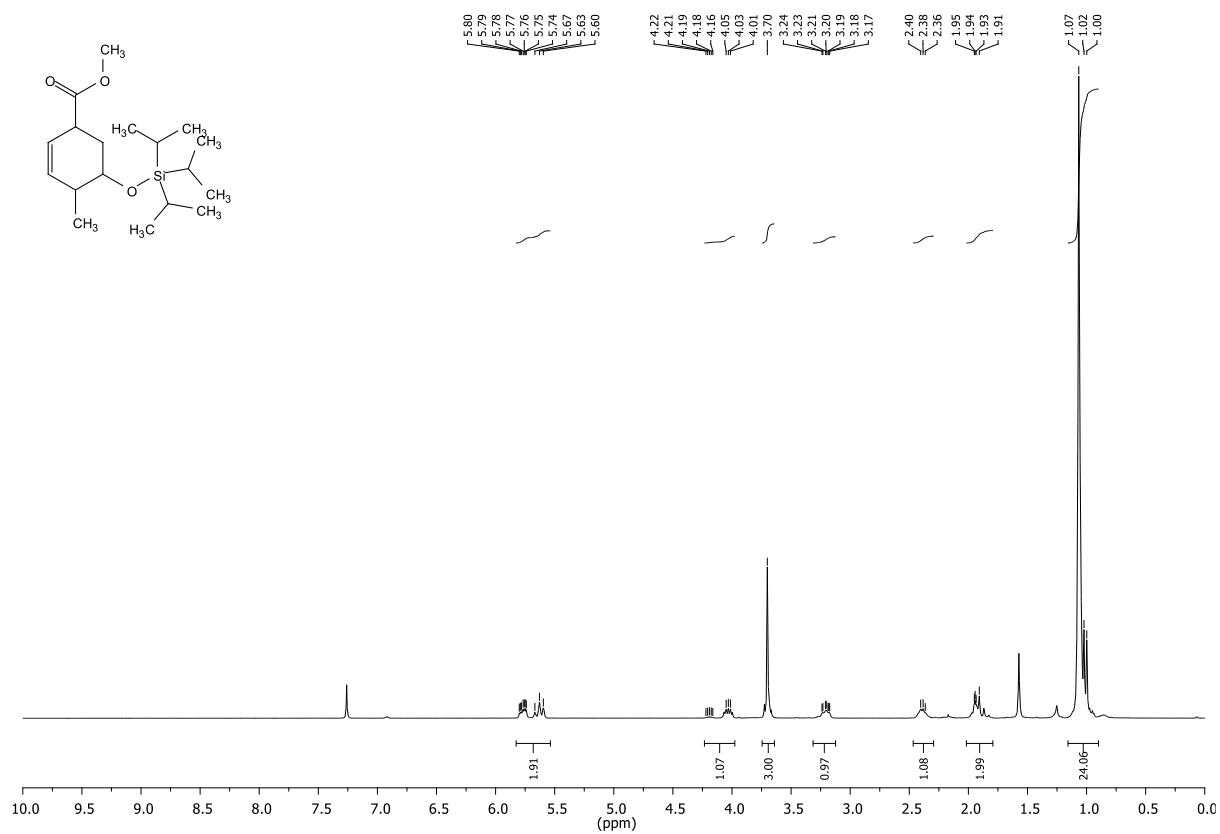


Figure 12.113: ¹H-NMR (300.36 MHz, CDCl₃) of compound **51**, additionally purified

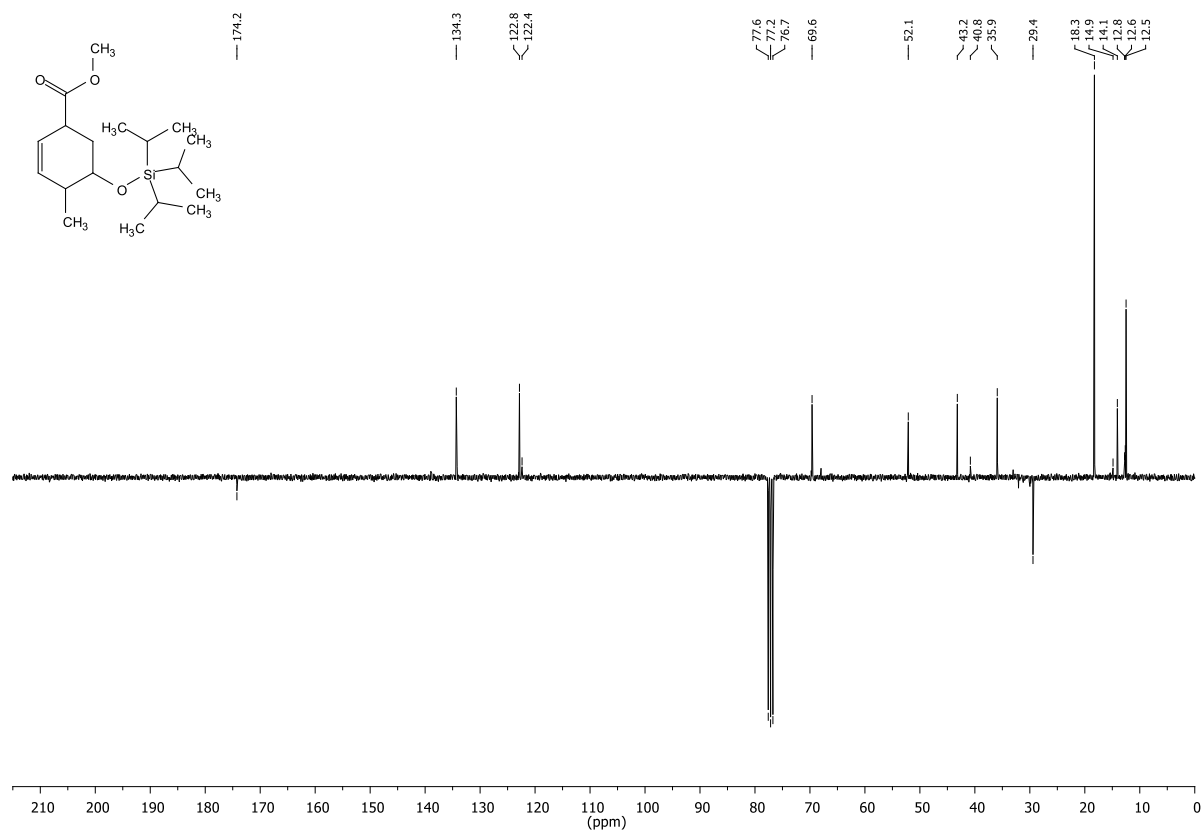


Figure 12.114: ¹³C-NMR,APT (75.53 MHz, CDCl₃) of compound **51**, additionally purified

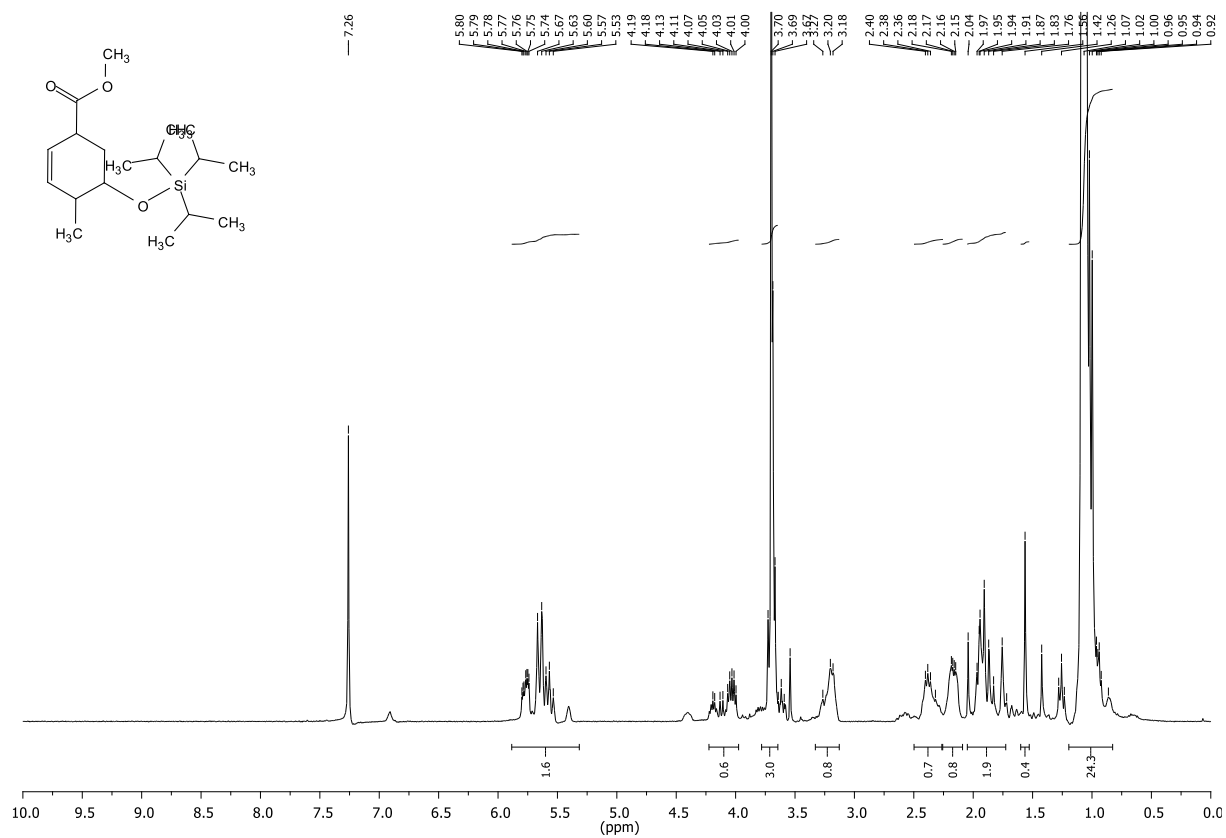


Figure 12.115: ¹H-NMR (300.36 MHz, CDCl₃) of compound **51**, impure

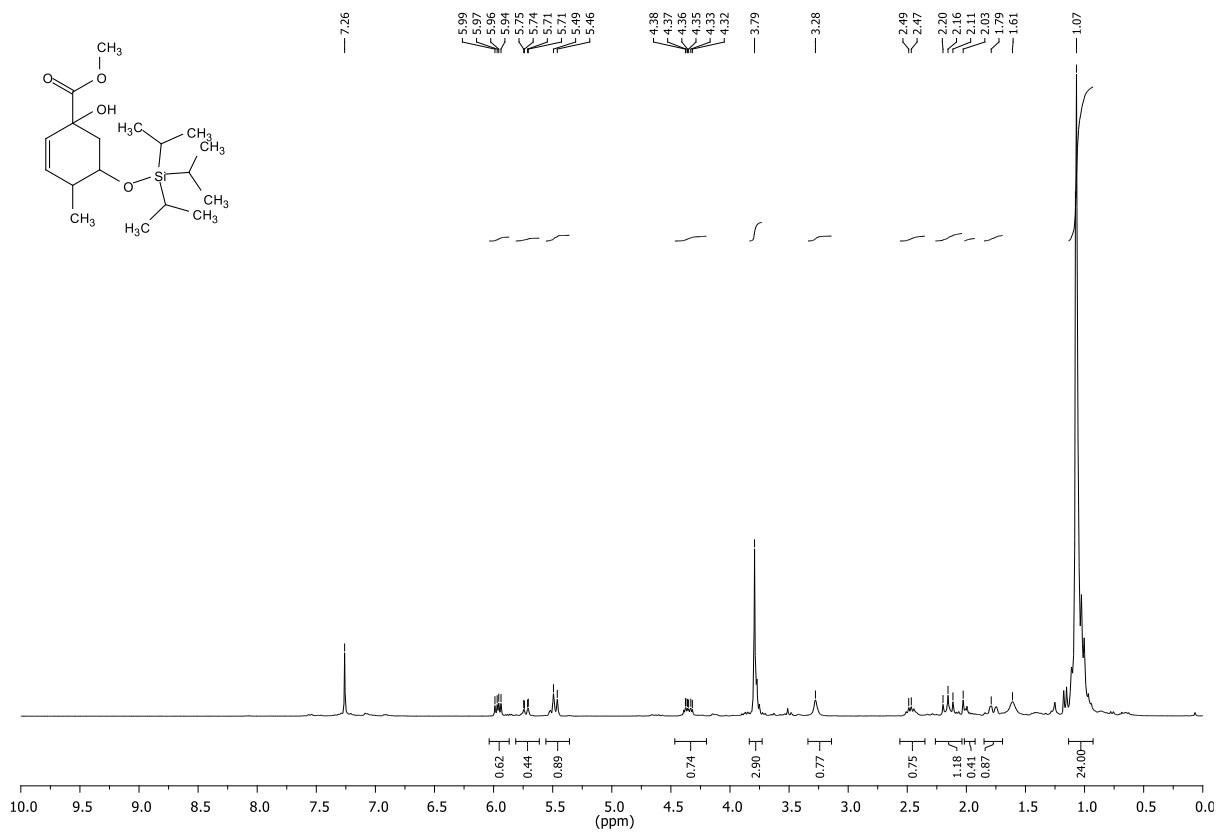


Figure 12.116: ¹H-NMR (300.36 MHz, CDCl₃) of compound 52.

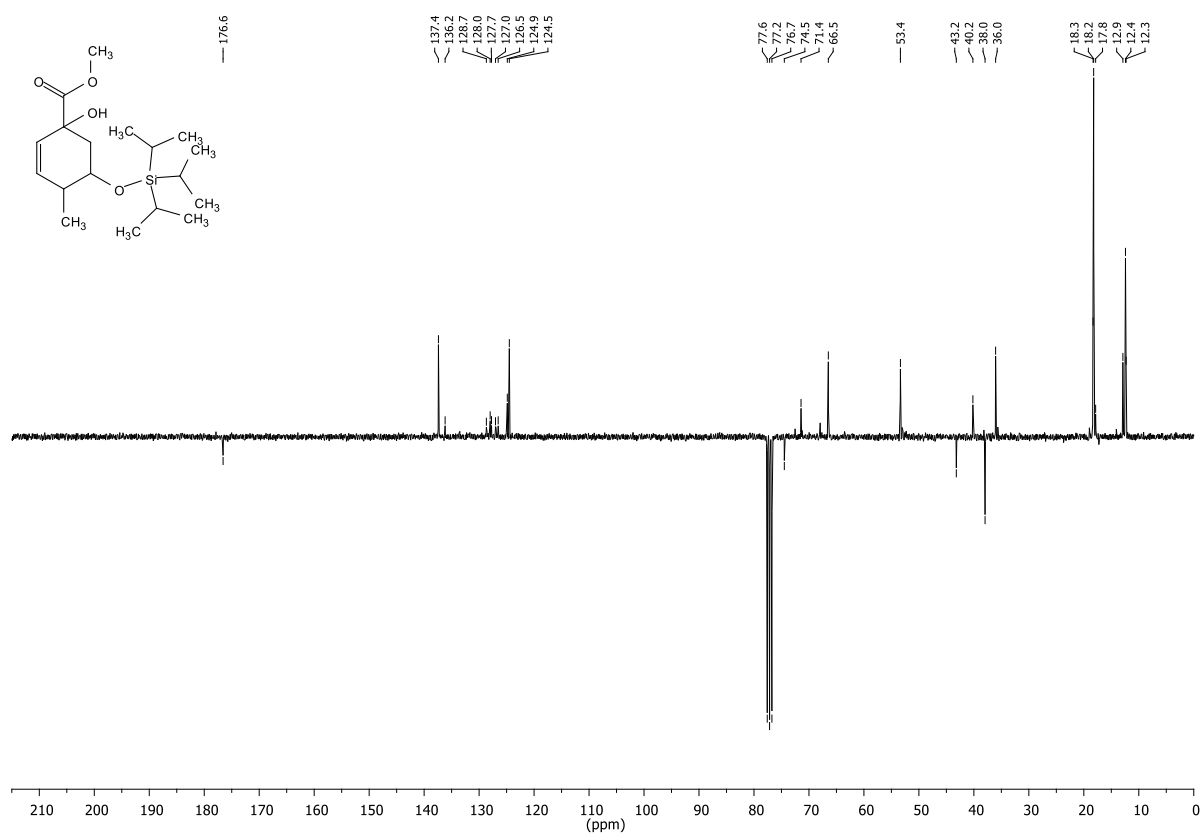
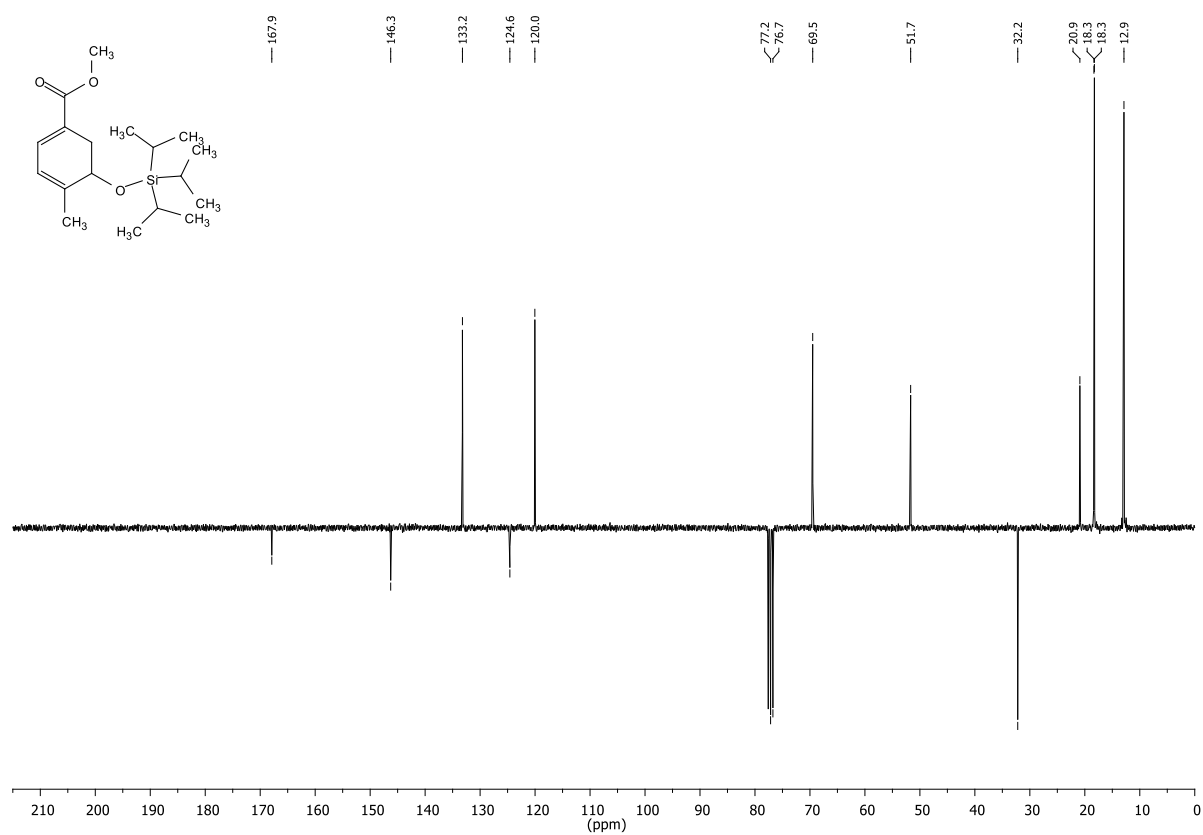
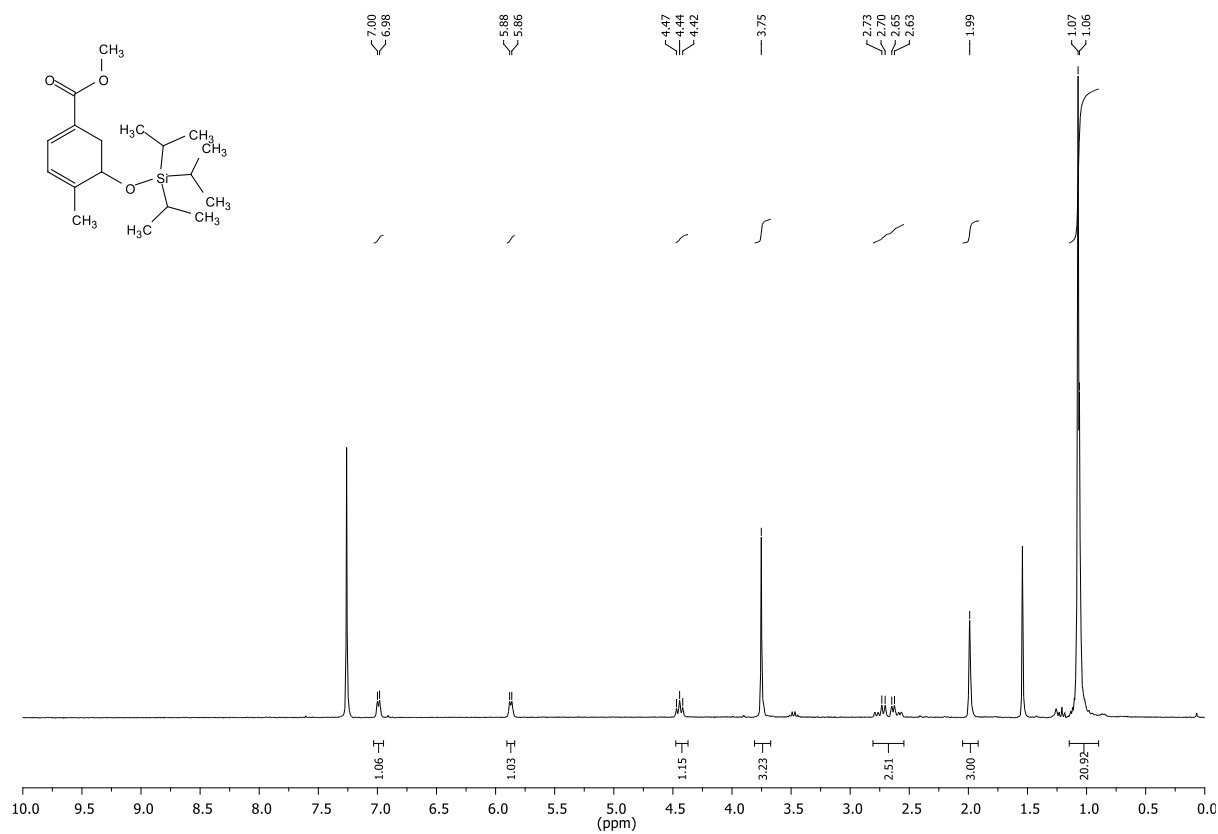
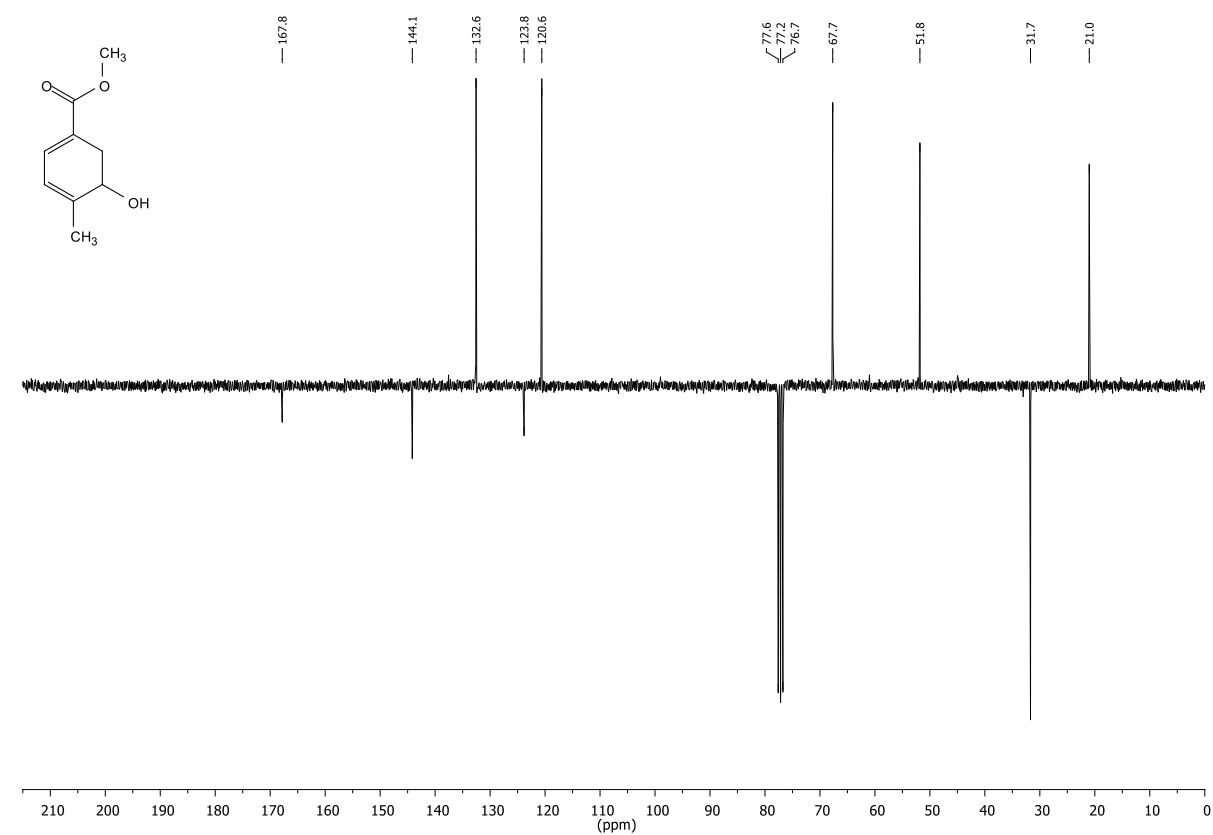
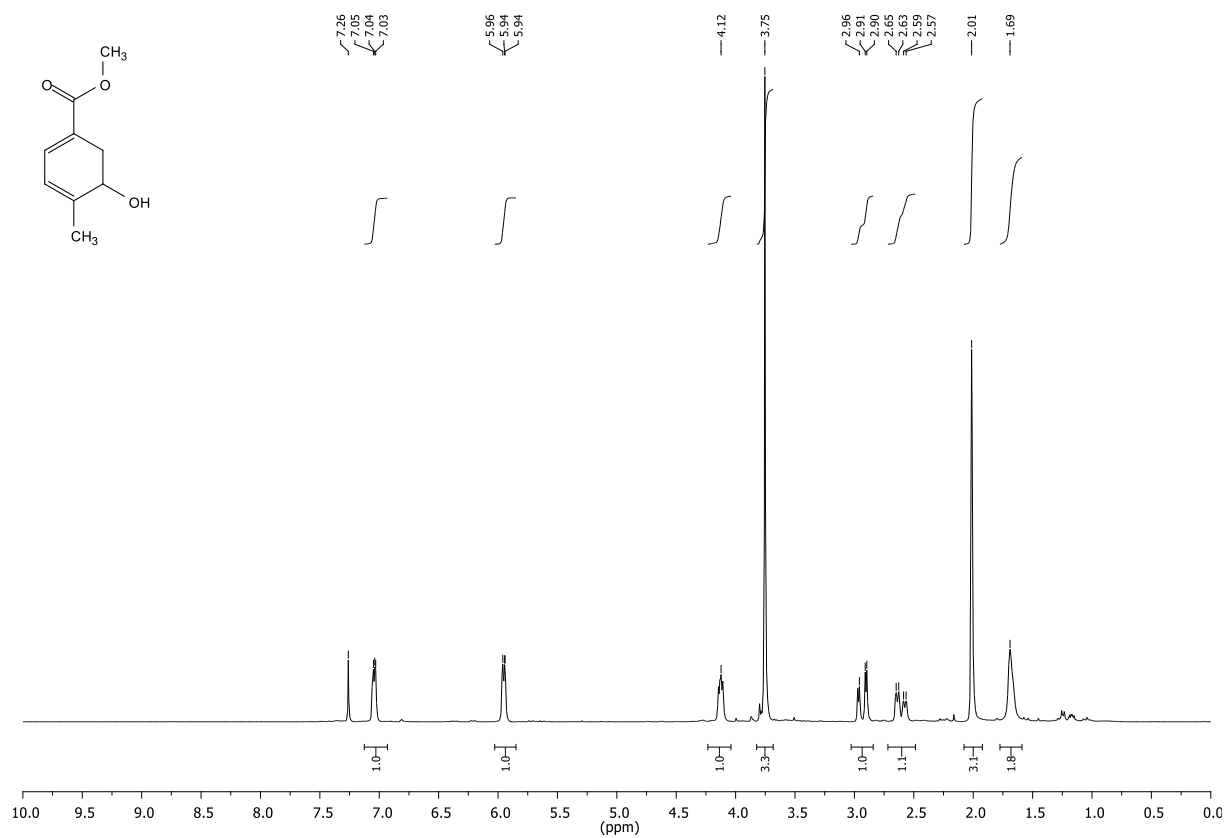


Figure 12.117: ¹³C-NMR,APT (75.53 MHz, CDCl₃) of compound 52.





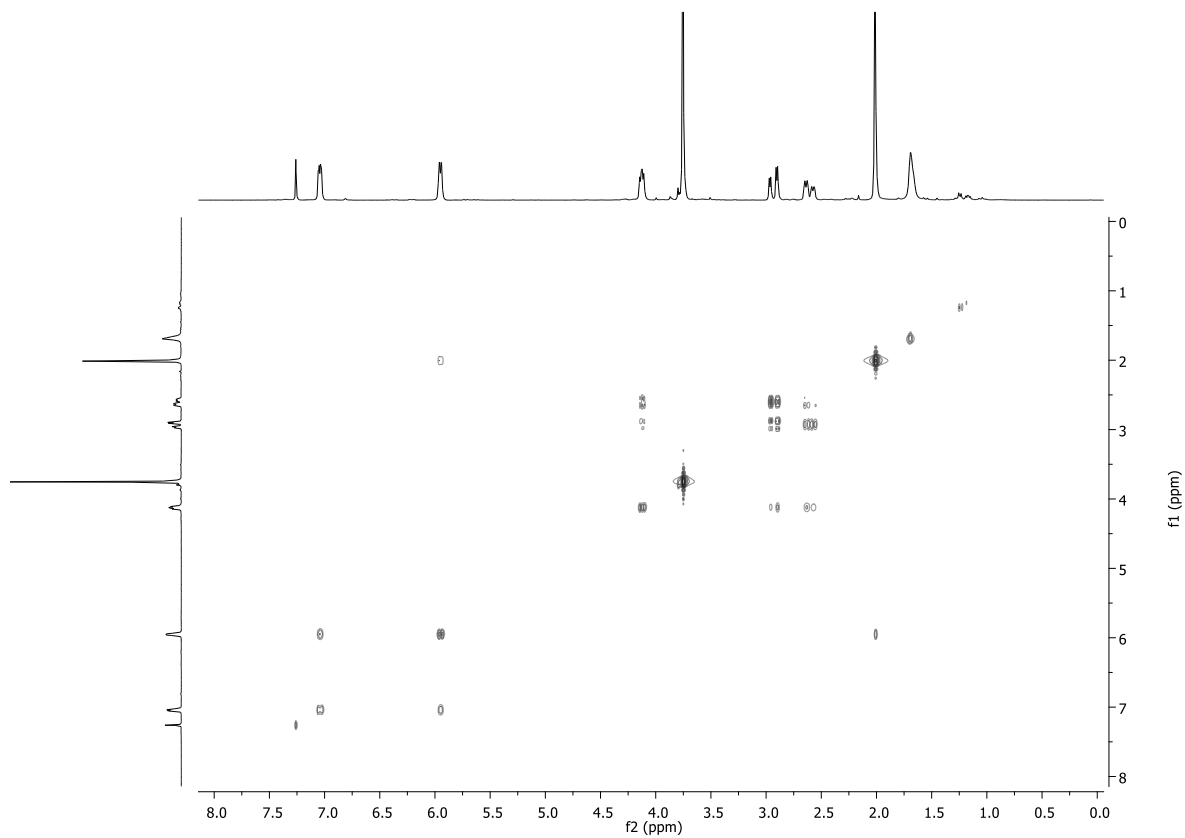


Figure 12.122: COSY-NMR (CDCl₃) of compound 54.

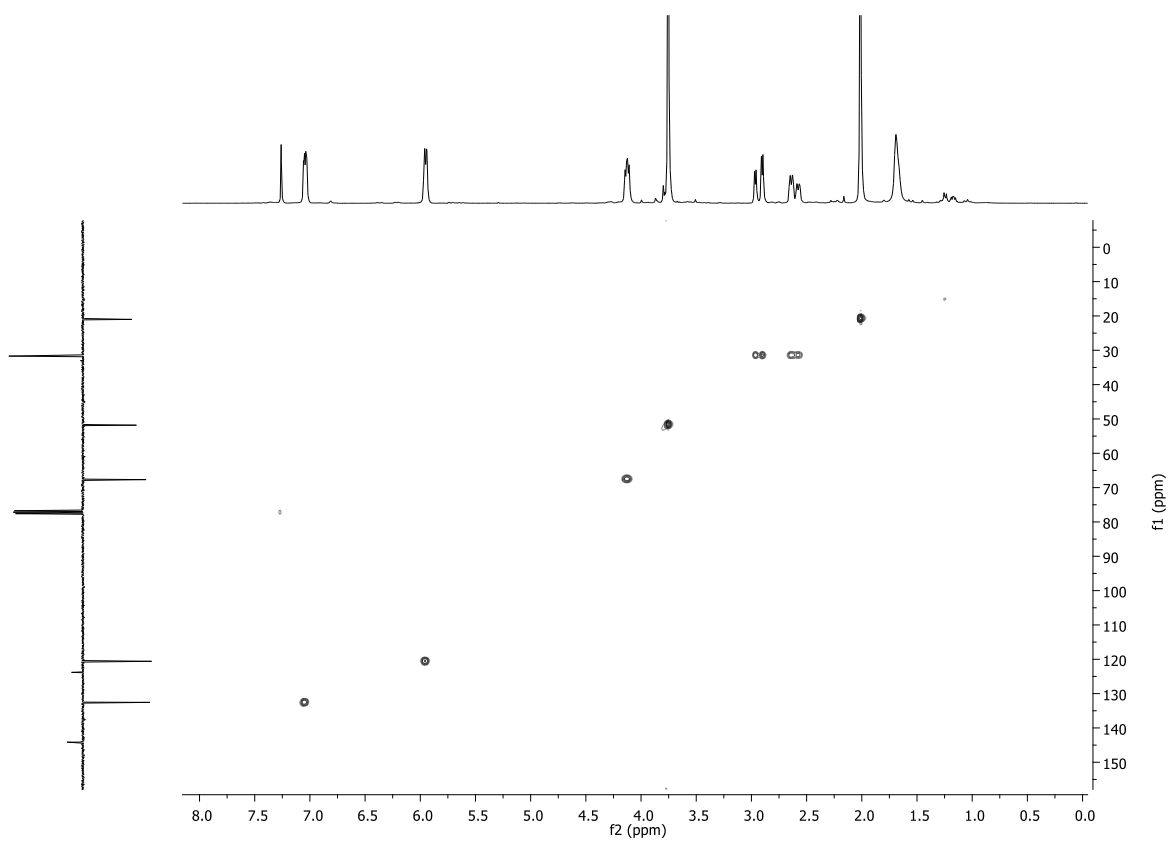


Figure 12.123: HSQC-NMR (CDCl₃) of compound 54.

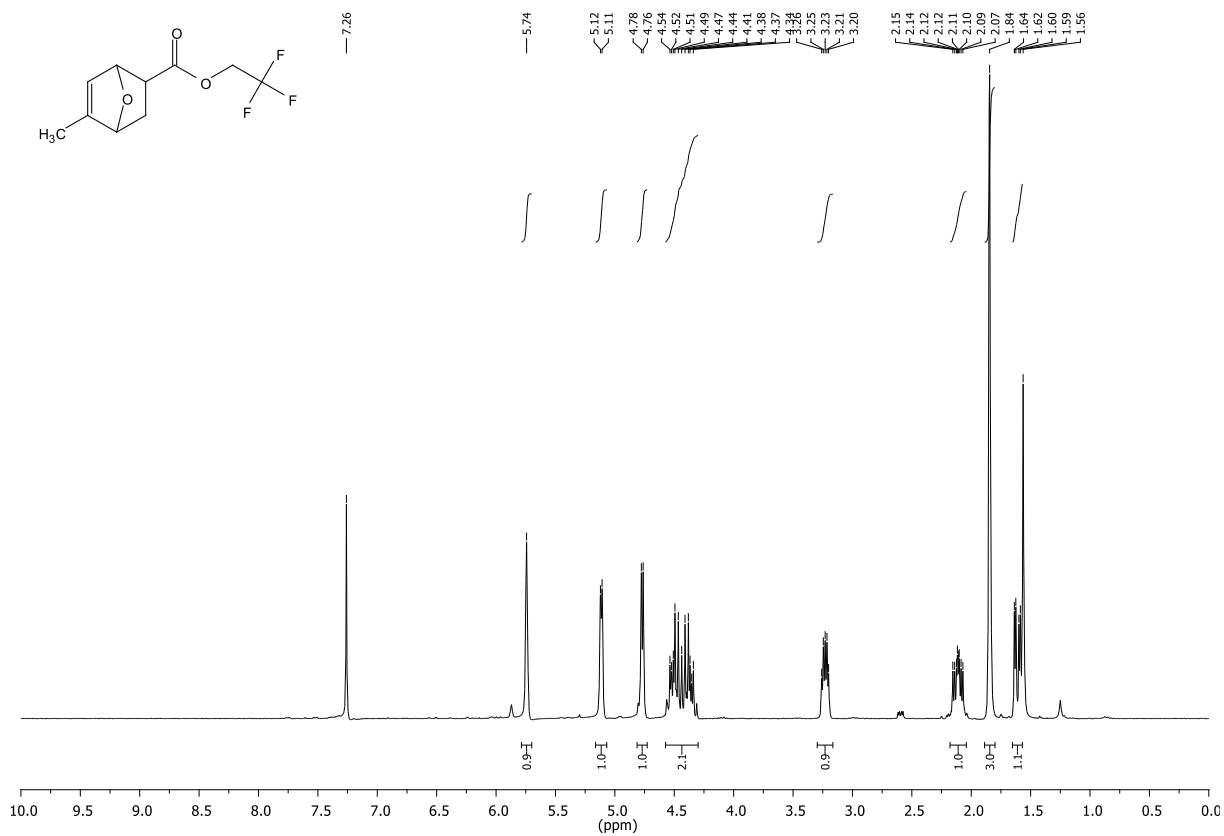


Figure 12.124: ¹H-NMR (300.36 MHz, CDCl₃) of compound 55.

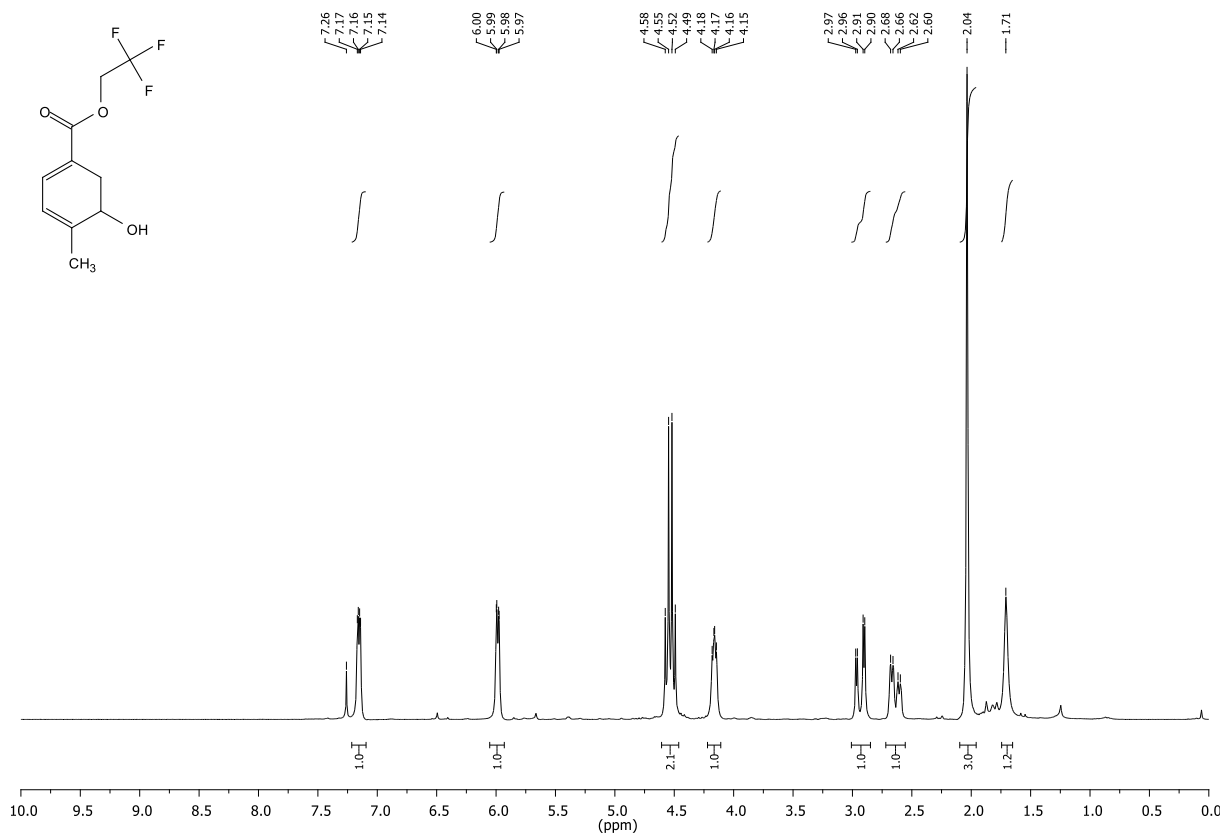


Figure 12.125: ¹H-NMR (300.36 MHz, CDCl₃) of compound 56.

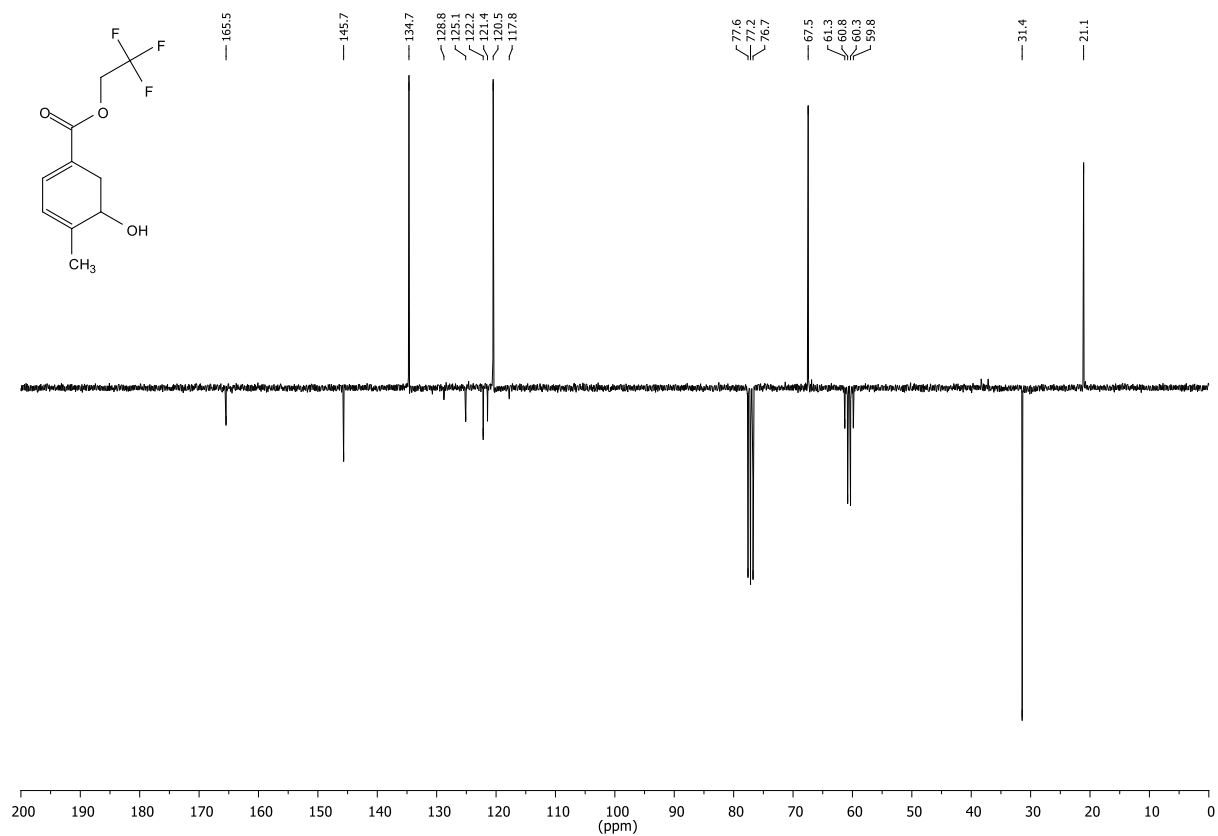


Figure 12.126: ¹³C-NMR,APT (75.53 MHz, CDCl₃) of compound 56.

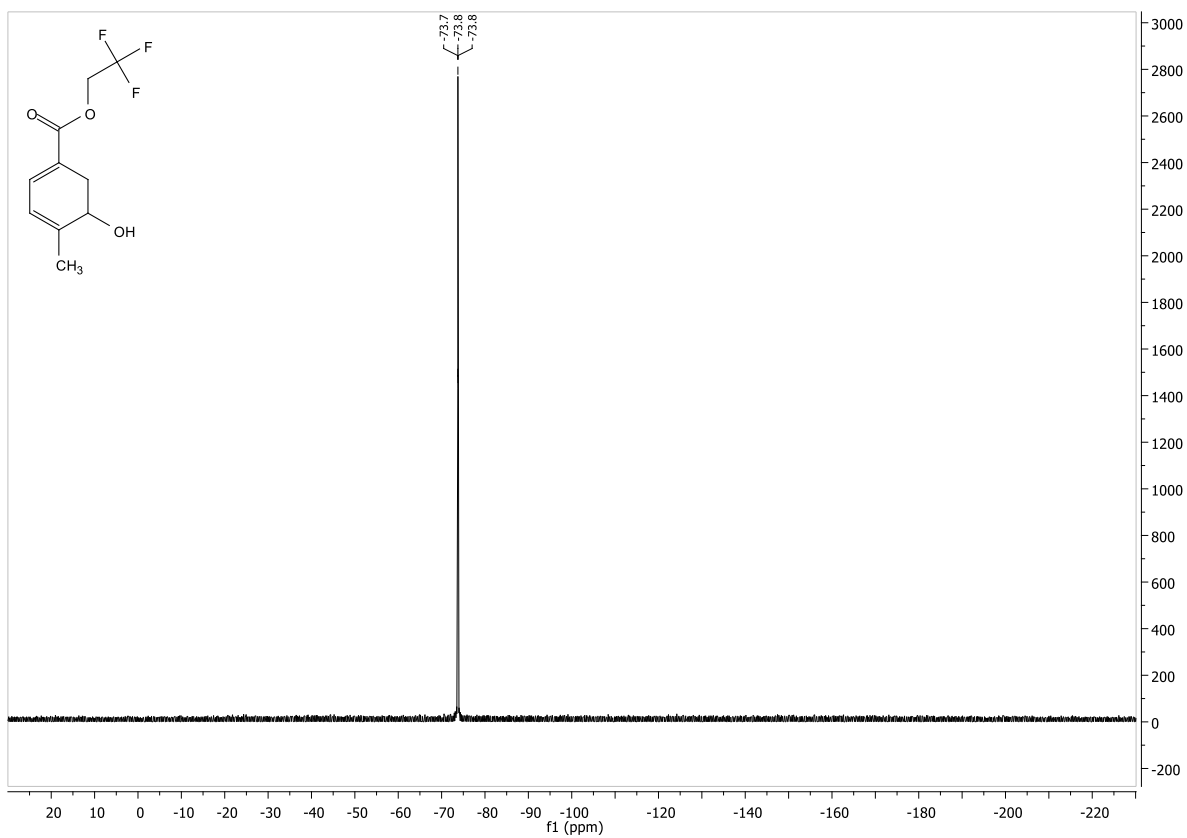


Figure 12.127: ^{19}F -NMR (470.35 MHz, CDCl_3) of compound **56**.

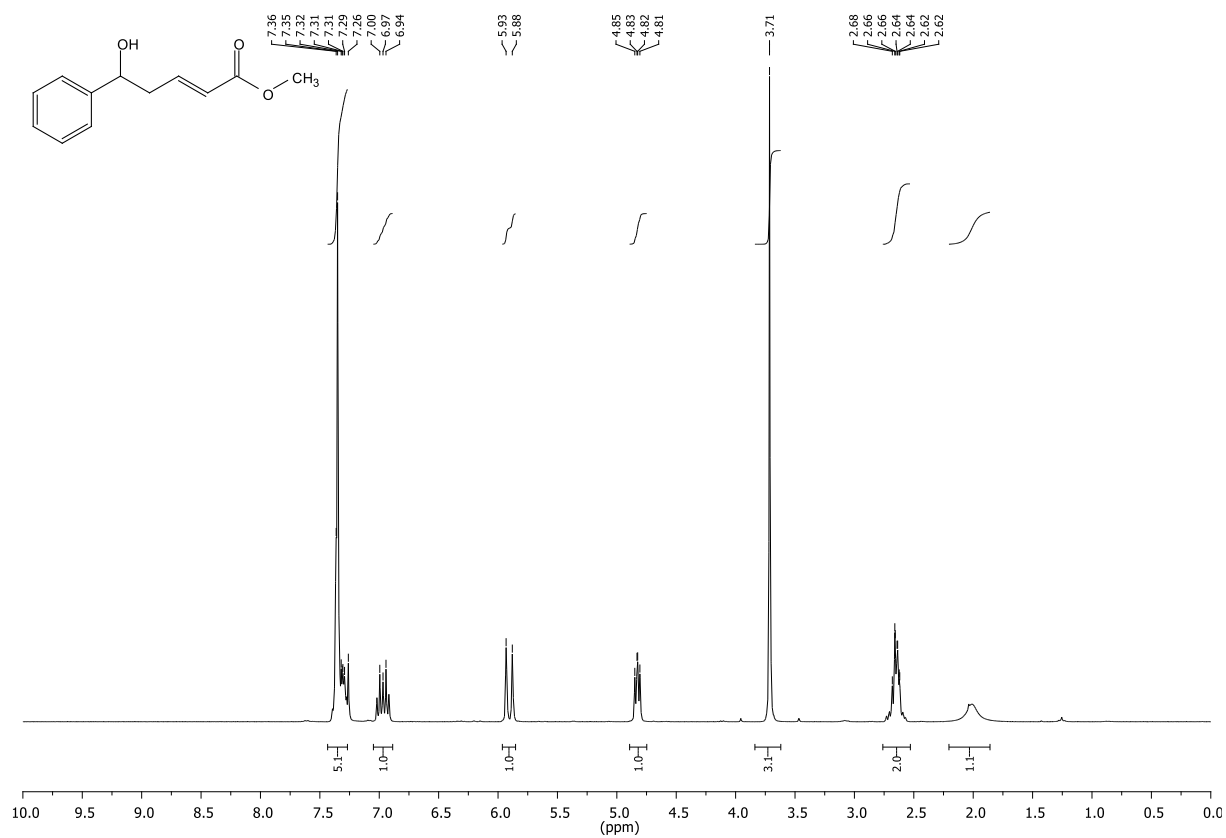


Figure 12.128: ¹H-NMR (300.36 MHz, D₂O) of compound 57.

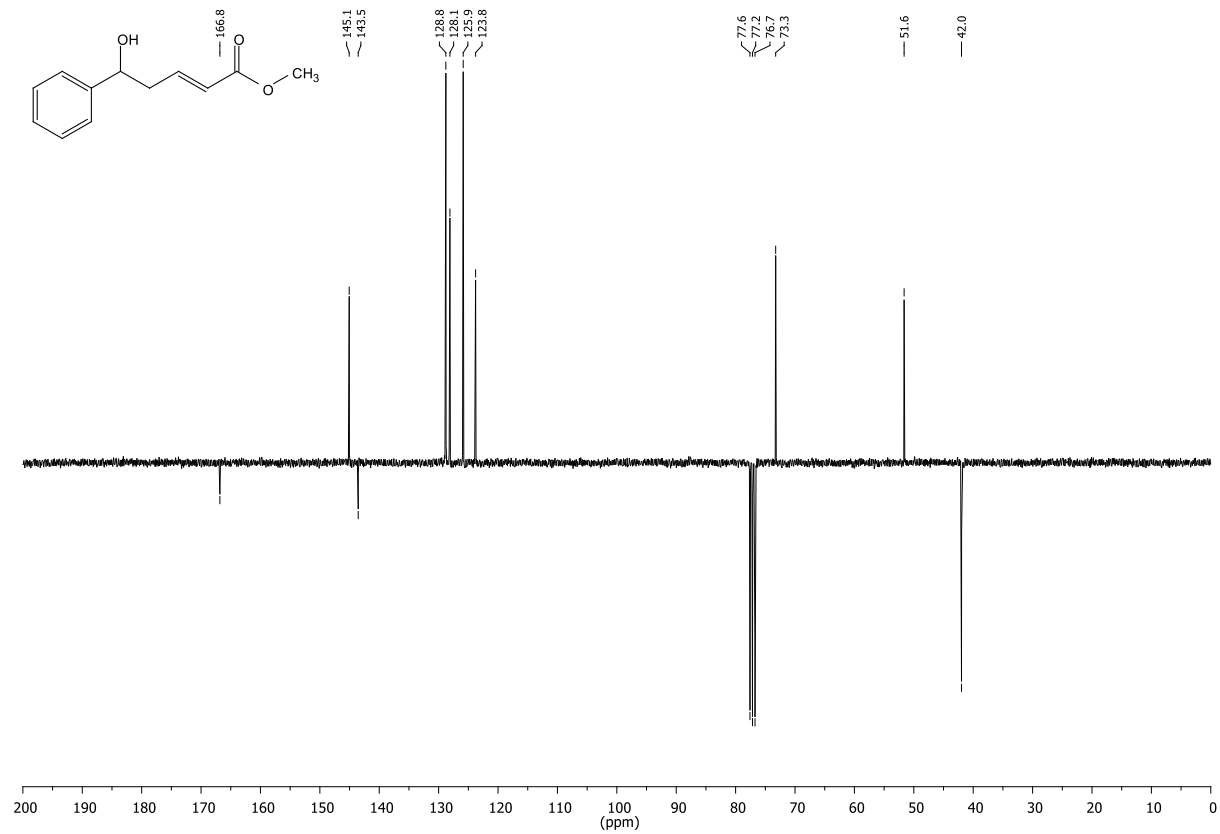


Figure 12.129: ¹³C-NMR, APT (75.53 MHz, CDCl₃) of compound 57.

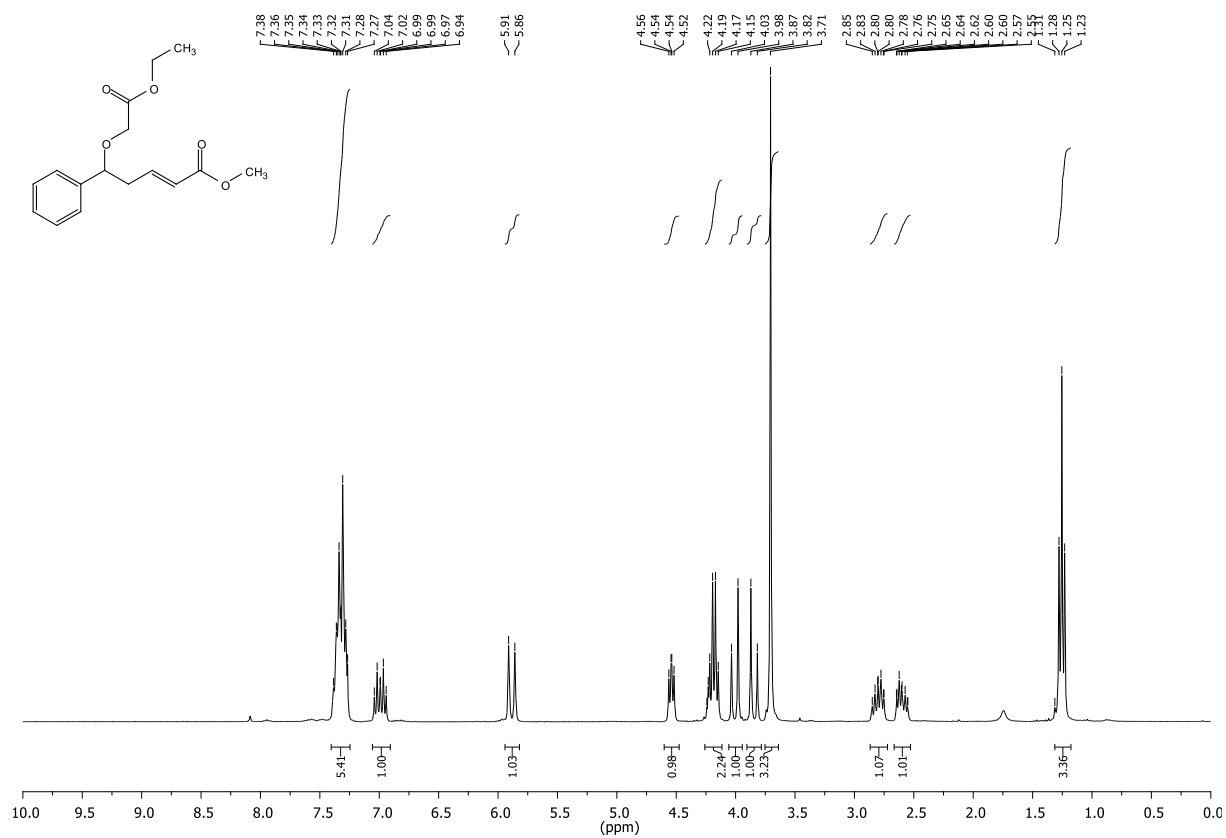


Figure 12.130: ¹H-NMR (300.36 MHz, CDCl₃) of compound 58.

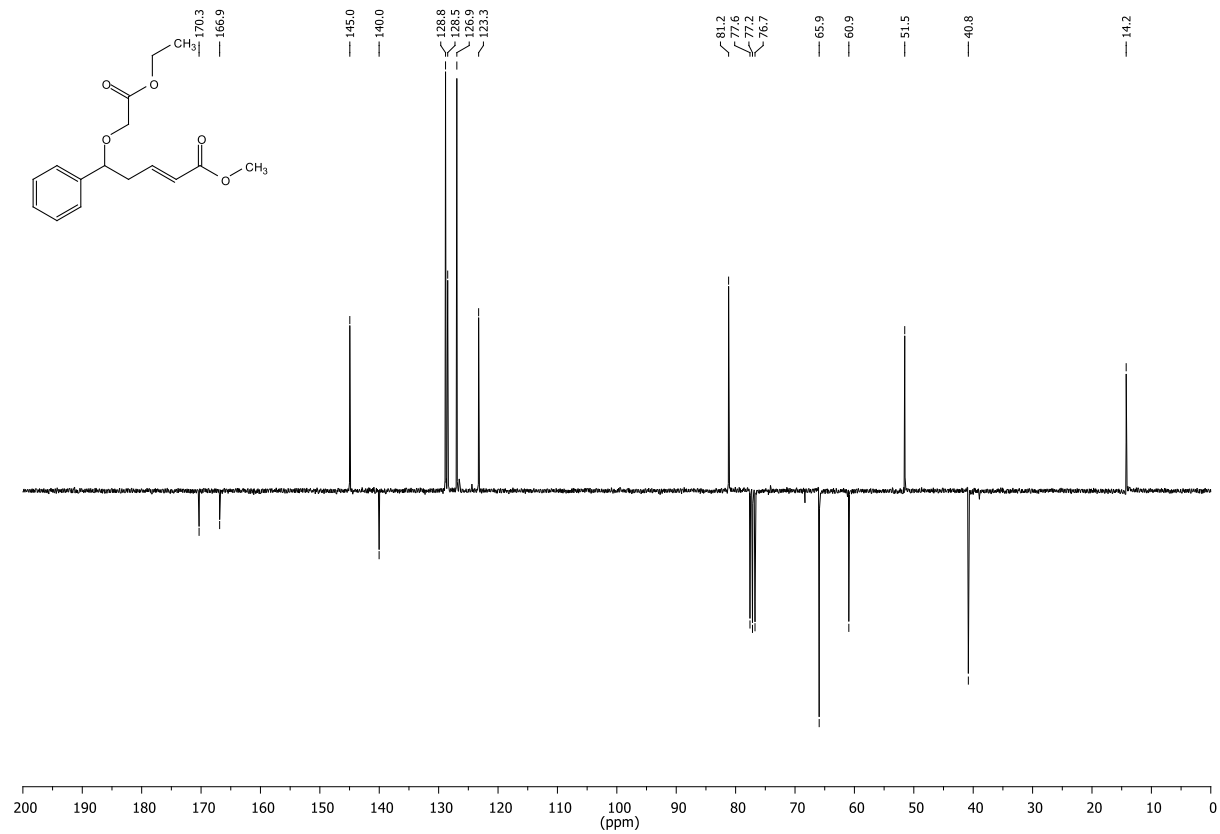


Figure 12.131: ¹³C-NMR, APT (75.53 MHz, CDCl₃) of compound 58.

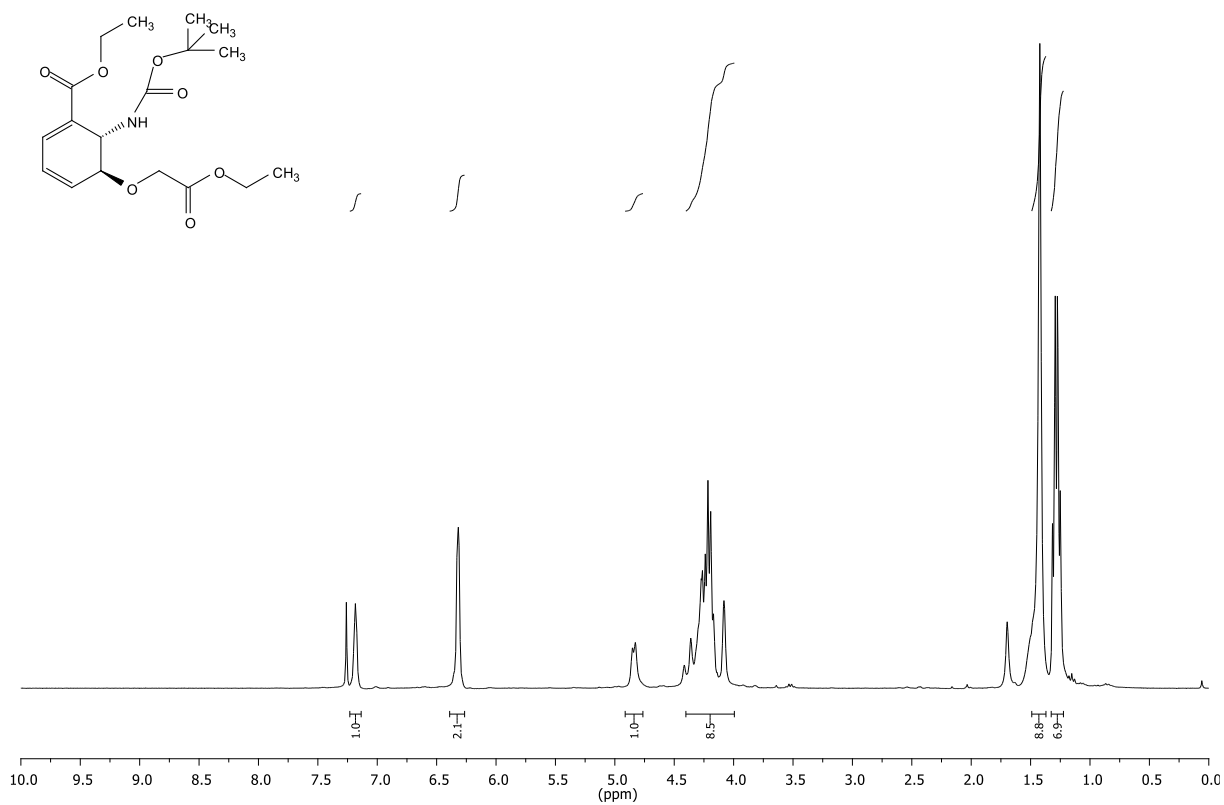


Figure 12.132: $^1\text{H-NMR}$ (300.36 MHz, CDCl_3) of compound **59**.

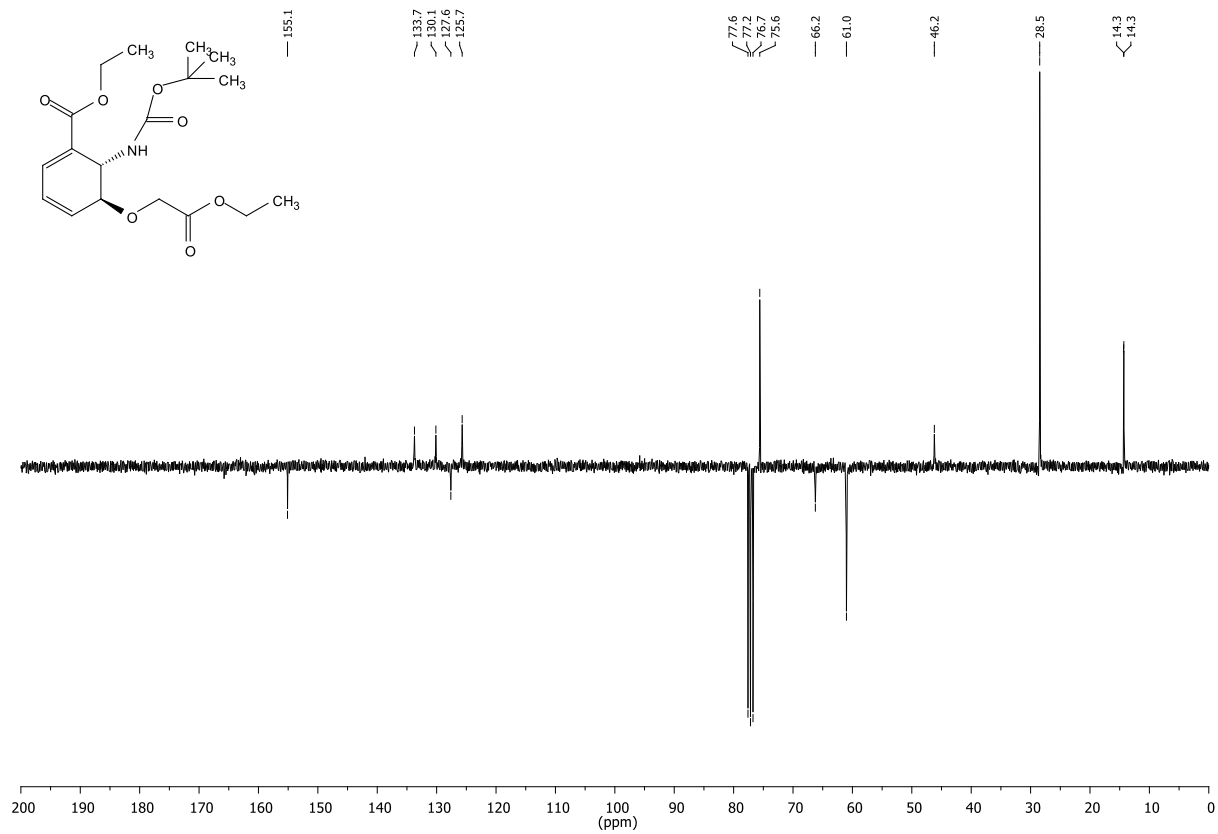


Figure 12.133: $^{13}\text{C-NMR}$,APT (75.53 MHz, CDCl_3) of compound **59**.

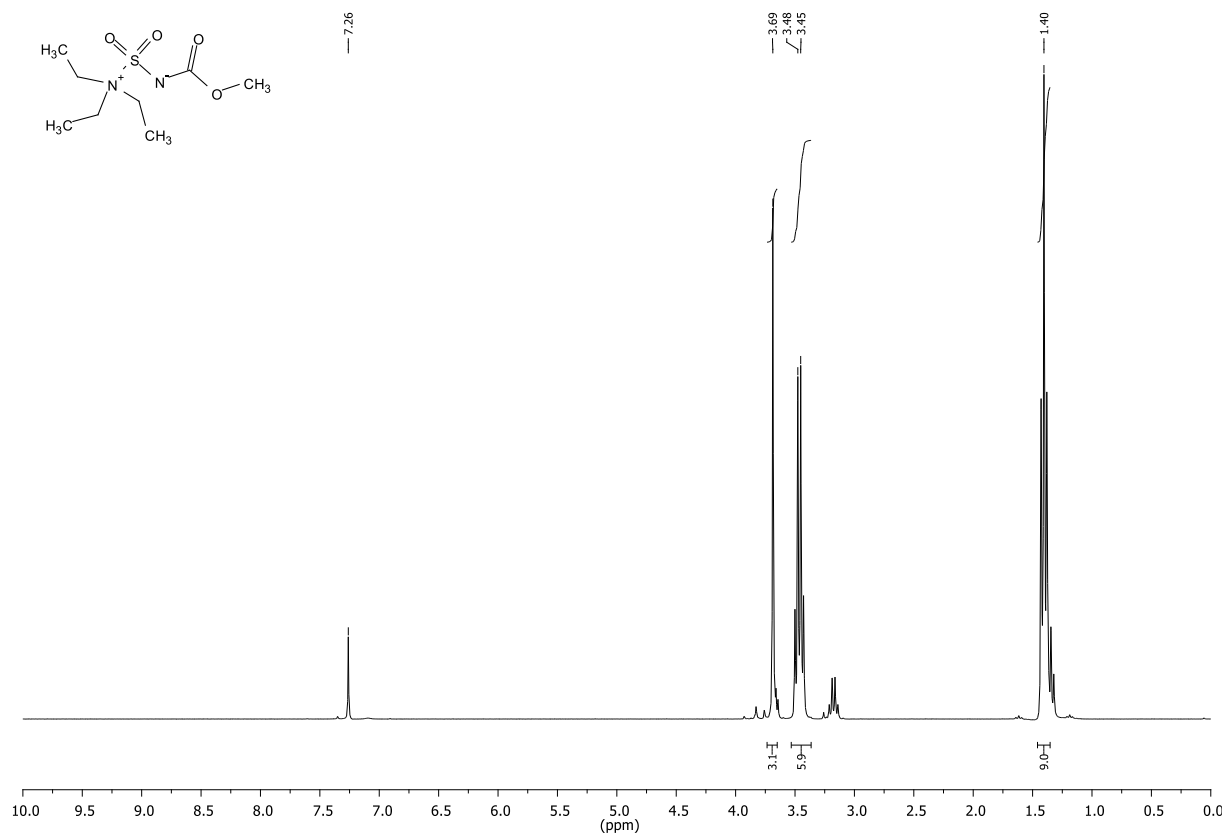


Figure 12.134: $^1\text{H-NMR}$ (300.36 MHz, CDCl_3) of Burgess reagent.

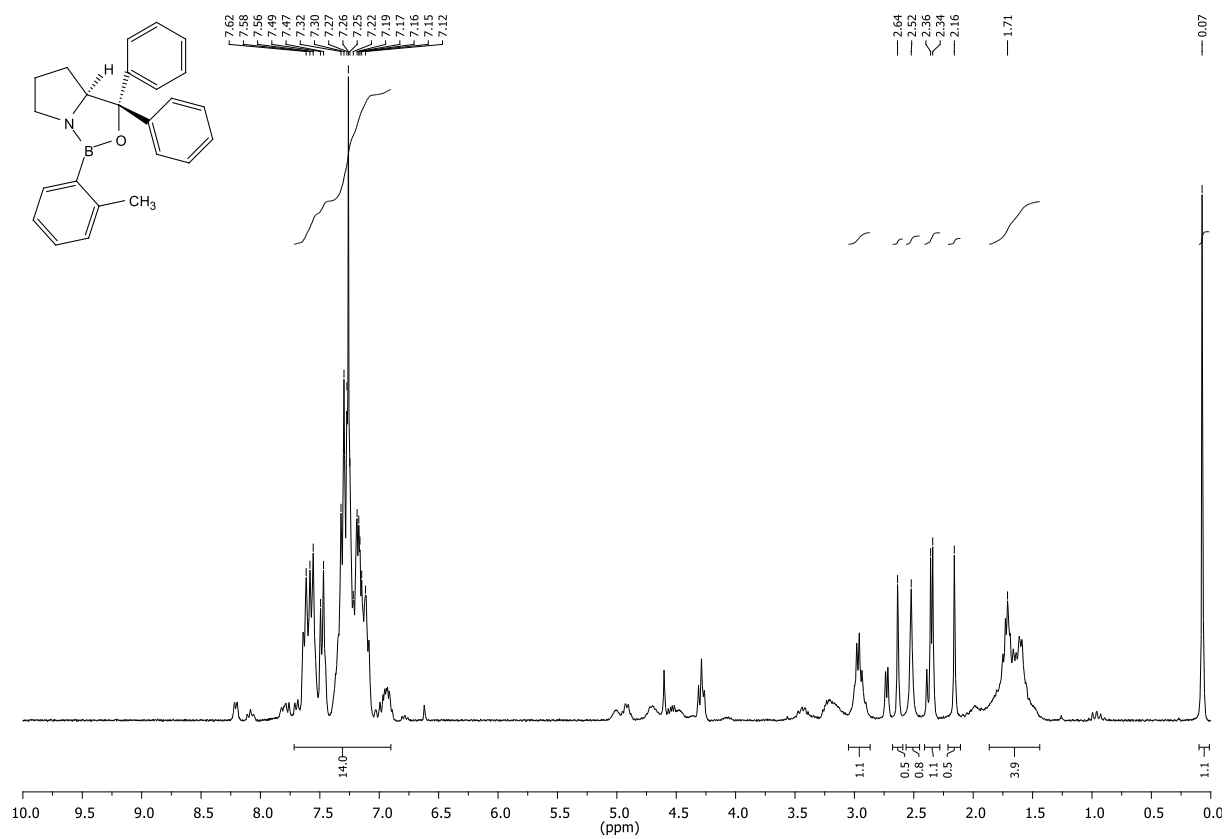


Figure 12.135: $^1\text{H-NMR}$ (300.36 MHz, CDCl_3) of Corey's oxazaborolidium catalyst.

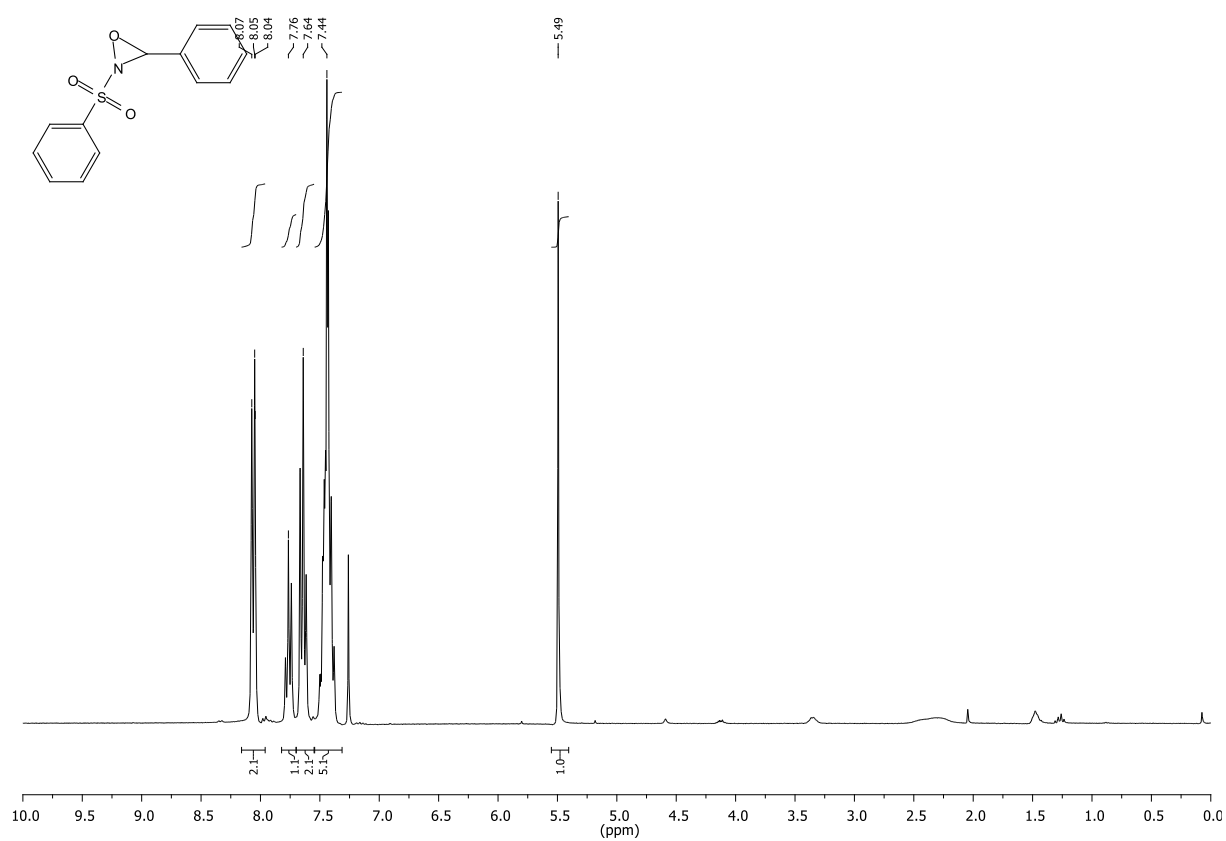


Figure 12.136: $^1\text{H-NMR}$ (300.36 MHz, CDCl_3) of Davis-Oxaziridine

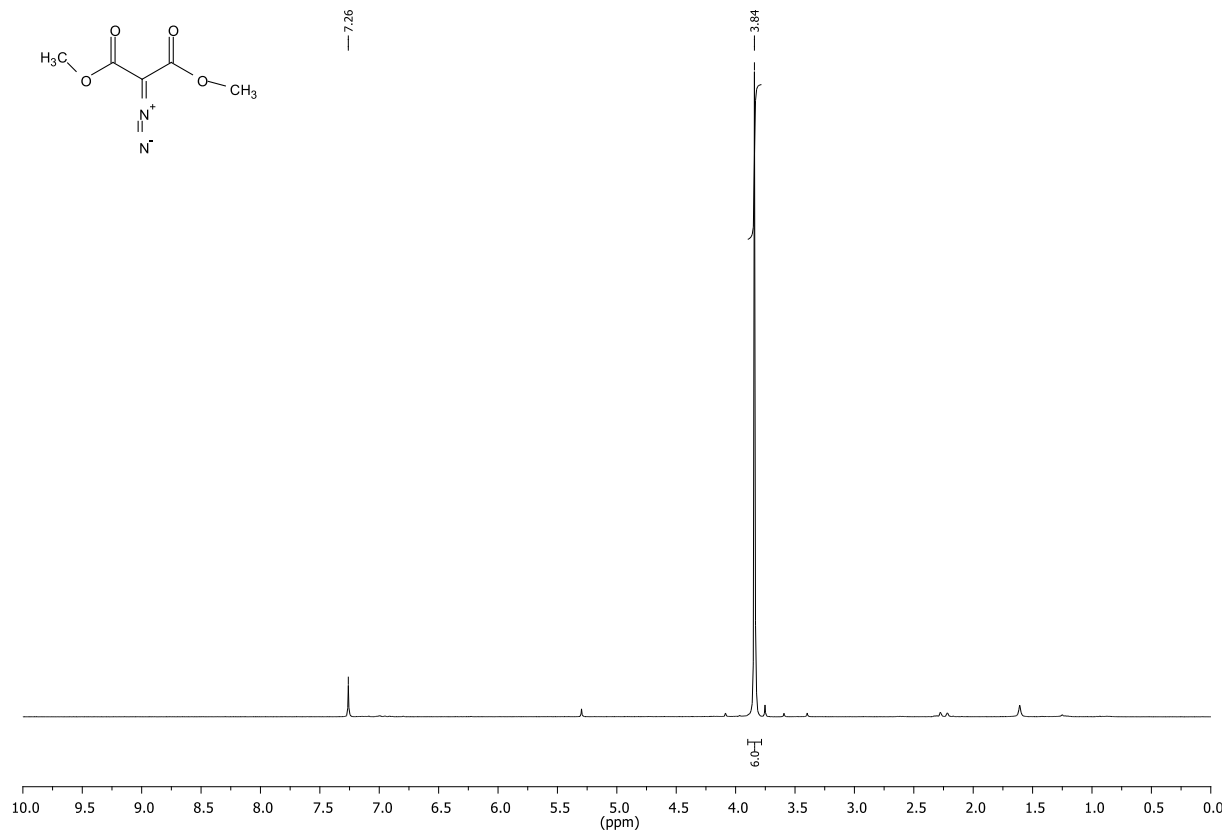


Figure 12.137: $^1\text{H-NMR}$ (300.36 MHz, CDCl_3) of dimethyl-2 diazomalonate

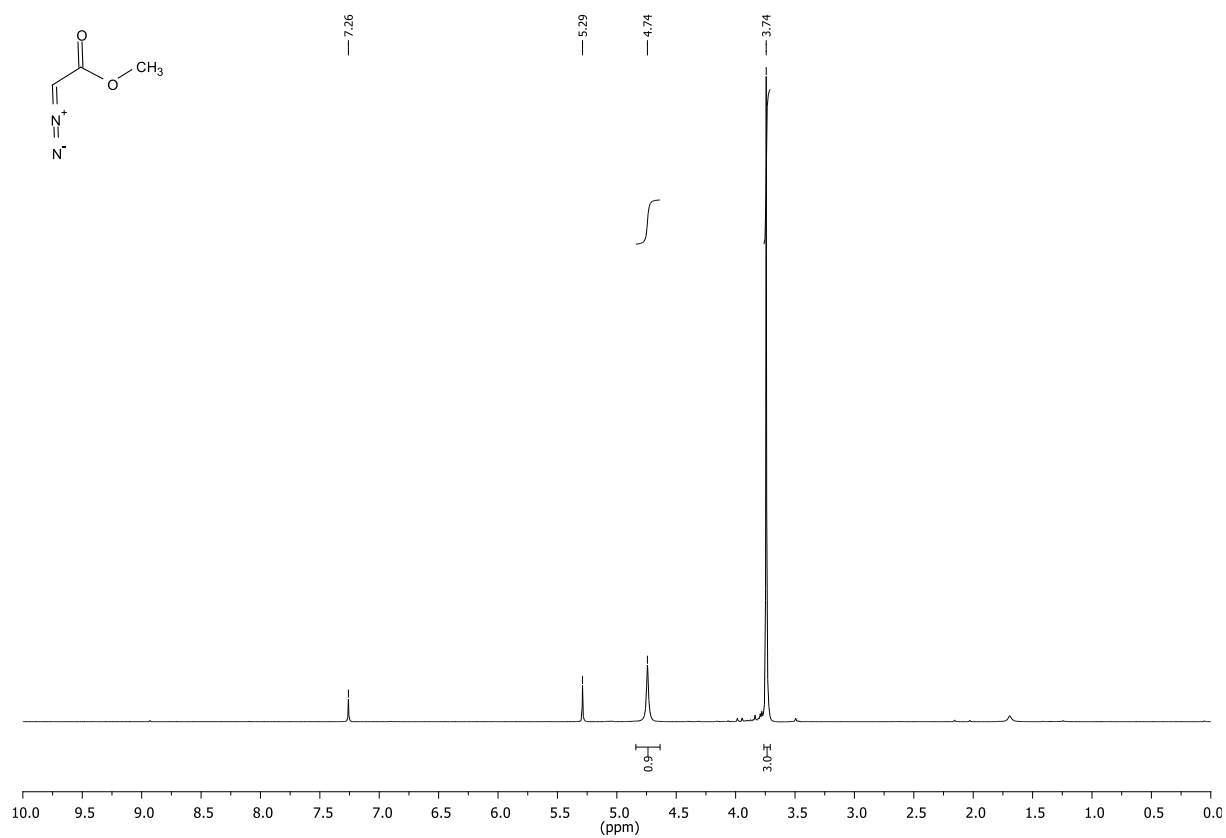


Figure 12.138: ¹H-NMR(300.36 MHz, CDCl₃) of methyl-2-diazoacetate

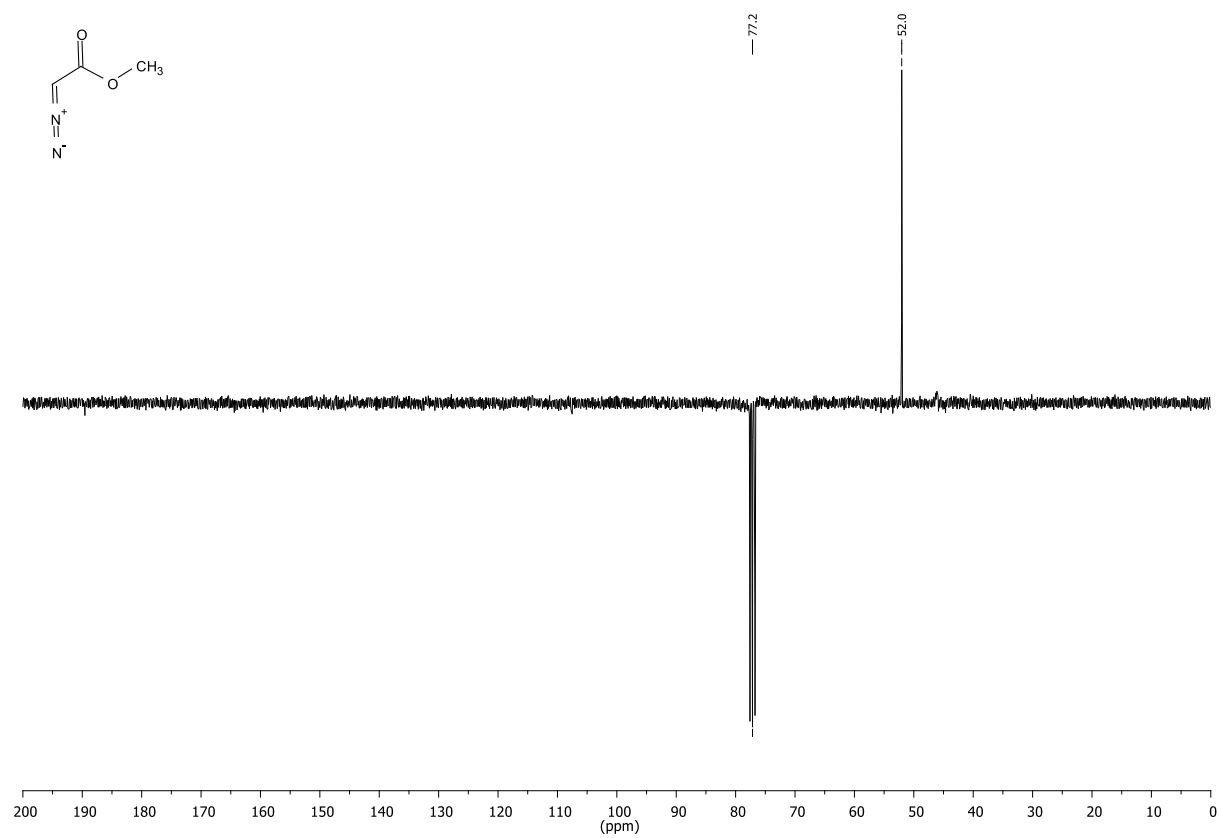


Figure 12.139: ¹³C-NMR, APT (75.53 MHz, CDCl₃) of methyl-2-diazoacetate

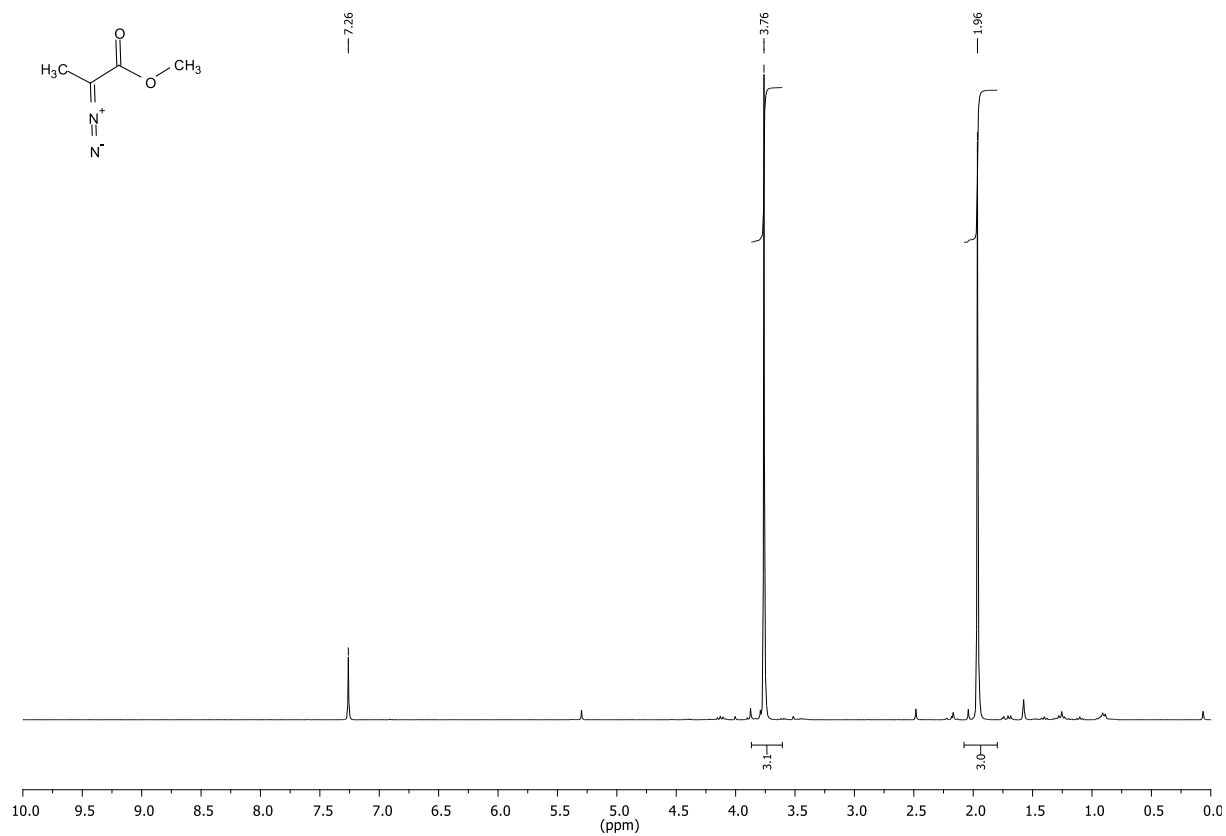


Figure 12.140: ¹H-NMR(300.36 MHz, CDCl₃) of methyl-2-diazopropionate.

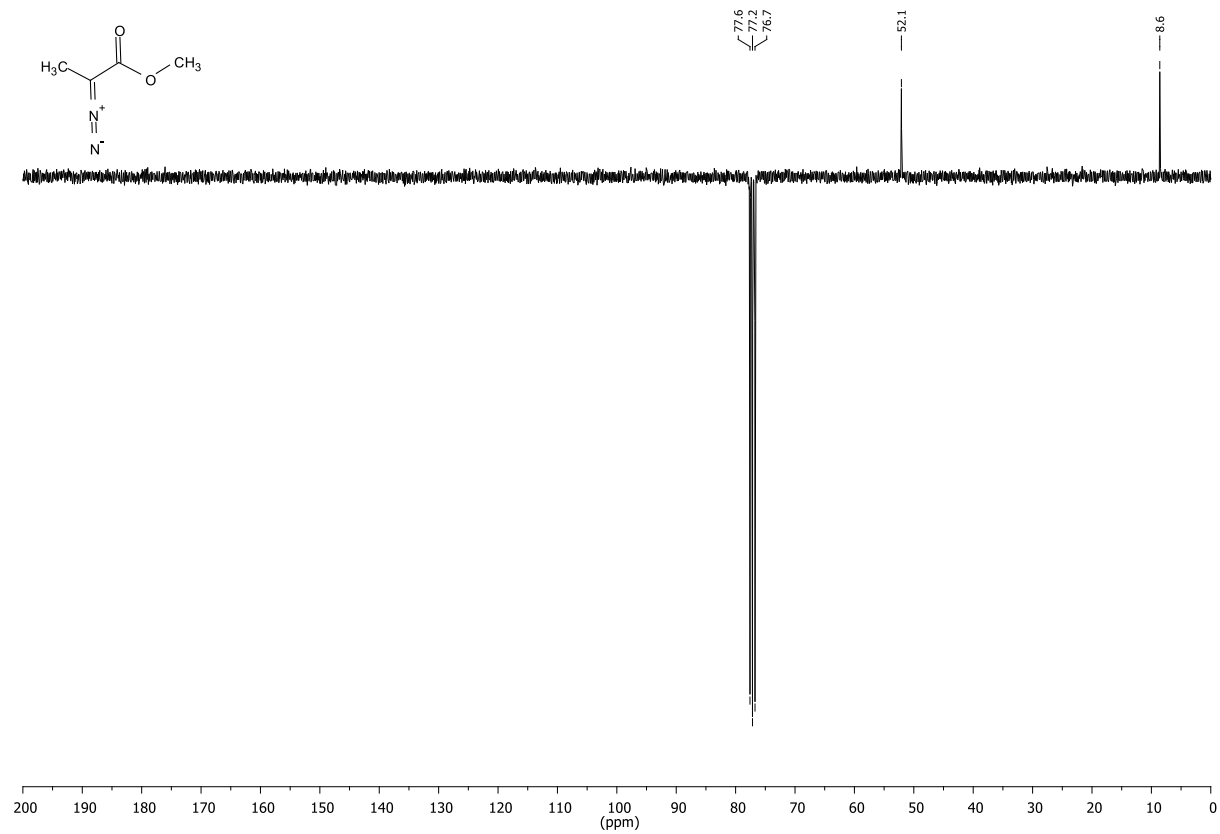


Figure 12.141: ¹³C-NMR,APT (75.53 MHz, CDCl₃) of methyl-2-diazopropionate.

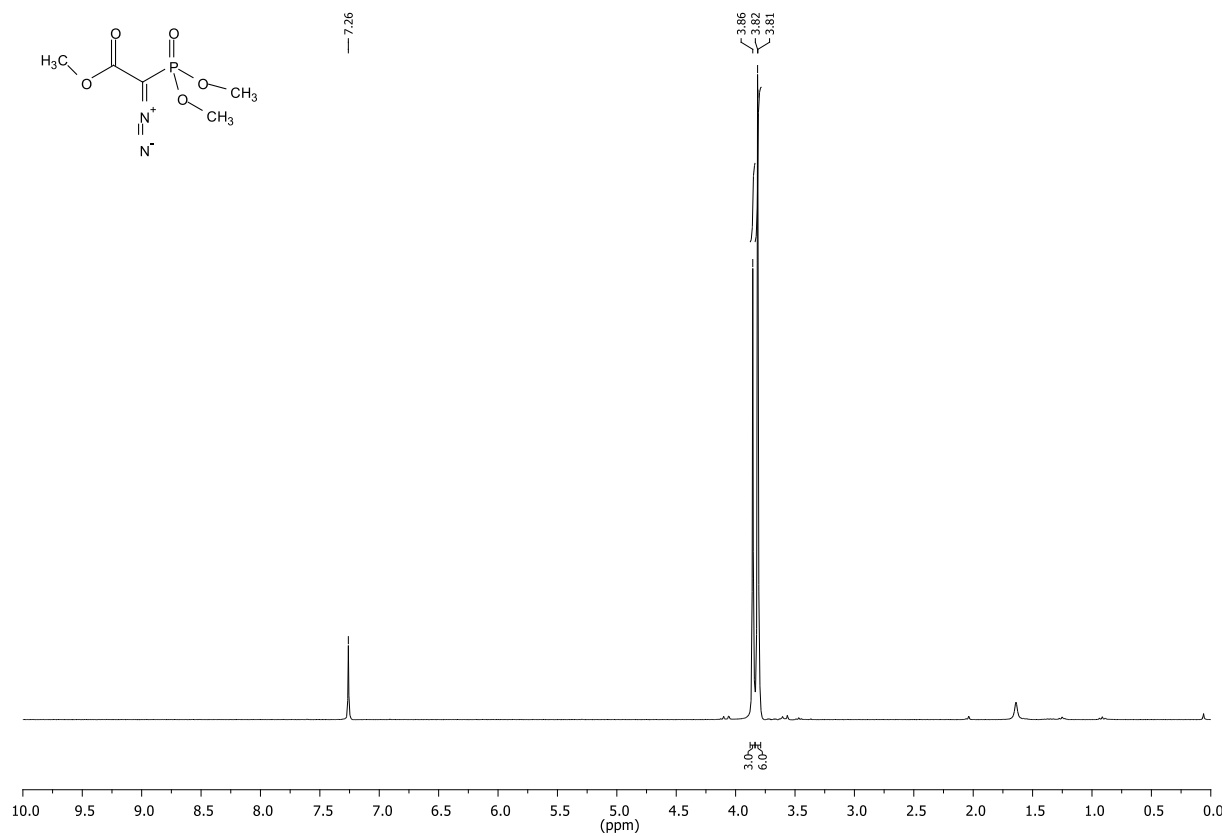


Figure 12.142: $^1\text{H-NMR}$ (300.36 MHz, CDCl_3) of methyl 2-diazo-2-(dimethoxyphosphoryl)acetate:

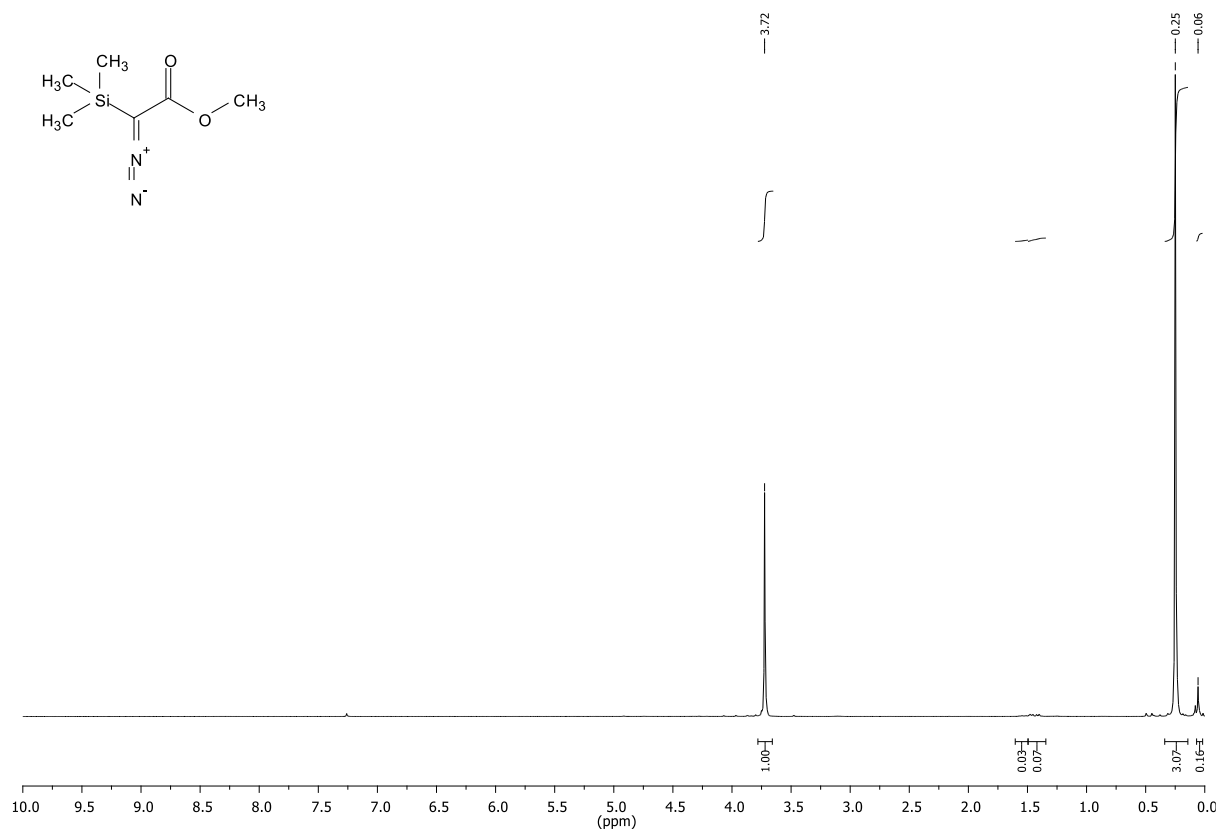


Figure 12.143: $^1\text{H-NMR}$ (300.36 MHz, CDCl_3) of methyl-2-diazo-2-(trimethylsilyl)acetate

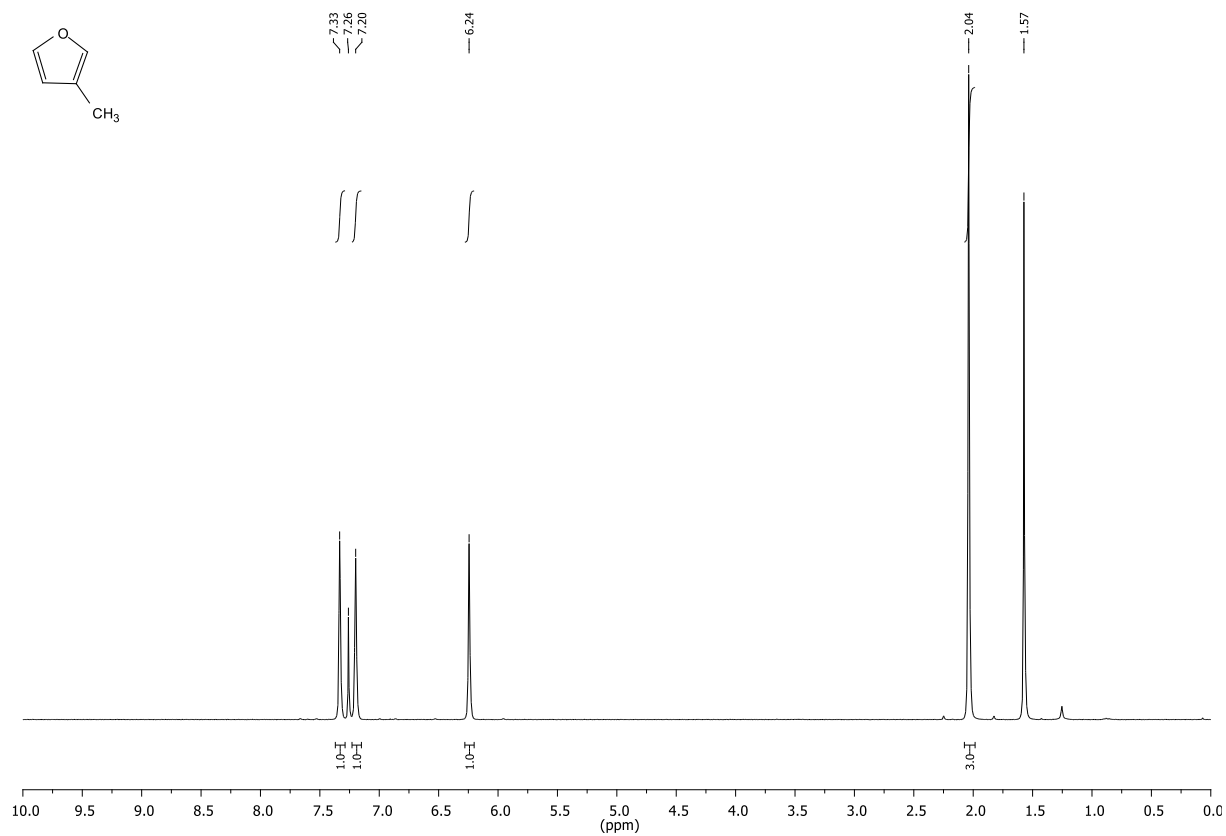


Figure 12.144: $^1\text{H-NMR}$ (300.36 MHz, CDCl_3) of 3-methylfuran

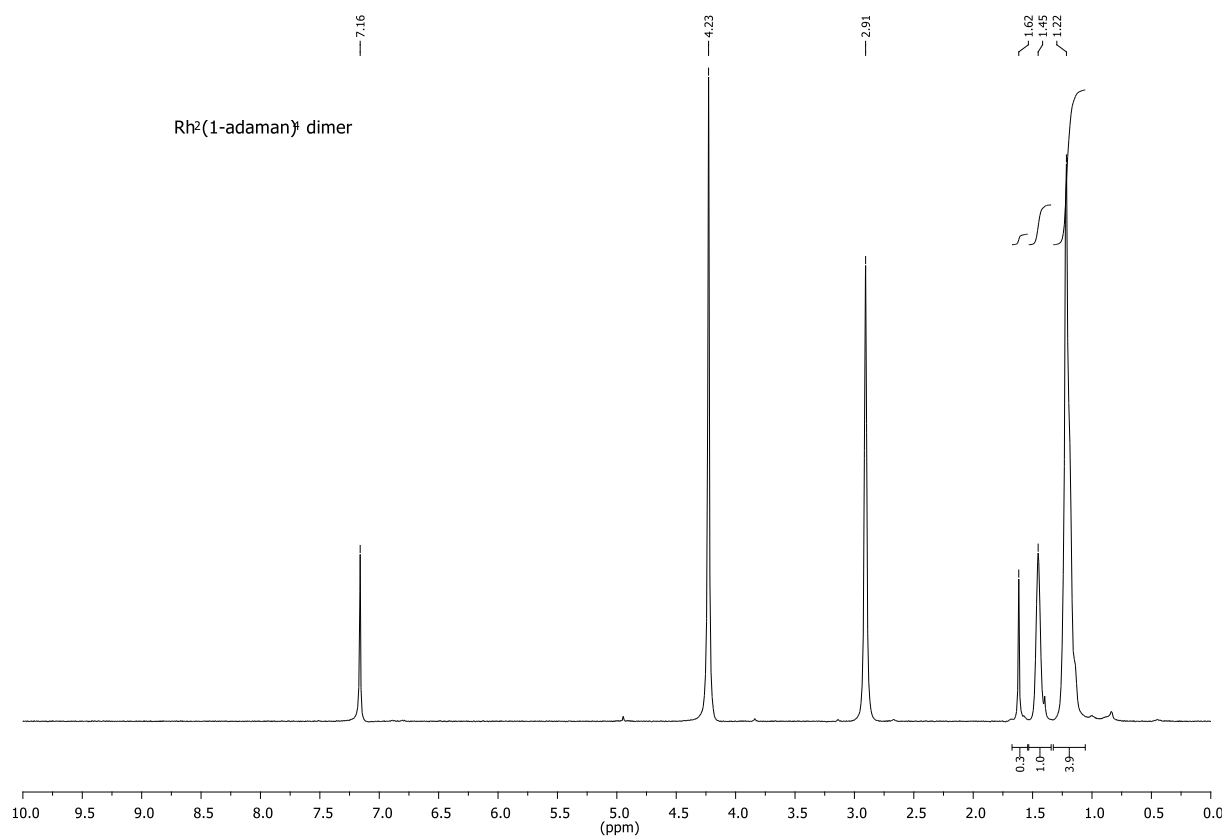


Figure 12.145: $^1\text{H-NMR}$ (300.36 MHz, $\text{MeOD}_4/\text{CDCl}_3$ mixture) of $\text{Rh}_2(1\text{-adaman})_4$ dimer

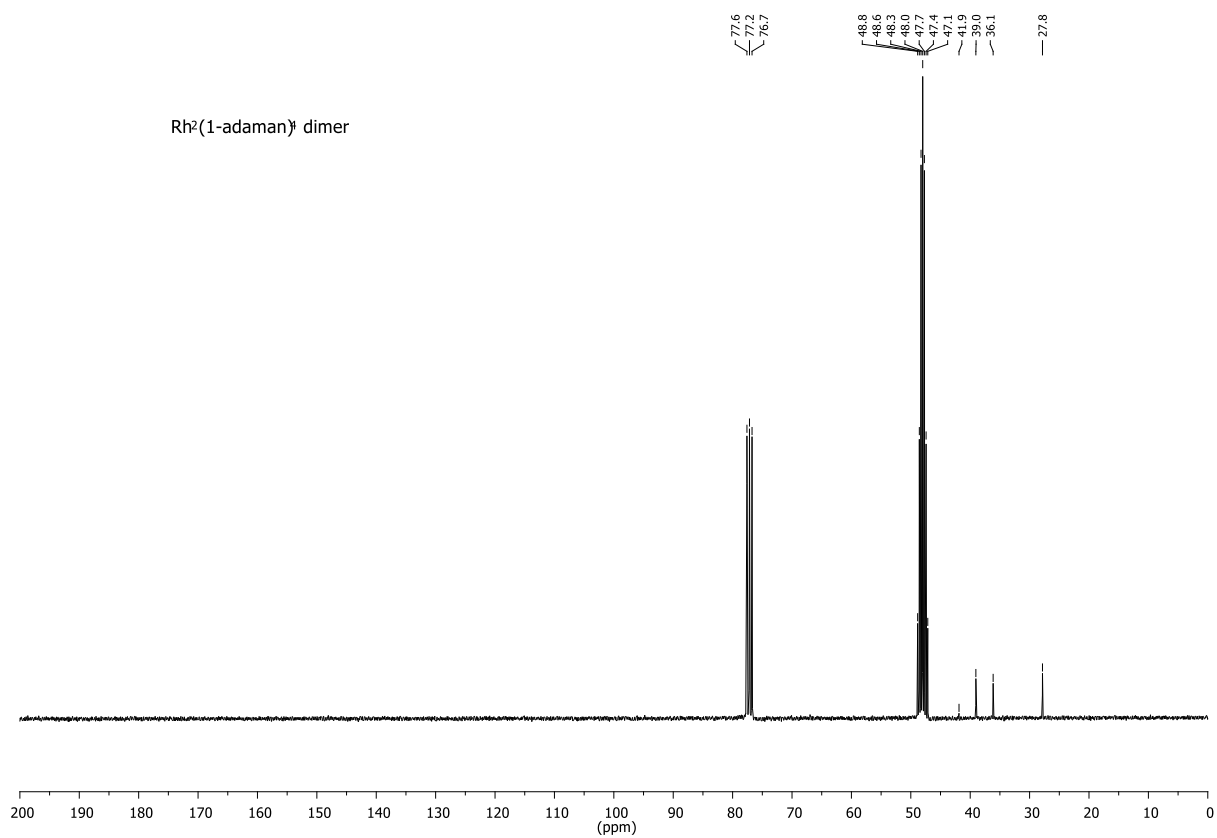


Figure 12.146: ¹³C-NMR,APT (75.53 MHz, MeOD₄/CDCl₃ mixture) of Rh₂(1-adaman)₄ dimer